INFLAMMATION IN CARDIOVASCULAR DISEASES: ROLE OF THE ENDOTHELIUM & EMERGING THERAPEUTICS

EDITED BY: Chen Huei Leo, Cheng Xue Helena Qin and Owen Llewellyn Woodman

PUBLISHED IN: Frontiers in Pharmacology

frontiers Research Topics

frontiers

ISSN 1664-8714
ISBN 978-2-88966-342-2
DOI 10.3389/978-2-88966-342-2

About Frontiers

Frontiers is more than just an open-access publisher of scholarly articles: it is a pioneering approach to the world of academia, radically improving the way scholarly research is managed. The grand vision of Frontiers is a world where all people have an equal opportunity to seek, share and generate knowledge. Frontiers provides immediate and permanent online open access to all its publications, but this alone is not enough to realize our grand goals.

Frontiers Journal Series

The Frontiers Journal Series is a multi-tier and interdisciplinary set of open-access, online journals, promising a paradigm shift from the current review, selection and dissemination processes in academic publishing. All Frontiers journals are driven by researchers for researchers; therefore, they constitute a service to the scholarly community. At the same time, the Frontiers Journal Series operates on a revolutionary invention, the tiered publishing system, initially addressing specific communities of scholars, and gradually climbing up to broader public understanding, thus serving the interests of the lay society, too.

Dedication to Quality

Each Frontiers article is a landmark of the highest quality, thanks to genuinely collaborative interactions between authors and review editors, who include some of the world's best academicians. Research must be certified by peers before entering a stream of knowledge that may eventually reach the public - and shape society; therefore, Frontiers only applies the most rigorous and unbiased reviews.
Frontiers revolutionizes research publishing by freely delivering the most outstanding research, evaluated with no bias from both the academic and social point of view. By applying the most advanced information technologies, Frontiers is catapulting scholarly publishing into a new generation.

What are Frontiers Research Topics?

Frontiers Research Topics are very popular trademarks of the Frontiers Journals Series: they are collections of at least ten articles, all centered on a particular subject. With their unique mix of varied contributions from Original Research to Review Articles, Frontiers Research Topics unify the most influential researchers, the latest key findings and historical advances in a hot research area! Find out more on how to host your own Frontiers Research Topic or contribute to one as an author by contacting the Frontiers Editorial Office: researchtopics@frontiersin.org

INFLAMMATION IN CARDIOVASCULAR DISEASES: ROLE OF THE ENDOTHELIUM & EMERGING THERAPEUTICS

Topic Editors:
Chen Huei Leo, Singapore University of Technology and Design, Singapore
Cheng Xue Helena Qin, Monash University, Australia
Owen Llewellyn Woodman, Monash University, Australia

Citation: Leo, C. H., Qin, C. X. H., Woodman, O. L., eds. (2021). Inflammation in Cardiovascular Diseases: Role of the Endothelium & Emerging Therapeutics. Lausanne: Frontiers Media SA. doi: 10.3389/978-2-88966-342-2

Table of Contents

frontiers in Pharmacology

EDITORIAL
published: 17 November 2020
doi: 10.3389/fphar.2020.614387

Editorial: Inflammation in Cardiovascular Diseases: Role of the Endothelium and Emerging Therapeutics

Cheng Xue Qin[1,2]*, *Owen L. Woodman*[1] and *Chen Huei Leo*[1,3]

[1]Drug, Discovery Biology, Monash Institute of Pharmaceutical Sciences, Monash University, Parkville, VIC, Australia, [2]Baker Heart & Diabetes Institute, Melbourne, VIC, Australia, [3]Science, Math and Technology, Singapore University of Technology & Design, Singapore, Singapore

Keywords: endothelial dysfunction, inflammation, cardiovascular disease, pharmacotherapeutics, vascular homeostasis and remodeling

Editorial on the Research Topic

Inflammation in Cardiovascular Diseases: Role of the Endothelium and Emerging Therapeutics

Endothelial cells, lining the interior surface of all blood vessels, not only participate in the maintenance of the delivery of blood to all vital organs but are also involved in the maintenance of vascular homeostasis. Specifically, endothelial cells play an important role in physiological processes such as the control of vasomotor tone, angiogenesis, leukocyte trafficking, and both innate and adaptive immunity. A great bulk of evidence suggests that multiple diseases, such as atherosclerosis, ischemia, hypertension or diabetes have detrimental effect on endothelium, contributing to the development of cardiovascular diseases (CVD). One of the key common central mechanisms that links all of these diseases is an exaggerated inflammatory response within the endothelium. In all cases, the interaction between inflammatory cells and the endothelium plays a role crucial to the initiation of the pathological condition. Indeed, endothelial dysfunction often encompasses a pro-inflammatory endothelium, contributing to reduced vasodilation, and increased vascular stiffness. Therefore, the main goal of this Research Topic is to provide new mechanistic insights on (patho)physiological events driving inflammation within the endothelium in conditions of multiple diseases, including atherosclerosis, ischemia, hypertension and diabetes.

As a critical contributor to vascular health endothelial function is an important contributor to the regulation of vascular tone, platelet aggregation and leukocyte adhesion. It is well established that endothelial dysfunction is linked with cardiovascular disease and assessment of endothelial function, for example through the assessment of flow mediated vasodilatation, has become an important clinical tool in the prediction of adverse cardiovascular events (Xu et al., 2014). There are multiple endothelium-derived vasodilators such as nitric oxide (NO•), nitroxyl (HNO), hydrogen sulfide (H_2S) and mediators of endothelium-dependent hyperpolarisation (EDH). Much attention has been paid to the impaired activity of NO•, due to the impaired activity of the synthetic enzyme endothelial nitric oxide synthase (eNOS) and its increased inactivation by oxidative stress, in cardiovascular disease (Förstermann and Münzel, 2006). Here Sun et al. and Velagic et al. review the less well documented roles of endothelium-derived H_2S and HNO, respectively. It is suggested by Sun et al. that H_2S may be an important inhibitor of endothelial inflammation suggesting a potential role for improved H_2S donors as therapeutics for CVD. Unlike NO• and H_2S, Velagic et al. discuss the preservation of responses to both endogenous and exogenous HNO in the presence of diabetes-

OPEN ACCESS

Edited and reviewed by:
Eliot Ohlstein,
Drexel University, United States

***Correspondence:**
Cheng Xue Qin
Helena.qin@monash.edu

Specialty section:
This article was submitted to Cardiovascular and Smooth Muscle Pharmacology, a section of the journal Frontiers in Pharmacology

Received: *06 October 2020*
Accepted: *15 October 2020*
Published: *17 November 2020*

Citation:
Qin CX, Woodman OL and Leo CH (2020) Editorial: Inflammation in Cardiovascular Diseases: Role of the Endothelium and Emerging Therapeutics. Front. Pharmacol. 11:614387. doi: 10.3389/fphar.2020.614387

induced oxidative stress and postulate that HNO donors may offer better efficacy than traditional NO-donors in the treatment of vascular disease. Tran et al. focus on metabolic syndrome as a precursor to diabetes and provide a thorough review of animal models that might be best employed to better understand the mechanisms of endothelial dysfunction, making the important point that the role of vasoconstrictor prostanoids is worthy of further investigation. The role of chemokine receptor 5 (CCR5) in metabolic disease and endothelial inflammation is explored by Zhang et al. who consider both the possibilities and difficulties of targeting CCR5 and its ligands in cardiovascular disease. The role of endothelial dysfunction in the genesis of age-related macular degeneration is considered by Yeo et al. who review the mechanisms of choroidal neovascularization and animal models that may advance knowledge in this area. In further consideration of vascular remodeling, Liu et al. investigate changes in pulmonary veins in a hypoxia pulmonary artery hypertension model in mice. In an elegant series of experiments it is demonstrated that hypoxia leads to inhibition of SERCA2 activity to promote calcium influx through the TRPC6 channel resulting in cell proliferation, migration and inhibition of apoptosis. Ding et al. review the rapidly developing area of endothelial and smooth muscle senescence as a contributor to vascular pathology and consider how epigenetic mechanisms may contribute to vascular inflammation and aging.

In the last 2–3 decades, many scientists have interrogated the mechanisms of action of the inflammatory signaling processes that are actively engaged to promote inflammation in the cardiovascular system. A great bulk of evidence suggests that multiple diseases, such as atherosclerosis, ischemia and diabetes, have detrimental effects on the endothelium, contributing to the development of CVD. One of the key common central mechanisms that links all of these diseases is an exaggerated inflammatory cytokine production and response.

The review by Ye et al. summarizes the role of interleukin-12 family members, a class of inflammatory cytokine, in their regulation and progression of various cardiovascular diseases, including atherosclerosis, hypertension, aortic dissection, cardiac hypertrophy, myocardial infarction, and acute cardiac injury. The authors highlight key knowledge gaps in the molecular and cellular mechanisms of interleukin-12 biology, and suggest that a better understanding of these disease processes is critical for the identification of possible targets for prevention which could lead to clinical treatment of a variety of cardiovascular diseases.

Sepsis-induced cardiomyopathy is one of the major predictors of morbidity and mortality of sepsis, present in more than 40% of cases of sepsis and its appearance can increase the mortality rate up to 70%. The review by Lin et al. provides a comprehensive summary of the recent progress in the pathophysiological characterization, diagnosis and current treatments (both pharmacological and non-drug) of septic cardiomyopathy. Furthermore, the authors also introduced several potential novel treatments for septic cardiomyopathy, which includes gene therapy, mitochondrial targeted therapy and inhibition of inflammatory mediators. In addition, the original study reported by Zhang et al. describes the protective actions of the novel anti-inflammatory agent, resolvin E1, an omega-3 polyunsaturated fatty acid-derived metabolite in an animal model of sepsis-induced cardiomyopathy. This exciting study reveals experimental evidence that resolvin E1 treatment inhibits mitogen-activated protein kinase (MAPK) and Nuclear factor kappa B (NF-κB) inflammatory signaling pathways, modulates macrophage polarization and reduces myocardial apoptosis leading to resolution of cardiac inflammation in sepsis-induced cardiomyopathy. This suggests that resolvin E1 may be a novel lipid mediator for the treatment of sepsis-induced cardiomyopathy.

Inflammation is also widely regarded as a key culprit for the pathogenesis of abdominal aortic aneurysm and diabetic cardiomyopathy. The original study by Yan et al. provides experimental evidence for bazedoxifene, a clinically approved therapy for the prevention and treatment of postmenopausal osteoporosis, as a potentially novel treatment for abdominal aortic aneurysm. In their study, Yan et al. indicated that bazedoxifene downregulated the IL-6/GP130/STAT3-dependent inflammatory signaling pathway and attenuated the formation of abdominal aortic aneurysm in angiotensin II-infused $ApoE^{-/-}$ mice. In another original study by Zou et al., the team investigated the potential of a natural compound derived from a Chinese herb, sophocarpine to protect against diabetic cardiomyopathy. Specifically, *in vitro* and *in vivo* experiments revealed that sophocarpine treatment protected myocardial cells from hyperglycemia-induced injury by improving mitochondrial function, suppressing NF-κB-dependent inflammatory signaling pathways and inhibiting cardiac apoptosis. In addition to sophocarpine, other natural products such as flavonoids, are also widely studied as potential treatment for cardiovascular diseases in the context of various disease settings including diabetes. In this regard, Choy et al. elegantly reviewed the therapeutic potential of flavonoids by acting as natural anti-inflammatory agents which target NF-κB inflammatory signaling pathways. The review provides a comprehensive update of the mechanisms underlying NF-κB-induced inflammation in various cardiovascular pathologies and discusses how flavonoids may inhibit the activation of NF-κB and mitigate the inflammatory responses in these disease processes.

Myocardial ischemia/reperfusion injury (I/R) is a complex and multifactorial pathophysiological process in which excess oxidative stress and inflammatory response are essential to the development of both acute and long-term consequences after the ischemic insult. This initial insult to the myocardium is often followed by a pro-inflammatory phase, a proliferative phase and a subsequent remodeling phase. Thus, the development of effective pharmacotherapies, especially by targeting the oxidative stress, inflammatory and remodeling pathways, may improve the clinical outcome of patients in cardiac emergency (Heusch, 2020).

Zhang et al. demonstrated that activation of aldehyde dehydrogenase 2 (ALDH2) is cardioprotective against post-cardiac arrest myocardial dysfunction by attenuating mitochondrial ROS in a rat cardiac arrest model. These observations provided novel evidence for the role of excess aldehyde-induced ROS production in the mitochondria,

suggesting that therapeutic targeting of ALDH2 may be an innovative approach for treating post-cardiac arrest-induced myocardial dysfunction. Yin et al. investigated whether overexpression of inhibitor of differentiation 2 (Id2, a transcriptional repressor) could preserve cardiac function and ameliorate cardiac fibrosis and apoptosis through modulation of TGF-β1/Smad3/hypoxia induced factor-1 alpha (HIF-1α)/interleukin (IL)-11 pathway. These observations suggest that Id2 could provide another novel target for cardiac fibrosis after myocardial infarction. Liu et al. evaluated the efficacy and safety of AFC1, a novel derivative from tanshinone IIa (a natural compound derived from Salvia miltiorrhiza) in a mouse model of myocardial ischemia/reperfusion (I/R) injury, likely by reducing platelet-derived growth factor receptors (PDGFR) and STAT signaling. This result confirmed that AFC1 exerts anti-hypertensive and anti-fibrotic effects against myocardial I/R injury and suggest that AFC1 may be a novel approach for patients suffering myocardial I/R injury.

Finally, we wish to highlight that this wealth of knowledge regarding the breadth of the impact of vascular inflammation in this Research Topic, which has provided new mechanistic insights on (patho)physiological events driving inflammation within the endothelium in CVD, including atherosclerosis, ischemia, hypertension, sepsis or diabetes. Emerging therapeutic strategies (small molecules, peptides, medical devices, natural products) that specifically target the inflammatory pathways or processes in the endothelium have been highlighted. In conclusion, deep knowledge on the endothelium in the cardiovascular system could accelerate the development of novel pharmacotherapies for cardiovascular disease.

AUTHOR CONTRIBUTIONS

CQ and CL conceived and designed the special issue. CXQ, OW, and CL drafted, edited and revised the manuscript. All authors approved the final version of the manuscript.

FUNDING

CXQ received a National Heart Foundation Future Leader Fellowship.

REFERENCES

Förstermann, U., and Münzel, T. (2006). Endothelial nitric oxide synthase in vascular disease: from marvel to menace. *Circulation* 13, 1708–1714. doi:10.1161/CIRCULATIONAHA.105.602532

Heusch, G. (2020). Myocardial ischaemia–reperfusion injury and cardioprotection in perspective. *Nat. Rev. Cardiol.* doi:10.1038/s41569-020-0403-y

Xu, Y., Arora, R. C., Hiebert, B. M., Lerner, B., Szwajcer, A., McDonald, K., et al. (2014). Non-invasive endothelial function testing and the risk of adverse outcomes: a systematic review and meta-analysis. *Eur. Heart J. Cardiovasc. Imaging* 15, 736–746. doi:10.1093/ehjci/jet256

Conflict of Interest: The authors declare that the research was conducted in the absence of any commercial or financial relationships that could be construed as a potential conflict of interest.

frontiers in Pharmacology

ORIGINAL RESEARCH
published: 15 October 2019
doi: 10.3389/fphar.2019.01142

AFC1 Compound Attenuated MI/R-Induced Ventricular Remodeling *via* Inhibiting PDGFR and STAT Pathway

Jie Liu[1,2†], Xiaohui Zhou[1,3†], Qingshu Meng[1,3†], Kevin W. Huang[4], Jing Liu[1,2], Jinjun Tie[1,2], Rulin Zhuang[1,2], Guohan Chen[2], Yuhui Zhang[5], Lu Wei[1,3], Li Huang[4], Chun Guang Li[6], Binghui Wang[3,4], Huimin Fan[1,2,3,7*] and Zhongmin Liu[1,2,3,7]*

[1] Research Center for Translational Medicine, Shanghai East Hospital, Tongji University School of Medicine, Shanghai, China, [2] Department of Cardiovascular and Thoracic Surgery, Shanghai East Hospital, Tongji University School of Medicine, Shanghai, China, [3] Shanghai Heart Failure Research Center, Shanghai East Hospital, Shanghai, China, [4] Monash Centre of Cardiovascular Research and Education in Therapeutics, Department of Epidemiology and Preventive Medicine, Monash University, Melbourne, VIC, Australia, [5] Department of Ultrasound, Shanghai East Hospital, Tongji University School of Medicine, Shanghai, China, [6] NICM Health Research Institute, Western Sydney University, Westmead, NSW, Australia, [7] Department of Heart Failure, Shanghai East Hospital, Tongji University School of Medicine, Shanghai, China

OPEN ACCESS

Edited by:
Cheng Xue Helena Qin, Baker Heart and Diabetes Institute, Australia

Reviewed by:
Neil Macritchie, University of Glasgow, United Kingdom
Francesco Rossi, University of Campania Luigi Vanvitelli, Italy

***Correspondence:**
Binghui Wang
bing.wang@monash.edu
Huimin Fan
Frankfan@tongji.edu.cn

†These authors have contributed equally to this work

Specialty section:
This article was submitted to Cardiovascular and Smooth Muscle Pharmacology, a section of the journal Frontiers in Pharmacology

Received: *12 May 2019*
Accepted: *04 September 2019*
Published: *15 October 2019*

Citation:
Liu J, Zhou X, Meng Q, Huang KW, Liu J, Tie J, Zhuang R, Chen G, Zhang Y, Wei L, Huang L, Li CG, Wang B, Fan H and Liu Z (2019) AFC1 Compound Attenuated MI/R-Induced Ventricular Remodeling via Inhibiting PDGFR and STAT Pathway. Front. Pharmacol. 10:1142. doi: 10.3389/fphar.2019.01142

Background: Effective interventions to improve the outcome of patients subjected to myocardial ischemia reperfusion (MI/R) are urgent in clinical settings. Tanshinone IIA (TSA) is reported to attenuate myocardial injury and improve ventricular remodeling post MI/R. Here, we evaluated the efficacy of AFC1 compound that is similar to TSA structure in murine MI/R models. We found that AFC1 had a comparable effect of improving murine cardiac function after MI/R while it was superior to TSA in safety profile. Administration of AFC1 reduced reactive oxygen species (ROS) production, inflammatory cells infiltration, and the expression of platelet derived growth factor receptors (PDGFR) in infarcted myocardium. Treatment with AFC1 also attenuated MI/R-induced cardiac remodeling and contributed to the recovery of cardiac function. Additionally, AFC1 reversed the elevation of PDGFR expression induced by PDGF-AB in both neonatal rat cardiomyocytes (NCMs) and neonatal rat cardiac fibroblasts (NCFs) and suppressed PDGF-AB induced NCM hypertrophy *via* STAT3 pathway and NCF collagen synthesis through p38-MAPK signaling *in vitro*. Similarly, AFC1 may contribute to the recovery of cardiac function in mice post MI/R *via* suppressing STAT signaling. Our results confirmed that AFC1 exerts anti-hypertrophic and anti-fibrotic effects against MI/R-induced cardiac remodeling, and suggest that AFC1 may have a promising potential in improving the outcome of patients who suffered from MI/R.

Keywords: AFC1 compound, myocardial ischemia reperfusion, platelet derived growth factor, platelet derived growth factor receptor, ventricular remodeling

INTRODUCTION

Ischemic heart disease (IHD) has been a leading cause to high morbidity and mortality in developed countries with increasing incidence in developing countries (Chan et al., 2011). Although timely intervention can restore coronary flow, the reperfusion process triggers myocardium injury (Yellon and Hausenloy 2007), known as myocardial ischemia reperfusion (MI/R) injury, and cardiac remodeling, and subsequent heart failure (HF), which are the predominant contributors of death

worldwide (Murdoch et al., 2006; Sun, 2009; Wang et al., 2015a). Therefore, effective prevention and treatment strategies to attenuate or reverse MI/R-induced remodeling is of great clinical value in IHD patients.

Recently, the protective role and relatively less adverse reaction of traditional Chinese medicine (TCM) in IHD have been highlighted. *Danshen,* the dry roots and rhizome of *Salvia miltiorrhiza Bge.*, has been widely used either alone or in combination with other herbal ingredients for patients with IHD and other cardiovascular diseases in both China and other countries because of its efficacy in improving microcirculation and protecting against myocardial ischemia (Cheng, 2007). For example, results from meta-analysis demonstrated the potential benefits of compound *Danshen* dripping pill (CDDP) for treating coronary heart disease (Luo et al., 2015; Huang et al., 2016). However, the overall quality of the evidences in the systematic reviews was poor and high-quality evidence is warranted to support the clinical application of CDDP in treating IHD. Tanshinone IIA (TSA) is the most abundant and active diterpenoid quinone compound among lipophilic components extracted from *Danshen* (Wu et al., 2013). It is reported that TSA can attenuate myocardial injury and improve ventricular remodeling post MI/R *via* reducing reactive oxygen species (ROS) generation in mitochondria (Zhou et al., 2003; Jin and Li, 2013; Jin et al., 2013). However, in clinical settings, the efficacy of TSA is limited because of its lipid-soluble property, low bioavailability, and short half-life (Liu et al., 2013). Therefore, TSA modification targeting the above shortcomings is a promising strategy for its development in MI/R therapy.

Recently our team has investigated various compounds with similar core structure of TSA, including AFC1. In this study, we proved its potential role in cardiac protective effect against cardiac cell injury, hypertrophy, and fibrosis *in vitro* and *in vivo*. Thus, AFC1 compound may become a novel therapeutic pharmaceutical for patients subjected to MI/R. Accordingly it is important to study the effect of AFC1 *in vivo* to evaluate its efficacy and possible mechanism of actions.

Previous studies have demonstrated the importance of growth factors in IHD (Liu et al., 2014; Pello et al., 2015). High level of platelet derived growth factor (PDGF) in infarcted hearts contributed to myocardial inflammation and fibrosis in rats (Zhao et al., 2011). PDGF family is composed of four kinds of isoforms, -A, -B, -C, and -D, which comprised homodimers of PDGF-AA, -BB, -CC, and –DD and heterodimer of PDGF-AB (Price et al., 2003). PDGF exerts its biological activities through two distinct subtypes of tyrosine kinase receptors, PDGF receptors (PDGFR)-α and -β expressed on cardiomyocytes (Vantler et al., 2010). Excessive expression of PDGF could result in deposition of extracellular matrix and further induces cardiac remodeling (Vantler et al., 2010; Zhao et al., 2011). PDGF could induce H_2O_2 (kind of ROS) generation in mouse embryonic fibroblasts (MEFs) by binding PDGFR (Choi et al., 2005). On the other hand, the inhibition of PDGF/PDGFR pathway could attenuate the vascular remodeling *via* reducing the inflammatory response in the hypertensive rat with myocardial fibrosis (Fan et al., 2013). Therefore, PDGF/PDGFR may promote the development of cardiac remodeling after MI/R by mediating oxidative stress and inflammatory response.

Our present study demonstrated for the first time that treatment with AFC1 compound effectively attenuates MI/R-induced cardiac remodeling, accompanied by decreased PDGFR expression, oxidative stress, and inflammatory response in hearts post MI/R. Moreover, AFC1 compound inhibited NCM hypertrophy and NCF collagen synthesis induced by PDGF-AB and contributed to the recovery of cardiac function post MI/R *via* regulating STAT3 pathway.

MATERIALS AND METHODS

Animals

Specific pathogen-free, male C57BL/6 mice (8–10 weeks) were purchased from Slac Laboratory Animal Co. Ltd (Shanghai, China). All experiments were conducted in accordance with protocols approved by the Institutional Animal Care and Use Committee of Tongji University.

Establishment of Myocardial Ischemia Reperfusion Murine Models

Echocardiography was performed before the establishment of MI/R models. Mice with EF above 50% were included in the *in vivo* experiment. MI/R models were established as described previously (Pu et al., 2013). Regional ischemia was achieved by ligation of LAD using a 10-0 silk suture with a section of silica gel tube. Successful myocardial ischemia was achieved when the anterior wall of the left ventricular (LV) turned pale. After 30 min of ischemia, the ligation was relieved and the successful reperfusion was confirmed by epicardial hyperemia. TSA (5 mg/kg) or AFC1 compound (7 or 14 mg/kg) were intraperitoneally administrated daily for 1 week following MI/R. Mice with the heart exposed through left thoracic incision without ligation of left anterior descending coronary artery (LAD) were included in the sham group. Mice with LAD ligation for 30 min and then reperfusion for 2 weeks were randomly assigned to the following groups (5 mice in each group): Sham, MI/R, MI/R+TSA (5 mg/kg), MI/R+AFC1-L (7 mg/kg), and MI/R+AFC1-H (14 mg/kg). Each experiment was repeated at least three times. The AFC1 compound was synthesized by CG LI's lab at Western Sydney University.

Echocardiography

On day 14 post MI/R, the mice were anesthetized using isoflurane then M-mode echocardiography was performed in mice with echocardiographic imaging system (Visualsonics, Canada) equipped with a 15-MHz linear transducer. Parameters of cardiac function were measured digitally on the M-mode tracings. All echocardiographic procedures were performed by a qualified investigator who was blinded to the grouping and treatment. The long-axis and short-axis view in B-mode were obtained. The B-mode guided M-mode view at the papillary muscle level was obtained for the evaluation of parameters. The end-systolic and end-diastolic LV dimensions were captured to calculate the LV ejection fraction (EF) and fractional shortening (FS) as previously described (Lin et al., 2013).

Histology

After the reperfusion, fresh heart biopsies were fixed in 4% paraformaldehyde overnight at 4°C and embedded in paraffin. Sections into 5-μm slices were stained with hematoxylin-eosin (H&E) or Masson's trichrome for assessment of fibrosis. Tissues for immunofluorescence were submerged in liquid nitrogen and then embedded in optimal cutting temperature (OCT) solution (Sakura Finetek, USA) on dry ice to be frozen completely. Cardiomyocyte hypertrophy was examined in the peri-infarct zone. Myocyte cross-sectional areas were measured using Image J software (National Institutes of Health) in frozen sections stained with 5 μg/ml wheat germ agglutinin (WGA-Alexa Fluor® 488 conjugate, Invitrogen, USA). Five parts were chosen in the WGA images (200X) including left top, right top, middle, left bottom, and right bottom, and six cells were analyzed for each part. In other experiments, the hearts were excised for Masson staining to evaluate the cardiac remodeling. For inflammatory cell infiltration and PDGFR protein expression, immunofluorescence staining with anti-CD45 (Cell Signaling Technology, USA) and anti-PDGFRα (Cell Signaling Technology, USA) in frozen sections was conducted. Then the number of CD45+ cells/field were quantified by Image J software (National Institutes of Health, USA).

ROS Production

ROS production was evaluated with dihydroethidium (DHE, Sigma, USA) on frozen myocardial sections. Heart slices were incubated at 37°C for 30 min with 10 μmol/L DHE in phosphate-buffered saline (PBS). Staining was captured by fluorescence microscope (Leica, Germany). Fluorescence intensity was quantified by using Image J software (National Institutes of Health, USA).

Isolation and Culture of Primary Cardiomyocytes and Cardiac Fibroblasts

NCM and NCF were isolated from 1-day-old pups with enzymatic digestion as described previously (Thomas et al., 2002; Tzanidis et al., 2003). Purified NCMs were seeded at high density of 1×10^6 in 6-well plate and 3×10^5 in 12-well plate and maintained in serum-free DMEM (Gibco, USA) supplemented with 5 mg/ml insulin, 10 mg/ml apo-transferrin, and 50 mM KCl. Bromodeoxyuridine (0.1 mM, Sigma, USA) was applied for the first 3 days. NCF were seeded at a density of 3×10^5 in 6-well plate and 5×10^4 in12-well plate and cultured in DMEM HG supplemented with 0.5% BSA and 1% L-ascorbic acid (Sigma, USA). On the fourth day, 1 h after pretreatment with AFC1 (0.1, 1.0, 3.0, 10.0 μM), PDGF-AB (10 ng/ml, PEPROTECH, USA) was added to induce hypertrophy in NCM and collagen synthesis in NCF. After 48 h of PDGF-AB stimulation, cells were harvested to determine hypertrophy and fibrosis, defined as a significant increase in protein content *via* ^{3}H-Leucine or ^{3}H-Proline incorporation. Cells were treated with AFC1 or DMSO for 1 h and then PDGF-AB for another 15 min for protein sample collection and Western blot detection.

^{3}H-Leucine and ^{3}H-Proline Incorporation

On the fourth day, after addition of PDGF-AB, NCMs were labeled with ^{3}H-Leucine (1 μCi) and NCF with ^{3}H-Proline (5 μCi) (PerkinElmer, USA) for 48 h. The experiment was terminated by washing the cells with cold PBS for three times then precipitating with 10% trichloroacetic acid (TCA, Sigma, USA) for 30 min. Cells were then lysed in 1 M NaOH overnight in 4°C. After neutralization with 1 M HCl and addition of scintillation fluid (PerkinElmer, USA), radioactivity was captured in a liquid scintillation counter (HIDEX 300 SL, Finland). The results represent at least three separate experiments done in triplicate for each condition.

MTT Assay

Cell viability was determined with colorimetric method using the MTT assay. NCFs were seeded at a density of 1.5×10^3 and human umbilical vein endothelial cells (HUVECs, PromoCell) at 1×10^4 cells per well in 96-well plate. After treatments for 48 h, cells were incubated with 10 μl of 5 mg/ml MTT (3-(4,5-dimethyl-2-thiazolyl)-2,5-diphenyl-2-H tetrazolium bromide (Sigma, USA) solution at 37°C for 4 h. The formazan crystals were dissolved in 100 μl of isopropanol for 20 min at 37°C, and absorbance at 570 nm was detected on a Microplate Reader (SpectraMax, USA).

Quantitative RT-PCR (q-PCR)

Total RNA (1 μg) extracted from myocardium, NCM, and NCF were reverse transcribed with PrimeScript RT reagent Kit with gDNA Eraser (TaKaRa, Japan), and q-PCR was performed on the 7900HT Fast Real Time PCR System (Applied Biosystems, UK) with the SYBR mastermix (Applied Biosystems, UK). All primer sequences were listed in **Table 1**.

Comparison of gene expression in different samples was calculated as follows. Each sample was related to an internal control gene (GAPDH). For example, Sample A was the control sample and Sample B was the treated one.

$\Delta\Delta Ct$ = (Ct gene of interest - Ct_{GAPDH})sample B - (Ct gene of interest - Ct_{GAPDH})sample A.

Finally, relative quantification of gene expression (Sample B) = $2^{-\Delta\Delta Ct}$.

Western Blot

Protein was extracted from NCM, NCF, and homogenized myocardium tissue in lysis buffer. Protein lysate concentrations were determined *via* Pierce BCA Protein Assay Kit (Termo Scientific, USA). Equal amount of protein sample (20–30 μg/lane) from each group was subjected to 10% SDS-PAGE and transferred onto nitrocellulose membranes. After blocking with 5% bovine serum albumin (BSA), membranes were incubated overnight with primary antibodies (1:1,000, Cell Signaling Technology, USA) against p-JAK2, p-STAT3, STAT3, p-p38, GAPDH, and pan-actin. On the second day, the membranes were incubated with fluorescent secondary antibody DyLight 800-Goat Anti-Rabbit IgG (H+L) (KPL,

TABLE 1 | Quantitative polymerase chain reaction primers.

Gene	Forward primer (5'-3')	Reverse primer (5'-3')
mPDGF-A	GAGGAAGCCGAGATACCCC	TGCTGTGGATCTGACTTCGAG
mPDGF-B	CATCCGCTCCTTTGATGATCTT	GTGCTCGGGTCATGTTCAAGT
mPDGFR-α	ACACGTTTGAGCTGTCAACC	CCCGACCACACAAGAACAGG
mPDGFR-β	TTCCAGGAGTGATACCAGCTT	AGGGGGCGTGATGACTAGG
mIL-1β	CGAGGCTAATAGGCTCATCT	GTTTGGAAGCAGCCCTTCAT
mTNF-α	AGCCGATGGGTTGTACCTTGTCTA	TGAGATAGCAAATCGGCTGACGGT
mIL-6	TGATGCACTTGCAGAAAACA	ACCAGAGGAAATTTTCAATAGGC
mGAPDH	AACTTTGGCATTGTGGAAGG	ACACATTGGGGGTAGGAACA
rPDGF-A	TTCTTGATCTGGCCCCCAT	TTGACGCTGCTGGTGTTACAG
rPDGF-B	GCAAGACGCGTACAGAGGTG	GAAGTTGGCATTGGTGCGA
rPDGF-C	CAGCAAGTTGCAGCTCTCCA	GACAACTCTCTCATGCCGGG
rPDGF-D	ATCGGGACACTTTTGCGACT	GTGCCTGTCACCCGAATGTT
rPDGFR-α	GCTACACGTTTGAGCTGTCAAC	ATGGTGGTCATCCACAAGC
rPDGFR-β	TCTCTCATCATCCTCATCATGC	CCTTCCATCGGATCTCATAGC
rANP	GAGGAGAAGATGCCGGTAG	CTAGAGAGGGAGCTAAGTG
rα-SKA	GCATGCAGAAGGAGATCACA	CATAGCACGATGGTCGATTG
rβMHC	AGATCGAGGACCTGATGGTG	GATGCTCTTCCCAGTTGAGC
rCol Type I	CATGTTCAGCTTTGTGGACCT	GCAGCTGACTTCAGGGATGT
rCol Type III	GGTCACTTTCACTGGTTGACGA	TTGAATATCAAACACGCAAGGC
rGAPDH	ACAAGATGGTGAAGGTCGGTG	AGAAGGCAGCCCTGGTAACC

USA). The membranes were scanned by ODYSSEY infrared imaging system (LI-COR Biosciences, USA). After incubation of phosphorylated proteins, we used stripping buffer (beyotime, China) to extract antibodies. Then we did the blocking and the following incubation procedures to obtain total protein quantification.

Statistical Analysis

Data, all presented as mean ± SEM, were analyzed using SPSS software, version 11.0 (SPSS Inc., Chicago, IL, USA). For *in vivo* experiments, the Mann-Whitney U test was used for comparisons between different groups. One-way analysis of variance with a Bonferroni *post hoc* test was used for multiple comparisons. $P < 0.05$ was considered statistically significant.

RESULTS

Safety Profile of AFC1 *In Vivo*

To determine the safety of AFC1 *in vivo*, we evaluated the pathology of liver, kidney, spleen, and lung from mice administrated with AFC1 compound for 14 days. As shown by **Figure 1A**, there are no significant morphological changes in these organs. Besides, AFC1 administration did not change the body weight of mice on day 14 (**Figure 1B**). Previous study showed the cytotoxic effect of TSA on human umbilical vein endothelial cells (HUVECs) in a dose-dependent manner (Nizamutdinova et al., 2012). Then we treated the HUVECs with AFC1 or TSA. MTT data showed no difference in HUVECs viability between AFC1 and TSA group when both concentrations are 0.1, 1.0, and 3.0 μM (**Figure 1C**). However, AFC1 treated cells showed higher viability than the TSA group at 10 μM ($p < 0.05$) (**Figure 1C**).

Administration of AFC1 Contributed to the Recovery of Cardiac Function After MI/R in Murine Models

Further cardiac function data showed that both high dose AFC1 (14 mg/kg) compound and TSA (5 mg/kg) significantly improved the EF and FS and systolic left ventricular interior diameters (LVIDs) in MI/R hearts (**Figure 1D**). However, there was no significance when AFC1 and TSA treated groups were compared. Then we assessed whether low (7 mg/kg) and high dose (14 mg/kg) of AFC1 have equal protective role in murine MI/R models. As shown by **Figure 1E**, only high dose of AFC1 increased the EF as well as FS and decreased LVIDs compared to the MI/R group on day 14 post operation.

AFC1 Compound Attenuated Mi/R-Induced Cardiac Remodeling

Both dosages of AFC1 reduced the heart to body weight ratio (HW/BW) of mice effectively in comparison to MI/R group on day 14 ($p < 0.0001$) (**Figure 2A**). WGA staining data revealed significant myocyte hypertrophy in MI/R group compared to the sham ($p < 0.0001$) and treatment with AFC1 greatly inhibited cardiac hypertrophy ($p < 0.01$ and $p < 0.001$) (**Figures 2B**, **C**). Furthermore, AFC1 treated mice showed alleviated cardiac fibrosis compared to the mice without treatment on day 14 following surgery (**Figures 2D**, **E**).

Antioxidant and Anti-Inflammatory Effects of AFC1 Compound on Infarcted Myocardium Following MI/R *In Vivo*

It is well established that oxidative stress and inflammation response contribute to cardiac remodeling and dysfunction following MI/R. We then detected the production of ROS in

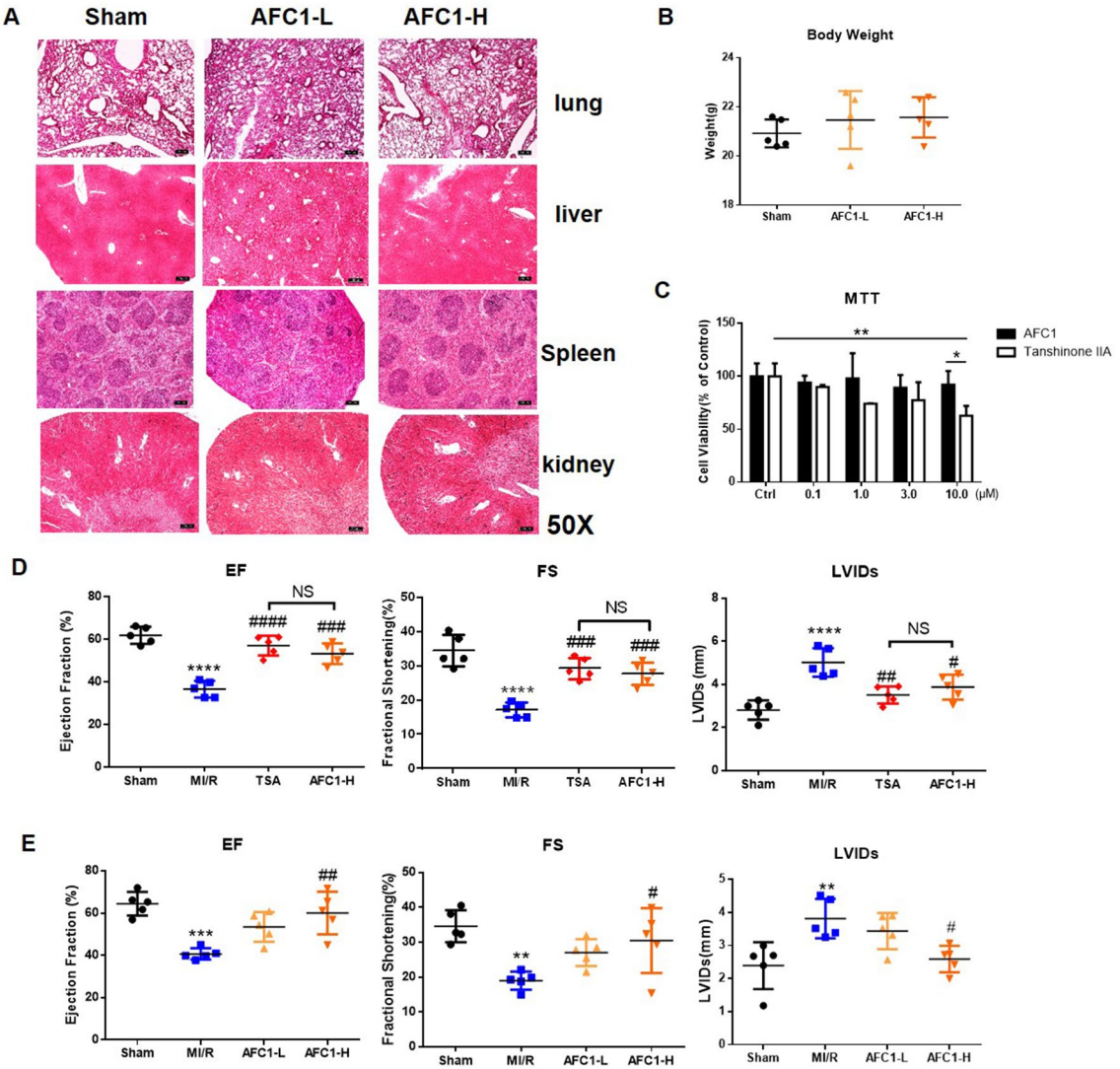

FIGURE 1 | Administration of AFC1 contributed to the recovery of cardiac function after MI/R in murine models. Mice were injected with low (7 mg/kg), high-dosage (14 mg/kg) of AFC1 compound or TSA (5 mg/kg) intraperitoneally for 7 days after MI/R (n = 5). **(A)** Lung, liver, spleen, and kidney sections were harvested on day 14 for H&E staining. Figures showed the representative data. Magnification was ×50. **(B)** Body weight change of mice after AFC1 administration was analyzed on day 14. **(C)** HUVECs were seeded at a concentration of 1×10^4/well in 96-well plate and treated with DMSO, AFC1 compound, or TSA for 24 h. Then cell viability was evaluated by MTT assay. **(D)** EF, FS, and LVIDs were measured by echocardiography on day 14 following MI/R. **(E)** Average values for EF, FS, and LVIDs. Each experiment was repeated for at least three times and results indicated mean ± SEM of one independent experiment. *$p < 0.05$, **$p < 0.01$, ***$p < 0.001$, ****$p < 0.0001$ versus sham or selected group; $^{\#}p < 0.05$, $^{\#\#}p < 0.01$, $^{\#\#\#}p < 0.001$ versus MI/R. *represent the significant different between MI/R group vs the sham group; $^{\#}$represent the significant different between treatment group and MI/R group.

hearts of different groups. MI/R significantly increased the ROS level, while AFC1 treatment greatly decreased ROS accumulation in the infarcted area ($p < 0.05$) (**Figures 3A**, **B**). **Figures 3C** and **D** showed that high dosage of AFC1 dramatically decreased the CD45+ cell infiltrations in heart post MI/R ($p < 0.0001$). Moreover, both high and low dosages of AFC1 compound significantly down-regulated mRNA levels of inflammatory cytokines including IL-1β, IL-6, and TNF-α in MI/R hearts (**Figure 3E**). These results suggested that AFC1 can attenuate MI/R-induced inflammatory responses in the heart.

AFC1 Inhibited the Expression of PDGFR in Murine Heart Following MI/R

Previous study revealed that PDGFs are involved in myocardial remodeling following infarction (Zhao et al., 2011). To verify whether MI/R could lead to an up-regulation of PDGF-related signaling, we measured the expression of PDGF-A, PDGF-B, and PDGFR isoforms in infarcted myocardium. As shown by **Figure 4A**, 30 min of ischemia followed by 2 weeks reperfusion markedly elevated mRNA levels of PDGFRα, -β, PDGF-A, and PDGF-B (**Figures 4A**, **B**). Next, we treated the MI/R mice with AFC1 and data showed high dose of AFC1 down-regulated

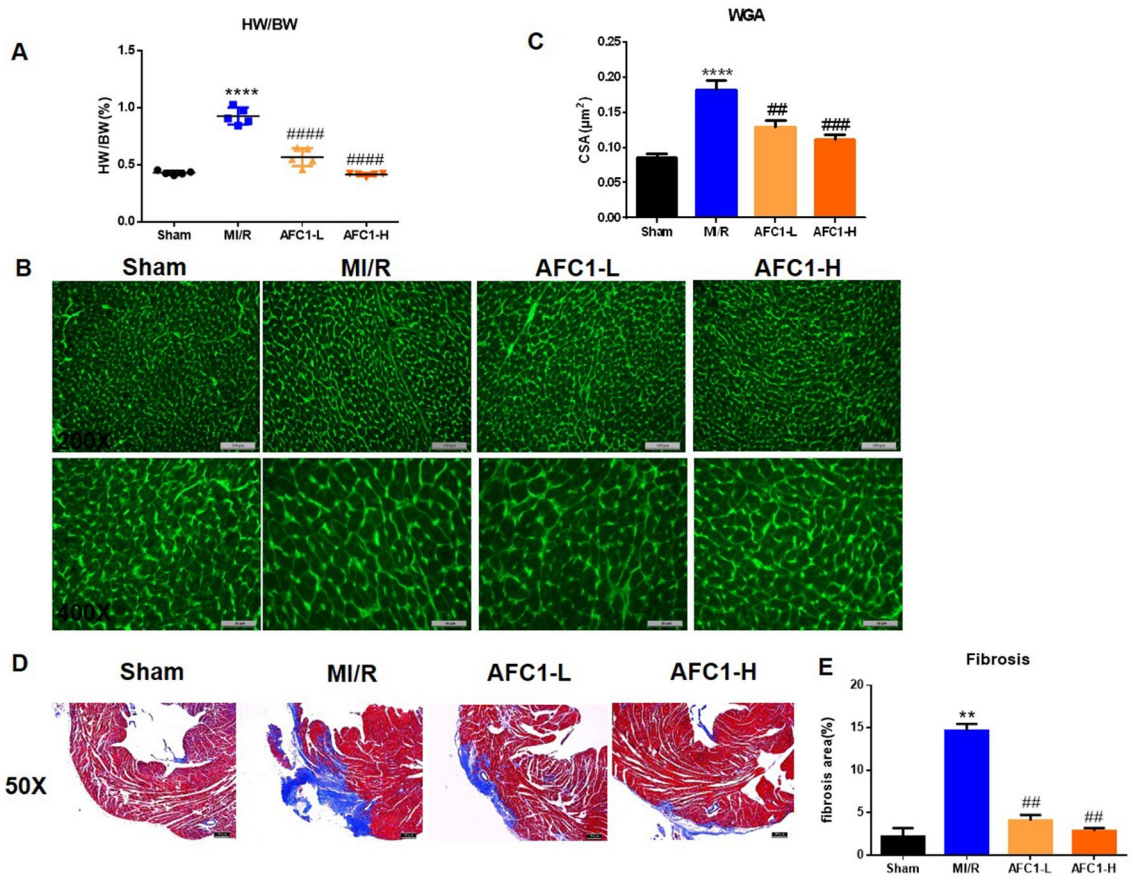

FIGURE 2 | AFC1 Compound attenuated MI/R-induced cardiac remodeling. Heart sections were harvested as mentioned above (n = 5). **(A)** Heart to body weight ratio (HW/BW%) was measured on day 14. **(B)** Representative photomicrographs illustrating ventricular myocyte cross-sections stained WGA. **(C)** Cross-sectional area quantification was shown in statistic graph. **(D)** Hearts were sliced and stained with Masson's trichrome to assess fibrosis. **(E)** Percent of fibrosis area in each group was shown in statistics. Each experiment was repeated for at least three times and results indicated mean ± SEM of one independent experiment. $^{**}p < 0.01$, $^{****}p < 0.0001$ versus sham; $^{\#\#}p < 0.01$, $^{\#\#\#}p < 0.001$, $^{\#\#\#\#}p < 0.0001$ versus MI/R.

both PDGFRα and -β mRNA levels in MI/R hearts. Low dose of AFC1 also decreased the expression of PDGFRα ($p < 0.05$). However, AFC1 did not affect PDGF-A or PDGF-B expression in hearts subjected to MI/R. Then we determined the PDGFRα protein level by immunofluorescence. As shown in **Figure 4C**, PDGFRα protein expression in the heart increased after MI/R, while it decreased after treatment with AFC1. (Nizamutdinova et al., 2012).

Effect of PDGF Stimulation on PDGFR Expression in NCM and NCF *In Vitro*

To further elucidate the role of PDGF signaling on heart remodeling, we treated NCM and NCF with different isoforms of PDGF for 48 or 72 h *in vitro*. As shown by **Figure 5A**, addition of PDGF-AA, PDGF-AB, PDGF-BB, or PDGF-CC all increased the mRNA levels of PDGFRα in NCM compared to the control media. Besides, PDGF-AB or PDGF-BB treatment up-regulated the PDGFRβ mRNA expression in NCM (**Figure 5B**). **Figure 5C** showed that NCM stimulated with PDGF-AB, PDGF-BB, or PDGF-CC for 48 h showed significant elevation of protein content in comparison to control cells. Moreover, administration of PDGF-AB or PDGF-BB triggered collagen synthesis in NCF (**Figure 5D**).

AFC1 Reversed the Elevation of PDGFR Induced by PDGF-AB in Both NCM and NCF *In Vitro*

Next, we treated NCM and NCF with PDGF-AB and AFC1 to determine whether AFC1 compound exerts its protective effect *via* regulating PDGF signaling *in vitro*. As shown by **Figures 6A** and **B**, addition of AFC1 greatly decreased both PDGFRα and PDGFRβ mRNA expression in NCM stimulated with PDGF-AB. Moreover, high dose of AFC1 reversed the up-regulation of PDGFRβ mRNA levels induced by PDGF-AB in NCF (**Figure 6C**). MTT data (**Figure 6D**) showed that AFC1 did not affect the viabilities of NCF, further confirming that AFC1 inhibits the levels of PDGFRα and PDGFRβ stimulated by PDGF-AB in viable NCF cells.

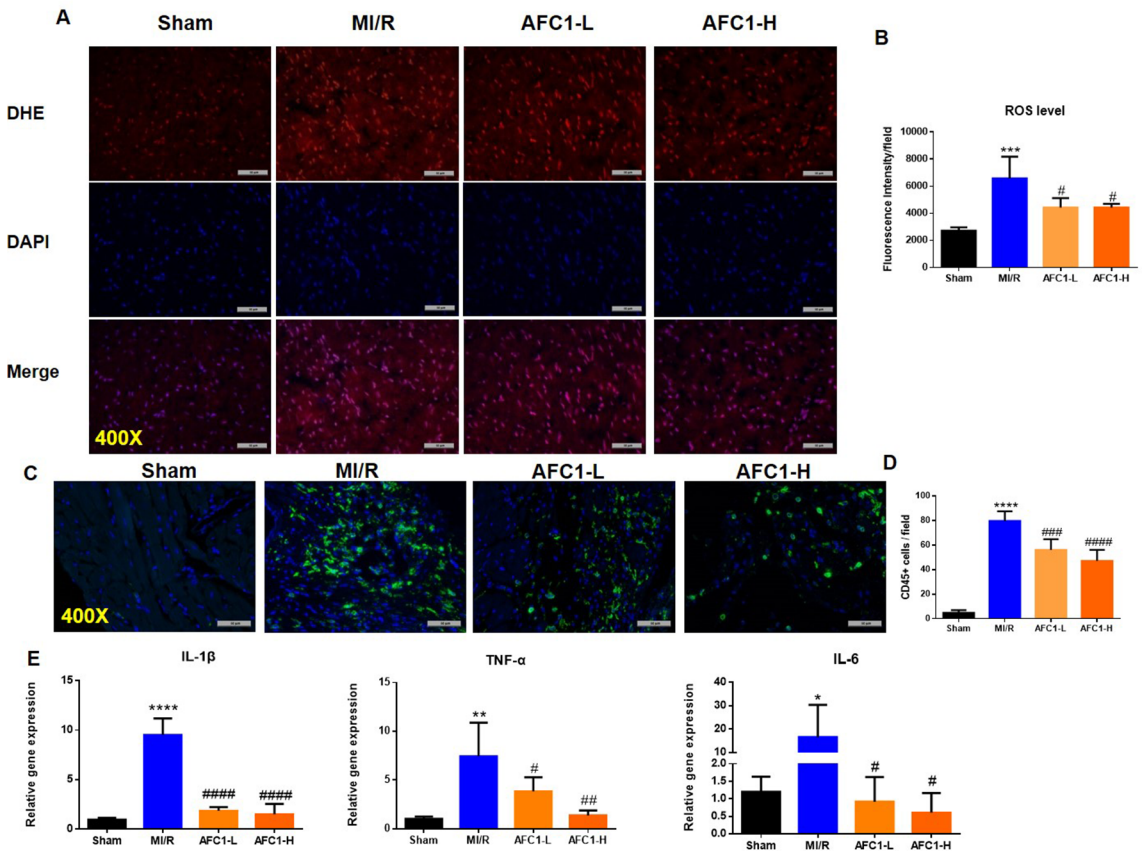

FIGURE 3 | Antioxidant and anti-inflammatory Effects of AFC1 compound on infarcted myocardium following MI/R *in vivo*. Heart sections were harvested and frozen as mentioned above (n = 5). **(A)** Reactive oxygen species production was assessed by dihydroethidium (DHE) conversion to red fluorescent ethidium. **(B)** Fluorescence intensity was evaluated to determine ROS level. **(C)** Immunofluorescence staining of CD45 in transverse section of heart (400×). **(D)** CD45+ cells were quantified in the field. **(E)** Hearts were homogenized and q-PCR was performed to quantify IL-1β, TNF-α, and IL-6 mRNA levels. Results indicated mean ± SEM of one representative experiment and the experiment was repeated three times. $^{*}p < 0.05$, $^{**}p < 0.01$, $^{***}p < 0.001$, $^{****}p < 0.0001$ versus sham; $^{\#}p < 0.05$, $^{\#\#}p < 0.01$, $^{\#\#\#}p < 0.001$, $^{\#\#\#\#}p < 0.0001$ versus MI/R.

AFC1 Suppressed NCM Hypertrophy and NCF Collagen Synthesis Induced by PDGF-AB

To determine whether AFC1 compound can inhibit PDGF-AB induced NCM hypertrophy and NCF collagen synthesis, we examined the protein content *via* liquid scintillation detector to evaluate cardiac remodeling *in vitro*. **Figure 7A** showed that addition of AFC1 (1.0–10 μM) significantly decreased NCM hypertrophy induced by PDGF-AB in a dose-dependent manner. Furthermore, AFC1 (3.0 and 10 μM) reversed the elevations of ANP, β-MHC, and α-SKA mRNA levels stimulated by PDGF-AB in NCM (**Figure 7B**). AFC1 also inhibited the collagen synthesis (**Figure 7C**) as well as the mRNA expression of Col I and Col III in NCF stimulated by PDGF-AB (**Figure 7D**).

AFC Modulated Signaling Pathways Involved in Cardiac Function and MI/R

Previous reports revealed that STAT signaling pathway played a vital role in myocardial remodeling (Aboulhoda, 2017, Wincewicz and Sulkowski, 2017), and P38MAPK pathway is involved in cellular inflammatory response and apoptosis under the condition of ischemia and hypoxia (Owona et al., 2013). We cultured NCM and NCF with PDGF-AB with or without JAK inhibitor JI1 (JAKs inhibitor I-Calbiochem, Darmstadt, Germany) and p38 inhibitor 979 (Cai et al., 2018). As shown by **Figures 8A** and **B**, both 10 μM JI1 and 3 μM 979 inhibited NCM hypertrophy and NCF collagen synthesis induced by PDGF-AB. Western blots analysis of protein expression of p-JAK2, p-STAT3, and p-p38 in cells revealed that PDGF-AB treatment greatly activated the phosphorylation of STAT3 in NCM and p-38 in NCF. Addition of AFC1 dramatically decreased the levels of p-STAT3 in NCM and p-p38 in NCF induced by PDGF-AB (**Figures 8C**, **D**). No significant difference was observed in the expression of p-JAK2 in these groups.

For *in vivo* study, MI/R increased the ratio of p-STAT3/GAPDH without affecting p-STAT3/STAT3 and STAT3/GAPDH in infarcted myocardium. Treatment with high dose of AFC1 markedly reversed the elevation of both p-STAT3/GAPDH and p-STAT3/STAT3 without affecting the ratio of STAT3/GAPDH (**Figures 8E**, **F**).

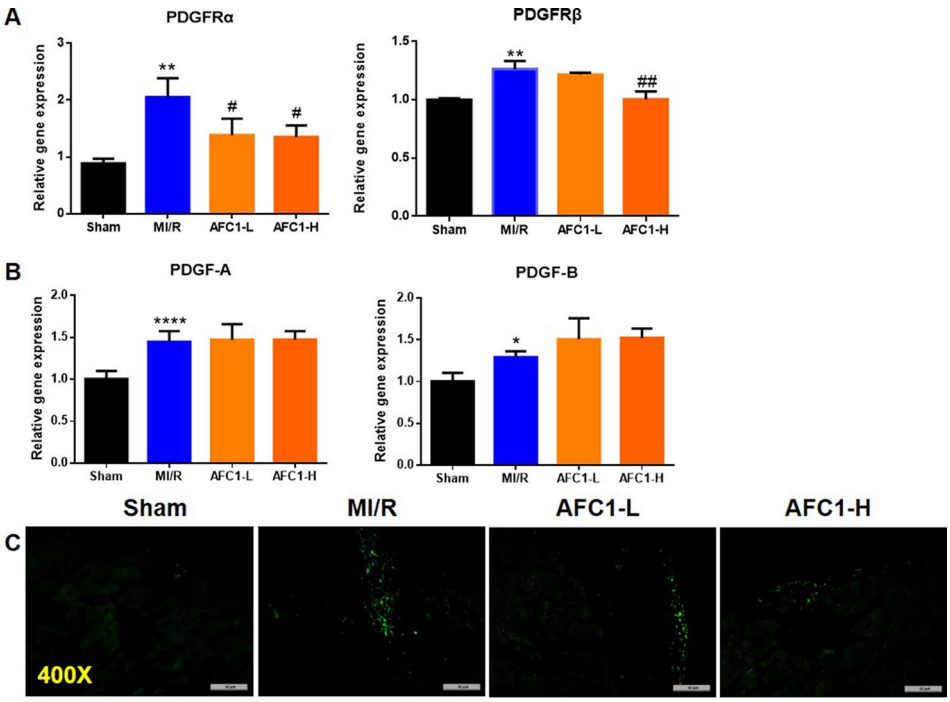

FIGURE 4 | AFC1 inhibited the expression of PDGFR in heart following MI/R (n = 5). Total RNA was extracted from hearts in each group and q-PCR was performed to quantify PDGFRα, PDGFRβ **(A)**, PDGF-A, and PDGF-B **(B)** mRNA levels. **(C)** Immunofluorescence staining of PDGFRα in transverse section of heart (400×). Each experiment was repeated for at least three times and results indicated mean ± SEM of one representative experiment. *p < 0.05, **p < 0.01, ****p < 0.0001 versus sham; #p < 0.05, ##p < 0.01 versus MI/R.

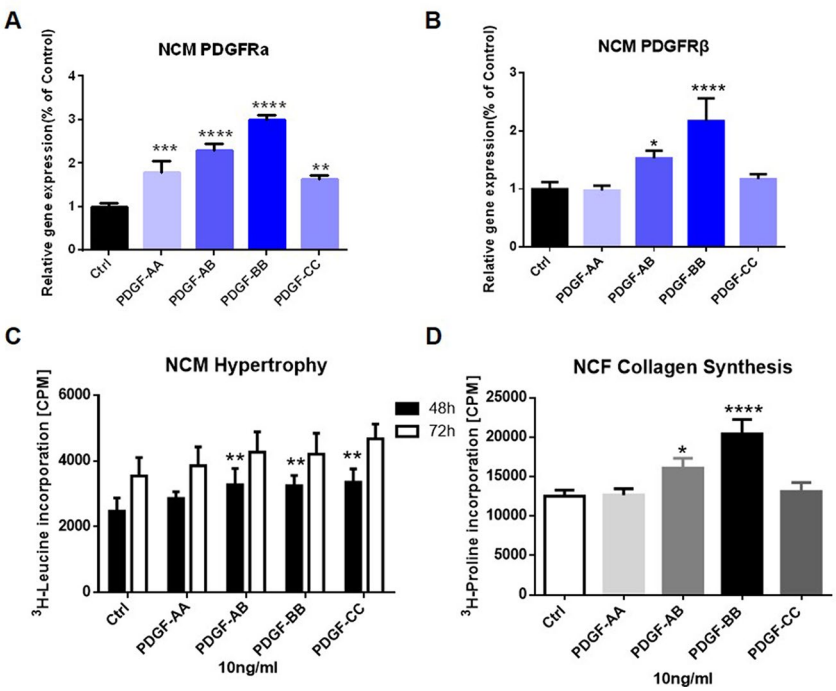

FIGURE 5 | Effect of PDGF stimulation on PDGFR expression in NCM and NCF *in vitro*. PDGFRα **(A)** and PDGFRβ **(B)** mRNA expression in NCM were assessed by q-PCR. NCM hypertrophy **(C)** was measured by ^{3}H-leucine incorporation and NCF collagen synthesis **(D)** measured by ^{3}H-proline incorporation on different PDGF isoform stimulation. Each experiment was repeated for four times and results indicated mean ± SEM of one representative experiment. *p < 0.05, **p < 0.01, ***p < 0.001, ****p < 0.0001 versus control.

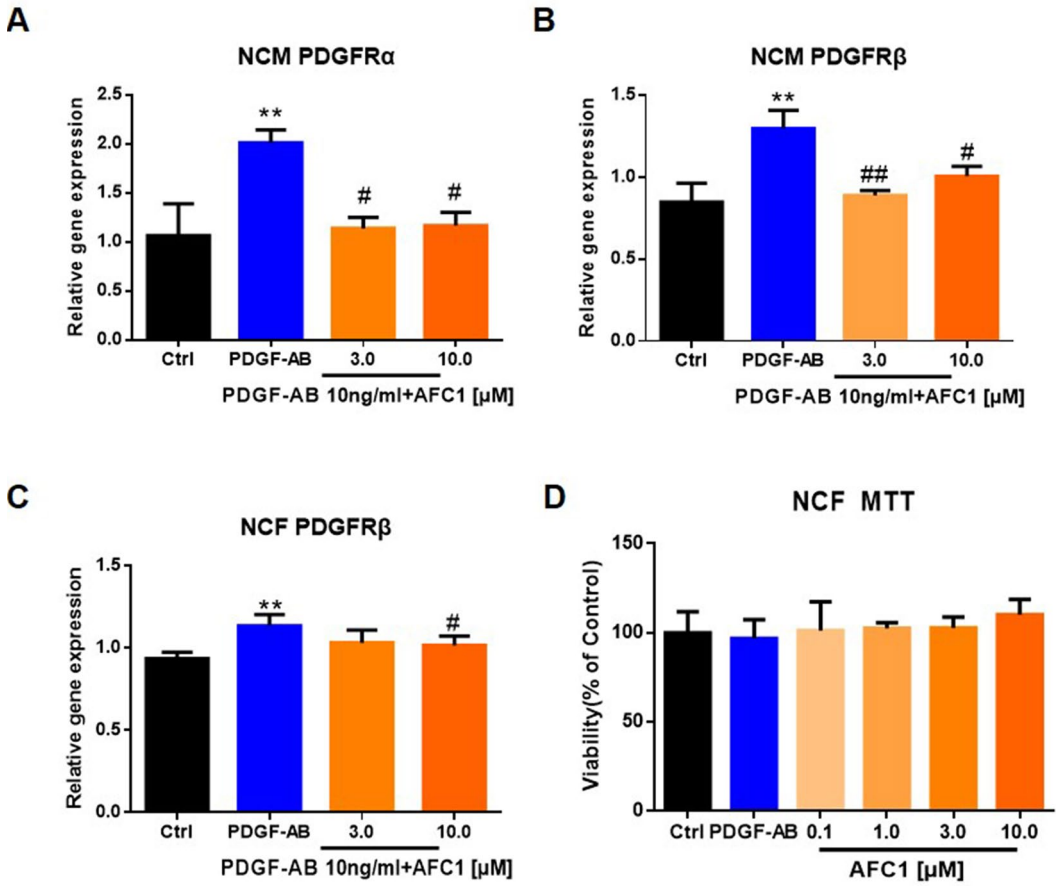

FIGURE 6 | AFC1 reversed the elevation of PDGFR induced by PDGF-AB in both NCM and NCF *in vitro*. PDGFR expression in NCM **(A**, **B)** and NCF **(C)** were quantified by q-PCR. **(D)** Viability of NCF stimulated with PDGF-AB or AFC1 compound (0.1, 1.0, 3.0, 10.0 μM) was evaluated by MTT assay. This experiment was repeated four times and results indicated mean ± SEM of one independent experiment and representative pictures. $^{**}p < 0.01$ versus control; $^{\#}p < 0.05$, $^{\#\#}p < 0.01$ versus PDGF-AB.

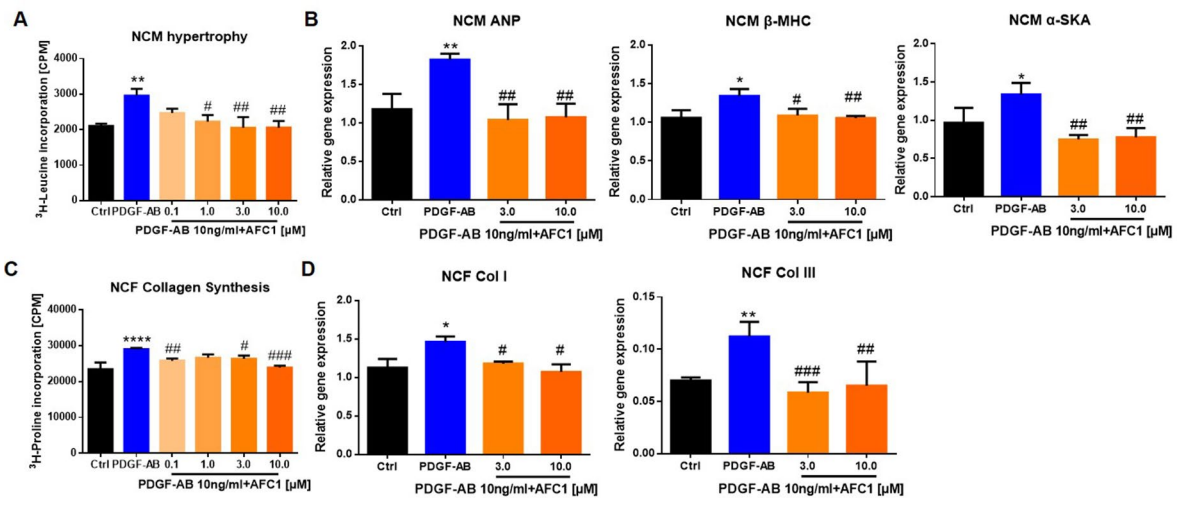

FIGURE 7 | AFC1 suppressed PDGF-AB induced NCM hypertrophy and NCF collagen synthesis. NCM hypertrophy **(A)** was measured by ^{3}H-leucine incorporation and NCF collagen synthesis **(C)** measured by ^{3}H-proline incorporation on different concentration of AFC1 after PDGF-AB (10 ng/ml) stimulation. mRNA levels of ANP, β-MHC, α-SKA in NCM **(B)**, and Col I, Col III in NCF **(D)** were measured by q-PCR. This experiment was repeated four times and results indicated mean ± SEM of one independent experiment. $^{*}p < 0.05$, $^{**}p < 0.01$, $^{****}p < 0.0001$ versus control; $^{\#}p < 0.05$, $^{\#\#}p < 0.01$, $^{\#\#\#}p < 0.001$ versus PDGF-AB.

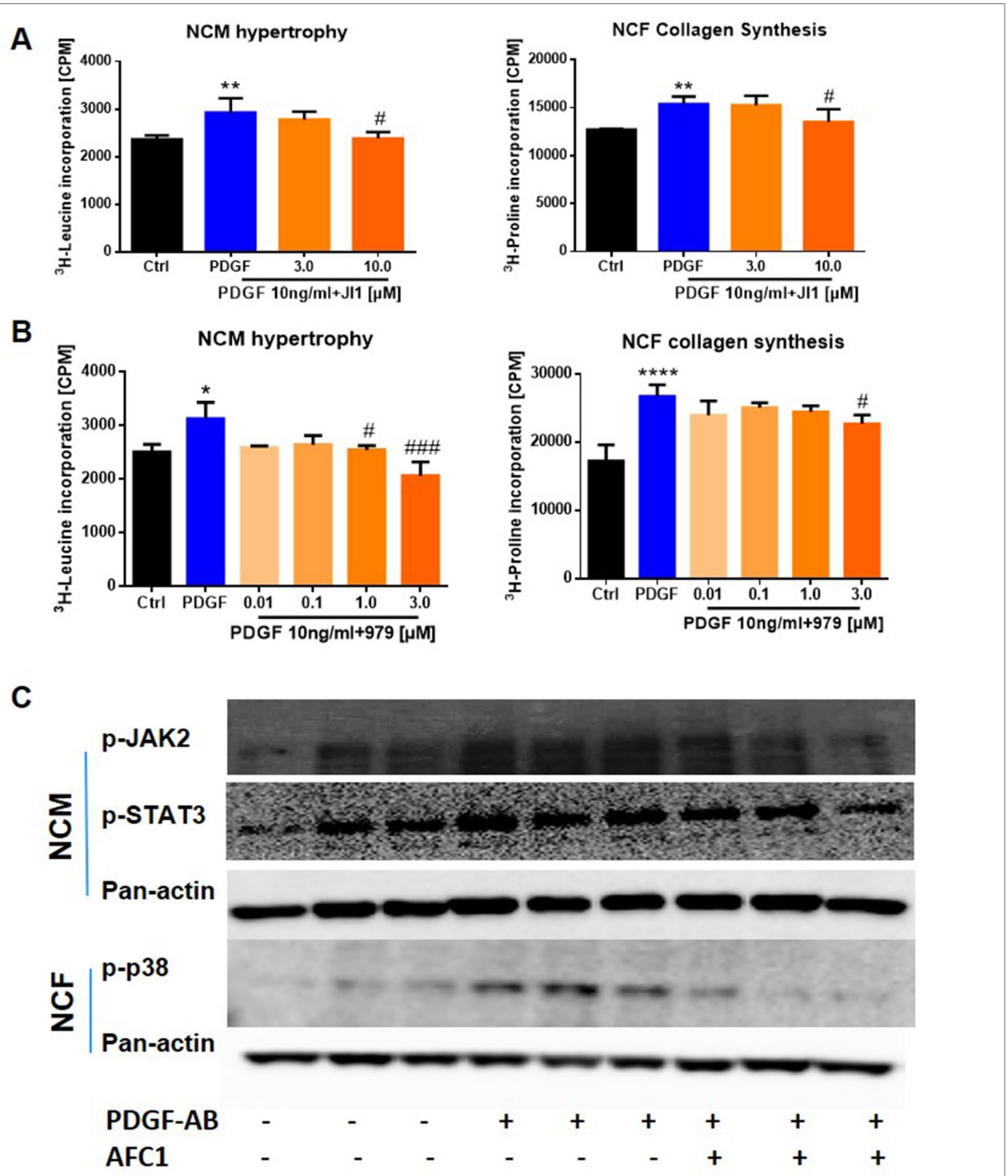

FIGURE 8 | Continued

DISCUSSION

Early and effective intervention strategies have greatly decreased the mortality of IHD; however, reperfusion could cause myocardium damage, even exacerbate the cardiac function and structure (Wang et al., 2015b). Innovative pharmacotherapies to improve the outcomes especially left ventricular remodeling in patients who suffered from MI are still an urgent need (Della Rocca et al., 2012; Chew et al., 2018). Recently, TCMs have received much attention due to their functions in reduction of myocardial injury (Mo et al., 2015; Yang et al., 2016). Many studies demonstrated the cardioprotective effect of TSA and

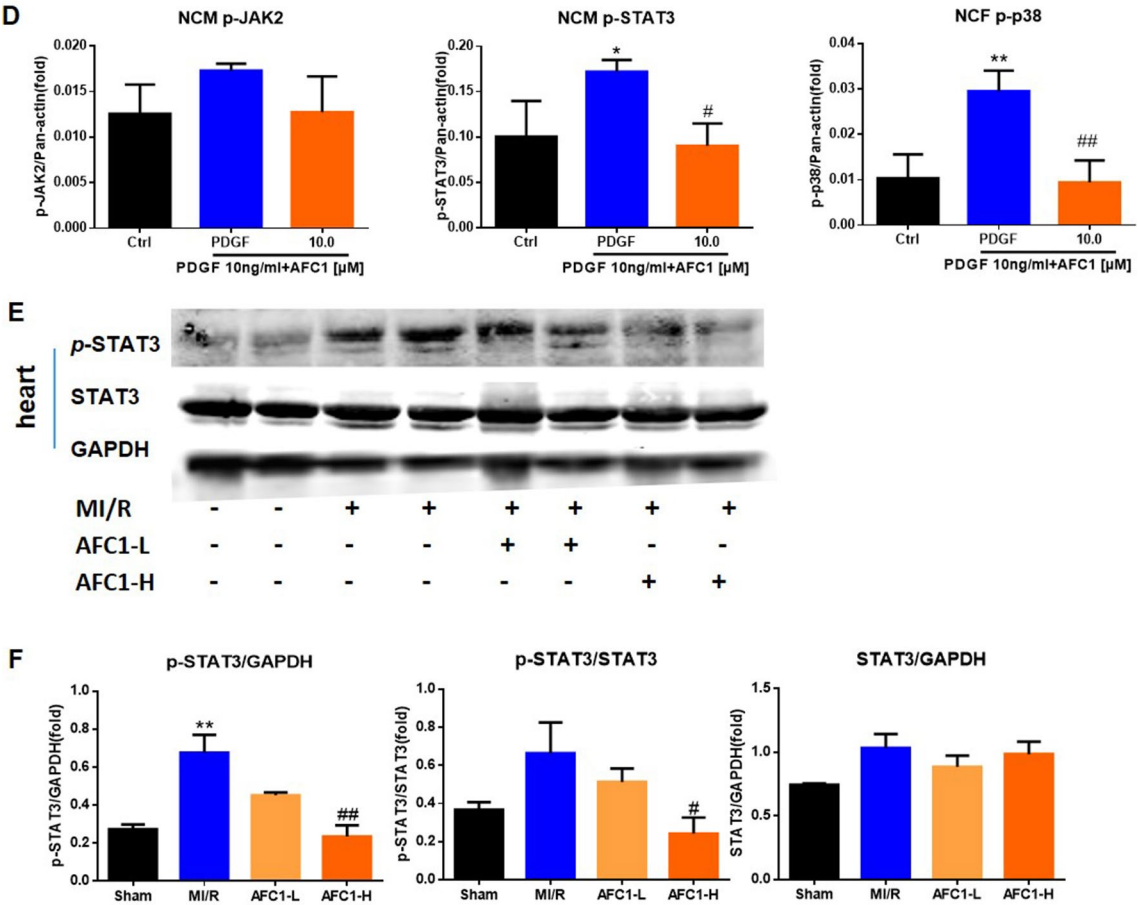

FIGURE 8 | Potential mechanism of the protective function of AFC1 treatment *in vitro* and *in vivo* n = 5. After being treated with JI1 **(A)** or 979 **(B)** and then stimulated with PDGF-AB, NCM hypertrophy was measured by ^{3}H-leucine incorporation and NCF collagen synthesis measured by ^{3}H-proline incorporation. **(C, D)** Protein levels of p-JAK2, p-STAT3 in NCM and p-p38 in NCF were determined *via* Western blot analysis. **(E)** Infarct area of heart in each group was lysed and p-STAT3, STAT3 protein levels were determined *via* Western blot. **(F)** p-STAT3/STAT3, p-STAT3/GAPDH, and STAT3/GAPDH were analyzed with image J software. Two or three samples were randomly selected from each group for Western blot experiment. Each experiment was repeated for at least three times and results indicated mean ± SEM of one independent experiment and the representative pictures. *$p < 0.05$, **$p < 0.01$, ****$p < 0.0001$ versus control or sham; $^{\#}p < 0.05$, $^{\#\#}p < 0.01$, $^{\#\#\#}p < 0.001$ versus PDGF-AB or MI/R.

sodium TSA sulfonate in myocardial ischemia/reperfusion injury animal models (Zhang et al., 2010; Zhang et al., 2013; Wei et al., 2014; Li Q et al., 2016; Pan et al., 2017). Results from the recent clinical trial indicated that sodium TSA sulfonate in combination with current therapies may significantly reduce adverse LV remodeling and potentially improve clinical outcomes, providing important evidence on the efficacy of sodium TSA sulfonate treatment in patients (Mao et al., 2015a; Mao et al., 2015b). Another trail named "Sodium Tanshinone IIA Sulfonate in Left Ventricular Remodeling Secondary to Acute Myocardial Infarction" is going on in Guangzhou, China (ClinicalTrials.gov Identifier: NCT02524964)(https://www.clinicaltrials.gov).

We have been searching new TCM-based cardioprotective agents and identified series AFC compounds with TSA mimic effects. In this study, we reported for the first time the cardioprotective actions of AFC1 in murine MI/R models. Ventricular remodeling including cardiac hypertrophy and fibrosis is the leading cause contributing to cardiac dysfunction after MI/R (Konishi et al., 2013). The key findings of the present study are that administration of AFC1 effectively reduced the cardiac myocyte hypertrophy and fibrosis on day 30 post MI/R, accompanied by significant improvement of cardiac function, and also inhibited MI/R-induced cardiac remodeling *in vivo*. The effect of AFC1 may be mediated by its inhibition of production of ROS and inflammation mediators and regulation of key signaling pathways, including PDGF, STAT3, and p38 signaling pathways.

MI/R is a complex multifactorial pathophysiological process that oxidative stress and inflammatory response are key contributors to the following cardiac remodeling. The damage of oxygen free radical on vessel and myocardium after perfusion could result in myocardial injury and finally accelerate the development of MI/R (Duan et al., 2015). MI/R activated sterile inflammatory response characterized by the recruitment and activation of immune cells (Yan et al., 2013). Numerous studies have demonstrated that inhibition of neutrophil recruitment mediated by macrophage reduced tissue damage

and infarct size in ischemic myocardium (Romson et al., 1983; de Lorgeril et al., 1989; Hatori et al., 1991; Li et al., 2016; Wang et al., 2016). Excessive neutrophil infiltration in the infarct site is detrimental to cardiomyocyte survival for secreting ROS, which further aggravates structural damage of tissue (Hansen, 1995). Our data showed that AFC1 compound inhibited the production of ROS, the infiltration of inflammatory cells, as well as the content of inflammatory cytokines, such as IL-1β, TNF-α, and IL-6 in infarcted myocardium, which implied that AFC1 compound may play an important role in improving ventricular remodeling after MI/R *via* suppressing oxidative stress and inflammatory responses.

Previously, evidences indicated the crucial role of PDGF on stimulating fibrosis in many pathological conditions (Choi et al., 2005; Fan et al., 2013). Hypoxia could cause murine pulmonary vascular medial hypertrophy *via* increasing PDGF concentration (Zhang et al., 2012). PDGF-AB released by myofibroblast could cause myocyte structural and electromechanical remodeling in ovine persistent atrial fibrillation (PAF) through reducing calcium transients (Musa et al., 2013). The expression of PDGF is closely related to inflammation and fibrosis in infarcted myocardium (Zhao et al., 2011). In addition, PDGF can induce ROS production in MEFs (Choi et al., 2005). Therefore, PDGF may induce cardiac remodeling following MI/R *via* promoting oxidative stress and inflammatory response. The present result showed much higher expressions of PDGF-A, PDGF-B, PDGFRα, and PDGFRβ in murine MI/R myocardium in MI/R heart than that in the sham group. Previous report from the MI rat models (Liu et al., 2014) revealed similar findings. Our results further indicated that AFC1 compound can effectively decrease the levels of PDGFR without affecting the expression of PDGF-A and PDGF-B in the heart post MI/R. Besides, AFC1 treatment greatly reduced PDGF-AB-stimulated PDGFR mRNA expression in NCM and NCF, as well as inhibited PDGF-AB-stimulated NCM hypertrophy and NCF collagen synthesis *in vitro*. These data suggested that cardio-protective function of AFC1 may attribute to the inhibition of PDGFR signaling *in vivo* and *in vitro*.

It is proved that Janus kinase/signal transduction and activators of transcription (JAK/STAT) pathway can be activated by ischemic stress stimuli and cardiac hypertrophy agonist PDGF (Goodman et al., 2011; Wu et al., 2012). Tyrosine kinase could phosphorylate receptor tyrosine residues expressed on cardiomyocytes and activate the STAT phosphorylation. The activated STAT then transferred to nucleus and bonded to the target gene to regulate the expression of transcription factors or genes associated with hypertrophy and fibrosis, such as p21waf1 and c-fibrinogen (Wagner and Siddiqui, 2012). Inhibition of JAK/STAT pathway could reduce the myocardial infarct size and cardiomyocyte apoptosis induced by MI/R in rat models (Mascareno et al., 2001). Besides, PDGF-AB stimulated proliferation of human airway smooth muscle cells, which contribute to airway remodeling through the JAK/STAT pathway (Simon et al., 2002). Studies revealed that the PDGF/PDGFR pathway is involved in the regulation of cardiac function and the development of ventricular remodeling in MI/R *via* JAK/STAT downstream pathway (Wang et al., 2000; Booz et al., 2002). On the other hand, as an important intracellular signaling enzyme, P38MAPK is activated by myocardial ischemia and hypoxia to induce cellular apoptosis, and results in impaired cardiac function and amplifies the inflammatory cascade in the heart following MI/R. Our *in vitro* data showed that stimulation of PDGF-AB increased STAT3 phosphorylation in NCM and p38 phosphorylation in NCF, and addition of AFC1 compound significantly decreased both proteins' phosphorylation, as well as suppressed NCM hypertrophy and NCF collagen synthesis. Moreover, in murine MI/R models, the expression of p-STAT3 up-regulated in murine infarcted myocardium and this elevation can be dramatically decreased by AFC1 treatment, indicating the possible downstream pathway in which AFC1 exerts its role in cardiac myocyte. We therefore proposed that AFC1 compound may attenuate MI/R-induced cardiac remodeling *via* regulating PDGFR signaling and inhibiting the phosphorylation of STAT3. It is also possible that AFC1 may act on other singling pathways, but further study is needed to elucidate this.

Importantly, AFC1 showed neither detrimental impact on morphological and histological changes of murine lung, liver, kidney, and spleen, nor the cytotoxicity in HUVEC viability. It showed less cytotoxicity than TSA in high doses, indicating it may have a better safety profile than TSA. Since TSA has been widely used clinically with excellent safety profile, AFC1 may also be a potential clinical agent for treating MI/R. But further study is needed on its pharmacokinetic profile and more detailed evaluation of its toxicity *in vivo*. In addition, further investigations are needed to explore the role of AFC1 in other cardiovascular diseases and further in clinical trials.

CONCLUSIONS

AFC1 compound had comparable effect with TSA in improving cardiac function after MI/R. Administration of AFC1 suppressed STAT signaling and attenuated MI/R-induced cardiac remodeling in murine MI/R models. AFC1 suppressed PDGF-AB induced NCM hypertrophy *via* STAT3 pathway and NCF collagen synthesis through p38 signaling. Therefore, AFC1 may be a novel therapeutic option with anti-hypertrophic and anti-fibrotic effect against MI/R-induced cardiac remodeling in patients who suffered from MI/R.

DATA AVAILABILITY STATEMENT

The raw data supporting the conclusions of this manuscript will be made available by the authors, without undue reservation, to any qualified researcher.

ETHICS STATEMENT

This study was carried out in accordance with the recommendations of the Institutional Animal Care and Use Committee of Tongji University. The protocol was approved

by the Institutional Animal Care and Use Committee of Tongji University.

AUTHOR CONTRIBUTIONS

XZ, BW, and HF contributed to the conception and design of the study. JieL, XZ, QM, KH, JingL, JT, RZ, GC, YZ, LW, and LH contributed to acquisition, analysis, and interpretation of the data. JieL, XZ, CL, ZL, and BW wrote and revised the MS.

FUNDING

The study was supported by the National Key Research and Development Program of China (2017YFA0105600), the National Natural Science Foundation of China (81370434; 81670458; 81470393), the Shanghai Municipal Health and Family Planning Commission (ZY3-LCPT-2-1003-2014ZYJB0502), Key Discipline Project of Pudong Health Bureau of Shanghai (PWZxk2017-01), and the Science and Technology Commission of Shanghai Municipality (17431906600).

REFERENCES

Aboulhoda, B. E. (2017). Age-related remodeling of the JAK/STAT/SOCS signaling pathway and associated myocardial changes: from histological to molecular level. *Ann. Anat.* 214, 21–30. doi: 10.1016/j.aanat.2017.07.003

Booz, G. W., Day, J. N., and Baker, K. M. (2002). Interplay between the cardiac renin angiotensin system and JAK-STAT signaling: role in cardiac hypertrophy, ischemia/reperfusion dysfunction, and heart failure. *J. Mol. Cell Cardiol.* 34 (11), 1443–1453. doi: 10.1006/jmcc.2002.2076

Cai, Y., Lu, C., Xu, T., Ma, Y., Min, S., Scammells, P., et al. (2018). Diffusion tensor imaging evaluation of axonal/white matter remodeling in a mouse model of diabetic stroke treated with novel p38 MAPK inhibitor, VCP979. *J. Biomed. Nanotechnol.* 14 (3), 585–593. doi: 10.1166/jbn.2018.2522

Chan, E., Liu, X. X., Guo, D. J., Kwan, Y. W., Leung, G. P., Lee, S. M., et al. (2011). Extract of Scutellaria baicalensis Georgi root exerts protection against myocardial ischemia-reperfusion injury in rats. *Am. J. Chin. Med.* 39 (4), 693–704. doi: 10.1142/S0192415X11009135

Cheng, T. O. (2007). Cardiovascular effects of Danshen. *Int. J. Cardiol.* 121 (1), 9–22. doi: 10.1016/j.ijcard.2007.01.004

Chew, D. S., Heikki, H., Schmidt, G., Kavanagh, K. M., Dommasch, M., Bloch Thomsen, P. E., et al. (2018). Change in left ventricular ejection fraction following first myocardial infarction and outcome. *JACC Clin. Electrophysiol.* 4 (5), 672–682. doi: 10.1016/j.jacep.2017.12.015

Choi, M. H., Lee, I. K., Kim, G. W., Kim, B. U., Han, Y. H., Yu, D. Y., et al. (2005). Regulation of PDGF signalling and vascular remodelling by peroxiredoxin II. *Nature* 435 (7040), 347–353. doi: 10.1038/nature03587

de Lorgeril, M., Basmadjian, A., Lavallee, M., Clement, R., Millette, D., Rousseau, G., et al. (1989). Influence of leukopenia on collateral flow, reperfusion flow, reflow ventricular fibrillation, and infarct size in dogs. *Am. Heart J.* 117 (3), 523–532. doi: 10.1016/0002-8703(89)90724-2

Della Rocca, D. G., Willenberg, B. J., Ferreira, L. F., Wate, P. S., Petersen, J. W., Handberg, E. M., et al. (2012). A degradable, bioactive, gelatinized alginate hydrogel to improve stem cell/growth factor delivery and facilitate healing after myocardial infarction. *Med. Hypotheses* 79 (5), 673–677. doi: 10.1016/j.mehy.2012.08.006

Duan, Z. Z., Li, Y. H., Li, Y. Y., Fan, G. W., Chang, Y. X., Yu, B., et al. (2015). Danhong injection protects cardiomyocytes against hypoxia/reoxygenation- and H2O2-induced injury by inhibiting mitochondrial permeability transition pore opening. *J. Ethnopharmacol.* 175, 617–625. doi: 10.1016/j.jep.2015.08.033

Fan, B., Ma, L., Li, Q., Wang, L., Zhou, J., and Wu, J. (2013). Correlation between platelet-derived growth factor signaling pathway and inflammation in desoxycorticosterone-induced salt-sensitive hypertensive rats with myocardial fibrosis. *Int. J. Clin. Exp. Pathol.* 6 (11), 2468–2475.

Goodman, M. D., Koch, S. E., Afzal, M. R., and Butler, K. L. (2011). STAT subtype specificity and ischemic preconditioning in mice: is STAT-3 enough? *Am. J. Physiol. Heart Circ. Physiol.* 300 (2), H522–H526. doi: 10.1152/ajpheart.00231.2010

Hansen, P. R. (1995). Role of neutrophils in myocardial ischemia and reperfusion. *Circulation* 91 (6), 1872–1885. doi: 10.1161/01.CIR.91.6.1872

Hatori, N., Roberts, R. L., Tadokoro, H., Ryden, L., Satomura, K., Fishbein, M. C., et al. (1991). Differences in infarct size with lidocaine as compared with bretylium tosylate in acute myocardial ischemia and reperfusion in pigs. *J. Cardiovasc. Pharmacol.* 18 (4), 581–588. doi: 10.1097/00005344-199110000-00015

Huang, J., Tang, X., Ye, F., He, J., and Kong, X. (2016). Clinical therapeutic effects of aspirin in combination with Fufang Danshen Diwan, a traditional Chinese medicine formula, on coronary heart disease: a systematic review and meta-analysis. *Cell Physiol. Biochem.* 39 (5), 1955–1963. doi: 10.1159/000447892

Jin, H. J., and Li, C. G. (2013). Tanshinone IIA and cryptotanshinone prevent mitochondrial dysfunction in hypoxia-induced H9c2 cells: association to mitochondrial ROS, intracellular nitric oxide, and calcium levels. *Evid. Based Complement Alternat. Med.* 2013, 610694. doi: 10.1155/2013/610694

Jin, H. J., Xie, X. L., Ye, J. M., and Li, C. G. (2013). TanshinoneIIA and cryptotanshinone protect against hypoxia-induced mitochondrial apoptosis in H9c2 cells. *PLoS ONE* 8 (1), e51720. doi: 10.1371/journal.pone.0051720

Konishi, K., Dohi, K., Tanimura, M., Sato, Y., Watanabe, K., Sugiura, E., et al. (2013). Quantifying longitudinal right ventricular dysfunction in patients with old myocardial infarction by using speckle-tracking strain echocardiography. *Cardiovasc. Ultrasound* 11, 23. doi: 10.1186/1476-7120-11-23

Li, Q., Shen, L., Wang, Z., Jiang, H. P., and Liu, L. X. (2016). Tanshinone IIA protects against myocardial ischemia reperfusion injury by activating the PI3K/Akt/mTOR signaling pathway. *Biomed. Pharmacother.* 84, 106–114. doi: 10.1016/j.biopha.2016.09.014

Li, W., Hsiao, H. M., Higashikubo, R., Saunders, B. T., Bharat, A., Goldstein, D. R., et al. (2016). Heart-resident CCR2+ macrophages promote neutrophil extravasation through TLR9/MyD88/CXCL5 signaling. *JCI Insight* 1 (12), E87135. doi: 10.1172/jci.insight.87315

Lin, S. Q., Wei, X. H., Huang, P., Liu, Y. Y., Zhao, N., Li, Q., et al. (2013). QiShenYiQi Pills(R) prevent cardiac ischemia-reperfusion injury via energy modulation. *Int. J. Cardiol.* 168 (2), 967–974. doi: 10.1016/j.ijcard.2012.10.042

Liu, C., Zhao, W., Meng, W., Zhao, T., Chen, Y., Ahokas, R. A., et al. (2014). Platelet-derived growth factor blockade on cardiac remodeling following infarction. *Mol. Cell Biochem.* 397 (1-2), 295–304. doi: 10.1007/s11010-014-2197-x

Liu, X., An, C., Jin, P., Liu, X., and Wang, L. (2013). Protective effects of cationic bovine serum albumin-conjugated PEGylated tanshinone IIA nanoparticles on cerebral ischemia. *Biomaterials* 34 (3), 817–830. doi: 10.1016/j.biomaterials.2012.10.017

Luo, J., Song, W., Yang, G., Xu, H., and Chen, K. (2015). Compound Danshen (Salvia miltiorrhiza) dripping pill for coronary heart disease: an overview of systematic reviews. *Am. J. Chin. Med.* 43 (1), 25–43. doi: 10.1142/S0192415X15500020

Mao, S., Li, X., Wang, L., Yang, P. C., and Zhang, M. (2015a). Rationale and design of sodium Tanshinone IIA sulfonate in left ventricular remodeling secondary to acute myocardial infarction (STAMP-REMODELING) trial: a randomized controlled study. *Cardiovasc. Drugs Ther.* 29 (6), 535–542. doi: 10.1007/s10557-015-6625-2

Mao, S., Wang, L., Zhao, X., Shang, H., Zhang, M., and Hinek, A. (2015b). Sodium tanshinone IIA sulfonate for reduction of periprocedural myocardial injury during percutaneous coronary intervention (STAMP trial): rationale and design. *Int. J. Cardiol.* 182, 329–333. doi: 10.1016/j.ijcard.2014.12.166

Mascareno, E., El-Shafei, M., Maulik, N., Sato, M., Guo, Y., Das, D. K., et al. (2001). JAK/STAT signaling is associated with cardiac dysfunction during ischemia and reperfusion. *Circulation* 104 (3), 325–329. doi: 10.1161/01.CIR.104.3.325

Mo, W. L., Chai, C. Z., Kou, J. P., Yan, Y. Q., and Yu, B. Y. (2015). Sheng-Mai-San attenuates contractile dysfunction and structural damage induced by chronic intermittent hypoxia in mice. *Chin. J. Nat. Med.* 13 (10), 743–750. doi: 10.1016/S1875-5364(15)30074-1

Murdoch, C. E., Zhang, M., Cave, A. C., and Shah, A. M. (2006). NADPH oxidase-dependent redox signalling in cardiac hypertrophy, remodelling and failure. *Cardiovasc. Res.* 71 (2), 208–215. doi: 10.1016/j.cardiores.2006.03.016

Musa, H., Kaur, K., O'Connell, R., Klos, M., Guerrero-Serna, G., Avula, U. M., et al. (2013). Inhibition of platelet-derived growth factor-AB signaling prevents electromechanical remodeling of adult atrial myocytes that contact myofibroblasts. *Heart Rhythm* 10 (7), 1044–1051. doi: 10.1016/j.hrthm.2013.03.014

Nizamutdinova, I. T., Kim, Y. M., Jin, H., Son, K. H., Lee, J. H., Chang, K. C., et al. (2012). Tanshinone IIA inhibits TNF-alpha-mediated induction of VCAM-1 but not ICAM-1 through the regulation of GATA-6 and IRF-1. *Int. Immunopharmacol.* 14 (4), 650–657. doi: 10.1016/j.intimp.2012.09.017

Owona, B. A., Njayou, N. F., Laufer, S. A., Schluesener, H. J., and Moundipa, P. F. (2013). Entada africana fraction CH(2)Cl(2)/MEOH 5% inhibits inducible nitric oxide synthase and pro-inflammatory cytokines gene expression induced by lipopolysaccharide in microglia. *BMC Complement. Altern. Med.* 13, 254. doi: 10.1186/1472-6882-13-254

Pan, Y., Qian, J. X., Lu, S. Q., Chen, J. W., Zhao, X. D., Jiang, Y., et al. (2017). Protective effects of tanshinone IIA sodium sulfonate on ischemia-reperfusion-induced myocardial injury in rats. *Iran J. Basic Med. Sci.* 20 (3), 308–315. doi: 10.22038/ijbms.2017.8361

Pello, A. M., Cristobal, C., Tarin, N., Huelmos, A., Acena, A., Carda, R., et al. (2015). Differential profile in inflammatory and mineral metabolism biomarkers in patients with ischemic heart disease without classical coronary risk factors. *J. Cardiol.* 66 (1), 22–27. doi: 10.1016/j.jjcc.2014.11.006

Price, R. L., Haley, S. T., Bullard, T. A., Goldsmith, E. C., Simpson, D. G., Thielen, T. E., et al. (2003). Effects of platelet-derived growth factor-AA and -BB on embryonic cardiac development. *Anat. Rec. A Discov. Mol. Cell Evol. Biol.* 272 (1), 424–433. doi: 10.1002/ar.a.10054

Pu, J., Yuan, A., Shan, P., Gao, E., Wang, X., Wang, Y., et al. (2013). Cardiomyocyte-expressed farnesoid-X-receptor is a novel apoptosis mediator and contributes to myocardial ischaemia/reperfusion injury. *Eur. Heart J.* 34 (24), 1834–1845. doi: 10.1093/eurheartj/ehs011

Romson, J. L., Hook, B. G., Kunkel, S. L., Abrams, G. D., Schork, M. A., and Lucchesi, B. R. (1983). Reduction of the extent of ischemic myocardial injury by neutrophil depletion in the dog. *Circulation* 67 (5), 1016–1023. doi: 10.1161/01.CIR.67.5.1016

Simon, A. R., Takahashi, S., Severgnini, M., Fanburg, B. L., and Cochran, B. H. (2002). Role of the JAK-STAT pathway in PDGF-stimulated proliferation of human airway smooth muscle cells. *Am J. Physiol. Lung Cell Mol. Physiol.* 282 (6), L1296–L1304. doi: 10.1152/ajplung.00315.2001

Sun, Y. (2009). Myocardial repair/remodelling following infarction: roles of local factors. *Cardiovasc. Res.* 81 (3), 482–490. doi: 10.1093/cvr/cvn333

Thomas, W. G., Brandenburger, Y., Autelitano, D. J., Pham, T., Qian, H., and Hannan, R. D. (2002). Adenoviral-directed expression of the type 1A angiotensin receptor promotes cardiomyocyte hypertrophy via transactivation of the epidermal growth factor receptor. *Circ. Res.* 90 (2), 135–142. doi: 10.1161/hh0202.104109

Tzanidis, A., Hannan, R. D., Thomas, W. G., Onan, D., Autelitano, D. J., See, F., et al. (2003). Direct actions of urotensin II on the heart: implications for cardiac fibrosis and hypertrophy. *Circ. Res.* 93 (3), 246–253. doi: 10.1161/01.RES.0000084382.64418.BC

Vantler, M., Karikkineth, B. C., Naito, H., Tiburcy, M., Didie, M., Nose, M., et al. (2010). PDGF-BB protects cardiomyocytes from apoptosis and improves contractile function of engineered heart tissue. *J. Mol. Cell Cardiol.* 48 (6), 1316–1323. doi: 10.1016/j.yjmcc.2010.03.008

Wagner, M. A., and Siddiqui, M. A. (2012). The JAK-STAT pathway in hypertrophic stress signaling and genomic stress response. *JAKSTAT* 1 (2), 131–141. doi: 10.4161/jkst.20702

Wang, J., Hu, X., and Jiang, H. (2015a). HDAC inhibition: a novel therapeutic target for attenuating myocardial ischemia and reperfusion injury by reversing cardiac remodeling. *Int. J. Cardiol.* 190, 126–127. doi: 10.1016/j.ijcard.2015.04.172

Wang, J., Hu, X., and Jiang, H. (2015b). The Nrf-2/ARE-HO-1 axis: an important therapeutic approach for attenuating myocardial ischemia and reperfusion injury-induced cardiac remodeling. *Int. J. Cardiol.* 184, 263–264. doi: 10.1016/j.ijcard.2015.02.073

Wang, Y., Yan, X., Mi, S., Li, Z., Wang, Y., Zhu, H., et al. (2016). Naoxintong attenuates ischaemia/reperfusion injury through inhibiting NLRP3 inflammasome activation. *J. Cell Mol. Med.* 21 (1), 4–12. doi: 10.1111/jcmm.12915

Wang, Y. Z., Wharton, W., Garcia, R., Kraker, A., Jove, R., and Pledger, W. J. (2000). Activation of Stat3 preassembled with platelet-derived growth factor beta receptors requires Src kinase activity. *Oncogene* 19 (17), 2075–2085. doi: 10.1038/sj.onc.1203548

Wei, B., Li, W. W., Ji, J., Hu, Q. H., and Ji, H. (2014). The cardioprotective effect of sodium tanshinone IIA sulfonate and the optimizing of therapeutic time window in myocardial ischemia/reperfusion injury in rats. *Atherosclerosis* 235 (2), 318–327. doi: 10.1016/j.atherosclerosis.2014.05.924

Wincewicz, A., and Sulkowski, S. (2017). Stat proteins as intracellular regulators of resistance to myocardial injury in the context of cardiac remodeling and targeting for therapy. *Adv. Clin. Exp. Med.* 26 (4), 703–708. doi: 10.17219/acem/62693

Wu, Q., Wang, W., Li, S., Nagarkatti, P., Nagarkatti, M., Windust, A., et al. (2012). American ginseng inhibits vascular smooth muscle cell proliferation via suppressing Jak/Stat pathway. *J. Ethnopharmacol.* 144 (3), 782–785. doi: 10.1016/j.jep.2012.09.046

Wu, W. Y., Wang, W. Y., Ma, Y. L., Yan, H., Wang, X. B., Qin, Y. L., et al. (2013). Sodium tanshinone IIA silate inhibits oxygen-glucose deprivation/recovery-induced cardiomyocyte apoptosis via suppression of the NF-kappaB/TNF-alpha pathway. *Br. J. Pharmacol.* 169 (5), 1058–1071. doi: 10.1111/bph.12185

Yan, X., Anzai, A., Katsumata, Y., Matsuhashi, T., Ito, K., Endo, J., et al. (2013). Temporal dynamics of cardiac immune cell accumulation following acute myocardial infarction. *J. Mol. Cell Cardiol.* 62, 24–35. doi: 10.1016/j.yjmcc.2013.04.023

Yang, M., Orgah, J., Zhu, J., Fan, G., Han, J., Wang, X., et al. (2016). Danhong injection attenuates cardiac injury induced by ischemic and reperfused neuronal cells through regulating arginine vasopressin expression and secretion. *Brain Res.* 1642, 516–523. doi: 10.1016/j.brainres.2016.04.046

Yellon, D. M., and Hausenloy, D. J. (2007). Myocardial reperfusion injury. *N. Engl. J. Med.* 357 (11), 1121–1135. doi: 10.1056/NEJMra071667

Zhang, L., Ma, J., Shen, T., Wang, S., Ma, C., Liu, Y., et al. (2012). Platelet-derived growth factor (PDGF) induces pulmonary vascular remodeling through 15-LO/15-HETE pathway under hypoxic condition. *Cell Signal.* 24 (10), 1931–1939. doi: 10.1016/j.cellsig.2012.06.007

Zhang, M. Q., Zheng, Y. L., Chen, H., Tu, J. F., Shen, Y., Guo, J. P., et al. (2013). Sodium tanshinone IIA sulfonate protects rat myocardium against ischemia-reperfusion injury via activation of PI3K/Akt/FOXO3A/Bim pathway. *Acta Pharmacol. Sin.* 34 (11), 1386–1396. doi: 10.1038/aps.2013.91

Zhang, Y., Wei, L., Sun, D., Cao, F., Gao, H., Zhao, L., et al. (2010). Tanshinone IIA pretreatment protects myocardium against ischaemia/reperfusion injury through the phosphatidylinositol 3-kinase/Akt-dependent pathway in diabetic rats. *Diabetes Obes. Metab.* 12 (4), 316–322. doi: 10.1111/j.1463-1326.2009.01166.x

Zhao, W., Zhao, T., Huang, V., Chen, Y., Ahokas, R. A., and Sun, Y. (2011). Platelet-derived growth factor involvement in myocardial remodeling following infarction. *J. Mol. Cell Cardiol.* 51 (5), 830–838. doi: 10.1016/j.yjmcc.2011.06.023

Zhou, G., Jiang, W., Zhao, Y., Ma, G., Xin, W., Yin, J., et al. (2003). Sodium tanshinone IIA sulfonate mediates electron transfer reaction in rat heart mitochondria. *Biochem. Pharmacol.* 65 (1), 51–57. doi: 10.1016/S0006-2952(02)01447-8

Conflict of Interest: The authors declare that the research was conducted in the absence of any commercial or financial relationships that could be construed as a potential conflict of interest.

frontiers in Pharmacology

MINI REVIEW
published: 31 October 2019
doi: 10.3389/fphar.2019.01295

Flavonoids as Natural Anti-Inflammatory Agents Targeting Nuclear Factor-Kappa B (NFκB) Signaling in Cardiovascular Diseases: A Mini Review

Ker Woon Choy[1], Dharmani Murugan[2]*, Xin-Fang Leong[3], Razif Abas[4], Aspalilah Alias[5] and Mohd Rais Mustafa[2,6]**

[1] Department of Anatomy, Faculty of Medicine, Bioscience and Nursing, MAHSA University, Jenjarom, Malaysia, [2] Department of Pharmacology, Faculty of Medicine, University of Malaya, Kuala Lumpur, Malaysia, [3] Centre for Craniofacial Diagnostics and Biosciences, Faculty of Dentistry, Universiti Kebangsaan Malaysia, Kuala Lumpur, Malaysia, [4] Department of Human Anatomy, Faculty of Medicine and Health Sciences, Universiti Putra Malaysia, Serdang, Malaysia, [5] Department of Basic Sciences and Oral Biology, Faculty of Dentistry, Universiti Sains Islam Malaysia, Kuala Lumpur, Malaysia, [6] Centre for Natural Product research and Drug Discovery (CENAR), Wellness Research Cluster, University of Malaya, Kuala Lumpur, Malaysia

OPEN ACCESS

Edited by:
Cheng Xue Helena Qin, Baker Heart and Diabetes Institute, Australia

Reviewed by:
Agnieszka Barbara Najda, University of Life Sciences of Lublin, Poland
Zakiah Jubri, National University of Malaysia, Malaysia

***Correspondence:**
Ker Woon Choy
celine_kerwoon@yahoo.com
Dharmani Murugan
dharmani79@um.edu.my
Mohd Rais Mustafa
rais@um.edu.my

Specialty section:
This article was submitted to Inflammation Pharmacology, a section of the journal Frontiers in Pharmacology

Received: *16 August 2019*
Accepted: *10 October 2019*
Published: *31 October 2019*

Citation:
Choy KW, Murugan D, Leong X-F, Abas R, Alias A and Mustafa MR (2019) Flavonoids as Natural Anti-Inflammatory Agents Targeting Nuclear Factor-Kappa B (NFκB) Signaling in Cardiovascular Diseases: A Mini Review. Front. Pharmacol. 10:1295. doi: 10.3389/fphar.2019.01295

Cardiovascular diseases (CVDs) such as angina, hypertension, myocardial ischemia, and heart failure are the leading causes of morbidity and mortality worldwide. One of the major transcription factors widely associated with CVDs is nuclear factor-kappa B (NFκB). NFκB activation initiates the canonical and non-conical pathways that promotes activation of transcription factors leading to inflammation, such as leukocyte adhesion molecules, cytokines, and chemokines. Flavonoids are bioactive polyphenolic compounds found abundantly in various fruits, vegetables, beverages (tea, coffee), nuts, and cereal products with cardiovascular protective properties. Flavonoids can be classified into six subgroups based on their chemical structures: flavanones, flavones, flavonols, flavan-3-ols, isoflavones, and anthocyanidins. As NFκB inhibitors, these flavonoids may modulate the expression of pro-inflammatory genes leading to the attenuation of the inflammatory responses underlying various cardiovascular pathology. This review presents an update on the anti-inflammatory actions of flavonoids *via* inhibition of NFκB mechanism supporting the therapeutic potential of these natural compounds in various CVDs.

Keywords: flavonoids, nuclear factor-kappa B signalling, anti-inflammatory, cardiovascular diseases, natural compounds

INTRODUCTION

Cardiovascular diseases (CVDs) represent the major burden of mortality and morbidity in the developed countries (Benjamin et al., 2017). The most common pathogeneses of CVDs are inflammatory processes (Ruparelia et al., 2017). Various transcription factors are related to inflammatory responses in CVDs such as T-bet (Haybar et al., 2019), signal transducer and activator of transcription 3 (STAT3) (Kurdi et al., 2018), interferon regulatory factors (IRFs), activator protein 1 (AP-1) (Smale and Natoli, 2014), and transcription factor Bcl11b (Daher et al., 2019). However, the key player in the regulation of inflammation is the transcription factor nuclear factor kappa B (NFκB) (Van Der Heiden et al., 2010).

The inhibition of NFκB pathway has been demonstrated to show beneficial effect in various CVDs including hypertension (Koeners et al., 2016), myocardial infraction (Zhao et al., 2017), and arteriosclerosis (Wang et al., 2016). These findings support that targeted inhibition of NFκB appears to be a promising strategy in reducing cardiovascular complications.

Flavonoids are plant polyphenolic compound derivatives from natural origin found in fruits, grains, vegetables, roots, bark, flowers, stems, tea, and wine (Zeinali et al., 2017). Non-plant natural products such as mushrooms and honey, plant extracts, plant juices, plant powders, and essential oils have shown to possess anti-inflammatory activities and many of these plant natural products have polyphenols as their major compound (Khalil and Sulaiman, 2010; Azab et al., 2016). However, the protective effects of flavonoid in CVDs *via* inhibition of NFκB are yet to be reviewed. Therefore, in this mini-review, we focused on the anti-inflammatory actions of flavonoids *via* inhibition of NFκB mechanism in CVDs.

FLAVONOIDS AND ITS SUBCLASS

Flavonoids are categorized into six subclasses depending on its chemical structures: flavones, flavonols, flavanones, isoflavones, flavan-3-ols, and anthocyanidins (Panche et al., 2016).

Flavones are found abundant in flowers, fruits, and leaves such as red peppers, celery, parsley, chamomile, mint, and ginkgo biloba (Manach et al., 2004). The most studied flavones are luteolin, apigenin, and tangeritin (Manach et al., 2004).

Flavonols such as kaempferol, myricetin, quercetin, rutin, fisetin, silymarin, and isorhamnetin are ubiquitous in foods such as saffron, onions, kale, lettuce, tomatoes, apples, grapes, berries, red wine, and tea (Pollastri and Tattini, 2011).

Flavanones widely present in all citrus fruits, which gives the bitter taste of the juice and its peel. Oranges, lemons, and grapes are rich sources of flavanones and major compounds are hesperitin, naringenin, and eriodictyol (Barreca et al., 2017).

Isoflavones are unique in that they resemble estrogen in structure and, therefore, are classified as phytoestrogens. There are found abundantly in soy products such as tofu, roasted soy nuts, and miso (Marzocchella et al., 2011).

Flavan-3-ols, also called as dihydroflavonols, include catechin, epicatechin, gallocatechin, epigallocatechin, epicatechingallate, epigallocatechingallate, and procyanidin (Alkhalidy et al., 2018). The most commonly associated food with the flavan-3-ol compounds is black and green tea and fruits such as bananas, apples, blueberries, peaches, and pears (Osakabe, 2013).

Anthocyanins are rich in outer cell layers of fruits such as merlot grapes, raspberries, cranberries, red grapes, strawberries, blueberries, bilberries, and blackberries. The most commonly studied anthocyanins are cyanidin, delphinidin, malvidin, pelargonidin, and peonidin (Khoo et al., 2017).

NFκB INDUCED INFLAMMATION AND CVDS

There are a few cellular redox pathways involved in the development of the chronic inflammatory CVD, which includes NFκB. NFκB is a transcription factor that activates inhibitor of kappa B (IκB) kinase in the cytosol upon being stimulated by inflammatory stimuli (Brasier, 2010). Subsequent signaling pathways *via* canonical or non-canonical lead to migration of NFκB toward the nucleus and hence initiates the targeting gene such as pro-inflammatory cells, monocytes, macrophages, and T and B cells (**Figure 1**).

The canonical NFκB pathway responds rapidly to stimuli and activates NFκB, which increases pro-inflammatory cytokines such as interleukin (IL)-1β, IL-6, and tumor necrosis factor alpha (TNF-α), which results in cell apoptosis. TNF-α receptor signaling plays an important role in the canonical pathway of NFκB in cell death *via* Jun N-terminal kinases (JNK), p38, and caspase 8 cascades (Ghosh et al., 2009). Furthermore, NFκB also activates angiotensin II, endothelin-1, and phenylephrine as hypertrophic agonist *via* IκB degradation and p65 nuclear translocation.

A central signaling component of the non-canonical NFκB pathway is NFκB-inducing kinase, which induces p100 phosphorylation through kinase IKKα in a slow manner (Sun, 2017). Ligands of a subset of tumor necrosis factor receptor (TNFR) superfamily members are typical inducers of the non-canonical NFκB pathway (Shih et al., 2011).

ANTI-INFLAMMATORY EFFECTS OF FLAVONOIDS IN CVDS *VIA* MODULATION OF NFκB SIGNALING

Quercetin

Quercetin or 3, 3′, 4′, 5, 7-pentahydroxyflvanone that falls into the category of flavonol is widely found in plants such as Ginkgo biloba, *Hypericum perforatum*, and *Sambucus canadensis* as well as vegetables such as apples, berries, grapes, onions, shallots, and tomatoes (Li et al., 2016).

In a clinical study involving patients with chronic systemic inflammation (CSI) in stable coronary artery disease (CAD), quercetin showed anti-inflammatory effects with reduction in indicators of CSI (Chekalina et al., 2018). Quercetin decreased IL-1β and TNF-α levels in blood serum, in addition to decreasing the transcriptional activity of NFκB in blood mononuclear cells (Chekalina et al., 2018). In leptin-induced inflammation model using human umbilical vein endothelial cells (HUVECs), quercetin significantly suppressed the upregulation of Ob-Ra (leptin receptor) expression, ERK1/2 phosphorylation, NFκB, and TNF-α (Indra et al., 2013). Furthermore, in a neonatal rat cardiac fibroblast, quercetin inhibited TNF-α, IL-1β, and IL-6 secretion by inhibiting the activation of NFκB and Akt induced by lipopolysaccharide (LPS) (Tang et al., 2014).

Luteolin

Luteolin or 3', 4', 5, 7-tetrahydroxyflavone is one of the most prevalent flavones widely found in fruits and vegetables such as carrots, cabbages, parsley, broccoli, celery, and apple skins (Weng and Yen, 2012).

In an *in-vivo* sodium fluoride-induced hypertensive model, administration of luteolin increased nitric oxide (NO)

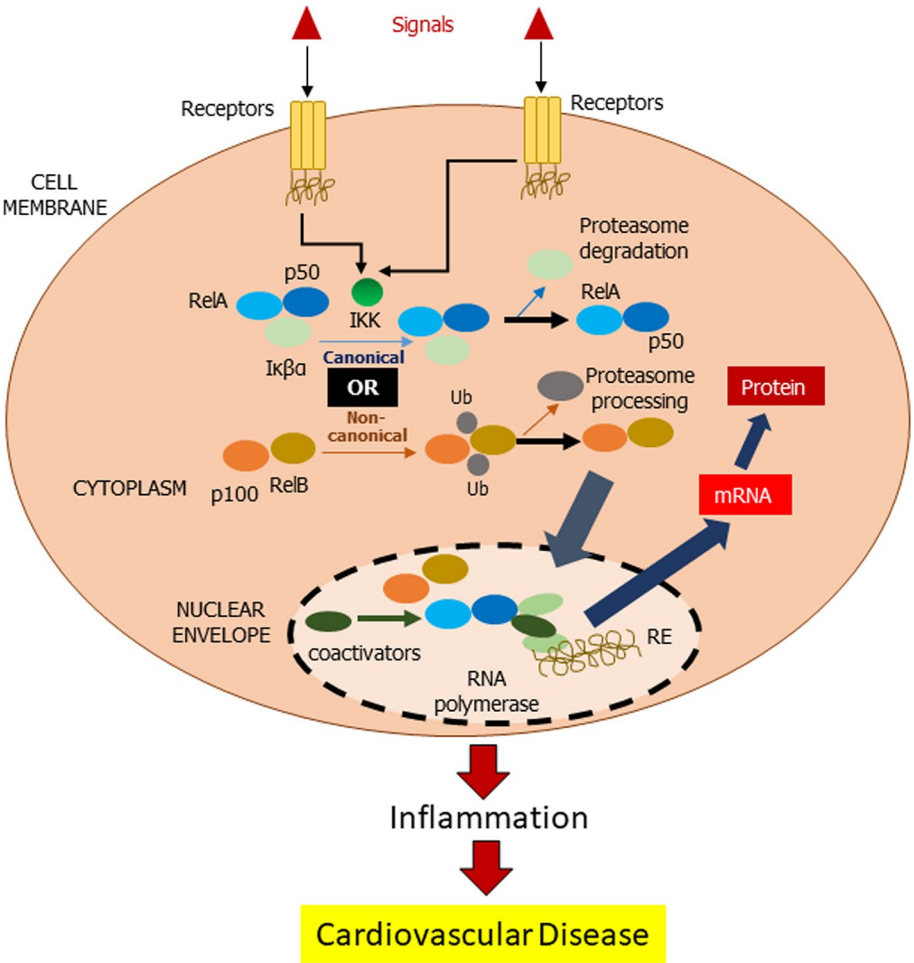

FIGURE 1 | Mechanism of NFκB action. In inactivated state, NF-κβ, which consists of Rel and p50 proteins, is located in the cytosol complexed with the inhibitory protein Iκβα. IκB kinase (IKK) is activated by extracellular signals *via* membrane receptors. Subsequently, IKK phosphorylates the Iκβα protein resulting in ubiquitination of Iκβα and eventually by the proteasome for Iκβα degradation (canonical pathway). In non-canonical pathway, RelB favors the activation of NF-κβ *via* RelB. Activated NF-κβ is further translocated into the nucleus for DNA bindings, called response elements (RE). The DNA/NF-κβ complex attracts coactivators and RNA polymerase, which transcribe the DNA into mRNA resulting in a cell transformation.

bioavailability, reversed prolongation of QT and QTc intervals, and reduced the expressions of kidney injury marker 1 (Kim-1), NFκB, and cardiac troponin I (CTnI), which eventually normalized the blood pressure (Oyagbemi et al., 2018a). Previous study in neonatal rat cardiac myocytes exposed to LPS showed luteolin reduced the TNF-α levels in the medium, downregulated the TNF-α mRNA in myocytes, inhibited degradation of IκB-β and nuclear translocation of NFκB, as well as reduced NFκB DNA binding, proposing the therapeutic potential of luteolin the management of inflammation-related myocardial diseases (Lv et al., 2011).

Fisetin

Fisetin or 3, 3c,4c,7-tetrahydroxyflavone is a bioactive molecule found in fruits such as strawberry, apple, persimmon, and grape and vegetables such as onion and cucumber (Arai et al., 2000).

Garg et al. (2019) reported the protective effect of fisetin against isoproterol-induced myocardial injury by suppressing myocardial injury markers, creatine kinase-muscle/brain (CK-MB), lactate dehydrogenase (LDH), and inflammatory markers (TNF-α and IL-6) in the blood serum as well as normalization of histological and ultrastructure of the heart. In addition, fisetin regulated the balance between pro- or anti-oxidants and pro- or anti-apoptotics proteins in the myocardial tissue (Garg et al., 2019). These protective effects of fisetin are attributed to the downregulation of receptor for advanced glycation end products (RAGE) and NFκB (Garg et al., 2019).

Fisetin attenuated the development of diabetic cardiomyopathy by attenuating the expression of myocardial NFκB and the pro-inflammatory cytokines IL-1β, IL-6, and TNF-α in the heart of diabetic rats. These result in reduction of cardiac function markers such as CK-MB, LDH, and cTn as well as normalization heart morphology (Althunibat et al., 2019).

Apigenin

Apigenin, a flavone, is found widely available in fruits and vegetables, such as grapefruits, oranges, celeries, and onions (Ren et al., 2018).

In LPS-treated macrophages, apigenin has been shown to reduce toll-like receptor 4 (TLR-4), MyD88, and p-IκB-α expression levels *via* nuclear NFκB p65 signaling pathway (Ren et al., 2018). Similarly, in LPS-challenged apoE-/- mice, treatment with apigenin increased expression of ATP binding cassette A1 (ABCA1), which alleviated extra lipid accumulation, reduced miR-33, TLR-4, and NFκB p65 levels, lessened the macrophages and smooth muscle cell contents in the atherosclerotic region, and improved plasma lipid profile (Ren et al., 2018). These results suggested that apigenin attenuates atherogenesis by inhibition of nuclear NFκB p65 that up-regulates ABCA1-mediated cholesterol efflux (Ren et al., 2018).

Apigenin was also shown to improve cardiac dysfunction and fibrosis in diabetic cardiomyopathy. Apigenin blunted the activity of NFκB and downregulated the activity of caspase3 accompanying with decreasing oxidative stress marker, glutathione peroxidase (GSH-Px), malondialdehyde (MAD), and superoxide dismutase (SOD) (Huangjun et al., 2016).

Isoliquiritigenin

Isoliquiritigenin is extracted from root of licorice and has been used traditionally for the treatment of inflammatory or pulmonary diseases (Peng et al., 2015). In HUVECS exposed to TNF-α, isoliquiritigenin blocked the involvement of NFκB at the transcriptional levels, and thus attenuated the downstream expression of VCAM-1, E-selectin, THP-1 monocyte adhesion, IκB-α, and PECAM-1, suggesting the protective effects of isoliquiritigenin through NFκB-dependent mechanisms (Kwon et al., 2007). In angiotensin II induced hypertension model, isoliquiritigenin attenuated inflammation cytokines including IL-1β and TNF-α, excessive deposition of extracellular matrix, and oxidative stress-induced apoptosis *via* nuclear factor E2-related factor 2 (Nrf2) and NFκB pathways (Xiong et al., 2018).

Rutin

Rutin is a flavonol that presents in buckwheat and citrus fruits. In a sodium fluoride-induced hypertensive rats, administration of rutin reduced blood pressure elevation by enhancing NO bioavailability *via* down-regulation of NFκB expression and up-regulation of Nrf2 (Oyagbemi et al., 2018b).

In carfilzomib-induced cardiotoxicity in rat, rutin protected against myocardial hypertrophy by upregulating IκB-α and downregulating NFκB expression, resulting in attenuation of β-myosin heavy chain, reduction in B-type natriuretic peptide mRNA expressions, and normalization of cardiac muscle fiber morphology (Imam et al., 2017).

In addition, rutin increased activities of Nrf, decreased activation of NFκB in human embryonic kidney reporter cell line, and preserved relaxation of fetal placental arteries derived from human chorionic plate (Sthijns et al., 2017).

In high mobility group box 1 (HMGBI)-induced inflammatory response in HUVECs, rutin attenuated NFκB and ERK1/2, which, in turn, reduced IL-6 and TNF-α levels (Yoo et al., 2014). Up-regulation of VCAM-1, intercellular adhesion molecule-1 (ICAM-1), and E-selectin induced by HMGB1 were similarly inhibited by rutin, suggesting that the protective effect of rutin on vascular inflammation is by inhibiting the HMGB1 and NFκB pathways.

In LPS-induced inflammation in HUVECs, rutin reversed barrier disruption, expression of cell adhesion molecules, and adhesion and migration of monocytes in endothelial cells. The barrier protective effects of rutin were linked to a down-regulation of TNF-α, deactivation of NFκB, and reduced phosphorylation of IκB-α (Lee et al., 2012).

Chrysin

Chrysin (5,7-dihydroxyflavone) is a flavone, which is found in the blue passion flower, honey, and propolis (Mantawy et al., 2017). Chrysin prevented doxorubicin (DOX)-induced cardiomyopathy including disturbance of cardiac conduction, increased serum cardiac markers and histopathological alteration in heart of rat *via* downregulation of NFκB, mitogen-activated protein kinase (MAPK), suppression of AKT pathway and its upstream activator, vascular endothelial growth factor (VEGF) (Mantawy et al., 2017).

In a rat model of monocrotaline-induced pulmonary arterial hypertension (PAH), chrysin reduced right ventricular systolic pressure and mean pulmonary artery pressure. In addition to suppression of right ventricular remodeling, chrysin abolished increased expression of collagen I, collagen III, and NFκB (Li et al., 2015).

In isoprenaline-induced myocardial injury in rats, chrysin relieved hemodynamic and ventricular dysfunction as well as reduced ultrastructural myocardial damage *via* inhibition of NFκB, IκKβ expression, and TNF-α level as well as increased peroxisome proliferator-activated receptor-gamma (PPAR-γ) expression (Rani et al., 2016).

In a rat model of myocardial infarction, fibrosis in the interstitial and perivascular regions and expression of collagen was reduced following chrysin treatment (Yang et al., 2018). This effect is associated with increased PPAR-γ expression and decreased NFκB expression *via* inhibition of IκKβ phosphorylation, leading to reduction of matrix metalloproteinase-2 (MMP-2), MMP-9 levels, and suppression of activator protein 1 (AP-1) level.

Genistein

Genistein under the subgroup of an isoflavone [4′,5,7-trihydroxyisoflavone,5,7-dihydroxy-3-(4-hydroxyphenyl)-4-H-1-benzopyran-4-one] is primarily found in soy-based foods, legumes, and red clover. In homocysteine-induced endothelial cell inflammatory injury, genistein prevented endothelial damage *via* blockade of activation of NFκB, expression of inflammatory cytokine and adhesion molecule, IL-6, and ICAM-1 (Han et al., 2015).

Xu et al. (2019) explored the effect of genistein on angiotensin II-induced vascular smooth muscle cell inflammation. Angiotensin II-induced expression of NFκB, C-reactive protein (CRP), MMP-9, phosphorylation of ERK1/2 and p-38, which lead to atherosclerotic inflammatory damage, were reversed following genistein treatment. Furthermore, genistein enhanced expression of PPAR-γ, suggesting cardiovascular protective effect by the isoflavone is through regulation of p38/ERK1/2-PPARγ-NFκB signaling pathway (Xu et al., 2019).

Silymarin

Silymarin is a flavonolignan extracted from the milk thistle. Silymarin augmented relaxation of pulmonary arteries isolated from a lung ischemia-reperfusion (I/R) injury model (Jin et al., 2016). Vascular protective effect of silymarin is due to inhibition of NFκB, thus suppressing the serum concentration of inflammatory cytokines and reducing protein expression of hypoxia inducible factor-1α (HIF-1α) and iNOS.

Silibinin, a major active constituent of silymarin, was able to reduce the abnormal size of cardiac myocytes and prevent hypertrophy by alleviating the production of epidermal growth factor receptor (EGFR) (Ai et al., 2010). Silibilin exerted its anti-inflammatory effect by suppressing the activation of NFκB stimulated by angiotensin II in cardiac myocytes or in the aortic banding male mice. Furthermore, silibilin interfered with the phosphorylation and degradation of IκB-α and activation of IκKβ *in vivo*.

Kaempferol

Kaempferol (3,4′,5,7-tetrahydroxyflavone) is a flavonol that is present widely in fruits, vegetables, and herbs, including grapes, tomatoes, and tea. In cardiac fibroblasts stimulated with LPS, kaempferol decreased release of pro-inflammatory cytokines by inhibiting AKT phosphorylation and NFκB activation (Tang et al., 2015). In isoprenaline-induced cardiac damage, kaempferol improved the hemodynamic and left ventricular functions in male rats, which abated the increased serum concentration of CK-MB and LDH, preserved the morphology of myocardium, and reduced the levels of pro-inflammatory cytokines (Suchal et al., 2016a). Similarly, kaempferol prevented cardiac damage by inhibiting the protein expression of NFκB, p38, and JNK (Suchal et al., 2016b) suggesting that cardioprotective and

TABLE 1 | Effect of flavonoids in CVDs.

No	Flavonoids	Models	Mechanisms	Reference
1	Quercetin	Clinical study: CAD patients	↓ NFκB, IL-1β, TNF-α, IkBα	(Chekalina et al., 2018)
		In vitro: leptin-induced inflammation and endothelial dysfunction in HUVECs	↓ ERK1/2 phosphorylation, NFκB, TNF-α	(Indra et al., 2013)
		In vitro: neonatal rat cardiac fibroblast inflammatory	↓ NFκB, TNF-α, IL-1β, IL-6, AKT	(Tang et al., 2014)
2	Luteolin	*In vivo*: NaF-induced hypertension	↑NO ↓ Nrf2, Kim-1, NFκB, CTnI	(Oyagbemi et al., 2018a)
		In vitro: Neonatal rat cardiac myocytes inflammatory	↓ NFκB, TNF-α, ↑ IκB-β	(Lv et al., 2011)
3	Fisetin	*In vivo*: Isoprenaline-induced cardiac ischemic injury	↓NFκB, RAGE, TNF-α, IL-6, CK-MB, LDH	(Garg et al., 2019)
		In vivo: Hyperglycemia-induced cardiac injury	↓NFκB, IL-1β, IL-6, TNF-α	(Althunibat et al., 2019)
4	Apigenin	*In vitro*: LPS-treated macrophages *In vivo*: LPS-challenged apoE-/- mice	↓ NFκB p65, TLR-4, MyD88, p-IκB-α ↑ ABCA1	(Ren et al., 2018)
		In vivo: diabetic cardiomyopathy	↓ NFκB, caspase3, GSH-Px, MDA, SOD	(Huangjun et al., 2016)
5	Isoliquiriti-genin	*In vitro*: TNF-α induced inflammation in HUVECs	↓ NFκB, VCAM-1, E-selectin, THP-1 monocyte adhesion, IκB-α, PECAM-1	(Kwon et al., 2007)
		In vivo: Angiotensin II-induced hypertension	↓ NFκB, IL-1β and TNF-α Nrf2,	(Xiong et al., 2018)
6	Rutin	*In vivo:* Sodium fluoride induced hypertension in rat	↓ NFκB ↑ Nrf2	(Oyagbemi et al., 2018b)
		In vivo: carfilzomib-induced cardiotoxicity in rat	↓ NFκB ↑ IκB-α	(Imam et al., 2017)
		In vitro: hydrogen peroxide induced oxidative stress in HUVECS	↓ NFκB ↑ Nrf2	(Sthijns et al., 2017)
		In vitro: HMGBI-induced inflammatory in HUVECS	↓ NFκB, ERK1/2, TNFα, IL-6, ICAM-1, VCAM-1, E-selectin	(Yoo et al., 2014)
		In vitro: LPS induced inflammation in HUVECS	↓ NFκB, IκB-α, TNF-α, ICAM-1, VCAM-1, E-selectin	(Lee et al., 2012)
7	Chrysin	*In vivo:* DOX-induced cardiotoxicity in rat	↓ p38, JNK, NFκB ↑ VEGF, AKT	(Mantawy et al., 2017)
		In vivo: monocrotaline-induced pulmonary arterial hypertension in rat	↓ NFκB	(Li et al., 2015)
		In vivo: ISO-induced myocardial injury in rat	↑ PPAR-γ ↓ NFκBp65, IκK-β, TNF-α	(Rani et al., 2016)
		In vivo: MI in rat	↑ PPAR-γ ↓ NFκB, IκK-β, MMP-2, MMP-9, AP-1	(Yang et al., 2018)
8	Genistein	*In vitro*: Homocysteine-induced endothelial cell inflammation in HUVECS	↓ NFκBp65, IL-6, ICAM-1	(Han et al., 2015)
		In vitro: angiotensin II-induced VSMCs inflammation	↑ PPAR-γ ↓ ERK1/2, p38, NFκB, CRP, MMP-9	(Xu et al., 2019)
9	Silymarin	*In vivo:* I/R injury in rat	↓ NFκB, HIF-1α, iNOS, TNFα, IL-1β, IL-6	(Jin et al., 2016)
		In vivo: Cardiac hypertrophy model in mouse	↓ NFκB, EGFR, IκB-α, IκKβ	(Ai et al., 2010)
10	Kaempferol	*In vitro*: LPS+ATP stimulated cardiac fibroblasts inflammation	↓ AKT, NFκBp65, TNF-α, IL-1β, IL-6, IL-18	(Tang et al., 2015)
		In vivo: I/R cardiac injury in rat	↓ p38, JNK, NFκBp65, TNF-α, IL-6	(Suchal et al., 2016a; Suchal et al., 2016b)

anti-inflammatory action of kaempferol was associated with NFκB signaling pathway.

Table 1 summarizes the effects and mechanisms of action of flavonoids in CVD.

CONCLUSION

The actions of flavonoids in mitigating inflammation by modulation of NFκB offer potential agents for the treatment of CVDs. However, several of these actions reported *in vitro* may yet to be fully recognized due to their low bioavailabilities following oral administration (Hollman and Katan, 1998; Thilakarathna and Rupasinghe, 2013). Flavonoids have shown promising results in reducing atherosclerosis in several animal experimental models; however, conflicting results were reported in human clinical trials (Arts and Hollman, 2005; Zordoky et al., 2015). The low bioavailability and clinical efficacy of flavonoids are attributed to their poor absorption, metabolism by the metabolizing enzymes in the intestine and liver, and structural modifications by the colonic bacteria remain as the major problems. Continuous investigation is required to enhance the bioavailability and efficacy of the flavonoids to tap the full potential of these natural agents.

AUTHOR CONTRIBUTIONS

All authors contributed to the writing. KC, DM, and MM conceived, designed, and revised the manuscript.

FUNDING

This study was funded by Government Agency grant GA001-2017, MAHSA University and USIM research project code: PPPI/FPG/0118/051000/15618 Universiti Kebangsaan Malaysia and Universiti Putra Malaysia. The funding agencies played no role in the design of the study and collection, analysis, and interpretation of data and in writing the manuscript, which are fully the responsibilities of the authors.

REFERENCES

Ai, W., Zhang, Y., Tang, Q. Z., Yan, L., Bian, Z. Y., Liu, C., et al. (2010). Silibinin attenuates cardiac hypertrophy and fibrosis through blocking EGFR-dependent signaling. *J. Cell. Biochem.* 110, 1111–1122. doi: 10.1002/jcb.22623

Alkhalidy, H., Wang, Y., and Liu, D. (2018). Dietary flavonoids in the prevention of t2d: an overview. *Nutrients* 10, 1–33. doi: 10.3390/nu10040438

Althunibat, O. Y., Al Hroob, A. M., Abukhalil, M. H., Germoush, M. O., Bin-Jumah, M., and Mahmoud, A. M. (2019). Fisetin ameliorates oxidative stress, inflammation and apoptosis in diabetic cardiomyopathy. *Life Sci.* 221, 83–92. doi: 10.1016/j.lfs.2019.02.017

Arai, Y., Watanabe, S., Kimira, M., Shimoi, K., Mochizuki, R., and Kinae, N. (2000). Dietary intakes of flavonols, flavones and isoflavones by Japanese women and the inverse correlation between quercetin intake and plasma LDL cholesterol concentration. *J. Nutr.* 130, 2243–2250. doi: 10.1093/jn/130.9.2243

Arikawa, M., Kakinuma, Y., Noguchi, T., Todaka, H., and Sato, T. (2016). Donepezil, an acetylcholinesterase inhibitor, attenuates LPS-induced inflammatory response in murine macrophage cell line RAW 264.7 through inhibition of nuclear factor kappa B translocation. *Eur. J. Pharmacol.* 789, 17–26. doi: 10.1016/j.ejphar.2016.06.053

Arts, I. C., and Hollman, P. C. (2005). Polyphenols and disease risk in epidemiologic studies. *Am. J. Clin. Nutr. 81* (1 Suppl), 317s–325s. doi: 10.1093/ajcn/81.1.317S

Azab, A., Nassar, A., and Azab, A. N. (2016). Anti-inflammatory activity of natural products. *Molecules* 21, 1–19. doi: 10.3390/molecules21101321

Barreca, D., Gattuso, G., Bellocco, E., Calderaro, A., Trombetta, D., Smeriglio, A., et al. (2017). Flavanones: Citrus phytochemical with health-promoting properties. *Biofactors* 43, 495–506. doi: 10.1002/biof.1363

Benjamin, E. J., Blaha, M. J., Chiuve, S. E., Cushman, M., Das, S. R., Deo, R., et al. (2017). Heart disease and stroke statistics-2017 update: a report from the american heart association. *Circulation* 135, e146–e603. doi: 10.1161/CIR.0000000000000485

Brasier, A. R. (2010). The nuclear factor-κB-interleukin-6 signalling pathway mediating vascular inflammation. *Cardiovasc. Res.* 86, 211–218. doi: 10.1093/cvr/cvq076

Chekalina, N., Burmak, Y., Petrov, Y., Borisova, Z., Manusha, Y., Kazakov, Y., et al. (2018). Quercetin reduces the transcriptional activity of NF-kB in stable coronary artery disease. *Indian Heart J.* 70, 593–597. doi: 10.1016/j.ihj.2018.04.006

Da Silva Franco, N., Lubaczeuski, C., Guizoni, D. M., Victorio, J. A., Santos-Silva, J. C., Brum, P. C., et al. (2017). Propranolol treatment lowers blood pressure, reduces vascular inflammatory markers and improves endothelial function in obese mice. *Pharmacol. Res.* 122, 35–45. doi: 10.1016/j.phrs.2017.05.018

Daher, M. T., Mougenot, N., Rohr, O., Bausero, P., Liu, P., Li, Z., et al. (2019). Role of the transcription factor Bcl11b in cardiac homeostasis and remodeling. *Arch. Cardiovasc. Dis. Suppl.* 11, 231. doi: 10.1016/j.acvdsp.2019.02.109

Di Raimondo, D., Tuttolomondo, A., Butta, C., Miceli, S., Licata, G., and Pinto, A. (2012). Effects of ACE-inhibitors and angiotensin receptor blockers on inflammation. *Curr. Pharm. Des.* 18, 4385–4413. doi: 10.2174/138161212802481282

Garg, S., Malhotra, R. K., Khan, S. I., Sarkar, S., Susrutha, P. N., Singh, V., et al. (2019). Fisetin attenuates isoproterenol-induced cardiac ischemic injury in vivo by suppressing RAGE/NF-kappaB mediated oxidative stress, apoptosis and inflammation. *Phytomedicine* 56, 147–155. doi: 10.1016/j.phymed.2018.09.187

Ghosh, J., Das, J., Manna, P., and Sil, P. C. (2009). Taurine prevents arsenic-induced cardiac oxidative stress and apoptotic damage: Role of NF-κB, p38 and JNK MAPK pathway. *Toxicol. Appl. Pharmacol.* 240, 73–87. doi: 10.1016/j.taap.2009.07.008

Han, S., Wu, H., Li, W., and Gao, P. (2015). Protective effects of genistein in homocysteine-induced endothelial cell inflammatory injury. *Mol. Cell. Biochem.* 403, 43–49. doi: 10.1007/s11010-015-2335-0

Haybar, H., Rezaeeyan, H., Shahjahani, M., Shirzad, R., and Saki, N. (2019). T-bet transcription factor in cardiovascular disease: attenuation or inflammation factor? *J. Cell Physiol.* 234, 7915–7922. doi: 10.1002/jcp.27935

Hollman, P. C., and Katan, M. B. (1998). Bioavailability and health effects of dietary flavonols in man. *Arch. Toxicol. Suppl.* 20, 237–248.

Huangjun, L., Zheng, Y., Wei, D., and Qizhu, T. (2016). GW27-e0367 Apigenin attenuates the cardiac remodeling in experimental diabetic cardiomyopathy. *J. Am. Coll. Cardiol.* 68, 1–10. doi: 10.1016/j.jacc.2016.07.054

Imam, F., Al-Harbi, N. O., Al-Harbia, M. M., Korashy, H. M., Ansari, M. A., Sayed-Ahmed, M. M., et al. (2017). Rutin attenuates carfilzomib-induced cardiotoxicity through inhibition of NF-κB, hypertrophic gene expression and oxidative stress. *Cardiovasc. Toxicol.* 17, 58–66. doi: 10.1007/s12012-015-9356-5

Indra, M. R., Karyono, S., Ratnawati, R., and Malik, S. G. (2013). Quercetin suppresses inflammation by reducing ERK1/2 phosphorylation and NF kappa B activation in Leptin-induced Human Umbilical Vein Endothelial Cells (HUVECs). *BMC Res. Notes* 6, 275–275. doi: 10.1186/1756-0500-6-275

Jin, Y., Zhao, X., Zhang, H., Li, Q., Lu, G., and Zhao, X. (2016). Modulatory effect of silymarin on pulmonary vascular dysfunction through HIF-1α-iNOS following rat lung ischemia-reperfusion injury. *Exp. Therapeutic Med.* 12, 1135–1140. doi: 10.3892/etm.2016.3370

Khalil, M. I., and Sulaiman, S. A. (2010). The potential role of honey and its polyphenols in preventing heart diseases: a review. *Afr. J. Tradition. Complementary Alternative Med.: AJTCAM* 7, 315–321. doi: 10.4314/ajtcam.v7i4.56693

Khoo, H. E., Azlan, A., Tang, S. T., and Lim, S. M. (2017). Anthocyanidins and anthocyanins: colored pigments as food, pharmaceutical ingredients, and the potential health benefits. *Food Nutr. Res.* 61, 1361779–1361779. doi: 10.1080/16546628.2017.1361779

Koeners, M. P., Wesseling, S., Sanchez, M., Braam, B., and Joles, J. A. (2016). Perinatal Inhibition of NF-KappaB has long-term antihypertensive and renoprotective effects in fawn-hooded hypertensive rats. *Am. J. Hypertens.* 29, 123–131. doi: 10.1093/ajh/hpv065

Kurdi, M., Zgheib, C., and Booz, G. W. (2018). Recent developments on the crosstalk between STAT3 and inflammation in heart function and disease. *Front. Immunol.* 9, 1–10. doi: 10.3389/fimmu.2018.03029

Kwon, H. M., Choi, Y. J., Choi, J. S., Kang, S. W., Bae, J. Y., Kang, I. J., et al. (2007). Blockade of cytokine-induced endothelial cell adhesion molecule expression by licorice isoliquiritigenin through NF-kappaB signal disruption. *Exp. Biol. Med. (Maywood)* 232, 235–245. doi: 10.3181/00379727-207-2320235

Lee, W., Ku, S.-K., and Bae, J.-S. (2012). Barrier protective effects of rutin in LPS-induced inflammation *in vitro* and *in vivo*. *Food Chem. Toxicol.* 50, 3048–3055. doi: 10.1016/j.fct.2012.06.013

Li, X., Guo, B., Shen, Y., and Yang, J. (2015). Effect of chrysin on expression of NOX4 and NF-κB in right ventricle of monocrotaline-induced pulmonary arterial hypertension of rats. *Yao Xue Xue Bao= Acta Pharma. Sin.* 50, 1128–1134. doi: 10.1016/j.jash.2017.03.008

Li, Y., Yao, J., Han, C., Yang, J., Chaudhry, M. T., Wang, S., et al. (2016). Quercetin, Inflammation and Immunity. *Nutrients* 8, 167–167. doi: 10.3390/nu8030167

Lin, X., Wu, M., Liu, B., Wang, J., Guan, G., Ma, A., et al. (2015). Candesartan ameliorates acute myocardial infarction in rats through inducible nitric oxide synthase, nuclear factorkappaB, monocyte chemoattractant protein1, activator protein1 and restoration of heat shock protein 72. *Mol. Med. Rep.* 12, 8193–8200. doi: 10.3892/mmr.2015.4432

Lv, L., Lv, L., Zhang, Y., and Kong, Q. (2011). Luteolin prevents LPS-induced TNF-alpha expression in cardiac myocytes through inhibiting NF-kappaB signaling pathway. *Inflammation* 34, 620–629. doi: 10.1007/s10753-010-9271-7

Manach, C., Scalbert, A., Morand, C., Remesy, C., and Jimenez, L. (2004). Polyphenols: food sources and bioavailability. *Am. J. Clin. Nutr.* 79, 727–747. doi: 10.1093/ajcn/79.5.727

Mantawy, E. M., Esmat, A., El-Bakly, W. M., Eldin, R.a.S., and El-Demerdash, E. (2017). Mechanistic clues to the protective effect of chrysin against doxorubicin-induced cardiomyopathy: plausible roles of p53, MAPK and AKT pathways. *Sci. Rep.* 7, 4795. doi: 10.1038/s41598-017-05005-9

Marzocchella, L., Fantini, M., Benvenuto, M., Masuelli, L., Tresoldi, I., Modesti, A., et al. (2011). Dietary flavonoids: molecular mechanisms of action as anti-inflammatory agents. *Recent Pat. Inflamm. Allergy Drug Discov.* 5, 200–220. doi: 10.2174/187221311797264937

Osakabe, N. (2013). Flavan 3-ols improve metabolic syndrome risk factors: evidence and mechanisms. *J. Clin. Biochem. Nutr.* 52, 186–192. doi: 10.3164/jcbn.12-130

Oyagbemi, A. A., Omobowale, T. O., Ola-Davies, O. E., Asenuga, E. R., Ajibade, T. O., Adejumobi, O. A., et al. (2018a). Luteolin-mediated Kim-1/NF-kB/Nrf2 signaling pathways protects sodium fluoride-induced hypertension and cardiovascular complications. *BioFactors* 44, 518–531. doi: 10.1002/biof.1449

Oyagbemi, A. A., Omobowale, T. O., Ola-Davies, O. E., Asenuga, E. R., Ajibade, T. O., Adejumobi, O. A., et al. (2018b). Ameliorative effect of Rutin on sodium fluoride-induced hypertension through modulation of Kim-1/NF-κB/Nrf2 signaling pathway in rats. *Environ. Toxicol.* 33, 1284–1297. doi: 10.1002/tox.22636

Panche, A. N., Diwan, A. D., and Chandra, S. R. (2016). Flavonoids: an overview. *J. Nutr. Sci.* 5, e47–e47. doi: 10.1017/jns.2016.41

Peng, F., Du, Q., Peng, C., Wang, N., Tang, H., Xie, X., et al. (2015). A review: the pharmacology of isoliquiritigenin. *Phytother. Res.* 29, 969–977. doi: 10.1002/ptr.5348

Pollastri, S., and Tattini, M. (2011). Flavonols: old compounds for old roles. *Ann. Bot.* 108, 1225–1233. doi: 10.1093/aob/mcr234

Quintana-Villamandos, B., Goukassian, D. A., Sasi, S. P., and Delgado-Baeza, E. (2018). Short-term treatment with esmolol reverses left ventricular hypertrophy in adult spontaneously hypertensive rats *via* inhibition of Akt/NF-κB and NFATc4. *BioMed. Res. Int.* 2018, 9. doi: 10.1155/2018/2691014

Rani, N., Bharti, S., Bhatia, J., Nag, T., Ray, R., and Arya, D. S. (2016). Chrysin, a PPAR-γ agonist improves myocardial injury in diabetic rats through inhibiting AGE-RAGE mediated oxidative stress and inflammation. *Chemico-Biol. Interact.* 250, 59–67. doi: 10.1016/j.cbi.2016.03.015

Ren, K., Jiang, T., Zhou, H. F., Liang, Y., and Zhao, G. J. (2018). Apigenin retards atherogenesis by promoting abca1-mediated cholesterol efflux and suppressing inflammation. *Cell Physiol. Biochem.* 47, 2170–2184. doi: 10.1159/000491528

Ruparelia, N., Chai, J. T., Fisher, E. A., and Choudhury, R. P. (2017). Inflammatory processes in cardiovascular disease: a route to targeted therapies. *Nat. Rev. Cardiol.* 14, 133–144. doi: 10.1038/nrcardio.2016.185

Shih, V. F.-S., Tsui, R., Caldwell, A., and Hoffmann, A. (2011). A single NFκB system for both canonical and non-canonical signaling. *Cell Res.* 21, 86–102. doi: 10.1038/cr.2010.161

Smale, S. T., and Natoli, G. (2014). Transcriptional control of inflammatory responses. *Cold Spring Harb. Perspect. Biol.* 6, a016261. doi: 10.1101/cshperspect.a016261

Sthijns, M. M., Schiffers, P. M., Janssen, G. M., Lemmens, K. J., Ides, B., Vangrieken, P., et al. (2017). Rutin protects against H2O2-triggered impaired relaxation of placental arterioles and induces Nrf2-mediated adaptation in human umbilical vein endothelial cells exposed to oxidative stress. *Biochim. Biophys. Acta (BBA)-General Subjects* 1861, 1177–1189. doi: 10.1016/j.bbagen.2017.03.004

Suchal, K., Malik, S., Gamad, N., Malhotra, R. K., Goyal, S. N., Bhatia, J., et al. (2016a). Kampeferol protects against oxidative stress and apoptotic damage in experimental model of isoproterenol-induced cardiac toxicity in rats. *Phytomedicine* 23, 1401–1408. doi: 10.1016/j.phymed.2016.07.015

Suchal, K., Malik, S., Gamad, N., Malhotra, R. K., Goyal, S. N., Chaudhary, U., et al. (2016b). Kaempferol attenuates myocardial ischemic injury via inhibition of MAPK signaling pathway in experimental model of myocardial ischemia-reperfusion injury. *Oxidative Med. Cell. Longevity* 2016, 1–1. doi: 10.1155/2016/7580731

Sun, S.-C. (2017). The non-canonical NF-κB pathway in immunity and inflammation. *Nat. reviews. Immunol.* 17, 545–558. doi: 10.1038/nri.2017.52

Tang, X.-l., Liu, J.-x., Dong, W., Li, P., Li, L., Hou, J.-c., et al. (2015). Protective effect of kaempferol on LPS plus ATP-induced inflammatory response in cardiac fibroblasts. *Inflammation* 38 (1), 94–101. doi: 10.1007/s10753-014-0011-2

Tang, X.-L., Liu, J.-X., Dong, W., Li, P., Li, L., Zheng, Y.-Q., et al. (2014). Intervention effect of quercetin on inflammatory secretion of cardiac fibroblasts.

Thilakarathna, S. H., and Rupasinghe, H. P. V. (2013). Flavonoid bioavailability and attempts for bioavailability enhancement. *Nutrients* 5 (9), 3367–3387. doi: 10.3390/nu5093367

Van Der Heiden, K., Cuhlmann, S., Luong Le, A., Zakkar, M., and Evans, P. C. (2010). Role of nuclear factor kappaB in cardiovascular health and disease. *Clin. Sci. (Lond)* 118, 593–605. doi: 10.1042/CS20090557

Wang, X., Chen, Q., Pu, H., Wei, Q., Duan, M., Zhang, C., et al. (2016). Adiponectin improves NF-kappaB-mediated inflammation and abates atherosclerosis progression in apolipoprotein E-deficient mice. *Lipids Health Dis.* 15, 33. doi: 10.1186/s12944-016-0202-y

Weng, C. J., and Yen, G. C. (2012). Flavonoids, a ubiquitous dietary phenolic subclass, exert extensive *in vitro* anti-invasive and *in vivo* anti-metastatic activities. *Cancer Metastasis Rev.* 31, 323–351. doi: 10.1007/s10555-012-9347-y

Xiong, D., Hu, W., Ye, S.-T., and Tan, Y.-S. (2018). Isoliquiritigenin alleviated the Ang II-induced hypertensive renal injury through suppressing inflammation cytokines and oxidative stress-induced apoptosis *via* Nrf2 and NF-κB pathways. *Biochem. Biophysical Res. Commun.* 506, 161–168. doi: 10.1016/j.bbrc.2018.09.013

Xu, L., Liu, J.-T., Li, K., Wang, S.-Y., and Xu, S. (2019). Genistein inhibits Ang II-induced CRP and MMP-9 generations *via* the ER-p38/ERK1/2-PPARγ-NF-κB signaling pathway in rat vascular smooth muscle cells. *Life Sci.* 216, 140–146. doi: 10.1016/j.lfs.2018.11.036

Yang, M., Xiong, J., Zou, Q., Wang, D.-D., and Huang, C.-X. (2018). Chrysin attenuates interstitial fibrosis and improves cardiac function in a rat model of acute myocardial infarction. *J. Mol. histology* 49, 555–565. doi: 10.1007/s10735-018-9793-0

Yoo, H., Ku, S.-K., Baek, Y.-D., and Bae, J.-S. (2014). Anti-inflammatory effects of rutin on HMGB1-induced inflammatory responses *in vitro* and *in vivo*. *Inflammation Res.* 63, 197–206. doi: 10.1007/s00011-013-0689-x

Zeinali, M., Rezaee, S. A., and Hosseinzadeh, H. (2017). An overview on immunoregulatory and anti-inflammatory properties of chrysin and flavonoids substances. *Biomed Pharmacother* 92, 998–1009. doi: 10.1016/j.biopha.2017.06.003

Zhao, H., Shen, R., Dong, X., and Shen, Y. (2017). Murine double minute-2 inhibition attenuates cardiac dysfunction and fibrosis by modulating nf-kappab pathway after experimental myocardial infarction. *Inflammation* 40, 232–239. doi: 10.1007/s10753-016-0473-5

Zordoky, B. N. M., Robertson, I. M., and Dyck, J. R. B. (2015). Preclinical and clinical evidence for the role of resveratrol in the treatment of cardiovascular diseases. Biochimica et Biophysica Acta (BBA) - Molecular Basis of Disease 1852 (6), 1155–1177. doi: 10.1016/j.bbadis.2014.10.016

Conflict of Interest: The authors declare that the research was conducted in the absence of any commercial or financial relationships that could be construed as a potential conflict of interest.

The reviewer ZJ declared a shared affiliation, with no collaboration, with one of the authors, XFL, to the handling editor at time of review

frontiers in Pharmacology

ORIGINAL RESEARCH
published: 31 October 2019
doi: 10.3389/fphar.2019.01219

Sophocarpine Suppresses NF-κB-Mediated Inflammation Both *In Vitro* and *In Vivo* and Inhibits Diabetic Cardiomyopathy

Fang Zou[1†], Ling Wang[2†], Han Liu[1], Wei Wang[1], Longlong Hu[3], Xiaoying Xiong[3], Lijuan Wu[3], Yunfeng Shen[1] and Renqiang Yang[3*]*

[1] Department of Endocrinology and Metabolism, The Second Affiliated Hospital of Nanchang University, Nangchang, China, [2] Department of Clinical Laboratory, The Second Affiliated Hospital of Nanchang University, Nangchang, China, [3] Department of Cardiovascular Disease, The Second Affiliated Hospital of Nanchang University, Nangchang, China

OPEN ACCESS

Edited by:
Cheng Xue Helena Qin,
Baker Heart and Diabetes Institute,
Australia

Reviewed by:
Nazareno Paolocci,
Johns Hopkins University,
United States
Bin-Nan Wu,
Kaohsiung Medical University,
Taiwan

***Correspondence:**
Yunfeng Shen
yunfengshen783ab@163.com
Renqiang Yang
yangrenqiangcn@163.com

†These authors have contributed equally to this work and share first authorship

Specialty section:
This article was submitted to Cardiovascular and Smooth Muscle Pharmacology, a section of the journal Frontiers in Pharmacology

Received: 24 June 2019
Accepted: 23 September 2019
Published: 31 October 2019

Citation:
Zou F, Wang L, Liu H, Wang W, Hu L, Xiong X, Wu L, Shen Y and Yang R (2019) Sophocarpine Suppresses NF-κB-Mediated Inflammation Both In Vitro and In Vivo and Inhibits Diabetic Cardiomyopathy. Front. Pharmacol. 10:1219. doi: 10.3389/fphar.2019.01219

Diabetic cardiomyopathy (DCM) is a leading cause of mortality in patients with diabetes. DCM is a leading cause of mortality in patients with diabetes. We used both *in vitro* and *in vivo* experiments to investigate the hypothesis that sophocarpine (SPC), a natural quinolizidine alkaloid derived from a Chinese herb, could protect against DCM. We used hyperglycemic myocardial cells and a streptozotocin (STZ)-induced type 1 diabetes mellitus mouse model. SPC protected myocardial cells from hyperglycemia-induced injury by improving mitochondrial function, suppressing inflammation, and inhibiting cardiac apoptosis. The SPC treatment significantly inhibited the activation of nuclear factor kappa-light-chain-enhancer of activated B cells (NF-κB) signaling in high-glucose-stimulated inflammatory responses. Moreover, SPC significantly slowed the development and progression of DCM in STZ-induced diabetic mice. These results show that SPC suppresses NF-κB-mediated inflammation both *in vitro* and *in vivo* and may be used to treat DCM.

Keywords: sophocarpine, NF-κB, inflammation, diabetes, cardiomyopathy—diagnostics

INTRODUCTION

Cardiovascular disease is a major cause of morbidity and mortality worldwide, especially for patients with diabetes (Tall and Levine, 2017; He et al., 2019; Tall and Jelic, 2019). Previous studies have reported that more than half of these patients die from diabetic cardiomyopathy (DCM), which is characterized by changes in myocardial structure and function such as ventricular hypertrophy, cardiac fibrosis, and heart failure (Ye et al., 2018; Kang et al., 2019; Knapp et al., 2019; Zheng et al., 2019). Due to the increased prevalence of DCM-related mortality, an understanding of the mechanism of DCM pathogenesis and effective therapies are needed urgently (Sun et al., 2019; Zheng et al., 2019; Wu et al., 2019b). The pathophysiology of DCM is complex; however, inflammatory upstream events that are mainly induced by hyperglycemia are important. The downstream events that eventually lead to heart failure include elevated oxidative stress, cardiac inflammation, cardiomyocyte apoptosis, interstitial fibrosis, and myocardial remodeling (Ye et al., 2018; Zhang et al., 2018a; Bombicz et al., 2019; Wu et al., 2019b). Therefore, suppressing inflammation is a promising strategy for treating DCM (Ye et al., 2018; Zheng et al., 2018; Bombicz et al., 2019; Wu et al., 2019b).

Sophocarpine (SPC) is a natural quinolizidine alkaloid derived from *Sophora flavescens*, a traditional Chinese herb that has been used to treat illnesses for nearly 2,000 years (Zhou et al., 2018; Wu et al., 2019a). SPC attenuates wear particle-induced implant loosening (Zhou et al., 2018), and both *in vitro* and *in vivo* studies suggest that it has strong anti-inflammatory and pharmacological effects on a variety of human diseases including viral infections, allergies, and cancer (Huang et al., 2016; Zhang et al., 2016; Sang et al., 2017; Zhu and Zhu, 2017; Liu et al., 2017b; Jiang et al., 2018; Li et al., 2018; Zhou et al., 2018; Zhang et al., 2018b; Wu et al., 2019a). Moreover, several previous studies reported that SPC can protect against cardiovascular diseases (Li et al., 2011; Zhang et al., 2012; Li et al., 2014). (Li et al., 2014) reported that oral SPC protected rat hearts against pressure-overload-induced cardiac fibrosis (Li et al., 2014). Zhang *et al.* reported that SPC attenuates the Na^+-dependent Ca^{2+} overload induced by *Anemonia sulcata* toxin-increased late sodium current in rabbit ventricular myocytes (Zhang et al., 2012). In another study, administering SPC to rats preserved myocardial function following ischemia-reperfusion by inactivating nuclear factor kappa-light-chain-enhancer of activated B cells (NF-κB) (Li et al., 2011). However, it is unclear whether SPC has cardioprotective effects against DCM.

Because of its effect on inflammatory responses and cardioprotective properties, here we conducted both *in vitro* and *in vivo* experiments to explore: (1) the effect of SPC on high glucose (HG)-induced mitochondrial dysfunction, inflammation, apoptosis of myocardial cells; (2) the effect of SPC on collagen deposition, fibrosis, left ventricular remodeling and cardiac dysfunction in DCM mice; and (3) the underlying mechanism.

RESULTS

SPC Protects Against HG-Induced Inflammatory Responses in Myocardial Cells

To investigate the cytotoxicity of SPC, H9c2 cells were treated with several doses (0–10 mM) (Zhou et al., 2018) of SPC for 48 and 96 h. As is shown in **Supplementary Figures 1**, no toxic effects of SPC were found on H9c2 cells, up to the maximal concentration of 10 mM. To assess the effect of SPC on HG-induced inflammatory responses, biomarkers of hypertrophy, cell fibrosis, and apoptosis were assessed by western blot assay after treatment. As in shown in **Figure 1**, HG stimulation for 12 h remarkably increased the expression of pro-fibrotic biomarkers including collagen 1 (COL-1), matrix metalloproteinase 9 (MMP-9), and transforming growth factor-β (TGF-β); hypertrophy biomarker myosin heavy chain (MyHC); and cell apoptotic biomarker Bax, which was then significantly inhibited by SPC in a dose dependent manner (**Figure 1B**). The results of qPCR further confirmed the findings of western blot analysis (**Figures 1C–F**). By conducting TUNEL (terminal deoxynucleotidyl transferase-mediated dUTP nick end labeling) staining, we found that the increased apoptosis of H9c2 cells was effectively attenuated by 1 mM SPC (**Figure 1G**), which was also confirmed by flow cytometry apoptosis assay (**Figure 1H**).

To confirm our findings about the effects of SPC on myocardial cells, we also applied additional experiments using neonatal mouse cardiomyocytes (NMCMs). As is shown in **Supplementary Figure 2**, SPC also attenuated HG-stimulated inflammatory responses and apoptosis in NMCMs, which was consistent with what we found in H9c2 cells.

SPC Attenuated HG-Stimulated Mitochondrial Dysfunction in H9c2 Cells

To uncover the possible underlying mechanism of the anti-apoptotic effect of SPC on H9c2 cells, the mitochondrial-mediated apoptotic pathway, which plays a vital role in HG-stimulated H9c2 cell apoptosis (Guo et al., 2018), was analyzed. As is shown in **Figure 2**, HG induction for 12 h significantly increased reactive oxygen species (ROS) production, which was effectively inhibited by 1 mM SPC treatment (**Figures 2A**, **B**). Similarly, the cytochrome c release and caspase-3/9 activation induced by HG were also inhibited by SPC. Moreover, we determined the effect of SPC on Bcl-2 family proteins expression. HG stimulation up-regulated the expression of pro-apoptotic Bax and down-regulated the expression of anti-apoptotic Bcl-2, whereas these changes were attenuated by application with expression (**Figures 2C**, **D**).

SPC Suppressed the Activation of the NF-κB Signaling in HG-Stimulated Inflammatory Responses

To further confirm the protective effects of SPC on HG-induced H9c2 cells were related with anti-inflammatory, the transcription factor NF-κB signaling pathway is investigated. First, we determined the effect of SPC on IκBα degradation in H9c2 cells incubated with HG. The results showed that incubation with HG (33 mM) for 12 h remarkably induced IκBα degradation, and this alteration was significantly reversed by SPC treatment (1 mM). Then, we analyzed the expression of p65 protein in both the nucleus and cytoplasm. HG stimulation markedly increased the nuclear translocation of NF-κB/p65, which was abolished by SPC treatment (**Figures 3A**, **B**).

To explore the possible mechanism underlying the regulation of SPC on Bcl-2 and Bax expression, small interfering RNAs (siRNAs) targeting p65 were used. As is shown in **Figures 3C**, **D**, the WB analysis showed successful knockdown of p65 using siRNAs. Based on the results of WB analysis, p65 siRNA#2 was chosen for subsequent experiments. As is shown in **Figures 3E–K**, p65 knockdown using siRNA partially mimicked the anti-inflammatory (**Figure 3G**) and anti-apoptotic effects (**Figures 3E**, **F**, **H**, **I**) and anti-oxidative stress (**Figure 3J**) of SPC, as SPC treatment (1 mM) together with p65 knockdown further augmented these effects. Thus, SPC treatment regulated the expression of Bcl-2 and Bax and protected against HG-induced cardiomyocyte apoptosis partially through the inhibition of NF-κB p65.

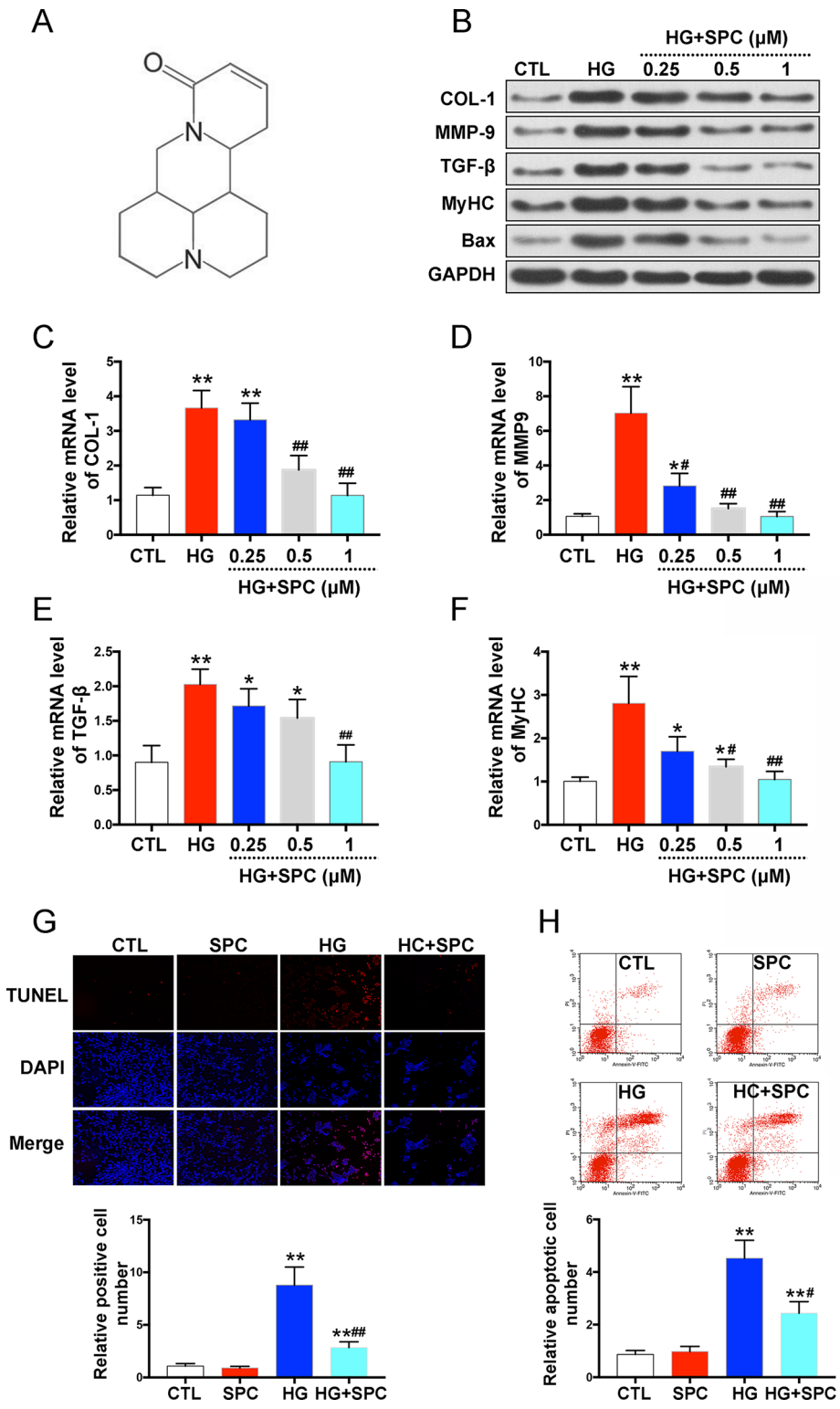

FIGURE 1 | SPC protects against HG-induced inflammatory responses in H9c2 cells. **(A)** The chemical structure of SPC. **(B)** Western blot analysis showed that HG stimulation for 12 h remarkebly increased the expression of COL-1, MMP-9, TGF-β, MyHC, and Bax, which was then significantly inhibited by SPC in a dose dependent manner. **(C–F)** The results of qPCR further confirmed the findings of western blot analysis. **(G)** TUNEL staining showed that the increased apoptosis of H9c2 cells was effectively attenuated by SPC. Figures are magnified as 100×. **(H)** Flow cytometry assay confirmed the results of TUNEL staining. CTL, control group; SPC, Sophocarpine; HG, high glucose. *P < 0.05 when compared with the results of control group; **P < 0.01 when compared with the results of control group; #P < 0.05 when compared with the results of HG group; ##P < 0.01 when compared with the results of HG group.

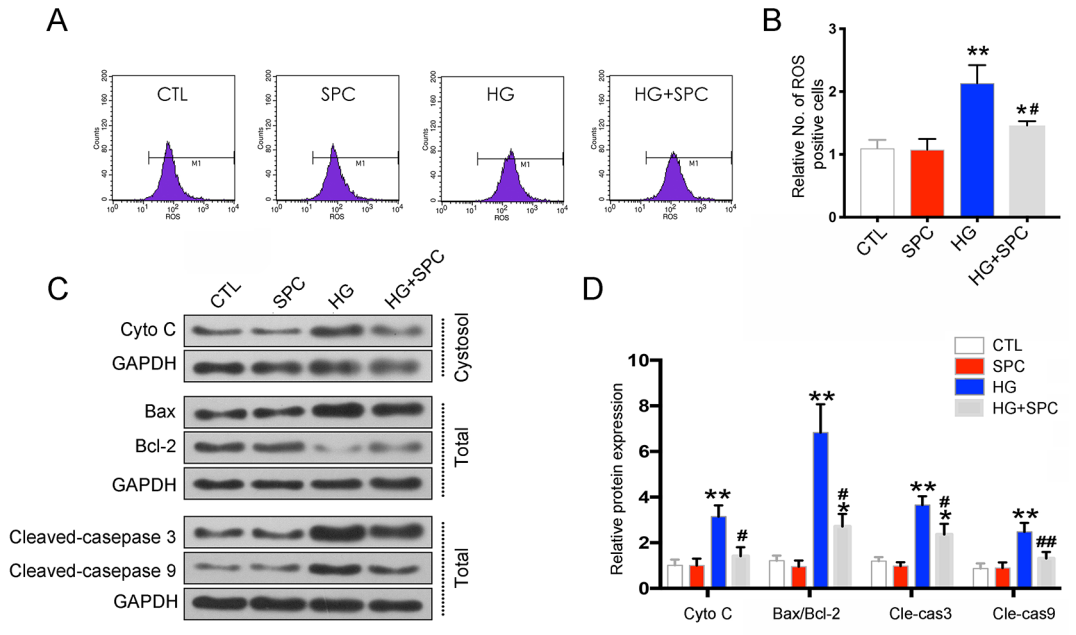

FIGURE 2 | SPC attenuated HG-stimulated mitochondrial dysfunction in H9c2 cells. **(A** and **B)** Effects of SPC (1 mM) treatment on ROS production using flow cytometry assay. **(C)** Western blot analysis showed that HG induction for 12 h significantly increased cytochrome c release and caspase-3/9 activation, which was effectively inhibited by SPC. Moreover, HG stimulation upregulated the expression of pro-apoptotic Bax and downregulated the expression of anti-apoptotic Bcl-2, whereas these changes were attenuated by application with expression. **(D)** Quantification of the western blot analysis. CTL, control group; SPC, Sophocarpine; HG, high glucose, ROS, reactive oxygen species. *P < 0.05 when compared with the results of control group; **P < 0.01 when compared with the results of control group; #P < 0.05 when compared with the results of HG group; ##P < 0.01 when compared with the results of HG group.

SPC Treatment Attenuated Diabetes-Induced Cardiac Dysfunction

Using a type 1 diabetic mouse model, we assessed the *in vivo* effect of SPC on DCM. As is shown in **Figures 4A–E**, the results of echocardiography demonstrated that mice in the DM group exhibited significant cardiac dysfunction compared to mice in the control group, with significantly decreased E/A velocity ratio, left ventricular ejection fraction (LVEF), fractional shortening (FS), and increased value of left ventricular end-diastolic diameter (LVEDD) and left ventricular end-systolic diameter (LVESD). After SPC treatment, all these parameters improved when compared to DM group. Moreover, the increased blood glucose level (**Figure 4F**) and serum inflammatory factor [tumor necrosis factor-α (TNF-α), interleukin-1β (IL-1β), IL-6] levels (**Figures 4G–I**) induced by DM were also effectively inhibited after SPC treatment. Taken together, these evidences suggested that SPC administration attenuated the diabetes-induced cardiac dysfunction.

SPC Relieved Diabetes-Induced Cardiac Remodeling

We then applied histological analysis to find out the *in vivo* role of SPC on fibrosis and histopathology of diabetic hearts. As shown in **Figures 4J–K**, hematoxylin and eosin (H&E) staining and Masson trichrome staining showed obvious structural abnormalities and collagen accumulation in the myocardial tissues from DM group, while SPC treatment remarkably reduced the collagen deposition and fibrosis. Consistent with the evidence from H&E staining and Masson trichrome staining, the results of α-SMA IHC staining showed a significant increase of α-SMA protein expression in the DM group, which again indicated obvious fibrosis of myocardial tissues. As expected, the protein expression level of α-SMA was decreased after SPC treatment (**Figure 4L**). In addition, the expression of pro-fibrotic biomarker TGF-β was also decreased after the treatment of SPC (**Figure 4M** and **Figures 5B**, **C**). As is shown in **Figure 5D**, heart tissue samples from mice in diabetes mellitus group have significantly higher Collagen I and Collagen III protein expression than samples from the control group, which was remarkably inhibited by SPC treatment. Taken together, these results indicated that SPC treatment reduces collagen deposition and fibrosis, eventually contributing to relieve diabetes-induced cardiac remodeling.

SPC Mitigated Diabetes-Induced Cardiac Inflammation and Myocardium Apoptosis

We next examined the role of SPC in alleviating inflammation and myocardium apoptosis in diabetic hearts. Consistent with the histomorphometric observation, the results of IHC staining and western blot analysis revealed a marked elevation in the protein expression of pro-inflammatory biomarker TNF-α in diabetic myocardial tissues compared with the control group. After SPC treatment, the protein expression of TNF-α was significantly reduced (**Figure 4I** and **Figures 5B**, **C**). We finally applied

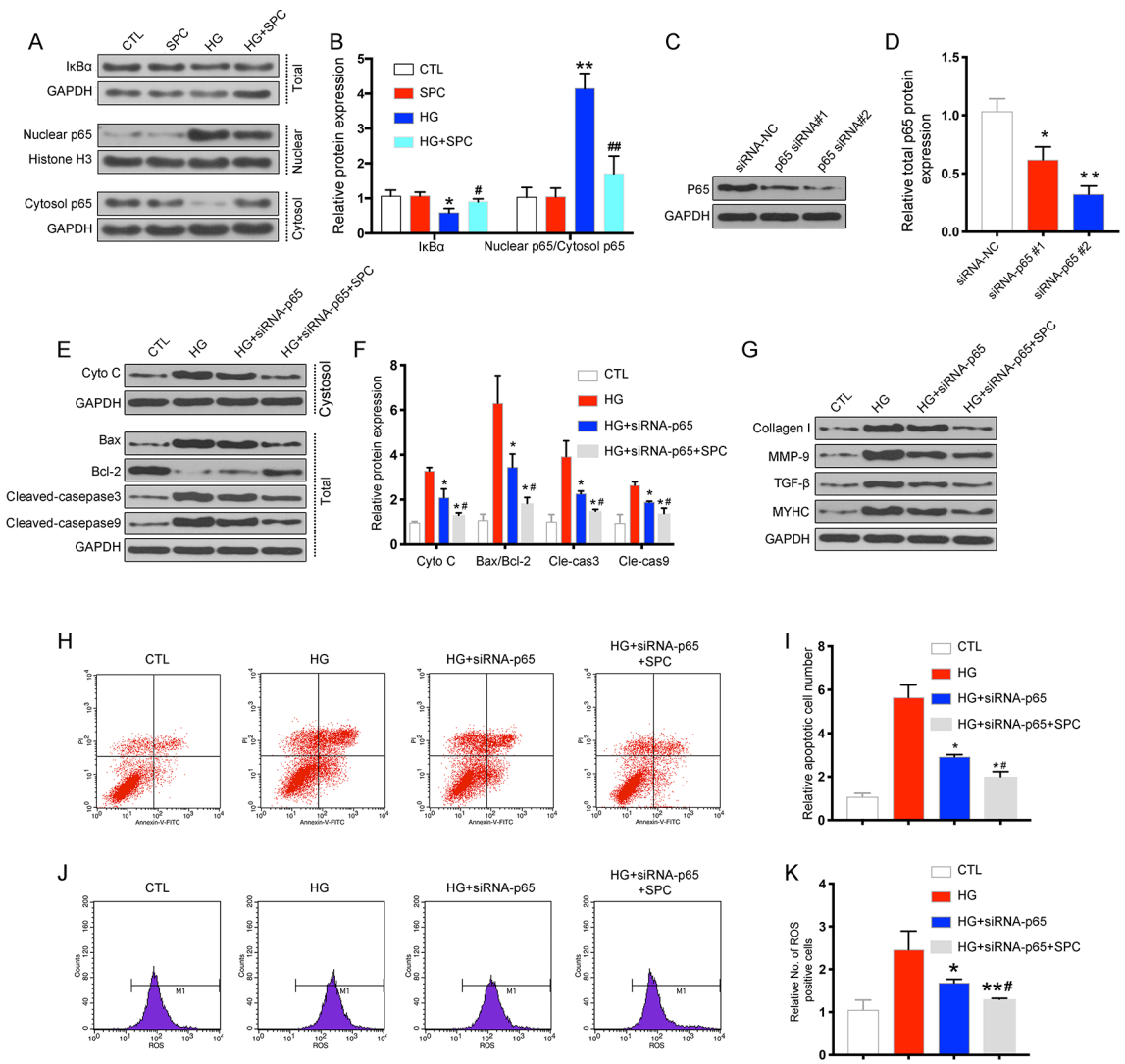

FIGURE 3 | SPC suppressed the activation of the NF-κB signaling in HG-stimulated inflammatory responses in H9c2 cells. **(A)** The results of western blot analysis showed that incubation with HG for 12 h remarkblely induced IκBα degradation, and this alteration was significantly reversed by SPC treatment. HG stimulation markedly increased the nuclear translocation of NF-κB/p65, which was abolished by SPC treatment (1 mM). **(B)** Quantification of the western blot analysis. *P < 0.05 when compared with the results of control group; **P < 0.01 when compared with the results of control group; #P < 0.05 when compared with the results of HG group; ##P < 0.01 when compared with the results of HG group. **(C** and **D)** The WB analysis showed successful knockdown of p65 using siRNAs. **(E–G)** WB analysis showed p65 knockdown using siRNA partially mimicked the anti-apoptotic and anti-inflammatory effects of SPC treatment. **(H** and **I)** The results of flow cytometry apoptosis assay. **(J** and **K)** The results of flow cytometry ROS production assay. *P < 0.05 when compared with the results of the HG group; **P < 0.01 when compared with the results of the HG group; #P < 0.05 when compared with the results of the HG + siRNA-P65 group; ##P < 0.01 when compared with the results of the HG+siRNA-P65 group. CTL, control group; SPC, Sophocarpine; HG, high glucose; ROS, reactive oxygen species.

TUNEL staining to investigate the anti-apoptotic effect of SPC in diabetic myocardial tissues. We observed significantly increased cell apoptosis (TUNEL-positive cells) in diabetic heart samples, which was remarkably mitigated by SPC treatment (**Figure 5A**).

DISCUSSION

The results of this study demonstrated that SPC protected H9c2s cell from hyperglycemia-induced injury. SPC treatment also slowed the development and progression of DCM in streptozotocin (STZ)-induced diabetic mice. SPC was able to protect against DCM by improving mitochondrial function, suppressing inflammation, and inhibiting cardiac apoptosis. Moreover, SPC treatment inhibited the activation of NF-κB signaling in high-glucose-stimulated inflammatory responses, which suggests that SPC suppressed the inflammatory response and prevented cardiac dysfunction in diabetic mice by inhibiting the NF-κB signaling pathway (**Figure 5E**).

Several physiological factors are reportedly associated with the development of DCM, including cardiac inflammation, oxidative stress, and cardiac cell apoptosis. Among these, chronic and

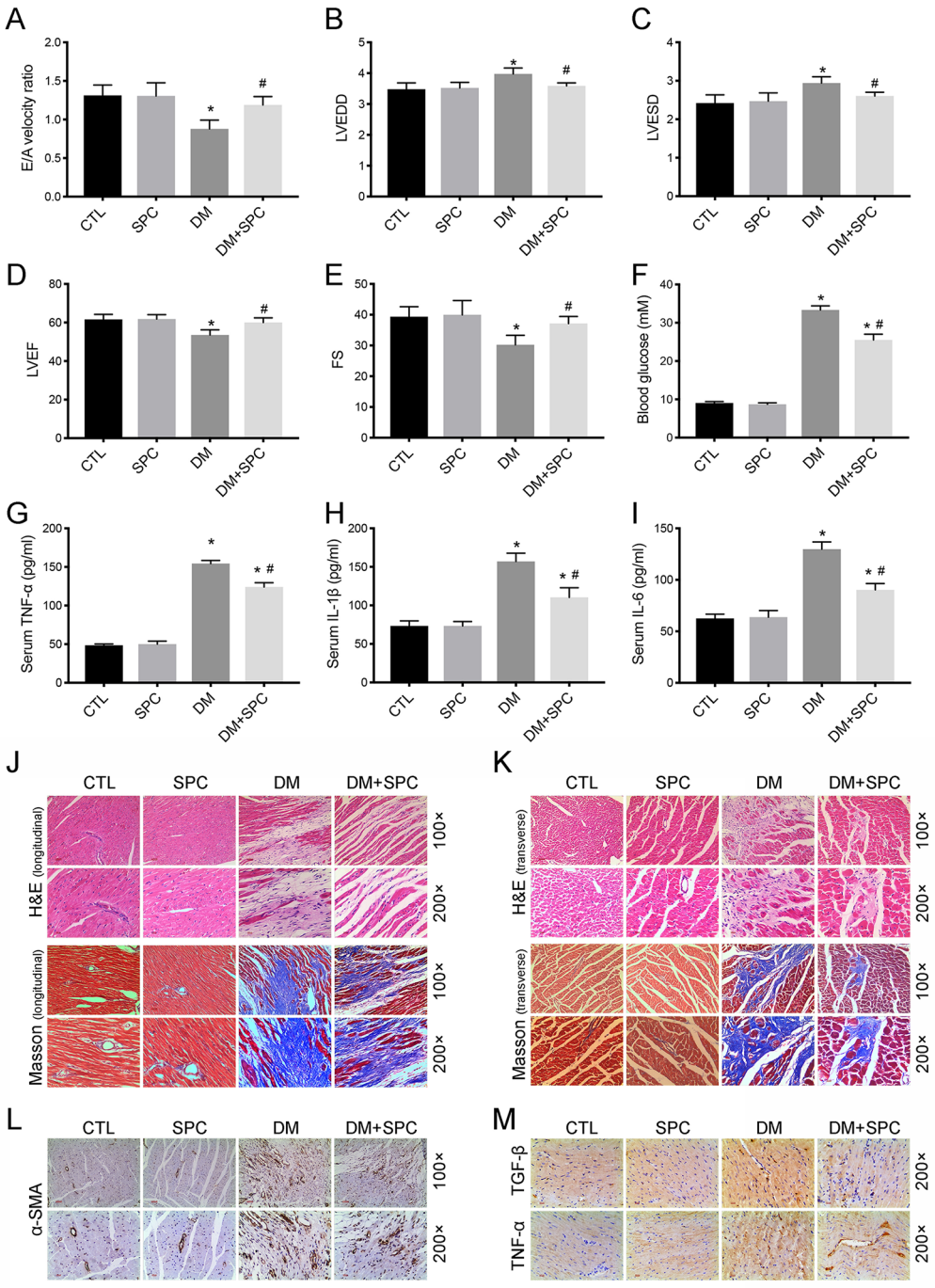

FIGURE 4 | SPC treatment attenuated diabetes-induced cardiac dysfunction and cardiac remodeling. **(A–E)** The results of echocardiography demonstrated that mice in the DM group exhibited significant cardiac dysfunction compared to mice in the control group, with significantly decreased E/A velocity ratio, LVEF, FS, and increased value of LVEDD and LVEDD. After SPC treatment, all these parameters improved notably when compared to DM group. **(F)** The increased blood glucose level induced by DM was effectively inhibited after SPC treatment. **(G–I)** Serum inflammatory factor (TNF-α, IL-1β, IL-6) levels were also effectively inhibited after SPC treatment. **(J** and **K)** H&E staining and Masson trichrome staining (longitudinal view on the left and transverse view on the right) showed obvious structural abnormalities and collagen accumulation in the myocardial tissues from DM group, while SPC treatment remarkably reduced the collagen deposition and fibrosis. **(L)** The results of α-SMA IHC staining showed a significant increase of α-SMA protein expression in the DM group, and the protein expression level of α-SMA was decreased after SPC treatment. **(M)** The expression of TGF-β and TNF-α was also decreased after the treatment of SPC. E/A velocity ratio: the ratio of early to late mitral valve flow velocity E/A velocity ratio; LVEF, left ventricular ejection fraction; FS, percentage of fractional shortening; LVESD, left ventricular end-systolic diameter; LVEDD, left ventricular end-diastolic diameter; IHC staining, immunohistochemical staining; CTL, control group; SPC, Sophocarpine; DM, diabetes mellitus group. *$P < 0.05$ when compared with the results of control group; #$P < 0.05$ when compared with the results of DM group.

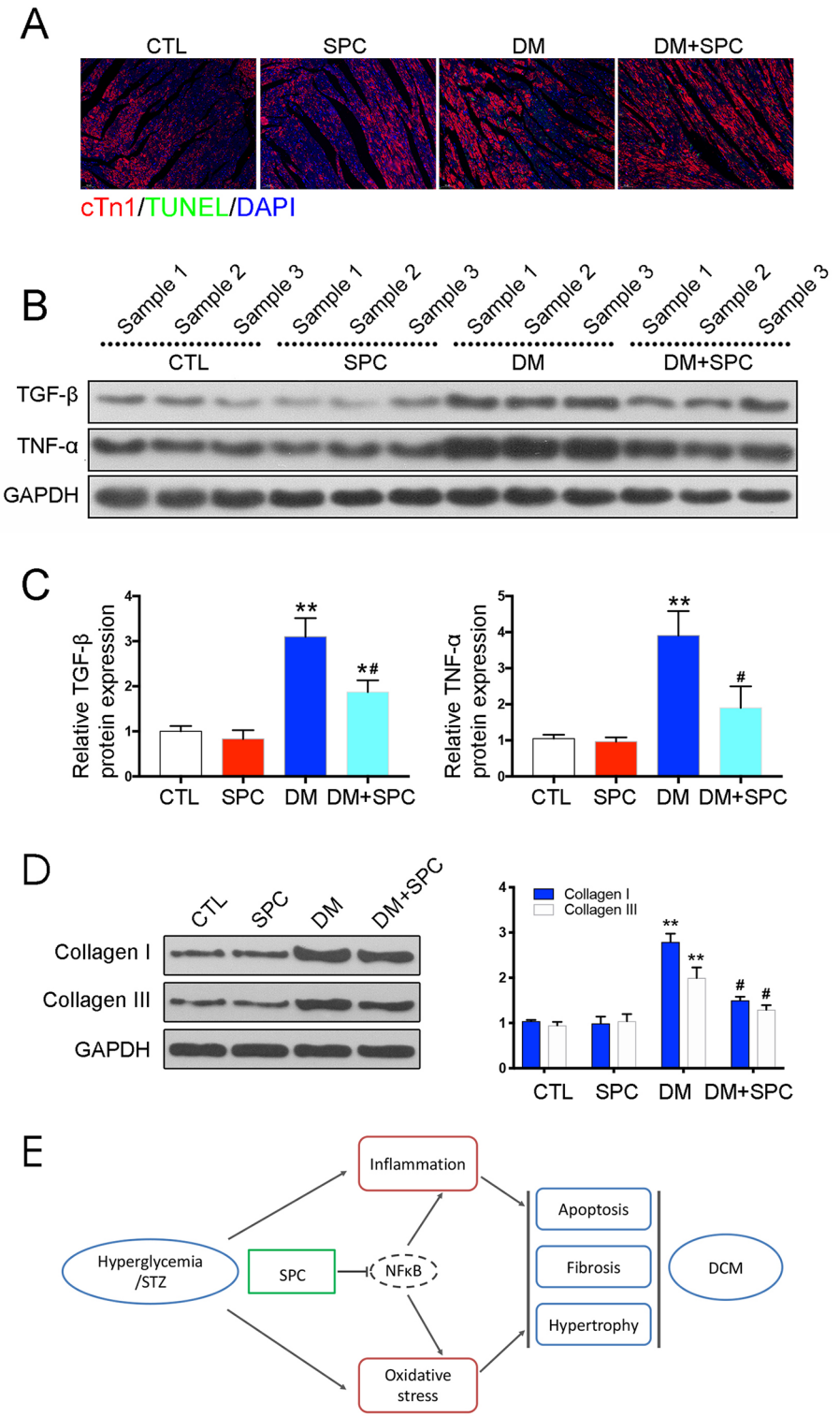

FIGURE 5 | SPC mitigated diabetes-induced cardiac inflammation and myocardium apoptosis. **(A)** TUNEL staining showed significantly increased cell apoptosis (TUNEL-positive cells) in diabetic hearts, which was remarkably mitigated by SPC treatment. Figures are magnified as 100×. **(B)** The results of western blot analysis revealed a marked elevation in the protein expression of TNF-α in diabetic myocardial tissues compared with the control group. After SPC treatment, the protein expression of TNF-α was significantly reduced. **(C)** Quantification of the western blot analysis. **(D)** Heart tissue samples from mice in diabetes mellitus group have significantly higher Collagen I and Collagen III protein expression than samples from the control group, which was remarkably inhibited by SPC treatment. **(E)** A diagram recapitulating the main findings of this study. CTL, control group; SPC, Sophocarpine; DM, diabetes mellitus group. *P < 0.05 when compared with the results of control group; **P < 0.01 when compared with the results of control group; #P < 0.05 when compared with the results of DM group.

sustained inflammation is the major reason that hyperglycemia leads to changes in the structure and function of cardiac muscle (Lee et al., 2018; Yan et al., 2018; Ye et al., 2018; Ying et al., 2018; Althunibat et al., 2019). Hyperglycemia increases the expression of pro-inflammatory cytokines such as IL-6, IL-1β, TNF-α, and TGF-β. Indeed, anti-inflammatory therapeutic strategies have generally been beneficial in treating DCM (Ye et al., 2018; Zheng et al., 2018; Zhang et al., 2018a; Knapp et al., 2019). Zhang et al. reported that H3 relaxin protects against DCM by suppressing inflammation (Zhang et al., 2017). Feng et al. studied DCM in endothelial-specific microRNA (miR)-146a-overexpressing transgenic mice and found that miR-146a inhibits DCM by suppressing inflammatory changes (Feng et al., 2017). Similarly, deletion of the kinin receptor B1 gene reportedly slowed the development of DCM by suppressing cardiac inflammation (Westermann et al., 2009). Treatment with drugs that are based on natural products has some advantages over using artificial chemical compounds and genetic approaches. The clinical potential of drugs such as SPC may be enhanced if the cost is low, side effects are few, and availability is high.

The NF-κB signaling pathway plays a critical role in the pathology of DCM (Bombicz et al., 2019; Kang et al., 2019; Knapp et al., 2019). Hyperglycemia triggers IκBα degradation, allowing cytoplasmic NF-κB/p65 to be translocated into the nucleus. This promotes physiological processes associated with DCM including cell hypertrophy, apoptosis, and fibrosis. Recent studies have shown that inactivating the NF-κB pathway is an effective treatment for DCM (Li et al., 2011; Guo et al., 2018; Tang et al., 2018). In our study, hyperglycemia increased NF-κB activity and promoted cardiac apoptosis and fibrosis. These results are consistent with those from previous studies using H9c2 myocardial cells and STZ-induced diabetes mellitus models (Liu et al., 2017a; You et al., 2018). We also showed that SPC inhibited IκBα degradation and p65 translocation. In addition, our *in vivo* experiments demonstrated that myocardial apoptosis and fibrosis were significantly attenuated. Together, these data suggest that SPC protects against DCM at least partly by suppressing NF-κB-mediated inflammation.

Interestingly, other studies have shown that SPC has anti-inflammatory activity in various cell types and disease models. SPC decreased the expression of pro-inflammatory cytokines in both *in vitro* and *in vivo* experiments on chondrocytes, providing effective protection against osteoarthritis (Wu et al., 2019a). In mice hepatocytes, SPC inhibited lipopolysaccharide-induced septic liver injury by downregulating the NF-κB signaling pathway and suppressing inflammation (Jiang et al., 2018). SPC also inhibited the production of TNF-α and IL-6 in murine primary macrophages and prevented cachexia-related symptoms induced by colon 26 adenocarcinoma in mice (Zhang et al., 2008). In addition, SPC can stabilize prostheses by binding to IκB kinases, suppressing NF-κB/p65 activation and thus inhibiting osteoclast formation and implant loosening (Zhou et al., 2018). Our study is consistent with previous research and describes a novel method for treating DCM by using SPC. Our results may provide important information to support the clinical application of SPC.

This study had some limitations. First, the pathological processes associated with DCM are complex, and although we investigated the effects of SPC on inflammation, apoptosis, and myocardial fibrosis, we did not investigate other processes such as autophagy. Second, we did not demonstrate that SPC inhibits NF-κB signaling *in vivo*. Third, we did not apply extra osmotic cells group in which mannitol was added to keep the same osmolarity as that under conditions of HG. Thus, further studies will be needed to confirm the results of this study.

CONCLUSIONS

Our study suggests that SPC has therapeutic potential and protects H9c2 cells from hyperglycemia-induced injury *in vitro*. Our mouse model experiments also show that SPC can be used to treat DCM *in vivo*. SPC may be effective against DCM because it can suppress inflammation and inhibit the NF-κB signaling pathway. These findings suggest that SPC may be effective in preventing DCM.

MATERIALS AND METHODS

Reagents

SPC was purchased from Selleck Chemicals [Houston, USA; purity (%) = 99.80%]. It was dissolved in dimethyl sulfoxide (DMSO) and stored in the dark. The chemical structure of SPC is shown in **Figure 1A**.

Cell Culture

The embryonic rat heart-derived cell line, H9c2, was obtained from ATCC (American Type Culture Collection, Manassas, VA, USA) and cultured in DMEM medium supplemented with 10% Fetal bovine serum (FBS), 100 mg/ml streptomycin, and 100 U/ml penicillin (Gibco, Waltham, MA, USA). Cells in the SPC treated group were pre-treated with SPC for 1 h and then exposed to high D-glucose concentration (33 mM, HG) or normal D-glucose (5.5 mM) DMEM medium, while cells in the control (CTL) group received same volume DMSO. The final concentration of DMSO in the medium of each group was less than 0.1% (v:v).

Quantitative Real-Time PCR

Total RNA of H9c2 cells was extracted using TRIZOL (Invitrogen, Carlsbad, CA), following the procedure of standard protocol. Reverse transcription was performed using a Double-Strand cDNA Synthesis Kit (Takara, Dalian, China). qPCR was performed using a SYBR Green Master Mix kit (Takara). Primers were synthesized and obtained from Sangon Biotech (Shanghai, China). The details of primers used in this study were listed in **Table S1**.

Cell Viability

H9c2 cells were seeded into 96-well plates at a density of 2×10^4 cells/well for 24 h. After that, cells were treated with/without various

doses of SPC (0.01–10 mM) for 48 or 96 h. After treatment, CCK-8 assay (Dojindo, Kumamoto, Japan) was carried out by adding 15 μl of CCK-8 buffer into each well. The plates were incubated 37°C for additional 4 h. The absorbance was detected at 450 nm on a microplate reader (Bio-Tek Instr., Winooski, VT, USA).

Flow Cytometry Assay

Flow cytometry assay was performed to determine the apoptosis of H9c2 cells using an FITC Annexin V Apoptosis Detection Kit (BD Biosciences, USA). According to the manufacturer's protocol, H9c2 cells were harvested and washed three times with phosphate buffer saline (PBS). After being incubated with FITC Annexin-V and propidium iodide (PI), cells were analyzed with a flow cytometry system (Becton Dickinson). In addition, ROS production was also measured by flow cytometry system (Becton Dickinson) using a DCFH-DA ROS assay kit (Sbjbio® life science, Nanjing, China), according to the manufacturer's instructions.

Western Blot Assay

Cells or tissue samples were lysed with protein extraction reagent RIPA (Beyotime, Haimen, China), and protein amounts were assessed using a BCA-kit (Thermo fisher Scientific, MA, USA). In addition, a nuclear and cytoplasmic protein extraction kit (P00028; Beyotime) was applied to obtain nuclear and cytoplasmic protein samples. According to the manufacturer's instructions, protein samples were then separated by SDS-PAGE gel and then transferred to polyvinylidene fluoride (PVDF) membranes (Millipore, MA, USA). After being blocked with 5% milk in TBST for 1.5 h at room temperature, the membranes were incubated overnight at 4°C with the following antibodies: COL-1 [1:1000, Cell Signaling Technology (CST), Danvers, MA, USA], MMP-9 (1:1000, Abcam, Shanghai, China), TGF-β (1:1000, CST), MyHC (1:1000, Abcam), B-cell lymphoma-2 (Bcl-2, 1:1000, Abcam), BCL2-associated X (Bax, 1:1000, CST), NF-κB/p65 (1:1000, CST), IkBα (1:1000, Abcam), cytochrome c (Cyto-C, 1:1000, Abcam), cleaved-caspase-3 (Cle-cas3), cleaved-caspase-9 (Cle-cas9), tumor necrosis factor-α (TNF-α, 1:1000, Abcam), glyceraldehyde-3-phosphate dehydrogenase (GAPDH, 1:1000, Abcam), and histone H3 (1:1000, CST) antibodies. Specific bands were detected by using an enhanced chemiluminescence kit (Bio-Rad, CA, USA) and were quantified by densitometry (Quantity One software, Bio-Rad).

siRNA Construction and Infection

To explore the mechanism by which SPC inhibits NF-κB signaling pathway, two siRNAs against p65 and negative control (NC) were obtained from GenePharma (Shanghai, China). H9c2 cells were incubated with p65 siRNAs or the negative control siRNAs using standard methods. WB analysis was used to confirm the successful knockdown of p65.

Isolation and Culture of NMCMs

NMCMs were prepared from newborn C57BL/6J mice (1–2 days old), as previously described (Brand et al., 2010; Xu et al., 2019). In brief, hearts of mice were cut into small pieces and digested with DMEM (Gibco) containing 0.03% trypsin and 0.03% collagenase II (Sigma). NMCMs were then isolated and cultured in DMEM with 20% FBS (Gibco) and 1% penicillin/streptomycin. After purification by 1.5 h differential preplating to allow cardiac fibroblast adherence, NMCMs were seeded onto dishes for 48 h and maintained in DMEM with 10% FBS and BrdU (0.1 mM, Sigma). After that, NMCMs were treated with HG and SPC, following the methods introduced above.

Animal Experiments

The study protocols for all animal studies were approved by the Institutional Animal Care and Use Committee of the second affiliated hospital of Nanchang University and complied with the NIH guidelines for the care and use of laboratory animals. Male C57BL/6 mice (6–8 weeks old, weighing 18–22 g) used in this study were purchased from Animal Center of Nanchang University. In total, 40 mice were randomly divided into four groups (n = 10 each group): control group (CTL), SPC treatment group (SPC), diabetes mellitus group (DM), and DM plus SPC group (DM+SPC). Firstly, the DM mice were induced by daily intraperitoneal (i.p.) injection of 50 mg/kg STZ (dissolved in 100 mM citrate buffer, pH 4.5) for 5 consecutive days (Liu et al., 2017a; Tang et al., 2018), while mice in the CTL group and SPC group received same volume of sodium citrate buffer. One week later, mice with fasting blood glucose levels ≥250 mg/dl were defined as successful establishment of diabetes mellitus. Then, mice in the SPC and DM+SPC group received daily i.p. injection of SPC (20 mg/kg) (Li et al., 2011; Zhou et al., 2018), while mice in the CTL group and DM group received same volume of PBS. Sixteen weeks after the administration, blood glucose level was measured by tail vein blood using an automated analyzer (Beckman, CA, USA). After that, mice were euthanized under anesthesia, and heart tissues were collected and kept in liquid nitrogen or 4% paraformaldehyde for further analysis. Blood samples were collected from mice eye socket vEin. Serum was obtained by centrifugalization and kept at −80°C. Then, serum inflammatory factor (TNF-α, IL-1β, IL-6) levels were determined using enzyme-linked immunosorbent assay (ELISA) kits (BD Biosciences, CA, USA), according to the manufacturer's protocol.

Cardiac Function Assessment

Cardiac function was determined by M-mode echocardiography in anaesthetized mice 1 day before termination. An echocardiography system together with a 15-MHz linear transducer (VisualSonics Vevo 2100, Toronto, Canada) was applied. LVEF, percentage of FS [FS (%)], LVESD, LVEDD, and the ratio of early to late mitral valve flow velocity E/A velocity ratio (E/A velocity ratio) were measured using the machine by the same personnel.

TUNEL Assay

The TUNEL apoptosis detection kit (R&D Systems, MN, USA) assay was also applied to detect cell apoptosis. H9c2

cells were washed three times with PBS and fixed with 4% paraformaldehyde, permeabilized with 0.1% TritonX-100, and then stained with TUNEL reagent. Following washing with PBS, cells were counterstained with DAPI (Sigma-Aldrich, USA) at room temperature for 5 min. For tissues, the sections of mice heart samples were treated for 60 min with TUNEL reagent (In Situ Cell Death Detection Kit; Roche Diagnostics) and DAPI for 5 min according to the manufacturer's instructions. In addition, staining using a monoclonal antibody against Troponin I (cTnI, Santa Cruz) was also performed to identify the myocardium. Images were finally captured under a fluorescence microscope and quantified by Image J software. All morphometric measurements were conducted on five randomly selected fields for each sample.

Histological Analysis

After being fixed in 4% paraformaldehyde for 48 h, mice heart samples were paraffin-embedded and sectioned at 5 μm thick for H&E, Masson trichrome staining, TUNEL staining, and immunohistochemical (IHC) staining as standard protocols. For IHC staining of α-SMA, TNF-α, and TGF-β, serial tissue sections were deparaffinized, rehydrated, and treated with 0.3% H_2O_2 for 30 min. After being blocked with 3% bovine serum albumin (BSA) in PBS for 30 min, the slides were then incubated with primary antibody at 4°C overnight (α-SMA, 1:200, CST; TNF-α, 1:100, Abcam; TGF-β, 1:250, Abcam). After that, a peroxidase-conjugated secondary antibody (Beyotime, China, 1:100) was applied for 1 h at room temperature. Finally, diaminobenzidine (DAB; Sigma-Aldrich, USA) was used to visualize the peroxidase binding sites and hematoxylin was used to visualize nuclears. Image-Pro Plus 6.0 (IPP 6.0) software was used to analyze the density of positive staining.

Statistical Analysis

All data from at least three independent experiments were expressed as mean ± SDs. All statistical analyses were performed with SPSS 14.0 software (SPSS, Chicago, IL, USA). Statistical comparisons among different groups were evaluated using one-way ANOVA followed by multiple comparisons test with Bonferroni correction. P value <0.05 was considered statistically significant.

DATA AVAILABILITY STATEMENT

The datasets generated for this study are available on request to the corresponding author.

ETHICS STATEMENT

The animal study was reviewed and approved by The Institutional Animal Care and Use Committee of the second affiliated hospital of Nanchang University.

AUTHOR CONTRIBUTIONS

Conception and design of the research: YS and RY. Acquisition of data: HL, LH, WW and XX. Analysis and interpretation of data: FZ and LWa. Statistical analysis: LWu. Obtaining funding: YS, FZ, and RY. Drafting the manuscript: FZ and LWa. Revision of manuscript for important intellectual content: YS and RY.

FUNDING

This study was funded by National Natural Science Foundation of China (No. 81860151, 81560145, 81400815, and 81660063), National Key R&D Program of China (No. 2016YFC0900400), and Natural Science Foundation of Jiangxi province (20171BAB205041).

SUPPLEMENTARY MATERIAL

The Supplementary Material for this article can be found online at: https://www.frontiersin.org/articles/10.3389/fphar.2019.01219/full#supplementary-material

REFERENCES

Althunibat, O. Y., Al Hroob, A. M., Abukhalil, M. H., Germoush, M. O., Bin-Jumah, M., and Mahmoud, A. M. (2019). Fisetin ameliorates oxidative stress, inflammation and apoptosis in diabetic cardiomyopathy. *Life Sci.* 221, 83–92. doi: 10.1016/j.lfs.2019.02.017

Bombicz, M., Priksz, D., Gesztelyi, R., Kiss, R., Hollos, N., Varga, B., et al. (2019). The drug candidate BGP-15 delays the onset of diastolic dysfunction in the Goto-Kakizaki rat model of diabetic cardiomyopathy. *Molecules* 24 (3), pii: E586. doi: 10.3390/molecules24030586

Brand, N. J., Lara-Pezzi, E., Rosenthal, N., and Barton, P. J. (2010). Analysis of cardiac myocyte biology in transgenic mice: a protocol for preparation of neonatal mouse cardiac myocyte cultures. *Methods Mol. Biol.* 633, 113–124. doi: 10.1007/978-1-59745-019-5_9

Feng, B., Chen, S., Gordon, A. D., and Chakrabarti, S. (2017). miR-146a mediates inflammatory changes and fibrosis in the heart in diabetes. *J. Mol. Cell Cardiol.* 105, 70–76. doi: 10.1016/j.yjmcc.2017.03.002

Guo, Y., Zhuang, X., Huang, Z., Zou, J., Yang, D., Hu, X., et al. (2018). Klotho protects the heart from hyperglycemia-induced injury by inactivating ROS and NF-kappaB-mediated inflammation both *in vitro* and *in vivo*. *Biochim. Biophys. Acta Mol. Basis Dis.* 1864 (1), 238–251. doi: 10.1016/j.bbadis.2017.09.029

He, S., Kahles, F., Rattik, S., Nairz, M., McAlpine, C. S., Anzai, A., et al. (2019). Gut intraepithelial T cells calibrate metabolism and accelerate cardiovascular disease. *Nature* 566 (7742), 115–119. doi: 10.1038/s41586-018-0849-9

Huang, Y. Q., Li, P. Y., Wang, J. B., Zhou, H. Q., Yang, Z. R., Yang, R. C., et al. (2016). Inhibition of sophocarpine on poly I: C/D-GalN-induced immunological liver injury in mice. *Front. Pharmacol.* 7, 256. doi: 10.3389/fphar.2016.00256

Jiang, Z., Meng, Y., Bo, L., Wang, C., Bian, J., and Deng, X. (2018). Sophocarpine attenuates LPS-induced liver injury and improves survival of mice through suppressing oxidative stress, inflammation, and apoptosis. *Mediators Inflamm.* 2018, 5871431. doi: 10.1155/2018/5871431

Kang, Y., Wang, S., Huang, J., Cai, L., and Keller, B. B. (2019). Right ventricular dysfunction and remodeling in diabetic cardiomyopathy. *Am. J. Physiol. Heart Circ. Physiol.* 316 (1), H113–H122. doi: 10.1152/ajpheart.00440.2018

Knapp, M., Tu, X., and Wu, R. (2019). Vascular endothelial dysfunction, a major mediator in diabetic cardiomyopathy. *Acta Pharmacol. Sin.* 40 (1), 1–8. doi: 10.1038/s41401-018-0042-6

Lee, M. M. Y., McMurray, J. J. V., Lorenzo-Almoros, A., Kristensen, S. L., Sattar, N., Jhund, P. S., et al. (2018). Diabetic cardiomyopathy. *Heart* 0, 1–9. doi: 10.1136/heartjnl-2016-310342

Li, C., Gao, Y., Tian, J., Shen, J., Xing, Y., and Liu, Z. (2011). Sophocarpine administration preserves myocardial function from ischemia-reperfusion in rats *via* NF-kappaB inactivation. *J. Ethnopharmacol.* 135 (3), 620–625. doi: 10.1016/j.jep.2011.03.052

Li, J., Li, L., Chu, H., Sun, X., and Ge, Z. (2014). Oral sophocarpine protects rat heart against pressure overload-induced cardiac fibrosis. *Pharm. Biol.* 52 (8), 1045–1051. doi: 10.3109/13880209.2013.877038

Li, X., Wang, M., Hong, H., Luo, C., Liu, Z., and Yang, R. (2018). Sophocarpine attenuates murine lupus nephritis *via* inhibiting NLRP3 inflammasome and NF-kappaB activation. *Immunol. Res.* 66 (4), 521–527. doi: 10.1007/s12026-018-9012-9

Liu, H. J., Fan, Y. L., Liao, H. H., Liu, Y., Chen, S., Ma, Z. G., et al. (2017a). Apigenin alleviates STZ-induced diabetic cardiomyopathy. *Mol. Cell. Biochem.* 428 (1-2), 9–21. doi: 10.1007/s11010-016-2913-9

Liu, W., Zhang, B., Chen, G., Wu, W., Zhou, L., Shi, Y., et al. (2017b). Targeting miR-21 with sophocarpine inhibits tumor progression and reverses epithelial-mesenchymal transition in head and neck cancer. *Mol. Ther.* 25 (9), 2129–2139. doi: 10.1016/j.ymthe.2017.05.008

Sang, X. X., Wang, R. L., Zhang, C. E., Liu, S. J., Shen, H. H., Guo, Y. M., et al. (2017). Sophocarpine protects mice from ConA-induced hepatitis *via* inhibition of the IFN-Gamma/STAT1 pathway. *Front. Pharmacol.* 8, 140. doi: 10.3389/fphar.2017.00140

Sun, X., Zhao, D., Lu, F., Peng, S., Yu, M., Liu, N., et al. (2019). Hydrogen sulfide regulates muscle RING finger-1 protein S-sulfhydration at Cys44 to prevent cardiac structural damage in diabetic cardiomyopathy. *Br. J. Pharmacol.* doi: 10.1111/bph.14601

Tall, A. R., and Jelic, S. (2019). How broken sleep promotes cardiovascular disease. *Nature* 566 (7744), 329–330. doi: 10.1038/d41586-019-00393-6

Tall, A. R., and Levine, R. L. (2017). Cardiovascular disease: commonality with cancer. *Nature* 543 (7643), 45–47. doi: 10.1038/nature21505

Tang, S. G., Liu, X. Y., Ye, J. M., Hu, T. T., Yang, Y. Y., Han, T., et al. (2018). Isosteviol ameliorates diabetic cardiomyopathy in rats by inhibiting ERK and NF-kappaB signaling pathways. *J. Endocrinol.* 238 (1), 47–60. doi: 10.1530/JOE-17-0681

Westermann, D., Walther, T., Savvatis, K., Escher, F., Sobirey, M., Riad, A., et al. (2009). Gene deletion of the kinin receptor B1 attenuates cardiac inflammation and fibrosis during the development of experimental diabetic cardiomyopathy. *Diabetes* 58 (6), 1373–1381. doi: 10.2337/db08-0329

Wu, D., Zhu, X., Kang, X., Huang, H., Yu, J., Pan, J., et al. (2019a). The protective effect of sophocarpine in osteoarthritis: an *in vitro* and *in vivo* study. *Int. Immunopharmacol.* 67, 145–151. doi: 10.1016/j.intimp.2018.11.046

Wu, S., Lu, Q., Ding, Y., Wu, Y., Qiu, Y., Wang, P., et al. (2019b). Hyperglycemia-driven inhibition of AMP-activated protein kinase alpha2 induces diabetic cardiomyopathy by promoting mitochondria-associated endoplasmic reticulum membranes *in vivo*. *Circulation* 139 (16), 1913–1936. doi: 10.1161/CIRCULATIONAHA.118.033552

Xu, L., Su, Y., Zhao, Y., Sheng, X., Tong, R., Ying, X., et al. (2019). Melatonin differentially regulates pathological and physiological cardiac hypertrophy: crucial role of circadian nuclear receptor RORalpha signaling. *J. Pineal. Res.* 67 (2), e12579. doi: 10.1111/jpi.12579

Yan, X. L., Wang, Y. Y., Yu, Z. F., Tian, M. M., and Li, H. (2018). Peroxisome proliferator-activated receptor-gamma activation attenuates diabetic cardiomyopathy *via* regulation of the TGF-beta/ERK pathway and epithelial-to-mesenchymal transition. *Life Sci.* 213, 269–278. doi: 10.1016/j.lfs.2018.09.004

Ye, P., Gu, Y., Zhu, Y. R., Chao, Y. L., Kong, X. Q., Luo, J., et al. (2018). Exogenous hydrogen sulfide attenuates the development of diabetic cardiomyopathy *via the* FoxO1 pathway. *J. Cell Physiol.* 233 (12), 9786–9798. doi: 10.1002/jcp.26946

Ying, Y., Jin, J., Ye, L., Sun, P., Wang, H., and Wang, X. (2018). Phloretin prevents diabetic cardiomyopathy by dissociating Keap1/Nrf2 complex and inhibiting oxidative stress. *Front. Endocrinol. (Lausanne)* 9, 774. doi: 10.3389/fendo.2018.00774

You, S., Qian, J., Sun, C., Zhang, H., Ye, S., Chen, T., et al. (2018). An Aza resveratrol-chalcone derivative 6b protects mice against diabetic cardiomyopathy by alleviating inflammation and oxidative stress. *J. Cell. Mol. Med.* 22 (3), 1931–1943. doi: 10.1111/jcmm.13477

Zhang, B., Zhang, J., Zhang, C., Zhang, X., Ye, J., Kuang, S., et al. (2018a). Notoginsenoside R1 protects against diabetic cardiomyopathy through activating estrogen receptor alpha and its downstream signaling. *Front. Pharmacol.* 9, 1227. doi: 10.3389/fphar.2018.01227

Zhang, J., Li, C., Zhang, J., and Zhang, F. (2018b). In vitro inhibitory effects of sophocarpine on human liver cytochrome P450 enzymes. *Xenobiotica* 49 (10), 1127–1132. doi: 10.1080/00498254.2018.1468047

Zhang, P. P., Wang, P. Q., Qiao, C. P., Zhang, Q., Zhang, J. P., Chen, F., et al. (2016). Differentiation therapy of hepatocellular carcinoma by inhibiting the activity of AKT/GSK-3beta/beta-catenin axis and TGF-beta induced EMT with sophocarpine. *Cancer Lett.* 376 (1), 95–103. doi: 10.1016/j.canlet.2016.01.011

Zhang, S., Ma, J. H., Zhang, P. H., Luo, A. T., Ren, Z. Q., and Kong, L. H. (2012). Sophocarpine attenuates the Na(+)-dependent Ca2(+) overload induced by Anemonia sulcata toxin-increased late sodium current in rabbit ventricular myocytes. *J. Cardiovasc. Pharmacol.* 60 (4), 357–366. doi: 10.1097/FJC.0b013e318262c932

Zhang, X., Pan, L., Yang, K., Fu, Y., Liu, Y., Chi, J., et al. (2017). H3 relaxin protects against myocardial injury in experimental diabetic cardiomyopathy by inhibiting myocardial apoptosis, fibrosis and inflammation. *Cell Physiol. Biochem.* 43 (4), 1311–1324. doi: 10.1159/000481843

Zhang, Y., Wang, S., Li, Y., Xiao, Z., Hu, Z., and Zhang, J. (2008). Sophocarpine and matrine inhibit the production of TNF-alpha and IL-6 in murine macrophages and prevent cachexia-related symptoms induced by colon26 adenocarcinoma in mice. *Int. Immunopharmacol.* 8 (13–14), 1767–1772. doi: 10.1016/j.intimp.2008.08.008

Zheng, D., Zhang, Y., Hu, Y., Guan, J., Xu, L., Xiao, W., et al. (2019). Long noncoding RNA Crnde attenuates cardiac fibrosis *via* Smad3-Crnde negative feedback in diabetic cardiomyopathy. *FEBS J.* 286 (9), 1645–1655. doi: 10.1111/febs.14780

Zheng, J., Cheng, J., Zheng, S., Zhang, L., Guo, X., Zhang, J., et al. (2018). Physical exercise and its protective effects on diabetic cardiomyopathy: what is the evidence? *Front. Endocrinol. (Lausanne)* 9, 729. doi: 10.3389/fendo.2018.00729

Zhou, C. H., Shi, Z. L., Meng, J. H., Hu, B., Zhao, C. C., Yang, Y. T., et al. (2018). Sophocarpine attenuates wear particle-induced implant loosening by inhibiting osteoclastogenesis and bone resorption *via* suppression of the NF-kappaB signalling pathway in a rat model. *Br. J. Pharmacol.* 175 (6), 859–876. doi: 10.1111/bph.14092

Zhu, L., and Zhu, L. (2017). Sophocarpine suppress inflammatory response in human fibroblast-like synoviocytes and in mice with collagen-induced arthritis. *Eur. Cytokine Netw.* 28 (3), 120–126. doi: 10.1684/ecn.2017.0400

Conflict of Interest: The authors declare that the research was conducted in the absence of any commercial or financial relationships that could be construed as a potential conflict of interest.

frontiers in Pharmacology

ORIGINAL RESEARCH
published: 13 November 2019
doi: 10.3389/fphar.2019.01349

Over-Expression of Inhibitor of Differentiation 2 Attenuates Post-Infarct Cardiac Fibrosis Through Inhibition of TGF-β1/Smad3/HIF-1α/IL-11 Signaling Pathway

Lin Yin[1,2,3†], *Ming-xin Liu*[1,2,3†], *Wei Li*[1,2,3], *Feng-yuan Wang*[1,2,3], *Yan-hong Tang*[1,2,3] *and Cong-xin Huang*[1,2,3*]

[1] Department of Cardiology, Renmin Hospital of Wuhan University, Wuhan, China, [2] Cardiovascular Research Institute, Wuhan University, Wuhan, China, [3] Hubei Key Laboratory of Cardiology, Wuhan, China

OPEN ACCESS

Edited by:
Cheng Xue Helena Qin, Baker Heart and Diabetes Institute, Australia

Reviewed by:
Tamer M. A. Mohamed, University of Louisville, United States
Hui-Hua Li, Dalian Medical University, China

***Correspondence:**
Cong-xin Huang
huangcongxin@vip.163.com

†*These authors have contributed equally to this work*

Specialty section:
This article was submitted to Cardiovascular and Smooth Muscle Pharmacology, a section of the journal Frontiers in Pharmacology

Received: *02 May 2019*
Accepted: *24 October 2019*
Published: *13 November 2019*

Citation:
Yin L, Liu M-x, Li W, Wang F-y, Tang Y-h and Huang C-x (2019) Over-Expression of Inhibitor of Differentiation 2 Attenuates Post-Infarct Cardiac Fibrosis Through Inhibition of TGF-β1/Smad3/HIF-1α/IL-11 Signaling Pathway. Front. Pharmacol. 10:1349. doi: 10.3389/fphar.2019.01349

Background: Cardiac fibrosis after myocardial infarction mainly causes cardiac diastolic and systolic dysfunction, which results in fatal arrhythmias or even sudden death. Id2, a transcriptional repressor, has been shown to play an important role in the development of fibrosis in various organs, but its effects on cardiac fibrosis remain unclear. This study aimed to explore the effects of Id2 on cardiac fibrosis after myocardial infarction and its possible mechanisms.

Methods: This study was performed in four experimental groups: control group, treatment group (including TGF-β1, hypoxia or MI), treatment+GFP group and treatment+Id2 group. *In vitro* anoxic and fibrotic models were established by subjecting CFs or NRVMs to a three-gas incubator or TGF-β1, respectively. An animal myocardial infarction model was established by ligating of the left anterior descending coronary artery followed by directly injecting of Id2 adenovirus into the myocardial infarct's marginal zone.

Results: The results showed that Id2 significantly improved cardiac EF and attenuated cardiac hypertrophy. The mRNA and protein levels of α-SMA, Collagen I, Collagen III, MMP2 and TIMP1 were higher in treatment+Id2 group than those in treatment group as well as in treatment+GFP group both *in vivo* and *in vitro*. Immunofluorescence revealed that both α-SMA and vimentin were co-expressed in the treatment group and GFP group, but the co-expression were not detected in the control group and Id2 group. Additionally, our findings illustrated that Id2 had protective effects demonstrated by its ability to inhibit the TGF-β1/Smad3/HIF-1α/IL-11 signaling pathways. Besides, over-expression of Id2 reduced cardiomyocytes apoptosis.

Conclusion: In conclusion, this study demonstrated that over-expression of Id2 preserved cardiac function and ameliorated adverse cardiac remodeling, which might be a promising treatment target for cardiac fibrosis and apoptosis.

Keywords: inhibitor of differentiation 2, myocardial infarction, cardiac fibrosis, cell apoptosis, hypoxia induced factor-1 alpha (HIF-1α), interleukin (IL)-11

INTRODUCTION

Fibrosis is defined as the accumulation of fibrillar extracellular matrix (ECM) components in a tissue or an organ. The development of cardiac fibrosis after myocardial infarction (MI) is a continuous process (Chen et al., 2018). In the initial inflammatory phase, leukocytes are recruited, followed by the release of chemokines and growth factors, such as interleukin (IL)-11 and transforming growth factor-β1(TGF-β1). Myofibroblasts release matrix metalloproteinases (MMPs) which destroy basement membranes. The initial phase is followed by the proliferative phase. In this phase, myofibroblasts generate excessive ECM and endothelial cells form new blood vessels. In the subsequent remodeling phase, activated myofibroblasts (derived from local fibroblasts) stimulate wound contraction. This process confers protection by maintaining the left ventricular structure after infarction. On the other hand, myofibroblasts activation and excessive ECM accumulation ultimately lead to permanent cardiac fibrosis, which is often accompanied with cardiac systolic insufficiency, arrhythmia and adverse cardiovascular events (Jun and Lau, 2018). The two main approaches used to inhibit cardiac fibrosis after MI are as follows: preventing the cause such as alleviating endogenous EMT; slowing the rate of progression i.e., the rate at which cardiac fibroblasts are transformed into myofibroblasts cells and the rate at which ECM is stacked.

Inhibitor of differentiation (Id), known as DNA binding inhibitor, is a regulatory protein which functions as a negative transcription factor. This protein has four subtypes: Id1, Id2, Id3 and Id4 (Jen et al., 1996). Several studies have shown that Id2 plays an important role in cardiac development and fibrosis of various organs. For instance, the Id family is involved in the formation of cardiac mesoderm (Fraidenraich et al., 2004). Id2 knock-out during the embryonic E9.5–E14.5 stage results in severe cardiac developmental defects, including systemic and pulmonary circulation abnormalities, ventricular septal defect and myocardial hypoplasia (Jongbloed et al., 2011; Cunningham et al., 2017). Secondly, Id2 participates in the formation of fibrosis. Myofibroblasts are the major sources of ECM proteins (Afratis et al., 2018). Those cells directly secrete collagen, MMPs and tissue inhibitors of MMPs (TIMPs) to regulate the dynamics of ECM balance (Shih et al., 2018). In the presence of stimulating factors (such as MI), this balance is broken, triggering myocardial fibrosis. Id2 also stimulates the production of MMPs in many cancers and liver fibrosis (Tajima et al., 2007; Hossain et al., 2012; Kamata et al., 2016). Moreover, TGF-β1 plays an important role in the development of cardiac fibrosis (Blyszczuk et al., 2017). It was previously reported that Id2 was a downstream regulator of TGF-β1, and overexpression of Id2 could reduce the effect of TGF-β1, to some extent (Cao et al., 2009).

Based on the above discussion, we hypothesize that Id2 may participate in the development of fibrosis after myocardial infarction. Our study aims to discover the role of Id2 in cardiac fibrosis and reveal it possible mechanisms.

MATERIALS AND METHODS

Animals

Newborn male Sprague–Dawley(SD) rats (n = 40; age, 1–3 days; weight, 40–80 g) were purchased from Disease Control and Prevention of Hubei Provincial Center(Hubei, China) (Animal license number: SCXK (E) 2015-0018). Adult healthy male SD rats (n = 70; weight, 180–200 g) was acquired from the Experimental Animal Center of Wuhan University People's Hospital (Hubei, China). The SD rats were kept in four per cage with standard laboratory chow and given sterilized water. The room environment was controlled under a constant temperature (22 ± 2°C), constant humidity (55 ± 5%), and a 12:12 h light/dark cycle. The present study was approved by the Experimental Animal Committee of Wuhan University (Hubei, China; no. WDRM20180912). All experimental procedures were approved by the Ethics Committee of Animal Research, Wuhan University Health Science Center, and the investigation conformed to the Guide for the Care and Use of Laboratory Animals published by the US National Institutes of Health (NIH Publication, 8th Edition, 2011).

Adenovirus Construction and Purification

The adenoviral vector expressing GV315Ad-MSC-GFP-Id2 was constructed by inserting the human Id2 gene (positive clone sequence: ATGAAAGCCTTCAGTCCCGTGAGGTCCGTTA GGAAAAACAGCCTGTCGGACCACAGCCTGGGCATCTC CCGGAGCAAAACCCCTGTGGACGACCCGATGAGCCTG CTATACAACATGAACGACTGCTACTCCAAGCTCAAGGA GCTGGTGCCCAGCATCCCCCAGAAC AAGAAGGTGAGC A A G A T G G A A A T C C T G C A G C A C G T C A T C G A C TACATCTTGGACCTGCAGATCGCCCTGGACTCGCATC CCACT ATTGTCAGCCTGCATCACCAGAGACCCGGGCAG AACCAGGCG TCCAGGACGCCGCTGACCACCCTCAACA CGGATATCAGCATCCTGTCCTTGCAGGCTTCTGAATTCC CTTCTGAGTTAATGTCA AATGACAGCAAAGCACTGTGT GGCTGA) into GV315Ad-MSC-GFP vector (Shanghai Genechem Co., Ltd., Shanghai, China) using AgeI/NheI (cat. no. CON267) restriction sites, all of which obtained from Shanghai Genechem Co., Ltd. Ad-GFP and Ad-GFP-Id2 were measured as 10^{10} PFU/ml and 8×10^{10} PFU/ml respectively, which were preserved at -80°C.

Cell Culture

Primary rat CFs (cardiac fibroblasts) and primary neonatal rat cardiomyocytes (NRVMs) were isolated from ten 1–3-day-old SD pups as described previously with some modifications (Golden et al., 2012). Briefly, ventricles from rats were minced and digested with 0.125% trypsin (cat. no. C0201, Beyotime Institute of Biotechnology, Shanghai, China) at 37°C for 10 min and then mixed with liquor containing 0.125% trypsin and 0.08% collagenase II (cat. no. C6885; Sigma; Merck KGaA) 6–8 times at 37°C for 5 min each time. The digested tissue pieces were then centrifuged at 1,000 r/min. The CFs were isolated from NRVMs

after culturing for 1.5 h. This was followed by gently sucking out the NRVMs from the culture dish and were seeded in 6-well plates. The cell concentration was adjusted to 5×10^5/ml. During the first 48 h after seeding, 0.1 mmol/l bromodeoxyuridine (cat. no. B-5002, Sigma; Merck KGaA) was added to inhibit the mitosis of fibroblasts. CFs were cultured for 48 h and then were passaged to 3–6 generations for further experiments.

Cell Proliferation Assay and Flow Cytometric Analysis

Cell proliferation was assessed with Cell Counting Kit-8 (CCK-8) (Labgic Technology Co., Ltd., Beijing, China) reagent following the manufacturer's instructions. CFs were passaged in 96-well plates at the density of 8×10^3 cells/well. After culturing for 24 h, cells were treated with serum-free medium for another 24 h and then were placed on three-gas incubators environment (96% nitrogen, 5% carbon dioxide and 1% oxygen). After treatment with hypoxia for 12 h, 20 ul of CCK-8 reagent was added into each well and CFs were incubated at 37°C for another 2 h. The optical density was measured at a wavelength of 450 nm. Serum-free mediums in normal incubators served as the negative control.

The apoptosis of NRVMs after exposed to hypoxia was assessed by staining cells with Annexin V-fluorescein isothiocyanate (APC) Apoptosis Detection Kit (BD Biosciences). The cells were collected and then washed with cold PBS twice. Thereafter, they were resuspended in 100 ul of Annexin V binding buffer and incubated with 5 ul of APC-conjugated Annexin V and 5 ul of propidium iodide for 15 min in the dark. Annexin V binding buffer (200 ul) was then added to each tube. Finally, the cells were examined using a BD FACS-Canto II flow cytometer (BD Biosciences, CA). All experiments were repeated three times, independently.

Experimental Groups and Treatment

CFs were transfected with Ad-GFP or Ad-GFP-Id2 for 48 h, then anoxic and fibrotic models were established using a three-gas incubator for 12 h or Recombinant Human TGF-β1(Rocky Hill, NJ 08553, USA) for 24 h, respectively. The hypoxia model was divided into 4 groups: control group (control), hypoxia group (hypoxia), hypoxia+Ad-GFP group (hypoxia+GFP), hypoxia+Ad-GFP-Id2 group (hypoxia+Id2). Fibrosis model: control group (control), TGF-β1 group (10 ng/ml, 24 h) (TGF-β1), TGF-β1+Ad-GFP group (TGF-β1+GFP), TGF-β1+Ad-GFP-Id2 group (TGF-β1+Id2). Similarly, after adenovirus transfection for 48 h, NRVMs were cultured and treated with three-gas incubators environment (96% nitrogen, 5% carbon dioxide and 1% oxygen) for 6 h. This model was also divided into four groups: control groups (C), hypoxia groups (H), hypoxia+GFP groups (H+G) and hypoxia+Ad-GFP-Id2 (H+I).

In Vivo Gene Transfer and Rat MI Model

Male SD rats weighing 180–200 g were randomly divided into six groups: sham operation group (sham, n = 15), MI group (MI, n = 18), MI+Ad-GFP group (GFP, n = 15), MI+Ad-GFP-Id2 group (Id2, n = 15), Ad-GFP-Id2 group (n = 12), Ad-GFP group (n = 3). The detailed protocol was described previously (Liu et al., 2018). Briefly, rats were anesthetized with sodium pentobarbital 1% (50 mg/kg) by intraperitoneal injection and then intubated and mechanically ventilated during surgery. A left thoracotomy was performed through the fourth intercostal space, and the pericardium was opened. The left anterior descending coronary artery about 3–4 mm from the aortic root between the left atrial appendage and pulmonary artery was permanently ligated with a 6-0 noninvasive suture. Evidences of MI was that S-T segment elevation and the appearance of Q wave was visible on an electrocardiogram or distal cardiomyocytes of the LAD coronary artery ligation became pale. Rats in Ad-GFP-Id2+MI and Ad-GFP+MI groups received intramyocardial injections of 2×10^9 pfu of Ad-GFP-Id2 or Ad-GFP into the left ventricular wall *via* a 50-gauge needle. A total volume of 100 ul was injected into five separate areas in the viable myocardium bordering the infarct zone. The sham groups or the MI groups were injected with 100 ul PBS. Rats in the sham group underwent similar surgical procedures as those in treatment groups only differing in having unknotted sutures placed under the left anterior descending coronary artery.

Heart Weight Index and Hemodynamics Monitoring

Two weeks after AMI, the body weights (BW) of the rats were recorded. Rats were anesthetized with sodium pentobarbital 1% (50 mg/kg) by intraperitoneal injection and hemodynamic parameters were recorded. Briefly, the right common carotid artery was dissected and separated from the connective tissues. A catheter was inserted into the carotid, then blood pressure and heart rate were recorded by using LabChart 7. After hemodynamics monitoring, the hearts were removed quickly by thoracotomy, washed with saline, and then lung weight (LW) and heart weight (HW) were measured. Cardiac index = HW/BM (mg/g), Cardiopulmonary index = HW/LM (mg/mg) were calculated.

Western Blot Analysis and Quantitative Real-Time PCR

Western blot was performed as previously described (Shih et al., 2018). Myocardial tissues obtained after AMI for 2 weeks or CFs and NRVMs transfected with adenovirus for 3–5 days, were homogenized with RIPA lysis buffer (Beyotime Institute of Biotechnology, Haimen, China). The lysates were centrifuged at 10,000*g* for 10 min (4°C) and the supernatants were collected. Equal amounts of proteins (40 μg) were separated by SDS-PAGE and then transferred to polyvinylidene difluoride membranes. Membranes were incubated with primary antibodies overnight at 4°C and then probed with horseradish-peroxidase-conjugated secondary antibodies for 30 min at room temperature (**Table 1**). Blots were visualized with Enhanced chemiluminescence detection (ECL; Beyotime Institute of Biotechnology). β-actin was used as a loading control.

Total RNA extraction and real-time PCR study were performed as previously described (Liu et al., 2019; Yin et al., 2019). A total

TABLE 1 | Antibodies used in this study.

Antibodies name	Catalog number	Manufacturer name
β-Actin	AS1107	TDY
Cleaved caspase3	#9664	CST
Cleaved caspase9	AF5240	affbiotech
Bax	#2772	CST
Bcl-2	ab196495	abcam
Id2	sc-398104	santa
α-SMA	ab32575	Rabbit
Collagen I	ab34710	abcam
Collagen III	ab7778	abcam
TGF-β 1	AF1027	affbiotech
Smad3	#9523	CST
HIF-1α	ab1	abcam
IL-11	bs-1827R	BOAOSEN
MMP-2	ab92536	abcam
TIMP-1	ab61224	abcam
HRP-Goat anti Rabbit	AS1107	ASPEN
HRP-Goat anti Mouse	AS1106	ASPEN

mRNA was isolated from heart or cells by TRIzol Reagent (Invitrogen), and complementary DNA (cDNA) was synthesized from total RNA by the RevertAid First Strand cDNA Synthesis Kit (Toyobo, Tokyo, Japan). RT-qPCR was performed using gene-specific primers (**Table 2**) and SYBR Green (Takara Bio, Japan). Relative mRNA expression was quantitated by $2^{-\Delta\Delta Ct}$ comparative quantification method, normalized to β-actin expression. All western blot and PCR analyses were repeated at least three times to verify results.

Transthoracic Echocardiography Measurements

A noninvasive transthoracic echocardiography method was used to evaluate the morphology and function of left ventricle. Echocardiography was performed in anesthetized animals. M-mode echocardiography was conducted in parasternal long-axis view to obtain echocardiographic parameters using a High-Resolution Imaging System (GE Vivid E95, USA) equipped with a 12-MHz probe(12S).

Immunohistochemistry and Histological Staining

The hearts and cells were fixed with 4% paraformaldehyde and embedded in paraffin. CFs and NRVMs were permeabilized in 0.2% Triton X-100 in PBS. Deparaffinized sections (6-um thickness) were stained with Masson's trichrome, Hematoxylin and Eosin (HE) or TUNEL. Deparaffinized sections (6-um thickness) or CFs were stained with primary antibodies overnight at 4°C with anti-α-SMA and/or anti-Vimentin or HIF-1α, and NRVMs were stained with anti-caspase-3, respectively, followed by the secondary antibody for 2 h at 37°C. Nuclei were stained with 4',6-diamidino-2-phenylindole (DAPI, Sigma-Aldrich). The

TABLE 2 | Polymerase chain reaction primers used in this study.

Gene	Accession No.		Primer (5'—3')	Size (bp)
R-β-actin	NM_031144.3	sense	CGTTGACATCCGTAAAGACCTC	110
		antisense	TAGGAGCCAGGGCAGTAATCT	
R-IL-11	NM_133519.4	sense	GCCAGATAGAGTCGTTGCCC	188
		antisense	AGGTAGGTAGGGAGTCCAGATTG	
R-TGF-β1	NM_021578.2	sense	GTGGCTGAACCAAGGAGACG	195
		antisense	AGGTGTTGAGCCCTTTCCAG	
R-Smad3	NM_013095.3	sense	GGGAGACATTCCACGCTTCA	233
		antisense	CTGGTTGCAGTTGGGAGACTG	
R-HIF-1α	NM_024359.1	sense	AAGCCCAGAGTCACTGGGACT	118
		antisense	GTACTCACTGGGACTGTTAGGCTC	
R-BAX	NM_017059	sense	TGAACTGGACAACAACATGGAG	148
		antisense	AGCAAAGTAGAAAAGGGCAACC	
R-Bcl2	NM_016993.1	sense	TTGTGGCCTTCTTTGAGTTCG	214
		antisense	TTCAGAGACAGCCAGGAGAAATC	
R-caspase3	NM_012922	sense	ATGCTTACTCTACCGCACCCG	138
		antisense	GGTTAACACGAGTGAGGATGTGC	
R-caspase9	NM_031632.1	sense	GCCAGAGGTTCTCACACCAGA	171
antisense	GAAGGGCAGAAGTTCACGTTG			
H-Id2	NM_031632.1	sense	CCCAGAACAAGAAGGTGAGCA	245
		antisense	TATTCAGCCACACAGTGCTTTGC	
R-α-SMA	NM_031004.2	sense	TCCTGACCCTGAAGTATCCGAT	260
		antisense	ACCAGTTGTACGTCCAGAAGCA	
R-Collagen I	NM_053304.1	sense	TCCTGACCCTGAAGTATCCGAT	161
		antisense	ACCAGTTGTACGTCCAGAAGCA	
R-Collagen III	NM_032085.1	sense	AGAGGCTTTGATGGACGCAA	269
		antisense	GGTCCAACCTCACCCTTAGC	
R-Id2	NM_013060.3	sense	ACCTGGACAGAACCAAACGTC	108
		antisense	TCATTCGACATAAGCTCAGAAGG	

TGF-β1, Transforming growth factor-β1; α-SMA, alpha smooth muscle actin; HIF-1α, hypoxia induced factor-1 alpha; IL-11, interleukin 11; Id2, Inhibitor of differentiation 2. R, rat; H, human.

negative controls lacking the primary antibody were included. Fluorescence images were captured by the fluorescent microscope (BX51 systems, Olympus, Tokyo, Japan). Semiquantitative analysis of the tissue staining images was performed using the Image-Pro Plus 6.0 System (Media cybernetics, USA).

Statistical Analysis

Data were expressed as means ± SEM and were analyzed by GraphPad Prism 5. One-way analysis of variance (ANOVA) was performed for multiple groups, followed by Bonferroni's multiple comparison test. Unpaired Student's t-test was performed to compare two groups. All data were subjected to formal tests for normality. Data not following normal distribution were evaluated by non-parametric tests. A P-value of <0.05 was considered statistically significant.

RESULTS

Myocardial Fibrosis and Id2 Expression in Rat Hearts Post-MI

Masson's trichrome staining showed the presence of collagen deposition in the border and infarct zones in MI rats (**Figure 1A** and **Supplementary Table 1**). HE staining results confirmed cardiac hypertrophy in the infarct and border zones compared to the sham group (**Figure 1B**). Myofibroblasts, transformed from CFs and characterized by α-SMA and vimentin-positive, were not detected in the sham group but were strongly expressed in the border and infarct zones of post-MI rats (**Figure 1C** and **Supplementary Table 1**). Immunofluorescence showed that Id2 expression was increased in infarct zone and border zone (**Figure 1D**). Western blot analysis affirmed that Id2 protein expression increased after 24 h and 2 weeks MI at the border zone (**Figures 1E, F**). Ad-GFP-Id2 and Ad-GFP adenovirus were transfected to normal rat hearts. Frozen heart slices from the adenovirus injected areas showed a green fluorescence, and the protein expression of Id2 in those Ad-Id2 injected areas was significantly higher compared to GFP group after transfection for 3 days, 7 days, 2 weeks and 4 weeks(**Figures 1G, H**).

Adenoviral Id2 Delivery Improves Cardiac Function and Ameliorates Cardiac Remodeling After MI

Male SD rats were randomly divided into four groups: sham operation group (sham, n = 15), MI group (MI, n = 15), MI+Ad-GFP group (GFP, n = 15), and MI+Ad-GFP-Id2 group (Id2, n = 15). There was no difference in body weight (BW) and lung weight (LW) among the four groups after 2 weeks. The heart weight (HW), HW/BW ratio and HW/LW ratio were higher in MI group and GPF group compared to the sham group (**Figures 2A–E** and **Supplementary Table 2**). The echocardiography showed that LVEDD, LVESD, LVEDV and LVESV significantly increased, whereas FS and LVEF decreased in the MI group and GFP group relative to the sham group (**Figures 2F–L** and **Supplementary Table 2**), illustrating that cardiac function was deteriorated after MI. HW, HW/BW ratio, HW/LW ratio, LVEDD, LVESD, LVEDV, and LVESV were lower, while FS and LVEF were higher in Id2 group compared to MI group and GFP group. In addition, hemodynamic parameters such as systolic blood pressure (SBP) and mean blood pressure were markedly reduced in MI groups and in GFP groups, which were restored in rats that received Ad-Id2 delivery. There were no difference of heart rates among the four groups (**Supplementary Table 2**). These findings indicated that over-expression of Id2 can remodel cardiac structure and improve cardiac function.

Over-Expression of Id2 Reduces Cardiac Fibrosis Post-MI

Reactive myocardium remodeling after MI leads to cardiac fibrosis. This is associated with myofibroblast differentiation, ECM accumulation and impaired the balance of MMPs and TIMPs. HE and Masson staining showed that hypertrophy and collagen deposition were higher in MI group and GFP group compared to sham groups. The fibrotic area was 59.50 ± 1.4% and 56.64 ± 5.6% in MI group and GFP group, respectively, and Id2 treatment reduced the fibrotic size to 33.63 ± 3.7% ($P < 0.05$) (**Figures 3A–C** and **Supplementary Table 3**). Immunofluorescence revealed that α-SMA and vimentin were co-expression in MI group and GFP group, but the phenomenon was not detected in the sham group and Id2 group (**Figure 3D**). Western blot analysis further confirmed that the protein levels of α-SMA, Collagen I, Collagen III, MMP2 and TIMP1 were augmented after MI. Id2 treatment decreased the protein levels of α-SMA, Collagen I, Collagen III, modulated the balance between MMP2 and TIMP1 compared to GFP group and MI group (**Figures 3E, F**).

Determination of Optimal MOI and CCK-8 Incubation Time

Two days after cell isolation, NRVMs were transfected with either Ad-GFP-Id2 or Ad-GFP at different multiplicity of infection (MOI) values (MOI = 0, 10, 20, 50, 100, 200). CFs of passages 3–6 were digested in culture dishes and then inoculated in 24-well plates and 6-well pates. When cell confluence reached 70–80%, Ad-GFP-Id2 and Ad-GFP in DMEM/F12 were added to the cells at different MOI values (MOI = 0, 10, 20, 50, 100, 200). After 12 h of incubation period, a fresh complete medium was added. The cells were observed under a light and fluorescent microscope (BX51 systems; Olympus Corporation, Tokyo, Japan). After transfection for 24 h, the CFs and NRVMs exhibited a green fluorescence. The results showed that as the MOI increased, the fluorescence intensity of Ad-GFP-Id2 increased. The highest MOI that did not reduce the number of cells was chosen as the optimal MOI value for infection. As shown in **Figure S1A(1–6)** and **Figure S1C(1–6)**, the optimal MOI was 50 and 100 in NRVMs and CFs, respectively. Furthermore, immunohistochemistry staining was performed to establish the identity of the isolated cells. CFs were vimentin-positive and α-SMA-negative (**Figure S1D(1–4)**), while NRVMs displayed high expression of cardiac troponin-I(c-TnI) (**Figure S1B(1–3)**). The mRNA levels of Id2 were significantly higher in Id2 group than in the control group

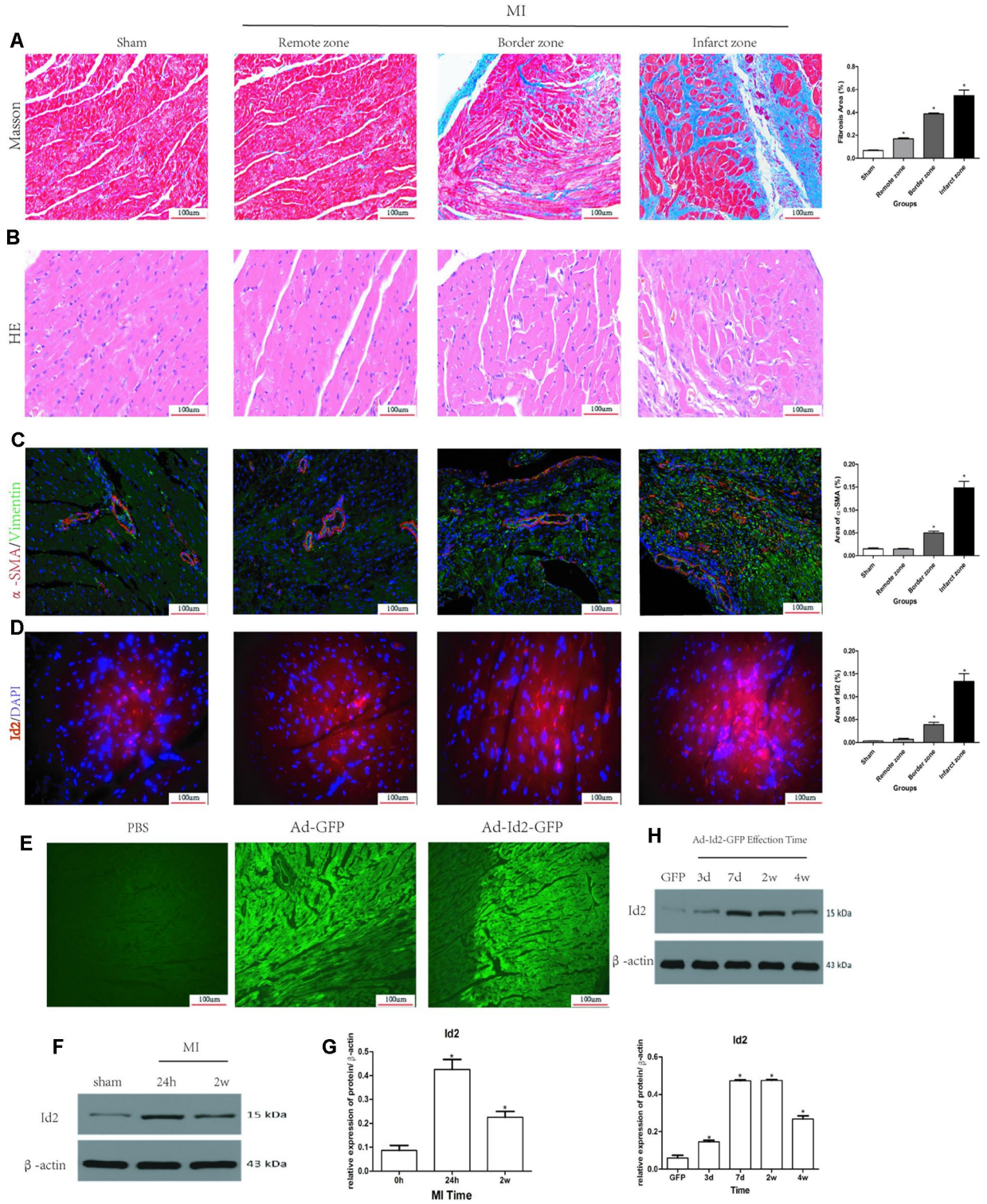

FIGURE 1 | Myocardial Fibrosis and Id2 expression in rat hearts post-MI. **(A)** Masson's trichrome staining post-MI after 2 weeks (n = 6). Blue staining represents fiber tissue. Scale bars represent 100 um. **(B)** HE staining post-MI after 2 weeks (n = 6). Scale bars represent 100 um. **(C)** Immunofluorescence images of myofibroblasts derived from CFs (n = 6). Green, vimentin; red, α-SMA; blue, nuclei. Scale bars represent 100 um (n = 6). **(D)** Immunofluorescence images show Id2 expressions in MI rats and sham rats. Red, Id2; blue, nuclei. Scale bars represent 100 um. **(E, F)** Id2 protein levels detected by western blot analysis after MI. **(G, H)** Rats were intramyocardially injected with Ad-GFP-Id2 or Ad-GFP for 3 days, 7 days, 2 weeks and 4 weeks. The fluorescence of Ad-GFP and Ad-GFP-Id2 in injected area of rat heart after transfected 2 weeks **(G)**. The protein levels of Id2 in left ventricular myocardium were examined by Western Blot **(H)**. h, hours; d, days; w, weeks. β-actin was used as the loading control. Data represent means ± SEM (n = 3). *,P < 0.05 VS Sham group, 0 h or GFP group.

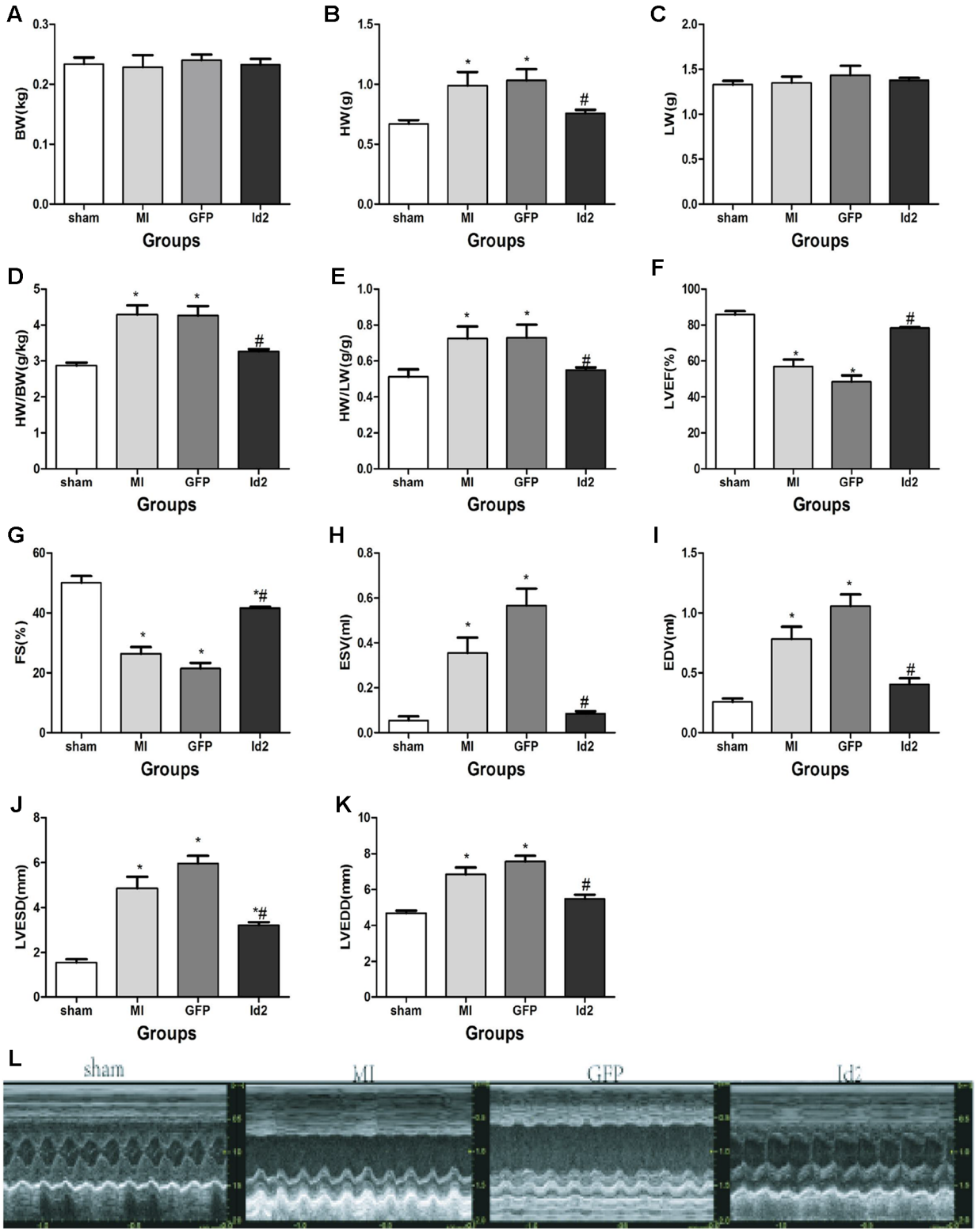

FIGURE 2 | Id2 improved cardiac structure and function. **(A–E)** Four groups' comparison represented Id2 can ameliorate cardiac structure by reducing the HW/BW or HW/LW ratio index. **(F–L)** Densitometric analysis of the data demonstrated a significantly improvement of cardiac function in Id2 groups. BW body weight, HW heart weight, Lung weight, FS fractional shortening, LVEF left ventricular ejection fraction, LVESD left ventricular end-systolic diameter, LVEDD left ventricular end-diastolic diameter, LVESV left ventricular end-systolic volume, LVEDV left ventricular end-diastolic volume, HR heart rate, Bp blood pressure. Data represent means ± SEM. Heart weight index (n = 10), Transthoracic echocardiography measurements (n = 7). *P <0.05, vs sham group; #P <0.05, vs MI group and GFP group.

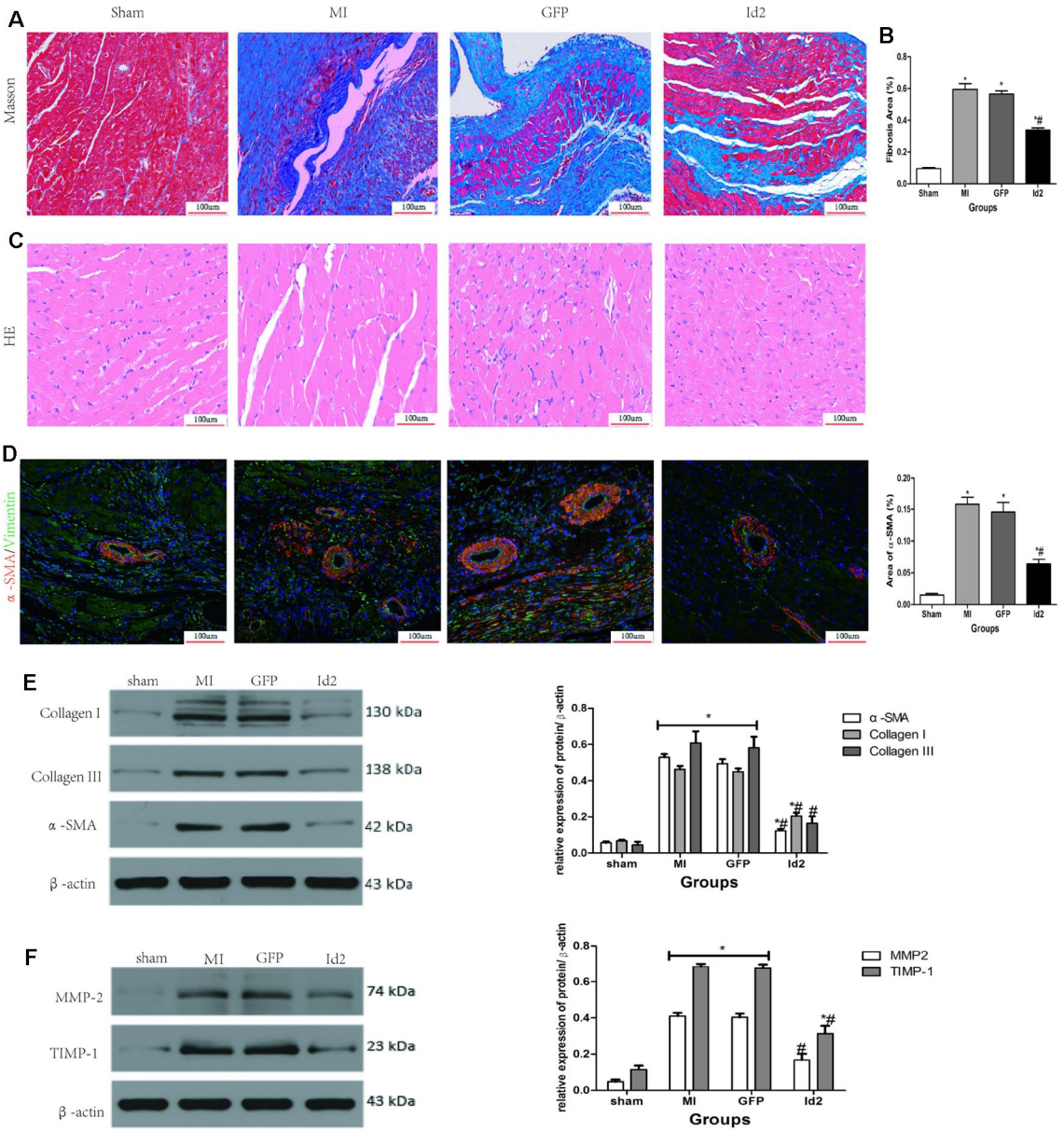

FIGURE 3 | Adenoviral Id2 delivery ameliorated cardiac remodeling post-MI. **(A**, **B)** Representative Masson's trichrome staining **(A)** and histogram of connective tissue percentage **(B)** of hearts. Blue staining indicates connective tissue (n = 6). Scale bars represent 100 um. **(C)** Representative HE staining images (n = 6). Scale bars indicate 100 um. **(D)** immunofluorescence images of myofibroblasts derived from CFs (n = 6). Green, vimentin; red, α-SMA; blue, nuclei. Scale bars represent 100 um. **(E**, **F)** Western blot analysis of protein expressions in rat hearts among the four groups (n = 3). β-actin was used as the loading control. Data represent means ± SEM. *,P < 0.05, vs sham group; # ,P < 0.05, vs MI group and GFP group; ⊢*⊣ in panel **(E)** including α-SMA, Collagen I, Collagen III in both MI and GFP group; ⊢*⊣ in panel **(E)** including MMP2, TIMP-1 in both MI and GFP group.

and GFP group at 48 h after transfection (**Figure S1E**). The results showed that Ad-GFP-Id2 transfection was successful and lead to a stable Id2 expression *in vitro*. Besides, the rate of CFs proliferation after incubation with CCK-8 reagent for 1 or 2 h was the same as that of the primary state. In contrast, incubation of CFs with CCK-8 reagent for 4 h increased CFs proliferation obviously, indicating that CCK-8 reagent did not have any effect on cell proliferation within 2 h. Thus, 2 h duration was regarded as the optimal incubation time (**Figure S1F**).

Id2 Protects CFs Against Cardiac Fibrosis *In Vitro*

Although Id2 expression increased after MI, the cellular source of Id2 was not known. Thus, we treated NRVMs and CFs in hypoxia environment for 6 h and 12 h, respectively. **Figures 4A–C** showed that the level of Id2 was not different between normal NRVMs and CFs. In the early hypoxia stage, the expression of Id2 was higher in NRVMs than in CFs, and overrode the level of Id2 in NRVMs at the late hypoxic stage. Thus,

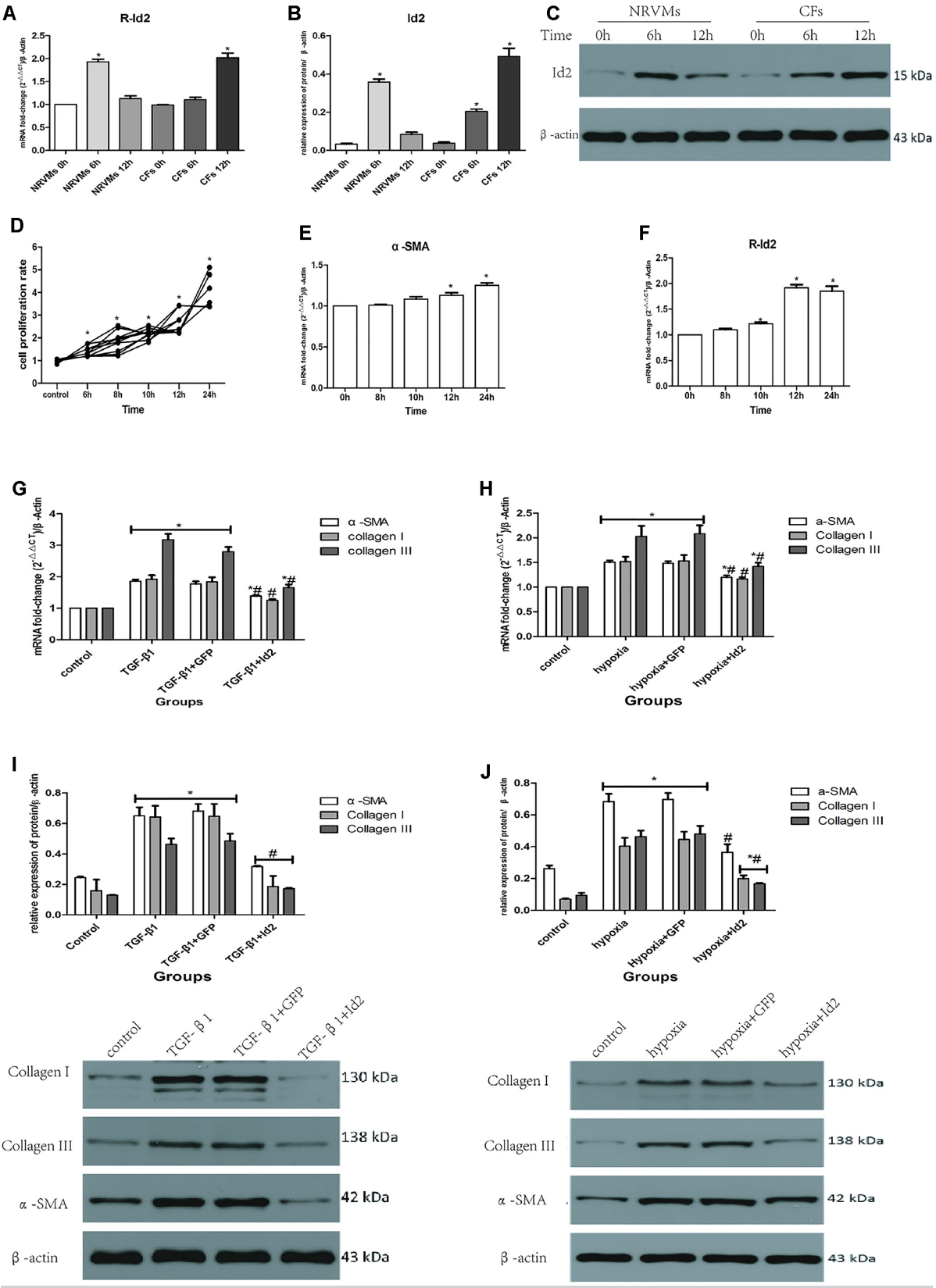

FIGURE 4 | Continued

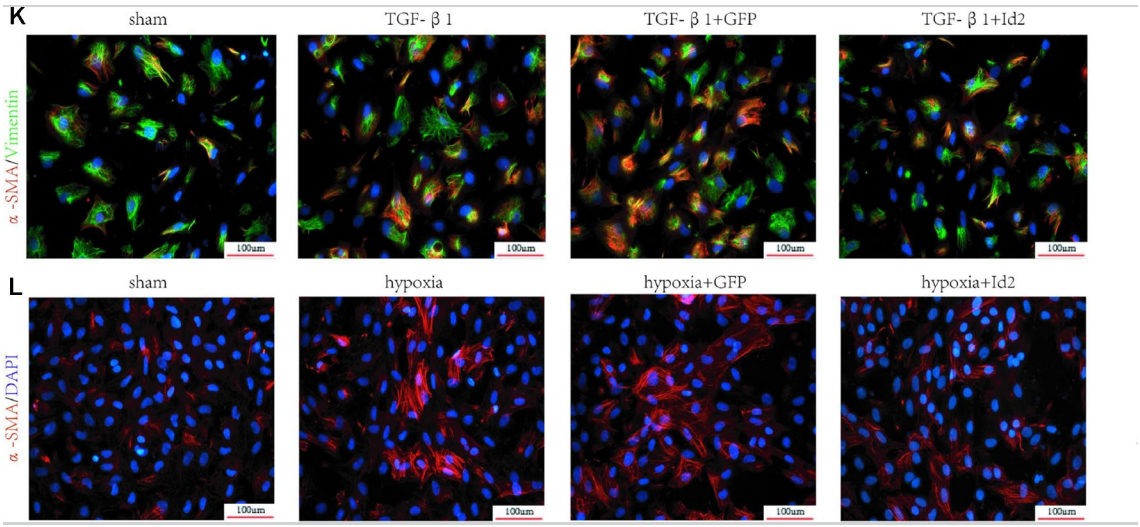

FIGURE 4 | NRVMs or CFs treated with hypoxia or TGF-β1. **(A–C)** Comparison of Id2 in NRVMs and in CFs (n = 3). **(D)** The proliferation rate of CFs in different hypoxia time (n = 5). **(E**, **F)** The mRNA levels of α-SMA **(E)** and rat Id2 **(F)** in CFs treated with the multi-hypoxia time (n = 3). **(G–J)** qRT-PCR and Western blot were performed to detect the mRNA levels of α-SMA, Collagen I, Collagen III in CFs treated with TGF-β1(10 ng/ml) for 24 **(G)** or hypoxia environment for 12 h **(H)** and the protein expressions of α-SMA, Collagen I, Collagen III in CFs treated with TGF-β1(10 ng/ml) for 24 h **(I)** or hypoxia environment for 12 h (J) (n = 3). **(K**, **L)** immunofluorescence images of myofibroblasts derived from CFs, which were treated with TGF-β1 **(G)** and put under hypoxia environment (**H**), respectively (n = 3). Green, vimentin; red, α-SMA; blue, nuclei. Scale bars represent 100 um. β-actin was used as the loading control. Data represent means ± SEM. *P < 0.05 VS control group or 0 h ; #P < 0.05 VS TGF-β1 group, TGF-β1+GFP group, hypoxia group, or hypoxia+GFP group; *| in panels **(G**, **I)** including α-SMA, Collagen I, Collagen III in both TGF-β1 group and TGF-β1+GFP group; *| in panels **(H**, **J)** including α-SMA, Collagen I, Collagen III in both hypoxia group and hypoxia+GFP group; #| in panel **(I)** including α-SMA, Collagen I, Collagen III in TGF-β1+Id2 group; *#| in panel **(J)** including Collagen I, Collagen III in hypoxia+Id2 group.

we inferred that NRVMs and CFs can express Id2 in a time-dependent manner.

Numerous studies have shown that myofibroblasts derived from CFs are markers of cardiac fibrosis. To clarify whether Id2 directly modulates myofibroblast differentiation, we treated CFs with TGF-β1 or hypoxia. The CFs were placed in incubators with hypoxic or normal conditions for 6, 8, 10, 12, and 24 h, after which the absorbance values were measured at 450 nm. It was observed that the proliferation of CFs increased along with the time of hypoxia (**Figure 4D**), so did the mRNAs of α-SMA (**Figure 4E**, **Supplementary Table 4**) and Id2 (**Figure 4F**). Since the mRNA levels of Id2 reached peak levels at 12 h, we chose 12 h as the optimal hypoxia time for CFs stimulation. The results showed that CFs exposed to hypoxic environment expressed higher mRNA and protein levels of α-SMA, Collagen I and Collagen III, then these effects were reversed by over-expression of Id2. Treatment with TGF-β1 (10 ng/ml) increased the expression of mRNA and protein levels of α-SMA, Collagen I and Collagen III in CFs compared to control groups. Id2 treated group expressed lower levels of α-SMA, Collagen I, and Collagen III levels in contrast to TGF-β1 group and TGF-β1+GFP group (**Figures 4G–J**). Similar findings were obtained by immunofluorescence analysis following hypoxia and TGF-β1 stimulation (**Figures 4K–L** and **Supplementary Table 5**).

Over-Expression of Id2 Reduces Cardiac Fibrosis *Via* TGF-β1/Smad3/HIF-1α/IL-11 Pathways

We further explored the mechanisms in which Id2 exhibits the anti-fibrotic effects. We detected that TGF-β1, smad3, HIF-1αand IL-11 highly expressed in MI hearts and GFP hearts compared to the sham group (**Figure 5A**). Moreover, treatment of CFs with TGF-β1 elevated the mRNA and protein levels of smad3, HIF-1αand IL-11 (**Figures 5B, C**), which matched with expression levels of CFs exposed to hypoxia (**Figures 5D–F**, **Supplementary Figure 2**). It was also found that the injections of Ad-GFP-Id2 into the myocardium and rat CFs decreased the expression of TGF-β1, smad3, HIF-1α and IL-11. Thus, we concluded that Id2 can inhibit cardiac fibrosis through TGF-β1/smad3/HIF-1α/IL-11 pathway.

To further examine the effect of TGF-β1/smad3/HIF-1α/IL-11 on Id2, Oltipraz, an inhibitor of HIF-1αactivation was used. This experiment was divided into six groups: control group (control), Ad-GFP-Id2 group (Id2), Oltipraz group (Oltipraz) (10 mmol/L), hypoxia group (hypoxia), hypoxia+Ad-GFP-Id2 group (hypoxia+Id2), and hypoxia+Oltipraz group (10 mmol/L) (hypoxia+Oltipraz). **Figures 5G–I** showed that Oltipraz and Ad-GFP-Id2 decreased the expression of HIF-1αin CFs at normal conditions. The protein level of HIF-1αwas lower in hypoxia+Id2 and hypoxia+Oltipraz compared to hypoxia group as reconfirmed by the immunofluorescence tests.

Id2 Decreases Apoptosis Both *In Vivo* and *In Vitro*

The apoptotic effects of Id2 were evaluated by the TUNEL staining. The number of apoptotic cells (TUNEL positive cells) were higher in MI group and GFP group than in the sham group and Id2 group. This implies that MI promoted cardiomyocyte apoptosis and over-expression of Id2 might prevent these adverse

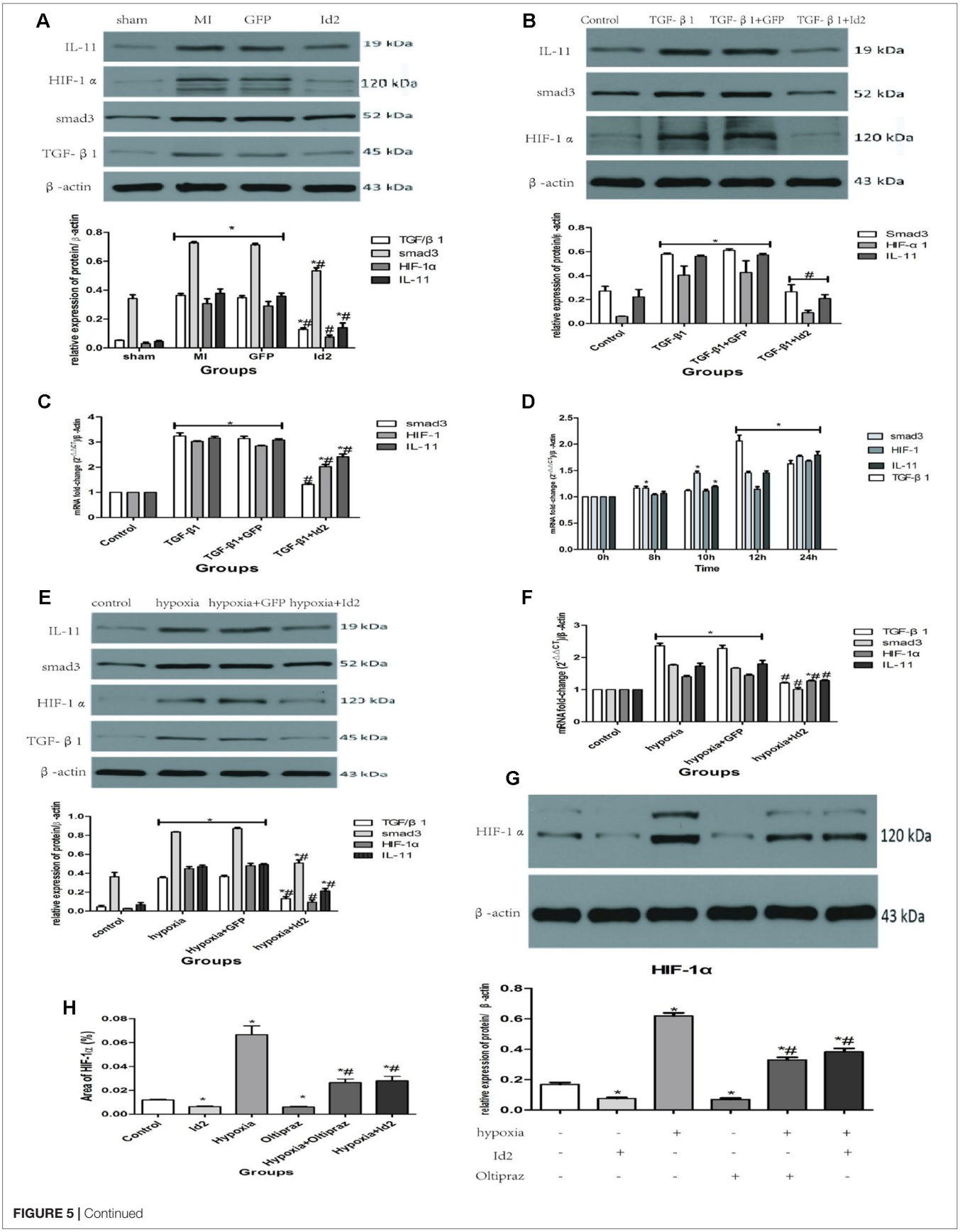

FIGURE 5 | Continued

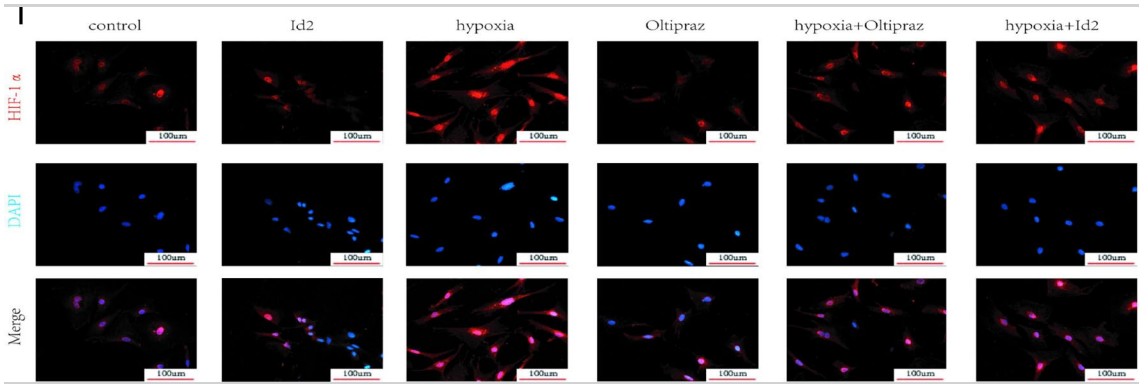

FIGURE 5 | Id2 inhibited myofibroblast differentiation via TGF-β1/smad3/HIF-1α/IL-11 pathways. **(A)** The protein levels of TGF-β1, smad3, HIF-1α, IL-11 in rat hearts. **(B**, **C)** qRT-PCR and Western blot were performed to detect the mRNA levels **(C)** or the protein expressions **(B)** of smad3, HIF-1α, IL-11 in CFs treated with TGF-β1 (10 ng/ml) for 24 h. **(D)**The mRNA levels of TGF-β1, smad3, HIF-1α, IL-11 in CFs treated with different hypoxia time. **(E–F)** qRT-PCR and Western blot were performed to detect the mRNA levels **(F)** or the protein expressions **(E)** of TGF-β1, smad3, HIF-1α, IL-11 in CFs treated with hypoxia for 12 h. **(G)** The protein levels of HIF-1α in six groups (n = 3). **(H**, **I)** immunofluorescence images of CFs among six groups *in vitro* (n = 6). Red, HIF-1α; blue, nuclei. Scale bars represent 100 um. β-actin was used as the loading control. Data represent means ± SEM (n = 3). *P < 0.05, vs sham group or control group. #P <0.05, vs MI group, GFP group, TGF-β1 group, TGF-β1+GFP group, hypoxia group, or hypoxia+GFP group; ⊢*⊣ in panel **(A)** including TGF-β1, smad3, HIF-1α, IL-11 in both MI group and GFP group; ⊢*⊣ in panels **(B**, **C)** including smad3, HIF-1α, IL-11 in both TGF-β1 group and TGF-β1+GFP group; ⊢#⊣ in panel **(B)** including smad3, HIF-1α, IL-11 in TGF-β1+Id2 group; ⊢*⊣ in panel **(D)** including TGF-β1, smad3, HIF-1α, IL-11 in both 12 h and 24 h; ⊢*⊣ in panels **(E**, **F)** including TGF-β1, smad3, HIF-1α, IL-11 in both hypoxia group and hypoxia+GFP group.

effects. The apoptotic cells displayed yellow-brown nuclei whereas normal cells had light blue nuclei. The rate of apoptosis was higher in MI group and GFP group compared to the sham group (MI 31.00% ± 0.9% vs GFP 31.70% ± 1.49% vs sham 7.20% ± 0.25%), and Id2 reversed these effects to some extent (Id2 17.30% ± 0.25%) (**Figures 6A, B** and **Supplementary Table 6**). In addition, Id2 protected against apoptosis post-MI from apoptosis by decreasing the expression of bax, bcl-2, cleaved-caspase3 and cleaved-caspase9 (**Figure 6C**). Furthermore, immunofluorescence assays confirmed that Id2 prevented the myocardium from apoptosis *in vivo* (**Figures 6D, E** and **Supplementary Table 7**).

To determine whether Id2 can reduce cell apoptosis *in vitro*, isolated NRVMs were exposed to hypoxia and then analyzed by flow cytometry. Results showed that the apoptosis rate of NRVMs increased with hypoxia exposure time and the mRNA level of Id2 reached the peak at 6 h (**Figures 7A–F**). Therefore, we chose 6 h as the optimal hypoxia exposure time. Besides, the expression levels of markers of cell apoptosis, bax/bcl-2, c-caspase3 and c-caspase9 were gradually increased along with the hypoxia time-course (**Figure 7G**). The hypoxic models were divided into four groups: control group (C), hypoxia group (h), hypoxia+GFP group (H+G) and hypoxia+Ad-GFP-Id2 group (H+I). The results showed that the mRNA and protein levels of bax/bcl, c-caspase3 and c-caspase9 were lower in H+I group compared to H group and H+G group (**Figures 7H, I**). Collectively, these results demonstrated that Id2 ameliorated myocardial apoptosis post-MI *in vivo* and attenuated apoptosis of NRVMs *in vitro*. To reveal the mechanism of Id2 in reducing apoptosis, the protein level of HIF-1α in the four groups was measured. **Figure 7J** shows that HIF-1α expression in NRVMs increased after exposure to hypoxic environment, while Id2 treatment inhibited it. We therefore inferred that Id2 inhibited apoptosis through HIF-1α.

DISCUSSION

Accumulating evidences indicate that Id2 plays a role in organic fibrotic diseases. A recent study by Vigolo et al. identified Id protein as the a key target of BMPR1A-SMAD1/5/8 signaling in renal fibrosis (Vigolo et al., 2019). Moreover, Id protein is stimulated by TGF-β1 and BMP7, and it acts as a molecular switch which determines the fate of cells by regulating the timing from cell proliferation to differentiation. Therefore, it might serve as a therapeutic target for corneal fibrosis (Izumi et al., 2006; Mohan et al., 2016). Id2 is a downstream target of BMP7 which antagonizes the TGF-β1-dependent fibro-genic activity in liver fibrosis and pulmonary myofibroblastic cells (Kinoshita et al., 2007). More importantly, Id is a member of the Id family associated with the Helicopter-loop-Helix (HLH) protein, which lacks the basic amino acid sequence necessary for DNA binding. Consequently, it can interact with the basic helix-loop-helix (Basic Helix-loop-Helix, bHLH) to form a heterodimer and inhibit the bHLH to link relevant DNA or other tissue-specific bHLH transcription factors (Lasorella et al., 2014). Id2 inhibits HLH transcriptional factors such as MyoD in liver fibrosis, thereby reducing differentiation of hepatic stellate cells and promoting cell proliferation. Finally, it has been reported that overexpression of Id2 attenuates pulmonary fibrosis by regulating c-Abl and Twist (Yang et al., 2015). The data described above show that Id2 is closely related with fibrosis.

The Id family proteins highly expressed in the early stage of embryonic growth and heart development. Particularly, Id1, Id2, and Id3 are detected in the heart, whereas Id4 is not. Fraidenraich et al. (2004) demonstrate that Id1 and Id3 regulate cardiac development for the first time and other several following studies have shown that Id family is involved in the formation

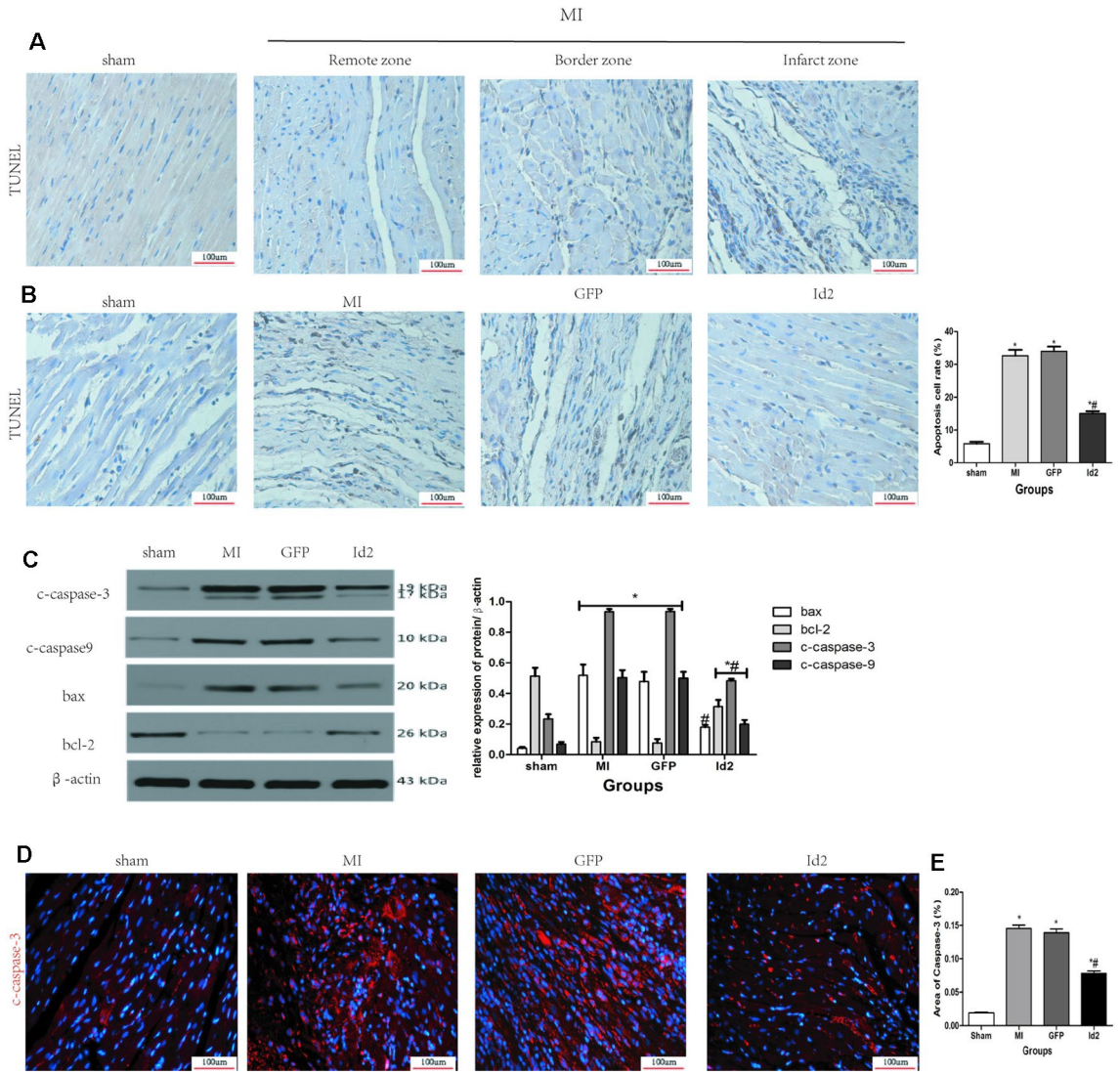

FIGURE 6 | Id2 reduced carmyocyte apoptosis post-MI. **(A**, **B)** Representative TUNEL staining. The apoptotic cells show yellow-brown nuclei, while the normal cells exhibit light blue nuclei. (n = 6). Scale bars represent 100 um. **(C)** The protein levels of c-caspase3, c-caspase9, bax and bcl-2 in rat hearts (n = 3). **(D)** The apoptotic cell rate in four groups. **(E)** Immunofluorescence images of cardiomyocytes among four groups *in vivo* (n = 6). Red, c-caspase3; blue, nuclei. Scale bars represent 100 um. β-actin was used as the loading control. Data represent means ± SEM. *P <0.05, vs control group. #P <0.05, vs MI group and GFP group; ⊢*⊣ in panel **(C)** including c-caspase3, c-caspase9, bax and bcl-2 in both MI group and GFP group; ⊢*#⊣ in panel **(C)** including c-caspase3, c-caspase9, and bcl-2 in Id2 group.

of the cardiac mesoderm (Cunningham et al., 2017). Id2 knock-out during embryonic E9.5-E14.5 leads to fatal defects in cardiac development, such as systemic and pulmonary circulation abnormalities, ventricular septal defect as well as myocardial hypoplasia.

Cardiac remodeling caused by MI is characterized by formation of α-SMA stress fibers, production of ECM proteins such as collagen I or collagen III, activation of TGF-β1 canonical and non-canonical pathway, myofibroblast differentiation and fibrosis of myocardial tissue (Frangogiannis, 2019). In this study, we found, for the first time, that Id2 over-expression after MI inhibited cardiac fibrosis. Results showed that Id2 improved cardiac function and attenuated cardiac fibrosis. These effects were associated with inhibition of myofibroblast differentiation, reduction of ECM accumulation and balance of MMP-TIMP system. Thus, Id2 over-expression influenced pathological cardiac remodeling post-MI.

We further explored the signaling molecules that mediate the anti-fibrotic effects of Id2. The TGF-β/Smad signaling pathway participates in the pathogenesis of cardiac fibrosis, and Smad3 plays a central role in TGF-β1-induced excessive accumulation of ECM components (Bujak et al., 2007; Hu et al., 2018; Zhang et al., 2018). As a key factor in organ fibrosis, TGF-β1 plays an indispensable role in cardiac fibrosis. Id2 is an inhibitory factor downstream of the TGF-β1 signaling. Secondly, HIF-1α, which increases following exposure to hypoxia, might be a target for

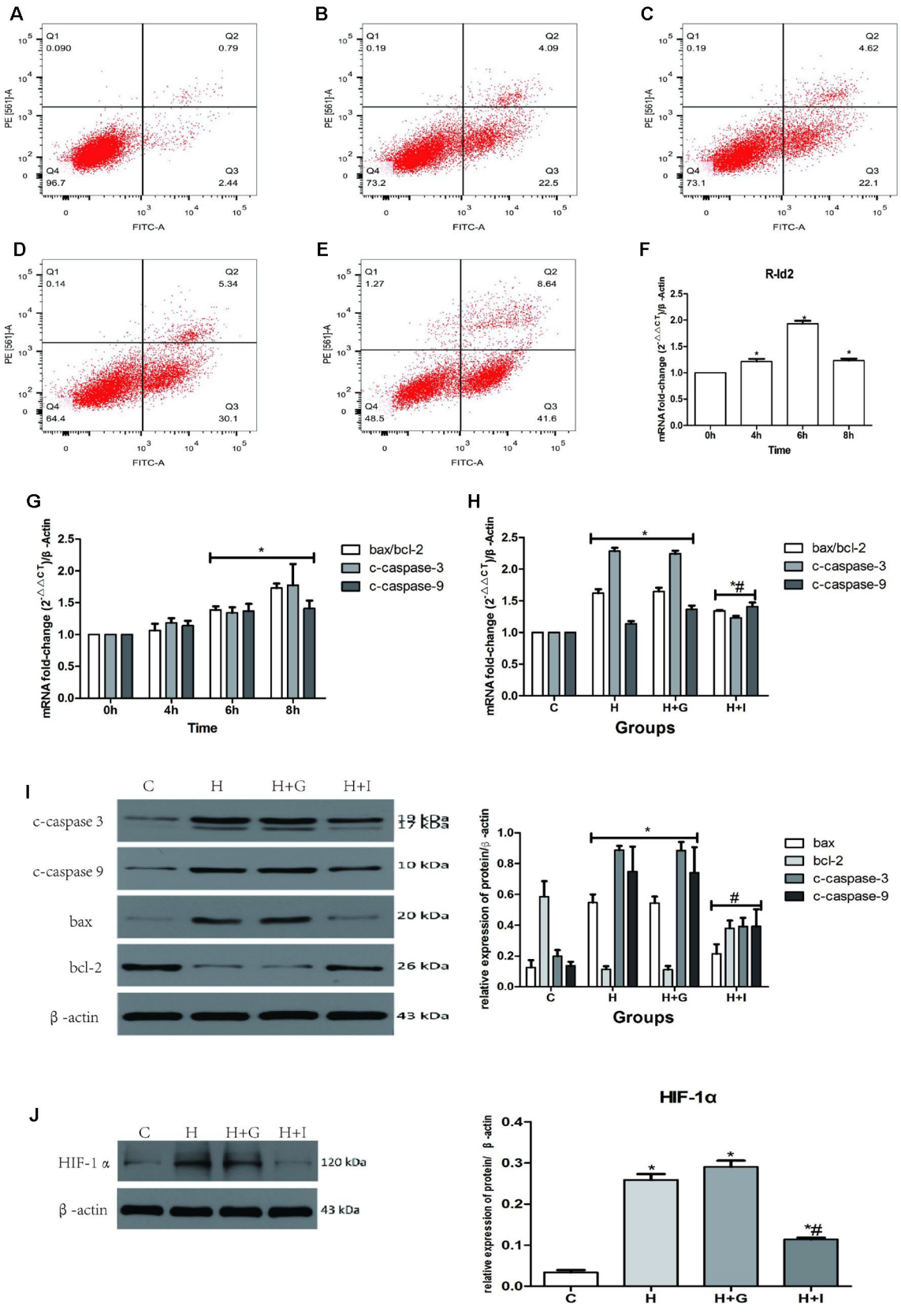

FIGURE 7 | Continued

FIGURE 7 | NRVMs treated with hypoxia.**(A–E)** Flow cytometry of NRVMs' apoptosis rate after treated with different hypoxia time (n = 3). **(A)** 0 h, **(B)** 4 h, **(C)** 6 h, **(D)** 8 h, **(E)** 12 h. **(F)** The mRNA levels of rat Id2 in NRVMs along with different hypoxia time. **(G)** The mRNA levels of bax/bcl, c-caspase3 and c-caspase9 in NRVMs with different hypoxia time. **(H**. **I)** qRT-PCR and Western blot were performed to detect the mRNA levels **(H)** or the protein expressions **(I)** of bax/bcl, c-caspase3 and c-caspase9 in NRVMs treated with hypoxia for 6 h. **(J)** The protein level of HIF-1α in NRVMs in four groups. β-actin was used as the loading control. Data represent means ± SEM (n = 3). *P <0.05, vs control groups or 0 h; #P <0.05, vs H groups and H+G groups; ⊢*⊣ in panel **(G)** including c-caspase3, c-caspase9, bax/bcl-2 in both 6 h and 8 h; ⊢*⊣ in panel **(H)** including c-caspase3, c-caspase9, bax/bcl-2 in both H group and H+G group; ⊢*#⊣ in panel **(H)** including c-caspase3, c-caspase9, and bax/bcl-2 in Id2 group; ⊢*⊣ in panel **(I)** including c-caspase3, c-caspase9, bax and bcl-2 in both H group and H+G group; ⊢#⊣ in panel **(I)** including c-caspase3, c-caspase9, bax, and bcl-2 in Id2 group.

preventing cardiac perivascular fibrosis by inhibiting endothelial-to-mesenchymal transition (Zhang et al., 2017). Besides, it is reported that HIF-1α-Smad3 transcriptional complexes regulate the transcription of several genes, e.g., pheromone in red blood cells or type-I collagen in human tubular epithelial cells (Sanchez-Elsner et al., 2004; Baumann et al., 2016). This complex is activated under hypoxic conditions or/and TGF-β1 stimulation. As a DNA binding inhibitor, Id2 binds to HIF-1α to form a heterodimer, which might block the effects of HIF-1α (Teng and Li, 2014). Recent studies have shown that IL-11 is a crucial determinant of cardiac fibrosis. Schafer et al. states that IL-11 together with other fibrotic factors can cause malignant myocardial fibrosis (Schafer et al., 2017). To further determine the effect of TGF-β1/smad3/HIF-1α/IL-11 on Id2, Oltipraz, an inhibitor of HIF-1α, was used. Results showed that Id2 inhibited HIF-1α, similar to the effects of Oltipraz in normal and hypoxia environment.

In addition, Id2 protected the myocardium from apoptosis, which is consistent with previous reports. Numerous studies have confirmed that Id family can reduce cell apoptosis (Sun et al., 2016; Zhao et al., 2016; Yin et al., 2017; Fan et al., 2018). However, it is also reported that Id2 can induce apoptosis in hypoxia- or ischemia-induced neuronal injury and lead to abnormal brain development (Park et al., 2013; Guo et al., 2015). Therefore, whether Id2 reduces or induces apoptosis requires further analysis. In this study, we found that Id2 reduced apoptosis in MI rat hearts and in NRVMs. To further explore the potential anti-apoptotic mechanisms of Id2, we detected the protein levels of HIF-1α in NRVMs. We found that HIF-1α was increased after exposure of cells to hypoxic environment, but Id2 inhibited this increase. Besides, other studies have illustrated that HIF-1α plays an essential role in NRVMs' apoptosis. Thus, we inferred that Id2 inhibited apoptosis by inhibiting HIF-1α.

However, we did not explore the interaction between HIF-1α and Id2. As mentioned above, Id2 was involved in cardiac fibrosis. Given that HIF-1α is a DNA-binding inhibitor, we hypothesize that Id2 may reduce the formation of HIF-1α-Smad3 transcriptional complexes, thereby promoting the transcription of IL-11. Further studies are required to pursue this possibility. Another limitation of this study is that we only focus on cardiac fibrosis induced by MI. In fact, many factors can lead to cardiac fibrosis, such as aging. In addition, we found that Id2 protected the myocardium from apoptosis *via* HIF-1α. But the exact role of Id2 in cell apoptosis remains unclear. Finally, our experiments were performed using SD rats while some of the previous researches mentioned above were performed in mice. We used rats because of their larger sizes. Compared to mice, the survival rate of rats post-MI is higher and the CFs and NRVMs isolated from rats are more stable. Thus, to validate the effects of Id2 on cardiac function, experiments should be performed in other animal species. The type of cells used in such experiments should be considered when interpreting the results since Id2 may have diverse effects in different cell-lines.

In conclusion, this study provided the first evidence that Id2 protected against cardiac fibrosis. The results showed that Id2 ameliorated cardiac fibrosis in rats post-MI by inhibiting TGF-β1/smad3/HIF-1α/IL-11 pathway. Thus, Id2 might be a therapeutic target for cardiac fibrosis after MI.

DATA AVAILABILITY STATEMENT

The raw data supporting the conclusions of this manuscript will be made available by the authors, without undue reservation, to any qualified researcher.

ETHICS STATEMENT

The present study was approved by the Experimental Animal Committee of Wuhan University (Hubei, China; no. WDRM20180912).

AUTHOR CONTRIBUTIONS

LY and MX-L made substantial contributions to the conception and design of the study, performed the experiments and wrote the paper. WL and F-YW assisted in the performance of experiments. Y-HT participated in research design and coordinated the study. C-XH revised the manuscript and gave final approval of the version to be published. All authors read and approved the final manuscript.

FUNDING

The present study was supported by the Fundamental Research Funds for the Central Universities of China (grant no. 2042015kf0229).

SUPPLEMENTARY MATERIAL

The Supplementary Material for this article can be found online at: https://www.frontiersin.org/articles/10.3389/fphar.2019.01349/full#supplementary-material

REFERENCES

Afratis, N. A., Klepfish, M., Karamanos, N. K., and Sagi, I. (2018). The apparent competitive action of ECM proteases and cross-linking enzymes during fibrosis: Applications to drug discovery. *Adv. Drug Delivery Rev.* 129, 4–15. doi: 10.1016/j.addr.2018.03.004

Baumann, B., Hayashida, T., Liang, X., and Schnaper, H. W. (2016). Hypoxia-inducible factor-1alpha promotes glomerulosclerosis and regulates COL1A2 expression through interactions with Smad3. *Kidney Int.* 90, 797–808. doi: 10.1016/j.kint.2016.05.026

Blyszczuk, P., Muller-Edenborn, B., Valenta, T., Osto, E., Stellato, M., Behnke, S., et al. (2017). Transforming growth factor-beta-dependent Wnt secretion controls myofibroblast formation and myocardial fibrosis progression in experimental autoimmune myocarditis. *Eur. Heart J.* 38, 1413–1425. doi: 10.1093/eurheartj/ehw116

Bujak, M., Ren, G., Kweon, H. J., Dobaczewski, M., Reddy, A., Taffet, G., et al (2007). Essential role of Smad3 in infarct healing and in the pathogenesis of cardiac remodeling. *Circulation* 116, 2127–2138. doi: 10.1161/CIRCULATIONAHA.107.704197

Cao, Y., Liu, X., Zhang, W., Deng, X., Zhang, H., Liu, Y., et al. (2009). TGF-beta repression of Id2 induces apoptosis in gut epithelial cells. *Oncogene* 28, 1089–1098. doi: 10.1038/onc.2008.456

Chen, D. Q., Feng, Y. L., Cao, G., and Zhao, Y. Y. (2018). Natural Products as a Source for Antifibrosis Therapy. *Trends Pharmacol. Sci.* 39, 937–952. doi: 10.1016/j.tips.2018.09.002

Cunningham, T. J., Yu, M. S., McKeithan, W. L., Spiering, S., Carrette, F., Huang, C. T., et al. (2017). Id genes are essential for early heart formation. *Genes Dev.* 31, 1325–1338. doi: 10.1101/gad.300400.117

Fan, Y., Huang, Z., Long, C., Ning, J., Zhang, H., Kuang, X., et al. (2018). ID2 protects retinal pigment epithelium cells from oxidative damage through p-ERK1/2/ID2/NRF2. *Arch. Biochem. Biophys.* 650, 1–13. doi: 10.1016/j.abb.2018.05.008

Fraidenraich, D., Stillwell, E., Romero, E., Wilkes, D., Manova, K., Basson, C. T., et al. (2004). Rescue of cardiac defects in id knockout embryos by injection of embryonic stem cells. *Science* 306, 247–252. doi: 10.1126/science.1102612

Frangogiannis, N. G. (2019). Cardiac fibrosis: Cell biological mechanisms, molecular pathways and therapeutic opportunities. *Mol. Aspects Med.* 65, 70–99. doi: 10.1016/j.mam.2018.07.001

Golden, H. B., Gollapudi, D., Gerilechaogetu, F., Li, J., Cristales, R. J., Peng, X., et al. (2012). Isolation of cardiac myocytes and fibroblasts from neonatal rat pups. *Methods Mol. Biol.* 843, 205–214. doi: 10.1007/978-1-61779-523-7_20

Guo, L., Yang, X., Lin, X., Lin, Y., Shen, L., Nie, Q., et al. (2015). Silencing of Id2 attenuates hypoxia/ischemia-induced neuronal injury *via* inhibition of neuronal apoptosis. *Behav. Brain Res.* 292, 528–536. doi: 10.1016/j.bbr.2015.07.018

Hossain, M. M., Banik, N. L., and Ray, S. K. (2012). Survivin knockdown increased anti-cancer effects of (-)-epigallocatechin-3-gallate in human malignant neuroblastoma SK-N-BE2 and SH-SY5Y cells. *Exp. Cell Res.* 318, 1597–1610. doi: 10.1016/j.yexcr.2012.03.033

Hu, H., Chen, D., Wang, Y., Feng, Y., Cao, G., Vaziri, N. D., et al. (2018). New insights into TGF-beta/Smad signaling in tissue fibrosis. *Chem.-Biol. Interact.* 292, 76–83. doi: 10.1016/j.cbi.2018.07.008

Izumi, N., Mizuguchi, S., Inagaki, Y., Saika, S., Kawada, N., Nakajima, Y., et al. (2006). BMP-7 opposes TGF-beta 1-mediated collagen induction in mouse pulmonary myofibroblasts through Id2. *Am. J. Physiol.-Lung C.* 290, L120–L126. doi: 10.1152/ajplung.00171.2005

Jen, Y., Manova, K., and Benezra, R. (1996). Expression patterns of Id1, Id2, and Id3 are highly related but distinct from that of Id4 during mouse embryogenesis. *Dev. Dyn.* 207, 235–252. doi: 10.1002/(SICI)1097-0177(199611)207:3<235::AID-AJA1<3.0.CO;2-I

Jongbloed, M. R., Vicente-Steijn, R., Douglas, Y. L., Wisse, L. J., Mori, K., Yokota, Y., et al. (2011). Expression of Id2 in the second heart field and cardiac defects in Id2 knock-out mice. *Dev. Dyn.* 240, 2561–2577. doi: 10.1002/dvdy.22762

Jun, J. I., and Lau, L. F. (2018). Resolution of organ fibrosis. *J. Clin. Invest.* 128, 97–107. doi: 10.1172/JCI93563

Kamata, Y. U., Sumida, T., Kobayashi, Y., Ishikawa, A., Kumamaru, W., and Mori, Y. (2016). Introduction of ID2 Enhances Invasiveness in ID2-null Oral Squamous Cell Carcinoma Cells *via the* SNAIL Axis. *Cancer Genomics Proteomics* 13, 493–497. doi: 10.21873/cgp.20012

Kinoshita, K., Iimuro, Y., Otogawa, K., Saika, S., Inagaki, Y., Nakajima, Y., et al. (2007). Adenovirus-mediated expression of BMP-7 suppresses the development of liver fibrosis in rats. *Gut* 56, 706–714. doi: 10.1136/gut.2006.092460

Lasorella, A., Benezra, R., and Iavarone, A. (2014). The ID proteins: master regulators of cancer stem cells and tumour aggressiveness. *Nat. Rev. Cancer* 14, 77–91. doi: 10.1038/nrc3638

Liu, X., Xu, Y., Deng, Y., and Li, H. (2018). MicroRNA-223 Regulates Cardiac Fibrosis After Myocardial Infarction by Targeting RASA1. *Cell. Physiol. Biochem.* 46, 1439–1454. doi: 10.1159/000489185

Liu, M., Yin, L., Li, W., Hu, J., Wang, H., Ye, B., et al. (2019). C1q/TNF-related protein-9 promotes macrophage polarization and improves cardiac dysfunction after myocardial infarction. *J. Cell. Physiol.* 234, 18731–18747. doi: 10.1002/jcp.28513

Mohan, R. R., Morgan, B. R., Anumanthan, G., Sharma, A., Chaurasia, S. S., and Rieger, F. G. (2016). Characterization of Inhibitor of differentiation (Id) proteins in human cornea. *Exp. Eye Res.* 146, 145–153. doi: 10.1016/j.exer.2015.12.003

Park, H. J., Hong, M., Bronson, R. T., Israel, M. A., Frankel, W. N., and Yun, K. (2013). Elevated Id2 expression results in precocious neural stem cell depletion and abnormal brain development. *Stem Cells* 31, 1010–1021. doi: 10.1002/stem.1351

Sanchez-Elsner, T., Ramirez, J. R., Sanz-Rodriguez, F., Varela, E., Bernabeu, C., and Botella, L. M. (2004). A cross-talk between hypoxia and TGF-beta orchestrates erythropoietin gene regulation through SP1 and Smads. *J. Mol. Biol.* 336, 9–24. doi: 10.1016/j.jmb.2003.12.023

Schafer, S., Viswanathan, S., Widjaja, A. A., Lim, W. W., Moreno-Moral, A., DeLaughter, D. M., et al. (2017). IL-11 is a crucial determinant of cardiovascular fibrosis. *Nature* 552, 110–115. doi: 10.1038/nature24676

Shih, Y. C., Chen, C. L., Zhang, Y., Mellor, R. L., Kanter, E. M., Fang, Y., et al. (2018). Endoplasmic Reticulum Protein TXNDC5 Augments Myocardial Fibrosis by Facilitating Extracellular Matrix Protein Folding and Redox-Sensitive Cardiac Fibroblast Activation. *Circ. Res.* 122, 1052–1068. doi: 10.1161/CIRCRESAHA.117.312130

Sun, W. Z., Li, M. H., Chu, M., Wei, L. L., Bi, M. Y., He, Y., et al. (2016). Id1 knockdown induces the apoptosis and inhibits the proliferation and invasion of ovarian cancer cells. *Eur. Rev. Med. Pharmacol. Sci.* 20, 2812–2818.

Tajima, K., Terai, S., Takami, T., Kawaguchi, K., Okita, K., and Sakaida, I. (2007). Importance of inhibitor of DNA binding/differentiation 2 in hepatic stellate cell differentiation and proliferation. *Hepatol. Res.* 37, 647–655. doi: 10.1111/j.1872-034X.2007.00089.x

Teng, Y., and Li, X. (2014). The roles of HLH transcription factors in epithelial mesenchymal transition and multiple molecular mechanisms. *Clin. Exp. Metastasis* 31, 367–377. doi: 10.1007/s10585-013-9621-6

Vigolo, E., Marko, L., Hinze, C., Muller, D. N., Schmidt-Ullrich, R., and Schmidt-Ott, K. M. (2019). Canonical BMP signaling in tubular cells mediates recovery after acute kidney injury. *Kidney Int.* 95, 108–122. doi: 10.1016/j.kint.2018.08.028

Yang, J., Velikoff, M., Agarwal, M., Disayabutr, S., Wolters, P. J., and Kim, K. K. (2015). Overexpression of inhibitor of DNA-binding 2 attenuates pulmonary fibrosis through regulation of c-Abl and Twist. *Am. J. Pathol.* 185, 1001–1011. doi: 10.1016/j.ajpath.2014.12.008

Yin, X., Tang, B., Li, J. H., Wang, Y., Zhang, L., Xie, X. Y., et al. (2017). ID1 promotes hepatocellular carcinoma proliferation and confers chemoresistance to oxaliplatin by activating pentose phosphate pathway. *J. Exp. Clin. Cancer Res.* 36, 166. doi: 10.1186/s13046-017-0637-7

Yin, L., Liu, M. X., Wang, F. Y., Wang, X., Tang, Y. H., Zhao, Q. Y., et al. (2019). Transcription Factor prrx1 Promotes Brown Adipose-Derived Stem Cells Differentiation to Sinus Node-Like Cells. *DNA Cell Biol.* 38, 1313–1322. doi: 10.1089/dna.2019.4998

Zhang, G. H., Yu, F. C., Li, Y., Wei, Q., Song, S. S., Zhou, F. P., et al. (2017). Prolyl 4-Hydroxylase Domain Protein 3 Overexpression Improved Obstructive Sleep Apnea-Induced Cardiac Perivascular Fibrosis Partially by Suppressing

Endothelial-to-Mesenchymal Transition. *J. Am. Heart Assoc.* 6, pii: e006680. doi: 10.1161/JAHA.117.006680

Zhang, Y., Cui, L., Guan, G., Wang, J., Qiu, C., Yang, T., et al. (2018). Matrine suppresses cardiac fibrosis by inhibiting the TGF-/Smad pathway in experimental diabetic cardiomyopathy. *Mol. Med. Rep.* 17, 1775–1781. doi: 10.3892/mmr.2017.8054

Zhao, Y., Luo, A., Li, S., Zhang, W., Chen, H., Li, Y., et al. (2016). Inhibitor of Differentiation/DNA Binding 1 (ID1) Inhibits Etoposide-induced Apoptosis in a c-Jun/c-Fos-dependent Manner. *J. Biol. Chem.* 291, 6831–6842. doi: 10.1074/jbc.M115.704361

Conflict of Interest: The authors declare that the research was conducted in the absence of any commercial or financial relationships that could be construed as a potential conflict of interest.

frontiers in Pharmacology

REVIEW
published: 29 November 2019
doi: 10.3389/fphar.2019.01363

Choroidal Neovascularization: Mechanisms of Endothelial Dysfunction

Natalie Jia Ying Yeo[1], *Ebenezer Jia Jun Chan*[2,3] *and Christine Cheung*[1,4]*

[1] *Lee Kong Chian School of Medicine, Nanyang Technological University, Singapore, Singapore,* [2] *Division of Psychology, School of Social Sciences, College of Humanities, Arts, and Social Sciences, Nanyang Technological University, Singapore, Singapore,* [3] *Duke-NUS Medical School, National University of Singapore, Singapore, Singapore,* [4] *Institute of Molecular and Cell Biology, Agency for Science, Technology and Research, Singapore, Singapore*

Many conditions affecting the heart, brain, and even the eyes have their origins in blood vessel pathology, underscoring the role of vascular regulation. In age-related macular degeneration (AMD), there is excessive growth of abnormal blood vessels in the eye (choroidal neovascularization), eventually leading to vision loss due to detachment of retinal pigmented epithelium. As the advanced stage of this disease involves loss of retinal pigmented epithelium, much less attention has been given to early vascular events such as endothelial dysfunction. Although current gold standard therapy using inhibitors of vascular endothelial growth factor (VEGF) have achieved initial successes, some drawbacks include the lack of long-term restoration of visual acuity, as well as a subset of the patients being refractory to existing treatment, alluding us and others to hypothesize upon VEGF-independent mechanisms. Against this backdrop, we present here a nonexhaustive review on the vascular underpinnings of AMD, implications with genetic and systemic factors, experimental models for studying choroidal neovascularization, and interestingly, on both endothelial-centric pathways and noncell autonomous mechanisms. We hope to shed light on future research directions in improving vascular function in ocular disorders.

Keywords: choroidal neovascularization, endothelial, vascular mechanisms, age-related macular degeneration, disease models

OPEN ACCESS

Edited by:
Owen Llewellyn Woodman, Baker Heart and Diabetes Institute, Australia

Reviewed by:
Carlos Alonso Escudero, University of the Bío Bío, Chile
Jason Hellmann, University of Louisville, United States

***Correspondence:**
Christine Cheung
ccheung@ntu.edu.sg

Specialty section:
This article was submitted to Cardiovascular and Smooth Muscle Pharmacology, a section of the journal Frontiers in Pharmacology

Received: *14 August 2019*
Accepted: *28 October 2019*
Published: *29 November 2019*

Citation:
Yeo NJY, Chan EJJ and Cheung C (2019) Choroidal Neovascularization: Mechanisms of Endothelial Dysfunction. Front. Pharmacol. 10:1363. doi: 10.3389/fphar.2019.01363

INTRODUCTION

Endothelial dysfunction underlies the crux of many conditions, which may implicate comorbidities. One example is choroidal neovascularization, a process in wet or exudative age-related macular degeneration (AMD), characterized by the abnormal intravasation of choroidal vasculature into the retinal epithelium or subretinal tissue. This often involves dysfunctional and leaky vessels, which then lead to the accumulation of fluid and blood in the macula (Chirco et al., 2017; Saini et al., 2017). AMD is the principal cause of permanent blindness among elderly over 60 years in industrialized countries (Stan et al., 2004; Pascolini and Mariotti 2012; Wong et al., 2014). It has a prevalence of 8.7% which will increase with ageing populations, adversely affecting the quality of life of 196 million people by 2020. As one would expect, it will incur substantial public health burden in the next few decades (Friedman et al., 2004; Seddon et al., 2005; Wong et al., 2014; Jonas et al., 2017). Among AMD cases with acute visual impairment, wet AMD is responsible for approximately 90%

of cases (Ferris et al., 1984). Despite the rising prevalence of this debilitating condition, current treatment strategies for wet AMD mostly revolve around inhibitors of vascular endothelial growth factor and photodynamic therapy. Both have considerable limitations such as lack of long-term improvement on visual acuity (Rofagha et al., 2013; Fernández-Robredo et al., 2014; Bracha et al., 2017; Dunn et al., 2017; Jaffe et al., 2017; Malek et al., 2018) and secondary inflammatory side effects (Ho et al., 2016). These bring to light the necessity for a deeper understanding of the disease (Fernández-Robredo et al., 2014; Bracha et al., 2017; Malek et al., 2018).

Endothelial dysfunction plays a role in many human diseases. Patients with early vascular abnormalities have been found to acquire AMD and associated cardiovascular and cerebrovascular diseases later in their lives (Cheung and Wong, 2014). Research on AMD has mainly focused on retinal pigmented epithelium deficit as that is the ultimate pathological change leading to vision loss, whereas mechanisms of endothelial dysfunction in choroidal neovascularization remain elusive. Limitations with the current gold standard treatment for wet AMD using inhibitors of vascular endothelial growth factor (VEGF) have revealed possibilities of VEGF-independent pathways (Huang et al., 2016). Despite advances in genome wide association studies (GWAS), risk variants associated with AMD are hardly translated into the intended development of diagnostics and treatment. It is slowly being recognized that genetic risk variants exert minuscule influences as they often have no direct relevance to the illness. In fact, they are postulated to act through complex regulatory networks to influence the activity of key genes that are more biologically connected to the disease (Boyle et al., 2017).

We recognize that emerging studies are discovering a significant involvement of endothelial pathology in choroidal neovascularization. Here, we provide a nonexhaustive review to address the vascular underpinnings of AMD, provide information on state-of-the-art experimental models of choroidal neovascularization, and interpret existing knowledge on endothelial mechanisms with heterotypic interplay of different cell types and environmental factors.

VASCULAR ETIOLOGY IN AGE-RELATED MACULAR DEGENERATION

Endothelial Dysfunction in Early Stages

While the pathogenesis of wet AMD is still poorly understood, several reports suggest a vascular etiology for the disease. The choroidal endothelial cells that form choriocapillaris vessel walls are lost even before the occurrence of retinal pigmented epithelium dysfunction, suggesting that vascular dysfunction could be the first trigger of wet AMD (Lutty et al., 2009; Bhutto and Lutty, 2012; Biesemeier et al., 2014; Mullins et al., 2014). Histologically, choriocapillaris tissue near the site of choroidal neovascular lesions exhibit decreased density without accompanying retinal pigmented epithelium disruption (Bhutto and Lutty 2012). Indeed, the choriocapillaris endothelium in aging macula is highly subject to complement activation stress and decreases in density with increasing drusen in dry or non-exudative AMD. Complement accumulation present in early stages may lead to choriocapillaris loss (Berenberg et al., 2012; Mullins et al., 2014). The resultant loss of vascular support to the retinal pigmented epithelium releases angiogenic signals which stimulate abnormal intravasation of choroidal vessels into subretinal layers, observed in some cases of nonexudative AMD which progress to wet AMD. Furthermore, it is well established that the functions of retinal pigmented epithelium and choriocapillaris show tight mutualistic dependence and atrophy of either structures leads to a dysfunction of the other (Blaauwgeers et al., 1999; Marneros et al., 2005; Biesemeier et al., 2014; Seddon et al., 2016; Chirco et al., 2017). Therefore, the pathogenesis of choroidal neovascularization may arise from initial structural changes in the vasculature (**Figure 1**).

Vasculopathy in Choroidal Neovascular Lesions

In addition to vascular degeneration in the early stages of AMD, vascular dysfunction is manifested in late stage neovascular outcomes, such as polypoidal choroidal vasculopathy (PCV). PCV is a subtype of wet AMD that is most prevalent in Asians (Wong et al., 2014; Huang et al., 2016). It is characterized by abnormal branching vascular networks and a presence of polypoidal or aneurysmal dilations at the terminal ends of these networks. These polypoidal lesions appear as hyperfluorescent nodules in fundus indocyanine angiography (Yannuzzi et al., 1990; Liu et al., 2016). Choroidal vessels in PCV display hyalinization, an arteriosclerotic phenotype characterized by the replacement of smooth muscle tissue with ill-defined basement membrane-like material, as observed in histopathological sections (Leishman 1957; Okubo et al., 2002; Kuroiwa et al., 2004; Nakashizuka et al., 2008). The aneurysmal dilations observed at terminal ends of aberrant networks also have vascular causes. They have been purported to be a result of dysfunction of elastin, homocysteine-associated oxidative stress and endothelial dysfunction (Cheng et al., 2014). The presence of hyalinization and aneurysms clearly indicate that PCV is a vasculopathy of the inner choroidal vasculature with arteriosclerotic features.

Wong et al. (2016) have presented a comprehensive review of the epidemiology, detailed risk factors and clinical manifestations of two wet AMD subtypes - PCV and typical choroidal neovascularization. Mechanisms that could lead to common vessel wall pathology in PCV and typical choroidal neovascularization include impaired extracellular matrix metabolism (Nakashizuka et al., 2008; Jones et al., 2011), involvement of the high-density lipoprotein pathway (Liu et al., 2014), choroidal vascular hyperpermeability associated with genetic polymorphisms *ARMS2 A69S* (rs10490924) and *CFH* (rs1329428) (Yoneyama et al., 2016), and choroidal venous congestion leading to thickened choroid and choroidal vascular hyperpermeability in PCV (Chung et al., 2013) (**Figure 1**). Notably, levels of VEGF in the aqueous humor of patients with typical choroidal neovascularization were found to be higher than that in PCV patients. It is postulated that the two wet AMD subtypes could have different pathological mechanisms, with

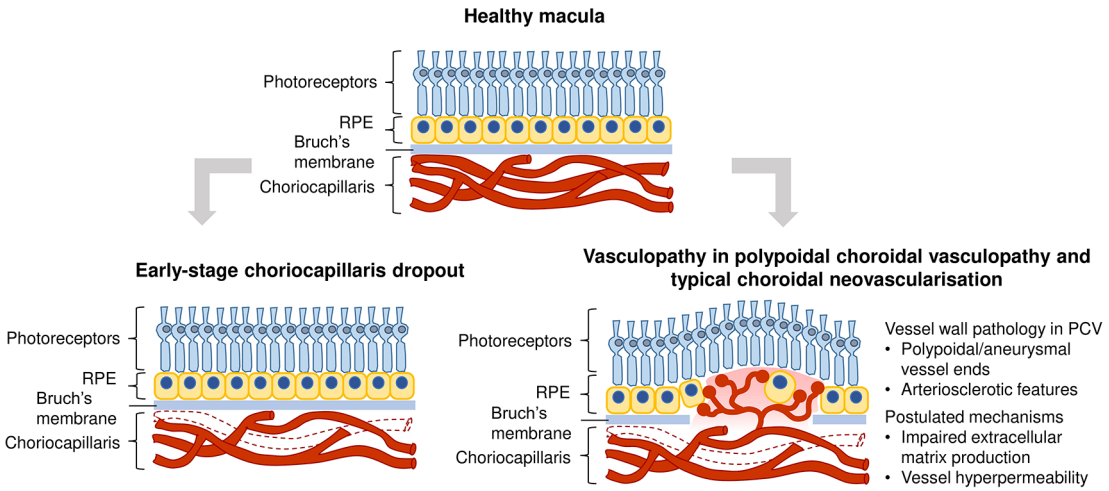

FIGURE 1 | Vascular contribution to wet age-related macular degeneration (AMD) pathogenesis. Top image: Healthy macula; Bottom left image: Vascular changes could occur early in disease progression, manifested as a reduction in choriocapillaris density through loss of endothelial cells; Bottom right image: Vasculopathy is also observed in polypoidal choroidal vasculopathy and typical choroidal neovascularization, such as polypoidal/aneurysmal dilations of vessels and arteriosclerotic features. Mechanisms in common vessel wall pathology in polypoidal choroidal vasculopathy (PCV) include impaired extracellular matrix production and choroidal vascular hyperpermeability.

typical choroidal neovascularization being more VEGF-driven than PCV (Tong et al., 2006).

Genetic Basis of Age-Related Macular Degeneration

In the past few decades, GWAS on AMD cohorts have revealed several disease-associated risk variants. The Genetics of AMD in Asians Consortium conducted a genome-wide and exome-wide association study to uncover the most common single nucleotide polymorphisms (SNPs) associated with wet AMD specifically in the East Asian population (Cheng et al., 2015). Consistent with previously identified variants, the SNPs *ARMS2-HTRA1* rs10490924, *CFH* rs10737680, *CETP* rs3764261, *ADAMTS9* rs6795735, *C2-CFB* rs429608, and *CFI* rs4698775 were the most significantly associated with wet AMD. In European and Asian populations, the most common SNPs seem to converge on the gene *HTRA1* and complement pathway-related genes. Advances in GWAS have generated more targets than biological interpretation can translate them into new therapeutics. Emerging functional studies are primarily focused on how those SNPs impact on retinal pigmented epithelium. We will further discuss how HTRA1 and complement factors could lead to aberrant vascular outcomes in a later section on *Vascular Mechanisms in Choroidal Neovascularization*.

The risk variant residing in proximity to the promoter region of *HTRA1* seems to be associated with elevated levels of HTRA1 in the retinal pigmented epithelium. It has been postulated that HTRA1 upregulation could lead to Bruch's membrane matrix breakdown, hence promoting choroidal vessel invasion (Yang et al., 2006; Jones et al., 2011). Variants in complement genes *CFH*, *CFB*, *C2*, *C3*, *C5*, and *SERPING1* also suggest important roles of complement dysregulation in AMD (Khandhadia et al., 2012). SNPs affecting *CFH* and *C3* result in decreased CFH inhibition, thus leading to increased alternative complement pathway activation (Nishida et al., 2006; Yu et al., 2014; Zhang et al., 2018), which might contribute to an angiogenic microenvironment favoring progression to choroidal neovascularization. **Table 1** represents a brief overview on the topmost variants with known molecular effects and implicated mechanisms contributing to AMD. Genetics of AMD and PCV have been reviewed extensively by our colleagues (Wong et al., 2016).

Limitation of Current Treatments

At present, gold standard therapy for wet AMD involves intravitreal administration of VEGF inhibitors such as bevacizumab, ranibizumab and aflibercept, based on the notion of VEGF being a main driver of angiogenesis (Xu and Chen, 2016; Siedlecki et al., 2017; Fogli et al., 2018). These are humanized monoclonal antibodies which act to decrease elevated VEGF at the site of neovascularization, eventually restoring retinal thickness and function (Golbaz et al., 2011). Other interventions for wet AMD include verteporfin photodynamic therapy, which is used in combination with anti-VEGF therapy to stimulate polyp regression in PCV (Cho et al., 2012; Qian et al., 2018). While anti-VEGF therapy has restored vision for many, the monotherapy does not improve visual acuity in a substantial number of AMD patients as a form of long-term management (Rofagha et al., 2013; Fernández-Robredo et al., 2014; Bracha et al., 2017; Dunn et al., 2017; Jaffe et al., 2017; Malek et al., 2018). Furthermore, approximately 15% of AMD patients do not respond to anti-VEGF treatment (Krebs et al., 2013). Zhang and colleagues have neatly reviewed potential mechanisms of resistance to anti-VEGF therapy (Zhang and Lai, 2018). In fact, the same anti-VEGF therapy tackling both PCV and typical wet AMD result in different treatment outcomes. PCV patients exhibit a poor response to anti-VEGF monotherapy compared

TABLE 1 | Common age-related macular degeneration (AMD) variants with known molecular effects and associated mechanisms.

Risk variant	Study references	Population/Type of cases	Effect of variant	Implicated mechanisms contributing to AMD
ARMS2-HTRA1 rs10490924	(DeWan et al., 2006)	Asia (Hong Kong)/wet AMD	In linkage disequilibrium with rs11200638; surrogate marker for functional polymorphism rs11200638 (DeWan et al., 2006)	–
	(Fritsche et al., 2013)	Europe and Asia (Meta-analysis of GWAS)/advanced AMD		
	(Yu et al., 2011)	Europe (Meta-analysis of GWAS)/advanced AMD		
	(Cheng et al., 2015)	East Asia/wet AMD		
HTRA1 rs11200638	(DeWan et al., 2006)	Asia (Hong Kong)/wet AMD	Increase in HTRA1 mRNA and protein [in RPE (DeWan, et al., 2006; Yang et al., 2006), in aqueous humor (Tosi et al., 2017) and in drusen (DeWan et al., 2006; Yang et al., 2006)]	Higher HTRA1 levels increase activity of degradative ECM enzymes and compromise Bruch membrane integrity, favoring choroidal invasion (Yang et al., 2006; Jones et al., 2011).
CFH rs10737680	(Fritsche et al., 2013)	Europe and Asia (Meta-analysis of GWAS)/advanced AMD	Loss of function mutation in CFH which disrupts binding of CFH to C3b *[Reported for common allele CFH Y402H and rare penetrant allele R1210C]* (Clark et al., 2010; Clark et al., 2013; Manuelian et al., 2003; Ferreira et al., 2009; Weismann et al., 2011)	Decreased CFH inhibition of C3b results in increased alternative complement pathway activation *[Reported for common allele CFH Y402H and rare penetrant allele R1210C]* (Clark et al., 2010; Clark et al., 2013; Manuelian et al., 2003; Ferreira et al., 2009; Weismann et al., 2011)
	(Cheng et al., 2015)	East Asia/wet AMD		
C3 rs2230199	(Fritsche et al., 2013)	Europe and Asia (Meta-analysis of GWAS)/advanced AMD	Alteration of configuration of first ring of macroglobulin domains, reducing binding of C3 to CFH (protein studies using electron microscopy) (Nishida et al., 2006; Zhang et al., 2018)	Reduced C3 binding to CFH increases complement activation (Zhang et al., 2018)

Amongst the large repertoire of AMD single nucleotide polymorphisms (SNPs) generated by genome wide association studies (GWAS), several such as ARMS2-HTRA1 rs10490924, HTRA1 rs11200638, CFH rs10737680, and C3 rs2230199 have been further interrogated for their molecular effects and mechanisms leading to AMD.

to typical wet AMD patients (Gomi et al., 2008; Lai et al., 2008; Liu et al., 2016; Zhang and Lai 2018). While it reduced subretinal fluid, visual acuity and retinal thickness, anti-VEGF monotherapy failed to eliminate polypoidal lesions after a year of treatment, which could lead to recurrence of exudative maculopathy (Gomi et al., 2008; Lai et al., 2008; Tsujikawa et al., 2010). Considering these limitations of anti-VEGF therapy, there might be a need for alternative strategies targeting wet AMD upon greater elucidation of the mechanisms of wet AMD.

Photodynamic therapy has several limitations. Firstly, the procedure has considerable side effects. Photodynamic therapy could cause secondary subretinal hemorrhage, retinal pigmented epithelium tears, and choroidal ischemia, resulting in further visual deficit (Lai et al., 2004; Lee et al., 2008; Teo et al., 2018). Administration of photodynamic therapy may also exacerbate existing intraocular inflammation in PCV (Ho et al., 2016). Secondly, photodynamic therapy does not entirely occlude the branching vascular network in PCV eyes, allowing new active polyps to emerge from persistent networks and hence triggering disease recurrence (Akaza et al., 2007; Lee et al., 2008). Therefore, photodynamic therapy does not prevent recurrence of PCV. Lee and colleagues proposed that polyps are more susceptible to photodynamic therapy than the branching vascular network because verteporfin is mainly taken up by proliferative endothelial cells that express high low-density lipoprotein receptors. Endothelial cells at polyp sites are more proliferative than those at the branching vascular network and are therefore more susceptible to verteporfin. Overall, the presence of secondary inflammatory side effects and its inability to prevent recurrence have rendered photodynamic therapy questionable as an efficacious treatment option. The aforementioned issues contributing to current treatment limitations for wet AMD surface a key question of whether we have sufficiently understood the mechanistic underpinnings of exudative macular degeneration and PCV, and whether alternative therapeutic angles are possible.

LINKING VASCULAR ASPECTS FROM OCULAR DISORDERS TO DISEASES OF THE BRAIN AND HEART

Scientists and clinicians have traditionally viewed AMD as a stand-alone disease that is confined to the eye. However, recent results from large-scale epidemiological studies have consistently shown that AMD is associated with several other disorders (Cheung and Wong, 2014). It is important to note that due to AMD's chronic degenerative nature, the disease tends to be associated with other chronic disorders such as cardiovascular and neurodegenerative disorders (Wong et al., 2006; Tan et al., 2008; Ohno-Matsui 2011; Lee et al., 2019). With accumulating evidence pointing to an increased risk of AMD in patients suffering from cardiovascular and neurodegenerative disorders and vice-versa, studies have started looking at common mechanisms that might underlie the associations. Here, we believe that blood vessels may provide some insights to the mechanistic link between AMD, cardiovascular, and neurodegenerative diseases.

AMD and Dementia

With a globally aging population, age-related diseases such as AMD and dementia have received unprecedented attention. These diseases have been known to contribute largely to our economic burden and healthcare expenses (Gordois et al., 2012). A recent meta-analysis of association between the two diseases proved that they tend to comorbid (Rong et al., 2019). Furthermore, a longitudinal study which followed 3,877 dementia-free participants who were diagnosed with eye disorders, found that those with AMD had a 50% increased risk of developing Alzheimer's disease later on (Lee et al., 2019). Interestingly, AMD and Alzheimer's disease share several degenerative and pathological features such as oxidative stress, inflammation, and deposition of amyloid-rich materials (Beatty et al., 2000; Golde 2002; Lin and Beal 2006; Hollyfield et al., 2008). Such common pathological features between the two diseases may be attributed to the close anatomical link between the retina and brain, explained by their shared developmental origin from the neural tube. Recognized as "the window to the brain," research have looked into using the blood vessels of the eye as a proxy to evaluate brain health (London et al., 2013; Lim et al., 2016; Yoon et al., 2019). While the vascular mechanisms that underlie the associations between AMD and dementia are largely still poorly described, here, we discuss two potential vascular links between AMD and dementia.

The first vascular link between AMD and dementia is highlighted by the deposition of vascular amyloid-β associated with tissue degeneration in both diseases. Traditionally, Alzheimer's disease, the most frequent cause of dementia, is hypothesized to arise due to an imbalance between amyloid-β production and clearance, resulting in increased levels of amyloid-β in the central nervous system. Amyloid-β accumulation subsequently causes neurotoxicity and cognitive impairment (Hardy and Selkoe 2002). Similarly, deposition of amyloid-β at the site of choroidal vessels and in extracellular deposits known as drusen, has been found in AMD patients (Dutescu et al., 2009; Kam et al., 2010; Ohno-Matsui 2011; Wang et al., 2011). Multiple reservoirs of amyloid-β have been found in the aging retinas of AMD patients and elevated amyloid-β levels were found to be associated with the key stages of AMD progression (Ohno-Matsui 2011). The similarities in brain and ocular amyloid-β deposition suggest that similar pathogenic mechanisms might underlie these two diseases. From a vascular angle, amyloid-β has toxic effects on the vascular unit in both brain and eye. In cerebral amyloid angiopathy, a vascular abnormality frequently accompanying Alzheimer's disease, amyloid-β directly hinders the adhesion of vascular smooth muscle cells to the basement membrane, leading to vascular damage (Mok et al., 2006). In the ageing retina, amyloid-β deposits from multiple reservoirs surrounding the retina exert pro-inflammatory and pro-angiogenic effects on the retinal pigmented epithelium, the choroidal vasculature and the neuroretina, which may lead to increased vascular permeability and triggering of choroidal neovascularization. This may occur on top of non-vascular effects of amyloid-β such as retinal pigmented epithelium degeneration and senescence and increased reactive oxygen species (Ratnayaka et al., 2015). Therefore, amyloid-β deposits may be a common mediator of vascular abnormalities in both AMD and Alzheimer's disease.

With multiple failed clinical trials targeted at removing amyloid-β from the brain, researchers have turned to other possible hypotheses to explain the cause of Alzheimer's disease (Holmes et al., 2008; Karran et al., 2011). The role of the blood vessel in cognitive dysfunction is well described by others (Snyder et al., 2015; Sweeney et al., 2018; Nortley et al., 2019). Cerebrovascular dysfunction might precede amyloid-β deposition in Alzheimer's disease. In a 25-year longitudinal study on dementia, the presence of vascular risk factors at midlife was associated with higher levels of amyloid-β at late-life, indicating the role of vascular disease early in Alzheimer's disease (Gottesman et al., 2017). Notably, adults with early cognitive dysfunction were found to develop brain microvascular damage independent of amyloid-β changes (Nation et al., 2019). Indeed, neuroimaging studies have found that patients with Alzheimer's disease exhibit neurovascular impairment such as lowered cerebral blood flow and atherosclerotic vessels (Arvanitakis et al., 2016; van de Haar et al., 2016; Kisler et al., 2017). Postmortem interrogations of cerebral microvasculature depict reduced density, length, and diameter in Alzheimer's disease compared with age-matched controls (Fischer et al., 1990; Buee et al., 1994; Bouras et al., 2006). These microvascular abnormalities show parallels to vascular dysfunction found in AMD. As described in an earlier section, such vascular dysfunction includes decreased choriocapillaris density in early stages of AMD and atherosclerotic features in choroidal vessels with polypoidal choroidal vasculopathy (Leishman 1957; Bhutto and Lutty 2012). Moreover, in Alzheimer's disease, the breakdown of the blood-brain barrier is observed, often caused by cerebrovascular dysfunction (Sweeney et al., 2018; Nation et al., 2019). In AMD, the breakdown of the outer blood-retinal barrier is observed, due to cumulative pathological events affecting its key component – the retinal pigmented epithelium – and surrounding tissues involved – Bruch's membrane and choroidal vasculature (Ambati, et al., 2013). These parallel pathologies may be explained by the functional and structural similarities of the blood-brain and blood-retinal barriers, both of which are derived from the developing neural tube (Ohno-Matsui 2011; London et al., 2013). Although we are still uncertain of the causative mechanisms that underlie AMD and Alzheimer's disease, the similarity of vascular pathology between the two diseases highlights a possible mechanistic link between AMD and neurodegenerative diseases.

AMD and Cardiovascular Diseases

Studies have found that changes in ocular microvascular pathology may be associated with underlying systemic vascular diseases such as cardiovascular disease. Increasing evidence has demonstrated that AMD may share identical risk factors and pathogenic mechanisms with cardiovascular diseases (Wu et al., 2014). In particular, both share several vascular-related factors highlighting the need to understand common mechanistic pathways that may result in an increased risk of developing one disease when one has the other (Tan et al., 2007; Yang et al., 2014; Pennington and DeAngelis 2016). For example,

having atherosclerotic carotid arteries and hypertension may be linked to a higher risk of AMD (Vingerling et al., 1995; Cheung et al., 2007; Hogg et al., 2008; Klein et al., 2013). Conversely, AMD and atherosclerotic retinal vessels have been suggested to be a predictor of coronary artery disease (Tedeschi-Reiner et al., 2005; Thomas et al., 2015). Additionally, it has been proposed that inflammatory markers in the eye are linked with activation of inflammatory pathways in the heart (Seddon et al., 2004). Studies have uncovered the involvement of vascular-related molecular mechanisms such as chronic inflammation, endothelial dysfunction, and oxidative stress between AMD and cardiovascular diseases (Cai and Harrison 2000; Machalińska et al., 2012; Klein et al., 2014).

Endothelial dysfunction often refers to a range of deteriorative endothelial responses that includes altered vascular inflammatory responses, vascular growth dysregulation, and vascular remodeling impairments (Gimbrone, 1995). Clinical trials and research data have shown that endothelial dysfunction is implicated in AMD through dysregulation of VEGF and soluble ICAM1 secretion that is linked to neovascularization (Lip et al., 2001; Schaumberg et al., 2007). Similarly, studies have found that endothelial dysfunction precedes the development of atherosclerosis (Davignon and Ganz 2004; Mudau et al., 2012) and may be temporally associated with myocardial ischemia (Hasdai et al., 1997). Most recently, attention has been given to characterizing circulating endothelial cells as a hallmark of vascular impairments. Circulating endothelial cells, once part of the vascular endothelial monolayer, enter the bloodstream due to damage in the blood vessels. Notably, elevated number of circulating endothelial cells have been detected in individuals affected by cardiovascular diseases and AMD, which reflects vasculopathy in both diseases (Boos et al., 2006; Erdbruegger et al., 2006; Machalińska et al., 2011). Taken together, vascular-related injury is a common pathological pathway implicated in the pathogenesis of AMD and cardiovascular diseases.

Investigations into the molecular mechanisms that link similar pathologies observed in AMD, dementia, and cardiovascular diseases are still in its infancy due to limited understanding of the causative mechanisms of these diseases. We propose that a closer look at the vascular mechanisms could yield answers on the purported associations. Specifically, studies on vascular endothelial cells, smooth muscle cells and pericytes of the eye, brain, and heart can potentially illuminate pathways that connect these diseases.

EXPERIMENTAL MODELS OF CHOROIDAL NEOVASCULARIZATION

As the causative mechanisms of AMD remain elusive, the use of experimental models that recapitulate clinical features accurately will greatly enhance our understanding of AMD etiology. Numerous *in vivo* and *in vitro* models have attempted to recapitulate the disease characteristics in its early and late stages. However, none have managed to recreate all the important pathological features seen in AMD owing to the disease's complex interplay of genetic and environmental factors. This complexity is furthermore compounded by the differences in the ocular anatomy between animal models, cellular models and humans. Despite the limitations, existing animal and cellular models have uncovered important findings on the role of vascular system in wet AMD (Rosenfeld et al., 2006; Jager et al., 2008). As mentioned in our earlier section, current therapies aim at targeting blood vessel growth and angiogenic factors (Couch and Bakri 2011; Lally et al., 2012), with greater success of anti-VEGF therapy in certain subtypes of wet AMD. The focus has been pivoted toward the vascular system and the involvement of vascular-related molecular mechanisms in AMD pathogenesis. In this section, we review existing models of choroidal neovascularization and suggest potential improvements that could better enable the study of AMD pathophysiology.

In Vivo Models

Animal models of choroidal neovascularization generally involve introducing a breach to the integrity of Bruch's membrane in the macula. This is achieved using laser and light, surgical methods, or manipulation through transgenic animals. Out of the three methods, models of laser-induced choroidal neovascularization are most widely adopted (Lambert et al., 2013). The first *in vivo* model of choroidal neovascularization was developed by Ryan (1979) using photocoagulation methods to induce a defect in the Bruch's membrane of the eyes of primates (Ryan, 1979). Building on this method, other groups were able to induce choroidal neovascularization with a higher rate of success in mouse models by modifying the different types of lasers (e.g., argon laser, krypton laser) and parameters targeted by the lasers (Dobi et al., 1989; Frank et al., 1989; Tobe et al., 1998).

The procedure to induce choroidal neovascularization in animal models starts with anesthetizing the animal and then dilating their pupils with an antimuscarinic drug, tropicamide. Laser photocoagulation is then performed to generate burns and laser spots in the areas of the eye surrounding the optic nerve. After laser treatment, the formation of a bubble at the burn spot indicates a rupture of the Bruch's membrane and this is necessary for choroidal neovascularization to occur. Laser spots with bubbles would be continually observed posttreatment for the occurrence of choroidal neovascularization using imaging methods such as confocal microscopy (Kramer et al., 2000). Laser-induced choroidal neovascularization models have become a standard for treatment evaluation and studying *in vivo* mechanisms (Grossniklaus et al., 2010; Lambert et al., 2013). The merits of the model are that it is highly reproducible, inexpensive, and time-efficient to create. However, like the limitations of any *in vivo* model, the findings in animals may not be translated to humans. Compared to human eyes, mice and rats do not possess a macula in their eyes which proves to be a huge limitation when studying AMD as the main area of degeneration occurs at the macula. Furthermore, it is important to note that there are stark anatomical differences between biologically developed choroidal neovascularization and laser induced choroidal neovascularization in animal models. For example, undergoing the laser treatment could damage the neural retina, which is not typically affected in an individual with AMD, and these

neuroretinal changes remove the biological similarity between experimental choroidal neovascularization and human choroidal neovascularization (Pennesi et al., 2012). In the end, it should be noted that laser induced acute injury does little to mimic the chronic onset of ocular neovascularization in diseases.

These laser-treated animal models have since been used to investigate the various molecular mechanisms of choroidal neovascularization and potential pharmacological interventions (Tobe et al., 1998; Bora et al., 2003; Tolentino et al., 2004; Jones et al., 2008). One of the more notable findings that led to current therapeutics was the importance of VEGF signaling in the development of choroidal neovascularization (Kwak et al., 2000). Treatments targeting VEGF signaling showed success in preventing vision loss and improving visual acuity for AMD patients at the early and late stages (Rosenfeld et al., 2006; CATT Research Group, 2011; Vogel et al., 2017). Apart from targeting VEGF, other studies open the possibility for therapeutics to inhibit and target other signaling pathways. Recently, apelin and TGF-β signaling were reported to play an essential role to trigger choroidal neovascularization in mouse models (Jiao et al., 2017; Wang et al., 2017). Additionally, transcriptional coactivator Yes-associated protein (YAP) was found to promote choroidal neovascularization formation by upregulating the proliferation of endothelial cells (Yan et al., 2018). Moreover, recent advances in nanotechnology have leveraged on choroidal neovascularization mouse models to pioneer a noninvasive method for treating choroidal neovascularization where local delivery of drugs are administered through light-triggered targeting (Wang et al., 2019). These findings underscore the value provided by *in-vivo* models of choroidal neovascularization.

Over the past few years, several optimizations and new developments have been made to augment existing *in vivo* models of laser-induced choroidal neovascularization (Poor et al., 2014; Gong et al., 2015). Recently, a preclinical mouse model of a complex heart disease was reported to accurately mimic the actual disease *in vivo* by combining the systematic manifestations of the disease instead of trying to recreate all the pathology (Schiattarella et al., 2019). In fact, AMD may be viewed as an manifestation of systematic disease (Cheung and Wong, 2014). Studies have widely reported associations between AMD and hypertension, cardiovascular disease, cerebrovascular disease, chronic kidney disease, and neurodegenerative disorders (Hogg et al., 2008; Nitsch et al., 2009; Kaarniranta et al., 2011; Chung et al., 2014). To the best of our knowledge, models of choroidal neovascularization created in combination with other stress paradigms such as metabolic perturbations have not been created. Perhaps scientists studying angiogenesis in ocular diseases such as AMD and diabetic retinopathy can apply similar principles to their animal models in order to account for systemic effects and interplay with other organ systems.

In Vitro Models

With the recent announcement of the closing of Wellcome Sanger Institute animal research facility, it has signaled a shift in the scientific community's preference for *in vitro* methods (Else 2019). Cellular systems are widely used as a working model for hypothesis testing due to their ease of handling, amenability to genetic manipulation and possibility to interrogate cell type-specific effects in isolation of other cofounding factors present in *in vivo* models. The use of primary choroidal endothelial cell lines has pinpointed signaling dysregulations in these cells as the main cause of new blood vessel formation in wet AMD (Wang and Hartnett 2016). However, human- and animal-derived choroidal endothelial cells can only be obtained post-mortem, making them a relatively scarce resource. Cells obtained from patients in advanced stage of AMD often limit their relevance in studying onset of choroidal neovascularization. Additionally, there are other constraints such as the difficulty in maintaining endothelial identity in long-term cell cultures (Rops et al., 2004).

The breakthrough by Takahashi and Yamanaka (2006) in discovering that differentiated cells can be reprogrammed back to its pluripotent state has revolutionized scientific research and allowed pluripotent stem cell derivatives to be used in place of primary cells (Takahashi and Yamanaka, 2006). Songstad et al. (2017) has reported success in generating choroidal endothelial cells from human pluripotent stem cells. They first reprogrammed human fibroblast from an individual with normal ocular history into induced pluripotent stem cells (iPSCs). These human iPSCs were differentiated alongside with a RF/6A cell line which was originally isolated from the choroid-retina of a rhesus macaque fetus (Lou and Hu, 1987). The differentiated choroidal endothelial cells expressed a choroid-restricted marker, carbonic anhydrase IV, and a fenestration marker. As part of the characterization, these differentiated cells were benchmarked against the transcriptomic signature of RF/6A cells (Songstad et al., 2017). However, a recent study led by Makin et al. (2018) conducted a rigorous characterization of the RF/6A cell line and found that RF/6A cells lack several key endothelial markers and phenotypic properties, hence limiting its use in validating iPSC-derived choroidal endothelial cells. It is still a common challenge in the iPSC field to achieve homogenous population of cell derivatives. Given that carbonic anhydrase IV is the closest and only known marker restricted to the choroid in the eye (Hageman et al., 1991), more research into specific cell fate markers would help in the generation of a pure population of these cells.

A recent study by Giacalone et al. (2019) discovered a way to immortalize human isolated choroidal endothelial cells by transducing them to express an endothelial cell specific promoter, CDH5p-hTERT/CDH5p-Tag. The immortalized choroidal endothelial cell line offers promise for a more reliable *in vitro* model as it expresses endothelial specific markers (vWF and CD34), the choroid-restricted marker carbonic anhydrase IV, AMD-related proteins (CFH), and display functional endothelial characteristics (Giacalone et al., 2019). On the other hand, scientists have cocultured choroidal endothelial cells with retinal pigmented epithelial cells to develop an *in vitro* disease model that more faithfully mimics the anatomical association of different cell types in the human eye [reviewed by Chichagova et al. (2018)]. As loss of functional cells occurs at the early stage of AMD, cell replacement therapy may potentially serve as a treatment for AMD (Veckeneer et al., 2017). Clinical trials for replacement with healthy retinal pigmented epithelial cells are

underway. There remains concerns for possible complications such as the uncontrolled proliferation of lab-grown cells which have slowed down some of the trials (Garber 2015). Nevertheless, with more advanced technology, bioengineers are leveraging on 3D printing methods to create scaffolds of blood vessels for laboratory and clinical use (Huang and Zhang, 2014). Recently, a group led by Wimmer et al. (2019) successfully developed 3D blood vessels organoids that functioned strikingly similar to real human blood vessels when transplanted into mice (Wimmer et al., 2019). These *in vitro* vascular platforms offer a promising and exciting outlook for enabling research on vasculopathy as research continues to push the frontiers of creating functional human-like blood vessels.

Both *in vivo* and *in vitro* models of choroidal neovascularization have been developed for researchers to study pathology from molecular to cellular and system level. Each model has its own strengths and weaknesses. Both *in vivo* and *in vitro* models are complementary and can be manipulated appropriately to address certain limitations as well as develop more fit-for-purpose models of ocular angiogenesis.

VASCULAR MECHANISMS IN CHOROIDAL NEOVASCULARIZATION

Here, we provide a nonexhaustive review of the known vascular mechanisms in choroidal neovascularization, ranging from the source of pathological endothelial cells to noncell and cell autonomous mechanisms leading to choroidal neovascularization. **Figure 2** provides an overview of our discussion in this section.

Source of Endothelial Cells in Choroidal Neovascularization

It was believed that all newly formed vessels in choroidal neovascularization arise from pre-existing choroidal vasculature (Ishibashi et al., 1987). However, in the 1990s, researchers discovered that circulating progenitor cells of bone marrow origin could in part contribute to postnatal vasculogenesis in both physiological and pathological neovascularization (Asahara et al., 1997; Asahara et al., 1999). Accumulating evidence then showed that circulating bone marrow progenitor cells contributed to newly generated endothelial cells specifically in choroidal neovascularization. Various groups have used the technique of transplanting EGFP-expressing bone marrow cells from EGFP donor mice into recipient mice and subsequently subjecting them to laser photocoagulation to induce injury in the choroid. The extent of donor derived GFP+ cells recruited to choroidal vasculatures or sites of Bruch membrane injury was then quantified. Often, GFP+ endothelial cells were found to give rise to different degrees of contribution to lesion endothelial cells (Sengupta et al., 2003; Tomita et al., 2004). Besides endothelial cells, a proportion of GFP+ cells was found to be immunoactive for vascular smooth muscle markers (Espinosa-Heidmann et al., 2003). Variability in levels of contribution to lesion endothelial cells was also observed depending on the stage of progression of choroidal neovascularization (Espinosa-Heidmann et al., 2005;

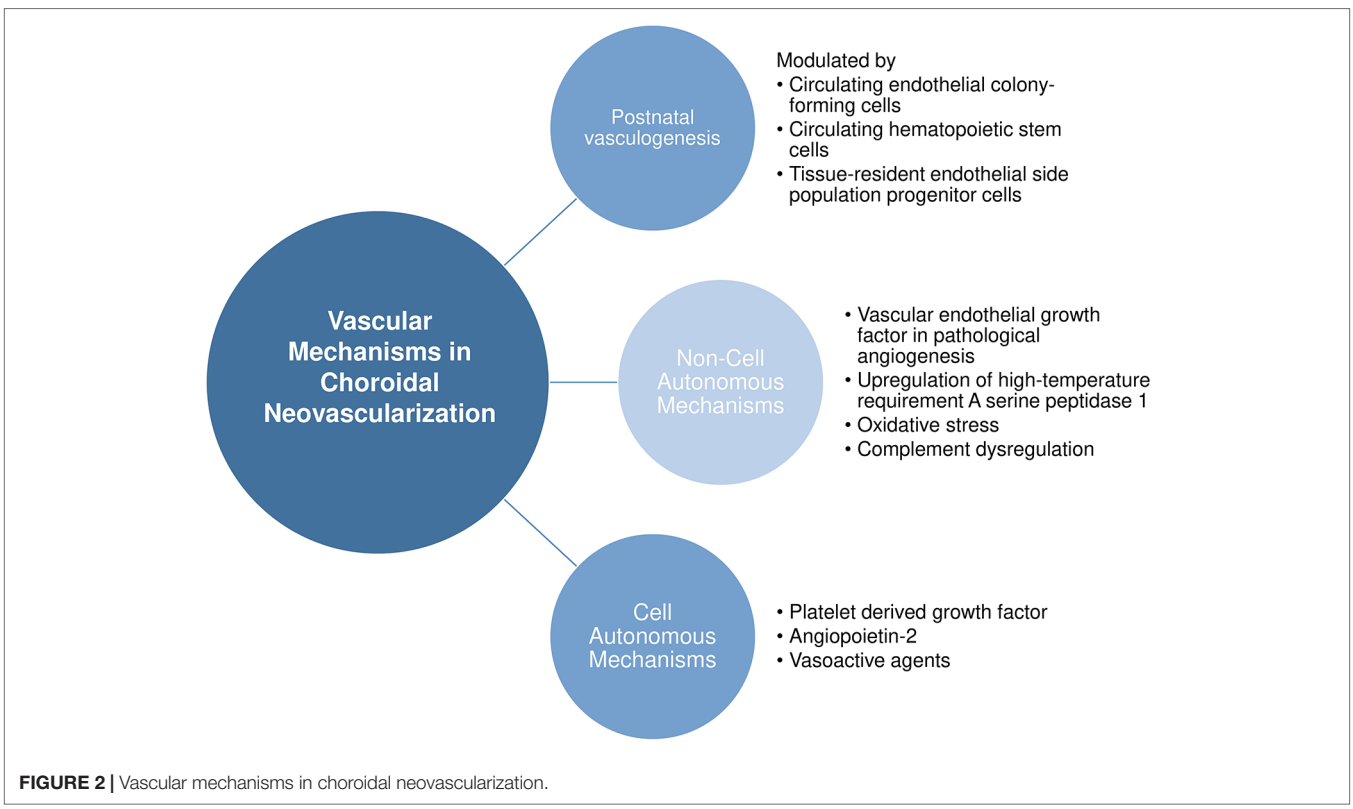

FIGURE 2 | Vascular mechanisms in choroidal neovascularization.

Hou et al., 2006). In addition, circulating adult hematopoietic stem cells are mobilized into the injury region and are able to form endothelial cells that are subsequently incorporated into choroidal neovasculature (Chan-Ling et al., 2006). Such hemangioblast activity was also observed in a murine model of retinal neovascularization (Grant et al., 2002). Similarly, evidence of bone marrow contribution to choroidal neovascularization was observed in humans. Using AC133 a putative marker of both human hematopoietic stem and bone marrow-derived progenitor cells, Sheridan et al. identified the presence of bone marrow-derived progenitor cells in excised human choroidal neovascularization sections, albeit in very low numbers (Sheridan et al., 2006). **Table 2** presents a summary of the aforementioned *in vivo* studies.

The mechanisms by which bone marrow progenitors are recruited to choroidal neovascularization sites have been described. Bone marrow derived cells incorporated into choroidal vasculature only at sites of laser-induced injury (Espinosa-Heidmann et al., 2003; Sengupta et al., 2003; Takahashi et al., 2004; Hou et al., 2006). This suggests that vascular injury is required for the mobilization of these cells and the microenvironment of the choroidal neovascular lesion might secrete molecular signals that assist in the recruitment and differentiation of circulating progenitor cells into vascular endothelial and smooth muscle cells *in situ* (Hou et al., 2006). Gao and colleagues have proposed that the process occurs in four phases: mobilization, migration, adhesion, and differentiation (Gao et al., 2016). Upon local tissue injury, the levels of various cytokines such as VEGF, granulocyte colony-stimulating factor (G-CSF), and erythropoietin (EPO) increase, which result in MMP9 activation, triggering the release of bone marrow cells from interacting stromal cells in the bone marrow (mobilization). The chemotactic gradients of cytokines then facilitate the migration of bone marrow cells to the local neovascular lesion site. Key chemokine mediators in choroidal neovascularization include the chemoattractant stromal derived factor (SDF-1), which is upregulated by retinal pigmented epithelium upon laser injury and binds to its concomitant receptor CXCR4 on bone marrow cells (Zhang et al., 2011). Cell adhesion molecules such as VCAM-1 and ICAM-1 then facilitate the adhesion of migrated bone marrow cells to existing endothelial cells at the site of choroidal neovascularization. The final phase of differentiation of the bone marrow progenitors to endothelial cells, smooth muscle cells, and macrophages then occur at the site of choroidal neovascularization. To summarize, choroidal neovascular injury specifically mobilizes and incorporates new vascular cells from the bone marrow into the injury site utilizing a complex repertoire of factors, pointing to the need to consider these processes in the pathological mechanisms of wet AMD.

Of note, there are also several studies that refute the contribution of bone marrow cells to postnatal vasculogenesis. Okuno and colleagues showed that bone marrow-derived cells did not contribute to the wound healing site as differentiated endothelial cells, but instead mainly as pro-angiogenic macrophages (Okuno et al., 2011). Grunwald et al. proposed that these recruited bone marrow cells are retained close to the neovasculature and exert proangiogenic effects on *in situ* endothelial cells (Grunewald et al., 2006). In line with the latter, Purhonen and colleagues demonstrated that during vasculogenesis none of the recruited bone marrow-derived cells contributed to the endothelium and contended that *in vivo* endothelial differentiation is a rare event for these cells (Purhonen et al., 2008). Alternatively, resident stem-like/progenitor cells have been discovered in pre-existing endothelium which demonstrate colony-forming ability (Naito et al., 2012). Wakabayashi and colleagues found that these resident progenitors (termed endothelial side population cells) did not originate from bone marrow and were thus distinct from bone marrow-derived endothelial progenitors. The endothelial side population cells isolated from murine choroidal tissue also displayed strong colony-forming ability *in vitro*, and increased proliferation upon laser-induced choroidal neovascularization *in vivo*, suggesting their ability to contribute to neovascular vessels (Wakabayashi et al., 2013). These studies highlight that postnatal vasculogenesis occurs to a significant extent in choroidal neovascularization. Taken together, endothelial cells

TABLE 2 | Summary of studies reporting bone marrow origin of endothelial cells in choroidal neovascularization.

Study references	Model species	Percentage of CD31+ endothelial cells in choroidal neovasculature that were bone-marrow derived	Total donor-derived bone marrow contribution to choroidal neovasculature	Percentage of bone marrow population in choroidal neovasculature that were endothelial
Tomita et al. (2004)	Murine	–	–	70%
Sengupta et al. (2003)	Murine	–	40 – 45%	–
Espinosa-Heidmann et al. (2003)	Murine	–	17%	41%
Takahashi et al. (2004)	Murine	5.3%	22% (total no. of cells: 154 ± 37; no. of marrow-derived cells: 34 ± 17)	20%
Espinosa-Heidmann et al. (2005)	Murine	65% in early choroidal neovascularization (3 days) 50% in late choroidal neovascularization (4 weeks)	20 – 40%	–
Hou et al. (2006)	Murine	70% in early choroidal neovascularization (7 days) 50% in late choroidal neovascularization (4 weeks)	–	31%
Sheridan et al. (2006)	Human	–	<0.1% stained for AC133	–

that participate choroidal neovascularization could potentially originate from these sources: (1) circulating bone marrow progenitors, (2) circulating hematopoietic stem cells that have hemangioblast activity, and (3) vessel-residing endothelial side population cells that have high colony-forming activity. **Figure 3** provides a graphical representation of our discussion above.

Noncell Autonomous Mechanisms

Vascular Endothelial Growth Factor in Pathological Angiogenesis

Dysregulation of VEGF signaling in lesion sites is known as one of the key stimuli for pathological angiogenesis (Kinnunen and Ylä-Herttuala, 2012). VEGF, existing as its various isoforms $VEGF_{121}$, $VEGF_{145}$, $VEGF_{165}$, $VEGF_{189}$, and $VEGF_{206}$, is a potent angiogenic molecule that is known to stimulate proliferation, migration, tube formation, and vascular permeability of endothelial cells (Ferrara et al., 1991; Papadopoulos et al., 2012). The physiological importance of VEGF in the outer retina is well known. During fetal development, the retinal pigmented epithelium constitutively releases VEGF and FGF2 that are crucial for development of the choriocapillaris (Saint-Geniez and D'Amore, 2004; Anand-Apte and Hollyfield, 2010). VEGF released from the basal side of the RPE monolayer is required for the formation of fenestrations in the choriocapillaris (Blaauwgeers et al., 1999; Marneros et al., 2005). These important structures serve a role of allowing large macromolecules to be transported in and out of choroidal circulation (Anand-Apte and Hollyfield, 2010). *In vivo* studies report that knock-out of *vegf* in the RPE resulted in total ablation of the choriocapillaris (Korte et al., 1984; Kurihara et al., 2012). Therefore, locally synthesized VEGF from the RPE is critical for the maintenance of the choriocapillaris. In physiological conditions, ocular levels of VEGF are low, but in pathological conditions like choroidal neovascularization, VEGF levels are significantly elevated in affected sites (Kvanta et al., 1996; Kinnunen and Ylä-Herttuala, 2012). Of note, the VEGF isoform found to participate predominantly in pathological angiogenesis is $VEGF_{164/165}$ (Ishida et al., 2003). In pathological angiogenesis, VEGF from hypoxic retina is believed to be the key driver (Miller et al., 1997; Papadopoulos et al., 2012). On top of its known functions of stimulating angiogenesis of choroidal vessels, elevated VEGF in the RPE leads to barrier integrity breakdown which could promote neovascularization (Ablonczy et al., 2011; Marneros 2013). As a proof of concept, treatment with VEGF antagonists have shown some success in reducing choroidal neovascularization lesion size and slowing the rate of vision loss (Schlingemann and Witmer, 2009; Kinnunen and Ylä-Herttuala, 2012; Papadopoulos et al., 2012). However, anti-VEGF drugs are not entirely effective to treat all choroidal neovascularization lesions in wet AMD and are also unable to prevent recurrence of symptoms, therefore pointing to the role of other interacting pathways of pathological neovascularization.

Upregulation of High-Temperature Requirement A Serine Peptidase 1

High-temperature requirement A serine peptidase 1 (HTRA1) is a multi-functional serine protease expressed in endothelium, epidermis, and neurons that regulates vascular growth and maintenance and is required for the normal development of vasculature in the brain and eye (De Luca et al., 2003; Jiang et al., 2012; Zhang et al., 2012). In 2006, it was reported that the SNP rs11200638 on the promoter sequence of *HTRA1* at chromosome 10q26 was the strongest casual genetic risk factor for AMD. The risk allele AA was associated with elevated levels of both *HTRA1* mRNA in lymphocytes of AMD donors and HTRA1 protein in retinal pigmented epithelium of AMD donors (DeWan et al., 2006; Yang et al., 2006). In line with these findings, Chan et al.

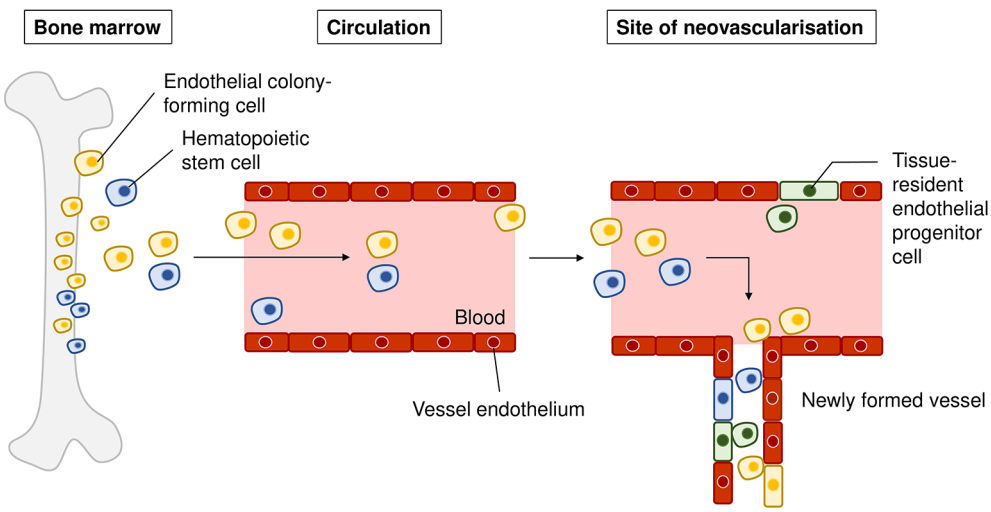

FIGURE 3 | Sources of recruited endothelial cells in choroidal neovascularization. Endothelial colony-forming cells (yellow) from the bone marrow can be mobilized from the bone marrow into the circulation, migrate to the site of neovascularization, and differentiate into vascular cells that form the new vasculature. Hematopoietic stem cells (blue) can be mobilized to the site of injury, differentiate into endothelial cells and be incorporated into newly formed vasculature. Tissue-resident endothelial side population cells (green) residing in choroidal endothelium have been proposed to contribute to choroidal neovascularization upon injury.

found that HTRA1 mRNA expression was higher in the macula of AMD eyes with the AA genotype compared to non-AMD eyes (Chan et al., 2007). Elevated HTRA1 levels was also observed in the aqueous humor of patients with wet AMD (Tosi et al., 2017). The overexpression of human HTRA1 in the RPE of mice has been shown to result in development of PCV (choroidal lesions with polypoidal structure), although classic choroidal neovascularization formation was not observed (Jones et al., 2011). Furthermore, presence of HTRA1 protein was observed in the drusen of AMD patients (DeWan et al., 2006; Yang et al., 2006). Several mechanisms have been proposed for how HTRA1 overexpression could lead to choroidal neovascularization observed in wet AMD. Firstly, HTRA1 has been suggested to increase activity of degradative extracellular matrix enzymes and thus promote matrix breakdown (Grau et al., 2006; Jones et al., 2011). *In vivo* studies of transgenic mice overexpressing HTRA1 in the RPE described ultrastructural changes in Bruch's membrane ECM (Vierkotten et al., 2011). It was therefore suggested that, in wet AMD, higher levels of HTRA1 compromise the integrity of Bruch's membrane, allowing infiltration of choroidal vasculature through the layered matrix (Yang et al., 2006). Secondly, HTRA1 is also known to inhibit the activity of transforming growth factor (TGF-ß) family proteins which have important roles in angiogenesis and extracellular matrix production (Oka et al., 2004; Zhang et al., 2012). Mathura et al. reported that the TGF-ß proteins BMP-2 and BMP-4 might serve as repressors of RPE growth and any dysregulation of the BMPs might lead to aberrant wound repair as observed in proliferative retinopathies (Mathura et al., 2000). Therefore, increased levels of HTRA1 in the RPE of AMD patients with risk genotype might result in pathological choroidal neovascularization through (1) promoting degradation of Bruch's membrane and compromising barrier function and (2) inhibiting BMP signaling thus removing a negative regulator for aberrant wound repair response.

Oxidative Stress

Antioxidants have been found to slow progression of progression from early AMD to advanced stages of AMD (wet AMD or severe geographic atrophy), thus highlighting the role of oxidative stress in AMD progression (Dong et al., 2009). Oxidative stress may facilitate in creating a pro-angiogenic environment in the outer retina and choroid, which coupled with altered integrity of Bruch's membrane may trigger the development of choroidal neovascularization as observed in wet AMD (Dong et al., 2009). In addition, oxidative stress is also known to stimulate premature senescence of RPE, a key event in the pathogenesis of AMD (Supanji et al., 2013). Senescent RPE has been found to increase the expression of VEGF and downregulate CFH, both of which are known to contribute to the development of choroidal neovascularization (Marazita et al., 2016; Kaarniranta et al., 2018). Of note, Supanji et al. showed that oxidative stress stimulated RPE cells to increase production of HTRA1 which when in excess accelerated premature senescence of the RPE cells (Supanji et al., 2013), suggesting that HTRA1 also has a role in influencing RPE senescence. These studies point to the complex role of oxidative stress in contributing to ocular neovascularization.

Complement Dysregulation

The complement system participates in the innate immune response as the first immediate acting system before cellular response is carried out by macrophages and neutrophils. It is composed of more than 30 small proteins and activation products with chemotactic, inflammatory, cytotoxic, and antimicrobial functions (Zipfel, 2009). Once fully activated, formation of the membrane attack complex will occur, which is then be able to destroy cells and pathogens (Xu and Chen, 2016). Membrane attack complex deposition occurs naturally in healthy aging choriocapillaris (Mullins et al., 2014; Chirco et al., 2016). With a physiological balance of activation and repression of the complement system, self-tissue destruction is avoided. In AMD pathogenesis, a lack of repression of the complement system is implicated (Maugeri et al., 2018). Multiple complement products, such as C3, C5b-9, CFH, and CFB have been found in AMD lesions and drusen (Nozaki et al., 2006; Xu and Chen, 2016). Furthermore, as revealed by GWAS, genetic polymorphisms in complement genes such as CFH, CFB, C2, C3, C5, and SERPING1 confer risk for AMD, suggesting the role of complement dysregulation in the pathogenesis of AMD (Khandhadia et al., 2012). However, while numerous components are involved in AMD, only C3 and C5 have been reported for their roles in choroidal neovascularization. Nozaki et al. showed that induction of choroidal neovascularization *in vivo* increased levels of C3a and C5a, and C3a and C5a induced increase in VEGF secretion by primary human RPE *in vitro* (Nozaki et al., 2006). Knock out of the C3 gene protected mice from choroidal neovascularization after laser treatment (Bora et al., 2005), and genetic ablation of both C3a and C5a receptors results in lower VEGF secretion by RPE cells leading to decreased choroidal neovascularization (Nozaki et al., 2006). Overall, build-up of membrane attack complex in the choriocapillaris and dysregulated complement activation might contribute to an angiogenic environment for the development of choroidal neovascularization.

Cell Autonomous Mechanisms

Platelet Derived Growth Factor

The long-term efficacy of anti-VEGF monotherapy on visual outcomes has been variable, with the need for repeated and lifelong treatment for patients with wet AMD (Singer et al., 2012; Rofagha et al., 2013; Silva et al., 2013). A common trend of initial visual improvement in the first few months followed by a plateau that lasts throughout the course of treatment has raised the notion of anti-VEGF resistance. In tumor studies, anti-VEGF resistance has been attributed to the secretion of platelet-derived growth factor (PDGF) by tumor cells which stimulate the recruitment and proliferation of pericytes to developing vasculature. On top of the physical stabilizing support rendered by pericytes, PDGF stimulates pericytes to upregulate VEGF which promote endothelial survival (Reinmuth et al., 2001; Franco et al., 2011). In choroidal neovascular sites, tip cells that form the vascular front express PDGF, causing recruitment of pericytes to the neovasculature and thereafter microvessel maturation. Newly recruited pericytes form a protective barrier

around the newly formed endothelium in the face of anti-VEGF therapy, reducing the effect of VEGF inhibitors and explaining the plateau phase in long term anti-VEGF treatment (Franco et al., 2011; Pachydaki et al., 2012). In line with this hypothesis, choroidal neovascular lesions from patients who were unresponsive to anti-VEGF therapy, were also found to be well-formed and "consistently exhibit pericytes" (Pachydaki et al., 2012).

Considering these findings, PDGF inhibitors were proposed in combination therapy with current anti-VEGF monotherapy for wet AMD. E10030 (Fovista; Ophthotech, New York, NY) is a DNA aptamer against PDGF that was recently assessed for its efficacy in combination therapy with the anti-VEGF treatment ranibizumab (Lucentis). The results from a phase 2b clinical trial showed that there was a 62% benefit from baseline with combination therapy compared with anti-VEGF monotherapy (Jaffe et al., 2017). However, much to the disappointment of clinical investigators, the following two phase 3 trials showed that Fovista in combination with ranibizumab showed no superiority over ranibizumab monotherapy. Further on, two other phase 2 studies investigating Fovista in combination with two other anti-VEGF approved drugs were terminated (Dunn et al., 2017). The failed anti-PDGF clinical trials have taught us a few lessons: firstly, that phase 3 trials should not be designed based on retrospective subgroup analyses of phase 2 trial results (as was done in Fovista phase 3 trials) (Rosenfeld and Feuer, 2018), and secondly, that failure with PDGF antagonists indicate the need to shift efforts to target other mechanisms of choroidal neovascularization in AMD.

Angiopoietin-2

Angiopoietin-2 (ANG2) is a proangiogenic cytokine that plays a role in both angiogenesis and immune activation, both of which are integral processes in the pathogenesis of wet AMD (Fiedler et al., 2006; Wolf and Langmann, 2019). ANG2 levels have been found to be upregulated in aqueous humor of wet AMD human donors and increasing with disease severity (Ng et al., 2017). Due to its additional role in inflammation that is implicated in wet AMD, ANG2 has become a potential therapeutic target in wet AMD beyond anti-VEGF therapies (Gahn and Khanani, 2018). *In vivo* experiments have recently demonstrated ANG2 and VEGF combinatory inhibition led to reduced neovascular lesion formation in a spontaneous chronic choroidal neovascularization mouse model (JR5558 mice) (Foxton et al., 2019). This has been carried forward to phase 1 and 2 clinical trials with the bispecific antibody anti-VEGF-A/ANG2 (RG7116; Roche/Genetech). Currently, RG7116, now known as faricimab, is being tested in phase 3 trials in comparison with the VEGF trap drug aflibercept (Eylea) (Wolf and Langmann 2019). The shift in efforts towards VEGF-independent pathways in wet AMD is promising; and it is hoped that more novel targetable candidates would be uncovered.

Vasoactive Agents

Endothelial cells produce a physiological balance of vasoactive substances to regulate vascular function, such as the vasoconstrictor endothelin-1 (ET-1) and the vasodilator nitric oxide (NO). ET-1 levels increase while NO availability decreases during aging, resulting in increased vasoconstriction and impaired vasodilation, which could lead to constriction of smaller vessels associated with ischemia of the choriocapillaris (decreased choroidal blood flow) seen in severe dry AMD (Stauffer et al., 2008; El Assar De La Fuente et al., 2012; Totan et al., 2015). Decreased choroidal blood flow in dry AMD has been correlated with severity of dry AMD, and could increase the risk for ischemia and hypoxia leading to choroidal neovascularization in wet AMD (Grunwald et al., 2005). Totan et al. showed that patients with wet AMD exhibit increased ET-1 and decreased NO in the plasma, indicating that endothelial dysfunction is apparent in these patients (Totan et al., 2015). With age being the largest risk factor for AMD, it is not surprising that age-related vascular dysfunction would contribute to the progression of AMD, as seen also in a number of age-related diseases (Ehrlich et al., 2009; Akpek and Smith, 2013). Therefore, endothelial dysfunction in the choriocapillaris could play a role in AMD pathogenesis.

CONCLUSION

With the great momentum in the study of choroidal neovascularization, there remains knowledge gaps which the scientific and clinical communities could address. We propose that further research on the following areas could be illuminating. (1) AMD subtypes could have different etiology, rendering it important to investigate subtype-specific mechanisms. Genomics distinguishing typical AMD and polypoidal choroidal vasculopathy may elucidate subtype-specific mechanisms. (2) Perturbations to choroidal vasculatures may have to be looked in the context of other influences. Existing experimental models could be adapted to recapitulate potential systemic/immune factors, as well as to study endothelial interplay with other cell types. (3) Finally, there is a need to explore both VEGF- and non-VEGF pathways to enhance the success of combinatorial treatment. We hope that vascular-targeting strategy will help advance therapy for early intervention.

AUTHOR CONTRIBUTIONS

CC provided the strategic focus for this review paper and edited the manuscript. NY and EC wrote and prepared the manuscript.

FUNDING

We are grateful for the funding support of an Academic Research Fund (AcRF) Tier 2 grant (MOE2018-T2-1-042) from the Ministry of Education, Singapore, as well as support from the SERI-IMCB Program in Retinal Angiogenic Diseases (SIPRAD) grant number SPF2014/002, a grant from A-STAR (Agency for Science Technology and Research, Singapore).

REFERENCES

Ablonczy, Z., Dahrouj, M., Tang, P. H., Liu, Y., Sambamurti, K., Marmorstein, A. D., et al. (2011). Human retinal pigment epithelium cells as functional models for the RPE in vivo. *Invest. Ophthalmol. Visual Sci.* 52 (12), 8614–8620. doi: 10.1167/iovs.11-8021

Akaza, E., Yuzawa, M., Matsumoto, Y., Kashiwakura, S., Fujita, K., and Mori, R. (2007). Role of photodynamic therapy in polypoidal choroidal vasculopathy. *Jpn J. Ophthalmol.* 51 (4), 270–277. doi: 10.1007/s10384-007-0452-3

Akpek, E. K., and Smith, R. A. (2013). Overview of age-related ocular conditions. *Am. J. Manag Care* 19 (5 Suppl), S67–S75.

Ambati, J., Atkinson, J. P., and Gelfand, B. D. (2013). Immunology of age-related macular degeneration. *Nat. Rev. Immunol.* 13 (6), 438. doi: 10.1038/nri3459

Anand-Apte, B., and Hollyfield, J. G. (2010). Developmental anatomy of the retinal and choroidal vasculature. In: Besharse, Joseph C. & Bok, Dean, eds. *The Retina and Its Disorders.* (San Diego, CA: Academic Press) 179–185. doi: 10.1016/B978-0-12-374203-2.00169-X

Arvanitakis, Z., Capuano, A. W., Leurgans, S. E., Bennett, D. A., and Schneider, J. A. (2016). Relation of cerebral vessel disease to Alzheimer's disease dementia and cognitive function in elderly people: a cross-sectional study. *Lancet Neurol.* 15 (9), 934–943. doi: 10.1016/S1474-4422(16)30029-1

Asahara, T., Murohara, T., Sullivan, A., Silver, M., van der Zee, R., Li, T., et al. (1997). Isolation of putative progenitor endothelial cells for angiogenesis. *Science* 275 (5302), 964–966. doi: 10.1126/science.275.5302.964

Asahara, T., Masuda, H., Takahashi, T., Kalka, C., Pastore, C., Silver, M., et al. (1999). Bone marrow origin of endothelial progenitor cells responsible for postnatal vasculogenesis in physiological and pathological neovascularization. *Circ. Res.* 85 (3), 221–228. doi: 10.1161/01.RES.85.3.221

Beatty, S., Koh, H.-H., Phil, M., Henson, D., and Boulton, M. (2000). The role of oxidative stress in the pathogenesis of age-related macular degeneration. *Survey Ophthalmol.* 45 (2), 115–134. doi: 10.1016/S0039-6257(00)00140-5

Berenberg, T. L., Metelitsina, T. I., Madow, B., Dai, Y., Ying, G.-S., Dupont, J. C., et al. (2012). The association between drusen extent and foveolar choroidal blood flow in age-related macular degeneration. *Retina (Philadelphia Pa.)* 32 (1), 25. doi: 10.1097/IAE.0b013e3182150483

Bhutto, I., and Lutty, G. (2012). Understanding age-related macular degeneration (AMD): relationships between the photoreceptor/retinal pigment epithelium/Bruch's membrane/choriocapillaris complex. *Mol. Aspects Med.* 33 (4), 295–317. doi: 10.1016/j.mam.2012.04.005

Biesemeier, A., Taubitz, T., Julien, S., Yoeruek, E., and Schraermeyer, U. (2014). Choriocapillaris breakdown precedes retinal degeneration in age-related macular degeneration. *Neurobiol. Aging* 35 (11), 2562–2573. doi: 10.1016/j.neurobiolaging.2014.05.003

Blaauwgeers, H. G., Holtkamp, G. M., Rutten, H., Witmer, A. N., Koolwijk, P., Partanen, T. A., et al. (1999). Polarized vascular endothelial growth factor secretion by human retinal pigment epithelium and localization of vascular endothelial growth factor receptors on the inner choriocapillaris: evidence for a trophic paracrine relation. *Am. J. Pathol.* 155 (2), 421–428. doi: 10.1016/S0002-9440(10)65138-3

Boos, C. J., Lip, G. Y., and Blann, A. D. (2006). Circulating endothelial cells in cardiovascular disease. *J. Am. Coll. Cardiol.* 48 (8), 1538–1547. doi: 10.1016/j.jacc.2006.02.078

Bora, P. S., Hu, Z., Tezel, T. H., Sohn, J.-H., Kang, S. G., Cruz, J. M., et al. (2003). Immunotherapy for choroidal neovascularization in a laser-induced mouse model simulating exudative (wet) macular degeneration. *Proc. Natl. Acad. Sci.* 100 (5), 2679–2684. doi: 10.1073/pnas.0438014100

Bora, P. S., Sohn, J.-H., Cruz, J. M., Jha, P., Nishihori, H., Wang, Y., et al. (2005). Role of complement and complement membrane attack complex in laser-induced choroidal neovascularization. *J. Immunol.* 174 (1), 491–497. doi: 10.4049/jimmunol.174.1.491

Bouras, C., Kovari, E., Herrmann, F. R., Rivara, C. B., Bailey, T. L., von Gunten, A., et al. (2006). Stereologic analysis of microvascular morphology in the elderly: Alzheimer disease pathology and cognitive status. *J. Neuropathol. Exp. Neurol.* 65 (3), 235–244. doi: 10.1097/01.jnen.0000203077.53080.2c

Boyle, E. A., Li, Y. I., and Pritchard, J. K. (2017). An expanded view of complex traits: from polygenic to omnigenic. *Cell* 169 (7), 1177–1186. doi: 10.1016/j.cell.2017.05.038

Bracha, P., Moore, N. A., and Ciulla, T. A. (2017). Induced pluripotent stem cell-based therapy for age-related macular degeneration. *Expert Opin. Biol. Ther.* 17 (9), 1113–1126. doi: 10.1080/14712598.2017.1346079

Buee, L., Hof, P. R., Bouras, C., Delacourte, A., Perl, D. P., Morrison, J. H., et al. (1994). Pathological alterations of the cerebral microvasculature in Alzheimer's disease and related dementing disorders. *Acta Neuropathol.* 87 (5), 469–480. doi: 10.1007/BF00294173

Cai, H., and Harrison, D. G. (2000). Endothelial dysfunction in cardiovascular diseases: the role of oxidant stress. *Circ. Res.* 87 (10), 840–844. doi: 10.1161/01.RES.87.10.840

CATT Research Group. (2011). Ranibizumab and bevacizumab for neovascular age-related macular degeneration. *New Engl. J. Med.* 364 (20), 1897–1908. doi: 10.1056/NEJMoa1102673

Chan, C.-C., Shen, D., Zhou, M., Ross, R. J., Ding, X., Zhang, K., et al. (2007). Human HtrA1 in the archived eyes with age-related macular degeneration. *Trans. Am. Ophthalmol. Soc.* 105, 92.

Chan-Ling, T., Baxter, L., Afzal, A., Sengupta, N., Caballero, S., Rosinova, E., et al. (2006). Hematopoietic stem cells provide repair functions after laser-induced Bruch's membrane rupture model of choroidal neovascularization. *Am. J. Pathol.* 168 (3), 1031–1044. doi: 10.2353/ajpath.2006.050697

Cheng, H.-C., Liu, J.-H., Lee, S.-M., and Lin, P.-K. (2014). Hyperhomocysteinemia in patients with polypoidal choroidal vasculopathy: a case control study. *PloS One* 9 (10), e110818. doi: 10.1371/journal.pone.0110818

Cheng, C.-Y., Yamashiro, K., Jia Chen, L., Ahn, J., Huang, L., Huang, L., et al. (2015). New loci and coding variants confer risk for age-related macular degeneration in East Asians. *Nat. Commun.* 6, 6063. doi: 10.1038/ncomms7063

Cheung, C., and Wong, T. (2014). "Is age-related macular degeneration a manifestation of systemic disease? New prospects for early intervention and treatment. *J. Internal Med.* 276 (2), 140–153. doi: 10.1111/joim.12227

Cheung, N., Liao, D., Islam, F. A., Klein, R., Wang, J. J., and Wong, T. Y. (2007). "Is early age-related macular degeneration related to carotid artery stiffness? The Atherosclerosis Risk in Communities Study. *Br. J. Ophthalmol.* 91 (4), 430–433. doi: 10.1136/bjo.2006.106054

Chichagova, V., Hallam, D., Collin, J., Zerti, D., Dorgau, B., Felemban, M., et al. (2018). Cellular regeneration strategies for macular degeneration: past, present and future. *Eye* 32 (5), 946. doi: 10.1038/s41433-018-0061-z

Chirco, K. R., Tucker, B. A., Stone, E. M., and Mullins, R. F. (2016). Selective accumulation of the complement membrane attack complex in aging choriocapillaris. *Exp. Eye Res.* 146, 393–397. doi: 10.1016/j.exer.2015.09.003

Chirco, K., Sohn, E., Stone, E., Tucker, B., and Mullins, R. (2017). Structural and molecular changes in the aging choroid: implications for age-related macular degeneration. *Eye* 31 (1), 10. doi: 10.1038/eye.2016.216

Cho, H., Kim, J., Lee, D., Cho, S., and Kim, C. (2012). Intravitreal bevacizumab and ranibizumab injections for patients with polypoidal choroidal vasculopathy. *Eye* 26 (3), 426. doi: 10.1038/eye.2011.324

Chung, S. E., Kang, S. W., Kim, J. H., and Kim, Y. T. (2013). Engorgement of vortex vein and polypoidal choroidal vasculopathy. *Retina* 33 (4), 834–840. doi: 10.1097/IAE.0b013e31826af540

Chung, S.-D., Ho, J.-D., Hu, C.-C., Lin, H.-C., and Sheu, J.-J. (2014). Increased risk of Parkinson disease following a diagnosis of neovascular age-related macular degeneration: a retrospective cohort study. *Am. J. Ophthalmol.* 157 (2), 464–469. doi: 10.1016/j.ajo.2013.09.026 e461

Clark, S. J., Perveen, R., Hakobyan, S., Morgan, B. P., Sim, R. B., Bishop, P. N., et al. (2010). Impaired binding of the age-related macular degeneration-associated complement factor H 402H allotype to Bruch's membrane in human retina. *J. Biol. Chem.* 285 (39), 30192–30202. doi: 10.1074/jbc.M110.103986

Clark, S. J., Ridge, L. A., Herbert, A. P., Hakobyan, S., Mulloy, B., Lennon, R., et al. (2013). Tissue-specific host recognition by complement factor H is mediated by differential activities of its glycosaminoglycan-binding regions. *J Immunol* 190 (5), 2049–2057. doi: 10.4049/jimmunol.1201751

Couch, S. M., Bakri, S. J., Couch, S. M., and Bakri, S. J. (2011). Review of combination therapies for neovascular age-related macular degeneration. Seminars in ophthalmology, Taylor & Francis. doi: 10.3109/08820538.2011.577130

Davignon, J., and Ganz, P. (2004). Role of endothelial dysfunction in atherosclerosis. *Circulation* 109 (23_suppl_1), III–27-III-32. doi: 10.1161/01.CIR.0000131515.03336.f8

De Luca, A., De Falco, M., Severino, A., Campioni, M., Santini, D., Baldi, F., et al. (2003). Distribution of the serine protease HtrA1 in normal human tissues. *J. Histochem. Cytochem.* 51 (10), 1279–1284. doi: 10.1177/002215540305101004

DeWan, A., Liu, M., Hartman, S., Zhang, S. S.-M., Liu, D. T., Zhao, C., et al. (2006). HTRA1 promoter polymorphism in wet age-related macular degeneration. *Science* 314 (5801), 989–992. doi: 10.1126/science.1133807

Dobi, E. T., Puliafito, C. A., and Destro, M. (1989). A new model of experimental choroidal neovascularization in the rat. *Arch. Ophthalmol.* 107 (2), 264–269. doi: 10.1001/archopht.1989.01070010270035

Dong, A., Xie, B., Shen, J., Yoshida, T., Yokoi, K., Hackett, S. F., et al. (2009). Oxidative stress promotes ocular neovascularization. *J. Cell. Physiol.* 219 (3), 544–552. doi: 10.1002/jcp.21698

Dunn, E. N., Hariprasad, S. M., and Sheth, V. S. (2017). An overview of the fovista and rinucumab trials and the fate of anti-PDGF medications. *Ophthalmic Surgery Lasers Imaging Retina* 48 (2), 100–104. doi: 10.3928/23258160-20170130-02

Dutescu, R. M., Li, Q.-X., Crowston, J., Masters, C. L., Baird, P. N., and Culvenor, J. G. (2009). Amyloid precursor protein processing and retinal pathology in mouse models of Alzheimer's disease. *Graefe's Arch. Clin. Exp. Ophthalmol.* 247 (9), 1213–1221. doi: 10.1007/s00417-009-1060-3

Ehrlich, R., Kheradiya, N. S., Winston, D. M., Moore, D. B., Wirostko, B., and Harris, A. (2009). Age-related ocular vascular changes. *Graefe's Arch. Clin. Exp. Ophthalmol.* 247 (5), 583. doi: 10.1007/s00417-008-1018-x

El Assar De La Fuente, M., Angulo Frutos, J., Vallejo Fernán, S., Peiró Vallejo, C., Sánchez-Ferrer, C., and Rodríguez-Mañas, L. (2012). Mechanisms involved in the aging-induced vascular dysfunction. *Front. In Physiol.* 3 (132), 1–13. doi: 10.3389/fphys.2012.00132

Else, H. (2019). Genomics institute to close world-leading animal facility. *Nature* 569 (7758), 612. doi: 10.1038/d41586-019-01685-7

Erdbruegger, U., Haubitz, M., and Woywodt, A. (2006). Circulating endothelial cells: a novel marker of endothelial damage. *Clinica Chimica Acta* 373 (1–2), 17–26. doi: 10.1016/j.cca.2006.05.016

Espinosa-Heidmann, D. G., Caicedo, A., Hernandez, E. P., Csaky, K. G., and Cousins, S. W. (2003). Bone marrow-derived progenitor cells contribute to experimental choroidal neovascularization. *Invest. Ophthalmol. Visual Sci.* 44 (11), 4914–4919. doi: 10.1167/iovs.03-0371

Espinosa-Heidmann, D. G., Reinoso, M. A., Pina, Y., Csaky, K. G., Caicedo, A., and Cousins, S. W. (2005). Quantitative enumeration of vascular smooth muscle cells and endothelial cells derived from bone marrow precursors in experimental choroidal neovascularization. *Exp. Eye Res.* 80 (3), 369–378. doi: 10.1016/j.exer.2004.10.005

Fernández-Robredo, P., Sancho, A., Johnen, S., Recalde, S., Gama, N., Thumann, G., et al. (2014). Current treatment limitations in age-related macular degeneration and future approaches based on cell therapy and tissue engineering. *J. Ophthalmol.* 2014, 510285. doi: 10.1155/2014/510285

Ferrara, N., Houck, K. A., Jakeman, L. B., Winer, J., and Leung, D. W. (1991). The vascular endothelial growth factor family of polypeptides. *J. Cell. Biochem.* 47 (3), 211–218. doi: 10.1002/jcb.240470305

Ferreira, V. P., Herbert, A. P., Cortés, C., McKee, K. A., Blaum, B. S., Esswein, S. T., et al. (2009). The binding of factor H to a complex of physiological polyanions and C3b on cells is impaired in atypical hemolytic uremic syndrome. *J. Immunol.* 182 (11), 7009–7018. doi: 10.4049/jimmunol.0804031

Ferris, F. L., Fine, S. L., and Hyman, X. X. X. L. (1984). Age-related macular degeneration and blindness due to neovascular maculopathy. *Arch. Ophthalmol.* 102 (11), 1640–1642. doi: 10.1001/archopht.1984.01040031330019

Fiedler, U., Reiss, Y., Scharpfenecker, M., Grunow, V., Koidl, S., Thurston, G., et al. (2006). Angiopoietin-2 sensitizes endothelial cells to TNF-α and has a crucial role in the induction of inflammation. *Nat. Med.* 12 (2), 235. doi: 10.1038/nm1351

Fischer, V. W., Siddiqi, A., and Yusufaly, Y. (1990). Altered angioarchitecture in selected areas of brains with Alzheimer's disease. *Acta Neuropathol.* 79 (6), 672–679. doi: 10.1007/BF00294246

Fogli, S., Del Re, M., Rofi, E., Posarelli, C., Figus, M., and Danesi, R. (2018). Clinical pharmacology of intravitreal anti-VEGF drugs. *Eye* 32 (6), 1010. doi: 10.1038/s41433-018-0021-7

Foxton, R. H., Uhles, S., Grüner, S., Revelant, F., and Ullmer, C. (2019). Efficacy of simultaneous VEGF-A/ANG-2 neutralization in suppressing spontaneous choroidal neovascularization. *EMBO Mol. Med.* 11 (5), e10204. doi: 10.15252/emmm.201810204

Franco, M., Roswall, P., Cortez, E., Hanahan, D., and Pietras, K. (2011). Pericytes promote endothelial cell survival through induction of autocrine VEGF-A signaling and Bcl-w expression. *Blood* 118 (10), 2906–2917. doi: 10.1182/blood-2011-01-331694

Frank, R. N., Das, A., and Weber, M. L. (1989). A model of subretinal neovascularization in the pigmented rat. *Curr. Eye Res.* 8 (3), 239–247. doi: 10.3109/02713688908997565

Friedman, D. S., O'Colmain, B. J., Munoz, B., Tomany, S. C., McCarty, C., De Jong, P., et al. (2004). Prevalence of age-related macular degeneration in the United States. *Arch. Ophthalmol* 122 (4), 564–572. doi: 10.1001/archopht.1941.00870100042005

Fritsche, L. G., Chen, W., Schu, M., Yaspan, B. L., Yu, Y., Thorleifsson, G., et al. (2013). Seven new loci associated with age-related macular degeneration. *Nat. Genet.* 45 (4), 433. doi: 10.1038/ng.2578

Gahn, G. M., and Khanani, A. M. (2018). New therapies of neovascular AMD beyond Anti-VEGF injections. *Vision* 2 (1), 15. doi: 10.3390/vision2010015

Gao, F., Hou, H., Liang, H., Weinreb, R. N., Wang, H., and Wang, Y. (2016). Bone marrow-derived cells in ocular neovascularization: contribution and mechanisms. *Angiogenesis* 19 (2), 107–118. doi: 10.1007/s10456-016-9497-6

Garber, K., and Garber, K. (2015). RIKEN suspends first clinical trial involving induced pluripotent stem cells, Nature Publishing Group. doi: 10.1038/nbt0915-890

Giacalone, J. C., Miller, M. J., Workalemahu, G., Reutzel, A. J., Ochoa, D., Whitmore, S. S., et al. (2019). Generation of an immortalized human choroid endothelial cell line (iChEC-1) using an endothelial cell specific promoter. *Microvascular Res.* 123, 50–57. doi: 10.1016/j.mvr.2018.12.002

Gimbrone, M. A. Jr. (1995). Vascular endothelium: an integrator of pathophysiologic stimuli in atherosclerosis. *Am. J. Cardiol.* 75 (6), 67B–70B. doi: 10.1016/0002-9149(95)80016-L

Golbaz, I., Ahlers, C., Stock, G., Schütze, C., Schriefl, S., Schlanitz, F., et al. (2011). Quantification of the therapeutic response of intraretinal, subretinal, and subpigment epithelial compartments in exudative AMD during anti-VEGF therapy. *Invest. Ophthalmol. Visual Sci.* 52 (3), 1599–1605. doi: 10.1167/iovs.09-5018

Golde, T. E. (2002). Inflammation takes on Alzheimer disease. *Nat. Med.* 8 (9), 936. doi: 10.1038/nm0902-936

Gomi, F., Sawa, M., Sakaguchi, H., Tsujikawa, M., Oshima, Y., Kamei, M., et al. (2008). Efficacy of intravitreal bevacizumab for polypoidal choroidal vasculopathy. *Br. J. Ophthalmol.* 92 (1), 70–73. doi: 10.1136/bjo.2007.122283

Gong, Y., Li, J., Sun, Y., Fu, Z., Liu, C.-H., Evans, L., et al. (2015). Optimization of an image-guided laser-induced choroidal neovascularization model in mice. *PloS One* 10 (7), e0132643. doi: 10.1371/journal.pone.0132643

Gordois, A., Cutler, H., Pezzullo, L., Gordon, K., Cruess, A., Winyard, S., et al. (2012). An estimation of the worldwide economic and health burden of visual impairment. *Global Public Health* 7 (5), 465–481. doi: 10.1080/17441692.2011.634815

Gottesman, R. F., Schneider, A. L. C., Zhou, Y., Coresh, J., Green, E., Gupta, N., et al. (2017). Association between midlife vascular risk factors and estimated brain amyloid depositionmidlife vascular risk factors and late-life brain amyloid depositionmidlife vascular risk factors and late-life brain amyloid deposition. *JAMA* 317 (14), 1443–1450. doi: 10.1001/jama.2017.3090

Grant, M. B., May, W. S., Caballero, S., Brown, G. A., Guthrie, S. M., Mames, R. N., et al. (2002). Adult hematopoietic stem cells provide functional hemangioblast activity during retinal neovascularization. *Nat. Med.* 8 (6), 607. doi: 10.1038/nm0602-607

Grau, S., Richards, P. J., Kerr, B., Hughes, C., Caterson, B., Williams, A. S., et al. (2006). The role of human HtrA1 in arthritic disease. *J. Biol. Chem.* 281 (10), 6124–6129. doi: 10.1074/jbc.M500361200

Grossniklaus, H. E., Kang, S. J., and Berglin, L. (2010). Animal models of choroidal and retinal neovascularization. *Prog. In Retinal Eye Res.* 29 (6), 500–519. doi: 10.1016/j.preteyeres.2010.05.003

Grunewald, M., Avraham, I., Dor, Y., Bachar-Lustig, E., Itin, A., Yung, S., et al. (2006). VEGF-induced adult neovascularization: recruitment, retention, and role of accessory cells. *Cell* 124 (1), 175–189. doi: 10.1016/j.cell.2005.10.036

Grunwald, J. E., Metelitsina, T. I., DuPont, J. C., Ying, G.-S., and Maguire, M. G. (2005). Reduced foveolar choroidal blood flow in eyes with increasing AMD severity. *Invest. Ophthalmol. Visual Sci.* 46 (3), 1033–1038. doi: 10.1167/iovs.04-1050

Hageman, G. S., Zhu, X. L., Waheed, A., and Sly, W. S. (1991). Localization of carbonic anhydrase IV in a specific capillary bed of the human eye. *Proc. Natl. Acad. Sci.* 88 (7), 2716–2720. doi: 10.1073/pnas.88.7.2716

Hardy, J., and Selkoe, D. J. (2002). The amyloid hypothesis of Alzheimer's disease: progress and problems on the road to therapeutics. *Science* 297 (5580), 353–356. doi: 10.1126/science.1072994

Hasdai, D., Gibbons, R. J., Holmes, D. R. Jr., Higano, S. T., and Lerman, A. (1997). Coronary endothelial dysfunction in humans is associated with myocardial perfusion defects. *Circulation* 96 (10), 3390–3395. doi: 10.1161/01.CIR.96.10.3390

Ho, M., Woo, D. C. F., Chan, V. C. K., Young, A. L., and Brelen, M. E. (2016). Treatment of polypoidal choroidal vasculopathy by photodynamic therapy, aflibercept and dexamethasone triple therapy. *Sci. Rep.* 6, 36870–36870. doi: 10.1038/srep36870

Hogg, R. E., Woodside, J. V., Gilchrist, S. E., Graydon, R., Fletcher, A. E., Chan, W., et al. (2008). Cardiovascular disease and hypertension are strong risk factors for choroidal neovascularization. *Ophthalmol.* 115 (6), 1046–1052. doi: 10.1016/j.ophtha.2007.07.031

Hollyfield, J. G., Bonilha, V. L., Rayborn, M. E., Yang, X., Shadrach, K. G., Lu, L., et al. (2008). Oxidative damage-induced inflammation initiates age-related macular degeneration. *Nat. Med.* 14 (2), 194. doi: 10.1038/nm1709

Holmes, C., Boche, D., Wilkinson, D., Yadegarfar, G., Hopkins, V., Bayer, A., et al. (2008). Long-term effects of Aβ42 immunisation in Alzheimer's disease: follow-up of a randomised, placebo-controlled phase I trial. *Lancet* 372 (9634), 216–223. doi: 10.1016/S0140-6736(08)61075-2

Hou, H.-Y., Wang, Y.-S., Xu, J.-F., Wang, Y.-C., and Liu, J.-P. (2006). The dynamic conduct of bone marrow-derived cells in the choroidal neovascularization microenvironment. *Curr. Eye Res.* 31 (12), 1051–1061. doi: 10.1080/02713680601100459

Huang, W., and Zhang, X. (2014). 3D printing: print the future of ophthalmology. *Invest. Ophthalmol. Visual Sci.* 55 (8), 5380–5381. doi: 10.1167/iovs.14-15231

Huang, L., Zhang, H., Cheng, C.-Y., Wen, F., Tam, P. O. S., Zhao, P., et al. (2016). A missense variant in FGD6 confers increased risk of polypoidal choroidal vasculopathy. *Nat. Genet.* 48, 640. doi: 10.1038/ng.3546

Ishibashi, T., Miller, H., Orr, G., Sorgente, N., and Ryan, S. (1987). Morphologic observations on experimental subretinal neovascularization in the monkey. *Invest. Ophthalmol. Visual Sci.* 28 (7), 1116–1130.

Ishida, S., Usui, T., Yamashiro, K., Kaji, Y., Amano, S., Ogura, Y., et al. (2003). VEGF164-mediated inflammation is required for pathological, but not physiological, ischemia-induced retinal neovascularization. *J. Exp. Med.* 198 (3), 483–489. doi: 10.1084/jem.20022027

Jaffe, G. J., Ciulla, T. A., Ciardella, A. P., Devin, F., Dugel, P. U., Eandi, C. M., et al. (2017). Dual antagonism of PDGF and VEGF in neovascular age-related macular degeneration: a phase IIb, multicenter, randomized controlled trial. *Ophthalmol.* 124 (2), 224–234. doi: 10.1016/j.ophtha.2016.10.010

Jager, R. D., Mieler, W. F., and Miller, J. W. (2008). Age-related macular degeneration. *New Engl. J. Med.* 358 (24), 2606–2617. doi: 10.1056/NEJMra0801537

Jiang, J., Huang, L., Yu, W., Wu, X., Zhou, P., and Li, X. (2012). Overexpression of HTRA1 leads to down-regulation of fibronectin and functional changes in RF/6A cells and HUVECs. *PloS One* 7 (10), e46115. doi: 10.1371/journal.pone.0046115

Jiao, J., Song, Y., Qin, D., and Jiang, Y. (2017). Apelin is essential for the development of laser-induced choroidal neovascularization model. *Int. J. Clin. Exp. Pathol.* 10 (2), 1104–1112.

Jonas, J. B., Cheung, C. M. G., and Panda-Jonas, S. (2017). Updates on the epidemiology of age-related macular Degeneration. *Asia Pac J. Ophthalmol. (Phila)* 6 (6), 493–497. doi: 10.22608/APO.2017251

Jones, C. A., London, N. R., Chen, H., Park, K. W., Sauvaget, D., Stockton, R. A., et al. (2008). Robo4 stabilizes the vascular network by inhibiting pathologic angiogenesis and endothelial hyperpermeability. *Nat. Med.* 14 (4), 448. doi: 10.1038/nm1742

Jones, A., Kumar, S., Zhang, N., Tong, Z., Yang, J.-H., Watt, C., et al. (2011). Increased expression of multifunctional serine protease, HTRA1, in retinal pigment epithelium induces polypoidal choroidal vasculopathy in mice. *Proc. Natl. Acad. Sci.* 108 (35), 14578–14583. doi: 10.1073/pnas.1102853108

Kaarniranta, K., Salminen, A., Haapasalo, A., Soininen, H., and Hiltunen, M. (2011). Age-related macular degeneration (AMD): Alzheimer's disease in the eye?. *J. Alzheimer's Dis.* 24 (4), 615–631. doi: 10.3233/JAD-2011-101908

Kaarniranta, K., Kajdanek, J., Morawiec, J., Pawlowska, E., and Blasiak, J. (2018). PGC-1α protects RPE cells of the aging retina against oxidative stress-induced degeneration through the regulation of senescence and mitochondrial quality control. the significance for AMD pathogenesis. *Int. J. Mol. Sci.* 19 (8), 2317. doi: 10.3390/ijms19082317

Kam, J. H., Lenassi, E., and Jeffery, G. (2010). Viewing ageing eyes: diverse sites of amyloid Beta accumulation in the ageing mouse retina and the up-regulation of macrophages. *PloS One* 5 (10), e13127. doi: 10.1371/journal.pone.0013127

Karran, E., Mercken, M., and De Strooper, B. (2011). The amyloid cascade hypothesis for Alzheimer's disease: an appraisal for the development of therapeutics. *Nat. Rev. Drug Discovery* 10 (9), 698. doi: 10.1038/nrd3505

Khandhadia, S., Cipriani, V., Yates, J., and Lotery, A. J. (2012). Age-related macular degeneration and the complement system. *Immunobiol.* 217 (2), 127–146. doi: 10.1016/j.imbio.2011.07.019

Kinnunen, K., and Ylä-Herttuala, S. (2012). Vascular endothelial growth factors in retinal and choroidal neovascular diseases. *Ann. Med.* 44 (1), 1–17. doi: 10.3109/07853890.2010.532150

Kisler, K., Nelson, A. R., Montagne, A., and Zlokovic, B. V. (2017). Cerebral blood flow regulation and neurovascular dysfunction in Alzheimer disease. *Nat. Rev. Neurosci.* 18 (7), 419. doi: 10.1038/nrn.2017.48

Klein, R., Cruickshanks, K. J., Myers, C. E., Sivakumaran, T. A., Iyengar, S. K., Meuer, S. M., et al. (2013). The relationship of atherosclerosis to the 10-year cumulative incidence of age-related macular degeneration: the Beaver Dam studies. *Ophthalmol.* 120 (5), 1012–1019. doi: 10.1016/j.ophtha.2012.11.003

Klein, R., Myers, C. E., Cruickshanks, K. J., Gangnon, R. E., Danforth, L. G., Sivakumaran, T. A., et al. (2014). Markers of inflammation, oxidative stress, and endothelial dysfunction and the 20-year cumulative incidence of early age-related macular degeneration: the Beaver Dam Eye Study. *JAMA Ophthalmol.* 132 (4), 446–455. doi: 10.1001/jamaophthalmol.2013.7671

Korte, G. E., Reppucci, V., and Henkind, P. (1984). RPE destruction causes choriocapillary atrophy. *Invest. Ophthalmol. Visual Sci.* 25 (10), 1135–1145.

Kramer, M., Mimouni, K., Priel, E., Yassur, Y., and Weinberger, D. (2000). Comparison of fluorescein angiography and indocyanine green angiography for imaging of choroidal neovascularization in hemorrhagic age-related macular degeneration. *Am. J. Ophthalmol.* 129 (4), 495–500. doi: 10.1016/S0002-9394(99)00388-8

Krebs, I., Glittenberg, C., Ansari-Shahrezaei, S., Hagen, S., Steiner, I., and Binder, S. (2013). Non-responders to treatment with antagonists of vascular endothelial growth factor in age-related macular degeneration. *Br. J. Ophthalmol.* 97 (11), 1443–1446. doi: 10.1136/bjophthalmol-2013-303513

Kurihara, T., Westenskow, P. D., Bravo, S., Aguilar, E., and Friedlander, M. (2012). Targeted deletion of Vegfa in adult mice induces vision loss. *J. Clin. Invest.* 122 (11), 4213–4217. doi: 10.1172/JCI65157

Kuroiwa, S., Tateiwa, H., Hisatomi, T., Ishibashi, T., and Yoshimura, N. (2004). Pathological features of surgically excised polypoidal choroidal vasculopathy membranes. *Clin. Exp. Ophthalmol.* 32 (3), 297–302. doi: 10.1111/j.1442-9071.2004.00827.x

Kvanta, A., Algvere, P., Berglin, L., and Seregard, S. (1996). Subfoveal fibrovascular membranes in age-related macular degeneration express vascular endothelial growth factor. *Invest. Ophthalmol. Visual Sci.* 37 (9), 1929–1934. doi: 10.1016/S0002-9394(14)70522-7

Kwak, N., Okamoto, N., Wood, J. M., and Campochiaro, P. A. (2000). VEGF is major stimulator in model of choroidal neovascularization. *Invest. Ophthalmol. Visual Sci.* 41 (10), 3158–3164.

Lai, T. Y., Chan, W. M., and Lam, D. S. (2004). Transient reduction in retinal function revealed by multifocal electroretinogram after photodynamic therapy. *Am. J. Ophthalmol.* 137 (5), 826–833. doi: 10.1016/j.ajo.2003.11.079

Lai, T. Y., Chan, W.-M., Liu, D. T., Luk, F. O., and Lam, D. S. (2008). Intravitreal bevacizumab (Avastin) with or without photodynamic therapy for the treatment of polypoidal choroidal vasculopathy. *Br. J. Ophthalmol.* 92 (5), 661–666. doi: 10.1136/bjo.2007.135103

Lally, D. R., Gerstenblith, A. T., and Regillo, C. D. (2012). Preferred therapies for neovascular age-related macular degeneration. *Curr. Opin. In Ophthalmol.* 23 (3), 182–188. doi: 10.1097/ICU.0b013e328352411c

Lambert, V., Lecomte, J., Hansen, S., Blacher, S., Gonzalez, M.-L. A., Struman, I., et al. (2013). Laser-induced choroidal neovascularization model to study age-related macular degeneration in mice. *Nat. Protoc.* 8 (11), 2197. doi: 10.1038/nprot.2013.13

Lee, W. K., Lee, P. Y., and Lee, S. K. (2008). Photodynamic therapy for polypoidal choroidal vasculopathy: vaso-occlusive effect on the branching vascular

network and origin of recurrence. *Jpn J. Ophthalmol.* 52 (2), 108–115. doi: 10.1007/s10384-007-0501-y

Lee, C. S., Larson, E. B., Gibbons, L. E., Lee, A. Y., McCurry, S. M., Bowen, J. D., et al. (2019). Associations between recent and established ophthalmic conditions and risk of Alzheimer's disease. *Alzheimer's Dementia* 15 (1), 34–41. doi: 10.1016/j.jalz.2018.06.2856

Leishman, R. (1957). The eye in general vascular disease: hypertension and arteriosclerosis. *Br. J. Ophthalmol.* 41 (11), 641–701. doi: 10.1136/bjo.41.11.641

Lim, J. K., Li, Q.-X., He, Z., Vingrys, A. J., Wong, V. H., Currier, N., et al. (2016). The eye as a biomarker for Alzheimer's disease. *Front. In Neurosci.* 10, 536. doi: 10.3389/fnins.2016.00536

Lin, M. T., and Beal, M. F. (2006). Mitochondrial dysfunction and oxidative stress in neurodegenerative diseases. *Nature* 443 (7113), 787. doi: 10.1038/nature05292

Lip, P.-L., Blann, A. D., Hope-Ross, M., Gibson, J. M., and Lip, G. Y. (2001). Age-related macular degeneration is associated with increased vascular endothelial growth factor, hemorheology and endothelial dysfunction. *Ophthalmol.* 108 (4), 705–710. doi: 10.1016/S0161-6420(00)00663-1

Liu, K., Chen, L. J., Lai, T. Y., Tam, P. O., Ho, M., Chiang, S. W., et al. (2014). Genes in the high-density lipoprotein metabolic pathway in age-related macular degeneration and polypoidal choroidal vasculopathy. *Ophthalmol.* 121 (4), 911–916. doi: 10.1016/j.ophtha.2013.10.042

Liu, R., Li, J., Li, Z., Yu, S., Yang, Y., Yan, H., et al. (2016). Distinguishing polypoidal choroidal vasculopathy from typical neovascular age-related macular degeneration based on spectral domain optical coherence tomography. *Retina* 36 (4), 778–786. doi: 10.1097/IAE.0000000000000794

London, A., Benhar, I., and Schwartz, M. (2013). The retina as a window to the brain-from eye research to CNS disorders. *Nat. Rev. Neurol.* 9 (1), 44. doi: 10.1038/nrneurol.2012.227

Lou, D.-A., and Hu, F. (1987). Specific antigen and organelle expression of a long-term rhesus endothelial cell line. *In Vitro Cell. Dev. Biol.* 23 (2), 75–85. doi: 10.1007/BF02623586

Lutty, G., Grebe, R., Bhutto, I., Taomoto, M., Merges, C., and McLeod, D. (2009). Death of choriocapillaris in age-related macular degeneration. *Invest. Ophthalmol. Visual Sci.* 50 (13), 3518–3518. doi: 10.1167/iovs.09-3639

Machalińska, A., Safranow, K., Dziedziejko, V., Mozolewska-Piotrowska, K., Paczkowska, E., Kłos, P., et al. (2011). Different populations of circulating endothelial cells in patients with age-related macular degeneration: a novel insight into pathogenesis. *Invest. Ophthalmol. Visual Sci.* 52 (1), 93–100. doi: 10.1167/iovs.10-5756

Machalińska, A., Kawa, M. P., Marlicz, W., and Machaliński, B. (2012). Complement system activation and endothelial dysfunction in patients with age-related macular degeneration (AMD): possible relationship between AMD and atherosclerosis. *Acta Ophthalmologica* 90 (8), 695–703. doi: 10.1111/j.1755-3768.2011.02295.x

Makin, R. D., Apicella, I., Nagasaka, Y., Kaneko, H., Turner, S. D., Kerur, N., et al. (2018). RF/6A chorioretinal cells do not display key endothelial phenotypes. *Invest. Ophthalmol. Visual Sci.* 59 (15), 5795–5802. doi: 10.1167/iovs.18-25215

Malek, G., Busik, J., Grant, M. B., and Choudhary, M. (2018). Models of retinal diseases and their applicability in drug discovery. *Expert Opin. Drug Discovery* 13 (4), 359–377. doi: 10.1080/17460441.2018.1430136

Manuelian, T., Hellwage, J., Meri, S., Caprioli, J., Noris, M., Heinen, S., et al. (2003) Mutations in factor H reduce binding affinity to C3b and heparin and surface attachment to endothelial cells in hemolytic uremic syndrome. *J. Clin. Invest.* 111 (8), 1181–1190. doi: 10.1172/JCI16651

Marazita, M. C., Dugour, A., Marquioni-Ramella, M. D., Figueroa, J. M., and Suburo, A. M. (2016). Oxidative stress-induced premature senescence dysregulates VEGF and CFH expression in retinal pigment epithelial cells: implications for age-related macular degeneration. *Redox Biol.* 7, 78–87. doi: 10.1016/j.redox.2015.11.011

Marneros, A. G., Fan, J., Yokoyama, Y., Gerber, H. P., Ferrara, N., Crouch, R. K., et al. (2005). Vascular endothelial growth factor expression in the retinal pigment epithelium is essential for choriocapillaris development and visual function. *Am. J. Pathol.* 167 (5), 1451–1459. doi: 10.1016/S0002-9440(10)61231-X

Marneros, A. G. (2013). NLRP3 inflammasome blockade inhibits VEGF-A-induced age-related macular degeneration. *Cell Rep.* 4 (5), 945–958. doi: 10.1016/j.celrep.2013.08.002

Mathura, J. R., Jafari, N., Chang, J. T., Hackett, S. F., Wahlin, K. J., Della, N. G., et al. (2000). Bone morphogenetic proteins-2 and-4: negative growth regulators in adult retinal pigmented epithelium. *Invest. Ophthalmol. Visual Sci.* 41 (2), 592–600.

Maugeri, A., Barchitta, M., Mazzone, M. G., Giuliano, F., and Agodi, A. (2018). Complement System and Age-Related Macular Degeneration: Implications of Gene-Environment Interaction for Preventive and Personalized Medicine. *BioMed. Res. Int.* 2018, 13. doi: 10.1155/2018/7532507

Miller, J. W., Adamis, A. P., and Aiello, L. P. (1997). Vascular endothelial growth factor in ocular neovascularization and proliferative diabetic retinopathy. *Diabetes/metabolism Rev.* 13 (1), 37–50. doi: 10.1002/(SICI)1099-0895(199703)13:1<37::AID-DMR174>3.0.CO;2-K

Mok, S. S., Losic, D., Barrow, C. J., Turner, B. J., Masters, C. L., Martin, L. L., et al. (2006). The beta-amyloid peptide of Alzheimer's disease decreases adhesion of vascular smooth muscle cells to the basement membrane. *J. Neurochem.* 96 (1), 53–64. doi: 10.1111/j.1471-4159.2005.03539.x

Mudau, M., Genis, A., Lochner, A., and Strijdom, H. (2012). Endothelial dysfunction: the early predictor of atherosclerosis. *Cardiovasc. J. Afr.* 23 (4), 222. doi: 10.5830/CVJA-2011-068

Mullins, R. F., Khanna, A., Schoo, D. P., Tucker, B. A., Sohn, E. H., Drack, A. V., et al. (2014). Is age-related macular degeneration a microvascular disease?. *Adv. Exp. Med. Biol.* 801, 283–289. doi: 10.1007/978-1-4614-3209-8_36

Naito, H., Kidoya, H., Sakimoto, S., Wakabayashi, T., and Takakura, N. (2012). Identification and characterization of a resident vascular stem/progenitor cell population in preexisting blood vessels. *EMBO J.* 31 (4), 842–855. doi: 10.1038/emboj.2011.465

Nakashizuka, H., Mitsumata, M., Okisaka, S., Shimada, H., Kawamura, A., Mori, R., et al. (2008). Clinicopathologic findings in polypoidal choroidal vasculopathy. *Invest. Ophthalmol. Visual Sci.* 49 (11), 4729–4737. doi: 10.1167/iovs.08-2134

Nation, D. A., Sweeney, M. D., Montagne, A., Sagare, A. P., D'Orazio, L. M., Pachicano, M., et al. (2019). Blood-brain barrier breakdown is an early biomarker of human cognitive dysfunction. *Nat. Med.* 25 (2), 270–276. doi: 10.1038/s41591-018-0297-y

Ng, D. S., Yip, Y. W., Bakthavatsalam, M., Chen, L. J., Ng, T. K., Lai, T. Y., et al. (2017). Elevated angiopoietin 2 in aqueous of patients with neovascular age related macular degeneration correlates with disease severity at presentation. *Sci. Rep.* 7, 45081. doi: 10.1038/srep45081

Nishida, N., Walz, T., and Springer, T. A. (2006). Structural transitions of complement component C3 and its activation products. *Proc. Natl. Acad. Sci.* 103 (52), 19737–19742. doi: 10.1073/pnas.0609791104

Nitsch, D., Evans, J., Roderick, P. J., Smeeth, L., and Fletcher, A. E. (2009). Associations between chronic kidney disease and age-related macular degeneration. *Ophthalmic Epidemiol.* 16 (3), 181–186. doi: 10.1080/09286580902863064

Nortley, R., Korte, N., Izquierdo, P., Hirunpattarasilp, C., Mishra, A., Jaunmuktane, Z., et al. (2019). Amyloid beta oligomers constrict human capillaries in Alzheimer's disease via signaling to pericytes. *Science* 365 (6450), eaav9518. doi: 10.1126/science.aav9518

Nozaki, M., Raisler, B. J., Sakurai, E., Sarma, J. V., Barnum, S. R., Lambris, J. D., et al. (2006). Drusen complement components C3a and C5a promote choroidal neovascularization. *Proc. Natl. Acad. Sci.* 103 (7), 2328–2333. doi: 10.1073/pnas.0408835103

Ohno-Matsui, K. (2011). Parallel findings in age-related macular degeneration and Alzheimer's disease. *Prog. In Retinal Eye Res.* 30 (4), 217–238. doi: 10.1016/j.preteyeres.2011.02.004

Oka, C., Tsujimoto, R., Kajikawa, M., Koshiba-Takeuchi, K., Ina, J., Yano, M., et al. (2004). HtrA1 serine protease inhibits signaling mediated by Tgfβ family proteins. *Dev.* 131 (5), 1041–1053. doi: 10.1242/dev.00999

Okubo, A., Sameshima, M., Uemura, A., Kanda, S., and Ohba, N. (2002). Clinicopathological correlation of polypoidal choroidal vasculopathy revealed by ultrastructural study. *Br. J. Ophthalmol.* 86 (10), 1093–1098. doi: 10.1136/bjo.86.10.1093

Okuno, Y., Nakamura-Ishizu, A., Kishi, K., Suda, T., and Kubota, Y. (2011). Bone marrow-derived cells serve as proangiogenic macrophages but not endothelial cells in wound healing. *Blood* 117 (19), 5264–5272. doi: 10.1182/blood-2011-01-330720

Pachydaki, S. I., Jakobiec, F. A., Bhat, P., Sobrin, L., Michaud, N. A., Seshan, S. V., et al. (2012). Surgical management and ultrastructural study of choroidal

neovascularization in punctate inner choroidopathy after bevacizumab. *J. ophthalmic Inflammation infection* 2 (1), 29–37. doi: 10.1007/s12348-011-0050-x

Papadopoulos, N., Martin, J., Ruan, Q., Rafique, A., Rosconi, M. P., Shi, E., et al. (2012). Binding and neutralization of vascular endothelial growth factor (VEGF) and related ligands by VEGF Trap, ranibizumab and bevacizumab. *Angiogenesis* 15 (2), 171–185. doi: 10.1007/s10456-011-9249-6

Pascolini, D., and Mariotti, S. P. (2012). Global estimates of visual impairment: 2010. *Br. J. Ophthalmol.* 96 (5), 614–618. doi: 10.1136/bjophthalmol-2011-300539

Pennesi, M. E., Neuringer, M., and Courtney, R. J. (2012). Animal models of age related macular degeneration. *Mol. aspects Med.* 33 (4), 487–509. doi: 10.1016/j.mam.2012.06.003

Pennington, K. L., and DeAngelis, M. M. (2016). Epidemiology of age-related macular degeneration (AMD): associations with cardiovascular disease phenotypes and lipid factors. *Eye Vision* 3 (1), 34. doi: 10.1186/s40662-016-0063-5

Poor, S. H., Qiu, Y., Fassbender, E. S., Shen, S., Woolfenden, A., Delpero, A., et al. (2014). Reliability of the mouse model of choroidal neovascularization induced by laser photocoagulation. *Invest. Ophthalmol. Visual Sci.* 55 (10), 6525–6534. doi: 10.1167/iovs.14-15067

Purhonen, S., Palm, J., Rossi, D., Kaskenpää, N., Rajantie, I., Ylä-Herttuala, S., et al. (2008). Bone marrow-derived circulating endothelial precursors do not contribute to vascular endothelium and are not needed for tumor growth. *Proc. Natl. Acad. Sci.* 105 (18), 6620–6625. doi: 10.1073/pnas.0710516105

Qian, T., Li, X., Zhao, M., and Xu, X. (2018). Polypoidal choroidal vasculopathy treatment options: a meta-analysis. *Eur. J. Clin. Invest.* 48 (1), e12840. doi: 10.1111/eci.12840

Ratnayaka, J. A., Serpell, L. C., and Lotery, A. J. (2015). Dementia of the eye: the role of amyloid beta in retinal degeneration. *Eye* 29 (8), 1013. doi: 10.1038/eye.2015.100

Reinmuth, N., Liu, W., Jung, Y. D., Ahmad, S. A., Shaheen, R. M., Fan, F., et al. (2001). Induction of VEGF in perivascular cells defines a potential paracrine mechanism for endothelial cell survival. *FASEB J.* 15 (7), 1239–1241. doi: 10.1096/fj.00-0693fje

Rofagha, S., Bhisitkul, R. B., Boyer, D. S., Sadda, S. R., Zhang, K., and Group, S.-U. S. (2013). Seven-year outcomes in ranibizumab-treated patients in ANCHOR, MARINA, and HORIZON: a multicenter cohort study (SEVEN-UP). *Ophthalmol.* 120 (11), 2292–2299. doi: 10.1016/j.ophtha.2013.03.046

Rong, S. S., Lee, B. Y., Kuk, A. K., Yu, X. T., Li, S. S., Li, J., et al. (2019). Comorbidity of dementia and age-related macular degeneration calls for clinical awareness: a meta-analysis. *Br. J. Ophthalmol.* 0, 1–7 doi: 10.1136/bjophthalmol-2018-313277

Rops, A. L., Van Der Vlag, J., Jacobs, C. W., Dijkman, H. B., Lensen, J. F., Wijnhoven, T. J., et al. (2004). Isolation and characterization of conditionally immortalized mouse glomerular endothelial cell lines. *Kidney Int.* 66 (6), 2193–2201. doi: 10.1111/j.1523-1755.2004.66009.x

Rosenfeld, P. J., and Feuer, W. J. (2018). Lessons from recent phase III trial failures: don't design phase III trials based on retrospective subgroup analyses from Phase II trials. *Ophthalmol.* 125 (10), 1488–1491. doi: 10.1016/j.ophtha.2018.06.002

Rosenfeld, P. J., Brown, D. M., Heier, J. S., Boyer, D. S., Kaiser, P. K., Chung, C. Y., et al. (2006). Ranibizumab for neovascular age-related macular degeneration. *New Engl. J. Med.* 355 (14), 1419–1431. doi: 10.1056/NEJMoa054481

Ryan, S. J. (1979). The development of an experimental model of subretinal neovascularization in disciform macular degeneration. *Trans. Am. Ophthalmol. Soc.* 77, 707–745.

Saini, J. S., Corneo, B., Miller, J. D., Kiehl, T. R., Wang, Q., Boles, N. C., et al. (2017). Nicotinamide ameliorates disease phenotypes in a human iPSC model of age-related macular degeneration. *Cell Stem Cell* 20 (5), 635–647. doi: 10.1016/j.stem.2016.12.015 e637.

Saint-Geniez, M., and D'Amore, P. A.Saint-Geniez, M., and D'Amore, P. A. (2004). Development and pathology of the hyaloid, choroidal and retinal vasculature. *Int. J. Dev. Biol.* 48(8–9),1045–1058. doi: 10.1387/ijdb.041895ms

Schaumberg, D. A., Christen, W. G., Buring, J. E., Glynn, R. J., Rifai, N., and Ridker, P. M. (2007). High-sensitivity C-reactive protein, other markers of inflammation, and the incidence of macular degeneration in women. *Arch. Ophthalmol.* 125 (3), 300–305. doi: 10.1001/archopht.125.3.300

Schiattarella, G. G., Altamirano, F., Tong, D., French, K. M., Villalobos, E., Kim, S. Y., et al. (2019). Nitrosative stress drives heart failure with preserved ejection fraction. *Nature* 568 (7752), 351. doi: 10.1038/s41586-019-1100-z

Schlingemann, R., and Witmer, A. (2009). Treatment of retinal diseases with VEGF antagonists. *Prog. Brain Res.* 175, 253–267. doi: 10.1016/S0079-6123(09)17517-9

Seddon, J. M., Gensler, G., Milton, R. C., Klein, M. L., and Rifai, N. (2004). Association between C-reactive protein and age-related macular degeneration. *JAMA* 291 (6), 704–710. doi: 10.1001/jama.291.6.704

Seddon, J. M., Cote, J., Page, W. F., Aggen, S. H., and Neale, M. C. (2005). The US twin study of age-related macular degeneration: relative roles of genetic and environmental influences. *Arch. Ophthalmol.* 123 (3), 321–327. doi: 10.1001/archopht.123.3.321

Seddon, J. M., McLeod, D. S., Bhutto, I. A., Villalonga, M. B., Silver, R. E., Wenick, A. S., et al. (2016). Histopathological insights into choroidal vascular loss in clinically documented cases of age-related macular degeneration. *JAMA Ophthalmol.* 134 (11), 1272–1280. doi: 10.1001/jamaophthalmol.2016.3519

Sengupta, N., Caballero, S., Mames, R. N., Butler, J. M., Scott, E. W., and Grant, M. B. (2003). The role of adult bone marrow-derived stem cells in choroidal neovascularization. *Invest. Ophthalmol. Visual Sci.* 44 (11), 4908–4913. doi: 10.1167/iovs.03-0342

Sheridan, C. M., Rice, D., Hiscott, P. S., Wong, D., and Kent, D. L. (2006). The presence of AC133-positive cells suggests a possible role of endothelial progenitor cells in the formation of choroidal neovascularization. *Invest. Ophthalmol. Visual Sci.* 47 (4), 1642–1645. doi: 10.1167/iovs.05-0779

Siedlecki, J., Wertheimer, C., Wolf, A., Liegl, R., Priglinger, C., Priglinger, S., et al. (2017). Combined VEGF and PDGF inhibition for neovascular AMD: anti-angiogenic properties of axitinib on human endothelial cells and pericytes in vitro. *Graefe's Arch. Clin. Exp. Ophthalmol.* 255 (5), 963–972. doi: 10.1007/s00417-017-3595-z

Silva, R., Axer-Siegel, R., Eldem, B., Guymer, R., Kirchhof, B., Papp, A., et al. (2013). The SECURE study: long-term safety of ranibizumab 0.5 mg in neovascular age-related macular degeneration. *Ophthalmol.* 120 (1), 130–139. doi: 10.1016/j.ophtha.2012.07.026

Singer, M. A., Awh, C. C., Sadda, S., Freeman, W. R., Antoszyk, A. N., Wong, P., et al. (2012). "HORIZON: an open-label extension trial of ranibizumab for choroidal neovascularization secondary to age-related macular degeneration. *Ophthalmol.* 119 (6), 1175–1183. doi: 10.1016/j.ophtha.2011.12.016

Snyder, H. M., Corriveau, R. A., Craft, S., Faber, J. E., Greenberg, S. M., Knopman, D., et al. (2015). Vascular contributions to cognitive impairment and dementia including Alzheimer's disease. *Alzheimer's Dementia* 11 (6), 710–717. doi: 10.1016/j.jalz.2014.10.008

Songstad, A. E., Worthington, K. S., Chirco, K. R., Giacalone, J. C., Whitmore, S. S., Anfinson, K. R., et al. (2017). Connective tissue growth factor promotes efficient generation of human induced pluripotent stem cell-derived choroidal endothelium. *Stem Cells Trans. Med.* 6 (6), 1533–1546. doi: 10.1002/sctm.16-0399

Stan, R. V., Tkachenko, E., and Niesman, I. R. (2004). PV1 is a key structural component for the formation of the stomatal and fenestral diaphragms. *Mol. Biol. Cell* 15 (8), 3615–3630. doi: 10.1091/mbc.e03-08-0593

Stauffer, B. L., Westby, C. M., and DeSouza, C. A. (2008). Endothelin-1, aging and hypertension. *Curr. Opin. In Cardiol.* 23 (4), 350–355. doi: 10.1097/HCO.0b013e328302f3c6

Supanji, Shimomachi, M., Hasan, M. Z., Kawaichi, M., and Oka, C. (2013). HtrA1 is induced by oxidative stress and enhances cell senescence through p38 MAPK pathway. *Exp. Eye Res.* 112, 79–92. doi: 10.1016/j.exer.2013.04.013

Sweeney, M. D., Sagare, A. P., and Zlokovic, B. V. (2018). Blood-brain barrier breakdown in Alzheimer disease and other neurodegenerative disorders. *Nat. Rev. Neurol.* 14, 133. doi: 10.1038/nrneurol.2017.188

Takahashi, K., and Yamanaka, S. (2006). Induction of pluripotent stem cells from mouse embryonic and adult fibroblast cultures by defined factors. *cell* 126 (4), 663–676. doi: 10.1016/j.cell.2006.07.024

Takahashi, H., Yanagi, Y., Tamaki, Y., Muranaka, K., Usui, T., and Sata, M. (2004). Contribution of bone-marrow-derived cells to choroidal neovascularization. *Biochem. Biophys. Res. Commun.* 320 (2), 372–375. doi: 10.1016/j.bbrc.2004.05.177

Tan, J. S., Mitchell, P., Smith, W., and Wang, J. J. (2007). Cardiovascular risk factors and the long-term incidence of age-related macular degeneration: the Blue Mountains Eye Study. *Ophthalmol.* 114 (6), 1143–1150. doi: 10.1016/j.ophtha.2006.09.033

Tan, J. S., Wang, J. J., Liew, G., Rochtchina, E., and Mitchell, P. (2008). Age-related macular degeneration and mortality from cardiovascular disease or stroke. *Br. J. Ophthalmol.* 92 (4), 509–512. doi: 10.1136/bjo.2007.131706

Tedeschi-Reiner, E., Strozzi, M., Skoric, B., and Reiner, Z. (2005). Relation of atherosclerotic changes in retinal arteries to the extent of coronary artery disease. *Am. J. Cardiol.* 96 (8), 1107–1109. doi: 10.1016/j.amjcard.2005.05.070

Teo, K. Y. C., Gillies, M., and Fraser-Bell, S. (2018). The use of vascular endothelial growth factor inhibitors and complementary treatment options in polypoidal choroidal vasculopathy: a subtype of neovascular age-related macular degeneration. *Int. J. Mol. Sci.* 19 (9), 2611. doi: 10.3390/ijms19092611

Thomas, J., Mohammad, S., Charnigo, R., Baffi, J., Abdel-Latif, A., and Ziada, K. M. (2015). Age-related macular degeneration and coronary artery disease in a VA population. *South. Med. J.* 108 (8), 502. doi: 10.14423/SMJ.0000000000000329

Tobe, T., Okamoto, N., Vinores, M. A., Derevjanik, N. L., Vinores, S. A., Zack, D. J., et al. (1998). Evolution of neovascularization in mice with overexpression of vascular endothelial growth factor in photoreceptors. *Invest. Ophthalmol. Visual Sci.* 39 (1), 180–188.

Tolentino, M. J., Brucker, A. J., Fosnot, J., Ying, G.-S., Wu, I.-H., Malik, G., et al. (2004). Intravitreal injection of vascular endothelial growth factor small interfering RNA inhibits growth and leakage in a nonhuman primate, laser-induced model of choroidal neovascularization. *Retina* 24 (1), 132–138. doi: 10.1097/00006982-200402000-00018

Tomita, M., Yamada, H., Adachi, Y., Cui, Y., Yamada, E., Higuchi, A., et al. (2004). Choroidal neovascularization is provided by bone marrow cells. *Stem Cells* 22 (1), 21–26. doi: 10.1634/stemcells.22-1-21

Tong, J.-P., Chan, W.-M., Liu, D. T., Lai, T. Y., Choy, K.-W., Pang, C.-P., et al. (2006). Aqueous humor levels of vascular endothelial growth factor and pigment epithelium-derived factor in polypoidal choroidal vasculopathy and choroidal neovascularization. *Am. J. Ophthalmol.* 141 (3), 456–462. doi: 10.1016/j.ajo.2005.10.012

Tosi, G. M., Caldi, E., Neri, G., Nuti, E., Marigliani, D., Baiocchi, S., et al. (2017). HtrA1 and TGF-β1 concentrations in the aqueous humor of patients with neovascular age-related macular degeneration. *Invest. Ophthalmol. Visual Sci.* 58 (1), 162–167. doi: 10.1167/iovs.16-20922

Totan, Y., Koca, C., Erdurmuş, M., Keskin, U., and Yiğitoğlu, R. (2015). Endothelin-1 and nitric oxide levels in exudative age-related macular degeneration. *J. ophthalmic Vision Res.* 10 (2), 151. doi: 10.4103/2008-322X.163765

Tsujikawa, A., Ooto, S., Yamashiro, K., Tamura, H., Otani, A., and Yoshimura, N. (2010). Treatment of polypoidal choroidal vasculopathy by intravitreal injection of bevacizumab. *Jpn J. Ophthalmol.* 54 (4), 310–319. doi: 10.1007/s10384-010-0813-1

van de Haar, H. J., Jansen, J. F., van Osch, M. J., van Buchem, M. A., Muller, M., Wong, S. M., et al. (2016). Neurovascular unit impairment in early Alzheimer's disease measured with magnetic resonance imaging. *Neurobiol. Aging* 45, 190–196. doi: 10.1016/j.neurobiolaging.2016.06.006

Veckeneer, M., Augustinus, C., Feron, E., Schauwvlieghe, P., Ruys, J., Cosemans, I., et al. (2017). OCT angiography documented reperfusion of translocated autologous full thickness RPE-choroid graft for complicated neovascular age-related macular degeneration. *Eye* 31 (9), 1274. doi: 10.1038/eye.2017.137

Vierkotten, S., Muether, P. S., and Fauser, S. (2011). Overexpression of HTRA1 leads to ultrastructural changes in the elastic layer of Bruch's membrane via cleavage of extracellular matrix components. *PloS One* 6 (8), e22959. doi: 10.1371/journal.pone.0022959

Vingerling, J. R., Dielemans, I., Bots, M. L., Hofman, A., Grobbee, D. E., and de Jong, P. T. (1995). Age-related macular degeneration is associated with atherosclerosis: the Rotterdam study. *Am. J. Epidemiol.* 142 (4), 404–409. doi: 10.1093/oxfordjournals.aje.a117648

Vogel, R. N., Davis, D. B., Kimura, B. H., Rathinavelu, S., Graves, G. S., Szabo, A., et al. (2017). Neovascular age-related macular degeneration with advanced visual loss treated with anti-vascular endothelial growth factor therapy. *Retina* 37 (2), 257–264. doi: 10.1097/IAE0000000000001150

Wakabayashi, T., Naito, H., Takara, K., Kidoya, H., Sakimoto, S., Oshima, Y., et al. (2013). Identification of vascular endothelial side population cells in the choroidal vessels and their potential role in age-related macular degeneration. *Invest. Ophthalmol. Visual Sci.* 54 (10), 6686–6693. doi: 10.1167/iovs.13-12342

Wang, H., and Hartnett, M. E. (2016). Regulation of signaling events involved in the pathophysiology of neovascular AMD. *Mol. Vision* 22, 189–202.

Wang, J., Zhu, C., Xu, Y., Liu, B., Wang, M., and Wu, K. (2011). Development and expression of amyloid-β peptide 42 in retinal ganglion cells in rats. *Anatomical Record: Adv. Integr. Anat. Evolutionary Biol.* 294 (8), 1401–1405. doi: 10.1002/ar.21438

Wang, X., Ma, W., Han, S., Meng, Z., Zhao, L., Yin, Y., et al. (2017). TGF-β participates choroid neovascularization through Smad2/3-VEGF/TNF-α signaling in mice with Laser-induced wet age-related macular degeneration. *Sci. Rep.* 7 (1), 9672. doi: 10.1038/s41598-017-10124-4

Wang, Y., Liu, C.-H., Ji, T., Mehta, M., Wang, W., Marino, E., et al. (2019). Intravenous treatment of choroidal neovascularization by photo-targeted nanoparticles. *Nat. Commun.* 10 (1), 804. doi: 10.1038/s41467-019-08690-4

Weismann, D, Hartvigsen, K., Lauer, N., Bennett, K. L., Scholl, H. P. N., Issa, P. C., et al. (2011). Complement factor H binds malondialdehyde epitopes and protects from oxidative stress. *Nature* 478 (7367), 76–81. doi: 10.1038/nature10449

Wimmer, R. A., Leopoldi, A., Aichinger, M., Wick, N., Hantusch, B., Novatchkova, M., et al. (2019). Human blood vessel organoids as a model of diabetic vasculopathy. *Nature*. 565 (7740), 505–510. doi: 10.1038/s41586-018-0858-8

Wolf, A., and Langmann, T. (2019). Anti-VEGF-A/ANG2 combotherapy limits pathological angiogenesis in the eye: a replication study. *EMBO Mol. Med.* 11 (5), e10362. doi: 10.15252/emmm.201910362

Wong, T. Y., Klein, R., Sun, C., Mitchell, P., Couper, D. J., Lai, H., et al. (2006). Age-related macular degeneration and risk for stroke. *Ann. Internal Med.* 145 (2), 98–106. doi: 10.7326/0003-4819-145-2-200607180-00007

Wong, W. L., Su, X., Li, X., Cheung, C. M. G., Klein, R., Cheng, C.-Y., et al. (2014). Global prevalence of age-related macular degeneration and disease burden projection for 2020 and 2040: a systematic review and meta-analysis. *Lancet Global Health* 2 (2), e106–e116. doi: 10.1016/S2214-109X(13)70145-1

Wong, C. W., Yanagi, Y., Lee, W. K., Ogura, Y., Yeo, I., Wong, T. Y., et al. (2016). Age-related macular degeneration and polypoidal choroidal vasculopathy in Asians. *Prog. Retin Eye Res.* 53, 107–139. doi: 10.1016/j.preteyeres.2016.04.002

Wu, J., Uchino, M., Sastry, S. M., and Schaumberg, D. A. (2014). Age-related macular degeneration and the incidence of cardiovascular disease: a systematic review and meta-analysis. *PloS One* 9 (3), e89600. doi: 10.1371/journal.pone.0089600

Xu, H., and Chen, M. (2016). Targeting the complement system for the management of retinal inflammatory and degenerative diseases. *Eur. J. Pharmacol.* 787, 94–104. doi: 10.1016/j.ejphar.2016.03.001

Yan, Z., Shi, H., Zhu, R., Li, L., Qin, B., Kang, L., et al. (2018). Inhibition of YAP ameliorates choroidal neovascularization via inhibiting endothelial cell proliferation. *Mol. Vision* 24, 83–93.

Yang, Z., Camp, N. J., Sun, H., Tong, Z., Gibbs, D., Cameron, D. J., et al. (2006). A variant of the HTRA1 gene increases susceptibility to age-related macular degeneration. *Science* 314 (5801), 992–993. doi: 10.1126/science.1133811

Yang, K., Wang, F.-H., Liang, Y.-B., Wong, T.-Y., Wang, J.-J., Zhan, S.-Y., et al. (2014). Associations between cardiovascular risk factors and early age-related macular degeneration in a rural Chinese adult population. *Retina* 34 (8), 1539–1553. doi: 10.1097/IAE.0000000000000118

Yannuzzi, L. A., Sorenson, J., Spaide, R. F., and Lipson, B. (1990). Idiopathic polypoidal choroidal vasculopathy (IPCV). *Retina* 10 (1), 1–8. doi: 10.1097/00006982-199010010-00001

Yoneyama, S., Sakurada, Y., Kikushima, W., Sugiyama, A., Tanabe, N., Mabuchi, F., et al. (2016). Genetic factors associated with choroidal vascular hyperpermeability and subfoveal choroidal thickness in polypoidal choroidal vasculopathy. *Retina* 36 (8), 1535–1541. doi: 10.1097/IAE.0000000000000964

Yoon, S. P., Grewal, D. S., Thompson, A. C., Polascik, B. W., Dunn, C., Burke, J. R., et al. (2019). Retinal microvascular and neurodegenerative changes in alzheimer's disease and mild cognitive impairment compared with control participants. *Ophthalmol. Retina* 3 (6), 489–499. doi: 10.1016/j.oret.2019.02.002

Yu, Y., Bhangale, T. R., Fagerness, J., Ripke, S., Thorleifsson, G., Tan, P. L., et al. (2011). Common variants near FRK/COL10A1 and VEGFA are associated with advanced age-related macular degeneration. *Hum. Mol. Genet.* 20 (18), 3699–3709. doi: 10.1093/hmg/ddr270

Yu, Y., Triebwasser, M. P., Wong, E. K. S., Schramm, E. C., Thomas, B., Reynolds, R., et al. (2014). Whole-exome sequencing identifies rare, functional CFH variants

in families with macular degeneration. *Hum. Mol. Genet.* 23 (19), 5283–5293. doi: 10.1093/hmg/ddu226

Zhang, X., and Lai, T. Y. (2018). Baseline predictors of visual acuity outcome in patients with wet age-related macular degeneration. *BioMed. Res. Int.* 2018, 10. doi: 10.1155/2018/9640131 2018.

Zhang, Z.-X., Wang, Y.-S., Shi, Y.-Y., Hou, H.-Y., Zhang, C., Cai, Y., et al. (2011). Hypoxia specific SDF-1 expression by retinal pigment epithelium initiates bone marrow-derived cells to participate in Choroidal neovascularization in a laser-induced mouse model. *Curr. Eye Res.* 36 (9), 838–849. doi: 10.3109/02713683.2011.593107

Zhang, L., Lim, S. L., Du, H., Zhang, M., Kozak, I., Hannum, G., et al. (2012). High temperature requirement factor A1 (HTRA1) gene regulates angiogenesis through transforming growth factor-β family member growth differentiation factor 6. *J. Biol. Chem.* 287 (2), 1520–1526. doi: 10.1074/jbc.M111.275990

Zhang, J., Li, S., Hu, S., Yu, J., and Xiang, Y. (2018). Association between genetic variation of complement C3 and the susceptibility to advanced age-related macular degeneration: a meta-analysis. *BMC Ophthalmol.* 18 (1), 274. doi: 10.1186/s12886-018-0945-5

Zipfel, P. F. (2009). Complement and immune defense: from innate immunity to human diseases. *Immunol. Lett.* 126 (1-2), 1–7. doi: 10.1016/j.imlet.2009.07.005

Conflict of Interest: The authors declare that the research was conducted in the absence of any commercial or financial relationships that could be construed as a potential conflict of interest.

frontiers in Pharmacology

REVIEW
published: 21 January 2020
doi: 10.3389/fphar.2019.01568

Role of Endothelial Dysfunction in Cardiovascular Diseases: The Link Between Inflammation and Hydrogen Sulfide

Hai-Jian Sun[1], *Zhi-Yuan Wu*[1], *Xiao-Wei Nie*[1] *and Jin-Song Bian*[1,2]*

[1] Department of Pharmacology, Yong Loo Lin School of Medicine, National University of Singapore, Singapore, Singapore,
[2] National University of Singapore (Suzhou) Research Institute, Suzhou, China

OPEN ACCESS

Edited by:
Owen Llewellyn Woodman,
Monash University,
Australia

Reviewed by:
Jiiang-Huei Jeng,
National Taiwan University,
Taiwan
Soon Yew Tang,
University of Pennsylvania,
United States
Joanne Hart,
University of Sydney,
Australia

***Correspondence:**
Jin-Song Bian
phcbjs@nus.edu.sg

Specialty section:
This article was submitted to Inflammation Pharmacology, a section of the journal Frontiers in Pharmacology

Received: 23 August 2019
Accepted: 03 December 2019
Published: 21 January 2020

Citation:
Sun H-J, Wu Z-Y, Nie X-W and Bian J-S (2020) Role of Endothelial Dysfunction in Cardiovascular Diseases: The Link Between Inflammation and Hydrogen Sulfide. Front. Pharmacol. 10:1568. doi: 10.3389/fphar.2019.01568

Endothelial cells are important constituents of blood vessels that play critical roles in cardiovascular homeostasis by regulating blood fluidity and fibrinolysis, vascular tone, angiogenesis, monocyte/leukocyte adhesion, and platelet aggregation. The normal vascular endothelium is taken as a gatekeeper of cardiovascular health, whereas abnormality of vascular endothelium is a major contributor to a plethora of cardiovascular ailments, such as atherosclerosis, aging, hypertension, obesity, and diabetes. Endothelial dysfunction is characterized by imbalanced vasodilation and vasoconstriction, elevated reactive oxygen species (ROS), and proinflammatory factors, as well as deficiency of nitric oxide (NO) bioavailability. The occurrence of endothelial dysfunction disrupts the endothelial barrier permeability that is a part of inflammatory response in the development of cardiovascular diseases. As such, abrogation of endothelial cell activation/inflammation is of clinical relevance. Recently, hydrogen sulfide (H_2S), an entry as a gasotransmitter, exerts diverse biological effects through acting on various targeted signaling pathways. Within the cardiovascular system, the formation of H_2S is detected in smooth muscle cells, vascular endothelial cells, and cardiomyocytes. Disrupted H_2S bioavailability is postulated to be a new indicator for endothelial cell inflammation and its associated endothelial dysfunction. In this review, we will summarize recent advances about the roles of H_2S in endothelial cell homeostasis, especially under pathological conditions, and discuss its putative therapeutic applications in endothelial inflammation-associated cardiovascular disorders.

Keywords: endothelial cell, gasotransmitters, hydrogen sulfide, inflammation, cardiovascular disease

INTRODUCTION

Currently, cardiovascular disease is identified to be a major cause of people death around the world, and this situation is estimated to remain for many years to come, thus bringing a considerable burden to the world's health resource (Mathers and Loncar, 2006). It is well known that poor diet, smoking, obesity, and physical inactivity are various modifiable risk factors for cardiovascular diseases, all of which lead to a proinflammatory state (Allende-Vigo, 2010). Actually, a wide range of

evidence supports a crucial role of inflammatory response in the pathogenesis of cardiovascular diseases through driving endothelial cell activation/dysfunction (Carter, 2012). Therefore, it is not unexpected that huge efforts have been made to identify therapeutically potential targets to halt endothelial cell inflammation.

The blood vessels are composed of connective tissue, fibroblasts, endothelial cells, and vascular smooth muscle cells (VSMCs). On the innermost side of blood vessels, the normal endothelium is a semipermeable layer between blood stream and blood vessel wall. Due to its tight specialized cell-to-cell junctions, the endothelium forms a barrier that selectively limits the movement of macromolecules (Rahimi, 2017). The barrier is critically involved in vascular tone, fluid homeostasis, and host defense (Zhang et al., 2018b). Activated endothelial cells may release various cytokines, chemokines, and growth factors that promote the proliferation, migration, and permeability of endothelial cells (Park-Windhol and D'amore, 2016). The endothelial cells with inflammatory phenotype cause inflammation in the blood vessels, resulting in endothelial dysfunction and following progression of cardiovascular diseases (Sun et al., 2016). In accordance with this notion, endothelial cell inflammation is directly responsible for various cardiovascular diseases, such as hypertension, atherosclerosis, aging, stroke, heart disease, diabetes, obesity, venous thrombosis, and intimal hyperplasia (Sun et al., 2017; Castro-Ferreira et al., 2018; Haybar et al., 2019; Zhong et al., 2019).

In the endothelium, hydrogen sulfide (H_2S), the third endogenous gaseous molecule after nitric oxide (NO) and carbon monoxide (CO), is synthesized and observed (Pan et al., 2017). Over the last decade, the roles of H_2S in the pathogenesis of endothelial dysfunction have grown exponentially. As a result, the current understanding of H_2S-mediated endothelial cell functions in both heath and disease continues to deepen. However, the potential molecular mechanisms that underlie H_2S-mediated cardiovascular homeostasis, especially endothelial inflammation, are not comprehensively elucidated. The present review focuses on the current progress regarding the roles of H_2S in endothelial inflammation-related cardiovascular disorders including hypertension, atherosclerosis and diabetes. Furthermore, we will discuss the possible challenges for developing H_2S-derived therapeutics to treat endothelial dysfunction in cardiovascular disorders.

ENDOTHELIAL DYSFUNCTION AND INFLAMMATION

The dysfunction of endothelial cells in the vasculature is profoundly implicated in the pathogenesis of cardiovascular disorders (Boulanger, 2016). Mounting evidence has shown that endothelial cell dysfunction is characterized by disrupted vascular tone and redox balance, and increased inflammatory reactions within the blood vessel wall (Ooi et al., 2018) (**Figure 1**). Most commonly, the impaired endothelium-dependent vasodilatation is defined as a hallmark of endothelial dysfunction, which is critically responsible for several cardiovascular disorders including diabetes mellitus, hypertension, atherosclerosis, aging and heart failure (Leung and Vanhoutte, 2017; Suryavanshi and Kulkarni, 2017). More recently, endothelial activation is also a prominent alteration in endothelial dysfunction, which refers to the upregulations of chemokines and adhesion molecules and other proteins involved

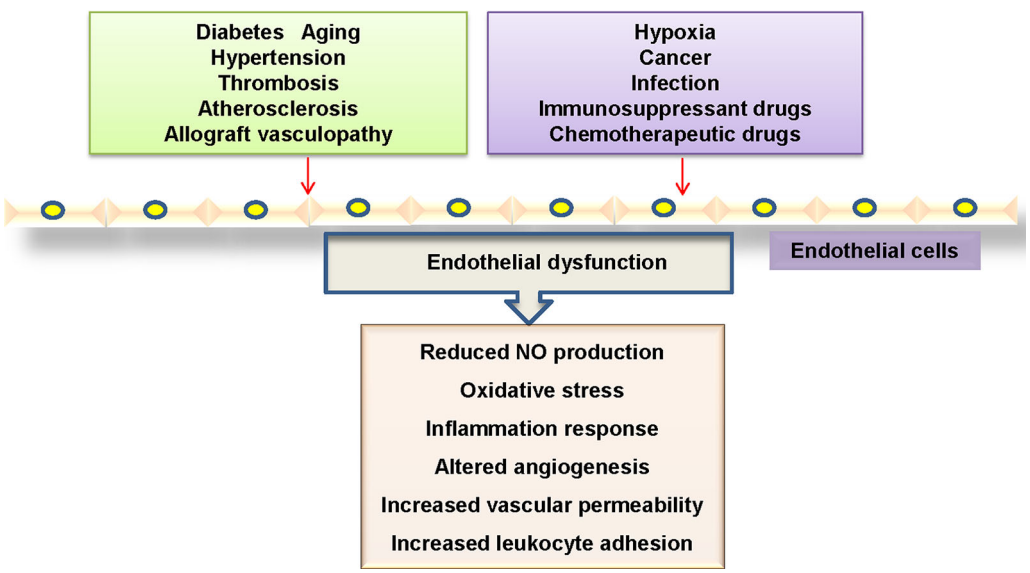

FIGURE 1 | Mechanisms linked to endothelial dysfunction. Several key mechanisms that promote endothelial dysfunction.

in cell–cell interactions (Weber and Noels, 2011; Ng et al., 2018), thus leading to the prothrombotic and proinflammatory circumstance in the blood vessels.

In activated endothelial cells, the expressions of proinflammatory cytokines, chemokines, enzymes, and adhesion molecules are substantially upregulated (Baghai et al., 2018). It is highly possible that endothelial cell inflammation plays an important role in the pathogenesis of endothelial dysfunction in cardiovascular disorders. Therefore, identification of endothelial cell-derived inflammatory factors and its underlying mechanisms may be effective in preventing the progression of cardiovascular diseases.

REGULATION OF ENDOTHELIAL FUNCTION BY H_2S UNDER PHYSIOLOGICAL CONDITION

As the third endogenous gasotransmitter, H_2S is primarily synthesized in mammalian tissues through enzymatic or non-enzymatic pathways (Li et al., 2011; Liu et al., 2012). The majority of endogenous H_2S is produced by three enzymes including cystathionine γ-lyase (CSE), cystathionine β-synthase (CBS) and 3-mercaptopyruvate sulfurtransferase (3-MST) in mammalian tissues (Liu et al., 2011) (**Figure 2**). In the vascular endothelium, H_2S is synthesized *via* the enzymatic metabolism of

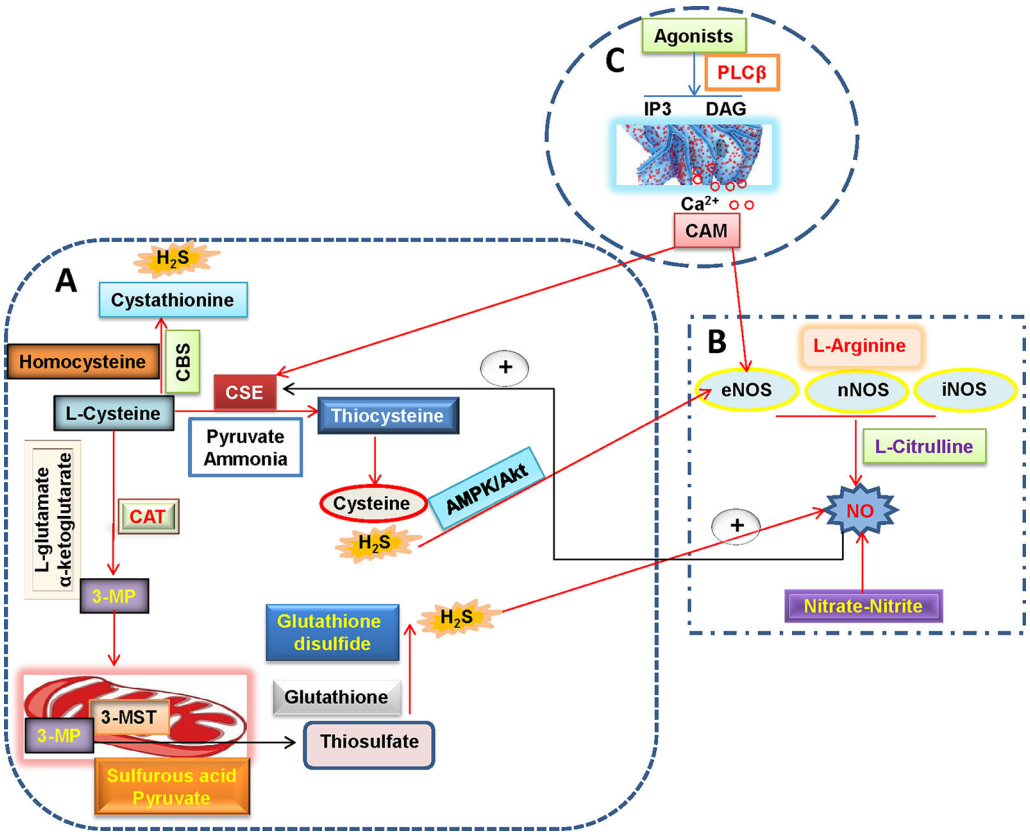

FIGURE 2 | H_2S and NO biosynthetic pathways in blood vessels. **(A)** L-cysteine is the substrate for the formation of H_2S through three H_2S-producing enzymes, L-cysteine is catalyzed by CSE to produce pyruvate, ammonia, and thiocysteine, the latter is then decomposed to cysteine and H_2S. The endogenous H_2S production by CBS is related with the condensation of homocysteine with L-cysteine, followed by the formation of cystathionine and H_2S. Direct reaction of L-cysteine and α-ketoglutarate by CAT yields the release of 3-MP and L-glutamate, 3-Mercaptopyruvate is transported into the mitochondria where it is catalyzed to sulfurous acid, pyruvate and thiosulfate by 3-MST. In the presence of reduced glutathione, the thiosulfate is reduced to glutathione disulfide and H_2S. It is well accepted that H_2S can increase eNOS activity and thereby subsequent NO production directly or through AMPK/Akt signaling pathway. **(B)** NO is produced in all tissues by NOS-dependent (L-arginine-NO pathway) and -independent (nitrate-nitrite-NO pathway) pathways. A recently discovered pathway for NO generation is the serial reduction of the inorganic anions nitrate and nitrite. With the assistance of three isoforms of NOS including nNOS, eNOS, and iNOS, L-arginine is oxidized into L-citrulline with NO. NO is found ro increase CSE activity and expression and then stimulate H_2S production. **(C)** In endothelial cells, vasoconstrictor agonists stimulate the release of Ca^{2+} and cause formation of calcium-calmodulin (CaM) *via* the PLCβ/IP3/DAG pathway. Then, CaM can simultaneously activate eNOS and CSE that yield NO and H_2S, respectively. H_2S, hydrogen sulfide; NO, nitric oxide; 3-MP, 3-mercaptopyruvate; CAT, cysteine aminotransferase; CSE, cystathionine γ-lyase; CBS, cystathionine β-synthase; 3-MST, 3-mercaptopyruvate sulfurtransferase; CaM, calcium-calmodulin; PLCβ, phospholipase Cβ; IP3, inositol-3-phosphate (IP3); DAG, diacylglycerol (DAG); eNOS, endothelial NO synthase; iNOS, inducible NO synthase; nNOS, neuronal NO synthase.

CBS/CSE using cysteine as the substrates (Tao et al., 2017; Mitidieri and Gurgone, 2019). Likewise, the involvement of 3-MST and cysteine aminotransferase (CAT) in endothelial generation of H_2S has been demonstrated (Wang, 2012).

The regulation of vascular tone by H_2S may be dependent on endothelium-independent and -dependent manners (Wang et al., 2015b). In the vasculature, H_2S has been shown to induce vasodilation in aorta (Zhao et al., 2001), gastric artery (Kubo et al., 2007), mesenteric artery (Cheng et al., 2004), and internal mammary artery (Webb et al., 2008). The underlying mechanism by which H_2S relaxes blood vessels is related with activation of vascular smooth muscle ATP-sensitive K^+ (KATP) channels (Zhao et al., 2001), independently of the endothelium. The involvement of KATP channels in H_2S-induced vasodilation is further confirmed by a finding that this relaxation is partially blocked by an inhibitor of KATP channels glibenclamide (Webb et al., 2008). Despite of these results, the exact mechanism of how KATP channels are directly activated by H_2S still remains unknown. It is also reported that 4-aminopyridine-sensitive K^+ channels are involved in H_2S-induced relaxation in the rat coronary artery (Cheang et al., 2010). The H_2S donor sodium hydrosulfide (NaHS) induces concentration-dependent vasorelaxation in both mesenteric arteries and aortas, which is blocked by the KCNQ-type Kv channel inhibitor XE991, suggesting the involvement of KCNQ channels in H_2S-mediated peripheral artery relaxation (Schleifenbaum et al., 2010). Moreover, Ca^{2+} channels or sparks (Jackson-Weaver et al., 2015), Cl(-)/HCO(3)(-) channels (Kiss et al., 2008), the NO pathway (Ali et al., 2006), phospholipase A2 (D'emmanuele Di Villa Bianca et al., 2011), transient receptor potential (TRP) channels (White et al., 2013), and metabolic/mitochondrial effects (Kiss et al., 2008), are also suggested to be implicated in H_2S-induced vasorelaxation. H_2S appears to play an important role in vasorelaxation *via* multidimensional mechanisms. In the endothelium, recent studies have provided several lines of evidence to support that H_2S might function as an endothelium-derived relaxing factor (EDRF), which shares many common traits with other EDRFs (Wang, 2009). Interestingly, the vasorelaxation actions of H_2S are more remarkable in peripheral resistance arteries than in large-conduit arteries, the effects require the membrane hyperpolarization of both VSMCs and endothelial cells, as well as activation of endothelial intermediate conductance (IK(Ca)) and small conductance (SK(Ca)) potassium channels (Mustafa et al., 2011; Tang et al., 2013). The definition of H_2S as an endogenous EDHF might shed light on possible therapeutic effects of H_2S on pathological abnormalities in the vascular system. Still, more extensive and mechanistic studies are needed to determine whether H_2S is a new EDRF in the future.

The endothelial cells also orchestrate tube formation and angiogenesis (Watson et al., 2017). H_2S is reported to stimulate endothelial proliferation, migration, and angiogenesis (Wang et al., 2010b) (**Figure 3**). Furthermore, administration of H_2S promotes angiogenesis in the Matrigel plug assay (Cai et al., 2007). However, it should be pointed out that high dose of H_2S loses the ability to induce angiogenesis (Cai et al., 2007). In a rat

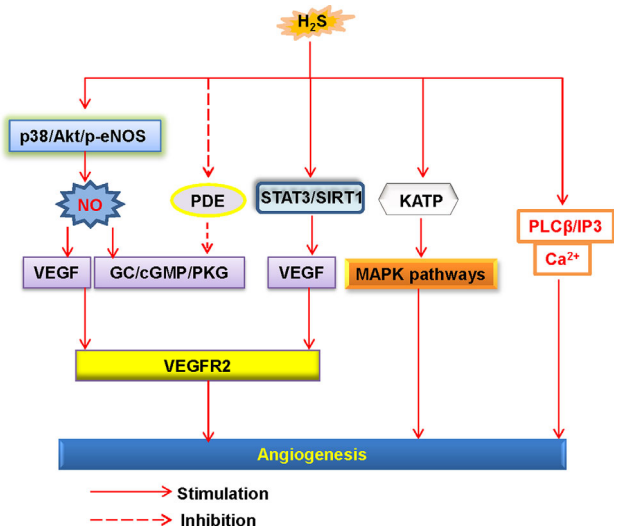

FIGURE 3 | Schematic illustration of the underlying mechanisms of H_2S-induced angiogenesis. H_2S, hydrogen sulfide; NO, nitric oxide; Akt, protein kinase B; p38, p38 mitogen-activated protein kinases; eNOS, endothelial NO synthase; VEGF, vascular endothelial growth factor; VEGFR2, vascular endothelial growth factor receptor 2; PDE, phosphodiesterase; GC, guanylate cyclase; cGMP, cyclic guanosine monophosphate; PKG, protein kinase G; SIRT1, sirtuin 1; KATP, ATP-sensitive K+ channels; MAPK, mitogen-activated protein kinase; STAT3, signal transducer and activator of transcription 3; PLCβ, phospholipase Cβ; IP3, inositol-3-phosphate (IP3).

model of chronic hindlimb ischaemia, intraperitoneal injection of the H_2S donor NaHS at the lower dose significantly improves capillary density, angiographic scores, thus improving hindlimb blood flow (Wang et al., 2010a). In line with the results discussed earlier, higher dose of the H_2S donor is found to be ineffective in this model (Wang et al., 2010a). On these grounds, we speculate that the effects of H_2S donors in angiogenesis may range from physiological, cytoprotective effects (low concentration) to cytotoxic effects (which are generally apparent at higher concentrations) (Szabo and Papapetropoulos, 2011). From a genetic perspective, mutant mice lacking CSE exhibit a variety of pathological features, including delayed wound healing secondary to inhibition of angiogenesis (Papapetropoulos et al., 2009). It has been reviewed that several cellular signaling pathways, such as the PI3K/Akt pathway, the mitogen activated protein kinase (MAPK) pathway, and ATP-sensitive potassium channels, are involved in H_2S-mediated angiogenic effects (Szabo and Papapetropoulos, 2011). In addition to this, further study has demonstrated that H_2S specifically disrupts cys1045-cys1024 disulfide bond in vascular endothelial growth factor receptor 2 (VEGFR2) and then stimulates its conformation for angiogenesis (Tao et al., 2013). As a molecular switch, H_2S is also reported to activate signal transducer and activator of transcription 3 (STAT3) (Kan et al., 2014), mammalian target of rapamycin (mTOR), and the VEGFR2 pathway (Zhou et al., 2016), then the endothelial cell proliferation and angiogenesis are observed. It is noteworthy that

due to its proangiogenic effects, H_2S might lead to pathological angiogenesis in atherosclerotic plaques, thus facilitating plaque vulnerability (Van Den Born et al., 2016). In spite of this, therapeutic angiogenesis is important for wound healing, organ ischaemia, or the reperfusion of previously ischaemic organs (Caporali and Emanueli, 2011; Dulmovits and Herman, 2012; Ng et al., 2018). For this reason, the reparative angiogenesis by H_2S may provide novel therapeutic avenues for post-ischemic neovascularization. Due to the physiological importance of H_2S in the endothelium, further research is indispensable to examine the novel roles of endogenous H_2S in the regulation of cardiovascular functions.

ROLE OF H_2S IN ENDOTHELIAL INFLAMMATION

Using intravital microscopy, H_2S donors are found to attenuate the leukocyte adherence in rat mesenteric arteries induced by aspirin, this effect may be likely dependent on activation of KATP channels (Zanardo et al., 2006; Zuidema and Korthuis, 2015). In accordance with this, blockade of endogenous H_2S exacerbates leukocyte-mediated inflammation in the endothelium (Zanardo et al., 2006). By contrast, NaHS promotes leukocyte rolling and adherence in mesenteric venules of mice with cecal ligation and puncture (CLP)-induced sepsis (Zhang et al., 2007). These conflicting results imply that H_2S acts as a pivotal regulator of leukocyte activation under different inflammatory states. However, in recent years, more studies support that H_2S could inhibit the process of endothelial cell inflammation (Wen et al., 2018). For instance, specific endothelial deletion of CSE is associated with the development of endothelial inflammation and atherosclerosis, effects that are reversed on treatment with a polysulfide donor (Bibli et al., 2019). H_2S treatment reduces the increases in inflammatory mediators such as vascular cell adhesionmolecule-1 (VCAM-1), intercellular adhesionmolecule-1 (ICAM-1) and monocyte chemoattractant protein-1 (MCP-1) in endothelial cell induced by tumour necrosis factor-α (TNF-α), and the underlying mechanism of this protective effect is primarily mediated by inhibition of soluble TNF-α shedding and its relevant MCP-1 release (Perna et al., 2013). Similarly, exogenous H_2S attenuates Ang II-induced inflammation response *via* inhibition of the nuclear transcription factor-κB (NF-κB) signaling pathway in endothelial cells (Hu et al., 2016). Inhibition of the NF-κB pathway is also required for H_2S to attenuate pulmonary endothelial cell inflammation and subsequent pulmonary hypertension (Feng et al., 2017b). Endogenous H_2S could directly induce sirtuin1 (SIRT1) sulfhydration and stability, thus reducing aortic inflammation and atherosclerotic plaque formation (Du et al., 2019). Deficiency of CSE increases endogenous sulfur dioxide (SO_2) level in endothelial cells, and blockade of endogenous SO_2 aggravates CSE knockdown-induced NF-κB pathway and its downstream inflammatory factors release in endothelial cells (Zhang et al., 2018a), suggesting that the increased endogenous SO_2 generation might act as a compensatory mechanism for the downregulated CSE/H_2S pathway in endothelial inflammatory response (Zhang et al., 2018a). It is concluded that the anti-inflammatory effects of H_2S donors show tremendous promise for the treatment of endothelial inflammation-related cardiovascular disorders.

In response to proinflammatory cytokines, the leukocyte or macrophages are activated and recruited to the endothelium, thus causing the development of endothelial dysfunction-related cardiovascular diseases (Fang et al., 2013). Fortunately, H_2S is found to alleviate vascular inflammation through various signaling pathways, including inhibition of NF-κB and nucleotide-binding oligomerization domain, leucine rich repeat, and pyrin domain-containing protein 3 (NLRP3) inflammasome, activation of KATP channels and voltage- and calcium-gated potassium (BKCa) channels (Fiorucci et al., 2005; Zanardo et al., 2006; Zuidema et al., 2010; Altaany et al., 2014; Bourque et al., 2018; Li et al., 2019). These possible mechanisms of H_2S may explain that H_2S can diminish vascular inflammation and attenuate the vascular injury, suggesting that the anti-inflammation effect of H_2S is a benefit for cardiovascular protection. Next, we will discuss the beneficial roles of H_2S-mediated suppression of endothelial dysfunction in cardiovascular disorders including atherosclerosis, diabetic cardiovascular complications and hypertension.

H_2S-RELATED ENDOTHELIAL DYSFUNCTION IN ATHEROSCLEROSIS

Atherosclerosis, a chronic vascular disease of large and medium arteries, involves various risk factors including lipid deposition, hypertension, inflammatory factors, and hyperhomocysteinemia, which synergistically elicit endothelial dysfunction (Baszczuk et al., 2014). Biochemical effects of these factors on the endothelium could lead to endothelial cell damage and vascular remodeling (Baszczuk et al., 2014). This important event induces endothelial inflammation, macrophage differentiation, foam cell formation, platelet deposition, and thrombus formation (Chistiakov et al., 2017; Rahman and Woollard, 2017). As such, correction of endothelial dysfunction could be a therapeutic strategy for management of atherosclerosis.

In recent years, considerable evidence indicates that the downregulated CSE/H2S pathway plays a pathophysiologic role in the development of atherosclerosis (Kanagy et al., 2017; Fan et al., 2019). CSE-knockout mice fed with atherogenic diet exhibt more severe atherosclerosis, suggesting that the disturbed CSE/H2S pathway predisposes the animals to the development of atherosclerosis (Mani et al., 2013). Macrophage inflammation directly contributes to necrotic core formation and plaque instability in atherosclerosis (Kavurma et al., 2017). In oxidized low density lipoprotein (ox-LDL)-treated macrophage, the levels of CSE mRNA and protein expression, as well as H2S production are remarkably decreased, thus, this finding indicates that alterations of the CSE/H2S pathway plays an important role in ox-LDL-stimulated macrophage inflammation and atherosclerosis (Wang et al., 2013b). It is worth noting that

CBS deficiency may cause hyperhomocysteinemia, which is an independent risk factor for the development of atherosclerosis (Zhang et al., 2012a; Yuan et al., 2017). In transgenic CBS-deficient mice, the emegence of hypercholesterolemia accelerates atherosclerotic lesions via oxidative stress and inflammatory monocyte generation (Zhang et al., 2009). On the other hand, vascular calcification and neointimal hyperplasia are also involved in the progression of atherosclerosis (Durham et al., 2018; Yu et al., 2018). Not surprisingly, the production of H2S and CSE protein expression are obviously decreased in rats with vascular calcification (Wu et al., 2006). The CSE expression and H2S production are impaired during the development of balloon injury-induced neointimal hyperplasia in rats, and this effect is obviously reversed by H2S treatment (Meng et al., 2007). In mice with high fat diet for 16 weeks, it is found that CSE protein level is downregulated in the liver, the lung, and the aortic endothelium, 3-MST was also reduced in the liver (Peh et al., 2014). By contrast, CBS expression was higher in the liver and the kidney (Peh et al., 2014). These results suggest that an abnormal H2S pathway may be an important factor for the pathophysiology of metabolic disorders and atherosclerosis.

The anti-atherosclerotic mechanisms of H_2S have been gradually described, including anti-inflammatory response, anti-oxidative action, endothelial function preservation, inhibition of foam cell formation and regulation of ion channels (Altaany et al., 2014; Mani et al., 2014; Xu et al., 2014; Wang et al., 2017; Barton and Meyer, 2019). Reduced CSE expressions at both mRNA and protein levels are detected in ox-LDL-treated endothelial cells and in aortas from apolipoprotein E knockout ($ApoE^{-/-}$) mice (Leucker et al., 2017). In this study, the authors demonstrated that increased histone deacetylase 6 (HDAC6) downregulated CSE and H_2S production *via* posttranslational modifications, thus leading to endothelial cell dysfunction and the development of atherosclerosis (Leucker et al., 2017). In cultured vascular endothelial cells, the expressions of miR-455-3p, endothelial nitric oxide synthase (eNOS) protein and NO production are augmented by H_2S. Besides, H_2S levels and miR-455-3p expressions are also increased in human atherosclerosis plaque, suggesting that the miR-455-3p/eNOS/NO axis is required to H_2S to circumvent the development of atherosclerosis (Li et al., 2017). Genetic deletion of CSE exaggerates atherosclerosis in $ApoE^{-/-}$ mice, and treatment of CSE-knockout mice with H_2S inhibits the development of atherosclerosis (Mani et al., 2013), pinpointing that endogenous H_2S may be of benefit in the treatment of atherosclerosis. In addition, the augmented expressions of selectins (P-selectin and E-selectin) and cell adhesion molecules (ICAM-1 and VCAM-1) are observed in vascular endothelial cells from CSE knockout mice (Mani et al., 2013). GYY4137, a novel slow-releasing H_2S compound, retards atherosclerotic plaque formation and partially restores endothelium-dependent relaxation in $ApoE^{-/-}$ mice through decreasing vascular inflammation and oxidative stress (Liu et al., 2013). Preconditioning with NaHS also grants a protection in atherosclerosis, as manifested by decreased atherosclerotic plaque size and aortic ICAM-1 levels (Wang et al., 2009). Supplementation with H_2S ameliorates, while inhibition of H_2S formation intensified aortic CX3CR1 and CX3CL1 expressions and the formation of atherosclerosis (Zhang et al., 2012b). Recently, H_2S induces S-sulfhydration of kelch-like ECH-associated protein 1 (Keap1) and nuclear factor erythroid 2-related factor 2 (Nrf2) dissociation from Keap1, followed by Nrf2 nuclear translocation and anti-oxidize effects in endothelial cells, contributing to the ameliorating effect of H_2S on atherosclerosis in the context of diabetes (Xie et al., 2016). Furthermore, in a mouse model of disturbed flow-induced atherosclerosis, application of H_2S donor NaHS considerably attenuates the severity of atherosclerosis via upregulating expressions of angiotensin converting enzyme 2 (ACE2), thus converting pro-atherosclerotic Ang II to anti-atherosclerotic angiotensin 1-7 (Ang-(1-7)) (Lin et al., 2017). At the cellular level, NaHS promotes the expression of ACE2 to exert anti-inflammatory properties in lipopolysaccharide (LPS)-stimulated endothelial cells, as pretreatment with a selective ACE2 inhibitor DX600 abrogates the anti-inflammatory effect of NaHS (Lin et al., 2017). The results showed that endogenous H_2S system was involved in the development of atherosclerosis. Exogenous H_2S could confer beneficial effects on the pathogenesis of atherosclerosis.

Also, H_2S is involved in shear stress and blood viscosity. The occurrence of atherosclerosis may be initiated due to changed patterns of blood flow and ensuing shear stress (Dunn et al., 2015). It is well established that atherosclerotic plaque formation in the endothelium is site specific, and disturbed blood flow formed at the lesser curvature of the aortic arch and branch points promotes plaque formation, whereas steady laminar flow at the greater curvature is indicated to be atheroprotective (Heo et al., 2016). The branches and curvatures of the blood vessels are predisposed to endothelial dysfunction and atherosclerosis progression (Zhou et al., 2014). Under oscillatory shear stress, H_2S treatment inhibits monocyte adhesion to endothelial cells *via* activating the NO-producing Akt/eNOS signaling pathway (Go et al., 2012). Conversely, H_2S impairs shear stress-induced dilation of isolated mouse coronary arteries by inhibition of NO generation (Chai et al., 2015). It is likely that both H_2S and NO are implicated in the shear stress-induced atherosclerosis. However, further investigation is required to help us obtain more novel insights into the underlying mechanisms.

H_2S-RELATED ENDOTHELIAL DYSFUNCTION IN DIABETIC VASCULAR COMPLICATIONS

Circulating levels of H_2S are markedly reduced in diabetic animal models, such as diabetic rats (Jain et al., 2010; Suzuki et al., 2011), diabetic mice (Brancaleone et al., 2008), and also in diabetic patients (Jain et al., 2013; Suzuki et al., 2017). However, the mRNA level of CSE in the aortas of diabetic rats is not altered (Denizalti et al., 2011). Likewise, the expressions of CSE, CBS, and 3-MST are unaltered in either high glucose-treated endothelial cells or in the aortas of diabetic rats (Jain et al.,

2010; Coletta et al., 2015). On the contrary, it has been demonstrated that both high glucose and palmitate inhibit CSE expression and H_2S production in rat aortic endothelial cells, while exogenous H_2S could protect endothelial cells against apoptosis under high glucose and palmitate stimulation *via* suppressing oxidative stress, decreasing mitochondrial fragments and promoting mitophagy (Liu et al., 2017). The CSE expression and H_2S content are significantly reduced in granulation tissues of wounds in obese diabetic mice when compared with control mice (Zhao et al., 2017). The expression of CSE and H_2S level are reduced after renal ischemia/reperfusion injury in diabetes mellitus (Chen et al., 2018). In comparison with control mice, the H_2S content and CSE expression in heart tissues of diabetic rats are also markedly lower (Guo et al., 2017). In progressive diabetic nephropathy, CSE expression is markedly reduced, whereas CBS expression is unaffected (Yamamoto et al., 2013). By contrast, the protein and mRNA expression of CBS are specifically decreased in the kidney, while CSE expression remains unchanged in obese diabetic mice (Liu et al., 2018). Interestingly, CSE expression is upregulated in cerebral microvessels of type I diabetic rats (Streeter et al., 2013). Although the data are conflicting, they raise the possibility that H_2S may be a double-edged sword under diabetic pathophysiology. Certainly, more research is needed to determine the molecular mechanisms underlying the changed or unchanged expressions of H_2S-generating enzymes/H_2S under diabetic conditions.

Despite of the aforementioned results, recent study has demonstrated that 3-MST activity is inhibited in endothelial cells during hyperglycemia, leading to reduced H_2S level, impaired angiogenesis, and suppressed mitochondrial function (Coletta et al., 2015). It is highly probable that inactivation of 3-MST and elevated H_2S depletion are putative mechanisms for the decreased circulating H_2S levels in hyperglycemic endothelial cells. The high glucose-incubated vascular rings exhibit impaired endothelium-dependent relaxation, and this effect is rescued by CSE overexpression or H_2S supplementation (Suzuki et al., 2011). In the same study, they have also shown that the vascular rings from mice with gene knockout of CSE display an aggravated impairment of endothelium-dependent relaxation in response to hyperglycemia (Suzuki et al., 2011). It is anticipated that genetic modulations of CSE, CBS or 3-MST levels are effective approaches to experimentally investigate the roles of H_2S in diabetic vascular complications.

Exposure to high glucose results in elevated ROS production and apoptosis, as well as decreased superoxide dismutase activity in endothelial cells, and all the above responses could be eliminated by pretreatment with H_2S (Guan et al., 2012). Exogenous H_2S alleviated the ROS overproduction and apoptosis in hyperglycemic endothelial cells through inhibiting necroptosis (Lin et al., 2018). In the aortas of diabetic rats, the connexin (Cx) 43 and 40 expressions are downregulated, while protein kinase C (PKC) and nicotinamide adenine dinucleotide phosphate-oxidase (NADPH) oxidase subunits are upregulated, H_2S appears to be effective in attenuating these abnormalities (Zheng et al., 2010). The novel mitochondria-targeted H_2S donors AP123 and AP39 are proven to prevent hyperglycemia-triggered oxidative stress and metabolic abnormalities in microvascular endothelial cells, suggesting that these compounds could be useful for the treatment of diabetic vascular complications (Gero et al., 2016). Induction of H_2S by Ginkgolide B alleviates endothelial dysfunction *via* inhibiting oxidative stress and increasing NO bioavailability in diabetic rats (Wang et al., 2015a). It is likely that the cardiovascular protective effects of H_2S in diabetes may be mediated by inhibition of oxidative stress.

Inhibition of the leptin/leptin receptor signal pathway contributes to the protective effects of H_2S on high-glucose-induced injuries in endothelial cells (Wu et al., 2016). Pretreatment with H_2S prevents high glucose-induced ICAM-1 levels as well as NF-κB activation in endothelial cells (Guan et al., 2013). Besides, stimulation of endothelial cells with high glucose significantly promotes the secretion of endothelin-1 with the concomitant suppression of H_2S production, and administration of H_2S attenuates the release of endothelin-1 induced by high glucose (Guan et al., 2015). The increasing recognitions of protective effects of H_2S in high glucose-induced endothelial inflammation provide a new avenue of antagonism towards diabetic vascular complications.

In addition, high glucose/palmitate-induced excessive autophagy in endothelial cells is rectified by H_2S, this may be mediated by the Nrf2-ROS-adenosine 5'-monophosphate (AMP)-activated protein kinase (AMPK) signaling pathway (Liu et al., 2016). However, another group demonstrates that exogenous H_2S inhibits mitochondrial apoptosis and promotes mitochondrial autophagy, thus protecting endothelial cells against apoptosis induced by high glucose and palmitate (Liu et al., 2017). These contradictory results suggest that additional research is necessary to ascertain the role of autophagy in H_2S-mediated protective actions on diabetic endothelial dysfunction.

H_2S-RELATED ENDOTHELIAL DYSFUNCTION IN HYPERTENSION

The abnormal levels of H_2S have been found to be correlated with hypertension (Szabo, 2007; Whiteman and Winyard, 2011). Specifically, in a clinical study, patients with severe hypertension exhibited lower plasma H2S level (Meng et al., 2015). In subjects with pulmonary hypertension, both CSE expression and H2S level are significantly lower than those in healthy population (Sun et al., 2014). *In situ* hybridization analysis has shown that the expression of CSE mRNA is downregulated in the pulmonary arteries of rats with pulmonary hypertension (Xiaohui et al., 2005). Likewise, the reduced protein contents of CSE and CBS are detected in pulmonary artery endothelial cells from tobacco smoke-induced emphysema and pulmonary hypertension (Han et al., 2011). It has been revealed a marked reduction in CBS and CSE expression as well as H2S production in mesenteric artery and carotid artery from dexamethasone-induced hypertensive rats (D'emmanuele Di Villa Bianca et al., 2015). By contrast, the suppressed CBS expression and reduced H2S concentration in the kidney are

observed in high salt-induced hypertension in Dahl rats (Huang et al., 2015). A decreased CSE/H2S activity is a potential contributor to the pathogenesis of maternal hypertension in preeclampsia (Wang et al., 2013a). Also, the plasma H2S level and CSE protein expression in thoracic aorta are all suppressed in spontaneously hypertensive rats (SHR) in comparison with normotensive rats (Yan et al., 2004; Ahmad et al., 2014). An intriguing study has illustrated that the blood pressure is enhanced by treatment with the combination of CSE inhibitor DL-propargylglycine (PAG) or the CBS inhibitor aminooxyacetic acid (AOA) in rats, while either compound alone has no any effect on the arterial pressure, suggesting that H2S plays a critical role in regulating blood pressure (Roy et al., 2012). Despite that the expression of 3-MST is still uncertain under hypensive condition, 3-MST gene therapy improves renovascular dysfunction in response to hyperhomocysteinemia (Sen et al., 2012). Thus, a better understanding of the biochemical functions of the H2S-producing enzyme 3-MST as well as its roles in hypertension may lead to new therapeutic targets based on modulation of H2S production. Overall, these studies suggest that endogenous H2S dysregulation plays an important role in regulating hypertneison-associated pathological processes.

As mentioned above, a close relationship between H_2S-related endothelial dysfunction and hypertension is confirmed by an observation that genetic deletion of CSE causes the development of hypertension in mice (Yang et al., 2008). In these CSE knockout mice, the endothelium-dependent relaxation of resistance mesenteric arteries is particularly impaired (Yang et al., 2008). In a mouse model of Ang II-induced hypertension, both aortic endothelial function and NO bioavailability are significantly attenuated, and these are reversed by treatment with H_2S (Al-Magableh et al., 2015). Conversely, blockade of endogenous H_2S exacerbates these abnormalities (Al-Magableh et al., 2015). In other studies, application of H_2S donors decrease blood pressure, reverse vascular remodeling *via* suppressing VSMC proliferation, and collagen deposition in the blood vessels (Zhao et al., 2001; Li et al., 2008; Wang, 2012; Meng et al., 2015; Tomasova et al., 2015). H_2S therapy markedly restores eNOS function and NO bioavailability in Nω-nitro-l-arginine methyl ester (L-NAME)-induced hypertensive rats (Ji et al., 2014). In agreement with this, the improvement of endothelial function by H_2S is largely attributed to inhibition of oxidative stress, suppression of renin angiotensin system (RAS), downregulation of BMP4/COX-2 pathway, or activation of the PPARδ/PI3K/Akt/AMPK/eNOS pathway, thus contributing to the antihypertensive mechanism of H_2S in renovascular hypertensive rats (Xue et al., 2015; Xiao and Dong, 2016; Xiao et al., 2018). In SHR, exogenous H_2S administration significantly reduces blood pressure and abrogated damaged endothelial dysfunction *via* inactivation of NLRP3 inflammasome and oxidative stress (Li et al., 2019). H_2S treatment blunts increases in systolic blood pressure and ameliorates endothelial dysfunction by inhibiting oxidative stress in lead-induced hypertensive rats (Possomato-Vieira and Goncalves-Rizzi, 2018). These results demonstrate that the H_2S pathway may provide potential therapeutic target for treating different hypertension models.

Importantly, supplementation with S-zofenopril ameliorates vascular endothelial dysfunction by potentiating the H_2S pathway in spontaneously hypertensive models (Bucci et al., 2014). Moreover, exercise training counteracts hypertension, ameliorates vascular remodeling, and endothelial dysfunction *via* restoring bioavailability of H_2S and NO in hypertensive rats (Gu et al., 2013). HDAC6 inhibitor tubastatin A alleviates Ang II-induced high blood pressure and vasoconstriction by preventing the protein degradation of CSE (Chi et al., 2019). Overall, these studies suggest that upregulation of H_2S may be considered as a promising strategy for preventing the progression of hypertension and its associated endothelial dysfunction (**Figure 4**). However, further in-depth research is still required to understand the precise underlying mechanisms, and this will be helpful to develop better therapeutic employment of H_2S in the treatment of hypertension.

EVIDENCE FOR H_2S/NO CROSSTALK IN ENDOTHELIAL INFLAMMATION

Due to the importance of H_2S and NO in cardiovascular disease, the interactive regulatory functions of H_2S and NO in endothelial dysfunction-associated cardiovascular disease may be a very attractive subject. In other words, the biological interactions of H_2S with NO could influence each other's fate in the endothelium as described previously (Wang et al., 2015b; Nagpure and Bian, 2016; Wu and Hu, 2018) (**Figure 2**).

Studies on H_2S/NO interaction in inflammation response, especially in endothelial cell inflammation, have been less extensive. Administration of LPS increases H_2S synthesis, upregulates CSE and iNOS expressions, and promotes myeloperoxidase activity in the liver, whereas the effects are inhibited by the NO donor, nitroflurbiprofen (Anuar et al., 2006). These results suggest that downregulation of H_2S biosynthesis is responsible for the augmented anti-inflammatory activity of nitroflurbiprofen in the liver (Anuar et al., 2006). In turn, pretreatment with H_2S is able to inhibit LPS-induced iNOS expression and NO production *via* heme oxygenase 1 (HO-1) expression in macrophages (Oh et al., 2006). In accordance with this finding, H_2S donor inhibits the release of the pro-inflammatory mediators and NO production, potentially *via* NF-κB inactivation in LPS-treated macrophages (Whiteman et al., 2010). The pulmonary CSE expression and H_2S levels are downregulated in a model of inflammatory lung disease (Chen et al., 2009; Whiteman and Winyard, 2011). NaHS, a donor for H_2S, significantly attenuates pulmonary iNOS activation in ovalbumin-treated rats (Chen et al., 2009). Moreover, H_2S is found to act as an anti-inflammatory agent contributing to gastrointestinal mucosal defense through NO-dependent pathway (Jensen et al., 2017). In cardiovascular system, vasodilation is impaired and endothelial H_2S content is decreased in vessels from obese mice, this may be attributed to

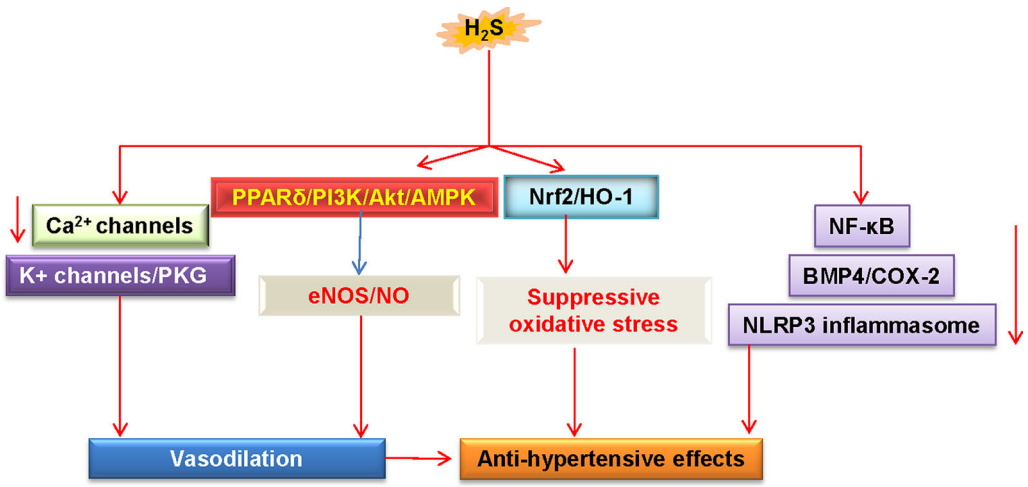

FIGURE 4 | Schematic illustration of underlying mechanisms in which H_2S protects against hypertension. H_2S lowers high blood pressure *via* vasodilatation by activation of vascular KATP channels and inhibition of Ca^{2+} influx. The PPARδ/PI3K/Akt/AMPK signaling pathway participates in H_2S-induced NO production. These above events cause vasodilation. H_2S inhibits ROS production *via* Nrf-2/HO-1 related redox sensitive signaling pathways. In addition, H_2S treatment blunts increases in systolic blood pressure by inhibiting inflammation-related signaling pathways. H_2S, hydrogen sulfide; NO, nitric oxide; Akt, protein kinase B; eNOS, endothelial NO synthase; PKG, protein kinase G; PI3K, phosphoinositide 3-kinase; PPARδ, peroxisome proliferators-activated receptor δ; AMPK, adenosine 5'-monophosphate (AMP)-activated protein kinase; Nrf2, nuclear factor erythroid 2-related factor 2; HO-1, heme oxygenase 1; NF-κB, nuclear factor-kappa B; BMP4, bone morphogenetic protein 4; COX-2, cyclooxygenase-2; NLRP3, nucleotide-binding oligomerization domain, leucine rich repeat, and pyrin domain-containing protein 3.

the increased iNOS activity in proinflammatory macrophages (Candela et al., 2017). This finding suggests that macrophages-derived iNOS promotes microvascular endothelial dysfunction through reducing the bioavailability of H_2S in the blood vessel (Candela et al., 2017). GYY4137, a novel slow-releasing H_2S compound, is reported to attenuate vascular inflammation and improve endothelial function *via* activating aortic eNOS phosphorylation in $ApoE^{-/-}$ mice (Liu et al., 2013). A number of studies have showed that H_2S strengthens endothelial NO production *via* activating eNOS phosphorylation (Predmore et al., 2011; Xiao et al., 2018), which results in ameliorating the development of hypertension (Xiao et al., 2018). Taken together, the above studies imply that a complex interaction between H_2S and NO might serve as an important regulator for endothelial inflammation and associated endothelial dysfunction. However, the potential mechanisms of the interactions between H_2S and NO in endothelial inflammation remain unclear. As research in this area progresses and more data are available, it will help us to better understand the underlying mechanisms.

ROLE OF H_2S IN INTESTINAL MICROBIOTA AND CIRCADIAN RHYTHMS

It should be emphasized that intestinal microbiota is also an emerging factor for human health and disease, including cardiovascular diseases (Tang et al., 2017). In recent years, both human and animal experiments have established that alterations in the composition, function, and metabolites of intestinal flora might induce gut microflora dysbiosis, contributing to the pathogenesis of cardiovascular disorders (Tang et al., 2019). Circadian rhythmicity is a characteristic of mammalian metabolism that orchestrates metabolic processes in living organisms based on day/night light cycles (Liu and Chang, 2017). Disturbance of circadian rhythmicity is associated with increased risk for metabolic obesity, diabetes, and cardiovascular dysfunction (Crnko et al., 2018). Similarly, the intestinal microbiota exhibits their own circadian rhythmicity in terms of composition and functions (Tahara et al., 2017). Circadian disorganization may affect the intestinal microbiota which may result in metabolic syndrome and cardiovascular diseases (Voigt et al., 2016). Accumulating evidence has indicated that circadian rhythm disruption in intestinal microbiota is involved in various human diseases, including cardiovascular diseases (Jin et al., 2019). Thereafter, interfering with the composition, function, and metabolites of the intestinal flora or recovery of the normal circadian rhythm in the intestinal flora may provide valuable insights into potential therapeutic strategies for cardiovascular diseases.

Notably, the cysteine degradation by the microbiota is taken as a dominant pathway for H_2S generation (Basic et al., 2017). Intestinal microbiota is a potential target of H_2S, and H_2S acts on gastrointestinal epithelium to modify the gut microbiota (Wallace et al., 2018). It has been reviewed that H_2S is a double-edge sword for the intestinal epithelium with beneficial effect at low concentration (nanomolar to low micromolar), but deleterious effects at higher concentrations (high micromolar to millimolar) (Blachier et al., 2019). Considering the critical importance of intestinal microbiota and H_2S in maintaining cardiovascular homeostasis, it is believed that intestinal microbiota-derived H_2S integrates microbial and circadian cues

for regulation of diurnal metabolic rhythms, thereby influencing the endothelial dysfunction in cardiovascular system. However, it is still largely unknown with respect to the roles of H_2S in intestinal microbiota-mediated endothelial dysfunction. The relationship between H_2S and intestinal microbiota in cardiovascular regulation may be a very interesting topic. As the gut microbiota leads to much more H_2S production from cysteine than endogenous metabolism, it is likely that H_2S from the bacterial or intestinal epithelium may be a critical determinant for cardiovascular health or disease. However, additional investigation is warranted to identify the exact roles of H_2S in intestinal microbiota and circadian rhythms. Our current understanding of the relationship between H_2S and intestinal microbiota in endothelial inflammation-related cardiovascular disorders is expanding continuously. The interaction between their signaling pathways is increasingly recognized as the future direction for the research in the gasotransmitters field.

CONCLUDING REMARKS AND FUTURE PERSPECTIVES

In addition to NO deficiency and intestinal flora, other factors including oxidative stress (Nakahira et al., 2011), endoplasmic reticulum stress (Battson et al., 2017; Luchetti et al., 2017), mitochondrial dysfunction (Gao et al., 2018), hypoxia (Feng et al., 2017a), homocysteine (Esse and Barroso, 2019), and immune activation (Pan et al., 2017) are also closely related with endothelial inflammation and dysfunction in cardiovascular diseases. With in-depth research, our knowledge on the underlying mechanisms of H_2S-mediated suppression of endothelial cell inflammation is expanding and it is now apparent that interactions between H_2S and endothelial inflammation-regulated pathways may be proposed as a promising approach for cardiovascular disease therapy. A better understanding of such interactions will be favorable to develop novel therapeutic strategies for endothelial dysfunction-related cardiovascular diseases.

Due to a myriad of biological functions of H_2S, there has been a growing interest regarding the enormously therapeutic potential of H_2S in various diseases including cardiovascular diseases. However, our current knowledge on cardiovascular protective effects of H_2S is mainly from animal or cell experiments using H_2S donors or inhibitors of H_2S-producing enzymes. Whether the promising effects of these chemicals in animal studies can be transferable to clinical studies warrants further studies. As such, it should be mentioned that clinical trial results will also pave the way to a better understanding of the effectiveness of H_2S in human diseases. In one completed clinical trial in healthy volunteers and subjects with impaired renal function received known concentrations of sodium sulfide (clinicaltrials.gov, NCT00879645). Despite that only some results have been announced so far, but the treatment could be considered safe because no serious adverse effects are occurred in the involved patients. However, some caution can be warranted as another clinical trial regarding the potential of H_2S in coronary artery bypass graft patients was terminated without undisclosed reasons (NCT00858936) and one had been withdrawn before enrollment (NCT01007461). Some other completed trials are completed to test the role of H_2S in inflammatory diseases such as ulcerative colitis (NCT01282905) or septic shock and stroke (NCT01088490). However, to date, no results are posted due to unknown reasons. Therefore, further results and information from those ongoing and future trials will help to elucidate the physiological and pathophysiological importance of H_2S in various diseases.

Until now, endothelial inflammation and dysfunction remain mortal factors for cardiovascular diseases. It is anticipated that a full understanding of the modulatory mechanisms of the link between endothelial inflammation and destructive H_2S bioavailability might promote the translation of H_2S biology to clinical management of endothelial dysfunction-related cardiovascular diseases. To achieve this, more original work remains to be experimentally evaluated in the future.

AUTHOR CONTRIBUTIONS

H-JS and J-SB designed the contents of this review article. H-JS, Z-YW, and X-WN conducted initial search of literature and prepared the figures. H-JS and J-SB drafted the manuscript. J-SB critically helped to revise the manuscript. All authors have read and approved the final manuscript.

FUNDING

This work was supported by the Ministry of Education of Singapore Tier 2 Research grant (MOE2017-T2-2-029), and the China Jiangsu Nature Science Foundation (BK20181185).

REFERENCES

Ahmad, F. U., Sattar, M. A., Rathore, H. A., Tan, Y. C., Akhtar, S., Jin, O. H., et al. (2014). Hydrogen sulphide and tempol treatments improve the blood pressure and renal excretory responses in spontaneously hypertensive rats. *Ren. Fail* 36, 598–605. doi: 10.3109/0886022X.2014.882218

Ali, M. Y., Ping, C. Y., Mok, Y. Y., Ling, L., Whiteman, M., Bhatia, M., et al. (2006). Regulation of vascular nitric oxide *in vitro* and *in vivo*; a new role for endogenous hydrogen sulphide? *Br. J. Pharmacol.* 149, 625–634. doi: 10.1038/sj.bjp.0706906

Allende-Vigo, M. Z. (2010). Pathophysiologic mechanisms linking adipose tissue and cardiometabolic risk. *Endocr. Pract.* 16, 692–698. doi: 10.4158/EP09340.RA

Al-Magableh, M. R., Kemp-Harper, B. K., and Hart, J. L. (2015). Hydrogen sulfide treatment reduces blood pressure and oxidative stress in angiotensin II-induced hypertensive mice. *Hypertens. Res.* 38, 13–20. doi: 10.1038/hr.2014.125

Altaany, Z., Moccia, F., Munaron, L., Mancardi, D., and Wang, R. (2014). Hydrogen sulfide and endothelial dysfunction: relationship with nitric oxide. *Curr. Med. Chem.* 21, 3646–3661. doi: 10.1097/SHK.0000000000000599

Anuar, F., Whiteman, M., Siau, J. L., Kwong, S. E., Bhatia, M., and Moore, P. K. (2006). Nitric oxide-releasing flurbiprofen reduces formation of proinflammatory hydrogen sulfide in lipopolysaccharide-treated rat. *Br. J. Pharmacol.* 147, 966–974. doi: 10.1038/sj.bjp.0706696

Baghai, T. C., Varallo-Bedarida, G., Born, C., Hafner, S., Schule, C., Eser, D., et al. (2018). Classical risk factors and inflammatory biomarkers: one of the missing biological links between cardiovascular disease and major depressive disorder. *Int. J. Mol. Sci.* 19, E1740. doi: 10.3390/ijms19061740

Barton, M., and Meyer, M. R. (2019). HuR-ry Up: how hydrogen sulfide protects against atherosclerosis. *Circulation* 139, 115–118. doi: 10.1161/CIRCULATIONAHA.118.036854

Basic, A., Blomqvist, M., Dahlen, G., and Svensater, G. (2017). The proteins of Fusobacterium spp. involved in hydrogen sulfide production from L-cysteine. *BMC Microbiol.* 17, 61. doi: 10.1186/s12866-017-0967-9

Baszczuk, A., Kopczynski, Z., and Thielemann, A. (2014). [Endothelial dysfunction in patients with primary hypertension and hyperhomocysteinemia]. *Postepy Hig. Med. Dosw (Online)* 68, 91–100. doi: 10.5604/17322693.1087521

Battson, M. L., Lee, D. M., and Gentile, C. L. (2017). Endoplasmic reticulum stress and the development of endothelial dysfunction. *Am. J. Physiol. Heart Circ. Physiol.* 312, H355–H367. doi: 10.1152/ajpheart.00437.2016

Bibli, S. I., Hu, J., Sigala, F., Wittig, I., Heidler, J., Zukunft, S., et al. (2019). Cystathionine gamma lyase sulfhydrates the RNA binding protein human antigen r to preserve endothelial cell function and delay atherogenesis. *Circulation* 139, 101–114. doi: 10.1161/CIRCULATIONAHA.118.034757

Blachier, F., Beaumont, M., and Kim, E. (2019). Cysteine-derived hydrogen sulfide and gut health: a matter of endogenous or bacterial origin. *Curr. Opin. Clin. Nutr. Metab. Care* 22, 68–75. doi: 10.1097/MCO.0000000000000526

Boulanger, C. M. (2016). Endothelium. *Arterioscler. Thromb. Vasc. Biol.* 36, e26–e31. doi: 10.1161/ATVBAHA.116.306940

Bourque, C., Zhang, Y., Fu, M., Racine, M., Greasley, A., Pei, Y., et al. (2018). H2S protects lipopolysaccharide-induced inflammation by blocking NFkappaB transactivation in endothelial cells. *Toxicol. Appl. Pharmacol.* 338, 20–29. doi: 10.1016/j.taap.2017.11.004

Brancaleone, V., Roviezzo, F., Vellecco, V., De Gruttola, L., Bucci, M., and Cirino, G. (2008). Biosynthesis of H2S is impaired in non-obese diabetic (NOD) mice. *Br. J. Pharmacol.* 155, 673–680. doi: 10.1038/bjp.2008.296

Bucci, M., Vellecco, V., Cantalupo, A., Brancaleone, V., Zhou, Z., Evangelista, S., et al. (2014). Hydrogen sulfide accounts for the peripheral vascular effects of zofenopril independently of ACE inhibition. *Cardiovasc. Res.* 102, 138–147. doi: 10.1093/cvr/cvu026

Cai, W. J., Wang, M. J., Moore, P. K., Jin, H. M., Yao, T., and Zhu, Y. C. (2007). The novel proangiogenic effect of hydrogen sulfide is dependent on Akt phosphorylation. *Cardiovasc. Res.* 76, 29–40. doi: 10.1016/j.cardiores.2007.05.026

Candela, J., Wang, R., and White, C. (2017). Microvascular endothelial dysfunction in obesity is driven by macrophage-dependent hydrogen sulfide depletion. *Arterioscler. Thromb. Vasc. Biol.* 37, 889–899. doi: 10.1161/ATVBAHA.117.309138

Caporali, A., and Emanueli, C. (2011). MicroRNA regulation in angiogenesis. *Vascul. Pharmacol.* 55, 79–86. doi: 10.1016/j.vph.2011.06.006

Carter, A. M. (2012). Complement activation: an emerging player in the pathogenesis of cardiovascular disease. *Scientifica (Cairo)* 2012, 402783. doi: 10.6064/2012/402783

Castro-Ferreira, R., Cardoso, R., Leite-Moreira, A., and Mansilha, A. (2018). The role of endothelial dysfunction and inflammation in chronic venous disease. *Ann. Vasc. Surg.* 46, 380–393. doi: 10.1016/j.avsg.2017.06.131

Chai, Q., Lu, T., Wang, X. L., and Lee, H. C. (2015). Hydrogen sulfide impairs shear stress-induced vasodilation in mouse coronary arteries. *Pflugers Arch.* 467, 329–340. doi: 10.1007/s00424-014-1526-y

Cheang, W. S., Wong, W. T., Shen, B., Lau, C. W., Tian, X. Y., Tsang, S. Y., et al. (2010). 4-aminopyridine-sensitive K+ channels contributes to NaHS-induced membrane hyperpolarization and relaxation in the rat coronary artery. *Vascul. Pharmacol.* 53, 94–98. doi: 10.1016/j.vph.2010.04.004

Chen, Y. H., Wu, R., Geng, B., Qi, Y. F., Wang, P. P., Yao, W. Z., et al. (2009). Endogenous hydrogen sulfide reduces airway inflammation and remodeling in a rat model of asthma. *Cytokine* 45, 117–123. doi: 10.1016/j.cyto.2008.11.009

Chen, Y., Zhao, L., Jiang, S., Hu, Z., Hu, B., Tong, F., et al. (2018). Cystathionine gamma-lyase is involved in the renoprotective effect of brief and repeated ischemic postconditioning after renal ischemia/reperfusion injury in Diabetes Mellitus. *Transplant. Proc.* 50, 1549–1557. doi: 10.1016/j.transproceed.2018.03.011

Cheng, Y., Ndisang, J. F., Tang, G., Cao, K., and Wang, R. (2004). Hydrogen sulfide-induced relaxation of resistance mesenteric artery beds of rats. *Am. J. Physiol. Heart Circ. Physiol.* 287, H2316–H2323. doi: 10.1152/ajpheart.00331.2004

Chi, Z., Byeon, H. E., Seo, E., Nguyen, Q. T., Lee, W., Jeong, Y., et al. (2019). Histone deacetylase 6 inhibitor tubastatin A attenuates angiotensin II-induced hypertension by preventing cystathionine gamma-lyase protein degradation. *Pharmacol. Res.* 146, 104281. doi: 10.1016/j.phrs.2019.104281

Chistiakov, D. A., Melnichenko, A. A., Myasoedova, V. A., Grechko, A. V., and Orekhov, A. N. (2017). Mechanisms of foam cell formation in atherosclerosis. *J. Mol. Med. (Berl)* 95, 1153–1165. doi: 10.1007/s00109-017-1575-8

Coletta, C., Modis, K., Szczesny, B., Brunyanszki, A., Olah, G., Rios, E. C., et al. (2015). Regulation of vascular tone, angiogenesis and cellular bioenergetics by the 3-mercaptopyruvate sulfurtransferase/H2S Pathway: functional impairment by hyperglycemia and restoration by DL-alpha-lipoic acid. *Mol. Med.* 21, 1–14. doi: 10.2119/molmed.2015.00035

Crnko, S., Cour, M., Van Laake, L. W., and Lecour, S. (2018). Vasculature on the clock: circadian rhythm and vascular dysfunction. *Vascul. Pharmacol.* 108, 1–7. doi: 10.1016/j.vph.2018.05.003

D'emmanuele Di Villa Bianca, R., Sorrentino, R., Coletta, C., Mitidieri, E., Rossi, A., Vellecco, V., et al. (2011). Hydrogen sulfide-induced dual vascular effect involves arachidonic acid cascade in rat mesenteric arterial bed. *J. Pharmacol. Exp. Ther.* 337, 59–64. doi: 10.1124/jpet.110.176016

D'emmanuele Di Villa Bianca, R., Mitidieri, E., Donnarumma, E., Tramontano, T., Brancaleone, V., Cirino, G., et al. (2015). Hydrogen sulfide is involved in dexamethasone-induced hypertension in rat. *Nitric. Oxide* 46, 80–86. doi: 10.1016/j.niox.2014.11.013

Denizalti, M., Bozkurt, T. E., Akpulat, U., Sahin-Erdemli, I., and Abacioglu, N. (2011). The vasorelaxant effect of hydrogen sulfide is enhanced in streptozotocin-induced diabetic rats. *Naunyn Schmiedebergs Arch. Pharmacol.* 383, 509–517. doi: 10.1007/s00210-011-0601-6

Du, C., Lin, X., Xu, W., Zheng, F., Cai, J., Yang, J., et al. (2019). Sulfhydrated Sirtuin-1 increasing its deacetylation activity is an essential epigenetics mechanism of anti-atherogenesis by hydrogen sulfide. *Antioxid. Redox Signal.* 30, 184–197. doi: 10.1089/ars.2017.7195

Dulmovits, B. M., and Herman, I. M. (2012). Microvascular remodeling and wound healing: a role for pericytes. *Int. J. Biochem. Cell Biol.* 44, 1800–1812. doi: 10.1016/j.biocel.2012.06.031

Dunn, J., Simmons, R., Thabet, S., and Jo, H. (2015). The role of epigenetics in the endothelial cell shear stress response and atherosclerosis. *Int. J. Biochem. Cell Biol.* 67, 167–176. doi: 10.1016/j.biocel.2015.05.001

Durham, A. L., Speer, M. Y., Scatena, M., Giachelli, C. M., and Shanahan, C. M. (2018). Role of smooth muscle cells in vascular calcification: implications in atherosclerosis and arterial stiffness. *Cardiovasc. Res.* 114, 590–600. doi: 10.1093/cvr/cvy010

Esse, R., and Barroso, M. (2019). The contribution of homocysteine metabolism disruption to endothelial dysfunction: state-of-the-Art. *Int. J. Mol. Sci.* 20, E867. doi: 10.3390/ijms20040867

Fan, J., Zheng, F., Li, S., Cui, C., Jiang, S., Zhang, J., et al. (2019). Hydrogen sulfide lowers hyperhomocysteinemia dependent on cystathionine gamma lyase S-sulfhydration in ApoE-knockout atherosclerotic mice. *Br. J. Pharmacol.* 176, 3180–3192. doi: 10.1111/bph.14719

Fang, F., Chen, D., Yu, L., Dai, X., Yang, Y., Tian, W., et al. (2013). Proinflammatory stimuli engage Brahma related gene 1 and Brahma in endothelial injury. *Circ. Res.* 113, 986–996. doi: 10.1161/CIRCRESAHA.113.301296

Feng, S., Bowden, N., Fragiadaki, M., Souilhol, C., Hsiao, S., Mahmoud, M., et al. (2017a). Mechanical activation of hypoxia-inducible factor 1alpha drives

endothelial dysfunction at atheroprone sites. *Arterioscler. Thromb. Vasc. Biol.* 37, 2087–2101. doi: 10.1161/ATVBAHA.117.309249

Feng, S., Chen, S., Yu, W., Zhang, D., Zhang, C., Tang, C., et al. (2017b). H2S inhibits pulmonary arterial endothelial cell inflammation in rats with monocrotaline-induced pulmonary hypertension. *Lab. Invest.* 97, 268–278. doi: 10.1038/labinvest.2016.129

Fiorucci, S., Antonelli, E., Distrutti, E., Rizzo, G., Mencarelli, A., Orlandi, S., et al. (2005). Inhibition of hydrogen sulfide generation contributes to gastric injury caused by anti-inflammatory nonsteroidal drugs. *Gastroenterology* 129, 1210–1224. doi: 10.1053/j.gastro.2005.07.060

Gao, F., Chen, J., and Zhu, H. (2018). A potential strategy for treating atherosclerosis: improving endothelial function *via* AMP-activated protein kinase. *Sci. China Life Sci.* 61, 1024–1029. doi: 10.1007/s11427-017-9285-1

Gero, D., Torregrossa, R., Perry, A., Waters, A., Le-Trionnaire, S., Whatmore, J. L., et al. (2016). The novel mitochondria-targeted hydrogen sulfide (H2S) donors AP123 and AP39 protect against hyperglycemic injury in microvascular endothelial cells *in vitro*. *Pharmacol. Res.* 113, 186–198. doi: 10.1016/j.phrs.2016.08.019

Go, Y. M., Lee, H. R., and Park, H. (2012). H(2)S inhibits oscillatory shear stress-induced monocyte binding to endothelial cells *via* nitric oxide production. *Mol. Cells* 34, 449–455. doi: 10.1007/s10059-012-0200-5

Gu, Q., Wang, B., Zhang, X. F., Ma, Y. P., Liu, J. D., and Wang, X. Z. (2013). Contribution of hydrogen sulfide and nitric oxide to exercise-induced attenuation of aortic remodeling and improvement of endothelial function in spontaneously hypertensive rats. *Mol. Cell Biochem.* 375, 199–206. doi: 10.1007/s11010-012-1542-1

Guan, Q., Zhang, Y., Yu, C., Liu, Y., Gao, L., and Zhao, J. (2012). Hydrogen sulfide protects against high-glucose-induced apoptosis in endothelial cells. *J. Cardiovasc. Pharmacol.* 59, 188–193. doi: 10.1097/FJC.0b013e31823b4915

Guan, Q., Wang, X., Gao, L., Chen, J., Liu, Y., Yu, C., et al. (2013). Hydrogen sulfide suppresses high glucose-induced expression of intercellular adhesion molecule-1 in endothelial cells. *J. Cardiovasc. Pharmacol.* 62, 278–284. doi: 10.1097/FJC.0b013e31829875ef

Guan, Q., Liu, W., Liu, Y., Fan, Y., Wang, X., Yu, C., et al. (2015). High glucose induces the release of endothelin-1 through the inhibition of hydrogen sulfide production in HUVECs. *Int. J. Mol. Med.* 35, 810–814. doi: 10.3892/ijmm.2014.2059

Guo, R., Wu, Z., Jiang, J., Liu, C., Wu, B., Li, X., et al. (2017). New mechanism of lipotoxicity in diabetic cardiomyopathy: Deficiency of Endogenous H2S Production and ER stress. *Mech. Ageing Dev.* 162, 46–52. doi: 10.1016/j.mad.2016.11.005

Han, W., Dong, Z., Dimitropoulou, C., and Su, Y. (2011). Hydrogen sulfide ameliorates tobacco smoke-induced oxidative stress and emphysema in mice. *Antioxid. Redox Signal.* 15, 2121–2134. doi: 10.1089/ars.2010.3821

Haybar, H., Shokuhian, M., Bagheri, M., Davari, N., and Saki, N. (2019). Involvement of circulating inflammatory factors in prognosis and risk of cardiovascular disease. *J. Mol. Cell Cardiol.* 132, 110–119. doi: 10.1016/j.yjmcc.2019.05.010

Heo, K. S., Berk, B. C., and Abe, J. (2016). Disturbed flow-induced endothelial proatherogenic signaling via regulating post-translational modifications and epigenetic events. *Antioxid. Redox Signal.* 25, 435–450. doi: 10.1089/ars.2015.6556

Hu, H. J., Jiang, Z. S., Zhou, S. H., and Liu, Q. M. (2016). Hydrogen sulfide suppresses angiotensin II-stimulated endothelin-1 generation and subsequent cytotoxicity-induced endoplasmic reticulum stress in endothelial cells *via* NF-kappaB. *Mol. Med. Rep.* 14, 4729–4740. doi: 10.3892/mmr.2016.5827

Huang, P., Chen, S., Wang, Y., Liu, J., Yao, Q., Huang, Y., et al. (2015). Down-regulated CBS/H2S pathway is involved in high-salt-induced hypertension in Dahl rats. *Nitric. Oxide* 46, 192–203. doi: 10.1016/j.niox.2015.01.004

Jackson-Weaver, O., Osmond, J. M., Naik, J. S., Gonzalez Bosc, L. V., Walker, B. R., and Kanagy, N. L. (2015). Intermittent hypoxia in rats reduces activation of Ca2+ sparks in mesenteric arteries. *Am. J. Physiol. Heart Circ. Physiol.* 309, H1915–H1922. doi: 10.1152/ajpheart.00179.2015

Jain, S. K., Bull, R., Rains, J. L., Bass, P. F., Levine, S. N., Reddy, S., et al. (2010). Low levels of hydrogen sulfide in the blood of diabetes patients and streptozotocin-treated rats causes vascular inflammation? *Antioxid. Redox Signal.* 12, 1333–1337. doi: 10.1089/ars.2009.2956

Jain, S. K., Manna, P., Micinski, D., Lieblong, B. J., Kahlon, G., Morehead, L., et al. (2013). In African American type 2 diabetic patients, is vitamin D deficiency associated with lower blood levels of hydrogen sulfide and cyclic adenosine monophosphate, and elevated oxidative stress? *Antioxid. Redox Signal.* 18, 1154–1158. doi: 10.1089/ars.2012.4843

Jensen, A. R., Drucker, N. A., Khaneki, S., Ferkowicz, M. J., and Markel, T. A. (2017). Hydrogen sulfide improves intestinal recovery following ischemia by endothelial nitric oxide-dependent mechanisms. *Am. J. Physiol. Gastrointest. Liver Physiol.* 312, G450–g456. doi: 10.1152/ajpgi.00444.2016

Ji, W., Liu, S., Dai, J., Yang, T., Jiang, X., Duan, X., et al. (2014). Hydrogen sulfide defends against the cardiovascular risk of Nw-nitro-L-argininemethyl ester-induced hypertension in rats *via the* nitric oxide/endothelial nitric oxide synthase pathway. *Chin. Med. J. (Engl)* 127, 3751–3757. doi: 10.3760/cma.j.issn.0366-6999.20141573

Jin, M., Qian, Z., Yin, J., Xu, W., and Zhou, X. (2019). The role of intestinal microbiota in cardiovascular disease. *J. Cell Mol. Med.* 23, 2343–2350. doi: 10.1111/jcmm.14195

Kan, J., Guo, W., Huang, C., Bao, G., Zhu, Y., and Zhu, Y. Z. (2014). S-propargyl-cysteine, a novel water-soluble modulator of endogenous hydrogen sulfide, promotes angiogenesis through activation of signal transducer and activator of transcription 3. *Antioxid. Redox Signal.* 20, 2303–2316. doi: 10.1089/ars.2013.5449

Kanagy, N. L., Szabo, C., and Papapetropoulos, A. (2017). Vascular biology of hydrogen sulfide. *Am. J. Physiol. Cell Physiol.* 312, C537–C549. doi: 10.1152/ajpcell.00329.2016

Kavurma, M. M., Rayner, K. J., and Karunakaran, D. (2017). The walking dead: macrophage inflammation and death in atherosclerosis. *Curr. Opin. Lipidol.* 28, 91–98. doi: 10.1097/MOL.0000000000000394

Kiss, L., Deitch, E. A., and Szabo, C. (2008). Hydrogen sulfide decreases adenosine triphosphate levels in aortic rings and leads to vasorelaxation *via* metabolic inhibition. *Life Sci.* 83, 589–594. doi: 10.1016/j.lfs.2008.08.006

Kubo, S., Kajiwara, M., and Kawabata, A. (2007). Dual modulation of the tension of isolated gastric artery and gastric mucosal circulation by hydrogen sulfide in rats. *Inflammopharmacology* 15, 288–292. doi: 10.1007/s10787-007-1590-4

Leucker, T. M., Nomura, Y., Kim, J. H., Bhatta, A., Wang, V., Wecker, A., et al. (2017). Cystathionine gamma-lyase protects vascular endothelium: a role for inhibition of histone deacetylase 6. *Am. J. Physiol. Heart Circ. Physiol.* 312, H711–H720. doi: 10.1152/ajpheart.00724.2016

Leung, S. W., and Vanhoutte, P. M. (2017). Endothelium-dependent hyperpolarization: age, gender and blood pressure, do they matter? *Acta Physiol. (Oxf)* 219, 108–123. doi: 10.1111/apha.12628

Li, L., Whiteman, M., Guan, Y. Y., Neo, K. L., Cheng, Y., Lee, S. W., et al. (2008). Characterization of a novel, water-soluble hydrogen sulfide-releasing molecule (GYY4137): new insights into the biology of hydrogen sulfide. *Circulation* 117, 2351–2360. doi: 10.1161/CIRCULATIONAHA.107.753467

Li, L., Rose, P., and Moore, P. K. (2011). Hydrogen sulfide and cell signaling. *Annu. Rev. Pharmacol. Toxicol.* 51, 169–187. doi: 10.1146/annurev-pharmtox-010510-100505

Li, X. H., Xue, W. L., Wang, M. J., Zhou, Y., Zhang, C. C., Sun, C., et al. (2017). H2S regulates endothelial nitric oxide synthase protein stability by promoting microRNA-455-3p expression. *Sci. Rep.* 7, 44807. doi: 10.1038/srep44807

Li, J., Teng, X., Jin, S., Dong, J., Guo, Q., Tian, D., et al. (2019). Hydrogen sulfide improves endothelial dysfunction by inhibiting the vicious cycle of NLRP3 inflammasome and oxidative stress in spontaneously hypertensive rats. *J. Hypertens.* 37, 1633–1643. doi: 10.1097/HJH.0000000000002101

Lin, Y., Zeng, H., Gao, L., Gu, T., Wang, C., and Zhang, H. (2017). Hydrogen sulfide attenuates atherosclerosis in a partially ligated carotid artery mouse model *via* regulating angiotensin converting enzyme 2 expression. *Front. Physiol.* 8, 782. doi: 10.3389/fphys.2017.00782

Lin, J., Chen, M., Liu, D., Guo, R., Lin, K., Deng, H., et al. (2018). Exogenous hydrogen sulfide protects human umbilical vein endothelial cells against high glucoseinduced injury by inhibiting the necroptosis pathway. *Int. J. Mol. Med.* 41, 1477–1486. doi: 10.3892/ijmm.2017.3330

Liu, F., and Chang, H. C. (2017). Physiological links of circadian clock and biological clock of aging. *Protein Cell* 8, 477–488. doi: 10.1007/s13238-016-0366-2

Liu, Y. H., Yan, C. D., and Bian, J. S. (2011). Hydrogen sulfide: a novel signaling molecule in the vascular system. *J. Cardiovasc. Pharmacol.* 58, 560–569. doi: 10.1097/FJC.0b013e31820eb7a1

Liu, Y. H., Lu, M., Hu, L. F., Wong, P. T., Webb, G. D., and Bian, J. S. (2012). Hydrogen sulfide in the mammalian cardiovascular system. *Antioxid. Redox Signal.* 17, 141–185. doi: 10.1089/ars.2011.4005

Liu, Z., Han, Y., Li, L., Lu, H., Meng, G., Li, X., et al. (2013). The hydrogen sulfide donor, GYY4137, exhibits anti-atherosclerotic activity in high fat fed apolipoprotein E(-/-) mice. *Br. J. Pharmacol.* 169, 1795–1809.doi: 10.1111/bph.12246

Liu, J., Wu, J., Sun, A., Sun, Y., Yu, X., Liu, N., et al. (2016). Hydrogen sulfide decreases high glucose/palmitate-induced autophagy in endothelial cells by the Nrf2-ROS-AMPK signaling pathway. *Cell Biosci.* 6, 33. doi: 10.1186/s13578-016-0099-1

Liu, N., Wu, J., Zhang, L., Gao, Z., Sun, Y., Yu, M., et al. (2017). Hydrogen Sulphide modulating mitochondrial morphology to promote mitophagy in endothelial cells under high-glucose and high-palmitate. *J. Cell Mol. Med.* 21, 3190–3203. doi: 10.1111/jcmm.13223

Liu, M., Deng, M., Su, J., Lin, Y., Jia, Z., Peng, K., et al. (2018). Specific downregulation of cystathionine beta-synthase expression in the kidney during obesity. *Physiol. Rep.* 6, e13630. doi: 10.14814/phy2.13630

Luchetti, F., Crinelli, R., Cesarini, E., Canonico, B., Guidi, L., Zerbinati, C., et al. (2017). Endothelial cells, endoplasmic reticulum stress and oxysterols. *Redox Biol.* 13, 581–587. doi: 10.1016/j.redox.2017.07.014

Mani, S., Li, H., Untereiner, A., Wu, L., Yang, G., Austin, R. C., et al. (2013). Decreased endogenous production of hydrogen sulfide accelerates atherosclerosis. *Circulation* 127, 2523–2534. doi: 10.1161/CIRCULATIONAHA.113.002208

Mani, S., Untereiner, A., Wu, L., and Wang, R. (2014). Hydrogen sulfide and the pathogenesis of atherosclerosis. *Antioxid. Redox Signal.* 20, 805–817. doi: 10.1089/ars.2013.5324

Mathers, C. D., and Loncar, D. (2006). Projections of global mortality and burden of disease from 2002 to 2030. *PloS Med.* 3, e442. doi: 10.1371/journal.pmed.0030442

Meng, Q. H., Yang, G., Yang, W., Jiang, B., Wu, L., and Wang, R. (2007). Protective effect of hydrogen sulfide on balloon injury-induced neointima hyperplasia in rat carotid arteries. *Am. J. Pathol.* 170, 1406–1414. doi: 10.2353/ajpath.2007.060939

Meng, G., Ma, Y., Xie, L., Ferro, A., and Ji, Y. (2015). Emerging role of hydrogen sulfide in hypertension and related cardiovascular diseases. *Br. J. Pharmacol.* 172, 5501–5511. doi: 10.1111/bph.12900

Mitidieri, E., and Gurgone, D. (2019). L-cysteine/cystathionine-beta-synthase-induced relaxation in mouse aorta involves a L-serine/sphingosine-1-phosphate/NO pathway. *Br. J. Pharmacol.* doi: 10.1111/bph.14654

Mustafa, A. K., Sikka, G., Gazi, S. K., Steppan, J., Jung, S. M., Bhunia, A. K., et al. (2011). Hydrogen sulfide as endothelium-derived hyperpolarizing factor sulfhydrates potassium channels. *Circ. Res.* 109, 1259–1268. doi: 10.1161/CIRCRESAHA.111.240242

Nagpure, B. V., and Bian, J. S. (2016). Interaction of hydrogen sulfide with nitric oxide in the cardiovascular system. *Oxid. Med. Cell. Longev.* 2016, 6904327. doi: 10.1155/2016/6904327

Nakahira, K., Haspel, J. A., Rathinam, V. A., Lee, S. J., Dolinay, T., Lam, H. C., et al. (2011). Autophagy proteins regulate innate immune responses by inhibiting the release of mitochondrial DNA mediated by the NALP3 inflammasome. *Nat. Immunol.* 12, 222–230. doi: 10.1038/ni.1980

Ng, H. H., Leo, C. H., Parry, L. J., and Ritchie, R. H. (2018). Relaxin as a therapeutic target for the cardiovascular complications of diabetes. *Front. Pharmacol.* 9, 501. doi: 10.3389/fphar.2018.00501

Oh, G. S., Pae, H. O., Lee, B. S., Kim, B. N., Kim, J. M., Kim, H. R., et al. (2006). Hydrogen sulfide inhibits nitric oxide production and nuclear factor-kappaB *via* heme oxygenase-1 expression in RAW264.7 macrophages stimulated with lipopolysaccharide. *Free Radic. Biol. Med.* 41, 106–119. doi: 10.1016/j.freeradbiomed.2006.03.021

Ooi, B. K., Chan, K. G., Goh, B. H., and Yap, W. H. (2018). The role of natural products in targeting cardiovascular diseases *via* Nrf2 pathway: novel molecular mechanisms and therapeutic approaches. *Front. Pharmacol.* 9, 1308. doi: 10.3389/fphar.2018.01308

Pan, L. L., Qin, M., Liu, X. H., and Zhu, Y. Z. (2017). The role of hydrogen sulfide on cardiovascular homeostasis: an overview with update on immunomodulation. *Front. Pharmacol.* 8, 686. doi: 10.3389/fphar.2017.00686

Papapetropoulos, A., Pyriochou, A., Altaany, Z., Yang, G., Marazioti, A., Zhou, Z., et al. (2009). Hydrogen sulfide is an endogenous stimulator of angiogenesis. *Proc. Natl. Acad. Sci. U. S. A.* 106, 21972–21977. doi: 10.1073/pnas.0908047106

Park-Windhol, C., and D'amore, P. A. (2016). Disorders of Vascular Permeability. *Annu. Rev. Pathol.* 11, 251–281. doi: 10.1146/annurev-pathol-012615-044506

Peh, M. T., Anwar, A. B., Ng, D. S., Atan, M. S., Kumar, S. D., and Moore, P. K. (2014). Effect of feeding a high fat diet on hydrogen sulfide (H2S) metabolism in the mouse. *Nitric. Oxide* 41, 138–145. doi: 10.1016/j.niox.2014.03.002

Perna, A. F., Sepe, I., Lanza, D., Capasso, R., Zappavigna, S., Capasso, G., et al. (2013). Hydrogen sulfide reduces cell adhesion and relevant inflammatory triggering by preventing ADAM17-dependent TNF-alpha activation. *J. Cell Biochem.* 114, 1536–1548. doi: 10.1002/jcb.24495

Possomato-Vieira, J. S., and Goncalves-Rizzi, V. H. (2018). Clinical and experimental evidences of hydrogen sulfide involvement in lead-induced hypertension. *BioMed. Res. Int.* 2018, 4627391. doi: 10.1155/2018/4627391

Predmore, B. L., Julian, D., and Cardounel, A. J. (2011). Hydrogen sulfide increases nitric oxide production from endothelial cells by an akt-dependent mechanism. *Front. Physiol.* 2, 104. doi: 10.3389/fphys.2011.00104

Rahimi, N. (2017). Defenders and challengers of endothelial barrier function. *Front. Immunol.* 8, 1847. doi: 10.3389/fimmu.2017.01847

Rahman, M. S., and Woollard, K. (2017). Atherosclerosis. *Adv. Exp. Med. Biol.* 1003, 121–144. doi: 10.1007/978-3-319-57613-8_7

Roy, A., Khan, A. H., Islam, M. T., Prieto, M. C., and Majid, D. S. (2012). Interdependency of cystathione gamma-lyase and cystathione beta-synthase in hydrogen sulfide-induced blood pressure regulation in rats. *Am. J. Hypertens.* 25, 74–81. doi: 10.1038/ajh.2011.149

Schleifenbaum, J., Kohn, C., Voblova, N., Dubrovska, G., Zavarirskaya, O., Gloe, T., et al. (2010). Systemic peripheral artery relaxation by KCNQ channel openers and hydrogen sulfide. *J. Hypertens.* 28, 1875–1882. doi: 10.1097/HJH.0b013e32833c20d5

Sen, U., Sathnur, P. B., Kundu, S., Givvimani, S., Coley, D. M., Mishra, P. K., et al. (2012). Increased endogenous H2S generation by CBS, CSE, and 3MST gene therapy improves ex vivo renovascular relaxation in hyperhomocysteinemia. *Am. J. Physiol. Cell Physiol.* 303, C41–C51. doi: 10.1152/ajpcell.00398.2011

Streeter, E. Y., Badoer, E., Woodman, O. L., and Hart, J. L. (2013). Effect of type 1 diabetes on the production and vasoactivity of hydrogen sulfide in rat middle cerebral arteries. *Physiol. Rep.* 1, e00111. doi: 10.1002/phy2.111

Sun, L., Sun, S., Li, Y., Pan, W., Xie, Y., Wang, S., et al. (2014). Potential biomarkers predicting risk of pulmonary hypertension in congenital heart disease: the role of homocysteine and hydrogen sulfide. *Chin. Med. J. (Engl)* 127, 893–899. doi:10.3760/cma.j.issn.0366-6999.20132694

Sun, H. J., Hou, B., Wang, X., Zhu, X. X., Li, K. X., and Qiu, L. Y. (2016). Endothelial dysfunction and cardiometabolic diseases: Role of long non-coding RNAs. *Life Sci.* 167, 6–11. doi: 10.1016/j.lfs.2016.11.005

Sun, H. J., Zhu, X. X., Cai, W. W., and Qiu, L. Y. (2017). Functional roles of exosomes in cardiovascular disorders: a systematic review. *Eur. Rev. Med. Pharmacol. Sci.* 21, 5197–5206. doi: 10.26355/eurrev_201711_13840

Suryavanshi, S. V., and Kulkarni, Y. A. (2017). NF-kappabeta: a potential target in the management of vascular complications of diabetes. *Front. Pharmacol.* 8, 798. doi: 10.3389/fphar.2017.00798

Suzuki, K., Olah, G., Modis, K., Coletta, C., Kulp, G., Gero, D., et al. (2011). Hydrogen sulfide replacement therapy protects the vascular endothelium in hyperglycemia by preserving mitochondrial function. *Proc. Natl. Acad. Sci. U. S. A.* 108, 13829–13834. doi: 10.1073/pnas.1105121108

Suzuki, K., Sagara, M., Aoki, C., Tanaka, S., and Aso, Y. (2017). Clinical implication of plasma hydrogen sulfide levels in Japanese patients with type 2 diabetes. *Intern. Med.* 56, 17–21. doi: 10.2169/internalmedicine.56.7403

Szabo, C., and Papapetropoulos, A. (2011). Hydrogen sulphide and angiogenesis: mechanisms and applications. *Br. J. Pharmacol.* 164, 853–865. doi: 10.1111/j.1476-5381.2010.01191.x

Szabo, C. (2007). Hydrogen sulphide and its therapeutic potential. *Nat. Rev. Drug Discovery* 6, 917–935. doi: 10.1038/nrd2425

Tahara, Y., Aoyama, S., and Shibata, S. (2017). The mammalian circadian clock and its entrainment by stress and exercise. *J. Physiol. Sci.* 67, 1–10. doi: 10.1007/s12576-016-0450-7

Tang, G., Yang, G., Jiang, B., Ju, Y., Wu, L., and Wang, R. (2013). H(2)S is an endothelium-derived hyperpolarizing factor. *Antioxid. Redox Signal.* 19, 1634–1646. doi: 10.1089/ars.2008.2117

Tang, W. H., Kitai, T., and Hazen, S. L. (2017). Gut microbiota in cardiovascular health and disease. *Circ. Res.* 120, 1183–1196. doi: 10.1161/CIRCRESAHA.117.309715

Tang, W. H. W., Backhed, F., Landmesser, U., and Hazen, S. L. (2019). Intestinal microbiota in cardiovascular health and disease: JACC state-of-the-art review. *J. Am. Coll. Cardiol.* 73, 2089–2105. doi: 10.1016/j.jacc.2019.03.024

Tao, B. B., Liu, S. Y., Zhang, C. C., Fu, W., Cai, W. J., Wang, Y., et al. (2013). VEGFR2 functions as an H2S-targeting receptor protein kinase with its novel Cys1045-Cys1024 disulfide bond serving as a specific molecular switch for hydrogen sulfide actions in vascular endothelial cells. *Antioxid. Redox Signal.* 19, 448–464. doi: 10.1089/ars.2012.4565

Tao, B., Wang, R., Sun, C., and Zhu, Y. (2017). 3-Mercaptopyruvate sulfurtransferase, not cystathionine beta-synthase nor cystathionine gamma-lyase, mediates hypoxia-induced migration of vascular endothelial cells. *Front. Pharmacol.* 8, 657. doi: 10.3389/fphar.2017.00657

Tomasova, L., Pavlovicova, M., Malekova, L., Misak, A., Kristek, F., Grman, M., et al. (2015). Effects of AP39, a novel triphenylphosphonium derivatised anethole dithiolethione hydrogen sulfide donor, on rat haemodynamic parameters and chloride and calcium Cav3 and RyR2 channels. *Nitric. Oxide* 46, 131–144. doi: 10.1016/j.niox.2014.12.012

Van Den Born, J. C., Mencke, R., Conroy, S., Zeebregts, C. J., Van Goor, H., and Hillebrands, J. L. (2016). Cystathionine gamma-lyase is expressed in human atherosclerotic plaque microvessels and is involved in micro-angiogenesis. *Sci. Rep.* 6, 34608. doi: 10.1038/srep34608

Voigt, R. M., Forsyth, C. B., Green, S. J., Engen, P. A., and Keshavarzian, A. (2016). Circadian rhythm and the gut microbiome. *Int. Rev. Neurobiol.* 131, 193–205. doi: 10.1016/bs.irn.2016.07.002

Wallace, J. L., Motta, J. P., and Buret, A. G. (2018). Hydrogen sulfide: an agent of stability at the microbiome-mucosa interface. *Am. J. Physiol. Gastrointest. Liver Physiol.* 314, G143–G149. doi: 10.1152/ajpgi.00249.2017

Wang, Y., Zhao, X., Jin, H., Wei, H., Li, W., Bu, D., et al. (2009). Role of hydrogen sulfide in the development of atherosclerotic lesions in apolipoprotein E knockout mice. *Arterioscler. Thromb. Vasc. Biol.* 29, 173–179. doi: 10.1161/ATVBAHA.108.179333

Wang, M. J., Cai, W. J., Li, N., Ding, Y. J., Chen, Y., and Zhu, Y. C. (2010a). The hydrogen sulfide donor NaHS promotes angiogenesis in a rat model of hind limb ischemia. *Antioxid. Redox Signal.* 12, 1065–1077. doi: 10.1089/ars.2009.2945

Wang, M. J., Cai, W. J., and Zhu, Y. C. (2010b). Mechanisms of angiogenesis: role of hydrogen sulphide. *Clin. Exp. Pharmacol. Physiol.* 37, 764–771. doi: 10.1111/j.1440-1681.2010.05371.x

Wang, K., Ahmad, S., Cai, M., Rennie, J., Fujisawa, T., Crispi, F., et al. (2013a). Dysregulation of hydrogen sulfide producing enzyme cystathionine gamma-lyase contributes to maternal hypertension and placental abnormalities in preeclampsia. *Circulation* 127, 2514–2522. doi: 10.1161/CIRCULATIONAHA.113.001631

Wang, X. H., Wang, F., You, S. J., Cao, Y. J., Cao, L. D., Han, Q., et al. (2013b). Dysregulation of cystathionine gamma-lyase (CSE)/hydrogen sulfide pathway contributes to ox-LDL-induced inflammation in macrophage. *Cell Signal* 25, 2255–2262. doi: 10.1016/j.cellsig.2013.07.010

Wang, G. G., Chen, Q. Y., Li, W., Lu, X. H., and Zhao, X. (2015a). Ginkgolide B increases hydrogen sulfide and protects against endothelial dysfunction in diabetic rats. *Croat. Med. J.* 56, 4–13. doi: 10.3325/cmj.2015.56.4

Wang, R., Szabo, C., Ichinose, F., Ahmed, A., Whiteman, M., and Papapetropoulos, A. (2015b). The role of H2S bioavailability in endothelial dysfunction. *Trends Pharmacol. Sci.* 36, 568–578. doi: 10.1016/j.tips.2015.05.007

Wang, Z. J., Wu, J., Guo, W., and Zhu, Y. Z. (2017). Atherosclerosis and the hydrogen sulfide signaling pathway - therapeutic approaches to disease prevention. *Cell Physiol. Biochem.* 42, 859–875. doi: 10.1159/000478628

Wang, R. (2009). Hydrogen sulfide: a new EDRF. *Kidney Int.* 76, 700–704. doi: 10.1038/ki.2009.221

Wang, R. (2012). Physiological implications of hydrogen sulfide: a whiff exploration that blossomed. *Physiol. Rev.* 92, 791–896. doi: 10.1152/physrev.00017.2011

Watson, E. C., Grant, Z. L., and Coultas, L. (2017). Endothelial cell apoptosis in angiogenesis and vessel regression. *Cell Mol. Life Sci.* 74, 4387–4403. doi: 10.1007/s00018-017-2577-y

Webb, G. D., Lim, L. H., Oh, V. M., Yeo, S. B., Cheong, Y. P., Ali, M. Y., et al. (2008). Contractile and vasorelaxant effects of hydrogen sulfide and its biosynthesis in the human internal mammary artery. *J. Pharmacol. Exp. Ther.* 324, 876–882. doi: 10.1124/jpet.107.133538

Weber, C., and Noels, H. (2011). Atherosclerosis: current pathogenesis and therapeutic options. *Nat. Med.* 17, 1410–1422. doi: 10.1038/nm.2538

Wen, Y. D., Wang, H., and Zhu, Y. Z. (2018). The drug developments of hydrogen sulfide on cardiovascular disease. *Oxid. Med. Cell. Longev.* 2018, 4010395. doi: 10.1155/2018/4010395

White, B. J., Smith, P. A., and Dunn, W. R. (2013). Hydrogen sulphide-mediated vasodilatation involves the release of neurotransmitters from sensory nerves in pressurized mesenteric small arteries isolated from rats. *Br. J. Pharmacol.* 168, 785–793. doi: 10.1111/j.1476-5381.2012.02187.x

Whiteman, M., and Winyard, P. G. (2011). Hydrogen sulfide and inflammation: the good, the bad, the ugly and the promising. *Expert Rev. Clin. Pharmacol.* 4, 13–32. doi: 10.1586/ecp.10.134

Whiteman, M., Li, L., Rose, P., Tan, C. H., Parkinson, D. B., and Moore, P. K. (2010). The effect of hydrogen sulfide donors on lipopolysaccharide-induced formation of inflammatory mediators in macrophages. *Antioxid. Redox Signal.* 12, 1147–1154. doi: 10.1089/ars.2009.2899

Wu, D., and Hu, Q. (2018). An update on hydrogen sulfide and nitric oxide interactions in the cardiovascular system. *Oxid. Med. Cell. Longev.* 2018, 4579140. doi: 10.1155/2018/4579140

Wu, S. Y., Pan, C. S., Geng, B., Zhao, J., Yu, F., Pang, Y. Z., et al. (2006). Hydrogen sulfide ameliorates vascular calcification induced by vitamin D3 plus nicotine in rats. *Acta Pharmacol. Sin.* 27, 299–306. doi: 10.1111/j.1745-7254.2006.00283.x

Wu, D. B., Chen, J. F., Xu, Q., Lin, J. Q., Liao, J. Q., and Wu, W. (2016). [Exogenous hydrogen sulfide inhibits high-glucose-induced injuries *via* regulating leptin/leptin receptor signaling pathway in human umbilical vein endothelial cells]. *Nan Fang Yi Ke Da Xue Xue Bao* 36, 1055–1061.

Xiao, L., and Dong, J. H. (2016). Hydrogen sulfide improves endothelial dysfunction *via* downregulating BMP4/COX-2 pathway in rats with hypertension. *Oxid. Med. Cell. Longev.* 2016, 8128957. doi: 10.1155/2016/8128957

Xiao, L., Dong, J. H., Teng, X., Jin, S., Xue, H. M., Liu, S. Y., et al. (2018). Hydrogen sulfide improves endothelial dysfunction in hypertension by activating peroxisome proliferator-activated receptor delta/endothelial nitric oxide synthase signaling. *J. Hypertens.* 36, 651–665. doi: 10.1097/HJH.0000000000001605

Xiaohui, L., Junbao, D., Lin, S., Jian, L., Xiuying, T., Jianguang, Q., et al. (2005). Down-regulation of endogenous hydrogen sulfide pathway in pulmonary hypertension and pulmonary vascular structural remodeling induced by high pulmonary blood flow in rats. *Circ. J.* 69, 1418–1424. doi: 10.1253/circj.69.1418

Xie, L., Gu, Y., Wen, M., Zhao, S., Wang, W., Ma, Y., et al. (2016). Hydrogen sulfide induces Keap1 S-sulfhydration and suppresses diabetes-accelerated atherosclerosis *via* Nrf2 activation. *Diabetes* 65, 3171–3184. doi: 10.2337/db16-0020

Xu, S., Liu, Z., and Liu, P. (2014). Targeting hydrogen sulfide as a promising therapeutic strategy for atherosclerosis. *Int. J. Cardiol.* 172, 313–317. doi: 10.1016/j.ijcard.2014.01.068

Xue, H., Zhou, S., Xiao, L., Guo, Q., Liu, S., and Wu, Y. (2015). Hydrogen sulfide improves the endothelial dysfunction in renovascular hypertensive rats. *Physiol. Res.* 64, 663–672.

Yamamoto, J., Sato, W., Kosugi, T., Yamamoto, T., Kimura, T., Taniguchi, S., et al. (2013). Distribution of hydrogen sulfide (H(2)S)-producing enzymes and the roles of the H(2)S donor sodium hydrosulfide in diabetic nephropathy. *Clin. Exp. Nephrol.* 17, 32–40. doi: 10.1007/s10157-012-0670-y

Yan, H., Du, J., and Tang, C. (2004). The possible role of hydrogen sulfide on the pathogenesis of spontaneous hypertension in rats. *Biochem. Biophys. Res. Commun.* 313, 22–27. doi:10.1016/j.bbrc.2003.11.081

Yang, G., Wu, L., Jiang, B., Yang, W., Qi, J., Cao, K., et al. (2008). H2S as a physiologic vasorelaxant: hypertension in mice with deletion of cystathionine gamma-lyase. *Science* 322, 587–590. doi: 10.1126/science.1162667

Yu, B., Chen, Q., Le Bras, A., Zhang, L., and Xu, Q. (2018). Vascular Stem/Progenitor Cell Migration and Differentiation in Atherosclerosis. *Antioxid. Redox Signal.* 29, 219–235. doi: 10.1089/ars.2017.7171

Yuan, S., Shen, X., and Kevil, C. G. (2017). Beyond a gasotransmitter: hydrogen sulfide and polysulfide in cardiovascular health and immune response. *Antioxid. Redox Signal.* 27, 634–653. doi: 10.1089/ars.2017.7096

Zanardo, R. C., Brancaleone, V., Distrutti, E., Fiorucci, S., Cirino, G., and Wallace, J. L. (2006). Hydrogen sulfide is an endogenous modulator of

leukocyte-mediated inflammation. *FASEB J.* 20, 2118–2120. doi: 10.1096/fj.06-6270fje

Zhang, H., Zhi, L., Moochhala, S. M., Moore, P. K., and Bhatia, M. (2007). Endogenous hydrogen sulfide regulates leukocyte trafficking in cecal ligation and puncture-induced sepsis. *J. Leukoc. Biol.* 82, 894–905. doi: 10.1161/CIRCULATIONAHA.109.866889

Zhang, D., Jiang, X., Fang, P., Yan, Y., Song, J., Gupta, S., et al. (2009). Hyperhomocysteinemia promotes inflammatory monocyte generation and accelerates atherosclerosis in transgenic cystathionine beta-synthase-deficient mice. *Circulation* 120, 1893–1902. doi: 10.1161/CIRCULATIONAHA.109.866889

Zhang, D., Fang, P., Jiang, X., Nelson, J., Moore, J. K., Kruger, W. D., et al. (2012a). Severe hyperhomocysteinemia promotes bone marrow-derived and resident inflammatory monocyte differentiation and atherosclerosis in LDLr/CBS-deficient mice. *Circ. Res.* 111, 37–49. doi: 10.1161/CIRCRESAHA.112.26947

Zhang, H., Guo, C., Wu, D., Zhang, A., Gu, T., Wang, L., et al. (2012b). Hydrogen sulfide inhibits the development of atherosclerosis with suppressing CX3CR1 and CX3CL1 expression. *PloS One* 7, e41147. doi: 10.1371/journal.pone.0041147

Zhang, D., Wang, X., Tian, X., Zhang, L., Yang, G., Tao, Y., et al. (2018a). The increased endogenous sulfur dioxide acts as a compensatory mechanism for the downregulated endogenous hydrogen sulfide pathway in the endothelial cell inflammation. *Front. Immunol.* 9, 882. doi: 10.3389/fimmu.2018.00882

Zhang, X., Sessa, W. C., and Fernandez-Hernando, C. (2018b). Endothelial transcytosis of lipoproteins in atherosclerosis. *Front. Cardiovasc. Med.* 5, 130. doi: 10.3389/fcvm.2018.00130

Zhao, W., Zhang, J., Lu, Y., and Wang, R. (2001). The vasorelaxant effect of H(2)S as a novel endogenous gaseous K(ATP) channel opener. *EMBO J.* 20, 6008–6016. doi: 10.1093/emboj/20.21.6008

Zhao, H., Lu, S., Chai, J., Zhang, Y., Ma, X., Chen, J., et al. (2017). Hydrogen sulfide improves diabetic wound healing in ob/ob mice *via* attenuating inflammation. *J. Diabetes Complications* 31, 1363–1369.doi: 10.1016/j.jdiacomp.2017.06.011

Zheng, Y. F., Dai, D. Z., and Dai, Y. (2010). NaHS ameliorates diabetic vascular injury by correcting depressed connexin 43 and 40 in the vasculature in streptozotocin-injected rats. *J. Pharm. Pharmacol.* 62, 615–621. doi: 10.1211/jpp/62.05.0009

Zhong, S., Li, L., Shen, X., Li, Q., Xu, W., Wang, X., et al. (2019). An update on lipid oxidation and inflammation in cardiovascular diseases. *Free Radic. Biol. Med.* 144, 266–278. doi: 10.1016/j.freeradbiomed

Zhou, J., Li, Y. S., and Chien, S. (2014). Shear stress-initiated signaling and its regulation of endothelial function. *Arterioscler. Thromb. Vasc. Biol.* 34, 2191–2198. doi: 10.1161/ATVBAHA.114.303422

Zhou, Y., Li, X. H., Zhang, C. C., Wang, M. J., Xue, W. L., Wu, D. D., et al. (2016). Hydrogen sulfide promotes angiogenesis by downregulating miR-640 *via the* VEGFR2/mTOR pathway. *Am. J. Physiol. Cell Physiol.* 310, C305–C317. doi: 10.1152/ajpcell.00230.2015

Zuidema, M. Y., and Korthuis, R. J. (2015). Intravital microscopic methods to evaluate anti-inflammatory effects and signaling mechanisms evoked by hydrogen sulfide. *Methods Enzymol.* 555, 93–125. doi: 10.1016/bs.mie.2014.11.022

Zuidema, M. Y., Yang, Y., Wang, M., Kalogeris, T., Liu, Y., Meininger, C. J., et al. (2010). Antecedent hydrogen sulfide elicits an anti-inflammatory phenotype in postischemic murine small intestine: role of BK channels. *Am. J. Physiol. Heart Circ. Physiol.* 299, H1554–H1567. doi: 10.1152/ajpheart.01229.2009

Conflict of Interest: The authors declare that the research was conducted in the absence of any commercial or financial relationships that could be construed as a potential conflict of interest.

frontiers in Pharmacology

ORIGINAL RESEARCH
published: 11 February 2020
doi: 10.3389/fphar.2019.01611

Role of TG2-Mediated SERCA2 Serotonylation on Hypoxic Pulmonary Vein Remodeling

*Bo Liu[1], Dong Wang[1], Erfei Luo[1], Jiantong Hou[1], Yong Qiao[1], Gaoliang Yan[1], Qingjie Wang[2] and Chengchun Tang[1]**

[1] Department of Cardiology, Zhongda Hospital, Southeast University, Nanjing, China, [2] Department of Cardiology, Changzhou No. 2 People's Hospital, Nanjing Medical University, Changzhou, China

Sarco-endoplasmic reticulum Ca2+ ATPase (SERCA) pumps take up Ca2+ from the cytoplasm to maintain the balance of intracellular Ca2+. A decline in expression or activity of SERCA results in persistent store-operated calcium entry (SOCE). In cardiomyocytes as well as vascular smooth muscle cells (SMCs), SERCA2 acts as an important regulator of calcium cycling. The purpose of this study is to identify and better understand the role of transglutaminases2 (TG2) as a key factor involved in SERCA2 serotonination (s-SERCA2) and to elucidate the underlying mechanism of action. Human pulmonary venous smooth muscle cell in normal pulmonary lobe were isolated and cultured *in vitro*. Establishment of hypoxic pulmonary hypertension model in wild type and TG2 knockout mice. SERCA2 serotonylation was analyzed by co-(immunoprecipitation) IP when the TG2 gene silenced or overexpressed under normoxia and hypoxia *in vivo* and *in vitro*. Intracellular calcium ion was measured by using Fluo-4AM probe under normoxia and hypoxia. Real-time (RT)-PCR and Western blot analyzed expression of TG2, TRPC1, and TRPC6 under normoxia and hypoxia. Bioactivity of cells were analyzed by using Cell Counting Kit (CCK)-8, flow cytometry, wound healing, RT-PCR, and Western blot under PST-2744 and cyclopiazonic acid. We confirmed that 1) hypoxia enhanced the expression and activity of TG2, and 2) hypoxia increased the basal intracellular Ca2+ concentration ([Ca2+]i) and SOCE through activating TRPC6 on human pulmonary vein smooth muscle cells (hPVSMC). Then, we investigated the effects of overexpression and downregulation of the TG2 gene on the activity of SERCA2, s-SERCA2, basal [Ca2+]i, and SOCE under normoxia and hypoxia *in vitro*, and investigated the activity of SERCA2 and s-SERCA2 *in vivo*, respectively. We confirmed that SERCA2 serotonylation inhibited the activity of SERCA2 and increased the Ca2+ influx, and that hypoxia induced TG2-mediated SERCA2 serotonylation both *in vivo* and *in vitro*. Furthermore, we investigated the effect of TG2 activity on the biological behavior of hPVSMC by using an inhibitor and agonist of SERCA2, respectively. Finally, we confirmed that chronic hypoxia cannot increase vessel wall thickness, the right ventricular systolic pressure (RVSP), and right ventricular hypertrophy index (RVHI) of vascular smooth muscle-specific Tgm2–/– mice. These results indicated that hypoxia promoted TG2-mediated SERCA2 serotonylation, thereby leading to inhibition of SERCA2 activity, which further increased the calcium influx through the TRPC6

OPEN ACCESS

Edited by:
Cheng Xue Helena Qin, Baker Heart and Diabetes Institute, Australia

Reviewed by:
Barbara Kathryn Kemp-Harper, Monash University, Australia
Haiyang Tang, University of Arizona, United States

***Correspondence:**
Chengchun Tang
tangchengchun@hotmail.com

Specialty section:
This article was submitted to Cardiovascular and Smooth Muscle Pharmacology, a section of the journal Frontiers in Pharmacology

Received: *09 May 2019*
Accepted: *10 December 2019*
Published: *11 February 2020*

Citation:
Liu B, Wang D, Luo E, Hou J, Qiao Y, Yan G, Wang Q and Tang C (2020) Role of TG2-Mediated SERCA2 Serotonylation on Hypoxic Pulmonary Vein Remodeling. Front. Pharmacol. 10:1611. doi: 10.3389/fphar.2019.01611

channel. Furthermore, tissue-specific conditional TG2 knockout mice prevents the development of pulmonary hypertension caused by hypoxia. In summary, we uncovered a new target (TG2) for treatment of chronic hypoxic pulmonary hypertension (CHPH).

Keywords: serotonylation, TG2, SERCA2, pulmonary venous smooth muscle cell, store-operated calcium entry, [Ca2+]i

INTRODUCTION

Pulmonary arterial hypertension (PAH) is a condition marked by high blood pressure in the lungs and vascular remodeling, which can lead to right heart failure (RHF), and even death. Vascular remodeling in the lungs is characterized by the excessive proliferation, movement, and blockage of apoptosis of pulmonary vascular smooth muscle cells (Dai et al., 2018). In previous studies, many researchers paid close attention to the role of pulmonary arteries on PAH, however more recently more and more studies have revealed that pulmonary veins (PVs) also play an important role on PAH (Jin et al.2013; Zhao et al.,1993; Kulik, 2014). Chronic hypoxic exposure, vasoconstriction, and structural alterations occur not only in pulmonary arteries (PAs) but also in PVs, each contributing significantly to total pulmonary vascular resistance (Raj and Chen, 1986; Zhao et al., 1993; Raj et al., 1990, 1992; Gao and Raj, 2005; Peng et al., 2010). In addition, intrapulmonary arteries and veins contributed to the increase in pulmonary vascular resistance during hypoxia (Aguero et al., 2016; Nelson et al., 2016; Sahoo et al., 2015). The abnormal proliferation and migration of pulmonary vein smooth muscle cells (PVSMCs) formed the pathological basis of pulmonary vein remodeling. In our previous study, we indicated that transient receptor potential cation 6 (TRPC6), not TRPC1, was functionally upregulated in rat PVs and PVSMCs in response to chronic hypoxia (CH). There is evidence to suggest that TRPC6 channels are activated, in the setting of hypoxia, by both stores operated and receptor operated mechanisms, however the relative contribution of each to TRPC6 activity remains contentious. It was widely believed that ROCE produced a large amount of calcium influx in a short time, causing acute pulmonary vessels vasoconstriction, and SOCE produced a small and persistent calcium influx which played an important role on chronic pulmonary vascular remodeling (Yuan et al., 2009; Xu et al., 2014; Peng et al., 2015). Hypoxia increased the proliferation and migration of PVSMCs, which was attenuated by siTRPC6 (Xu et al., 2014). After the endoplasmic reticulum (ER) has released Ca2+, the enhanced intracellular Ca2+ concentration ([Ca2+]i) is maintained by Ca2+ from the store-operated Ca2+ entry (SOCE). SOCE regulates adding Ca2+ back into the ER, which prevents Ca2+ from entering and enables restorative resting of Ca2+. This exhibits a mediating effect on [Ca2+]i, which facilitates the resting [Ca2+]i in the nanomolar range by way of sarco(endo)plasmic reticulum calcium ATPase (SERCA). SERCA activity increases upon the release of ER/sarcoplasmatic reticulum (SR) Ca2+, which allows for rapid re-uptake of cytosolic Ca2+ (Luo et al., 1994). Subtype SERCA2 was a key modulator of calcium cycling in both cardiomyocytes and vascular SMCs, and the pulmonary arterial SERCA2 expression is down-regulated in a rat monocrotaline model of PH as well as in humans with PAH (Sahoo et al., 2015). 5-Hydroxytryptamine (5-HT and serotonin) is a well-known small protein that plays a central role in the pathogenesis of PAH and vascular remodeling (Lee et al., 1991; Lee et al., 1998; Lee et al., 1999; Liu et al., 2011; Thomas et al., 2013; Penumatsa et al., 2014a). Previous research has found that the enzyme tissue transglutaminase 2 (TG2) regulates the cross-linking of proteins with 5-HT. This is a post-translational process of monoaminylation, which is known as "serotonylation" TG2 activity and is active in both smooth muscle proliferation and contraction produced by 5-HT (Penumatsa et al., 2014b; He et al., 2016; Yu et al., 2016; Chen et al., 2018; Liu et al., 2018). Moreover, in our previous study, we used tandem mass spectrometry and immunoprecipitation of cardiomyocytes to confirm that SERCA2 was another target protein for 5-HT, and was named SERCA2 serotonylation (Wang et al., 2016). We speculated that CH inhibits the activity of SERCA2 by serotonylation, thereby activating TRPC6-mediated SOCE to increase the intracellular calcium concentration and promote cell proliferation and migration.

Abbreviations: CAP, cyclopiazonic acid; SOCE, store-operated calcium entry; [Ca2+]i, intracellular Ca2+ concentration; SERCA, sarco-endoplasmic reticulum Ca2+ ATPase; s-SERCA2, SERCA2 serotonination; TG2, transglutaminases2; PAH, pulmonary arterial hypertension; RVSP, right ventricular systolic pressure; RVHI, right ventricular hypertrophy index; hPVSMC, human pulmonary venous smooth muscle cell; TRPC, transient receptor potential cation channel; 5-HT, serotonin, 5-hydroxytryptamine; WT, wild type; Tgm2 −/−, TG2 gene knockout.

MATERIALS AND METHODS

Reagents

Cyclopiazonic acid (CPA) and PST-2744 (SERCA2 agonists, Sigma-Aldrich, St. Louis, MO, USA), 5-BP, and Fluo-4 AM probes were from Life Technologies (Thermo Fisher Scientific, Waltham, MA, USA), culture–insert two well (ibidi GmbH, Germany).

Small Interfering Ribonucleic Acid and Recombinant Adenovirus

hPVSMCs at 70–80% confluence was transfected with siRNA and recombinant adenovirus. Takes 2.5 μl (six-well) Lipofectamine® RNAiMAX Reagent (Thermo Fisher Scientific) and 5 μl (six-well) siRNA into two centrifuge tubes with 250 μl serum-free and antibiotic-free DEME/F-12 medium separately, and blend by gently shaking. Then, add diluted siRNA to diluted Lipofectamine® RNAiMAX Reagent, and incubate for 5 min at room temperature. Add siRNA-lipid complex to hPVSMCs (six-well)

and then add 500 μl medium to six well for 1 ml. Replace fresh medium after 8 h and continue to culture hPVSMCs for 48 h.

Recombinant adenovirus (1×1,010 TU/ml) was diluted 1,000 times in medium. Add the diluted Recombinant Adenovirus to a six-well plate and add 1 ml to each well. Replace fresh medium after 12 h and continue to culture hPVSMCs for 72 h. hPVSMCs were treated with hypoxia after completing stable transfection. Small-interfering RNA (siRNA) molecules targeting human TRPC1, TRPC6, and TG2 messenger RNAs (mRNAs) were purchased from GenePharma biotech company, China. For TRPC1, TRPC6, and TG2 overexpression, adenoviral vectors were purchased from GenePharma biotech company, China. TRPC1 siRNA: sense strand: GGAUGUGCGGGAGGUG AAGTT; antisense strand: CUUCACCUCCCGCACAUCCTT; TRPC6 siRNA: sense strand: GCCACUCACUCAACG UUAATT; antisense strand: UUAACGUUGAGUGA GUGGCTT. TG2 siRNA: sense strand: GCCUGAUCCUU CUAGAUGUTT; antisense strand: ACAUCUAGAAGGA UCAGGCTT. The efficiency of the TG2 siRNA and adenovirus were about 68 and 230% mRNA, 15 and 170% protein. The efficiency of the TRPC1 siRNA and adenovirus were about 67 and 263% mRNA, 20 and 160% protein. The efficiency of the TRPC6 siRNA and adenovirus were about 71 and 233% mRNA, 17 and 211% protein. For specific analysis, please referred to **Supplementary Materials**.

Vascular Smooth Muscle-Specific Tg2 Knockout Mice

Vascular smooth muscle-specific Tgm2 knockout mice were generated using standard Cre-LoxP-based gene targeting strategies. The final targeting vector for Tgm2 conditional knockout was constructed and subsequently delivered to vascular smooth cells. Male adult Tgm2 conditional knockout mice and female adult Tg(Tagln-cre)1Her/J were purchased from The Jackson Laboratory (USA) on a C57BL/6J background. These Tgm2t/t floxed mice possessed loxP sites flanking exons 6–8 of the transglutaminase 2, C polypeptide (Tgm2) gene. Under the control of mouse transgelin (smooth muscle protein 22-alpha), the transgenic mice expressed Cre recombinase. Cre-mediated recombination, when crossed with a strain possessing the appropriate loxP site-flanked sequence, will delete the flanked sequence in vascular smooth muscle cells. Mice were housed in groups of four in standard polypropylene cages in 12-h light-dark cycle approved by the Nanjing Medical University animal welfare guidelines (Nanjing, China). Genotyping was performed *via* PCR using DNA extracted from tail clippings with a Direct PCR (Tail) Kit (ViaGen Biotech Inc, USA). In brief, 8 to 10-week old male mice were used for *in vivo* experiments. Mice were assigned to experimental groups based on their genotype and SM22α-Cre+/− status. Selection of animal for CH treatment was performed randomly and in a blinded manner.

Cell Isolation

Human pulmonary vein smooth muscle cells (hPVSMCs) were aseptically isolated from the intrapulmonary vein (fourth level) from surgical pulmonary lobectomy at room temperature. After removing adhering fat, connective tissue, and endothelial cells, the dissected media of the PVs was cut into small pieces (1–2 mm^2) and covered by autoclaved glass coverslips in cell culture dishes. Next, we cultured fourth level hPVSMCs in DMEM/F-12 (HyClone, USA) which was supplemented with 10% fetal bovine serum (FBS) (Biological Industries, Israel), and 1% Penicillin-Streptomycin liquid (Gibco, USA) at 37°C and 5% CO2. PVSMCs were identified by positive immunostaining with anti-α-SMA monoclonal antibody (Abcam, UK). Cells at passages 2–3 were used in experiments, and each experiment was repeated at least three times with different preparations of cells. While the cells cultured in a tri-gas incubator, we performed hypoxia preconditioning (Forma Series II 3131 Water Jacket CO2 Incubator, Thermo Scientific, USA) for 12 or 24 h with oxygen concentration in 1% (Weisel, et al., 2014).

Pulmonary Arterial Hypertension Model

In vivo, 8-week male wild-type (WT) mice (n = 6) and TG2 knockout (Tgm2−/−) mice (n = 6) were exposed to hypoxia (10% O2) in a normobaric chamber for 6 weeks, which represented the hypoxia group. Another set of identical WT mice (n = 6) and Tgm2−/− mice (n = 6) were kept under normal conditions for 6 weeks, and represented the normoxia groups. The chamber (AiPu XBS-02B, China) had an external oxygen controller, sensing the ambient oxygen concentration and replacing it with nitrogen when necessary. The chamber was partially ventilated. At the end of the treatment period, hemodynamic indexes were determined, and lung tissue of mice were collected (Chen et al., 2018; Liu et al., 2018).

Hemodynamic and Morphometric Measurements

Mice were anesthetized with 1% pentobarbital sodium (80 mg/kg ip). Then the RSVP was measured by closed-chest insertion into the right ventricle (RV), in order to measure the mean pulmonary arterial pressure of spontaneously breathing, anesthetized animals using a xiphocostal approach. This entailed using a 22-gauge needle that was connected to a pressure transducer, both of which were controlled by the PowerLab system (ADInstruments, Australia). In order to specify the position of the needle, we used the wave form and our data were recorded using the Chart program (part of the PowerLab system). We then extracted the heart and lungs from the mice and separately weighed the right ventricle and the left ventricle plus interventricular septum (LV+S). This allowed us to examine the extent of RV hypertrophy. We calculated the right ventricular hypertrophy index (RVHI) according to the following formula: RVHI = [RV/(LV+S)]. Lung sections from inferior lobe of right lung were prepared and processed using hematoxylin-eosin (HE) staining using a standard protocol. Tissue sections were observed under a light microscope. At 400× magnification small pulmonary vessels of at least three animals per group ranging from 50 to 100 μm in internal diameter were assessed. The percentage medial layer thickness [MT% = 100 x (medial layer thickness)/(vessel semidiameter)] and area [MA% = 100 (cross-sectional medial layer area)/(total cross-sectional vessel area)] of peripheral pulmonary arteries

were analyzed using a blind-method image-processing program (Image-Pro Plus, Version 6.0) (He et al., 2016; Chen et al., 2017).

Co-Immunoprecipitation Assay

To determine the interaction between SERCA2 and 5-HT *in vivo* and *in vitro*, hPVSMCs were lysed in an immunoprecipitation (IP) lysis buffer (KeyGen BioTech, China) after incubation with 5-HT (1 mM) and Ca2+(6.7 mM). Cell lysates were cleared by centrifugation at 10,000 rpm for 5 min at 4°C. Briefly, distal (≥2th generations) PV relative to atrium were dissected from lungs of male mice after finishing hypoxia. The thin layer of adventitia was carefully stripped off with fine forceps, and the endothelium was wiped off using a cotton swab. Total protein was extracted using an immunoprecipitation (IP) lysis buffer (KeyGen BioTech, China) for distal PV tissue. The protein content was measured using a bicinchoninic acid assay (BCA) protein assay (KeyGen BioTech, China). In brief, magnetic beads were resuspended in the vial. And 50 μl Protein A/G magnetic beads were added to a 1.5 ml tube, and 150 μl binding buffer (50 mM Tris, 150 mM NaCl, 0.1% Triton X-100, pH 7.5) was added into the tube twice to perform magnetic separation. Next, 200 μl of 30 μg/ml anti-SERCA2 mouse monoclonal antibody (Abcam, UK) was added to pretreat the magnetic beads. The tube was rotated for 1 h at room temperature or 4 h at 4°C, then resuspended thoroughly by pipetting up and down. Magnetic separation was performed and the supernatant was discarded twice. Tubes were removed from the magnetic separator and the sample containing the antigen (Ag) (200 μl) was added and gently pipetted to resuspend the Protein A/G magnetic beads-Ab complex. The mixture was incubated overnight at 4°C under rotation to allow Ag to bind to the Protein A/G magnetic Bbads-Ab complex. Next, the magnetic beads-Ab-Ag complex was washed three times using 300 μl binding buffer per wash. Magnetic separation was performed between each wash, supernatant was removed and resuspended by gentle pipetting. The Protein A/G magnetic beads-Ab-Ag complex was resuspended in 150 μl binding buffer and the bead suspension were transferred to a clean tube to avoid co-elution of the proteins bound to the tube wall. Then, the supernatant was discarded and 30 μl of 1× sodium dodecyl sulfate polyacrylamide gel electrophoresis (SDS-PAGE) loading buffer was added, mixed well, and heated at 95°C for 5 min. The supernatant was collected for SDS-PAGE detection by magnetic separation, then 5-HT and SERCA2 expression were evaluated in the final supernatant using Western blot analysis using an anti-serotonin antibody (Abcam, UK) and anti-SERCA2 rabbit polyclonal antibody (Abcam, UK).

SERCA2 Activity Assay

SERCA2 is a member of the ATPase family, which can decompose ATP into ADP and inorganic phosphorus. Analysis of the amount of inorganic phosphorus determined the level of ATPase activity by using ultramicro-Ca2+-ATPase detection kit (Jiancheng Bioengineering Institute, China). The treated hPVSMCs were digested, centrifuged, and the supernatant was removed, leaving layers of cells, and 200 μl of ultrapure water was added to each tube to prepare a 107/ml cell suspension, which was disrupted by an ultrasonic pulverizer. The prepared cell suspension did not centrifuge and the total protein concentration was measured by the BCA method. *In vivo*, pulmonary veins were isolated from WT and Tgm2−/− mice under hypoxia and normoxia. In brief, 9 vol of ultrapure water were added to the veins, and veins were mechanically disrupted in an ice bath, and centrifuged at 2,500 rpm for 10 min. Next, the supernatant was collected, diluted 10-fold, and the total protein concentration was measured by the BCA method. Enzymatic reactions and phosphorus determination were carried out according to the kit instructions. An UV spectrophotometer (Mapada UV-3100PC, China) was used to measure the absorbance of samples at a wavelength of 636 nm and 1 cm optical path after ultrapure water zero setting. The optical density (OD) value was used in the following formula to calculate the activity of ATPase. Activity of ATPase (U/mgprot) = (the OD value of the sample − the OD value of the control)/(OD value of standard-OD value of blank)×0.02 μmol/l×6×2.8÷total protein concentration of sample (mg protein/ml) (Guo et al., 2017).

TG2 Activity Assay

For measurement of TG2 activity, 5-BP (400 μM, Thermo Scientific, USA) activity was visualized with fluorochrome-labeled HRP-added streptavidin. In brief, hPVSMCs were grown at a rate of 80% on glass coverslips (CitoGlas, China). hPVSMCs were exposed to 5-BP for an h prior to the exposure to hypoxia/normoxia, after 24 h of free-serum starvation. As a negative control, the incubation of 5-BP was omitted. Following the hypoxia/normoxia treatment, cells were fixed with 4% formaldehyde (Biosharp, China) for 20 min at room temperature. Cells were treated with 0.1% Triton X-100 for 30 min after complete removal of paraformaldehyde. Then, cells were blocked with 5% BSA in 0.1% Triton X-100 for 1 h at 4°C. Then, cells were incubated with 2 μg/L Streptavidin Alexa Fluor 488 Streptavidin HRP (YeaSen Bio, China) overnight at 4°C. Finally, cells were treated with 4′,6-diamidino-2-phenylindole (DAPI) (Leagene Biotechnology, China) at 37°C for 5 min, and was then sealed with nail polish. We examined the stained sections under a light microscope (Nikon Eclipse TE2000-S, Japan). The green fluorescence intensity per cell was calculated using ImageJ software to quantitatively analyze the activity of TG2 (Occhiogrosso et al., 2012).

Measurements of [Ca2+]i and Store-Operated Calcium Entry

In order to quantify the [Ca2+]i in groups of hPVSMCs using an Infinite M200 PRO plate-reader (Tecan, Switzerland), the hPVSMCs were seeded into 96-well plates, with each well containing 104 cells. After 2 days, the medium was replaced with DMEM/F12 (with no serum), and the cells were used after incubation for another 24 h. Cells were washed with HEPES [4-(2-hydroxyethyl)-1-piperazineethanesulfonic acid]-buffered saline (HBS: 135 mM NaCl, 5.9 mM KCl, 1.2 mM MgCl2, 1.5 mM CaCl2, 11.6 mM HEPES, 11.5 mM D-glucose, pH 7.3), and loaded with fluo-4 by incubation with Fluo-4-AM (2 μM) in HBS (100 μl per well). After 30 min at 37°C, HBS

replaced the medium at a rate of 100 μl per well, and the fluorescence from Fluo-4AM (excitation 485 nm, emission 525 nM) was recorded at 5-min intervals for 30 cycles using Tecan i-control. For the measurement of SOCE, hPVSMCs were treated as in the following four steps. Step one, hPVSMCs were treated with HBS solution for 5 min. Step two, hPVSMCs were treated with free-Ca2+ HBS solution included 5 μM nifedipine (Aladdin Industrial Corporation, China) and 10 μM CPA (Sigma-Aldrich, St. Louis, MO, USA). Step three, hPVSMCs were treated with free-Ca2+ HBS solution included 5 μM nifedipine and 10 μM CPA for 10 min. Step four, hPVSMCs were treated with HBS solution for 10 min. Fluorescence was only recorded in steps 2 and 3. The change in intracellular Ca2+ concentration was represented by the change of fluorescence intensity. The ratio of fluorescence intensity (F/F0) was used to compare intracellular Ca2+ concentration under different treatments (F: the average fluorescence intensity under different treatments, F0: the initial fluorescence intensity) (Dale et al., 2018; Zhu et al., 2018).

Real-Time Polymerase Chain Reaction

Total RNA from hPVSMCs with different treatments was isolated by using the RNAprep pure cell Kit (TianGen BioTech, China) according to the manufacturer's protocol. The RNA concentrations were determined using a NanoDrop ND-1000 spectrophotometer (Thermo Scientific). Equal amounts of total RNA were reversed transcribed using the FastQuant RT Kit (with gDNase) (TianGen BioTech, China). RT-PCR was performed with the SuperReal PreMix Plus (SYBR Green) (TianGen BioTech, China) and Prism 7500 SDS (Applied Biosystems; Thermo Fisher Scientific, USA). The primers for TRPC1 were: h-TRPC1-s ATGTGCTTGGGA GAA ATGCTG, h-TRPC1-a TCTTGATGATCGTTTTGGTCG. The primers for TRPC6 were: h-TRPC6-sACTCCTTCCT AATGAAACCAGCAC, h-TRPC6-a CAGATTTCTTTACATT CAGCCCATA. The primers for h-β-actin were: h-ACTIN-s CACCCAGCACAATGAAGATCA AGAT, h-β-actin-a CCAG TTTTTAAATCCTGAGTCAAGC. The primers for TG2 were: h-TG2-s TATGGCCAGTGCTGGGTCTTCGCC, h-TG2-a GGCTC CAGGGTTAGGTTGAGCAGG. The relative gene expression values were calculated using the ΔΔCt method (ΔΔCt = ΔΔCt treated − ΔΔCt untreated control) and the equation y = 2 − ΔΔCt and β-actin served as the control.

Lung Tissue Immunohistochemistry

Lung tissues were fixed in 4% paraformaldehyde, processed, and embedded in paraffin. We carefully examined the cores and inserted them into new paraffin blocks, using Tissue Arrayer Minicore (Alphelus, Plaisir, France). We deparaffinized the sections with a thickness of 5 μm and washed them with 100% ethanol, 90% ethanol, 70% ethanol, and then distilled water. These sections were then prepared for antigen retrieval in a citrate buffer with a pH of 6.0 by heating them in a microwave for 5-min cycles. The sections were then incubated overnight at a temperature of 4°C with a 1:200 diluted Anti-TG2 antibody (Abcam, USA), after which we incubated them with biotin-labeled Rabbit Anti-Mouse IgG H&L preabsorbed (Abcam, USA) for immunostaining (Chihong, et al., 2017).

Western Blot Analysis

Protein samples were prepared in a similar way as was described for co-IP analysis. In brief, 30 μg of protein was loaded per lane, with a buffer of 8% SDS-PAGE gel subsequently transferred to polyvinylidene fluoride or polyvinylidene difluoride (PVDF) membranes. Following the transfer, the membranes were incubated overnight at 4°C with anti-TG2 monoclonal antibody (1:1,000, Abcam, UK), anti-osteopontin polyclonal antibody (1:1,000, Abcam, UK), anti-SM22α polyclonal antibody (1:1,000, Abcam, UK), anti-β-actin monoclonal antibody (1:1,000, Abcam, UK), and anti-calponin polyclonal antibody (1:1,000, Abcam, UK). Then, membranes were washed and incubated with an HRP-conjugated secondary antibody and developed using a ECL Substrate Kit (Invent Biotechnology, USA). The subsequent processes were performed according to the manufacturer's instructions. The image was taken by a Tanon-4600 Chemiluminescent Imaging System (Tanon, China) for 1–3 min. Specific bands were analyzed according to apparent molecular sizes.

Cell Proliferation Assay and Apoptosis Detection

FBS-free medium starvation for 24 h, hPVSMCs were treated with 10 μM cyclopiazonic acid (CPA) (SERCA2 inhibitor, Sigma-Aldrich, St. Louis, MO, USA) and 5 μM PST-2744 (SERCA2 agonists, Sigma-Aldrich, St. Louis, MO, USA) for 24 and 48 h, respectively. The proliferation of cells was examined using a Cell Counting Kit-8 assay (Dojindo, Japan). Cells were seeded at 5,000 cells/well into 96-well plates with 100 μl culture medium. Then, 10 μl of CCK-8 solution was added to the cells at specific time points and cells were incubated for 3 h at 37°C. Then, the absorbance at 450 nm was measured using a Microplate Reader (Bio-Rad, USA). Cells were seeded at 5×104 cells/well into six-well plates in 2,000 μl culture medium. Apoptosis was examined by flow cytometric analysis. An Annexin V-EGFP/PI double stain assay (KeyGen BioTech, China) was performed following the manufacturer's protocol.

Wound Scratch Assays

A total of 5 × 105 cells/ml hPVSMCs suspension was prepared as usual. Then, 70 μl of the suspension was placed into a culture–insert two well (ibidi GmbH, Germany). Shaking is avoided as this will result in an inhomogeneous cell distribution. Cells were incubated at 37°C and 5% CO2. After appropriate cell adherence (24 h), the culture–insert two well was gently removed by using sterile tweezers, and the outer area was filled with cell culture medium. In brief, hPVSMCs were seeded on two-wells silicone inserts with a defined cell-free gap culture dish, incubate at 37°C and 5% CO2 as usual, after appropriate cell attachment (24 h) gently remove the Culture-Insert 2 Well by using sterile tweezers. Grab a corner of the Culture-Insert 2 Well. Fill the used well or dish with cell free medium. The scratch healing area of cells was detected after 12 and 24 h and imaged under a microscope (Olympus, Japan).

STATISTICAL ANALYSIS

Data are expressed as the mean ± SE; for at least three independent replicates (n ≥ 3). Data analyses were performed using either the

Turkey and Dunnett test or the Student's t test. A p value of less than 0.05 was considered statistically significant. Statistical analysis of the data was employed by one-way analysis of variance (ANOVA) using a post-test depending on the requirement.

RESULTS

Effects on TG2 Expression and Activity From Hypoxia

As shown in **Figure 1A**, no differences in expression of TG2 protein and mRNA were observed at various time points under normoxia. Compared with the normoxia group, expression of TG2 mRNA and protein significantly increased after hypoxia treatment for 12, 24, and 48 h and was time-dependent. As shown in **Figure 1B**, cells were stained with Alexa Fluor 488 Streptavidin-conjugated horseradish peroxidase (HRP) to detect TG2 localization. No differences in cytosolic fluorescence was observed at various time points under normoxia (**Figure 1B-b**). The streptavidin staining for (biotinamido)pentylamine (BP) incorporation showed a time dependent increased cytosolic fluorescence under hypoxia compared to the normoxia group (**Figure 1B-a**). The graph presented in (**Figure 1B-c**) shows the quantification of the relative 5-BP fluorescent intensities that are normalized to number of cells per image. Together, these data showed that hypoxia enhanced the expression and activity of TG2 and was time -dependent.

Effect of Hypoxia on the Activity of SERCA2 and Expression of SERCA2 Serotonylation

In vitro, cells produced more organic phosphorus (IP) when the TG2 gene was silenced, whereas cells produced less organic phosphorus when the TG2 gene overexpressed under normoxia. In addition, our findings showed that hypoxia significantly prevented cells from producing inorganic phosphorus, which was regulated by TG2. When compared to the normoxia group, silencing of the TG2 gene did not increase the production of inorganic phosphorus under hypoxic conditions (**Figure 2A**). Next, we used co-IP to analyze the level of s-SERCA2 protein. Our data showed that the expression of s-SERCA2 protein was significantly increased when the TG2 gene was overexpressed, whereas the expression of s-SERCA2 protein decreased when the TG2 gene was silenced under normoxic conditions. When compared to the normoxia group, the expression of s-SERCA2 protein significantly increased under hypoxia, however the expression did not significantly increase when the TG2 gene was silenced under hypoxia. When comparing the two groups of cells regarding TG2 gene overexpression or TG2 gene silencing, we found that the activity

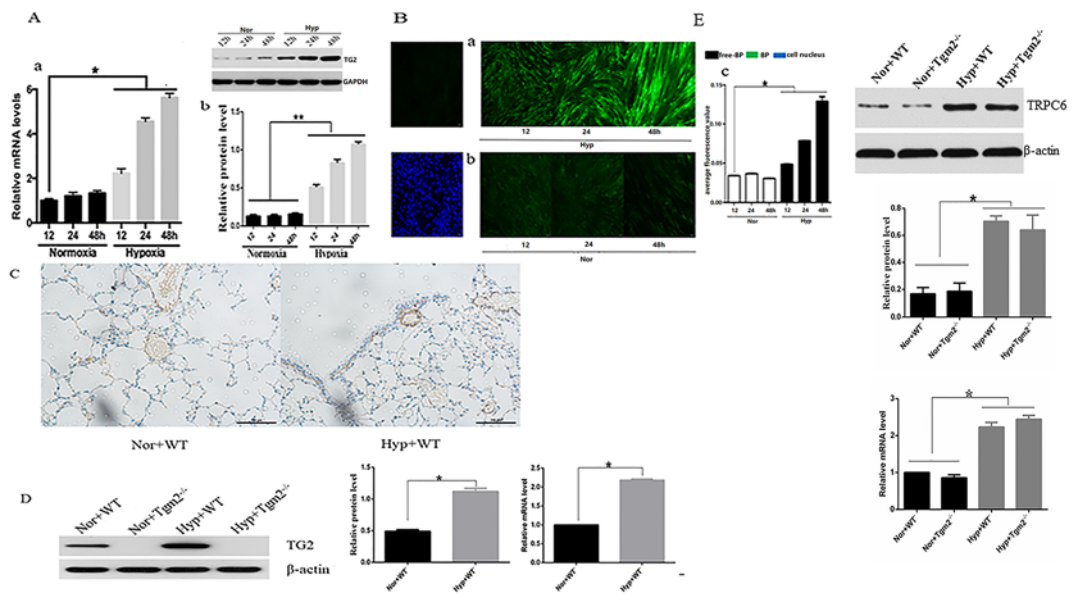

FIGURE 1 | Effects of hypoxia on the expression and activity of TG2 *in vivo* and *in vitro*. All values are presented as the mean ± S.E.M. Nor, normoxia; Hyp, hypoxia; WT, wild type; Tgm2–/–. **(A**-a**)** The level of TG2 messenger RNA (mRNA) (n = 3, *p < 0.05 compared with the normoxic group). **(A**-b**)** TG2 protein band and the level of TG2 protein (n = 3, *p < 0.05 compared with the normoxic group, **p < 0.05 compared with normoxia). **(B)** Cells were exposed to 5-BP for 1 h prior to exposure to hypoxia/normoxia after 24 h of free-serum starvation. As a negative control, 5-BP incubation was omitted. Cells were then exposed to hypoxia or normoxia for 12, 24, and 48 h, and stained with streptavidin-conjugated BP incorporation, and 4′,6-diamidino-2-phenylindole (DAPI). The image shows the overlay of TG2 and 5-BP staining, which indicates the co-localization. **(B**-a**)** The green fluorescence was stronger after treatment with hypoxia and time-dependent. **(B**-b**)** Green fluorescence was weak and no marked differences in the normoxic group were observed. **(B**-c**)** The figure shows the relative fluorescence intensity (n = 3, *p < 0.05 as compared to the normoxic group). **(C)** TG2 location on the pulmonary vessels by using immunohistochemistry. **(D)** The level of TG2 protein and mRNA expression on the pulmonary veins under normoxia and hypoxia (n = 6, *p < 0.05 compared with the normoxic group). **(E)** The level of TRPC6 protein and mRNA expression on the pulmonary veins under normoxia and hypoxia (n = 6, *p < 0.05 compared with the normoxic group).

of TG2 played a key role in serotonylation *in vitro* (**Figure 2B**). *In vivo*, $Tgm2^{-/-}$ mice produced more organic phosphorus than WT mice under normoxic and hypoxic conditions, however there no differences were observed in the production of organic phosphorus between WT mice under normoxia and $Tgm2^{-/-}$ mice under hypoxia (**Figure 2C**). The levels of SERCA2-s on the PV were detected by co-IP. The expression of s-SERCA2 protein in WT mice was higher when compared to that in TG2 mice under normoxia. Hypoxia increased the expression of s-SERCA2 protein in WT mice, but did not affect the expression of s-SERCA2 protein in $Tgm2^{-/-}$ mice. Similarly, when comparing the two groups of WT mice or the two groups of $Tgm2^{-/-}$ mice, we found that the activity of TG2 played a key role in serotonylation *in vivo* (**Figure 2D**). Combined, these findings showed that serotonylation of SERCA2 inhibited the activity of SERCA2, and hypoxia induced serotonylation of SERCA2, which was modulated by the key enzyme of TG2 *in vivo* and *in vitro*. Furthermore, the activity of TG2 may play a key role in SERCA2 serotonylation both *in vivo* and *in vitro*.

Effect of SERCA2 Serotonylation on [Ca2+]i and Store-Operated Calcium Entry in Human Pulmonary Vein Smooth Muscle Cells

As shown in **Figure 3B**, hypoxia (1% O2) induced a marked increase in basal [Ca2+]i from 6.81 ± 1.14 to 13.88 ± 0.26. In the normoxia group, the cell basal [Ca2+]i decreased from 6.81 ± 1.14 to 1.40 ± 0.04 when the TG2 gene was silenced, and increased from 6.81 ± 1.14 to 8.30 ± 0.03 when the TG2 gene was overexpressed. In the hypoxia group, the cell basal [Ca2+]i decreased from 13.88 ± 0.26 to 6.95 ± 0.16 when the TG2 gene was silenced, and increased to 20.48 ± 0.25 when the TG2 gene was overexpressed. Thus, both groups showed a similar trend. Further comparison of the two groups showed that hypoxia did not significantly reduce the basal [Ca2+]i when the TG2 gene was silenced. Our data showed that nifedipine specifically blocked the L-type voltage-dependent calcium channel (VDCC). CPA promoted the release of calcium ions from the sarcoplasmic reticulum, causing a brief increase in [Ca2+]i that allowed for large amounts of calcium ions to flow into cells through the SOCE channel after restoring the extracellular calcium concentration. As shown in **Figures 3A, C**, semi-quantitative detection of SOCE by Δfluorescence [the difference in fluorescence intensity between cells that were perfused Hank's Balanced Salt Solution (HBSS) and Ca2+-free HBSS] under normoxia and hypoxia. We established a time course curvilinear of time−Δfluorescence by GraphPad software to analyze dynamic changes in [Ca2+]i. Hypoxia induced a marked increase in the peak of time−Δfluorescence curve from 164.33 ± 7.64 to 228.00 ± 14.42. In the normoxia group, the peak Δ[Ca2+]i decreased from 164.33 ± 7.64 to 130.33 ± 4.51 when the TG2 gene was silenced, and increased to 207.00 ± 6.25 when the TG2 gene was overexpressed. In addition, in the hypoxia group, the peak Δ[Ca2+]i decreased from 228.00 ± 14.42 to 165.33 ± 11.01 when the TG2 gene was silenced, and increased to 383.67 ± 13.50 when the TG2 gene was overexpressed. Further comparison of the two groups showed that hypoxia did not significantly increase the calcium influx when the TG2 gene was silenced. Thus, these data showed that TG2-mediated SERCA2 serotonylation can promote calcium ion influx through SOCE.

Effect of TRPC1 and TRPC6 on [Ca2+]i and Store-Operated Calcium Entry in Human Pulmonary Vein Smooth Muscle Cells Under Hypoxia

Many studies have shown that hypoxia increased expression of TRPC6, not TRPC1, on pulmonary artery smooth muscle cells (Lu et al., 2008; Xia et al., 2014; Wang et al., 2016). When compared to the control group, the expression of TRPC6 mRNA and protein was significantly increased and time-dependent under hypoxia, whereas the expression of TRPC1 mRNA and protein was not significantly increased or decreased under hypoxia (**Figure 4A**). As one of the main channels mediating the extracellular calcium influx on the cell membrane, the TRPC channel was an indispensable molecule during the formation of chronic hypoxic pulmonary hypertension (CHPH). We analyzed [Ca2+]i and SOCE by silencing and overexpression of the TRPC1 and TRPC6 genes under hypoxia. Semi-quantitative analysis of basal [Ca2+]i by F/F0 and SOCE was performed by time-Δfluorescence curve under hypoxia. As shown in **Figure 4B-b**, the basal [Ca2+]i increased from 2.81 ± 0.29 to 5.04 ± 0.05 after TRPC6 gene overexpression, but decreased to 1.64 ± 0.06 after TRPC6 gene silencing. The basal [Ca2+]i of silencing and overexpressing of the TRPC1 gene were 2.82 ± 0.25 and 2.73 ± 0.29, respectively. When compared with normal cells, [Ca2+]i was not significantly different when the TRPC1 gene was silenced or overexpressed. Next, we measured the peak of time-Δfluorescence curve to analyze SOCE. As shown in **Figure 4B-a, c**, the peak fluorescence increased from 193.00 ± 4.00 to 314.67 ± 2.89 after TRPC6 gene overexpression, and decreased to 114.33 ± 2.31 after TRPC6 gene silencing. The peak fluorescence of silencing and overexpressing TRPC1 gene were 200.67 ± 10.60 and 206.00 ± 5.00, respectively. In fact, silencing or overexpressing TRPC1 did not effect peak fluorescence. Combined, these data showed that hypoxia activated TRPC6-mediated SOCE to promote the extracellular calcium influx.

Effect of Cyclopiazonic Acid and PST-2744 on Human Pulmonary Vein Smooth Muscle Cell Proliferation, Apoptosis, Migration, [Ca2+]i, Store-Operated Calcium Entry, and Cell Phenotype

Proliferation, Apoptosis, and Migration

When compared to the control group, CPA promoted proliferation of hPVSMCs in a time-dependent manner, but PST-2744 inhibited proliferation of hPVSMCs in a timely fashion (**Figure 5A**). Secondly, examined the rate of cell apoptosis by using flow cytometry. When compared to the control group, CPA inhibited apoptosis of hPVSMCs in a time-dependent manner, however PST-2744 promoted apoptosis of hPVSMCs in a time-dependent manner (**Figure 5B**). Thirdly, we analyzed migration of cells by using Culture-Insert 2 Well (ibidi, German). Compared to control group, CPA promoted cell migration and resulted in a reduced wound left by the insert. However, PST-2744 prevented cells

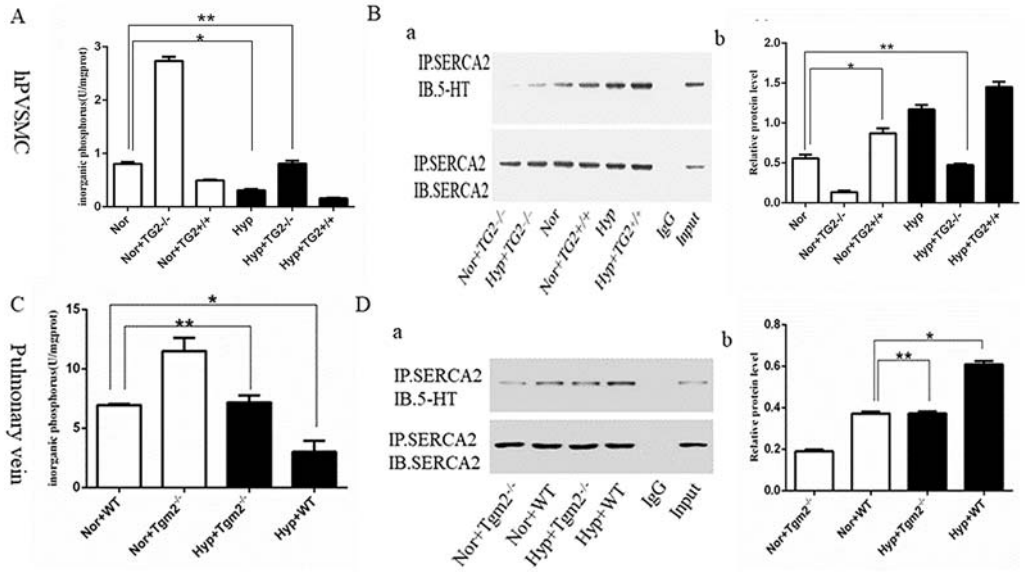

FIGURE 2 | The inorganic phosphorus production and s-SERCA2 protein expression of human pulmonary vein smooth muscle cells (hPVSMCs) and the pulmonary vein. Cells were treated with Ca2+ (6.7 mM), 5-HT (1 mM), and hypoxia (1%) for 24 h. Mice were housed under hypoxic conditions (10% O2) for 6 weeks. All values are presented as the mean ± S.E.M. Inorganic phosphorus, IP; Hyp, hypoxia; Nor, normoxia; TG2–/–, TG2 gene silencing; TG2+/+, TG2 gene overexpression; WT, wild type mice; Tgm2–/–, vascular smooth muscle-specific TG2 knockout mice. **(A)** Analysis of inorganic phosphorus produced by six groups of hPVSMCs. Hypoxia significantly prevented cells from producing inorganic IP (n = 3, $*p < 0.05$ *vs.* normoxia). When compared to the normoxia group, silencing of the TG2 gene did not increase IP under hypoxia (n = 3, $**p > 0.05$ compared with normoxia). **(B)** Co-IP analyzing the expression of s-SERCA2 protein *in vitro*. Relative expression of s-SERCA2 protein. Hypoxia significantly increased s-SERCA2 protein expression on hPVSMCs (n = 3, $*p < 0.05$ *vs.* normoxia). When silencing TG2 gene, hypoxia did not affect s-SERCA2 protein expression under hypoxia (n = 3, $**p > 0.05$ compared with normoxia). **(C)** Analysis of inorganic phosphorus produced by WT and Tgm2–/– mice. WT mice produced more IP under normoxia than under hypoxia (n = 6, $*p < 0.05$ *vs*. normoxia). There no differences were observed in the production of IP between WT mice under normoxia and Tgm2–/– mice under hypoxia (n = 6, $**p > 0.05$ compared with WT mice under normoxia). **(D)** Co-IP analyzed expression of s-SERCA2 protein *in vivo*. Relative expression of s-SERCA2 protein. Hypoxia significantly increased s-SERCA2 protein expression (n = 6, $*p < 0.05$ *vs*. WT mice under normoxia). Hypoxia increased the expression of s-SERCA2 protein in WT mice, but did not affect the expression of s-SERCA2 protein in $Tgm2^{-/-}$ mice (n = 6, $**p > 0.05$ compared with WT mice under normoxia).

migration and resulted in a residual wound by the insert (**Figure 5C**). These data showed that CPA inhibited cell apoptosis, and promoted cell proliferation and migration, whereas PST-2744 promoted cell apoptosis, and inhibited cell proliferation and migration.

[Ca2+]i and Store-Operated Calcium Entry

SERCA is an ion pump that takes up calcium ions from the cytoplasm of the endoplasmic reticulum. The decreased expression or activity of SERCA2 was the main cause of persistent SOCE. Time-Δfluorescence curve (**Figure 5E**) showed that the normal [Ca2+]i was 6.97 ± 1.16. Moreover, the [Ca2+]i of cells treated with CPA for 12 and 24 h was 8.69 ± 0.43 and 14.82 ± 0.88, respectively. In addition, the [Ca2+]i of cells treated with PST-2744 for 12 and 24 h was 5.36 ± 0.46 and 4.03 ± 0.19, respectively. As shown in **Figure 5D**, the peak of time-Δfluorescence curve was measured to analyze SOCE. The normal peak fluorescence was 171.33 ± 6.11. The peak fluorescence of cells treated with CPA for 12 and 24 h were 221.67 ± 8.62 and 265.00 ± 6.00, respectively, and the peak fluorescence the of cells treated with PST-2744 for 12 and 24 h was 143.67 ± 5.69 and 116.67 ± 6.51, respectively. Combined, these data showed that inhibition of the SERCA2 activity promoted extracellular calcium influx in a time-dependent manner, whereas and increase in SERCA2 activity decreased the extracellular calcium influx in a time-dependent manner.

Cell Phenotype

Unlike skeletal muscle and cardiomyocytes, vascular smooth muscle cells (VSMCs) are non-terminally differentiated cells with a strong plastic phenotype. The VSMCs of normal adult animals were mainly contractile phenotypes. Under the influence of various stimulating factors, the phenotype of VSMCs can be transformed from a differentiated phenotype with a contractile function to a dedifferentiated phenotype with a strong proliferation and migration ability. In this study, we focused on contractile phenotype protein markers, calopnin, and secreted protein marker, osteopontin, which were evaluated by Western blot analysis. PST-2744 suppressed the expression of osteopontin protein, but promoted the expression of calopnin protein. In addition, CPA suppressed the expression of calopnin protein, but promoted expression of osteopontin protein (**Figure 5F**). These data showed that CPA promoted transformation from a differentiated phenotype to a dedifferentiated phenotype, and PST-2744 promoted transformation from a dedifferentiated phenotype to a differentiated phenotype.

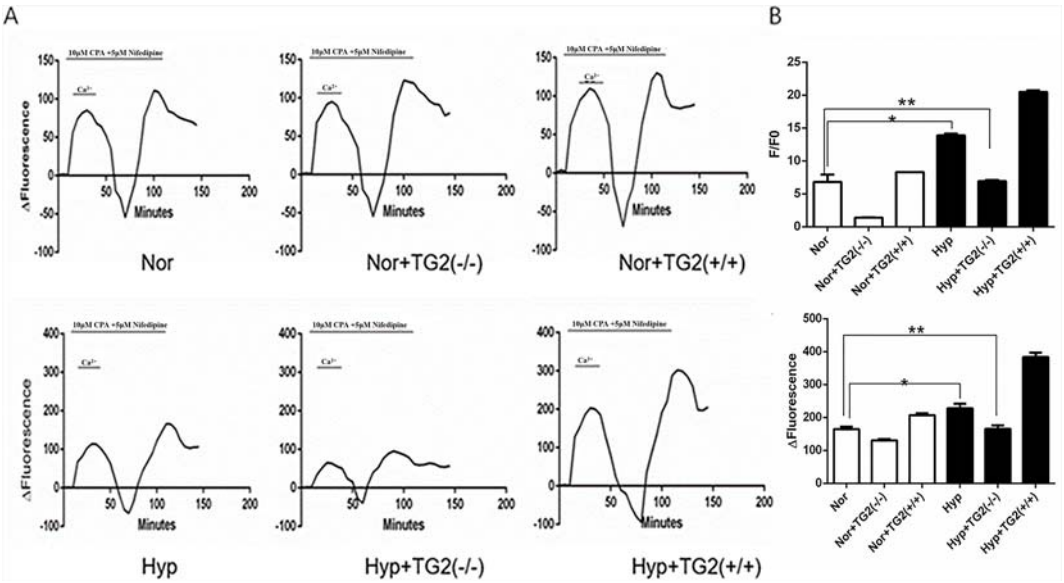

FIGURE 3 | Effect of SERCA2 serotonylation on [Ca2+]i and store-operated calcium entry (SOCE) in human pulmonary vein smooth muscle cells (hPVSMCs). The ratio of the fluorescence intensity (F/F0) was used to compare [Ca2+]i. The difference in fluorescence intensity was used to compare SOCE. L-type voltage-dependent calcium channel (VDCC) antagonist, nifedipine. SERCA2 antagonist, cyclopiazonic acid (CPA). All values are presented as the mean ± S.E.M. **(A)** Time course curvilinear of time–Δfluorescence by GraphPad software to analyze SOCE. ΔFluorescence, the difference in fluorescence intensity between cells perfused with Hank's Balanced Salt Solution (HBSS) and Ca2+-free HBSS. **(B)** Semi-quantitative analysis of intracellular basal [Ca2+]i by F/F0 (n = 3, *p < 0.05 compared with the normoxic group). **(C)** Histogram analysis of the peak-to-valley value of the time-fluorescence curve (n = 3, **p > 0.05 compared with normoxic group).

TG2 Reverses Hypertension of the Right Ventricle and Remodeling Vascular

In vivo, as shown in **Figure 6A**, based on mouse tail genetic identification, heterozygous and SM22α-Cre– was considered wild-type (WT), homozygous and SM22α-Cre+ was considered a Tgm2 complete knock-out (Tgm2–/– type). Three WT and Tgm2–/– mice were randomly selected to identify the expression of TG2 protein by Western blot (WB) analysis, which indicated that TG2 protein was normally expressed in the PV of WT mice but not in that of Tgm2–/– mice. As shown in **Figures 6C**, **D** we measured the right ventricular systolic pressure (RVSP) of mice by using a closed-chest insertion into the right ventricle (RV) and a xiphocostal angle approach under hypoxia for 6 weeks. We found that the RVSP of Tgm2–/– mice and WT mice was 18.15 ± 0.45 mmHg and 18.35 + 0.76 mmHg, respectively, under normoxia, which was not significantly different between groups. The RVSP of WT mice increased from 18.15 ± 0.45 mmHg to 34.05 ± 0.99 mmHg after hypoxia exposure for 6 weeks, and we noticed some differences between WT mice under normoxia and Tgm2–/– mice under hypoxia. The RVSP of Tgm2–/– mice under hypoxia 22.79 ± 6.79 mmHg was slightly higher when compared to that of WT mice under normoxia, however no statistical significance was achieved. After measurement of RVSP, heart and lung tissues were collected. Weights of the RV and the left ventricle (LV) plus interventricular septum (LV+S) were measured separately. The RVHI of Tgm2–/– mice and WT mice were 0.20 ± 0.010 and 0.21 + 0.009 under normoxia, respectively. Moreover, the RVHI of Tgm2–/– mice and WT mice were 0.25 ± 0.063 and 0.34 + 0.055 under hypoxia. The trend of RHVI was consistent with that of RVSP. As shown in **Figure 6B**, hematoxylin and eosin (H&E) staining showed that MT % of Tgm2–/– mice and WT mice were 9.90 ± 0.30 and 10.37 ± 0.67, and MA% of Tgm2–/– mice and WT mice were 19.13 ± 1.00 and 18.40 ± 0.62 under normoxia respectively. The MT% of Tgm2–/– mice and WT mice were 9.63 ± 0.70 and 43.30 ± 1.67, and MA% of Tgm2–/– mice and WT mice were 8.97 ± 0.47 and 70.67 ± 0.50 under hypoxia respectively. The data showed that there was no significant difference in vessel wall thickness between Tgm2–/– and WT mice under normoxia. However, vascular wall thickness of WT mice significantly increased after hypoxic treatment, whereas vascular wall thickness of Tgm2–/– mice was not significantly increased after hypoxic treatment. Together, these data showed that TG2 reversed hypertension of the right ventricle and vascular remodeling.

DISCUSSION

Here, we revealed a novel mechanism in which TG2 alleviated hypoxia-induced pulmonary vein remodeling. Our findings demonstrated that the activity of SERCA2 was regulated by a new post-translational modification (PTM) "serotonylation" and SERCA2 serotonylation inhibited activity of SERCA2. Cytoplasmic Ca2+ storage was depleted when the activity of SERCA2 was inhibited, then TRPC6 was activated which further increased SOCE to lead to a continuous increase of intracellular calcium, consequently promoting proliferation and migration of hPVSMCs. Moreover, we demonstrated that the activity of SERCA2 played an important role on the biological behavior of hPVSMCs.

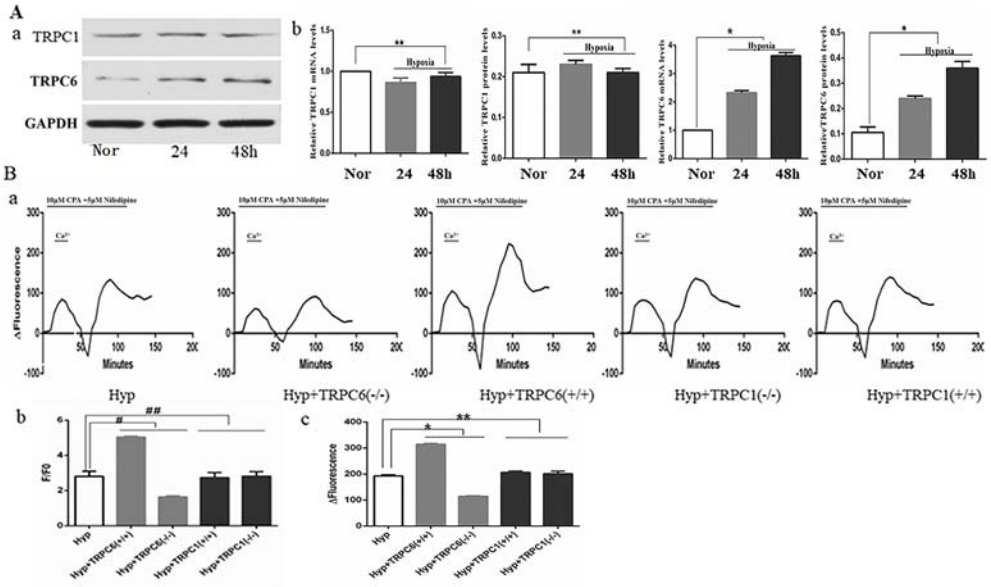

FIGURE 4 | Expression of TRPC1, TRPC6, and the effect of TRPC1 and TRPC6 on [Ca2+]i and store-operated calcium entry (SOCE) in human pulmonary vein smooth muscle cells (hPVSMCs) under hypoxia. L-type voltage-dependent calcium channel (VDCC) antagonist, nifedipine. SERCA2 antagonist, cyclopiazonic acid (CPA). Nor, normoxia; Hyp, hypoxia; TRPC(–/–), TRPC gene silencing; TRPC(+/+), TRPC overexpression. ΔFluorescence, difference in fluorescence intensity between cells perfused with Hank's Balanced Salt Solution (HBSS) and Ca2+-free HBSS. All values are presented as the mean ± S.E.M. **(A**-a**)** TRPC1 and TRPC6 protein bands and the level of TG2 protein. **(A**-b**)** The relative level of TRPC1 messenger RNA (mRNA) and protein (n = 3, **p > 0. 05 as compared to the normoxic group). **(A**-c**)** The relative level of TRPC6 mRNA and protein (n = 3, *P < 0. 05 as compared to the normoxic group). **(B)** The ratio of fluorescence intensity (F/F0) was used to compare [Ca2+]i. Time-Δfluorescence curve was used to compare SOCE. **(B**-a**)** Time course curvilinear of time-Δfluorescence by GraphPad software to analyze SOCE. **(B**-b**)** Semi-quantitative analysis of [Ca2+]i by F/F0 (n = 3, $^{\#}$p < 0.05 as compared to hypoxia group, $^{\#\#}$p > 0.05 as compared to the hypoxia group). **(B**-c**)** Histogram analysis of the peak-to-valley value of the time-fluorescence curve (n = 3, *p < 0.05 as compared to hypoxia group).

It is well known that 5-HT plays an important role on the development of HPAH. In order to understand the molecular mechanism involved, most studies focused on the 5-HT transporter and 5-HT receptor. For example, some evidence indicated that 5-HT-related stimulation of pulmonary artery smooth muscle cell (PASMC) proliferation required 5-HT internalization through the 5-HT transporter (5-HTT) (Lee et al., 1991; Lee et al., 1998; Lee et al., 1999; Eddahibi et al., 2001; Abid et al., 2012). In addition, 5-HT2A and 5-HT2B were also involved in hypoxia-induced pulmonary artery remodeling and proliferation of human pulmonary artery smooth muscle cells (hPASMC) (Keegan et al., 2001; Welsh et al., 2004; Maclean and Dempsie, 2010; Occhiogrosso et al., 2012). New insight regarding the possible mechanism by which intracellular 5-HT might exert an intracellular effect stems from our *in vitro* studies with SMCs, which showed that 5-HT serotonylates (transaminates) take up intracellular proteins through the enzyme transglutaminase (TGase) (Liu et al., 2011).

As previously mentioned, transglutaminase2 (TG2) is a ubiquitous multifunctional protein that catalyzed the post-translational modification of proteins *via* a calcium-dependent transglutamidation reaction. Modification of TG2 substrate proteins by transamidation has been shown to be important in cell survival, apoptosis, and cytoskeleton organization (Watts et al., 2009; Kumar and Mehta, 2012; Gundemir et al., 2013; Penumatsa and Fanburg, 2014). Moreover, its expression is finely regulated at the transcriptional level by cytokines, retinoids, NFκB, and by inflammatory and hypoxic stimuli (Ientile et al., 2007; Nurminskaya and Belkin, 2012; Eckert et al., 2014). In fact, as early as in 2003, Walther et al. firstly demonstrated that serotonin (5-HT) was transamidated to small GTPases by transglutaminases during activation and aggregation of platelets, rendering these GTPases constitutively active, and provided evidence for a receptor-independent signaling mechanism, termed here as "serotonylation" for the first time (Walther et al., 2003). Several studies have demonstrated that the serotonylation of RhoA, fibronectin, and smooth muscle b-actin all play important roles in aortic vascular contractility (Guilluy et al., 2007; Guilluy et al., 2009; Liu et al., 2011).

It is well known that the ryanodine receptor (RyR) and SERCA play an important role in hypoxia-induced pulmonary vascular remodeling by regulating calcium influx. Chronically high levels of intracellular calcium in pulmonary SMCs trigger signaling pathways that allow cellular proliferation, migration, and dedifferentiation, all of which are factors that contribute to hypertrophic vascular remodeling (Kuhr et al., 2012), and SERCA2 was a key modulator of calcium cycling in both cardiomyocytes and vascular SMCs (Kawase and Hajjar, 2008). Hypoxia reduced SERCA2 activity, however its mechanism of action was unclear, involving a variety of accessory proteins and kinases, and SERCA2 had multiple PTM of protein sites. PTM was an important way to regulate its activity (Vangheluwe et al., 2005). More importantly,

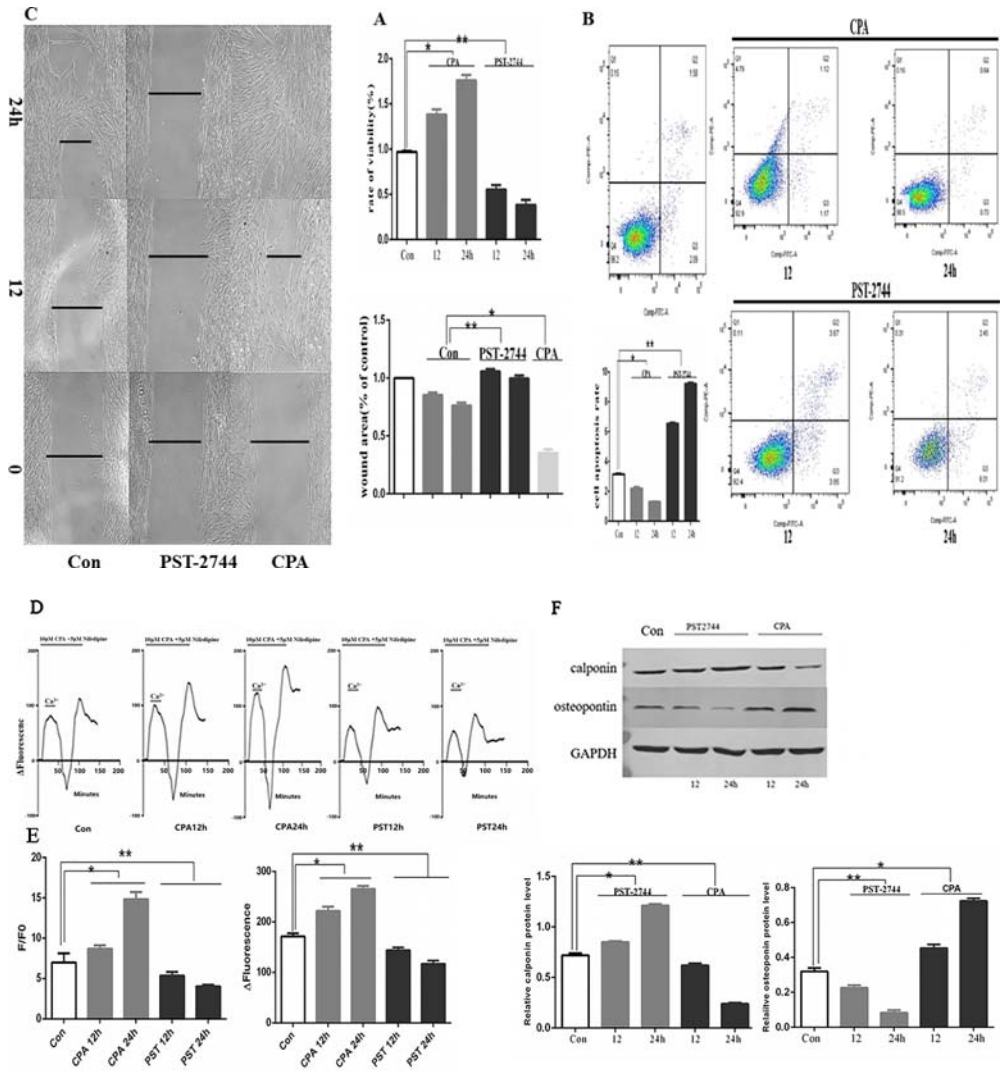

FIGURE 5 | Effect of cyclopiazonic acid (CPA) and PST-2744 on cell proliferation, apoptosis, migration, [Ca2+]i, store-operated calcium entry (SOCE), and cell phenotype. PST, PST-2744; Con, control. 12, 12 h. 24, 24 h. ΔFluorescence, difference in fluorescence intensity between cells perfused with Hank's Balanced Salt Solution (HBSS) and Ca2+-free HBSS. All values were presented as the mean ± S.E.M. **(A)** Rate of proliferation measured by Cell Counting Kit (CCK)-8 assay. CPA promoted cell proliferation in a time-dependent manner. PST-2744 suppressed cell proliferation in a time-dependent manner (n = 3, *p < 0.05 as compared to the control group, **p < 0.05 as compared to the control group). **(B)** Apoptosis rate measured by flow cytometry. CPA suppressed cell apoptosis in a time-dependent manner. PST-2744 promoted cell apoptosis in a timely fashion. Quantitative analysis of the apoptosis rate (n = 3, *p < 0.05 as compared to the control group, **p < 0.05 as compared to the control group). **(C)** Wound healing assay for human pulmonary vein smooth muscle cells (hPVSMCs). CPA promoted wound healing, whereas PST-2744 prevented wound healing. **(C)** Quantification of wound-healed area of hPVSMCs (n = 3, *p < 0.05 as compared to the control group, **p < 0.05 as compared to the control group). **(D)** Time-Δfluorescence curve was used to compare SOCE. Time course curvilinear of time-Δfluorescence by GraphPad software to analyze SOCE. Histogram analysis of the peak-to-valley value of the time-fluorescence curve (*p < 0.05 as compared to the control group, **p < 0.05 as compared to the control group). **(E)** The ratio of fluorescence intensity (F/F0) was used to compare [Ca2+]i. Semi-quantitative analysis of [Ca2+]i by F/F0 (n = 3, *p < 0.05 compared with the control group, *p < 0.05 compared with the control group). **(F)** Western blot analysis for the expression of calopnin and osteopontin protein. PST-2744 suppressed the expression of osteopontin protein, but promoted expression of calopnin protein. CPA suppressed the expression of calopnin protein, but promoted expression of osteopontin protein. Quantitative analysis of the relative expression of calopnin and osteopontin protein (n = 3, *p < 0.05 compared with the control group, **p < 0.05 compared with the control, *p < 0.05 compared with the control, **p < 0.05 compared with the control group).

once the activity was inhibited, it was difficult to reverse (Tong et al., 2010). Our study firstly proposed a new PTM of SERCA2, SERCA2 serotonylation. We demonstrated that hypoxia enhanced SERCA2 serotonation, expression, and activity of TG2 both *in vivo* and *in vitro*. Conversely, hypoxia inhibited the activity of SERCA2 *in vivo* and *in vitro*. To further investigate the effect of serotonation on the activity of SERCA2, we established vascular smooth muscle-specific TG2 knockout (Tgm2−/−) mice, overexpressed, and silenced TG2 gene on cells, and the results demonstrated that TG2-mediated serotonation inhibited SERCA2 activity under hypoxia. As

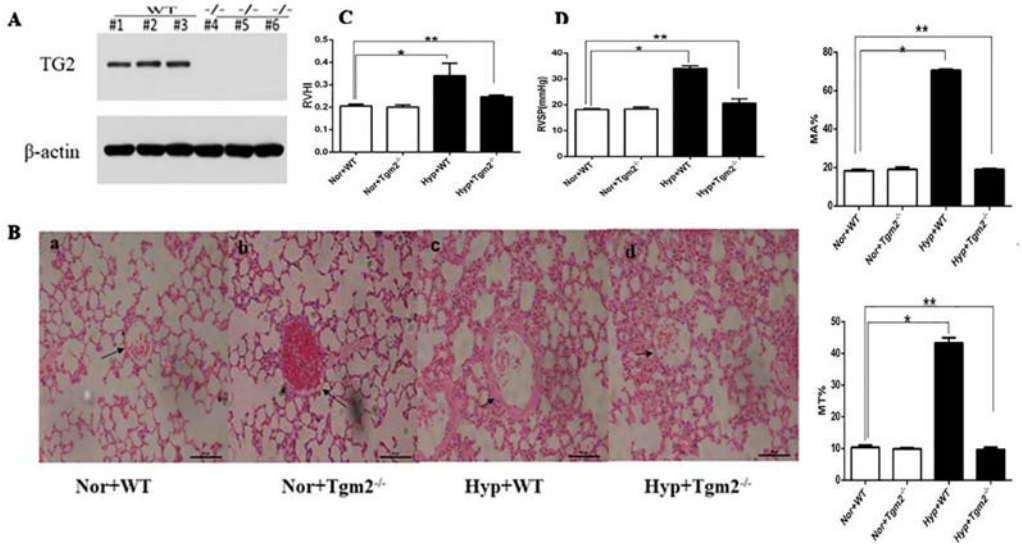

FIGURE 6 | TG2 reverses right ventricle pressure and vessel remodeling. WT, wild type; Hyp, hypoxia; Nor, normoxia; Tgm2–/–, TG2 gene knockout. MT% = 100×(medial layer thickness)/(vessel semidiameter) and area [MA% = 100×(cross-sectional medial layer area)/(total cross-sectional vessel area)]. All values are denoted as the mean ± S.E.M. **(A)** Homozygous mice-SM22α-Cre+. Western blot analysis of pulmonary veins using an anti-TG2 polyclonal antibody. **(B)** Hematoxylin-eosin (H&E) staining in mice pulmonary vessels. No difference in vessel wall thickness was observed between WT and Tgm2$^{-/-}$ mice under normoxia. The wall thickness of pulmonary vessels significantly increased in WT mice after 6 weeks of hypoxia (n = 6, *P > ;0.05 compared with under normoxia, **P > 0.05 compared with under normoxia). **(C, D)** The measurement of right ventricular systolic pressure (RVSP) and right ventricular hypertrophy index (RVHI) in wild-type (WT) and TG2 knockout mice were treated with normoxia and hypoxia (5% O2, 6 weeks) (n = 6, *P > ;0.05 compared with under normoxia, **P > 0.05 compared with under normoxia).

mentioned earlier, our results confirmed that TG2 was a ubiquitous multifunctional protein that catalyzed the PTM, which was consistent with the increased activity of TG2 that promoted fibronectin (sFn) serotonylation in the sera of humans with pulmonary arterial hypertension (PAH) and in the sera and lungs of experimental rodent models of PH (Penumatsa et al., 2014a). In fact, there was a potential cross-talking between serotonylation and other relevant signal pathway. According to Wu et al., during early reperfusion, the ROS/JAK2/STAT3 pathways play a crucial role in i) IHH (intermittent hypobaric hypoxia)-maintained intracellular CA(2+) homeostasis by improving postischemic SERCA2 activity, by increasing SR Bcl-2 and its interaction with SERCA2; and ii) the IHH-improved mitochondrial functioning (Yuan et al., 2009). Oxidative stress influences various proteins. Oxidative stress influences various proteins and biological processes, and there was also cross-interaction between oxidative stress and SUMOylation (Rigato et al.,2002; Feligioni et al., 2011; Leitao et al., 2011; Wu et al., 2015). The intensity of SUMOylation of many proteins was affected by oxidative stress (Shishido et al., 2008; Pandey et al., 2011; Shrivastava et al., 2014; Sahin et al., 2014). SUMOylation enhances the stability and activity of SERCA2a (Feligioni and Nistico, 2013). Upgrading the intensity of SERCA2a-SUMOylation increases the protein level of SERCA2a and improves cardiac function in animal models with heart failure (HF) (Feligioni and Nistico, 2013). Although the relation between oxidative stress and SERCA2a-SUMOylation still needs to be investigated, Jing Yao et al. suggested the possible role of SERCA2a-SUMOylation on the obesity-induced cardiac dysfunction and PA-induced cardiomyocyte dysfunction (Kho et al., 2011).

It was generally believed that SOCE was a small and persistent calcium influx, often associated with chronic hypoxic pulmonary vascular remodeling (Yuan et al., 2009; Wu et al., 2015). We found that TRPC6, not TRPC1 was highly expressed in hPVSMCs after hypoxia treatment, and basal [Ca2+]i and SOCE were increased and decreased when the TRPC6 gene silenced and overexpressed, respectively. However, silencing or overexpression of the TRPC1 gene did not have an effect on [Ca2+]i and SOCE. These results suggested that CH may increase SOCE and [Ca2+]i through activating the TRPC6 channel on hPVSMCs, however the mechanism was not clear. Our study highly suggested that SERCA2 serotonination may be a new mechanism for hypoxia-induced imbalance of intracellular calcium ions. We further demonstrated that the activity of SERCA2 was closely related to proliferation, migration, and phenotype of cells by using an inhibitor and agonist of SERCA2. Furthermore, we demonstrated that the activity of TG2 played a key role in serotonylation *in vivo* and *in vitro*.

Finally, we analyzed the vascular remodeling of Tgm2–/– mice under hypoxia. The index of morphology and hemodynamics of WT mice was consistent with pathological features of CHPH under hypoxia for 6 weeks. However, after the same treatment of hypoxia, the above-mentioned indexes of Tgm2–/– mice did not significantly increase, although it did not reach the level of WT mice under normoxia. Therefore, we speculated that TG2 can reverse pulmonary vascular remodeling, which provided a novel

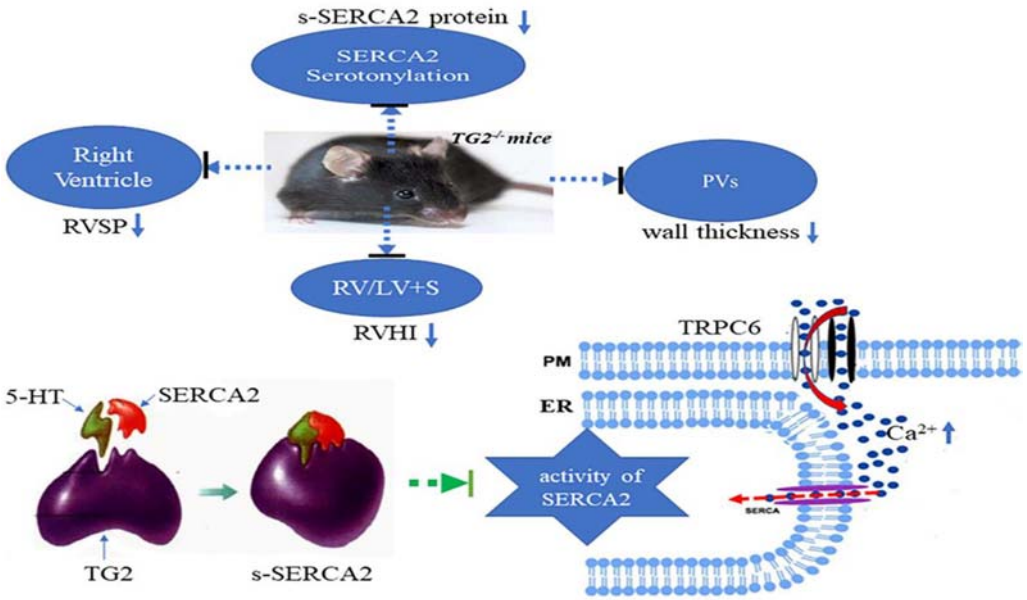

FIGURE 7 | A model for TG2-mediated SERCA2 serotonylation on hypoxic pulmonary vein remodeling. Upon depletion of ER Ca2+ stores, store-operated calcium entry (SOCE) channels and TRPC6 channels promoting entry of Ca2+ across the plasma membrane (PM). Hypoxia promoted TG2-mediated SERCA2 serotonylation, leading to inhibition of SERCA2 activity, which further increased the calcium influx through the TRPC6 channel, which eventually resulted in excessive cell proliferation, migration, and blockage of apoptosis, thereby promoting pulmonary vascular remodeling. Right ventricular systolic pressure (RVSP), right ventricular hypertrophy index (RVHI), and wall thickness of pulmonary veins (PVs) of Tgm2−/− mice did not significantly increase under hypoxia for 6 weeks.

target and orientation for treatment of CHPH. A limitation of the current experimental design was the low replicates (n = 3) in the cell-based experiments, albeit statistical significance was reached.

CONCLUSIONS

We firstly demonstrated that hypoxia promoted TG2-mediated SERCA2 serotonylation, leading to inhibition of SERCA2 activity, which further increased the calcium influx through the TRPC6 channel, which eventually resulted in excessive cell proliferation, migration, and blockage of apoptosis, thereby promoting pulmonary vascular remodeling (**Figure 7**).

DATA AVAILABILITY STATEMENT

The raw data supporting the conclusions of this manuscript will be made available by the authors, without undue reservation, to any qualified researcher.

ETHICS STATEMENT

All of the procedures carried out on animals were approved by the Animal Care and Use Committee of Nanjing Medical University, under animal protocol number IACUC11445. All protocols concerning the use of patient samples in this study were approved by the Ethics Committee of Zhongda Hospital, Southeast University.

AUTHOR CONTRIBUTIONS

CT and DW designed the study, and BL wrote the manuscript with support from EL, JH, YQ, GY, and QW. BL performed the *in vitro* experiments and the *in vivo* experiments. BL contributed to data interpretation and manuscript preparation. All authors read and approved the final manuscript.

FUNDING

This research was supported by the National Natural Science Foundation of China (Grant Number 81670237) and the Changzhou Health Commission of Science and Research (Grant Number QN201713).

ACKNOWLEDGMENTS

The authors thank Dr. Dong Wang for the technical assistance with the laboratory experiments.

SUPPLEMENTARY MATERIAL

The Supplementary Material for this article can be found online at: https://www.frontiersin.org/articles/10.3389/fphar.2019.01611/full#supplementary-material

REFERENCES

Abid, S., Houssaini, A., Chevarin, C., Marcos, E., Tissot, C. M., Gary-Bobo, G., et al. (2012). Inhibition of gut- and lung-derived serotonin attenuates pulmonary hypertension in mice. *Am. J. Physiol. Lung Cell Mol. Physiol.* 303, L500–L508. doi: 10.1152/ajplung.00049.2012

Aguero, J., Ishikawa, K., Hadri, L., Santos-Gallego, C. G., Fish, K. M., Kohlbrenner, E., et al. (2016). Intratracheal gene delivery of SERCA2a ameliorates chronic post-capillary pulmonary hypertension: a large animal model. *J. Am. Coll. Cardiol.* 67, 2032–2046. doi: 10.1016/j.jacc.2016.02.049

Chen, J., Wang, Y. X., Dong, M. Q., Zhang, B., Luo, Y., W1, N., et al. (2017). Reoxygenation reverses hypoxic pulmonary arterial remodeling by inducing smooth muscle cell apoptosis *via* reactive oxygen species-mediated mitochondrial dysfunction. *J. Am. Heart Assoc.* 6 (6), e005602. doi: 10.1161/JAHA.117.005602

Chen, G., Zuo, S., Tang, J., Zuo, C., Jia, D., Liu, Q., et al. (2018). Inhibition of CRTH2-mediated Th2 activation attenuates pulmonary hypertension in mice. *J. Exp. Med.* 215, 2175–2195. doi: 10.1084/jem.20171767

Chihong, Z., Yutian, L., Danying, W., Ruibin, J., Huaying, S., Linhui, G., et al. (2017). Prognostic value of Transglutaminase 2 in non-small cell lung cancer patients. *Oncotarget* 8, 45577–45584. doi: 10.18632/oncotarget.17374

Dai, Z., Zhu, M. M., Peng, Y., Machireddy, N., Evans, C. E. , Machado, R., et al. (2018). Therapeutic targeting of vascular remodeling and right heart failure in PAH with HIF-2alpha inhibitor. *Am. J. Respir. Crit. Care Med.* 198, 1423–1434. doi: 10.1164/rccm.201710-2079OC

Dale, P., Head, V., Dowling, M. R., and Taylor, C. W. (2018). Selective inhibition of histamine-evoked Ca(2+) signals by compartmentalized cAMP in human bronchial airway smooth muscle cells. *Cell Calcium.* 71, 53–64. doi: 10.1016/j.ceca.2017.12.002

Eckert, R. L., Kaartinen, M. T., Nurminskaya, M., Belkin, A. M., Colak, G., Johnson, G. V., et al. (2014). Transglutaminase regulation of cell function. *Physiol. Rev.* 94, 383–417. doi: 10.1152/physrev.00019.2013

Eddahibi, S., Humbert, M., Fadel, E., Raffestin, B., Darmon, M., Capron, F., et al. (2001). Adnot Serotonin transporter overexpression is responsible for pulmonary artery smooth muscle hyperplasia in primary pulmonary hypertension. *J. Clin. Invest.* 108, 1141–1150. doi: 10.1172/JCI12805

Feligioni, M., and Nistico, R. (2013). Sumo: a (oxidative) stressed protein. *Neuromo. Mole. Med.* 15, 707–719. doi: 10.1007/s12017-013-8266-6

Feligioni, M., Brambilla, E., Camassa, A., Sclip, A., Arnaboldi, A., and Morelli, F. (2011). Crosstalk between JNK and SUMO signaling pathways: desumoylation is protective against H2O2-induced cell injury. *PloS One* 6, e28185. doi: 10.1371/journal.pone.0028185

Gao, Y., and Raj, J. U. (2005). Role of veins in regulation of pulmonary circulation. *Am. J. Physiol. Lung Cell Mol. Physiol.* 288, L213–L226. doi: 10.1152/ajplung.00103.2004

Guilluy, C., Rolli-Derkinderen, M., Tharaux, P. L., Melino, G., Pacaud, P., and Loirand, G. (2007). Transglutaminase-dependent RhoA activation and depletion by serotonin in vascular smooth muscle cells. *J. Biol. Chem.* 282, 2918–2928. doi: 10.1074/jbc.M604195200

Guilluy, C., Eddahibi, S., Agard, C., Guignabert, C., Izikki, M., Tu, L., et al. (2009). RhoA and Rho kinase activation in human pulmonary hypertension: role of 5-HT signaling. *Am. J. Respir. Crit. Care Med.* 179, 1151–1158. doi: 10.1164/rccm.200805-691OC

Gundemir, S., Colak, G., Feola, J., Blouin, R., and Johnson, G. V. (2013). Transglutaminase 2 facilitates or ameliorates HIF signaling and ischemic cell death depending on its conformation and localization. *Biochim. Biophys. Acta* 1833, 1–10. doi: 10.1016/j.bbamcr.2012.10.011

Guo, H., Wang, Y., Zhang, X., Zang, Y., Zhang, Y., Wang, L., et al. (2017). Astragaloside IV protects against podocyte injury *via* SERCA2-dependent ER stress reduction and AMPKα-regulated autophagy induction in streptozotocin-induced diabetic nephropathy. *Sci. Rep.* 7, 6852. doi: 10.1038/s41598-017-07061-7

He, Y. Y., Liu, C. L., Li, X., Li, R. J., Wang, L. L., and He, K. L. (2016). Salubrinal attenuates right ventricular hypertrophy and dysfunction in hypoxic pulmonary hypertension of rats. *Vasc. Pharmacol.* 87, 190–198. doi: 10.1016/j.vph.2016.09.009

Ientile, R., Caccamo, D., and Griffin, M. (2007). Tissue transglutaminase and the stress response. *Amino. Acids* 33, 385–394. doi: 10.1007/s00726-007-0517-0

Jin, Y., Chen, B., Calvert, T. J., Chicoine, L. G., Liu, Y., and Nelin, L. D. (2013). Chronic hypoxia decreases arterial and venous compliance in isolated perfused rat lungs: an effect that is reversed by exogenous L-arginine. *Am. J. Physiol. Heart Circulatory Physiol.* 304, H195–H205. doi: 10.1152/ajpheart.00188.2012

Kawase, Y., and Hajjar, R. J. (2008). The cardiac sarcoplasmic/endoplasmic reticulum calcium ATPase: a potent target for cardiovascular diseases. *Nat. Clin. Pract. Cardiovasc. Med.* 5, 554–565. doi: 10.1038/ncpcardio1301

Keegan, A., Morecroft, I., Smillie, D., Hicks, M. N., and MacLean, M. R. (2001). Contribution of the 5-HT(1B) receptor to hypoxia-induced pulmonary hypertension: converging evidence using 5-HT(1B)-receptor knockout mice and the 5-HT(1B/1D)-receptor antagonist GR127935. *Circ. Res.* 89, 1231–1239. doi: 10.1161/hh2401.100426

Kho, C., Lee, A., Jeong, D., Oh, J. G., Chaanine, A. H., Kizana, E., et al. (2011). Sumo1-dependent modulation of SERCA2a in heart failure. *Nature* 477, 601–605. doi: 10.1038/nature10407

Kuhr, F. K., Smith, K. A., Song, M. Y., Levitan, I., and Yuan, J. X. (2012). New mechanisms of pulmonary arterial hypertension: role of Ca(2)(+) signaling. *Am. J. Physiol. Heart Circ. Physiol.* 302, H1546–H1562. doi: 10.1152/ajpheart.00944.2011

Kulik, T. J. (2014). Pulmonary hypertension caused by pulmonary venous hypertension. *Pulmon. Circ.* 4, 581–595.

Kumar, S., and Mehta, K. (2012). Tissue transglutaminase constitutively activates HIF-1alpha promoter and nuclear factor-kappa B *via a* non-canonical pathway. *PloS One* 7, e49321. doi: 10.1371/journal.pone.0049321

Lee, S. L., Wang, W. W., Moore, B. J., and Fanburg, B. L. (1991). Dual effect of serotonin on growth of bovine pulmonary artery smooth muscle cells in culture. *Circ. Res.* 68, 1362–1368. doi: 10.1161/01.res.68.5.1362

Lee, S. L., Wang, W. W., and Fanburg, B. L. (1998). Superoxide as an intermediate signal for serotonin-induced mitogenesis. *Free Radic. Biol. Med.* 24, 855–858. doi: 10.1016/s0891-5849(97)00359-6

Lee, S. L., Wang, W. W., Finlay, G. A., and Fanburg, B. L. (1999). Serotonin stimulates mitogen-activated protein kinase activity through the formation of superoxide anion. *Am. J. Physiol.* 277, L282–L291. doi: 10.1152/ajplung.1999.277.2.L282

Leitao, B. B., Jones, M. C., and Brosens, J. J. (2011). .The sumo e3-ligase pias1 couples reactive oxygen species-dependent JNK activation to oxidative cell death. *FASEB J.* 25, 3416–3425. doi: 10.1096/fj.11-186346

Liu, Y., Wei, L., Laskin, D. L., and Fanburg, B. L. (2011). Role of protein transamidation in serotonin-induced proliferation and migration of pulmonary artery smooth muscle cells. *Am. J. Respir. Cell Mol. Biol.* 44, 548–555. doi: 10.1165/rcmb.2010-0078OC

Liu, J., Wang, W., Wang, L., Chen, S., Tian, B., Huang, K., et al. (2018). IL-33 initiates vascular remodelling in hypoxic pulmonary hypertension by up-regulating HIF-1alpha and VEGF expression in vascular endothelial cells. *EBioMedicine* 33, 196–210. doi: 10.1016/j.ebiom.2018.06.003

Lu, W., Wang, J., Shimoda, L. A., and Sylvester, J. T. (2008). Differences in STIM1 and TRPC expression in proximal and distal pulmonary arterial smooth muscle are associated with differences in Ca2+ responses to hypoxia. *Am. J. Physiol. Lung Cell. Mol. Physiol.* 295, L104–L113.

Luo, W., Grupp, I. L., Harrer, J., Ponniah, S., Grupp, G., Duffy, J. J., et al. (1994). Targeted ablation of the phospholamban gene is associated with markedly enhanced myocardial contractility and loss of beta-agonist stimulation. *Circ. Res.* 75, 401–409. doi: 10.1161/01.res.75.3.401

Müller, M. S., Fox, R., Schousboe, A., Waagepetersen, H. S., and Bak, L. K. (2014). Astrocyte glycogenolysis is triggered by store-operated calcium entry and provides metabolic energy for cellular calcium homeostasis. *Glia* 62, 526–534. doi: 10.1002/glia.22623

Maclean, M. R., and Dempsie, Y. (2010). The serotonin hypothesis of pulmonary hypertension revisited. *Adv. Exp. Med. Biol.* 661, 309–322. doi: 10.1007/978-1-60761-500-2_20

Nelson, B. R., Makarewich, C. A., Anderson, D. M., Winders, B. R., Troupes, C. D., Wu, F., et al. (2016). A peptide encoded by a transcript annotated as long noncoding RNA enhances SERCA activity in muscle. *Science* 351, 271–275. doi: 10.1126/science.aad4076

Nurminskaya, M. V., and Belkin, A. M. (2012). Cellular functions of tissue transglutaminase. *Int. Rev. Cell Mol. Biol.* 294, 1–97. doi: 10.1016/B978-0-12-394305-7.00001-X

Occhiogrosso, M., Omran, S. S., and Altemus, M. (2012). Persistent pulmonary hypertension of the newborn and selective serotonin reuptake inhibitors.

lessons from clinical and translational studies. *Am. J. Psychiatry* 169, 134–140. doi: 10.1176/appi.ajp.2011.11040553

Pandey, D., Chen, F., Patel, A., Wang, C. Y., Dimitropoulou, C., and Patel, V. S. (2011). Sumo1 negatively regulates reactive oxygen species production from nadph oxidases. Arterioscler Thromb. Vasc. *Biol* 31, 1634–1642. doi: 10.1161/ATVBAHA.111.226621

Peng, G., Lu, W., Li, X., Chen, Y., Zhong, N., Ran, P., et al. (2010). Expression of store-operated Ca2+ entry and transient receptor potential canonical and vanilloid-related proteins in rat distal pulmonary venous smooth muscle. *Am. J. Physiol. Lung Cell Mol. Physiol.* 2995, L621–L630. doi: 10.1152/ajplung.00176.2009

Peng, G., Li, S., Hong, W., Hu, J., Jiang, Y., Hu, G., et al. (2015). Chronic hypoxia increases intracellular Ca(2+) concentration *via* enhanced Ca(2+) entry through receptor-operated Ca(2+) channels in pulmonary venous smooth muscle cells. *Circ. J.* 79, 2058–2068. doi: 10.1253/circj.CJ-15-0067

Penumatsa, K. C., and Fanburg, B. L. (2014). Transglutaminase 2-mediated serotonylation in pulmonary hypertension. *Am. J. Physiol. Lung Cell Mol. Physiol.* 306, L309–L315. doi: 10.1152/ajplung.00321.2013

Penumatsa, K., Abualkhair, S., Wei, L., Warburton, R., Preston, I., Hill, N. S., et al. (2014a). Tissue transglutaminase promotes serotonin-induced AKT signaling and mitogenesis in pulmonary vascular smooth muscle cells. *Cell Signal.* 26, 2818–2825. doi: 10.1016/j.cellsig.2014.09.002

Penumatsa, K. C., Toksoz, D., Warburton, R. R., Hilmer, A. J., Liu, T., Khosla, C., et al. (2014b). Role of hypoxia-induced transglutaminase 2 in pulmonary artery smooth muscle cell proliferation. *Am. J. Physiol. Lung Cell Mol. Physiol.* 307, L576–L585.

Raj, J. U., and Chen, P. (1986). Micropuncture measurement of microvascular pressures in isolated lamb lungs during hypoxia. *Circ. Res.* 59, 398–404. doi: 10.1161/01.res.59.4.398

Raj, J. U., Hillyard, R., Kaapa, P., Gropper, M., and Anderson, J. (1990). Pulmonary arterial and venous constriction during hypoxia in 3- to 5-wk-old and adult ferrets. *J. Appl. Physiol.* (1985). 69, 2183–2189. doi: 10.1152/jappl.1990.69.6.2183

Raj, J. U., Toga, H., and Ibe, B. O. (1992). Effects of endothelin, platelet activating factor and thromboxane A2 in ferret lungs. *Respir. Physiol.* 88, 129–140. doi: 10.1016/0034-5687(92)90034-t

Rigato, F., Garwood, J., Calco, V., Heck, N., Faivre-Sarrailh, C., and Faissner, A. (2002). Tenascin-C promotes neurite outgrowth of embryonic hippocampal neurons through the alternatively spliced fibronectin type III BD domains *via* activation of the cell adhesion molecule F3/contactin. *J. Neurosci.* 22, 6596–6609. doi: 10.1523/JNEUROSCI.22-15-06596.2002

Sahin, U., Ferhi, O., Jeanne, M., Benhenda, S., Berthier, C., and Jollivet, F. (2014). Oxidative stress-induced assembly of PML nuclear bodies controls sumoylation of partner proteins. *J. Cell Biol.* 204, 931–945. doi: 10.1083/jcb.201305148

Sahoo, S. K., Shaikh, S. A., Sopariwala, D. H., Bal, N. C., Bruhn, D. S., Kopec, W., et al. (2015). The N terminus of sarcolipin plays an important role in uncoupling sarco-endoplasmic Reticulum Ca2+-ATPase (SERCA) ATP Hydrolysis from Ca2+ Transport. *J. Biol. Chem.* 290, 14057–14067. doi: 10.1074/jbc.M115.636738

Shishido, T., Woo, C. H., Ding, B., McClain, C., Molina, C. A., Yan, C., et al. (2008). Effects of MEK5/ERK5 association on small ubiquitin-related modification of ERK5: implications for diabetic ventricular dysfunction after myocardial infarction. *Circ. Res.* 102, 1416–1425. doi: 10.1161/CIRCRESAHA.107.168138

Shrivastava, V., Marmor, H., Chernyak, S., Goldstein, M., Feliciano, M., Vigodner, M., et al. (2014). Cigarette smoke affects posttranslational modifications and inhibits capacitation-induced changes in human sperm proteins. *Reprod. Toxicol.* 43, 125–129. doi: 10.1016/j.reprotox.2013.12.001

Thomas, M., Ciuclan, L., Hussey, M. J., and Press, N. J. (2013). Targeting the serotonin pathway for the treatment of pulmonary arterial hypertension. *Pharmacol. Ther.* 138, 409–417. doi: 10.1016/j.pharmthera.2013.02.002

Tong, X., Hou, X., Jourd'Heuil, D., Weisbrod, R. M., and Cohen, R. A. (2010). Upregulation of Nox4 by TGF{beta}1 oxidizes SERCA and inhibits NO in arterial smooth muscle of the prediabetic Zucker rat. *Circ. Res.* 107, 975–983. doi: 10.1161/CIRCRESAHA.110.221242

Vangheluwe, P., Raeymaekers, L., Dode, L., and Wuytack, F. (2005). Modulating sarco(endo)plasmic reticulum Ca2+ ATPase 2 (SERCA2) activity: cell biological implications. *Cell Calcium.* 38, 291–302. doi: 10.1016/j.ceca.2005.06.033

Walther, D. J., Peter, J. U., Winter, S., Holtje, M., Paulmann, N., Grohmann, M., et al. (2003). Serotonylation of small GTPases is a signal transduction pathway that triggers platelet alpha-granule release. *Cell* 115, 851–862. doi: 10.1016/s0092-8674(03)01014-6

Wang, Q., Wang, D., Yan, G., Qiao, Y., Sun, L., Zhu, B., et al. (2016). SERCA2a was serotonylated and may regulate sino-atrial node pacemaker activity. *Biochem. Biophys. Res. Commun.* 480, 492–497. doi: 10.1016/j.bbrc.2016.10.082

Watts, S. W., Priestley, J. R., and Thompson, J. M. (2009). Serotonylation of vascular proteins important to contraction. *PloS One* 4, e5682. doi: 10.1371/journal.pone.0005682

Weisel, F. C., Kloepping, C., Pichl, A., Sydykov, A., Kojonazarov, B., Wilhelm, J., et al. (2014). Impact of S-adenosylmethionine decarboxylase 1 on pulmonary vascular remodeling. *CIRCULATION* 129, 1510–1523. doi: 10.1161/CIRCULATIONAHA.113.006402

Welsh, D. J., Harnett, M., MacLean, M., and Peacock, A. J. (2004). Proliferation and signaling in fibroblasts: role of 5-hydroxytryptamine2A receptor and transporter. *Am. J. Respir. Crit. Care Med.* 170, 252–259. doi: 10.1164/rccm.200302-264OC

Wu, L., Tan, J. L., Wang, Z. H., Chen, Y. X., Gao, L., Liu, J. L., et al. (2015). ROS generated during early reperfusion contribute to intermittent hypobaric hypoxia-afforded cardioprotection against postischemia-induced Ca(2+) overload and contractile dysfunction *via the* JAK2/STAT3 pathway. *J. Mol. Cell Cardiol.* 81, 150–161. doi: 10.1016/j.yjmcc.2015.02.015

Xia, Y., Yang, X. R., Fu, Z., Paudel, O., Abramowitz, J., Birnbaumer, L., et al. (2014). Classical transient receptor potential 1 and 6 contribute to hypoxic pulmonary hypertension through differential regulation of pulmonary vascular functions. *Hypertension* 63, 173–180.

Xu, L., Chen, Y., Yang, K., Wang, Y., Tian, L., Zhang, J., et al. (2014). Chronic hypoxia increases TRPC6 expression and basal intracellular Ca2+ concentration in rat distal pulmonary venous smooth muscle. *PloS One* 9, e112007. doi: 10.1371/journal.pone.0112007

Yao, J., Shao, X. H., Song, G. Y., Zhao, Z. Y., Teng, S. Y., and Wu, Y. J. (2015). The expression of Ubc9 and the intensity of SERCA2a-SUMOylation were reduced in diet-induced obese rats and partially restored by trimetazidine. *J. Cardiovasc. Pharmacol.* 65, 47–53. doi: 10.1097/FJC.0000000000000162

Yu, C., Tang, W., Wang, Y., Shen, Q., Wang, B., Cai, C., et al. (2016). Downregulation of ACE2/Ang-(1-7)/Mas axis promotes breast cancer metastasis by enhancing store-operated calcium entry. *Cancer Lett.* 376, 268–277. doi: 10.1016/j.canlet.2016.04.006

Yuan, J. P., Kim, M. S., Zeng, W., Shin, D. M., Huang, G., Worley, P. F., et al. (2009). TRPC channels as STIM1-regulated SOCs. *Channels (Austin.)* 3, 221–225. doi: 10.4161/chan.3.4.9198

Zhao, Y., Packer, C. S., and Rhoades, R. A. (1993). Pulmonary vein contracts in response to hypoxia. *Am. J. Physiol.* 265, L87–L92. doi: 10.1152/ajplung.1993.265.1.L87

Zhu, Z. D., Yu, T., Liu, H. J., Jin, J., and He, J. (2018). SOCE induced calcium overload regulates autophagy in acute pancreatitis *via* calcineurin activation. *Cell Death Dis.* 9, 50. doi: 10.1038/s41419-017-0073-9

Conflict of Interest: The authors declare that the research was conducted in the absence of any commercial or financial relationships that could be construed as a potential conflict of interest.

frontiers in Pharmacology

MINI REVIEW
published: 03 March 2020
doi: 10.3389/fphar.2020.00210

Current Status of Septic Cardiomyopathy: Basic Science and Clinical Progress

Huan Lin[1], Wenting Wang[1], Madeline Lee[2], Qinghe Meng[3] and Hongsheng Ren[1]**

[1] Department of Intensive Care Unit, Shandong Provincial Hospital Affiliated to Shandong University, Jinan, China, [2] Dartmouth College, Hanover, NH, United States, [3] Department of Surgery, SUNY Upstate Medical University, Syracuse, NY, United States

Septic cardiomyopathy (SCM) is a complication that is sepsis-associated cardiovascular failure. In the last few decades, there is progress in diagnosis and treatment despite the lack of consistent diagnostic criteria. According to current studies, several hypotheses about pathogenic mechanisms have been revealed to elucidate the pathophysiological characteristics of SCM. The objective of this manuscript is to review literature from the past 5 years to provide an overview of current knowledge on pathogenesis, diagnosis and treatment in SCM.

Keywords: sepsis, heart failure, septic cardiomyopathy, pathogenesis, treatment, diagnosis, left ventricular ejection fraction

OPEN ACCESS

Edited by:
Owen Llewellyn Woodman, Monash University, Australia

Reviewed by:
Satish Ramalingam, SRM Institute of Science and Technology, India
Chuanfu Li, East Tennessee State University, United States

****Correspondence:***
Qinghe Meng
mengq@upstate.edu
Hongsheng Ren
hongsheng-ren@163.com

Specialty section:
This article was submitted to Inflammation Pharmacology, a section of the journal Frontiers in Pharmacology

Received: *21 August 2019*
Accepted: *14 February 2020*
Published: *03 March 2020*

Citation:
Lin H, Wang W, Lee M, Meng Q and Ren H (2020) Current Status of Septic Cardiomyopathy: Basic Science and Clinical Progress. Front. Pharmacol. 11:210. doi: 10.3389/fphar.2020.00210

INTRODUCTION

Sepsis is defined as a life-threatening organ dysfunction due to a dysregulated immune response to an infection (Singer et al., 2016) and has become one of the top ten leading causes of death in developed and developing countries (Hawiger, 2018), with a mortality rate as high as 30% (Morin et al., 2015). Septic shock is defined as hypotension with lactic acid >2 mmol/L after adequate fluid resuscitation (Singer et al., 2016) and its death rate can be as high as 50% (Lu et al., 2019). First described over 40 years ago, septic cardiomyopathy (SCM) is an acute cardiac disorder caused by sepsis (Beesley et al., 2018), which is reversible and can be restored at an early stage of sepsis (Lu et al., 2019). The reported incidence of SCM in patients with sepsis or septic shock is inconsistent, ranging from 13.8 to 40% due to lack of large-scale studies and uniform diagnostic criteria (Li et al., 2019; Lu et al., 2019). In patients with sepsis combined with SCM, the mortality is increased 2–3 times, up to 70–90% (Ehrman et al., 2018; Fan and Zhang, 2018; Li et al., 2019). Epidemiological studies have shown that male, younger age, higher lactate level and previous history of heart failure/coronary heart disease as well as lactic acid level (>4.0 mmol/L) when admitted to ICU are associated with SCM (Sato et al., 2016; Li et al., 2019). Other evidences have shown that acute physiology and chronic health evaluation system II score (Caser et al., 2014) and the application of catecholamine were positively correlated with occurrence of SCM (Wang and Li, 2015).

The myocardial depressant factors (MDFs) have been proposed since the 1950s (Lefer, 1982; Fan and Zhang, 2018), referring to active substances that suppress the action of the heart. Currently, recognized MDFs include cytokines, the complement system, nitric oxide (NO), lipopolysaccharides (LPS) etc. Cytokines include tumor necrosis factor-α (TNF-α), interleukin-1β (IL-1β), interleukin-6 (IL-6), and high mobility protein box 1 (HMGB1) (Beesley et al., 2018; Lu et al., 2019). Moreover, the activations of Toll like receptors (TLRs) and nuclear factor kappa B (NF-κB) contribute to pathogenesis of SCM (Martin et al., 2019). In general, SCM is defined as the decrease

in left ventricular ejection fraction (LVEF) and ventricular dilatation during sepsis (Beesley et al., 2018). Clinically, in addition to proper management of infection and sepsis control, maintenance of hemodynamic stability is the first step for patients with SCM. The currently recommended treatment strategy is symptomatic, and there is no specific treatment in septic patients with SCM.

Some progress has been made in understanding the pathogenesis of SCM. In recent years, there are excellent review articles regarding the pathophysiology of cardiomyopathy, present review focuses on the current the evidence on pathogenic mechanism of SCM and the potential of diagnoses and treatments for SCM.

PATHOGENESIS

Presently, the pathogenesis of SCM is still in its exploration stage. The role of inflammatory cytokines in the pathogenesis of sepsis was identified. But all antibodies based on specific pro-inflammatory cytokines as targets have failed in clinical trials (Kumar, 2019). This indicates that some others factors are involved in the pathogenesis of SCM like mitochondrial dysfunction and exosomes in cardiac myocytes, suggesting that SCM is caused by many contributing factors. We will highlight recent discoveries of pathogenic mechanisms that are associated with SCM.

The Complement System

Sepsis can lead to the activation of the complement system, resulting in increasing the amount of complement component 5 (C5a). C5a reacts with its receptor, leading to cytokine storm, lymphocyte apoptosis, neutrophilic innate immune function loss, cardiomyopathy, disseminated intravascular coagulation, etc. Meanwhile, C5a also affects intracellular calcium homeostasis (Fattahi et al., 2018a; Ward and Fattahi, 2019). SCM is associated with decreased levels of three key enzymes (serca2, NCX, and Na+/K+-atpase) in cardiomyocytes, which are complement receptor-dependent (Fattahi et al., 2018a). Some studies have suggested that histones may be a target for reducing cardiac dysfunction in sepsis. Interestingly, the investigation of mechanism has found that extracellular histones appearing in sepsis plasma require C5a receptors (Kalbitz et al., 2015). A study evaluated the cardiac function and contractility of cardiomyocytes in rats with cecal ligation and puncture (CLP). The left ventricular pressure decreased significantly. These defects were prevented in CLP rats by blocking antibody against C5a. After the addition of recombinant rat C5a, both sham and CLP myocardial cells showed significant systolic dysfunction. These data indicates that CLP induces the generation of C5a receptor by cardiomyocytes, and the production of C5a leads to the interaction of C5a-C5a receptor, leading to the dysfunction of cardiomyocytes, then resulting in the impairment of cardiac function, suggesting interventions directly targeted at C5a interception or C5a receptor blockade may be a new and promising treatment for patients with SCM (Niederbichler et al., 2006). A study from Keshari et al. has shown that inhibition of C5 protects organ failure and reduces mortality in baboon model of sepsis via decreasing plasma LPS concentration and inhibiting the production of inflammatory cytokines. In addition, C5 inhibitor attenuated sepsis-increased soluble uPAR, thrombomodulin and angiopoietin-2 in plasma, suggesting that C5 inhibition may also protect against endothelial cell dysfunction (Keshari et al., 2017). Another study using Soliris (Eculizumab), an FDA-approved C5 inhibitor, for the treatment of paroxysmal nocturnal hemoglobinuria (PNH) has shown that Eculizumab application in a septic child rescued the sepsis-induced multiorgan failure, including cardiac dysfunction (Galic et al., 2019). All the above studies indicate that C5 is closely related to the occurrence of SCM, and suggesting that a C5 inhibitor may be a promising treatment for patients with SCM.

Mitochondrial Dysfunction in Cardiac Myocytes

Cardiomyocytes have a high mitochondrial density, which allows them to produce adenosine triphosphate (ATP) quickly. ATP provides the energy for both energy-consuming endergonic reactions and energy-releasing exergonic reactions. Mitochondrial dysfunction can seriously affect heart function in sepsis. Mitochondrial damage occurs in SCM, mainly manifested as morphological and functional changes, including interrupted oxidative phosphorylation, impaired mitochondrial respiration rate, free radical production of mitochondria, decreased mitochondrial membrane potential, attenuated autophagy, and apoptosis (Tan Y. et al., 2019). Takasu et al. (2013) conducted autopsies on 17 patients who died of sepsis and have found that six of them had mitochondrial micro-structural damage including mitochondrial swelling, ridge loss, as well as rupture of inner and outer membrane. They have demonstrated that the integrity of the mitochondrial micro-structure is necessary to ensure that mitochondria produces enough energy. When the micro-structure is damaged, mitochondria becomes dysfunctional. Durand et al. (2017) have discussed mitochondrial oxidative phosphorylation disorder in SCM, and pointed out that reactive oxygen species (ROS) and other substances, such as cytochrome C produced in mitochondria, were considered as a signal related to apoptosis. BAP31, a B cell receptor-related protein, may affect mitochondrial homeostasis and endoplasmic reticulum function. The transcription of BAP31 was inhibited in LPS-treated cardiomyocytes. While melatonin could up-regulate the expression of BAP31, this effect depends on the MAPK-ERK pathway. Inhibition of the ERK pathway and/or inhibition of BAP31 could diminish the beneficial effects of melatonin on mitochondrial function and endoplasmic reticulum homeostasis under LPS stress, suggesting that ERK-BAP31 pathway can be a regulator of mitochondrial function and endoplasmic reticulum homeostasis (Zhang et al., 2019). Yes- related protein (Yap), a transcriptional activator in the Hippo signaling, plays an important role in mitochondrial function, especially mitochondrial fission function, which is associated with a variety of cardiovascular diseases. In a mouse model of SCM, LPS down-regulated the expression of Yap, while Yap overexpression can maintain cardiac function and reduce myocardial cell death

via regulating mitochondrial fission (Yu et al., 2019). Chen et al. (2019a) found that the myocardial cells in septic mice were significantly overexpression of long non-coding RNA (LncRNA) SOX2 overlapping transcript (SOX2OT), suggesting that SOX2OT contributed to mitochondrial dysfunction in SCM. Receptor-interacting protein kinase3 (Ripk3) may regulate signaling pathways that are related to mitochondrial injury, endoplasmic reticulum stress, and cell scaffold balance. Zhong et al. (2019) found that Ripk3 expression was increased in LPS-infected cardiomyocytes. Mitochondrial autophagy plays an integral role in cardiac dysfunction. A study has shown that Beclin-1, an autophagy protein, modulates inflammation and improves cardiac function in the LPS-induced animal sepsis (Sun et al., 2018).

In summary, the findings from experimental animal models have shown that changes in mitochondrial morphology and function are involved in the pathogenesis of SCM. Understanding molecular mechanisms of mitochondrial injury may provide evidence for developing new therapeutic targets for SCM.

Toll-Like Receptors in Cardiomyocytes

Toll-like receptors (TLRs), a trans-membrane glycoprotein on the surface of the cell membrane, is an important part of the immune system that can identify different pathogen associated molecular patterns (PAMPs). The stimulation of TLRs by PAMPs causes the nuclear translocation of nuclear factor kappa B (NF-κB), and then leads to the expression of inflammatory mediators, such as TNF-α and interleukins (ILs) (Dalton and Shahul, 2018). Signaling regulated by TLRs is classified MyD88-dependent and MyD88-independent pathways. TLRs form homodimers, and one or more adaptor proteins such as MyD88, MAL/TIRAP, TRIF or TRAM, which are then recruited into the cytoplasm after the binding of TLRs to their respective ligands. MyD88 dependent pathway is utilized by most TLRs except TLR3 (Feng and Chao, 2011). In MyD88-dependent pathway, MyD88 binds IRAK4, IRAK1, and/or IRAK2, and promotes their binding to TRAF6, then leads to the activation of TAK1 by TRAF6. After a series of activations/reactions, this eventually leads to nuclear translocation of NF-κB, which activates the expression of various inflammatory genes (called gene storms), causing host dysfunction and multiple organ dysfunction (Hawiger, 2018). In MyD88 independent pathways, such as Trif-dependent pathways, Trif interacts with TRAF3 to activate TBK1 and IKKi, and then cause the phosphorylation of IRF3. Phosphitylated IRF3 is transferred into the nucleus to activate type I IFN and IFN-induced gene transcription. Myocardial cells express TLR2, TLR3, TLR4, and TLR9 (Vallejo, 2011). A study by Fattahi et al. (2018b) has shown that LVEF was increased and plasma pro-inflammatory cytokines (TNF-α, IL-1, IL-6) were decreased significantly in a mouse septic model with TLR9 and TLR3 deletion, suggesting that TLR9 and TLR3 activation is associated with dysfunction of heart in sepsis. TLR4 can bind to LPS, and then cause the release of a variety of inflammatory factors, finally insults in cardiac dysfunction (Vallejo, 2011). TLR4 regulates oxidative stress in ryanodine receptor 2 (RyR2), leading to increased Ca^{2+} leakage in the sarcoplasmic reticulum (SR) of cardiac myocytes (Yang et al., 2018). Chen et al. (2019b) analyzed gene expression in septic patients compared with control, showing that TNF-α, JAK and transcriptional activation (STAT) signaling pathways were up-regulated. Cirulis et al. (2019) provided the evidence for the role of interferon signaling in SCM using a human study. The linkage between activations of TLRs/its downstream signals and SCM has been established from current investigations. Inhibition of TLR4 has shown protective effect on SCM in experimental animal models (Fenhammar et al., 2014; Yang et al., 2018). Based on those findings, targeting TLRs to develop new therapeutic approaches is promising.

Nitric Oxide and Nitric Oxide Synthase in Cardiac Myocytes

Nitric oxide is synthesized by the oxidation of L-arginine by nitric oxide synthase (NOS) expressed in cardiac myocytes. NOS can be divided into three subtypes, namely neuronal nitric oxide synthase (nNOS), inducible nitric oxide synthase (iNOS), and endothelial nitric oxide synthase (eNOS) (Martin et al., 2019). The only small amount of NO produced by nNOS and eNOS are noted in physiological state, but NO produced by eNOS plays a protective role in vascular endothelium and vascular function (Mingjie and Zheng, 2018). iNOS are not responsible for producing NO in normal physiological state. However, iNOS will produce a large amount of NO when an inflammatory response occurs (Martin et al., 2019). In humans, neutrophils also express iNOS. Bacterial invasion leads to the activation of TLRs, which causes elevated inflammatory meditators (cytokines, chemokines etc.) that overstimulate neutrophils, then cause the expression of iNOS and subsequently increase the production of NO, finally result in up-regulation of G-protein-coupled receptor kinase 2 (GRK2), down-regulation of CXC chemokine receptor 2 (CXCR2), shedding of L-selectin, decrease in adhesion molecules, and influence of neutrophil chemotaxis (Spiller et al., 2019). A number of experiments have confirmed that the production of NO by iNOS can impair heart function, such as down-regulating adrenaline receptors, decrease sensitivity of myocardium to Ca^{2+} and also damage to mitochondria, etc. (Martin et al., 2019). We have discussed the role of mitochondrial dysfunction in cardiac myocytes in SCM previously. A study has shown that melatonin (an iNOS inhibitor) prevents the destruction of mitochondrial homeostasis after sepsis, restores ATP production and improves the survival rate of sepsis (Cimolai et al., 2015). This evidence supports the hypothesis that mitochondrial homeostasis and increased NO play a role in the pathogenesis of SCM.

Nicotinic Acetylcholine Receptor α7 Subunit

Alpha 7 nicotinic acetylcholine receptor (α7nAchR) is widely expressed in the cytokine-producing immune cells such as macrophages, dendritic cells and T cells (Souza et al., 2019). α7nAchR is an important element of the cholinergic anti-inflammatory pathway (CAP). Acetylcholine (Ach), a neurotransmitter released by stimulation of vagus nerve, binds to α7nAchR on cell surface and inhibits the degradation of NF-κB inhibitory proteins through a series of intracellular signals, preventing its separation from NF-κB, thereby inhibiting

the translocation of NF-κB and reducing the release of pro-inflammatory cytokines (Chao et al., 2015). The evidences from some studies have shown that the expression of α7nAchR in LPS-induced septic mouse model is significantly decreased compared with control group (Kong et al., 2017). At the same time, dexmedetomidine can reduce the expressions of apoptotic proteins, IL-6, IL-1, and TNF-α through α7nAchR activation, thus protecting the myocardium in septic mice. GTS-21, a synthetic selective stimulant of α7nAchR, has been shown to reduce myocardial injury via modulating inflammation (decreases in IL-6, IL-1β, TNF-α and activation of NF-κB P65) and apoptosis in LPS-induced sepsis in mice (Kong et al., 2018). Although there are a few studies on the activation of CAP in this area, the beneficial role of CAP activation in SCM will be emphasized in the future because α7nAchR is an essential mechanism for the CAP which has revealed potent immunomodulatory properties in various diseases including SCM.

The Effects of Exosomes on Cardiac Function in Sepsis

Exosomes are small cell-derived vesicles originate from leukocytes, platelets and dendritic cells, etc. (Monteiro et al., 2017). Exosomes are a double-edged sword that can protect and cause SCM. The roles of exosomes in SCM is mainly considered from two mechanisms that are exosomal nicotinamide adenine dinucleotide phosphate (NADPH) and microRNA-223 (Monteiro et al., 2017). A study has shown that exosomes can induce vascular apoptosis and myocardial dysfunction by the mechanisms that are related to inflammation and oxidative stress (Real et al., 2018). In patients with sepsis, increased platelet-derived exosomes containing NADPH oxidase subunits similar to phagocytes in blood can help to produce ROS. Therefore, inhibiting the secretion of platelet exosomes would be beneficial for patients with sepsis. A study used GW4869 (a neutral sphingomyelinase inhibitor for blocking exosome generation) to investigate the effects of blockade of exosome release on the production of inflammatory cytokines and sepsis-induced myocardial dysfunction, suggesting that GW4869 deceased production of pro-inflammatory cytokines *in vitro* and inflammatory response *in vivo* via the inhibition of exosome generation. In addition, the attenuation of cardiac dysfunction and improvement of survival are noted in septic mice (Essandoh et al., 2015). Also, another component from exosomes, iNOS, can produce NO that is related to myocardial dysfunction in sepsis (Monteiro et al., 2017; Spiller et al., 2019). **Figure 1** is the Illustration of the roles platelet-derived exosomes in SCM. On the contrary, MiRNAs are non-coding segments of RNA, which regulate the transcription of specific proteins. Studies have shown that miR-223 is down-regulated in patients who died of sepsis. miR-223 can inhibit the expression of endothelial cell adhesion molecule (ICAM-1) and negatively regulates transcription activator 3 (STAT3). Studies have shown that miR-223 found in exosomes and derived from mesenchymal stem cells (MSC) has a protective effect on cardiac function (Monteiro et al., 2017; Ge, 2019). Less amounts of miR-223 from MSC-derived exosomes are observed in blood in patients with septic shock, suggesting an impact of exosomes on cardiac dysfunction and mortality (Monteiro et al., 2017). Despite the inconsistencies regarding the role of exosomes in SCM, the association between SCM and exosomes has been established from current studies.

Imbalance of Calcium Homeostasis in Cardiac Myocytes

In sepsis, decrease in density of L-type calcium channels and down-regulated sensitivity to calcium in myocardia myofilaments lead to decreased intracellular free calcium concentration and imbalance of calcium homeostasis, which eventually leads to decreased calcium-binding troponin and contractility (Dalton and Shahul, 2018). High mobility group box (HMGB) protein increases intracellular ROS level by interacting with TLR4, thereby increasing oxidative stress and phosphorylation of ryanodine receptor in cardiac myocytes. Meanwhile, increased ROS can enhance Ca^{2+}-mediated Ca^{2+} leakage in SR, Ca^{2+} depletion from SR, and damage in myocardial excitation-contraction coupling (Kakihana et al., 2016). A study has shown beneficial effect of TLR4 inhibitor (TAK-242) through preventing SR Ca^{2+} leak in septic mice. Coincidentally, TLR4 deficiency significantly improved cardiac function and corrected abnormal Ca^{2+} handling in septic mice (Yang et al., 2018), which indicate that the critical role of TLR4-dependent SR Ca^{2+} leak in the development of SCM.

The pathogenesis of SCM is extremely complex and our manuscript tends to discuss various mechanisms involved in SCM. Current studies indicate that the occurrence of SCM is the result of multiple factors including superantigen interaction with TLRs, then increase expressions of TNF-α and IL-1β that stimulate the immunocytes to produce other pro-inflammatory factors such as IL-6 as well as ROS. A large number of inflammatory cytokines and ROS can cause a series of direct damage to cardiovascular dysfunction, disequilibrium of calcium homeostasis, mitochondrial dysfunction, down regulated expression of β adrenaline receptor, and eventually lead to cardiac dysfunction (**Figure 2**).

DIAGNOSIS OF SEPTIC CARDIOMYOPATHY

Currently, there is no unified international definition for SCM. In the 1980s, SCM was defined as the decrease in left ventricular ejection fraction (LVEF) and ventricular dilatation during sepsis (Beesley et al., 2018). However, LVEF depends profoundly on loading conditions, it has been increasingly acknowledged to be an inaccurate marker of intrinsic cardiac function largely. Now, some groups define SCM as an acute cardiac dysfunction syndrome caused by sepsis, which has nothing to do with ischemia (Beesley et al., 2018). In addition, it has one or more of the following characteristics: (i) decreased ventricular contractility; (ii) left ventricular dilation under normal or low filling pressure; (iii) right ventricular dysfunction and/or left ventricular dysfunction with a reduced response to fluid infusion (Martin et al., 2019). Currently, the challenges of defining SCM

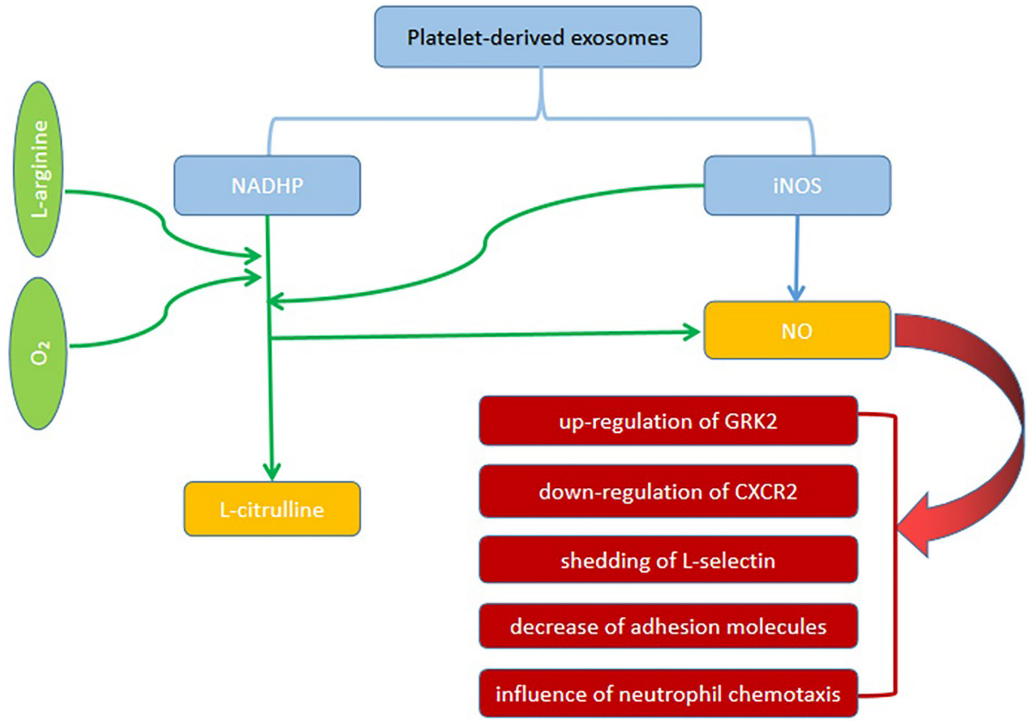

FIGURE 1 | The roles of platelet-derived exosomes in SCM. Platelet-derived exosomes contain NADPH oxidase subunits similar to phagocytes can produce NO. Also, another component from exosomes, iNOS, can produce NO that is related to myocardial dysfunction in sepsis. NO can cause the up-regulation of GRK2, down-regulation of CXCR2, shedding of L-selectin, decrease in adhesion molecules, and influence of neutrophil chemotaxis.

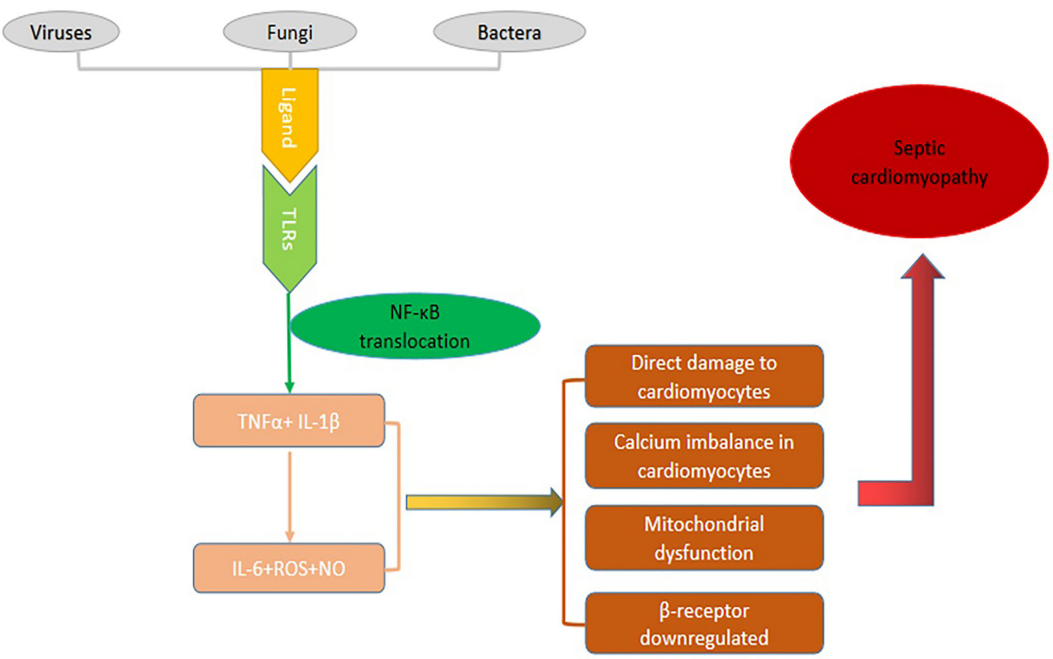

FIGURE 2 | The pathogenic mechanism of SCM. Specific components called ligands of viruses, bacteria or fungi bind to TLRs then go through a series of cascade reactions that cause NF-κB to be transcribed into the nucleus, causing the expression of inflammatory factor genes and producing a large number of inflammatory mediators. These inflammatory factors can cause a series of direct damage to cardiovascular dysfunction, disequilibrium of calcium homeostasis, mitochondrial dysfunction, down regulated expression of β adrenaline receptor, and eventually lead to cardiac dysfunction.

include: (i) how to evaluate cardiac function under the condition of high preload and postload; (ii) how to obtain longitudinal echocardiography data about cardiac function throughout the pathogenetic process (Sanfilippo et al., 2019).

To date, there is no gold diagnostic standard for SCM. Most clinical studies use LVEF < 50% as a diagnostic criteria (Ruian and Chen, 2018). Based on previous studies, diagnostic criteria of SCM should include two aspects: the presence of myocardial systolic and/or diastolic disorders, and the exclusion of other conditions leading to cardiac dysfunction. Here, with the exception of LVEF, we will discuss some other markers that may contribute to the diagnosis of SCM.

Indicators Used to Assess Cardiac Function

Echocardiogram: Echocardiography and doppler imaging can detect abnormalities in systolic and diastolic function of the heart in patients with severe sepsis or septic shock. There are three main indicators, namely myocardial performance index (MPI), mitral ring systolic displacement (MAPSE) and global longitudinal strain (GLS). MPI, also known as Tei index, is a parameter measured by echocardiography (Beesley et al., 2018). The formula for MPI is: MPI = (ventricular isometric systolic time + ventricular isometric diastolic time)/ejection time. Some studies have indicated that left ventricular MPI is positively correlated with BNP and cardiac Troponin I (cTnI), and negatively correlated with LVEF. In a study of 47 patients with sepsis, Nizamuddin et al. (2017) found that deterioration of MPI within 24 h of admission was associated with increased 90-day mortality. MAPSE is an indicator used to assess global and local systolic function of the left ventricle. A small sample prospective study by Havaldar (2018) showed that MAPSE could predict mortality from SCM. Recently, some studies on speckle tracking echocardiography (STE) are performed, which can monitor GLS that refers to the changes in the length of myocardium during the period of contraction and the end of diastole (Jiahui and Cai, 2018). A large amount of data shows that GLS is more helpful for the early recognition and diagnosis of SCM than LVEF reduction (defined as left ventricular systolic dysfunction) (Jiahui and Cai, 2018). Ehrman et al. (2019) proposed that GLS was the preferred method for studying the relationship between left ventricular systolic function and prognosis in the patients with SCM. However, no diagnostic criteria of GLS is available for SCM currently. Vasques-Novoa et al. (2019) also reported that myocardial edema detected by magnetic resonance imaging in three patients with SCM. Magnetic resonance may be a promising modality for the diagnosis of SCM. Although auxiliary instrumental examination is not specific for SCM, it is an adjunct to early detection of SCM in patients with sepsis.

Modified Shock Index (MSI) and Some Other Biological Markers

Modified shock index (MSI) refers to heart rate/mean arterial pressure, which can reflect both systolic and diastolic functions. Jayaprakash et al. (2018) conducted a retrospective study on 624 patients with severe sepsis or septic shock and concluded that the increase of MSI in the early stage (12 h) was correlated to the incidence of cardiac dysfunction, sequential organ failure assessment (SOFA) score and mortality. MSI was found to be promising predictors in febrile patients with sepsis. However, no single cut-off values of MSI was found to have an optimal accuracy for prediction of sepsis-related outcomes like SCM. Further studies are required to assess the incorporation of MSI in a multi-item scaling system for the prediction of SCM.

Some biological markers, such as B-type natriuretic peptide (BNP) and troponin I are elevated in patients with SCM, which have no diagnostic value specifically (Ruian and Chen, 2018). Chen et al. (2019b) analyzed the gene expressions from patients with SCM and proposed that CCL2, STAT3, MYC, and Serpine1 might be potential biomarkers or therapeutic targets for SCM. Although there is no conclusive evidence that these markers are associated with SCM, they may provide some clues for diagnosing SCM.

For the diagnosis of SCM, cardiac dysfunction caused by other diseases should be excluded. It is important to distinguish it from acute coronary syndrome. Coronary angiography and coronary computed tomography angiography (CCTA) can determine whether there is myocardial ischemia. But it is a risky examination for the patients with sepsis. Some studies have suggested using ultrasonic myocardial perfusion technology to examine myocardial perfusion abnormalities in the area of impaired myocardial wall in patients with sepsis. SCM and coronary syndromes can be distinguished by this method, but it is still invasive (Ruian and Chen, 2018). Also, other cardiomyopathies should be excluded, such as hypertrophic cardiomyopathy, dilated cardiomyopathy. These diseases usually have a long history and are slower to be developed.

TREATMENT

Due to the uncertainty of pathogenesis of SCM, no effective disease-modifying treatment is currently available. The strategies to deal with SCM is to control the primary disease to prevent the occurrence of secondary SCM. Specific treatment for SCM is still being developed. Currently some drugs and device-based therapy have been used clinically.

Clinical Treatment

Drug Therapy: Levosimendan, Natriuretic Peptide, Combination of Chinese and Western Medicine

Levosimendan is a calcium ion sensitizer, which can directly bind to troponin to increase myocardial contractility, but there is no significant change in heart rate and myocardial oxygen consumption. Studies have shown that levosimendan can effectively reduce the plasma lactic acid in sepsis and increase the myocardial contractility, but its application cannot reduce usage of norepinephrine and has no significant improvement in the mortality of SCM (Chang et al., 2018).

Natriuretic peptide, a recombinant human brain natriuretic peptide (rhBNP), can bind to human endogenous natriuretic peptide receptor. Natriuretic peptide not only can expand the arteries and veins, urinate and expel sodium to reduce the preload

and afterload of the heart, but also can inhibit renin-angiotensin-aldosterone system (RAAS) and sympathetic nervous system, which has been widely used clinically for treating heart failure via effectively relieving hemodynamic abnormalities and cardiac dysfunction. Shi et al. (2015) reported that a patient with SCM caused by intestinal obstruction and diffuse peritonitis was recovered using natriuretic peptide. Yin et al. (2016) conducted a prospective study to observe 42 patients with sepsis complicated with cardiac dysfunction, showing that natriuretic peptide significantly improved the heart rate, mean arterial pressure, BNP, acute physiology and chronic health evaluation (APACHE-II) score, peripheral vascular resistance index (SVRI) and extracellular pulmonary fluid index (ELWI).

Combination of Chinese and western medicine: Clinical studies have shown the application of anti-infection and organ support therapy (MOST) accompanied by traditional Chinese medicine (fu zheng jie du hua yu granules) can further reduce acute physiology and chronic health evaluation (APACHE-II) score and other indicators such as procalcitonin (PCT), BNP and cTnI, in patients with SCM (Haiyun et al., 2016). Animal experiments have also shown that tanshinone IIA, a member of the major lipophilic components extracted from the root of Salvia miltiorrhiza Bunge, has a protective effect on myocardial injury in septic rat model (Dekun et al., 2016). However, further investigations are needed to clarify its mechanism of beneficial effect in SCM.

Non-drug Therapy: ECMO, IABP, Blood Purification

ECMO

In septic patients complicated with SCM, extracorporeal membrane oxygenation (ECMO) is a feasible rescue strategy. Some approaches have been reported that application of anti-infection combined with ECMO has been used to treat the patient with SCM and septic shock caused by infection and hemorrhage of ileal diverticulum (Liu et al., 2017). Vogel et al. (2018) conducted retrospective analysis and concluded that the survival rate in patients with SCM could reach up to 75% after 4 days of veno-arterial-venous (VAV) ECMO treatment.

IABP

Intra-aortic balloon counter-pulsation (IABP) supports cardiac function by unloading contractions and enhancing relaxation. The former can lower systolic blood pressure and the latter can raise diastolic blood pressure. A retrospective study was performed among 38 cases with the application of IABP, suggesting that IABP is effective for the patients with cardiac shock by increasing mean arterial pressure and reducing dosage of catecholamine during the acute phase of sepsis. However, no improvement in long-term survival was observed (Takahashi et al., 2019). Kenshiro Wada also reported that a patient combined with chronic cardiac insufficiency was recovered using V-A ECMO and IABP (Wada et al., 2019).

Blood purification has long been used to treat sepsis. Recently, Andreja Sinkovic reported that a patient with lymphoma, splenectomy and autologous bone marrow transplant and receiving chemotherapy, and accompanying severe pneumococcal infections, septic shock, SCM and unacceptable drug therapy, was subjected to blood purification. The reductions in the level of IL-6, lactic acid deposition and the dosage of vascular vasopressors, improvement of left ventricular systolic function and clinical features were observed after treatment for 36 h (Sinkovic et al., 2018). CytoSorb is a non-temperature, sterile disposable endotoxin and cytokine sorbent that reduces circulating cytokines such as IL-1β, TNF-α, IL-6, etc. (Gruda et al., 2018; Ankawi et al., 2019). A retrospective study by Brouwer et al. (2019) showed that continuous renal replacement therapy (CRRT) combined with Cytosorb improved the 28-day survival rate for septic shock compared with CRRT alone. All those methods have been applied clinically. However, only a few cases have been reported. A large-scale randomized clinical trial and prospective study are needed to better understand and evaluate the value of these approaches to treat SCM.

Potential Treatments

Gene Therapy

Some studies suggested that the pathogenesis of sepsis is the damage of micro-vessels caused by "Genomic Storm"(Hawiger, 2018). Bacteria, fungi, infectious agents and viral nucleic acids bind to TLRs, causing the activation of stress response transcription factors (SRTFs), such as NF-κB, and activated protein 1 (AP-1), which in turn activate multiple genes encoding pro-inflammatory cytokines and chemokines, leading to septic shock and multiple organ dysfunction (Hawiger, 2018). Based on this observation, gene therapy for sepsis and SCM has been proposed. Studies have demonstrated that miR-21-3p inhibitors can improve cardiac dysfunction and mitochondrial ultrastructure damage caused by LPS, suggesting that miR-21-3p may be a potential target for SCM treatment (Wang et al., 2016). Zheng et al. (2017) proposed that miR-135a may serve as a therapeutic target in SCM because miR-135a can aggravate sepsis-induced inflammation and myocardial dysfunction possible via activation of p38 MAPK/NF-κB pathway. An et al. (2018) provided evidence that miR-146a can decrease pro-inflammatory cytokines and suppress apoptosis via inhibition of NF-κB activity by targeting TRAF6 and IRAK1. Cao et al. (2019) reported that miR-23b prevent NF-κB activation via inhibiting TRAF6 and IκκB, resulting in significant alleviation in cell injury induced by LPS as well as improvement in cell survival rate. We believe that gene therapy is the preferred method for SCM therapy in the future because it is targeted therapy with low side effects.

Mitochondrial Targeted Therapy

Structural and functional disorders of mitochondria affect the production of energy in cardiac myocytes, resulting in cardiac dysfunction. Maintaining the stability of mitochondrial structure and protecting its function have become the target of treating septic myocardium. Melatonin can restore the physiological functions of mitochondria and endoplasmic reticulum, maintain the stability of cytoskeleton, and thus improve cardiac function in septic mice (Zhang et al., 2019). The study on molecular mechanism has shown that melatonin attenuates the expression of BAP31 that interacts with mitochondria-localized proteins

and regulates mitochondrial function (Zhang et al., 2019; Zhong et al., 2019). Kokkinaki et al. (2019) showed that chemically synthesized diglucoside (LGM2605) can reduce the accumulation of cardiac ROS, protect mitochondrial function in heart, reverse myocardial injury, and improve the survival rate in a mouse model of sepsis.

Inhibition of Inflammatory Mediators

Independent growth factor I (GFI-I) can inhibit the expression of NF-κB and TNF-α, thus inhibiting LPS-induced inflammatory response and apoptosis of HPC2 cells (Zheng et al., 2017). 3,3′-Diindolylmethane (DIM) is a potential therapeutic drug with scavenging free radicals and antioxidant effects. Studies have shown that DIM can significantly inhibit the expression of IL-6 and TNF-α induced by LPS, suggesting that DIM may be a new perspective for treating SCM (Luo et al., 2018). Qiangxin 1 formula effectively inhibited the expression of IL-1β, TNF-α, thus protecting the cardiac function of sepsis (Xu et al., 2018). Tan's team demonstrated that hydrogen gas (H2) had a protective effect on cardiac insufficiency in LPS-induced sepsis in mice by blocking nuclear translocation of NF-κB (Tan S. et al., 2019). Supplementation of exogenous brain-derived neurotrophic factor (BDNF) can increase the level of BDNF in cardiac myocytes, improve cardiac dysfunction, reduce oxidative stress, and increase the survival rate in septic animals. Honda et al. found that the remote ischemic conditioner (RIC) could improve the ventricular function, cardiac output and survival rate in an LPS-induced septic mouse model (Honda et al., 2019). RIC may be a useful tool to improve the cardiomyopathy induced by sepsis clinically. Based on these observations, to reduce the level of inflammatory factors and regulate inflammatory signal are still the key for the treatment of SCM.

The treatments discussed in this section are only from animal experiments and have not been applied clinically. Whether or not the genetic response in animal models can mimic human inflammatory disease is controversial.

CONCLUSION

Septic cardiomyopathy, although it is reversible at early stage, has a high mortality rate because its pathogenesis is not well-understood. In terms of diagnosis and treatment, it is an important subject in clinical and basic research. Previous studies in this area have been limited by poor diagnostic strategies that only relied on LVEF reduction. In this review, we have not only discussed pathogenesis of SCM in detail, but also introduced some other approaches that are associated with the diagnosis of SCM. Early detection and intervention of SCM in patients with sepsis can reduce mortality. For example, MSI is considered as a "predictor" of SCM (Jayaprakash et al., 2018), and MAPSE can predict mortality in SCM (Havaldar, 2018). A large number of new studies are needed to improve the understanding pathogenesis of SCM. It is believed that in the near future, the pathogenesis of SCM can be clarified and specific targeted therapeutic drugs can be developed to reduce the mortality of SCM.

AUTHOR CONTRIBUTIONS

HL and WW conceived and wrote the manuscript. ML, QM, and HR revised the manuscript. All authors listed wrote the manuscript and approved for publication.

FUNDING

Shandong Provincial Research and Development Plan (item 2016 GSF 201052).

REFERENCES

An, R., Feng, J., Xi, C., Xu, J., and Sun, L. (2018). miR-146a attenuates sepsis-induced myocardial dysfunction by suppressing IRAK1 and TRAF6 via targeting ErbB4 expression. *Oxid. Med. Cell Longev.* 2018:7163057. doi: 10.1155/2018/7163057

Ankawi, G., Xie, Y., Yang, B., Xie, Y., Xie, P., and Ronco, C. (2019). What have we learned about the use of cytosorb adsorption columns? *Blood Purif.* 48, 196–202. doi: 10.1159/000500013

Beesley, S. J., Weber, G., Sarge, T., Nikravan, S., Grissom, C. K., Lanspa, M. J., et al. (2018). Septic cardiomyopathy. *Crit. Care Med.* 46, 625–634. doi: 10.1097/CCM.0000000000002851

Brouwer, W. P., Duran, S., Kuijper, M., and Ince, C. (2019). Hemoadsorption with CytoSorb shows a decreased observed versus expected 28-day all-cause mortality in ICU patients with septic shock: a propensity-score-weighted retrospective study. *Crit. Care* 23:317. doi: 10.1186/s13054-019-2588-1

Cao, C., Zhang, Y., Chai, Y., Wang, L., Yin, C., Shou, S., et al. (2019). Attenuation of sepsis-induced cardiomyopathy by regulation of MicroRNA-23b is mediated through targeting of MyD88-mediated NF-kappaB activation. *Inflammation* 42, 973–986. doi: 10.1007/s10753-019-00958-7

Caser, E. B., Zandonade, E., Pereira, E., Gama, A. M., and Barbas, C. S. (2014). Impact of distinct definitions of acute lung injury on its incidence and outcomes in Brazilian ICUs: prospective evaluation of 7,133 patients*. *Crit. Care Med.* 42, 574–582. doi: 10.1097/01.ccm.0000435676.68435.56

Chang, W., Xie, J. F., Xu, J. Y., and Yang, Y. (2018). Effect of levosimendan on mortality in severe sepsis and septic shock: a meta-analysis of randomised trials. *BMJ Open* 8:e019338. doi: 10.1136/bmjopen-2017-019338

Chao, R., Tong, Y., and Yao, Y. (2015). Research progress on the mechanism of cholinergic anti-inflammatory pathway disorder in severe sepsis. *Chin. J. Trauma* 31, 217–219.

Chen, M., Guan, Y., Li, A., Zhao, Y. Z., Zhang, L., Zhang, L., et al. (2019a). LncRNA SOX2OT mediates mitochondrial dysfunction in septic cardiomyopathy. *DNA Cell Biol.* 38, 1197–1206. doi: 10.1089/dna.2019.4839

Chen, M., Kong, C., Zheng, Z., and Li, Y. (2019b). Identification of biomarkers associated with septic cardiomyopathy based on bioinformatics analyses. *J. Comput. Biol.* 27, 69–80. doi: 10.1089/cmb.2019.0181

Cimolai, M. C., Alvarez, S., Bode, C., and Bugger, H. (2015). Mitochondrial mechanisms in septic cardiomyopathy. *Int. J. Mol. Sci.* 16, 17763–17778. doi: 10.3390/ijms160817763

Cirulis, M. M., Beesley, S. J., Wilson, E. L., Stubben, C., Olsen, T. D., Hirshberg, E. L., et al. (2019). The peripheral blood transcriptome in septic cardiomyopathy: an observational, pilot study. *Intensive Care Med. Exp.* 7:57. doi: 10.1186/s40635-019-0271-0

Dalton, A., and Shahul, S. (2018). Cardiac dysfunction in critical illness. *Curr. Opin. Anaesthesiol.* 31, 158–164. doi: 10.1097/ACO.0000000000000572

Dekun, W., Wei, H., and Peng, J. (2016). Influence and mechanism of tanshinone II A on the expression of HMGB–I and TNF-αof cardiomyocyte in rats with sepsis. *JETCM* 25, 1272–1284. doi: 10.3969/j.issn.1004-745x.2016.07.002

Durand, A., Duburcq, T., Dekeyser, T., Neviere, R., Howsam, M., Favory, R., et al. (2017). Involvement of mitochondrial disorders in septic cardiomyopathy. *Oxid. Med. Cell. Longev.* 2017:4076348. doi: 10.1155/2017/4076348

Ehrman, R. R., Moore, S. C., Favot, M. J., Akers, K. G., Gallien, J. Z., Welch, R. D., et al. (2019). Scientific letter to the editor: need for a definitive study of global longitudinal strain for prognostication in septic cardiomyopathy. *J. Am. Soc. Echocardiogr.* 32, 549.e3–552.e3. doi: 10.1016/j.echo.2018.12.005

Ehrman, R. R., Sullivan, A. N., Favot, M. J., Sherwin, R. L., Reynolds, C. A., Abidov, A., et al. (2018). Pathophysiology, echocardiographic evaluation, biomarker findings, and prognostic implications of septic cardiomyopathy: a review of the literature. *Crit. Care* 22:112. doi: 10.1186/s13054-018-2043-8

Essandoh, K., Yang, L., Wang, X., Huang, W., Qin, D., Hao, J., et al. (2015). Blockade of exosome generation with GW4869 dampens the sepsis-induced inflammation and cardiac dysfunction. *Biochim. Biophys. Acta* 1852, 2362–2371. doi: 10.1016/j.bbadis.2015.08.010

Fan, L., and Zhang, Q. (2018). Progress of pathogenesis in sepsis-induced cardiomyopathy. *Chin. Pediatr. Emerg. Med.* 25, 52–55, 60. doi: 10.3760/cma.j.issn.1673-4912.2018.01.013

Fattahi, F., Frydrych, L. M., Bian, G., Kalbitz, M., Herron, T. J., Malan, E. A., et al. (2018a). Role of complement C5a and histones in septic cardiomyopathy. *Mol. Immunol.* 102, 32–41. doi: 10.1016/j.molimm.2018.06.006

Fattahi, F., Russell, M. W., Malan, E. A., Parlett, M., Abe, E., Zetoune, F. S., et al. (2018b). Harmful roles of TLR3 and TLR9 in cardiac dysfunction developing during polymicrobial sepsis. *Biomed. Res. Int.* 2018:4302726. doi: 10.1155/2018/4302726

Feng, Y., and Chao, W. (2011). Toll-like receptors and myocardial inflammation. *Int. J. Inflamm.* 2011:170352. doi: 10.4061/2011/170352

Fenhammar, J., Rundgren, M., Hultenby, K., Forestier, J., Taavo, M., Kenne, E., et al. (2014). Renal effects of treatment with a TLR4 inhibitor in conscious septic sheep. *Crit. Care* 18:488. doi: 10.1186/s13054-014-0488-y

Galic, S., Csuka, D., Prohaszka, Z., Turudic, D., Dzepina, P., and Milosevic, D. (2019). A case report of a child with sepsis induced multiorgan failure and massive complement consumption treated with a short course of Eculizumab: a case of crosstalk between coagulation and complement? *Medicine* 98:e14105. doi: 10.1097/MD.0000000000014105

Ge, J. (2019). Research progress on the mechanism of exosomes in septic cardiomyopathy. *J. Electrocardiol. Circ.* 38, 157–159. doi: 10.12124/j.issn.2095-3933.2019.2.2019-3685

Gruda, M. C., Ruggeberg, K. G., O'Sullivan, P., Guliashvili, T., Scheirer, A. R., Golobish, T. D., et al. (2018). Broad adsorption of sepsis-related PAMP and DAMP molecules, mycotoxins, and cytokines from whole blood using CytoSorb(R) sorbent porous polymer beads. *PLoS One* 13:e0191676. doi: 10.1371/journal.pone.0191676

Haiyun, Z., Jianying, K., and Cao, S., (2016). CliIlical study of Fu zhengjie du Hua yugranuleon the treatment of septic cardiomyopathy. *Chin. J. TCM WM Crit. Care* 23, 245–247. doi: 10.3969/j.issn.1008-9691.2016.03.006

Havaldar, A. A. (2018). Evaluation of sepsis induced cardiac dysfunction as a predictor of mortality. *Cardiovasc. Ultrasound* 16:31. doi: 10.1186/s12947-018-0149-4

Hawiger, J. (2018). Heartfelt sepsis: microvascular injury due to genomic storm. *Kardiol. Pol.* 76, 1203–1216. doi: 10.5603/KP.a2018.0146

Honda, T., He, Q., Wang, F., and Redington, A. N. (2019). Acute and chronic remote ischemic conditioning attenuate septic cardiomyopathy, improve cardiac output, protect systemic organs, and improve mortality in a lipopolysaccharide-induced sepsis model. *Basic Res. Cardiol.* 114:15. doi: 10.1007/s00395-019-0724-3

Jayaprakash, N., Gajic, O., Frank, R. D., and Smischney, N. (2018). Elevated modified shock index in early sepsis is associated with myocardial dysfunction and mortality. *J. Crit. Care* 43, 30–35. doi: 10.1016/j.jcrc.2017.08.019

Jiahui, Y., and Cai, G. (2018). Research progress of left ventricular global longitudinal strain in the diagnosis of septic cardiomyopathy. *Prevent. Treat. Cardio Cereb. Vasc. Dis.* 18, 410–414. doi: 10.3969/j.issn.1009-816x.2018.05.017

Kakihana, Y., Ito, T., Nakahara, M., Yamaguchi, K., and Yasuda, T. (2016). Sepsis-induced myocardial dysfunction: pathophysiology and management. *J. Intensive Care* 4:22. doi: 10.1186/s40560-016-0148-1

Kalbitz, M., Grailer, J. J., Fattahi, F., Jajou, L., Herron, T. J., Campbell, K. F., et al. (2015). Role of extracellular histones in the cardiomyopathy of sepsis. *FASEB J.* 29, 2185–2193. doi: 10.1096/fj.14-268730

Keshari, R. S., Silasi, R., Popescu, N. I., Patel, M. M., Chaaban, H., Lupu, C., et al. (2017). Inhibition of complement C5 protects against organ failure and reduces mortality in a baboon model of *Escherichia coli* sepsis. *Proc. Natl. Acad. Sci. U.S.A.* 114, E6390–E6399. doi: 10.1073/pnas.1706818114

Kokkinaki, D., Hoffman, M., Kalliora, C. I, Kyriazis, D., Maning, J., Lucchese, A. M., et al. (2019). Chemically synthesized Secoisolariciresinol diglucoside (LGM2605) improves mitochondrial function in cardiac myocytes and alleviates septic cardiomyopathy. *J. Mol. Cell. Cardiol.* 127, 232–245. doi: 10.1016/j.yjmcc.2018.12.016

Kong, W., Kang, K., Gao, Y., Liu, H., Meng, X., Cao, Y., et al. (2018). GTS-21 protected against LPS-induced sepsis myocardial injury in mice through alpha7nAChR. *Inflammation* 41, 1073–1083. doi: 10.1007/s10753-018-0759-x

Kong, W., Kang, K., Gao, Y., Liu, H., Meng, X., Yang, S., et al. (2017). Dexmedetomidine alleviates LPS-induced septic cardiomyopathy via the cholinergic anti-inflammatory pathway in mice. *Am. J. Transl. Res.* 9, 5040–5047.

Kumar, V. (2019). Sepsis roadmap: what we know, what we learned, and where we are going. *Clin. Immunol.* 210:108264. doi: 10.1016/j.clim.2019.108264

Lefer, A. M. (1982). The pathophysiologic role of myocardial depressant factor as a mediator of circulatory shock. *Klin. Wochenschr.* 60, 713–716. doi: 10.1007/bf01716561

Li, Y., Li, H., and Zhang, D. (2019). Analysis Of incidence and risk factors Of septic cardjomyopathy. *Chin. J. Emerg. Med.* 28, 836–840. doi: 10.3760/cma.j.issn.1671-0282.2019.07.006

Liu, C., Zhu, R., Zhou, Z., Liu, H., Lin, J., Wen, S., et al. (2017). [Sepsis-induced cardiomyopathy complicated with cardiogenic shock patients supported with extracorporeal membrane oxygenation]. *Zhonghua Wei Zhong Bing Ji Jiu Yi Xue* 29, 1140–1143. doi: 10.3760/cma.j.issn.2095-4352.2017.12.018

Lu, N. F., Jiang, L., Zhu, B., Yang, D. G., Zheng, R. Q., Shao, J., et al. (2019). Elevated plasma histone H4 levels are an important risk factor for the development of septic cardiomyopathy. *Balkan Med. J.* doi: 10.4274/balkanmedj.galenos.2019.2019.8.40 [Epub ahead of print].

Luo, Q., Yang, A., Cao, Q., and Guan, H. (2018). 3,3′-Diindolylmethane protects cardiomyocytes from LPS-induced inflammatory response and apoptosis. *BMC Pharmacol. Toxicol.* 19:71. doi: 10.1186/s40360-018-0262-x

Martin, L., Derwall, M., Al Zoubi, S., Zechendorf, E., Reuter, D. A., Thiemermann, C., et al. (2019). The septic heart: current understanding of molecular mechanisms and clinical implications. *Chest* 155, 427–437. doi: 10.1016/j.chest.2018.08.1037

Mingjie, W., and Zheng, X. (2018). Effects of simvastatin nanoparticles on septic-associated acute lung injury in mice byregulating inducible nitric oxide synthase / endothelial nitric oxide synthase system. *Chin. J. Crit. Care Med.* 11, 393–399. doi: 10.3877/cma.j.issn.1674-6880.2018.06.007

Monteiro, V. V. S., Reis, J. F., de Souza Gomes, R., Navegantes, K. C., and Monteiro, M. C. (2017). Dual behavior of exosomes in septic cardiomyopathy. *Adv. Exp. Med. Biol.* 998, 101–112. doi: 10.1007/978-981-10-4397-0_7

Morin, E. E., Guo, L., Schwendeman, A., and Li, X. A. (2015). HDL in sepsis - risk factor and therapeutic approach. *Front. Pharmacol.* 6:244. doi: 10.3389/fphar.2015.00244

Niederbichler, A. D., Hoesel, L. M., Westfall, M. V., Gao, H., Ipaktchi, K. R., Sun, L., et al. (2006). An essential role for complement C5a in the pathogenesis of septic cardiac dysfunction. *J. Exp. Med.* 203, 53–61. doi: 10.1084/jem.20051207

Nizamuddin, J., Mahmood, F., Tung, A., Mueller, A., Brown, S. M., Shaefi, S., et al. (2017). Interval changes in myocardial performance index predict outcome in severe sepsis. *J. Cardiothorac. Vasc. Anesth.* 31, 957–964. doi: 10.1053/j.jvca.2016.11.007

Real, J. M., Ferreira, L. R. P., Esteves, G. H., Koyama, F. C., Dias, M. V. S., Bezerra-Neto, J. E., et al. (2018). Exosomes from patients with septic shock

convey miRNAs related to inflammation and cell cycle regulation: new signaling pathways in sepsis? *Crit. Care* 22:68. doi: 10.1186/s13054-018-2003-3

Ruian, D., and Chen, X. (2018). Research progress of sepsis cardiomyopathy. *J. Mod. Med. Health* 34:13. doi: 10.3969/j.issn.1009-5519.2018.13.019

Sanfilippo, F., Orde, S., Oliveri, F., Scolletta, S., and Astuto, M. (2019). The challenging diagnosis of septic cardiomyopathy. *Chest* 156, 635–636. doi: 10.1016/j.chest.2019.04.136

Sato, R., Kuriyama, A., Takada, T., Nasu, M., and Luthe, S. K. (2016). Prevalence and risk factors of sepsis-induced cardiomyopathy: a retrospective cohort study. *Medicine* 95:e5031. doi: 10.1097/MD.0000000000005031

Shi, H., Ma, J., Sun, J., and Guan, B. (2015). [Successful rescue of a patient with acute respiratory distress syndrome and septic shock with myocardial depression]. *Zhonghua Wei Zhong Bing Ji Jiu Yi Xue* 27:233.

Singer, M., Deutschman, C. S., Seymour, C. W., Shankar-Hari, M., Annane, D., Bauer, M., et al. (2016). The Third International Consensus definitions for sepsis and septic shock (sepsis-3). *JAMA* 315, 801–810. doi: 10.1001/jama.2016.0287

Sinkovic, A., Kit, B., and Markota, A. (2018). Successful use of combined blood purification techniques in splenectomised patient with septic shock in streptococcus pneumoniae infection - a case report. *BMC Infect. Dis.* 18:433. doi: 10.1186/s12879-018-3327-y

Souza, A. C. P., Souza, C. M., Amaral, C. L., Lemes, S. F., Santucci, L. F., Milanski, M., et al. (2019). Short-term high-fat diet consumption reduces hypothalamic expression of the nicotinic acetylcholine receptor alpha7 subunit (alpha7nAChR) and affects the anti-inflammatory response in a mouse model of sepsis. *Front. Immunol.* 10:565. doi: 10.3389/fimmu.2019.00565

Spiller, F., Oliveira Formiga, R., Fernandes da Silva Coimbra, J., Alves-Filho, J. C., Cunha, T. M., and Cunha, F. Q. (2019). Targeting nitric oxide as a key modulator of sepsis, arthritis and pain. *Nitric. Oxide* 89, 32–40. doi: 10.1016/j.niox.2019.04.011

Sun, Y., Yao, X., Zhang, Q. J., Zhu, M., Liu, Z. P., Ci, B., et al. (2018). Beclin-1-dependent autophagy protects the heart during sepsis. *Circulation* 138, 2247–2262. doi: 10.1161/CIRCULATIONAHA.117.032821

Takahashi, Y., Sonoo, T., Naraba, H., Hashimoto, H., and Nakamura, K. (2019). Effect of intra-arterial balloon pumping for refractory septic cardiomyopathy: a case series. *Indian J. Crit. Care Med.* 23, 182–185. doi: 10.5005/jp-journals-10071-23150

Takasu, O., Gaut, J. P., Watanabe, E., To, K., Fagley, R. E., Sato, B., et al. (2013). Mechanisms of cardiac and renal dysfunction in patients dying of sepsis. *Am. J. Respir. Crit. Care Med.* 187, 509–517. doi: 10.1164/rccm.201211-1983OC

Tan, S., Long, Z., Hou, X., Lin, Y., Xu, J., You, X., et al. (2019). H2 protects against lipopolysaccharide-induced cardiac dysfunction via blocking TLR4-mediated cytokines expression. *Front. Pharmacol.* 10:865. doi: 10.3389/fphar.2019.00865

Tan, Y., Chen, S., Zhong, J., Ren, J., and Dong, M. (2019). Mitochondrial injury and targeted intervention in septic cardiomyopathy. *Curr. Pharm. Des.* 25, 2060–2070. doi: 10.2174/1381612825666190708155400

Vallejo, J. G. (2011). Role of toll-like receptors in cardiovascular diseases. *Clin. Sci.* 121, 1–10. doi: 10.1042/CS20100539

Vasques-Novoa, F., Laundos, T. L., Madureira, A., Bettencourt, N., Nunes, J. P. L., Carneiro, F., et al. (2019). Myocardial edema: an overlooked mechanism of septic cardiomyopathy? *Shock* doi: 10.1097/SHK.0000000000001395 [Epub ahead of print].

Vogel, D. J., Murray, J., Czapran, A. Z., Camporota, L., Ioannou, N., Meadows, C. I. S., et al. (2018). Veno-arterio-venous ECMO for septic cardiomyopathy: a single-centre experience. *Perfusion* 33, 57–64. doi: 10.1177/0267659118766833

Wada, K., Bunya, N., Kakizaki, R., Kasai, T., Uemura, S., Harada, K., et al. (2019). Successful use of veno-arterial extracorporeal membrane oxygenation for septic cardiomyopathy in a patient with pre-existing chronic heart failure. *Acute Med. Surg.* 6, 301–304. doi: 10.1002/ams2.407

Wang, H., Bei, Y., Shen, S., Huang, P., Shi, J., Zhang, J., et al. (2016). miR-21-3p controls sepsis-associated cardiac dysfunction via regulating SORBS2. *J. Mol. Cell. Cardiol.* 94, 43–53. doi: 10.1016/j.yjmcc.2016.03.014

Wang, S., and Li, G. (2015). [Clinical research progress of septic cardiomyopathy]. *Zhonghua Wei Zhong Bing Ji Jiu Yi Xue* 27, 1019–1021. doi: 10.3760/cma.j.issn.2095-4352.2015.12.021

Ward, P. A., and Fattahi, F. (2019). New strategies for treatment of infectious sepsis. *J. Leukoc. Biol.* 106, 187–192. doi: 10.1002/JLB.4MIR1118-425R

Xu, X., Liu, Q., He, S., Zhao, J., Wang, N., Han, X., et al. (2018). Qiang-Xin 1 formula prevents sepsis-induced apoptosis in murine cardiomyocytes by suppressing endoplasmic reticulum- and mitochondria-associated pathways. *Front. Pharmacol.* 9:818. doi: 10.3389/fphar.2018.00818

Yang, J., Zhang, R., Jiang, X., Lv, J., Li, Y., Ye, H., et al. (2018). Toll-like receptor 4-induced ryanodine receptor 2 oxidation and sarcoplasmic reticulum Ca(2+) leakage promote cardiac contractile dysfunction in sepsis. *J. Biol. Chem.* 293, 794–807. doi: 10.1074/jbc.M117.812289

Yin, H.-Y., Min-shan, Q., Yong-hui, M., and Xiao-ling, Y. (2016). Curative effect of recombinant human brain natriuretic peptide for septic patients with cardiac in sufficiency. *Chin. J. Crit. Care Med.* 36, 673–678. doi: 10.3969/j.issn.1002-1949.2016.08.001

Yu, W., Mei, X., Zhang, Q., Zhang, H., Zhang, T., and Zou, C. (2019). Yap overexpression attenuates septic cardiomyopathy by inhibiting DRP1-related mitochondrial fission and activating the ERK signaling pathway. *J. Recept. Signal. Transduct. Res.* 39, 175–186. doi: 10.1080/10799893.2019.1641822

Zhang, J., Wang, L., Xie, W., Hu, S., Zhou, H., Zhu, P., et al. (2019). Melatonin attenuates ER stress and mitochondrial damage in septic cardiomyopathy: a new mechanism involving BAP31 upregulation and MAPK-ERK pathway. *J. Cell Physiol.* 235, 2847–2856. doi: 10.1002/jcp.29190

Zheng, G., Pan, M., Jin, W., Jin, G., and Huang, Y. (2017). MicroRNA-135a is up-regulated and aggravates myocardial depression in sepsis via regulating p38 MAPK/NF-kappaB pathway. *Int. Immunopharmacol.* 45, 6–12. doi: 10.1016/j.intimp.2017.01.029

Zhong, J., Tan, Y., Lu, J., Liu, J., Xiao, X., Zhu, P., et al. (2019). Therapeutic contribution of melatonin to the treatment of septic cardiomyopathy: a novel mechanism linking Ripk3-modified mitochondrial performance and endoplasmic reticulum function. *Redox Biol.* 26:101287. doi: 10.1016/j.redox.2019.101287

Conflict of Interest: The authors declare that the research was conducted in the absence of any commercial or financial relationships that could be construed as a potential conflict of interest.

frontiers in Pharmacology

REVIEW
published: 03 March 2020
doi: 10.3389/fphar.2020.00146

Chemokine Receptor 5, a Double-Edged Sword in Metabolic Syndrome and Cardiovascular Disease

Zhongwen Zhang[1,2†], Qiannan Wang[1,2†], Jinming Yao[1,2], Xiaojun Zhou[1,2], Junyu Zhao[1,2], Xiaoqian Zhang[1,2], Jianjun Dong[3] and Lin Liao[1,2*]*

[1] Department of Endocrinology, Shandong Provincial Qianfoshan Hospital, the First Hospital Affiliated with Shandong First Medical University, Jinan, China, [2] Division of Endocrinology, Department of Internal Medicine, Shandong Provincial QianFoShan Hospital, Shandong University, Jinan, China, [3] Division of Endocrinology, Department of Internal Medicine, Qilu Hospital of Shandong University, Jinan, China

The key characteristic of cardiovascular disease (CVD) is endothelial dysfunction, which is likely the consequence of inflammation. It is well demonstrated that chemokines and their receptors play a crucial role in regulating inflammatory responses, and recently, much attention has been paid to chemokine receptor 5 (CCR5) and its ligands. For example, CCR5 aggravates the inflammatory response in adipose tissue by regulating macrophage recruitment and M1/M2 phenotype switch, thus causing insulin resistance and obesity. Inhibition of CCR5 expression reduces the aggregation of pro-atherogenic cytokines to the site of arterial injury. However, targeting CCR5 is not always effective, and emerging evidence has shown that CCR5 facilitates progenitor cell recruitment and promotes vascular endothelial cell repair. In this paper, we provide recent insights into the role of CCR5 and its ligands in metabolic syndrome as related to cardiovascular disease and the opportunities and roadblocks in targeting CCR5 and its ligands.

Keywords: CCR5, inflammation, endothelial dysfunction, cardiovascular disease, metabolic syndrome

OPEN ACCESS

Edited by:
Owen Llewellyn Woodman, Monash University, Australia

Reviewed by:
Javier Angulo, Ramón y Cajal University Hospital, Spain
Carlos F. Sánchez-Ferrer, Autonomous University of Madrid, Spain
Cristiana Couto Garcia, Oswaldo Cruz Foundation, Brazil

***Correspondence:**
Jianjun Dong
cwc_ll@sdu.edu.cn
Lin Liao
liaolin@sdu.edu.cn

[†]These authors have contributed equally to this work and share first authorship

Specialty section:
This article was submitted to Cardiovascular and Smooth Muscle Pharmacology, a section of the journal Frontiers in Pharmacology

Received: *23 August 2019*
Accepted: *04 February 2020*
Published: *03 March 2020*

Citation:
Zhang Z, Wang Q, Yao J, Zhou X, Zhao J, Zhang X, Dong J and Liao L (2020) Chemokine Receptor 5, a Double-Edged Sword in Metabolic Syndrome and Cardiovascular Disease. Front. Pharmacol. 11:146. doi: 10.3389/fphar.2020.00146

INTRODUCTION

Metabolic syndrome (MetS), including obesity, hypertension, hyperglycemia, and dyslipidemia, has detrimental effects on the endothelium, contributing to the development of cardiovascular diseases (CVD) (Nikolopoulou and Kadoglou, 2014; Yao et al., 2014). One of the key common central mechanisms linking all of these diseases is underpinned by an exaggerated inflammatory response (Lumeng et al., 2007). In recent years, evidence has accumulated that chemokine receptor 5 (CCR5) and its ligands play a critical role in regulating the inflammatory response. For example, CCR5 aggravates the inflammatory response in mouse adipose tissue by regulating macrophage recruitment and M1/M2 phenotype switching, thus causing insulin resistance and obesity (Kitade et al., 2012). Inhibition of CCR5 expression reduces the accumulation of pro-atherogenic cytokines and monocytes to the site of arterial injury. However, therapies targeting CCR5 and its ligands have not performed consistently with regard to preventing metabolic syndrome related diseases (Kennedy et al., 2013; Slominski et al., 2017), indicating that CCR5 and its ligands might play a double-edged role in the progression of these diseases. More importantly, emerging evidence shows that CCR5 is specifically expressed in endothelial cells and endothelial progenitor cells (EPCs). CCR5 facilitates progenitor cell

recruitment and promotes vascular endothelial repair in a mouse model (Ishida et al., 2012; Suffee et al., 2012; Zhang et al., 2015b). Although inhibiting CCR5 expression reduces the inflammatory response, it also aggravates the endothelial damage, thus significantly limiting the actual effectiveness of therapeutic interventions. Therefore, studying the mechanisms of CCR5 and its ligands that control these processes in the endothelial cells and the inflammatory response will provide further understanding of the pathophysiology of cardiovascular disease and may be used to develop novel pharmacological strategies.

CCR5 AND ITS LIGANDS

CCR5, a member of the guanine nucleotide binding protein (G protein) coupled receptors (GPCR), has been known as a key player in HIV-1 entry into target cells from its discovery (Berger et al., 1999). CCR5 binds and responds to chemokine ligand 3 (CCL3) (**Table 1**), chemokine ligand 4 (CCL4), and chemokine ligand 5(CCL5). CCR5 is expressed in macrophages, activated T cells, natural killer cells, endothelial cells, and EPCs. CCR5 participates in the regulation of proinflammatory response by modulating the behavior, survival, and retention of immune cells in tissues (Kohlmeier et al., 2011). In addition, CCR5 can be expressed in non-immune system cells, notably in astrocytes, microglia, and neurons, which are involved in neuronal survival and differentiation (Sorce et al., 2011).

CCL3, also known as macrophage inflammatory protein-α (MIP-α), is released from activated platelets, mast cells, and neutrophils (Weber, 2005; Montecucco et al., 2008). Previous studies indicated that CCL3 activates neutrophils *via* the mediation of firm adherence and the (subsequent) transmigration of neutrophils as a result of lipid mediator production. CCL4 is also called macrophage inflammatory protein-β (MIP-β) and was first isolated from culture medium containing lipopolysaccharide-activated macrophages. CCL4 can induce the chemotaxis of different cell types, including natural killer cells, monocytes/macrophages, and coronary endothelial cells (Mirabelli-Badenier et al., 2011). The chemotactic activity of CCL5, initially considered to be a T cell-specific protein that is stored in and released from various cells, including endothelial cells, EPCs, monocytes/macrophages and fibroblasts, recruits activated T cells, NK cells, and basophils to the site of an inflammatory response (Appay and Rowland-Jones, 2001).

CCR5 AND ITS LIGANDS IN RELATION TO ENDOTHELIAL FUNCTION

Endothelial cells line the interior surface of all blood vessels and are involved not only in delivering blood to all vital organs but also in maintaining the homeostasis of the vasculature. A large body of evidence has shown that diabetes, ischemia, and atherosclerosis (Suffee et al., 2012; Zhang et al., 2015b; Ali and Woodman, 2019) have adverse effects on the endothelium, which contributes to the development of CVD. One of the key common central mechanisms linking all of these diseases is based on exaggerated inflammation. In all cases, the interaction between

TABLE 1 | Summary of data of CCR5 and its ligands, primary source, main effects, and main references.

Gene name	Expressed by/primary source	Main effects		References
		Pro-inflammation	Endothelium repair and angiogenesis	
CCL3	Monocytes/macrophages, T cells, vascular smooth muscle cells, eosinophils, coronary endothelial cells, and platelets.	Mediates the recruitment of macrophages into the injured site by binding with its receptor, CCR5.	CCL3 induces the infiltration of macrophages into the damaged retina and produces vascular endothelial growth factor (VEGF) by binding to CCR5, and eventually promotes corneal neovascularization.	Ridiandries et al., 2016; Menten et al., 2002; DiPietro et al., 1998; Lu et al., 2008.
CCL4	Monocyte, T cells, B lymphocytes, NK cells, dendritic cells, vascular smooth muscle cells, and neutrophils.	Chemoattractants for immature dendritic cells and macrophages/ monocytes, attracts macrophages to destroy islet cells.	Increases VEGF-C expression and promotes lymph angiogenesis in oral cancer cells.	Ridiandries et al., 2016; Menten et al., 2002; Chang and Chen, 2016; Lien et al., 2018.
CCL5	T-cells, epithelial cells and activated platelets	Mediates the macrophage recruitment and M1/M2 phenotype switching, recruits leukocytes and certain natural-killer cells, promotes smooth muscle cells phenotypic switching from the contractile to synthetic phenotype.	CCL5 is pro-angiogenic in the ischemic tissues and subcutaneous model, promotes the revascularization and muscle regeneration by binding to its receptor, CCR5.	Suffee et al., 2012; Liu et al., 2014; Zhang et al., 2015b; Ridiandries et al., 2016; Lin et al., 2018.
CCR5	Monocytes/macrophages, activated T cells, endothelial cells, endothelial progenitor cells (EPCs), natural killer cells, astrocytes, microglia, and neurons.	Promotes infiltration of monocytes/ macrophages to the injured site, aggravates hepatic steatosis and insulin resistance, and increases triglyceride synthesis.	Accelerates the homing of EPCs to damaged endothelial cells, promoting endothelial repair or the formation of neovascularization.	Suffee et al., 2017; Bjerregaard et al., 2019; Rookmaaker et al., 2007; Potteaux et al., 2006; Berres et al., 2010; Ishida et al., 2012; Kitade et al., 2012; Shen et al., 2013; Liu et al., 2014; Zhang et al., 2015b; Ridiandries et al., 2016; Perez-Martinez et al., 2018; Yan et al., 2019.

the endothelium and inflammatory cells plays a key role in the initiation of the pathological condition.

Previous studies have demonstrated that chemokines can directly regulate the migration and recruitment of cells to injury sites *via* inflammation. All CC-chemokines contain nuclear factor-kappa B (NF-κB) binding motifs, and their expression is significantly upregulated under inflammatory conditions (Werts et al., 2007; Ridiandries et al., 2016). CCL3, CCL4, and CCL5 are upregulated when induced by an inflammatory stimulus (Laurence, 2006; Zhang et al., 2015a; Ridiandries et al., 2016). Increased expression of CCL3/CCL4/CCL5 mediates the arrest and transmigration of monocytes/macrophages into the damaged endothelium by binding with its receptor CCR5 (Zhang et al., 2015b; Ridiandries et al., 2016), which is involved in the inflammatory response to endothelial injury. Blocking CCR5 alleviated myocardial ischemia–reperfusion injury in rats by regulating the cardiac inflammatory response (Shen et al., 2013). CCR5 deficiency could reduce macrophage aggregation into atherosclerotic plaques in a hypercholesterolemic mouse model (Potteaux et al., 2006).

In addition to their roles in mediating inflammation, CCL5 has also been shown to play a role in the process of ischemia-mediated physiological angiogenesis (Suffee et al., 2017; Bjerregaard et al., 2019) and endothelial repair (Maarten B. et al., 2007; Zhang et al., 2015b; Yan et al., 2019). CCL5/CCR5 is specifically expressed in endothelial cells and EPCs, and endothelial cell specific CCR5 is involved in the regulation of vascular regeneration in ischemic tissues (Suffee et al., 2017). Administration of CCL5-loaded microparticles could improve the clinical score of mice after limb injury as well as promote the revascularization and the muscle regeneration. Yan et al. (2019) verified that CCR5 expression was upregulated in vascular endothelial growth factor (VEGF) modified macrophage *in vitro* after treatment with VEGF-modified macrophages therapy accelerated reendothelialization and attenuated neointima formation in the wire-induced carotid artery injury mouse model. CCL5 is pro-angiogenic in a rat model of subcutaneous injury. One *in vitro* study found that the effects of CCL5-mediated angiogenesis are at least partially dependent on VEGF secretion by endothelial cells, as the effects are weaker when endothelial cells are incubated with anti-VEGF receptor antibodies (Suffee et al., 2012). According to the leucocyte subset chemokine expression, patients with age-related macular degeneration (AMD) of neovascularization have different responses to anti-VEGF receptor antibody treatment, with good responders to the anti-VEGF loading dose having higher CCR1 expression on monocytes and lower CCR5 expression on $CD14^+$ T cells, indicating that CCR5 may be an effective way to provide individualized treatment for neovascular AMD (Bjerregaard et al., 2019).

EPCs, as a kind of precursor cell derived from bone marrow that can differentiate into endothelial cells, play an important role in neovascularization during tissue repair (Zhang et al., 2015b). In a mouse skin injury model, deletion of the CCR5 gene reduced the accumulation of vascular EPCs and the formation of neovascularization, and it eventually delayed the healing of damaged skin. When EPCs carrying the CCR5 gene are transferred into $CCR5^{-/-}$ mice, EPCs accumulated at the site of injury and restored normal neovascularization (Ishida et al., 2012). CCL5 is involved in the homing of bone marrow-derived EPCs in glomerular endothelial repair. In a mouse model of reversible glomerulonephritis, administration of a CCR5 inhibitor (METRANTES) reduced the participation of EPCs in glomerular vascular repair (Rookmaaker et al., 2007). In a hypercholesterolemic $ApoE^{-/-}$ mouse model, overexpression of CCR5 contributes to the homing of EPCs to damaged endothelial cells, promoting endothelial repair, improving endothelial dysfunction, and ultimately stabilizing atherosclerotic plaques (Zhang et al., 2015b).

CCR5 and its ligands play an important role in regulating tissue angiogenesis, but the exact mechanism is still unclear. A study (Liu et al., 2014) on human chondrosarcoma cells revealed that pretreatment with a phosphatidylinositol 3-kinase (PI3K) inhibitor repressed the VEGF production and angiogenesis induced by CCL5/CCR5, suggesting that the PI3K-dependent pathway plays a crucial role in CCL5/CCR5-mediated angiogenesis.

In addition to CCL5, CCL3 and CCL4 are also involved in the process of revascularization. In alkali-induced corneal neovascularization of mouse models, CCL3 could induce the infiltration of macrophages into the damaged retina and the production VEGF by binding to CCR5, eventually promoting corneal neovascularization (Lu et al., 2008). Anti-CCL3 antiserum has been shown to decrease angiogenic activity in a murine wound repair model (DiPietro et al., 1998). CCL4 was proven to increase VEGF-C expression and promote lymphangiogenesis in oral cancer cells (Lien et al., 2018).

CCR5 AND ITS LIGANDS IN METABOLIC SYNDROME

Obesity

Obesity is characterized as low-grade systemic or chronic inflammation that is associated with an increased incidence of metabolic syndrome, cardiovascular disease, and tumor (Despres and Lemieux, 2006; Nikolopoulou and Kadoglou, 2014). Excessive fat tissue expansion triggers the secretion of cytokines and chemokines (Brownlee, 2005), which in turn attract various leukocytes, leading to fatty tissue inflammation.

The exact role of CCR5 and its ligands in the pathogenesis of obesity is still obscure, but there are several studies that have continuously reported this finding (Yao et al., 2014). Gao et al. (2015) noted that phosphatidyl-ethanol-amine-N-methyl transferase-deficient mice were resistant to high fat diet-induced obesity. This may result from decreased expression of CCL5. Similarly, Pisano et al. (2017) found that weight gain in patients on antipsychotics is associated with the extent of CCL5 expression. CCL5, as a neuroendocrine element, modulates food intake and body temperature of C57BL/6 mice through unidentified receptors in the hypothalamus (Chou et al., 2016), thus affecting the body weight. In a high-fat diet-induced obese mouse model (Kitade et al., 2012), CCR5 plays a critical role in adipose tissue macrophage recruitment and polarization.

Deletion of CCR5 reduces the transition of macrophages from the pro-inflammatory M1 phenotype to the anti-inflammatory M2 phenotype and ameliorated obesity-induced insulin resistance. This observation is consistent with previous studies that have indicated that CCR5 could directly induce the transition of the M1/M2 phenotype by modulating the alteration of Ly6C ^{high} and Ly6C ^{low} monocyte subsets (Soehnlein et al., 2013; Huh et al., 2018); further studies are required to clarify the details of this mechanism.

Hyperglycemia

CCR5 and its ligands have been shown to be associated with the pathogenesis of both type 1 diabetes mellitus (T1DM) and type 2 diabetes mellitus (T2DM). As we know, the main pathological mechanism of T1DM is the pancreatic islet β-cell death (Ashcroft and Rorsman, 2012). CCL4 is upregulated in the islet autoantibody-positive T1DM patients and relatives at high risk of developing T1DM, and increased expression of CCL4 aggravates β-cell death and early islet graft loss by stimulating the trafficking of macrophages into injured pancreatic islets (Hanifi-Moghaddam et al., 2006). Moreover, the extracellular regulated protein kinases and NF-kB pathway may be involved in the process of CCL4 production by stimulating CD40-CD40L interaction in human pancreatic islets (Barbe-Tuana et al., 2006).

In patients with diabetes, CCL5 and CCR5 are upregulated in the peripheral blood (Slominski et al., 2019; Inayat et al., 2019). Exogenous insulin supplementation may reduce concentrations of CCL5 in patients with newly diagnosed type 2 diabetes compared with the control subjects (Bogdanski et al., 2007). Epidemiological studies have indicated that CCR5 promoter function mutation (CCR5 59029 G to A alteration) could be a susceptibility factor for type 2 diabetes and the CCR5 59029 A positive genotype increased the risk for type 2 diabetes (Kochetova et al., 2019). The exact mechanism of CCR5 gene mutation and the pathogenesis of type 2 diabetes are still unclear. Since the metabolic hallmark of type 2 diabetes is insulin resistance, previous studies have shown that CCR5 gene knockout in mice could prevent insulin resistance and diabetes induced by a high-fat feeding. The beneficial effects of CCR5 deficiency were correlated with reduced recruitment and the M2-dominant shift of macrophages in adipose tissues (Kitade et al., 2012). However, this finding is contrary to Chou et al' s studies, which suggested that the CCR5 gene knockout in mice impairs the regulation of energy metabolism in the hypothalamus (Chou et al., 2016). Both *in vitro* tissue culture and *ex vivo* stimulation studies indicated that the activation of PI3K-Akt pathways and insulin signaling were impaired in the hypothalamus of CCR5 knockout mice. METRANTES, a CCR5 antagonist, abolished the dephosphorylation of insulin receptor substrates-1 (IRS-1)^{S302} and insulin signal activation. In addition, intracerebroventricular delivery of the CCR5 antagonist interrupted hypothalamic insulin signaling and led to glucose intolerance. In summary, CCR5 may be involved in the pathogenesis of type 2 diabetes through mediating insulin resistance and hypothalamic insulin signaling regulation. However, there are still many unanswered questions about the exact effect of CCR5 in the pathogenesis of type 2 diabetes. Additional research is needed in the future to confirm this conclusion.

Microvascular complications are the leading cause of death in diabetic patients. The recruitment of leukocytes to kidney tissue during T2DM is an early event in the pathogenesis of diabetic kidney disease (DKD). CCR5 mRNA was faintly detected in the normal tubulointerstitial compartment tissue (Mezzano et al., 2003). After the high glucose treatment, CCR5 expression was upregulated in the tubulointerstitial compartment during the process of diabetes. Since CCL5/CCR5 participates in the formation of inflammatory infiltrates during glomerulonephritis, inhibition of CCR5 exerts renal protection during early glomerulonephritis through its anti-inflammatory properties (Turner et al., 2008). The correlation between the CCR5 gene and the risk of DKD is conflicting and inconclusive. An oral CCR2/CCR5 antagonist (PF-04634817) slightly reduced albuminuria in adults with DKD (Gale et al., 2018). However, in ob/ob mice, treatment with a dual CCR2/CCR5 antagonist (MK-0812) showed no protective effect on DKD (O'Brien et al., 2017). Although adipose tissue inflammation was decreased in this mouse model, the improvement was insufficient to overcome the metabolic imbalances of type 2 diabetes. The mutations in the CCR5 gene promoter region (CCR5 59029 G to A alteration) and deletion of 32 nucleotides (CCR5-Δ32) lead to genetic inactivation of CCR5 (Nazir et al., 2014). Previous studies have found that CCR5-59029 G/A was an independent risk factor for DKD (Yahya et al., 2019). The CCR5 59029A-positive genotype was correlated with an increased risk for albuminuria (Zhang et al., 2016). Mlynarski et al. (2005) showed that the CCR5-Δ32 mutation increased the risk of kidney disease in men with type 1 diabetes; however, this outcome is contrary to that of Prasad et al. (2007) who found that CCR5-Δ32 was not related to nephropathic type 2 diabetes patients. Skrzypkowska et al. (2019) even indicated that 32 allele-bearing individuals exhibit more beneficial values of kidney function parameters. Specifically, the wt/Δ32 and Δ32/Δ32 carriers exhibited a higher number of $CD34^{+}VEGFR^{2+}$ and $CD34^{+}VEGFR^{2+}c\text{-}Kit^{+}$ cells than that in the wild type counterparts.

In addition, CCR5-Δ32 gene mutation was associated with retinopathy in patients with type 1 diabetes. Previous studies indicated that tumor necrosis factor (TNF)-α, vascular cell adhesion molecule (VCAM)-1, and intercellular cell adhesion molecule (ICAM)-1 were upregulated in diabetic patients with *CCR5*-Δ32 carriers (Joussen et al., 2002; Slominski et al., 2017). TNF-α plays a major role in the degeneration of retinal capillaries. Since ICAM-1 is the primary adhesion molecule involved in the pathogenesis of diabetic retinopathy (DR), the elevated level of ICAM-1 may facilitate the recruitment of leukocytes into the damaged retina (McLeod et al., 1995). Thus, the mutation of CCR5 gene (CCR5-Δ32) in the retina may lead to upregulating expression of other cytokines that exacerbate retinal damage.

Dyslipidemia

Diabetes is often accompanied by dyslipidemia as a result of insulin resistance. Dyslipidemia has been demonstrated to be detrimental to diabetes microvascular and macrovascular

complications (Cooper and Jandeleit-Dahm, 2005; Margeirsdottir et al., 2008).

Clinical research has shown that the expression levels of CCL5 and CCR5 were increased in the subcutaneous adipose tissue of obese individuals in comparison with those in the lean population, which could be reduced back to the normal levels through physical exercise (Baturcam et al., 2014). One study (Kim et al., 2018) reported that ultraviolet irradiation of human sun-protected subcutaneous fat *in vitro* could induce CXCL5 and CCL5 production; CCL5 treatment dose-dependently reduced triglyceride (TG) content and downregulated the expressions of acetyl CoA carboxylase (ACC), fatty acid synthase (FAS), stearoyl CoA desaturase (SCD), and sterol regulatory element-binding protein-1(SREBP-1) in human adipocytes. The changes could be reversed when the CCL5 receptor, the CCR5 gene, is deleted, suggesting that CCL5 impairs the synthesis of TG by reducing the expression of SREBP-1 and lipogenic enzymes through binding to its receptor, CCR5. In a nonalcoholic fatty liver disease mouse model, treatment with a CCR5 antagonist, maraviroc, could ameliorate hepatic steatosis *via* downregulation of dietary lipid absorption or *de novo* lipogenesis (Perez-Martinez et al., 2018). This also accords with Kitade et al.'s (2012) earlier observations, which showed that the deletion of the CCR5 gene reduced the content of TG and the lipogenic genes expression in mice. Similarly, Berres et al. (2010) even found that the administration of CCR5 antagonist markedly ameliorated hepatic fibrosis and accelerated fibrosis regression in mouse models of liver fibrosis. Epidemiological research (Hyde et al., 2010) has also shown that there was a significant positive correlation between the CCR5-Δ32 mutation and elevated serum high-density lipoprotein cholesterol (HDL) and reduced serum TG, both of which are beneficial from a cardiovascular perspective.

In addition to endothelial cells, dyslipidemia could drive the phenotypic modulation of smooth muscle cells (SMCs) and cause SMCs phenotypic alteration from the physiologically contractile to the pathophysiologically synthetic phenotype. CCR5 and CCL5 play crucial roles in the phenotypic modulation of SMCs. In HFD fed mouse model, the CCR5 and CCL5 gene knockouts showed significantly decreased levels of serum lipids and increased expressions of the SMCs contractile phenotype in the thoracoabdominal aorta as compared with the levels observed in wild-type mice. *In vitro*, CCL5 treated human aorta derived SMCs could induce cell proliferation and promote the phenotypic switching from the contractile to the synthetic phenotype (Lin et al., 2018).

Hypertension

Hypertension is an important risk factor for the development of cardiovascular diseases (Perticone et al., 2004). Previous studies have shown that angiotensin II (Ang II) promotes the infiltration of T cells and monocytes into perivascular adipose tissues (pVAT) (Mikolajczyk et al., 2016). Subsequent studies have demonstrated that the activation and recruitment of T cells and monocytes into pVAT is very important in the pathogenesis of renin-angiotensin system (RAS)-dependent hypertension (Guzik et al., 2007).

CCL5 is produced by several tissues that contribute to the regulation of the vasoconstriction and diastolic function, such as the vascular endothelium, vascular smooth muscle (Jordan et al., 1997), glomeruli (Wolf et al., 1997), renal tubules (Wada et al., 1999), and the central nervous system (Gouraud et al., 2011). CCL5 expression is upregulated in the aorta and pVAT during RAS-dependent hypertension. Previous studies have shown that there is a significant positive correlation between CCL5 expression and blood pressure in the Ang II-induced hypertension mouse model (Mikolajczyk et al., 2016). CCL5 could enhance the genesis of perivascular inflammation, thus affecting the development of hypertensive vascular dysfunction. The deletion of CCL5 reduces the infiltration of leukocytes and T lymphocytes into pVAT and importantly, this is independent of blood pressure changes.

Furthermore, the effects of CCL5 signaling on hypertensive organ damage appear to be tissue-and context-dependent. For example, CCL5 and CCR5 are possibly involved in the pathogenesis of pulmonary arterial hypertension (PAH). CCL5 can be released from endothelial cells and perivascular fibroblasts. Anti-endothelial cell antibody (AECA)-positive systemic sclerosis patients are associated with an increased risk of PAH, which may result from the increased CCL5 expression induced in endothelial cells by the stimulation with AECA. CCR5 is expressed in the macrophages, pulmonary artery endothelial cells, and pulmonary artery smooth muscle cells. Inhibition of CCR5 expression in mice model decreased perivascular macrophages recruitment and the proliferation of pulmonary-artery smooth muscle cell during hypoxia exposure (Mamazhakypov et al., 2019). However, this finding is contrary to previous studies which have suggested that CCL5 plays an important protective role in hypertension-induced renal injury. In the angiotensin II-induced hypertension mice model, CCL5 gene deficiency exhibited markedly aggravation of kidney damage, macrophage infiltration, and proinflammatory cytokine expression, which led to the aggravation of urinary albumin excretion (Rudemiller and Crowley, 2017). This may be explained by the blockade of one chemokine leading to the upregulated expressions of other cytokines that exacerbate RAS-dependent hypertension, as CCL2 blockade abrogates the enhanced renal macrophage infiltration and interstitial fibrosis in CCL5-deficient mice (Mikolajczyk et al., 2016; Rudemiller et al., 2016).

Atherosclerosis

Atherosclerosis is characterized by the accumulation of lipids, immune cells, and cell debris in the vessel wall, which form atherosclerotic lesions that can grow over time and eventually occlude the blood vessels, leading to ischemia and angina (Halvorsen et al., 2015; Pothineni et al., 2017). As a chronic inflammatory disease, atherosclerosis is associated with many chemokines and chemokine receptors (Zhang et al., 2015b; Andersen et al., 2019; Van der Vorst et al., 2019).

In recent years, much attention has been focused on the role of CCR5 and its ligands, which is crucial in the context of atherosclerosis initiation and progression (Pai et al., 2006; Afzal et al., 2008; Zhang et al., 2015a). CCR5 is expressed in the endothelial cells, monocytes/macrophages, and leukocytes

(Soehnlein et al., 2013). CCL5 may be released from activated platelets and T cells. During the progression of atherosclerotic disease, CCR5 and CCL5 proteins are faintly detected when there are no visible atherosclerotic plaques and are highly expressed in the stable plaques and advanced unstable plaques (Zhang et al., 2015b). Activated platelets release CCL5 (Gleissner et al., 2008), transferring CCL5 to the surface of injured endothelial cells and leading to increased monocyte/macrophage and leukocyte adhesion to the atherosclerotic vascular wall by binding with its receptor, CCR5 (Soehnlein et al., 2013; Zhang et al., 2015b), both of which are adverse effects from a cardiovascular perspective. The deletion of the CCR5 gene in apolipoprotein E-deficient ($ApoE^{-/-}$) mice has a protective effect on diet-induced atherosclerosis and reduces the infiltration of mononuclear and Th1 type immune response. CCR5 is also associated with a more stable plaque phenotype (Braunersreuther et al., 2007). Administration of the CC chemokine antagonist METRANTES (Veillard et al., 2004) or treatment with [^{44}AANA^{47}]-RANTES (Braunersreuther et al., 2008) inhibits the progression of atherosclerosis in a hyperlipidemic mouse model. This inhibition of lesions is associated with reduced infiltration of leukocytes into plaques and increased content of smooth muscle cells and collagen content, indicating a more stable plaque phenotype. Systemic CCL5 deficiency in $ApoE^{-/-}$ mice was found to cause reduced neointima formation after carotid artery injury (Czepluch et al., 2016). The atheroprotective effect of CCL5 deficiency might be mediated by the upregulation of kruppel-like factor 4 expression in smooth muscle cells. For HIV-infected patients, treatment with a CCR5 antagonist (Maraviroc) could significantly improve endothelial dysfunction, arterial stiffness, and early carotid atherosclerosis (Francisci et al., 2019). Matrix metalloproteinases (MMP) are involved in the vascular remodeling and immunomodulation during the process of atherosclerosis (Clemente et al., 2018). Studies have demonstrated that mice deficient for MT4-MMP have higher numbers of patrolling monocytes/macrophages adhered to inflamed endothelial cells, leading to larger lipid deposits in atherosclerotic plaques. Interestingly, these effects could be reversed by CCR5 inhibition (Clemente et al., 2018). However, epidemiological studies have shown that the association between CCR5 gene mutation and the risk of atherosclerosis-related diseases is conflicting and inconclusive. Previous studies have found that CCR5-Δ32 allele bearing individuals exhibit more beneficial values of cardiovascular function parameters (Pai et al., 2006; Afzal et al., 2008; Hyde et al., 2010). There was a significant positive correlation between CCR5-Δ32 allele bearing individuals and reduced susceptibility to CVD (Afzal et al., 2008) or development of CVD in a North Indian population (Pai et al., 2006). This may be due to CCR5 deficiency affecting lipid metabolism (Hyde et al., 2010). CCR5-Δ32 was significantly associated with higher levels of HDL-C and lower levels of TG, both of which are beneficial from a cardiovascular perspective. However, this outcome is contrary to those of Sharda et al. (2008) and Apostolakis et al. (2007) who found that there was no significant difference between the CCR5-Δ32 and the risk of CVD. Zhang et al. (2015a) even indicated that the CCR5-Δ32 increased the risk of atherosclerotic disease in Asian population (Zhang et al., 2015a). Moreover, previous studies have reported that a CCR5 gene promoter region mutation (CCR5-59029 G/A) was an independent risk factor for CVD (Simeoni et al., 2004; Vogiatzi et al., 2009). The CCR5 59029A-positive genotype was correlated with an increased risk of acute coronary syndrome (Ting et al., 2015). Considering that the role of CCR5 gene mutation in the risk of CVD is controversial, further studies with more focus on the association is therefore suggested.

In addition to CCL5, CCL3 and CCL4 have also been reported to participate in the process of atherosclerosis. CCL3 was highly expressed in atherosclerotic plaques, and the treatment with atorvastatin alleviated atherosclerotic lesions through inhibition of the 5-Lipoxygenase pathway and downregulation of CCL3 expressions in an atherosclerotic mouse model (Yang et al., 2013). CCL4 was also upregulated in vulnerable atherosclerosis plaques and was expressed by T cells in advanced atherosclerotic lesions in stroke patients (Montecucco et al., 2010). Studies has been conducted in a cohort of hypertensive patients for an average follow-up period of 37.2 ± 19.9 months; the result found that elevated serum CCL4 levels is an independent predictor of stroke and cardiovascular events (Tatara et al., 2009).

DISCUSSION

It is generally assumed that CCR5 and its ligands play a critical role in promoting inflammation by recruiting immune cells, such as monocytes and T cells. They may contribute to insulin resistance by M1/M2 phenotype switching of macrophages that infiltrate adipose tissues (Kitade et al., 2012). On the one hand, an impaired insulin signal *via* PI3K-Akt directly reduces endothelial NO synthase (eNOS) activation (Rask-Madsen and King, 2007), leading to endothelial dysfunction. On the other hand, long-term exposure of endothelial cells to high levels of glucose induces cellular dysfunction (Brownlee, 2005) and production of CCR5 and its ligands (Li et al., 2013). Adipokines, primarily adiponectin and TNF-α, secreted by fat tissue, also contribute to endothelial damage (Rask-Madsen and King, 2007), which is regarded as the initiation of cardiovascular diseases. CCR5 seems to be associated with endothelial dysfunction *via* proinflammatory activity (**Figure 1A**) (Yao, et al., 2014).

However, therapies targeting CCR5 and its ligands are not always satisfactory. Populations with CCR5-Δ32 are not consistently protected from diabetes and its complications. Deletion of CCR5 or treatment with a CCR5 antagonist in mouse model did not always reverse the inflammatory status in metabolic syndrome. One possible explanation may be that blockade of one chemokine leads to the upregulated expressions of other cytokines that exacerbate cellular dysfunction and inflammation. Another explanation may point to the potential therapeutic effect role of CCR5 in endothelial repair. The macrophages recruited by CCR5 may release various pro-angiogenic factors, including VEGF, basic fibroblast growth factor (bFGF), and platelet derived growth factor (PDGF) (**Figure 1B**) (Ridiandries et al., 2016). In addition, CCR5 facilitates the recruitment of EPCs into injured vessels and enhances

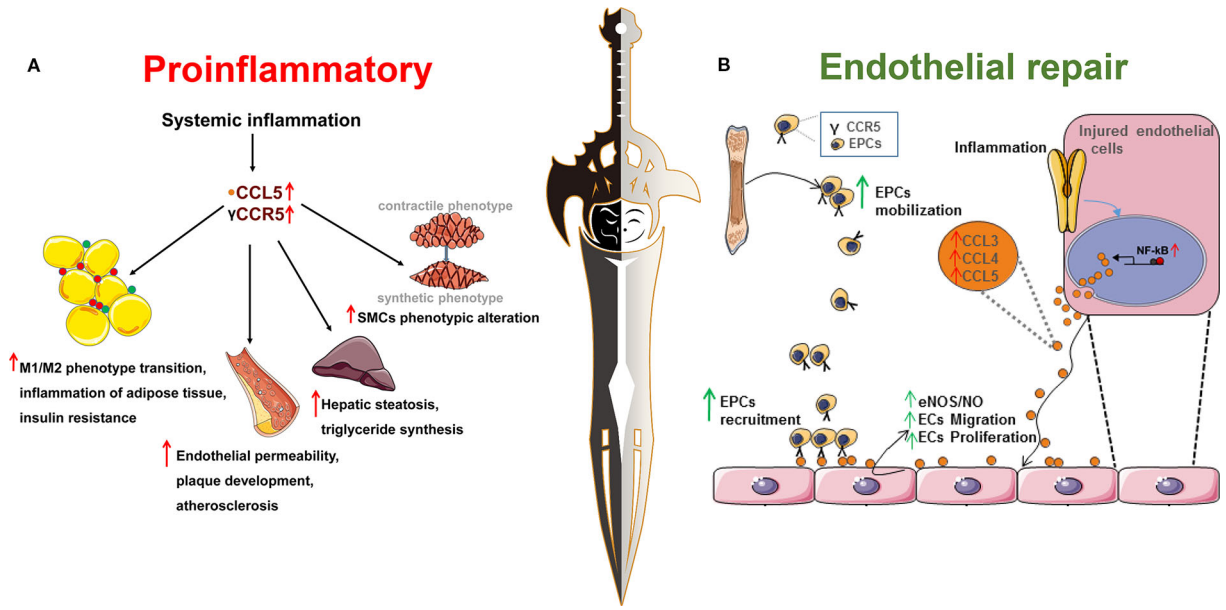

FIGURE 1 | Chemokine receptor 5, a double-edged sword in the inflammatory response and endothelial repair during the process of metabolic syndrome and cardiovascular disease. **(A)** The proinflammatory role of CCR5 and its ligands in metabolic syndrome and cardiovascular disease. As shown in section **(A)**, obesity is characterized as low-grade systemic or chronic inflammation that is associated with increased incidence of metabolic syndrome and cardiovascular disease. CCR5 and its ligands are associated with systemic inflammation. (1) CCR5 and its ligands promote the transition of macrophages from the pro-inflammatory M1 phenotype to the anti-inflammatory M2 phenotype and aggravate obesity-induced insulin resistance; (2) CCR5 and its ligands promote infiltration of leukocytes into plaques and endothelial permeability, decrease the content of smooth muscle cells and collagen content, indicating a more vulnerable plaque phenotype; (3) CCL5 increases the synthesis of triglyceride and hepatic steatosis through binding to its receptor, CCR5; (4) CCL5 could induce smooth muscle cell proliferation and promote the phenotypic switching from the contractile to the synthetic phenotype; **(B)** CCR5 and its ligands are involved in the endothelial repair during the process of endothelial damage. As shown in section **(B)**, CCL3, CCL4, and CCL5 contain NF-κB binding motifs and are upregulated when induced by an inflammatory stimulus. Increased expression of CCL3/CCL4/CCL5 mediates the mobilization and recruitment of bone marrow derived-endothelial progenitor cells into the damaged endothelium by binding with its receptor, CCR5. In addition, CCL3, CCL4, and CCL5 could directly stimulate injured cells, increase nitric oxide production, and promote endothelial cell migration and proliferation to the injured sites.

endothelial regeneration, which may also explain the genetic inactivation of CCR5 as an independent risk factor for DR and DKD (Slominski et al., 2017).

CCR5 is a double-edged sword for metabolism-related cardiovascular diseases, which may result from the patients with varying degrees of damage at different growth stages. In addition, the specificity of populations and organs should also be taken into consideration. Further studies are required to clarify the details of the mechanism.

AUTHOR CONTRIBUTIONS

LL and JD contributed to study conception and design, literature review, and preparation of the manuscript. JY, XZho, JZ, and XZha contributed to study conception and design. ZZ and QW drafted the manuscript, revised it critically for important intellectual content, gave final approval of the version to be sent, and read and approved the final manuscript.

FUNDING

This work was supported by the Key Research & Development Plan of Shandong Province (No. 2018GSF118176), the Natural Science Foundation of Shandong Province (No. ZR2016HQ26), the National Natural Science Foundation of China (81670757, 81770822), and the Bethune-Merck's Diabetes Research Foundation (No. G2016014).

REFERENCES

Afzal, A. R., Kiechl, S., Daryani, Y. P., Weerasinghe, A., Zhang, Y., Reindl, M., et al. (2008). Common CCR5-del32 frameshift mutation associated with serum levels of inflammatory markers and cardiovascular disease risk in the Bruneck population. *Stroke* 39, 1972–1978. doi: 10.1161/STROKEAHA.107.504381

Ali, S. F., and Woodman, O. L. (2019). Tocomin restores endothelium-dependent relaxation in the diabetic rat aorta by increasing NO bioavailability and improving the expression of eNOS. *Front. Physiol.* 4 (10), 186. doi: 10.3389/fphys2019.00186

Andersen, T., Ueland, T., Ghukasyan, L. T., Akerblom, A., Bertilsson, M., Aukrust, P., et al. (2019). C-X-C ligand 16 is an independent predictor of cardiovascular death

and morbidity in acute coronary syndromes. *Arterioscler. Thromb. Vasc. Biol.* 39, 2402–2410. doi: 10.1161/ATVBAHA.119.312633

Apostolakis, S., Baritaki, S., Kochiadakis, G. E., Igoumenidis, N. E., Panutsopulos, D., and Spandidos, D. A. (2007). Effects of polymorphisms in chemokine ligands and receptors on susceptibility to coronary artery disease. *Thromb. Res.* 119, 63–71. doi: 10.1016/j.thromres.2005.12.016

Appay, V., and Rowland-Jones, S. L. (2001). RANTES: a versatile and controversial chemokine. *Trends Immunol.* 22 (2), 83–87. doi: 10.1016/S1471-4906(00)01812-3

Ashcroft, F. M., and Rorsman, P. (2012). Diabetes mellitus and the beta cell: the last ten years. *Cell* 148 (6), 1160–1171. doi: 10.1016/j.cell.2012.02.010

Barbe-Tuana, F. M., Klein, D., Ichii, H., Berman, D. M., Coffey, L., Kenyon, N. S., et al. (2006). CD40-CD40 ligand interaction activates proinflammatory pathways in pancreatic islets. *Diabetes* 55 (9), 2437–2445. doi: 10.2337/db05-1673

Baturcam, E., Abubaker, J., Tiss, A., Abu-Farha, M., Khadir, A., Al-Ghimlas, F., et al. (2014). Physical exercise reduces the expression of RANTES and its CCR5 receptor in the adipose tissue of obese humans. *Mediators Inflamm.* 2014, 627150. doi: 10.1155/2014/627150

Berger, E. A., Murphy, P. M., and Farber, J. M. (1999). Chemokine receptors as HIV-1 coreceptors: roles in viral entry, tropism, and disease. *Annu. Rev. Immunol.* 17, 657–700. doi: 10.1146/annurev.immunol.17.1.657

Berres, M. L., Koenen, R. R., Rueland, A., Zaldivar, M. M., Heinrichs, D., Sahin, H., et al. (2010). Antagonism of the chemokine Ccl5 ameliorates experimental liver fibrosis in mice. *J. Clin. Invest.* 120, 4129–4140. doi: 10.1172/JCI41732

Bjerregaard, T., Krogh, N. M., Molbech, C. R., Subhi, Y., and Sorensen, T. L. (2019). Treatment failure in neovascular age-related macular degeneration is associated with a complex chemokine receptor profile. *BMJ Open Ophthalmol.* 4, e000307. doi: 10.1136/bmjophth-2019-000307

Bogdanski, P., Pupek-Musialik, D., Dytfeld, J., Jagodzinski, P. P., Jablecka, A., Kujawa, A., et al. (2007). Influence of insulin therapy on expression of chemokine receptor CCR5 and selected inflammatory markers in patients with type 2 diabetes mellitus. *Int. J. Clin. Pharmacol. Ther.* 45 (10), 563–567. doi: 10.5414/cpp45563

Braunersreuther, V., Zernecke, A., Arnaud, C., Liehn, E. A., Steffens, S., Shagdarsuren, E., et al. (2007). Ccr5 but not Ccr1 deficiency reduces development of diet-induced atherosclerosis in mice. *Arterioscler. Thromb. Vasc. Biol.* 27, 373–379. doi: 10.1161/01.ATV.0000253886.44609.ae

Braunersreuther, V., Steffens, S., Arnaud, C., Pelli, G., Burger, F., Proudfoot, A., et al. (2008). A novel RANTES antagonist prevents progression of established atherosclerotic lesions in mice. *Arterioscler. Thromb. Vasc. Biol.* 28, 1090–1096. doi: 10.1161/ATVBAHA.108.165423

Brownlee, M. (2005). The pathobiology of diabetic complications: a unifying mechanism. *Diabetes* 54 (6), 1615–1625. doi: 10.2337/diabetes.54.6.1615

Chang, T. T., and Chen, J. W. (2016). Emerging role of chemokine CC motif ligand 4 related mechanisms in diabetes mellitus and cardiovascular disease: friends or foes? *Cardiovasc Diabetol.* 15 (1), 117. doi: 10.1186/s12933-016-0439-9

Chou, S. Y., Ajoy, R., Changou, C. A., Hsieh, Y. T., Wang, Y. K., and Hoffer, B. (2016). CCL5/RANTES contributes to hypothalamic insulin signaling for systemic insulin responsiveness through CCR5. *Sci. Rep.* 6, 37659. doi: 10.1038/srep37659

Clemente, C., Rius, C., Alonso-Herranz, L., Martin-Alonso, M., Pollan, A., Camafeita, E., et al. (2018). MT4-MMP deficiency increases patrolling monocyte recruitment to early lesions and accelerates atherosclerosis. *Nat. Commun.* 9, 910. doi: 10.1038/s41467-018-03351-4

Cooper, M. E., and Jandeleit-Dahm, K. A. (2005). Lipids and diabetic renal disease. *Curr. Diabetes Rep.* 5 (6), 445–448. doi: 10.1007/s11892-005-0053-9

Czepluch, F. S., Meier, J., Binder, C., Hasenfuss, G., and Schafer, K. (2016). CCL5 deficiency reduces neointima formation following arterial injury and thrombosis in apolipoprotein E-deficient mice. *Thromb. Res.* 144, 136–143. doi: 10.1016/j.thromres.2016.06.013

Despres, J. P., and Lemieux, I. (2006). Abdominal obesity and metabolic syndrome. *Nature* 444 (7121), 881–887. doi: 10.1038/nature05488

DiPietro, L. A., Burdick, M., Low, Q. E., Kunkel, S. L., and Strieter, R. M. (1998). MIP-1alpha as a critical macrophage chemoattractant in murine wound repair. *J. Clin. Invest.* 101, 1693–1698. doi: 10.1172/JCI1020

Francisci, D., Pirro, M., Schiaroli, E., Mannarino, M. R., Cipriani, S., Bianconi, V., et al. (2019). Maraviroc intensification modulates atherosclerotic progression in HIV-suppressed patients at high cardiovascular risk. A randomized, crossover pilot study. *Open Forum Infect. Dis.* 6, ofz112. doi: 10.1093/ofid/ofz112

Gale, J. D., Gilbert, S., Blumenthal, S., Elliott, T., Pergola, P. E., Goteti, K., et al. (2018). Effect of PF-04634817, an oral CCR2/5 chemokine receptor antagonist, on albuminuria in adults with overt diabetic nephropathy. *Kidney Int. Rep.* 3, 1316–1327. doi: 10.1016/j.ekir.2018.07.010

Gao, X., van der Veen, J. N., Hermansson, M., Ordonez, M., Gomez-Munoz, A., Vance, D. E., et al. (2015). Decreased lipogenesis in white adipose tissue contributes to the resistance to high fat diet-induced obesity in phosphatidylethanolamine N-methyltransferase-deficient mice. *Biochim. Biophys. Acta* 1851 (2), 152–162. doi: 10.1016/j.bbalip.2014.11.006

Gleissner, C. A., von Hundelshausen, P., and Ley, K. (2008). Platelet chemokines in vascular disease. *Arterioscler. Thromb. Vasc. Biol.* 28, 1920–1927. doi: 10.1161/ATVBAHA.108.169417

Gouraud, S. S., Waki, H., Bhuiyan, M. E., Takagishi, M., Cui, H., Kohsaka, A., et al. (2011). Down-regulation of chemokine Ccl5 gene expression in the NTS of SHR may be pro-hypertensive. *J. Hypertens.* 29 (4), 732–740. doi: 10.1097/HJH.0b013e328344224d

Guzik, T. J., Hoch, N. E., Brown, K. A., McCann, L. A., Rahman, A., Dikalov, S., et al. (2007). Role of the T cell in the genesis of angiotensin II induced hypertension and vascular dysfunction. *J. Exp. Med.* 204, 2449–2460. doi: 10.1084/jem.20070657

Halvorsen, B., Espeland, M. Z., Andersen, G. O., Yndestad, A., Sagen, E. L., Rashidi, A., et al. (2015). Increased expression of NAMPT in PBMC from patients with acute coronary syndrome and in inflammatory M1 macrophages. *Atherosclerosis* 243, 204–210. doi: 10.1016/j.atherosclerosis.2015.09.010

Hanifi-Moghaddam, P., Kappler, S., Seissler, J., Muller-Scholze, S., Martin, S., Roep, B. O., et al. (2006). Altered chemokine levels in individuals at risk of Type 1 diabetes mellitus. *Diabetes Med.* 23 (2), 156–163. doi: 10.1111/j.1464-5491.2005.01743.x

Huh, J. H., Kim, H. M., Lee, E. S., Kwon, M. H., Lee, B. R., Ko, H. J., et al. (2018). Dual CCR2/5 antagonist attenuates obesity-induced insulin resistance by regulating macrophage recruitment and M1/M2 status. *Obesity (Silver Spring)* 26, 378–386. doi: 10.1002/oby.22103

Hyde, C. L., Macinnes, A., Sanders, F. A., Thompson, J. F., Mazzarella, R. A., Faergeman, O., et al. (2010). Genetic association of the CCR5 region with lipid levels in at-risk cardiovascular patients. *Circ. Cardiovasc. Genet.* 3 (2), 162–168. doi: 10.1161/CIRCGENETICS.109.897793

Inayat, H., Azim, M. K., and Baloch, A. A. (2019). Analysis of inflammatory gene expression profile of peripheral blood leukocytes in type 2 diabetes. *Immunol. Invest.* 48, 618–631. doi: 10.1080/08820139.2019.1586917

Ishida, Y., Kimura, A., Kuninaka, Y., Inui, M., Matsushima, K., Mukaida, N., et al. (2012). Pivotal role of the CCL5/CCR5 interaction for recruitment of endothelial progenitor cells in mouse wound healing. *J. Clin. Invest.* 122 (2), 711–721. doi: 10.1172/JCI43027

Jordan, N. J., Watson, M. L., Williams, R. J., Roach, A. G., Yoshimura, T., and Westwick, J. (1997). Chemokine production by human vascular smooth muscle cells: modulation by IL-13. *Br. J. Pharmacol.* 122 (4), 749–757. doi: 10.1038/sj.bjp.0701433

Joussen, A. M., Poulaki, V., Qin, W., Kirchhof, B., Mitsiades, N., Wiegand, S. J., et al. (2002). Retinal vascular endothelial growth factor induces intercellular adhesion molecule-1 and endothelial nitric oxide synthase expression and initiates early diabetic retinal leukocyte adhesion *in vivo*. *Am. J. Pathol.* 160 (2), 501–509. doi: 10.1016/S0002-9440(10)64869-9

Kennedy, A., Webb, C. D., Hill, A. A., Gruen, M. L., Jackson, L. G., and Hasty, A. H. (2013). Loss of CCR5 results in glucose intolerance in diet-induced obese mice. *Am. J. Physiol. Endocrinol. Metab.* 305 (7), E897–E906. doi: 10.1152/ajpendo.00177.2013

Kim, E. J., Kim, Y. K., Kim, S., Kim, J. E., Tian, Y. D., Doh, E. J., et al. (2018). Adipochemokines induced by ultraviolet irradiation contribute to impaired fat metabolism in subcutaneous fat cells. *Br. J. Dermatol.* 178 (2), 492–501. doi: 10.1111/bjd.15907

Kitade, H., Sawamoto, K., Nagashimada, M., Inoue, H., Yamamoto, Y., Sai, Y., et al. (2012). CCR5 plays a critical role in obesity-induced adipose tissue inflammation and insulin resistance by regulating both macrophage recruitment and M1/M2 status. *Diabetes* 61 (7), 1680–1690. doi: 10.2337/db11-1506

Kochetova, O. V., Avzaletdinova, D. S., Morugova, T. V., and Mustafina, O. E. (2019). Chemokine gene polymorphisms association with increased risk of type 2 diabetes mellitus in Tatar ethnic group, Russia. *Mol. Biol. Rep.* 46 (1), 887–896. doi: 10.1007/s11033-018-4544-6

Kohlmeier, J. E., Reiley, W. W., Perona-Wright, G., Freeman, M. L., Yager, E. J., Connor, L. M., et al. (2011). Inflammatory chemokine receptors regulate CD8 (+) T cell contraction and memory generation following infection. *J. Exp. Med.* 208 (8), 1621–1634. doi: 10.1084/jem.20102110

Laurence, A. D. (2006). Location, movement and survival: the role of chemokines in haematopoiesis and malignancy. *Br. J. Haematol* 132, 255–267. doi: 10.1111/j.1365-2141.2005.05841.x

Li, G., Zhu, G., Gao, Y., Xiao, W., Xu, H., Liu, S., et al. (2013). Neferine inhibits the upregulation of CCL5 and CCR5 in vascular endothelial cells during chronic high glucose treatment. *Inflammation* 36 (2), 300–308. doi: 10.1007/s10753-012-9547-1

Lien, M. Y., Tsai, H. C., Chang, A. C., Tsai, M. H., Hua, C. H., Wang, S. W., et al. (2018). Chemokine CCL4 induces vascular endothelial growth factor C expression and lymphangiogenesis by miR-195-3p in oral squamous cell carcinoma. *Front. Immunol.* 9, 412. doi: 10.3389/fimmu.2018.00412

Lin, C. S., Hsieh, P. S., Hwang, L. L., Lee, Y. H., Tsai, S. H., Tu, Y. C., et al. (2018). The CCL5/CCR5 axis promotes vascular smooth muscle cell proliferation and atherogenic phenotype switching. *Cell. Physiol. Biochem.* 47, 707–720. doi: 10.1159/000490024

Liu, G. T., Chen, H. T., Tsou, H. K., Tan, T. W., Fong, Y. C., Chen, P. C., et al. (2014). CCL5 promotes VEGF-dependent angiogenesis by down-regulating miR-200b through PI3K/Akt signaling pathway in human chondrosarcoma cells. *Oncotarget* 5 (21), 10718–10731. doi: 10.18632/oncotarget.2532

Lu, P., Li, L., Wu, Y., Mukaida, N., and Zhang, X. (2008). Essential contribution of CCL3 to alkali-induced corneal neovascularization by regulating vascular endothelial growth factor production by macrophages. *Mol. Vis.* 14, 1614–1622. doi: 10.1016/j.molcel.2008.07.018

Lumeng, C. N., Bodzin, J. L., and Saltiel, A. R. (2007). Obesity induces a phenotypic switch in adipose tissue macrophage polarization. *J. Clin. Invest.* 117 (1), 175–184. doi: 10.1172/JCI29881

Mamazhakypov, A., Viswanathan, G., Lawrie, A., Schermuly, R. T., and Rajagopal, S. (2019). The role of chemokines and chemokine receptors in pulmonary arterial hypertension. *Br. J. Pharmacol.* doi: 10.1111/bph.14826

Margeirsdottir, H. D., Larsen, J. R., Brunborg, C., Overby, N. C., and Dahl-Jorgensen, K. (2008). High prevalence of cardiovascular risk factors in children and adolescents with type 1 diabetes: a population-based study. *Diabetologia* 51 (4), 554–561. doi: 10.1007/s00125-007-0921-8

McLeod, D. S., Lefer, D. J., Merges, C., and Lutty, G. A. (1995). Enhanced expression of intracellular adhesion molecule-1 and P-selectin in the diabetic human retina and choroid. *Am. J. Pathol.* 147 (3), 642–653. doi: 10.1097/00000433-199509000-00020

Menten, P., Wuyts, A., and Van Damme, J. (2002). Macrophage inflammatory protein-1. *Cytokine Growth Factor Rev.* 13 (6), 455–481. doi: 10.1016/s1359-6101(02)00045-x

Mezzano, S., Droguett, A., Burgos, M. E., Ardiles, L. G., Flores, C. A., Aros, C. A., et al. (2003). Renin-angiotensin system activation and interstitial inflammation in human diabetic nephropathy. *Kidney Int. Suppl.* 64 (86), S64–S70. doi: 10.1046/j.1523-1755.64.s86.12.x

Mikolajczyk, T. P., Nosalski, R., Szczepaniak, P., Budzyn, K., Osmenda, G., Skiba, D., et al. (2016). Role of chemokine RANTES in the regulation of perivascular inflammation, T-cell accumulation, and vascular dysfunction in hypertension. *FASEB J.* 30 (5), 1987–1999. doi: 10.1096/fj.201500088R

Mirabelli-Badenier, M., Braunersreuther, V., Viviani, G. L., Dallegri, F., Quercioli, A., Veneselli, E., et al. (2011). CC and CXC chemokines are pivotal mediators of cerebral injury in ischaemic stroke. *Thromb. Haemost.* 105 (3), 409–420. doi: 10.1160/TH10-10-0662

Mlynarski, W. M., Placha, G. P., Wolkow, P. P., Bochenski, J. P., Warram, J. H., and Krolewski, A. S. (2005). Risk of diabetic nephropathy in type 1 diabetes is associated with functional polymorphisms in RANTES receptor gene (CCR5): a sex-specific effect. *Diabetes* 54, 3331–3335. doi: 10.2337/diabetes.54.11.3331

Montecucco, F., Steffens, S., Burger, F., Da, C. A., Bianchi, G., Bertolotto, M., et al. (2008). Tumor necrosis factor-alpha (TNF-alpha) induces integrin CD11b/CD18 (Mac-1) up-regulation and migration to the CC chemokine CCL3 (MIP-1alpha) on human neutrophils through defined signalling pathways. *Cell Signal* 20 (3), 557–568. doi: 10.1016/j.cellsig.2007.11.008

Montecucco, F., Lenglet, S., Gayet-Ageron, A., Bertolotto, M., Pelli, G., Palombo, D., et al. (2010). Systemic and intraplaque mediators of inflammation are increased in patients symptomatic for ischemic stroke. *Stroke* 41, 1394–1404. doi: 10.1161/STROKEAHA.110.578369

Nazir, N., Siddiqui, K., Al-Qasim, S., and Al-Naqeb, D. (2014). Meta-analysis of diabetic nephropathy associated genetic variants in inflammation and angiogenesis involved in different biochemical pathways. *BMC Med. Genet.* 15, 103. doi: 10.1186/s12881-014-0103-8

Nikolopoulou, A., and Kadoglou, N. P. (2014). Obesity and metabolic syndrome as related to cardiovascular disease. *Expert Rev. Cardiovasc. Ther.* 10 (7), 933–939. doi: 10.1586/erc.12.74

O'Brien, P. D., Hinder, L. M., Parlee, S. D., Hayes, J. M., Backus, C., Zhang, H., et al. (2017). Dual CCR2/CCR5 antagonist treatment attenuates adipose inflammation, but not microvascular complications in ob/ob mice. *Diabetes Obes. Metab.* 19, 1468–1472. doi: 10.1111/dom.12950

Pai, J. K., Kraft, P., Cannuscio, C. C., Manson, J. E., Rexrode, K. M., Albert, C. M., et al. (2006). Polymorphisms in the CC-chemokine receptor-2 (CCR2) and -5 (CCR5) genes and risk of coronary heart disease among US women. *Atherosclerosis* 186, 132–139. doi: 10.1016/j.atherosclerosis.2005.06.041

Perez-Martinez, L., Ochoa-Callejero, L., Rubio-Mediavilla, S., Narro, J., Bernardo, I., Oteo, J. A., et al. (2018). Maraviroc improves hepatic triglyceride content but not inflammation in a murine nonalcoholic fatty liver disease model induced by a chronic exposure to high-fat diet. *Transl. Res.* 196, 17–30. doi: 10.1016/j.trsl.2018.01.004

Perticone, F., Maio, R., Tripepi, G., and Zoccali, C. (2004). Endothelial dysfunction and mild renal insufficiency in essential hypertension. *Circulation* 110 (7), 821–825. doi: 10.1161/01.CIR.0000138745.21879.27

Pisano, S., Catone, G., Coppola, G., Carotenuto, M., Iuliano, R., Tiano, C., et al. (2017). Different immune signature in youths experiencing antipsychotic-induced weight gain compared to untreated obese patients. *J. Child Adolesc. Psychopharmacol.* 27 (9), 844–848. doi: 10.1089/cap.2016.0203

Pothineni, N. V. K., Subramany, S., Kuriakose, K., Shirazi, L. F., Romeo, F., Shah, P. K., et al. (2017). Infections, atherosclerosis, and coronary heart disease. *Eur. Heart J.* 38 (43), 3195–3201. doi: 10.1093/eurheartj/ehx362

Potteaux, S., Combadiere, C., Esposito, B., Lecureuil, C., Ait-Oufella, H., Merval, R., et al. (2006). Role of bone marrow-derived CC-chemokine receptor 5 in the development of atherosclerosis of low-density lipoprotein receptor knockout mice. *Arterioscler. Thromb. Vasc. Biol.* 26, 1858–1863. doi: 10.1161/01.ATV.0000231527.22762.71

Prasad, P., Tiwari, A. K., Kumar, K. M., Ammini, A. C., Gupta, A., Gupta, R., et al. (2007). Association of TGFbeta1, TNFalpha, CCR2 and CCR5 gene polymorphisms in type-2 diabetes and renal insufficiency among Asian Indians. *BMC Med. Genet.* 8, 20. doi: 10.1186/1471-2350-8-20

Rask-Madsen, C., and King, G. L. (2007). Mechanisms of disease: endothelial dysfunction in insulin resistance and diabetes. *Nat. Clin. Pract. Endocrinol. Metab.* 3 (1), 46–56. doi: 10.1038/ncpendmet0366

Ridiandries, A., Tan, J. T., and Bursill, C. A. (2016). The role of CC-Chemokines in the regulation of angiogenesis. *Int. J. Mol. Sci.* 17 (11), 1856. doi: 10.3390/ijms17111856

Rookmaaker, M. B., Verhaar, M. C., de Boer, H. C., Goldschmeding, R., Joles, J. A., Koomans, H. A., et al. (2007). Met-RANTES reduces endothelial progenitor cell homing to activated (glomerular) endothelium *in vitro* and *in vivo*. *Am. J. Physiol. Renal Physiol.* 293 (2), F624–F630. doi: 10.1152/ajprenal.00398.2006

Rudemiller, N. P., and Crowley, S. D. (2017). The role of chemokines in hypertension and consequent target organ damage. *Pharmacol. Res.* 119, 404–411. doi: 10.1016/j.phrs.2017.02.026

Rudemiller, N. P., Patel, M. B., Zhang, J. D., Jeffs, A. D., Karlovich, N. S., Griffiths, R., et al. (2016). C-C Motif Chemokine 5 Attenuates Angiotensin II-Dependent Kidney Injury by Limiting Renal Macrophage Infiltration. *Am. J. Pathol.* 186 (11), 2846–2856. doi: 10.1016/j.ajpath.2016.07.015

Sharda, S., Gilmour, A., Harris, V., Singh, V. P., Sinha, N., Tewari, S., et al. (2008). Chemokine receptor 5 (CCR5) deletion polymorphism in North Indian patients with coronary artery disease. *Int. J. Cardiol.* 124, 254–258. doi: 10.1016/j.ijcard.2006.12.021

Shen, B., Li, J., Gao, L., Zhang, J., and Yang, B. (2013). Role of CC-chemokine receptor 5 on myocardial ischemia-reperfusion injury in rats. *Mol. Cell. Biochem.* 378, 137–144. doi: 10.1007/s11010-013-1604-z

Simeoni, E., Winkelmann, B. R., Hoffmann, M. M., Fleury, S., Ruiz, J., Kappenberger, L., et al. (2004). Association of RANTES G-403A gene polymorphism with increased risk of coronary arteriosclerosis. *Eur. Heart J.* 25, 1438–1446. doi: 10.1016/j.ehj.2004.05.005

Skrzypkowska, M., Slominski, B., Ryba-Stanislawowska, M., Lawrynowicz, U., Gutknecht, P., and Siebert, J. (2019). New mechanisms of CCR5-Delta32 carriers' advantage - Impact on progenitor cells and renal function. *Int. J. Biochem. Cell Biol.* 108, 92–97. doi: 10.1016/j.biocel.2019.01.006

Slominski, B., Lawrynowicz, U., Mysliwska, J., Ryba-Stanislawowska, M., Skrzypkowska, M., and Brandt, A. (2017). CCR5-Delta32 gene polymorphism is associated with retinopathy in patients with type 1 diabetes. *Mol. Cell Endocrinol.* 439, 256–260. doi: 10.1016/j.mce.2016.09.009

Slominski, B., Lawrynowicz, U., Ryba-Stanislawowska, M., Skrzypkowska, M., Mysliwska, J., and Mysliwiec, M. (2019). CCR5-Delta32 polymorphism is a genetic risk factor associated with dyslipidemia in patients with type 1 diabetes. *Cytokine* 114, 81–85. doi: 10.1016/j.cyto.2018.11.005

Soehnlein, O., Drechsler, M., Doring, Y., Lievens, D., Hartwig, H., Kemmerich, K., et al. (2013). Distinct functions of chemokine receptor axes in the atherogenic mobilization and recruitment of classical monocytes. *EMBO Mol. Med.* 5, 471–481. doi: 10.1002/emmm.201201717

Sorce, S., Myburgh, R., and Krause, K. H. (2011). The chemokine receptor CCR5 in the central nervous system. *Prog. Neurobiol.* 93 (2), 297–311. doi: 10.1016/j.pneurobio.2010.12.003

Suffee, N., Hlawaty, H., Meddahi-Pelle, A., Maillard, L., Louedec, L., Haddad, O., et al. (2012). RANTES/CCL5-induced pro-angiogenic effects depend on CCR1, CCR5 and glycosaminoglycans. *Angiogenesis* 15 (4), 727–744. doi: 10.1007/s10456-012-9285-x

Suffee, N., Le Visage, C., Hlawaty, H., Aid-Launais, R., Vanneaux, V., Larghero, J., et al. (2017). Pro-angiogenic effect of RANTES-loaded polysaccharide-based microparticles for a mouse ischemia therapy. *Sci. Rep.* 7, 13294. doi: 10.1038/s41598-017-13444-7

Tatara, Y., Ohishi, M., Yamamoto, K., Shiota, A., Hayashi, N., Iwamoto, Y., et al. (2009). Macrophage inflammatory protein-1beta induced cell adhesion with increased intracellular reactive oxygen species. *J. Mol. Cell. Cardiol.* 47, 104–111. doi: 10.1016/j.yjmcc.2009.03.012

Ting, K. H., Ueng, K. C., Chiang, W. L., Chou, Y. E., Yang, S. F., and Wang, P. H. (2015). Relationship of Genetic Polymorphisms of the Chemokine, CCL5, and Its Receptor, CCR5, with Coronary Artery Disease in Taiwan. *Evid. Based Complement Alternat. Med.* 2015, 851683. doi: 10.1155/2015/851683

Turner, J. E., Paust, H. J., Steinmetz, O. M., Peters, A., Meyer-Schwesinger, C., Heymann, F., et al. (2008). CCR5 deficiency aggravates crescentic glomerulonephritis in mice. *J. Immunol.* 181 (9), 6546–6556. doi: 10.4049/jimmunol.181.9.6546

Van der Vorst, E., Peters, L., Muller, M., Gencer, S., Yan, Y., Weber, C., et al. (2019). G-protein coupled receptor targeting on myeloid cells in atherosclerosis. *Front. Pharmacol.* 10, 531. doi: 10.3389/fphar.2019.00531

Veillard, N. R., Kwak, B., Pelli, G., Mulhaupt, F., James, R. W., Proudfoot, A. E., et al. (2004). Antagonism of RANTES receptors reduces atherosclerotic plaque formation in mice. *Circ. Res.* 94, 253–261. doi: 10.1161/01.RES.0000109793.17591.4E

Vogiatzi, K., Voudris, V., Apostolakis, S., Kochiadakis, G. E., Thomopoulou, S., Zaravinos, A., et al. (2009). Genetic diversity of RANTES gene promoter and susceptibility to coronary artery disease and restenosis after percutaneous coronary intervention. *Thromb. Res.* 124, 84–89. doi: 10.1016/j.thromres.2008.12.043

Wada, T., Furuichi, K., Segawa-Takaeda, C., Shimizu, M., Sakai, N., Takeda, S. I., et al. (1999). MIP-1alpha and MCP-1 contribute to crescents and interstitial lesions in human crescentic glomerulonephritis. *Kidney Int.* 56 (3), 995–1003. doi: 10.1046/j.1523-1755.1999.00646.x

Weber, C. (2005). Platelets and chemokines in atherosclerosis: partners in crime. *Circ. Res.* 96 (6), 612–616. doi: 10.1161/01.RES.0000160077.17427.57

Werts, C., le Bourhis, L., Liu, J., Magalhaes, J. G., Carneiro, L. A., Fritz, J. H., et al. (2007). Nod1 and Nod2 induce CCL5/RANTES through the NF-kappaB pathway. *Eur. J. Immunol.* 37 (9), 2499–2508. doi: 10.1002/eji.200737069

Wolf, G., Ziyadeh, F. N., Thaiss, F., Tomaszewski, J., Caron, R. J., Wenzel, U., et al. (1997). Angiotensin II stimulates expression of the chemokine RANTES in rat glomerular endothelial cells. Role of the angiotensin type 2 receptor. *J. Clin. Invest.* 100 (5), 1047–1058. doi: 10.1172/JCI119615

Yahya, M. J., Ismail, P. B., Nordin, N. B., Akim, A., Yusuf, W., Adam, N., et al. (2019). Association of CCL2, CCR5, ELMO1, and IL8 Polymorphism with diabetic nephropathy in malaysian type 2 diabetic patients. *Int. J. Chronic Dis.* 2019, 2053015. doi: 10.1155/2019/2053015

Yan, D., Zhang, D., Lu, L., Qiu, H., and Wang, J. (2019). Vascular endothelial growth factor-modified macrophages accelerate reendothelialization and attenuate neointima formation after arterial injury in atherosclerosis-prone mice. *J. Cell. Biochem.* 120, 10652–10661. doi: 10.1002/jcb.28355

Yang, L. X., Heng, X. H., Guo, R. W., Si, Y. K., Qi, F., and Zhou, X. B. (2013). Atorvastatin inhibits the 5-lipoxygenase pathway and expression of CCL3 to alleviate atherosclerotic lesions in atherosclerotic ApoE knockout mice. *J. Cardiovasc. Pharmacol.* 62, 205–211. doi: 10.1097/FJC.0b013e3182967fc0

Yao, L., Herlea-Pana, O., Heuser-Baker, J., Chen, Y., and Barlic-Dicen, J. (2014). Roles of the chemokine system in development of obesity, insulin resistance, and cardiovascular disease. *J. Immunol. Res.* 2014, 181450. doi: 10.1155/2014/181450

Zhang, Z., Dong, J., Lobe, C. G., Gong, P., Liu, J., and Liao, L. (2015b). CCR5 facilitates endothelial progenitor cell recruitment and promotes the stabilization of atherosclerotic plaques in ApoE$^{-/-}$ mice. *Stem Cell Res. Ther.* 6, 36. doi: 10.1186/s13287-015-0026-0

Zhang, Z., Liu, J., Wang, H., Wu, H., Wu, X., Dong, J., et al. (2015a). Association between chemokine receptor 5 (CCR5) delta32 gene variant and atherosclerosis: a meta-analysis of 13 studies. *Int. J. Clin. Exp. Med.* 8, 658–665.

Zhang, Z., Zhang, X., Dong, J., Gao, W., Liu, F., Zhao, J., et al. (2016). Association of chemokine ligand 5/chemokine receptor 5 gene promoter polymorphisms with diabetic microvascular complications: A meta-analysis. *J. Diabetes Invest.* 7, 212–218. doi: 10.1111/jdi.12397

Conflict of Interest: The authors declare that the research was conducted in the absence of any commercial or financial relationships that could be construed as a potential conflict of interest.

frontiers in Pharmacology

MINI REVIEW
published: 04 March 2020
doi: 10.3389/fphar.2020.00148

The Vascular Consequences of Metabolic Syndrome: Rodent Models, Endothelial Dysfunction, and Current Therapies

Vivian Tran, T. Michael De Silva, Christopher G. Sobey, Kyungjoon Lim, Grant R. Drummond, Antony Vinh†* and Maria Jelinic*†*

Department of Physiology, Anatomy and Microbiology, La Trobe University, Bundoora, VIC, Australia

OPEN ACCESS

Edited by:
Chen Huei Leo, Singapore University of Technology and Design, Singapore

Reviewed by:
Wolfgang F. Graier, Medical University of Graz, Austria
Carlos F. Sánchez-Ferrer, Autonomous University of Madrid, Spain

***Correspondence:**
Antony Vinh
a.vinh@latrobe.edu.au

†These authors have contributed equally to this work

Specialty section:
This article was submitted to Cardiovascular and Smooth Muscle Pharmacology, a section of the journal Frontiers in Pharmacology

Received: *30 November 2019*
Accepted: *04 February 2020*
Published: *04 March 2020*

Citation:
Tran V, De Silva TM, Sobey CG, Lim K, Drummond GR, Vinh A and Jelinic M (2020) The Vascular Consequences of Metabolic Syndrome: Rodent Models, Endothelial Dysfunction, and Current Therapies. Front. Pharmacol. 11:148. doi: 10.3389/fphar.2020.00148

Metabolic syndrome is characterized by visceral obesity, dyslipidemia, hyperglycemia and hypertension, and affects over one billion people. Independently, the components of metabolic syndrome each have the potential to affect the endothelium to cause vascular dysfunction and disrupt vascular homeostasis. Rodent models of metabolic syndrome have significantly advanced our understanding of this multifactorial condition. In this mini-review we compare the currently available rodent models of metabolic syndrome and consider their limitations. We also discuss the numerous mechanisms by which metabolic abnormalities cause endothelial dysfunction and highlight some common pathophysiologies including reduced nitric oxide production, increased reactive oxygen species and increased production of vasoconstrictors. Additionally, we explore some of the current therapeutics for the comorbidities of metabolic syndrome and consider how these benefit the vasculature.

Keywords: endothelial dysfunction, vascular disease, cardiometabolic abnormalities, nitric oxide, reactive oxygen species

OVERVIEW

Metabolic syndrome is a growing epidemic affecting ~20% of adults (over a billion people) (O'Neill and O'Driscoll, 2015; Saklayen, 2018). This complex, multifactorial disorder arising from metabolic disturbances is characterized by visceral obesity, dyslipidemia, hyperglycemia and hypertension (Grundy et al., 2005). Another characteristic of metabolic syndrome is chronic low-grade inflammation (De Ferranti and Mozaffarian, 2008; Sharma, 2011). These factors all contribute to the elevated risk of cardiovascular disease, acute cardiovascular events (including stroke and myocardial infarction), type 2 diabetes mellitus (T2DM), or further complications such as renal disease (O'Neill and O'Driscoll, 2015; Tune et al., 2017). Vascular dysfunction is a key contributor to the pathogenesis of all of these disorders (Rajendran et al., 2013). Metabolic syndrome not only causes social and economic burdens, but significantly impacts morbidity and mortality. This review will describe how metabolic syndrome affects the regulation of vascular function and tone. Specifically, we will focus on rodent models of metabolic syndrome, highlighting the changes that occur to endothelial function and adipose tissue and

consider relevance to clinical translation in humans. We will also discuss potential areas for further research to advance knowledge on vascular pathophysiology in metabolic syndrome.

Current Rodent Models for Metabolic Syndrome

An ideal translational animal model for metabolic syndrome would closely resemble the human anatomy and pathophysiology of the disease (Emini Veseli et al., 2017). Thus, an important consideration when choosing an animal model is that it mimics the key clinical criteria that define metabolic syndrome. The International Diabetes Federation defines metabolic syndrome as central obesity and at least two of the following: dyslipidemia (>150 mg/dl plasma triglycerides and/or reduced high-density lipoproteins (HDL) < 40 mg/dl for men and <50 mg/dl for women), elevated blood pressure (≥130 mmHg systolic and/or ≥ 85 mmHg diastolic), or hyperglycemia (≥100 mg/dl fasting plasma glucose) (Alberti et al., 2006). Importantly, many patients do not present with all of these classifications, and similarly there is no one animal model that mimics all of these abnormalities of metabolic syndrome.

Genetic Mouse Models

Genetic models of obesity and diabetes allow for the evaluation of specific molecular mechanisms. C57BL/6J-*Lep*^{ob} mice, more commonly known as *ob/ob* mice, were one of the first genetic models of obesity. These mice lack leptin due to a spontaneous homozygous mutation on the leptin gene, causing marked obesity, hyperinsulinemia, and hyperglycemia by 12 weeks of age. By approximately 24 weeks of age, *ob/ob* mice develop left ventricular hypertrophy and cardiac fibrosis and are in a pro-inflammatory state (La Cava, 2017). The C57BL/KsJ-db/db (*db/db*) mouse is a related genetic mouse model, which has a defective leptin receptor (Wang et al., 2014). By 13 weeks of age, *db/db* mice are overweight and have hyperglycemia and dyslipidemia (increased plasma triglycerides, total cholesterol, and non-esterified fatty acids). Importantly, endothelium-dependent aortic relaxation to acetylcholine (ACh) is impaired whereas that to direct nitric oxide donors remains unaffected, indicating endothelial dysfunction (Dong et al., 2010). Additionally, *db/db* mice have elevated circulating leptin which promotes a pro-inflammatory state, linked to the increased activity of interleukin-6 (IL-6) (La Cava, 2017). Neither *ob/ob* nor *db/db* mice, however, display increased blood pressure—unlike a large proportion of humans with metabolic syndrome—and are therefore not ideal models for the many such people with metabolic syndrome (Mark et al., 1999).

Genetic Rat Models

Zucker Fatty rats are among the most common genetic rat models of metabolic syndrome and are deficient in the leptin receptor due to a missense mutation in the gene. This increases circulating leptin levels and rats are obese by 3–5 weeks of age (Aleixandre de Artinano and Miguel Castro, 2009). These rats variably develop hyperglycemia (the severity is variable between studies, and sometimes within the same cohort), dyslipidemia, and hypertension (Zucker and Zucker, 1961; Marsh et al., 2007; Yokoi et al., 2013; Wang et al., 2014; Wong et al., 2016). However, several studies also report conflicting data, with lower systolic blood pressure in Zucker fatty rats compared to the lean controls (Aleixandre de Artinano and Miguel Castro, 2009). Thus, while in some studies the model does appear to accurately reflect the presentation of metabolic syndrome patients in the clinic, inconsistencies between different studies make it difficult to develop definitive conclusions.

The Dahl salt-sensitive rat is widely used to study salt-induced hypertension and, when crossed with Zucker fatty rats, the resulting offspring are DahlS.Z-Lepr^{fa}/Lepr^{fa} (DS/obese) rats. DS/obese rats have hyperphagia and develop abdominal obesity, hypertension, dyslipidemia, and T2DM and thus, appear to be a useful model for advanced metabolic syndrome (Hattori et al., 2011). Obese spontaneously hypertensive rats (also known as Koletsky rats) are another animal model used to study metabolic syndrome. These rats are obese by 5 weeks of age and develop hyperlipidemia even when fed a normal chow diet. Mild hyperinsulinemia is present with only slight hyperglycemia. At 3 months of age, spontaneous hypertension occurs with mean arterial pressure rising to ≥180 mmHg (Aleixandre de Artinano and Miguel Castro, 2009).

Diet-Induced Rodent Models

Diet modifications are often used to study metabolic syndrome due to pronounced effects on metabolism and in turn, hormonal, glucose, and lipid pathways. Fructose-enriched diets are effective for inducing metabolic syndrome and act *via* several mechanisms to promote obesity (Johnson et al., 2007). Mechanisms relevant to the satiety center suggest that fructose stimulates the production of insulin and leptin but inhibits ghrelin (Teff et al., 2004). Other studies suggest that the addition of fructose simply makes food more appetizing and stimulates increased food intake and weight gain (Lowette et al., 2015). Simple and complex carbohydrates are essential nutrients and the main source of energy for the body. Adopting a sedentary lifestyle in conjunction with excessive carbohydrate consumption can result in an imbalance in energy, which increases blood glucose and increases release of insulin. This imbalance predisposes individuals to weight gain and decreases insulin sensitivity (Wong et al., 2016).

A high fat diet (HFD) can also be used to induce metabolic syndrome. Mice fed a HFD from 4 to 6 weeks of age develop obesity, hyperglycemia, and endothelial dysfunction after 10 weeks (Kobayasi et al., 2010; Liu et al., 2016). In some instances, systolic blood pressure is mildly raised (by ~10 mmHg), suggesting a pre-hypertensive state (Taylor et al., 2018). HFD mice have increased quantities of white adipose tissue, which enhances the expression of pro-inflammatory mediators such as tumor necrosis factor alpha (TNF-α). This mechanism is thought to be a key driver for insulin resistance in obesity (Makki et al., 2013). To date, numerous types of HFD regimens have been used, with variations in the amount of fat (20 to 60% of total energy) and its source (lard, beef tallow, olive, or coconut oil) as well as the duration of feeding and age of animals. The fat source appears to be particularly important. Fats derived from lard, coconut and olive oil increase body weight, plasma insulin and triglyceride and decrease plasma adiponectin concentrations in male Wistar rats (Buettner et al., 2006). Alternatively, beef tallow derived-fat increases plasma leptin, insulin, and lipid concentrations (Hsu et al., 2009).

HFD rodent models display most of the features of metabolic syndrome, but patients with metabolic syndrome would typically consume a higher proportion of simple carbohydrates than most HFD models in the literature (Panchal and Brown, 2011). Diets comprising both high fat and high carbohydrate components promote even more of the features of metabolic syndrome in rodents and are therefore more clinically representative than just HFD alone (Panchal and Brown, 2011). One potential criticism of these diet-induced models is that they rarely lead to atherosclerosis. Thus, HFD regimens are often combined with mice that are genetically dyslipidemic to incorporate the atherosclerotic phenotype in metabolic syndrome. For example, apolipoprotein E-deficient ($ApoE^{-/-}$) mice and low density lipoprotein receptor deficient ($LDLR^{-/-}$) mice show similar metabolic profiles to the diet-induced models described above, but have the added complication of advanced atherosclerosis (Emini Veseli et al., 2017).

Despite there being a variety of rodent models of metabolic syndrome available (summarized in **Table 1**), the precise mechanisms behind the progression to a diseased vascular state remain poorly understood. Obesity and the abnormalities associated with metabolic syndrome (i.e., hypertension, dyslipidemia, hyperglycemia) adversely impact vascular structure and function (Beckman et al., 2002). The remainder of this review will address this.

The Role of Metabolic Syndrome Comorbidities on Endothelial Dysfunction

Endothelial dysfunction predisposes the vasculature to a heightened contractile state due to an imbalance between endothelium-derived relaxing (e.g., NO, PGI_2, EDH downregulation) and contracting factors (e.g., TxA_2, ET-1 upregulation) (Guzik et al., 2000; Lerman and Zeiher, 2005). Endothelial dysfunction also promotes pro-inflammatory and oxidative stress pathways *via* endothelial mitochondrial reactive oxygen species (ROS) driving vascular growth and remodeling (Cai and Harrison, 2000; Shenouda et al., 2011; Widlansky and Gutterman, 2011). This fundamental switch of the endothelium in metabolic syndrome to a dysfunctional state, involves the host immune system and production of ROS (Deanfield et al., 2007), and the progression of diseases occurs *via* a variety of dynamic changes within the vasculature (**Figure 1**). There are many detailed reviews regarding the function of the endothelium in a physiological state (Cai and Harrison, 2000; Endemann and Schiffrin, 2004; Hadi et al., 2005; Rajendran et al., 2013), and thus, this review will focus on the mechanisms of endothelial dysfunction that accompany the comorbidities of metabolic syndrome. Some animal models of metabolic syndrome inherently present with multiple comorbidities—for example diet-induced models may present hyperglycemia, dyslipidemia, and obesity. However, the studies mentioned in this section focus on individual comorbidities and their effect on endothelial dysfunction.

Hyperglycemia

In *db/db and ob/ob* mice, endothelium-dependent vasodilatation is impaired in the coronary arterioles, aorta, and mesenteric arteries. This impairment is associated with enhanced superoxide production and the activation of immune responses downstream of the NACHT, LRR, and PYD domains-containing protein 3

TABLE 1 | Summary of different rodent models of metabolic syndrome and their effects on varying vessels.

Model	Age	Species	Sex	Vessel	Effect of metabolic syndrome	Ref
HFD (45% kcal from fat) for 32 weeks	37 weeks	C57BL/6J mice	M	MA	↑ Superoxide and NOX activity in PVAT	(Gil-Ortega et al., 2014)
WD (30% fructose, 20% lard, 18% protein, 5% cellulose) for 42 weeks	50 weeks	Sprague-Dawley rats	M	TA	↑ROCK pathway associated with insulin resistance	(Elrashidy et al., 2019)
High carbohydrate, HFD (% kcal from fat + 15% fructose in drinking water)	24 weeks	Sprague-Dawley rats	M	CA, MA	↑Insulin sensitivity and lipid profiles; ↓SBP	(Senaphan et al., 2015)
HFD (59% kcal from fat) for 16 weeks	24 weeks	Swiss mice	F	Aorta	↑ SBP and DBP; ↓ aortic relaxation to ACh but not SNP; ⟷ aortic IL-1β and IL-6 protein expression; ↓ aortic NF-kB	(Kobayasi et al., 2010)
HFD (42% kcal from fat) for 30 weeks	35 weeks	C57BL/6J mice	M	TA, CA	↑Prostanoids and vascular thromboxane receptor gene expression	(Traupe et al., 2002)
C57BL/6J-*Lep^{ob} (ob/ob)*	27–32 weeks	C57BL/6J mice	M	Aorta MA	↑Plasma insulin, PKC activity, GRK2 protein levels; ↓aortic insulin-induced relaxation, ACh-induced relaxation	(Winters et al., 2000; Taguchi et al., 2011)
C57BL/KsJ-db/db (*db/db*)	16 weeks	C57BL/KsJ mice	M	MA	↑Production of superoxide anions; ↓ACh-induced relaxation and BH_4 bioavailability	(Pannirselvam et al., 2002)
Zucker diabetic fatty (ZDF *fa/fa*) rat	9–11 weeks	Zucker diabetic fatty rats	M	Aorta	↑FFA-induced NADPH oxidase activation and ROS production	(Chinen et al., 2007)
Spontaneously hypertensive rats	14 months	Spontaneously hypertensive rats	M	TA	↑ROS formation, NADPH oxidase activity and protein expression of NOX 1 and NOX 2; ↓ACh-induced relaxation	(Wind et al., 2010)
HFD (20.5% protein, 35.7% carbohydrates, and 36.0% fat)	24–28 weeks	Dahl-Salt Sensitive rats	F and M	Aorta	↑HFD male and female SBP at 4 weeks and CD4+ T cells and T helper cells, greater CD3+ T cells in males, and greater % of pro-inflammatory T cells in males	(Taylor et al., 2018)

ACh, acetylcholine; BH_4, tetrahydrobiopterin; CA, carotid arteries; DBP, diastolic blood pressure; F, female; FFA, free fatty acid; GRK2, G protein-coupled receptor kinase 2; HFD, high fat diet; IL, interleukin; Kcal, kilocalorie; M, male; MA, mesenteric arteries; NF-kB, nuclear factor kappa beta; NOX, NADPH oxidase; PKC, protein kinase C; PVAT, perivascular adipose tissue; ROCK, Rho kinase; SBP, systolic blood pressure; SNP, sodium nitroprusside; TA, thoracic aorta; WD, western diet.

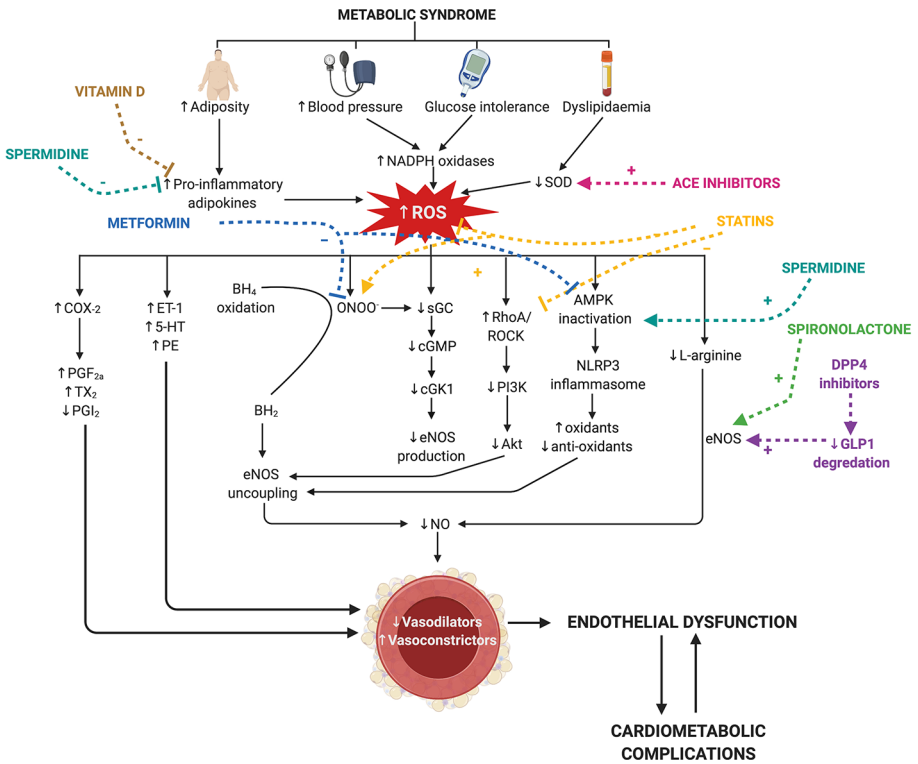

FIGURE 1 | Current therapies for the comorbidities of metabolic syndrome, targetting nitric oxide and reactive oxygen species signaling in endothelial dysfunction. Metabolic syndrome is characterized by an increase in visceral adiposity, blood pressure, glucose intolerance, and dyslipidemia. Individually, these co-morbidities induce endothelial dysfunction by increasing reactive oxygen species (ROS) and reducing nitric oxide (NO; pathways indicated in black). ROS is increased *via* increases in nicotinamide adenine dinucleotide phosphate (NADPH) oxidase and pro-inflammatory adipokines and reductions in superoxide dismutase (SOD). This reduces endothelial nitric oxide synthase (eNOS) production *via* two key mechanisms: reduced L-arginine conversion and soluble guanylate cyclase (sGC) activity. Uncoupling of eNOS occurs *via* two mechanisms [tetrahydrobiopterin (BH_4) and 5′-AMP-activated protein kinase (AMPK) inactivation] to further reduce eNOS activity. Increased cyclooxygenase-2 (COX-2) activity drives the production of vasoconstrictor prostanoids (PGF_{2a}, prostaglandin F2α; TXA_2, thromboxane A2) and decreases prostacyclin (PGI_2) production. ROS also drives the production of other endothelium-derived contracting factors (ET-1= endothelin-1, 5-HT= serotonin and PE= phenylephrine). Many first-line therapeutic drugs for the co-morbidities of metabolic syndrome (colored) target these mechanisms. Metformin (blue) reduces AMPK inactivation and peroxynitrite (ONOO-) production. Angiotensin converting enzyme (ACE) inhibitors (pink) reduce SOD activity. Statins (yellow) reduce AMPK inactivation and ROS production and increase sGC activity. Spironolactone and dipeptidyl peptidase-4 (DPP4) increase eNOS activity. Spermidine (turquoise) and vitamin D (dark yellow) inhibit the activation of pro-inflammatory adipokines released from adipose tissue, and spermidine promotes AMPK activation. BH_2, 7,8-dihydrobiopterin; cGMP, cyclic guanosine-3′,5′-monophosphate; cGK1, cGMP-dependent protein kinase-1; ROCK, RhoA associated protein kinase; GLP1, glucagon-like peptide 1. Created with BioRender.com.

inflammasome, which reduces the function of endothelium-dependent relaxing factors and the regulation of insulin (Bagi et al., 2003; Okon et al., 2003; Vandanmagsar et al., 2011). Endothelial dysfunction is not only a consequence of insulin resistance, but also impairs insulin signaling to further reduce insulin sensitivity, thereby resulting in a destructive cycle in metabolic syndrome and diabetes. In obese Zucker rats, altered insulin signaling disrupts insulin-mediated NO production (*via* downregulation of eNOS expression) to impair vasodilatation in resistance arteries. The involvement of ROS and subsequent degradation of BH_4 (a cofactor essential for NO synthesis from eNOS) synthesis in insulin resistance is thought to play a role in the impairment of NO-dependent vasodilatation (Eringa et al., 2007). In T2DM patients, ROS reduces the availability of BH_4 (Heitzer et al., 2000). Reduced interaction between BH_4 and eNOS leads to eNOS uncoupling and production of superoxide instead of NO (Heitzer et al., 2000). In that study, an infusion of BH_4 partially counteracted the reduced ACh-induced vasodilation, demonstrating that eNOS uncoupling and reduction of NO availability contribute to endothelial dysfunction in T2DM (Heitzer et al., 2000). An early study using female streptozotocin (STZ)-induced diabetic rats found impaired endothelial function in mesenteric arteries due mainly to altered production of vasodilators rather than ROS (Taylor et al., 1992). Endothelial dysfunction is region-specific in this model— as endothelial impairment was absent in the aortae of the diabetic animals (Taylor et al., 1994). The therapeutic potential of antioxidants has been a key area of interest in hyperglycemia research due to their ability to scavenge/neutralize ROS (Morrow et al., 2003; Davis et al., 2006; Versari et al., 2009). However, large clinical studies have investigated the effects of anti-oxidant vitamins (such as vitamin E and C) in diabetes, and these did not reduce the incidence of vascular disease (Heart Protection Study Collaborative

G, 2002; Xu and Zou, 2009). Furthermore, acute hyperglycemia promotes vasoconstrictor-prostanoid production and thus, an increased vascular smooth muscle cells (VSMC) contractility and vascular tone (Bagi et al., 2003; Okon et al., 2003).

There are a number of therapeutics available for the treatment of hyperglycemia. Pharmacological therapies such as thiazolidinediones, statins, and metformin not only improve insulin sensitivity, but also endothelium-dependent vasodilation in patients with type 2 diabetes (Paniagua et al., 2002; Yee A et al., 2004; Xu and Zou, 2009) and in diabetic rodent studies (Kanda M and Ichihara, 2003; Wong et al., 2006). Metformin is the first-line drug used for the treatment of hyperglycemia. Despite this, the precise mechanisms by which metformin lowers blood glucose levels are still unclear, but AMPK activation is thought to be a key target of action (Eriksson and Nystrom, 2014). AMPK is also thought to be a potential target in reversing endothelial dysfunction by promoting eNOS phosphorylation to stimulate NO production (Davis et al., 2006; Xu and Zou, 2009). Conversely, cell-culture studies indicate that this occurs independently of AMPK activation in mouse microvascular endothelial cells, but rather *via* eNOS and Akt phosphorylation (Ghosh et al., 2015). Thus, the involvement of AMPK in metformin therapy may require the involvement of other cell-types. A newer therapeutic strategy for hyperglycemia is glucagon-like peptide-1 receptor agonists and dipeptidyl peptidase-4 inhibitors. Glucagon-like peptide-1 is a direct endothelium-dependent vasodilator, and is also NOS-dependent. The vasoprotective effects of glucagon-like peptide-1 receptor agonists have been shown in a number of clinical studies too, however, there are also studies that show detrimental effects on the vasculature (Ban et al., 2008). Such detrimental effects appear to occur with chronic long-term administration (>4 weeks), highlighting the importance of determining long-term effects of hyperglycemia medications on the vasculature.

Dyslipidemia

Endothelial relaxation is impaired *via* multiple pathways in dyslipidemia. In humans with hypercholesterolemia, ACh-induced vasodilatation is reduced, whereas G_i-independent bradykinin-induced vasodilatation remains unchanged (Matsumoto et al., 2004; Gendron et al., 2007).This indicates a selective loss of some vasorelaxation pathways in hypercholesterolemia (Matsumoto et al., 2004; Gendron et al., 2007). Rodent models have been previously used to study lipid metabolism and its links to cardiovascular disease, however there are significant differences between lipid metabolism in rodents and humans. For example, mice carry the majority of plasma cholesterol in HDL, whereas humans carry it in low-density lipoproteins (LDL) (Gordon et al., 2015). However, there are similarities between the species that should be noted. For the protein diversity of HDL and LDL size ranges are similar in both humans and mice, and mice have minor proteins that are identified in humans which play a role in inflammation and innate immunity (Gordon et al., 2015). The majority of rodent dyslipidemia studies to date (characterized by increased triglycerides, decreased HDL and abnormal LDL) have been performed in $ApoE^{-/-}$ mice. Interestingly, despite severe hypercholesterolemia, young $ApoE^{-/-}$ mice have normal vascular function. Importantly, once challenged with either HFD or ageing to induce atherosclerotic lesions, relaxation (both endothelial-dependent and -independent) is impaired.

In non-rodent animal models, such as hypercholesterolemic rabbits, L-arginine treatment inhibits atherosclerosis and improves NO-mediated vasodilatation in thoracic and abdominal aortae and iliac arteries by enhanced NO synthesis and eNOS expression (Jeremy et al., 1996; Hayashi et al., 2005) The increased levels of oxidized low-density LDL in dyslipidemia has cytotoxic potential and atherogenic properties, and may also attenuate NO activity. In cultured human endothelial cells, oxidized LDL exposure decreased eNOS messenger RNA (mRNA) expression (Shi et al., 2014). In human umbilical vein endothelial cells, eNOS mRNA degradation is also linked to upregulation of the pro-inflammatory cytokine TNF-α in atherosclerotic lesions. Therefore, pro-inflammatory cytokines that interfere with eNOS mRNA levels may reduce eNOS activity and impair vasorelaxation in dyslipidemia (Yoshizumi et al., 1993). Transmembrane receptor LOX-1 can also directly mediate oxidized LDL inducing superoxide formation through the activation of nuclear factor kappa B (Cominacini et al., 2000; Sangle and Shen, 2010). Not only does this contribute to lipid accumulation through macrophages and inflammatory cytokines, high levels of circulating oxidized LDL acts on receptors that decrease L-arginine availability, thus altering NO production and ultimately endothelial function (Saraswathi and Hasty, 2006). Statins are used in the clinic to lower blood LDL cholesterol. An added benefit of statins is that they also reverse endothelial dysfunction in dyslipidemic patients (Bonetti et al., 2003). Cell culture studies confirm that statins stabilize eNOS mRNA to increase NO production in human endothelial cells (Bonetti et al., 2003). Additionally, statins λ also reduce nicotinamide adenine dinucleotide phosphate (NADPH) oxidase activity by downregulating NOX-1 mRNA expression, thus suppressing O_2^- generation in hypertensive rats further contributing to the protective effects of statins (Wassmann et al., 2002; Antonopoulos et al., 2012). Spermidine, a precursor to polyamines, has been shown to exert anti-inflammatory properties, and to inhibit age-related oxidative protein damage and ROS. To target lipid metabolism, spermidine induces AMPK pathway to regulate autophagy, in turn inhibiting expression of fatty acids (Gao et al., 2018).

Obesity

In obesity, the severity of endothelial dysfunction strongly correlates with the degree of visceral adiposity (Lobato et al., 2012). This is likely to be due to multiple pathways, such as adipocyte hypertrophy, hypoxia and macrophage infiltration (Leal Vde and Mafra, 2013). Similar to hypertensive conditions, visceral adiposity increases oxidative stress, and promotes changes in the pro-inflammatory adipokine profile resulting in eNOS uncoupling (Li et al., 2015). Specifically, circulating pro-inflammatory adipokines such as visfastin, apelin, retinol binding protein-4, vaspin, serum amyloid A, plasminogen activator inhibitor-1, angiotensinogen, chemerin and are increased in obesity. Conversely, obesity is associated with reduced adiponectin, omentin, and zinc-α2-glycoprotein (Leal Vde and Mafra, 2013). In obesity, NADPH oxidase upregulation also accentuates ROS production and induce endothelial dysfunction in

the aorta (Serpillon et al., 2009; Jiang et al., 2011). In endothelial cells, the nuclear factor-κB (NF-κB) pathway mediates inflammation by increasing ROS production and reducing NO production (Kobayasi et al., 2010). Additionally, surrounding adipocytes secrete products that stimulate the increase of adhesion molecules and apoptosis of endothelial cells (Kobayasi et al., 2010). Although obese patients present with elevated NF-κB expression, it is unknown whether the direct inhibition of this pathway improves endothelium-dependent relaxation (Silver et al., 2007). Weight loss is the primary objective for obese patients. In obese patients with essential hypertension, calorie restriction demonstrated beneficial effects and improvement in endothelium-dependent vasodilation stimulating an increased release of nitric oxide (Sasaki et al., 2002).

In diet-induced obese mice, vascular dysfunction (in the thoracic aorta and carotid artery) is associated with increased thromboxane gene expression and vasoconstrictor prostanoids (Traupe et al., 2002). Non-selective COX inhibition blocks ACh-induced contraction but selective inhibition of COX-2 is without effect (Traupe et al., 2002). Additionally, thromboxane synthase inhibitors did not affect ACh-induced contraction, indicating that vascular dysfunction in obesity is driven by upregulation of vascular thromboxane receptor and endothelium-dependent prostanoid vasoconstrictors (Traupe et al., 2002). COX-inhibition also altered ET-1-induced contraction (Traupe et al., 2002; Mundy et al., 2007). This provides evidence that, not surprisingly, multiple mechanisms are involved in endothelial dysfunction in obese rodents. Importantly though, diet-induced obese mice are normotensive, indicating that obesity-induced endothelial dysfunction is likely independent of changes to blood pressure.

Epidemiological studies indicate that low vitamin D levels are associated with all of aforementioned co-morbidities of metabolic syndrome (Snijder et al., 2005; Awad et al., 2012). *In vitro* studies demonstrate that vitamin D3 inhibits pre-adipocyte proliferation by downregulating adipogenesis genes (Zhuang et al., 2007) and reducing obesity-induced inflammation (Marcotorchino et al., 2012). Despite ample evidence that vitamin D hinders the development of adipose, the precise mechanism by which vitamin D influences obesity has not yet been elucidated.

Hypertension

The pathophysiology of hypertension is multifactorial and related to activation of the sympathetic nervous system, renin-angiotensin-aldosterone system, pro-inflammatory mediators, endothelial dysfunction, and increased oxidative stress (Oparil et al., 2003). Sustained elevated pressure in the vasculature promotes premature ageing and increased endothelial cell turnover (Bleakley et al., 2015). The regenerated endothelial cells have an impaired ability to release endothelium-derived relaxing factors (Tang and Vanhoutte, 2010). Endothelial dysfunction has been demonstrated in most animal models of hypertension including spontaneously hypertensive rats (SHRs), angiotensin II-induced hypertension, Dahl salt-sensitive rats, and the two-kidney one-clip model (Stankevicius et al., 2002; Yang et al., 2004; Michel et al., 2008). A sustained elevation of blood pressure is linked with decreased levels of NO and increased vascular ROS (Konukoglu and Uzun, 2017). Oxidative stress plays a major role in the pathophysiology of hypertension-induced endothelial dysfunction. ROS alone promote vasoconstriction and impair antioxidant production (Santilli et al., 2015). Superoxide and other ROS inhibit NO bioavailability in several ways. Superoxide can react directly with NO to form peroxynitrite. This leads to eNOS uncoupling, thus aggravating the reduced NO production and promoting endothelial dysfunction (Bakker et al., 2009). Peroxynitrite can also nitrate other proteins, altering their function (Pacher et al., 2007). This correlates with studies in hypertensive patients reporting decreased NO availability and increased serum malondialdehyde [a clinical indicator of elevated ROS; (Wattanapitayakul et al., 2000; Guzik et al., 2002; Armas-Padilla et al., 2007)]. Increased NADPH oxidase activity has been observed in angiotensin II-induced hypertension, deoxycorticosterone acetate-salt hypertension and SHRs. In angiotensin II-infused mice, increased ROS is linked to eNOS uncoupling, BH_4 oxidation and further increases in superoxide, impairing endothelial function. This is also associated with downregulation of downstream targets of NO, such as cyclic-GMP, soluble guanylate cyclase, protein kinase G-dependent phosphorylation, S-nitrosylation, and transnitrosylation (Mollnau et al., 2002; Zhang, 2017). Clinically, there is an abundance of pharmacological treatments for hypertension that directly target the renin angiotensin aldosterone system (incl. angiotensin converting enzyme inhibitors and angiotensin II receptor blockers). In addition to blocking renal sodium reabsorption and plasma volume expansion (Ferrario and Schiffrin, 2015), many of these also improve endothelial dysfunction. This occurs *via* inhibition of vascular angiotensin I and II conversion and by increasing NO bioavailability (Farquharson and Struthers, 2000). The precise mechanisms by which this occurs varies between the different types of drugs. Mineralocorticoid receptor antagonists such as spironolactone increases NO bioavailability *via* the upregulation of eNOS and downregulation of the proinflammatory cytokine TGF-ß (Adel et al., 2014). ACE inhibitors increase NO bioavailability *via* three key mechanisms: increased intracellular calcium to increase NO production; blocking natural endopeptidase to inhibit local bradykinin degradation; and enhancing activity of the antioxidant superoxide dismutase (Enseleit et al., 2003).

The transformation of arachidonic acid by cyclooxygenase results in the production of endoperoxides, releasing endothelial-derived contracting factors (Vanhoutte et al., 2005). Importantly, many rodent studies show evidence of increased vasoconstrictor prostanoid responses in hypertension (Vanhoutte et al., 2005; Vanhoutte and Tang, 2008). Conversely, blunted endothelium-dependent vasodilation is the key underlying cause of vascular dysfunction in hypertensive humans (Vanhoutte et al., 2005). Therefore, while the impact of hypertension on the vasculature is similar between species, the underlying mechanisms may differ. This highlights the challenge of translating pre-clinical findings to a clinical setting. Thus, identification and use of the most representative animal models of human disease are vital for progressing our understanding of these conditions.

CONCLUSION

Accompanying the global rise in obesity, metabolic syndrome is an escalating public health concern. Metabolic syndrome is a multifactorial disorder, and hence it is not surprising that numerous signaling pathways contribute to the subsequent endothelial dysfunction. Despite this, the majority of current therapies that treat the comorbidities of metabolic syndrome and improve endothelial dysfunction target NO and ROS signaling (**Figure 1**). Future studies should investigate the effects of therapeutics which target vasoconstrictor prostanoids, another key mechanism of endothelial dysfunction in metabolic syndrome.

AUTHOR CONTRIBUTIONS

VT, MJ and AV wrote the manuscript. VT and MJ created figure and table. All authors contributed to the planning and drafting of the review.

REFERENCES

Adel, H., Taye, A., and Khalifa, M. M. (2014). Spironolactone improves endothelial dysfunction in streptozotocin-induced diabetic rats. *Naunyn Schmiedebergs Arch. Pharmacol.* 387 (12), 1187–1197. doi: 10.1007/s00210-014-1048-3

Alberti, K. G., Zimmet, P., and Shaw, J. (2006). Metabolic syndrome: a new world-wide definition. a consensus statement from the international diabetes federation. *Diabetes Med.* 23 (5), 469–480. doi: 10.1111/j.1464-5491.2006.01858.x

Aleixandre de Artinano, A., and Miguel Castro, M. (2009). Experimental rat models to study the metabolic syndrome. *Br. J. Nutr.* 102 (9), 1246–1253. doi: 10.1017/S0007114509990729

Antonopoulos, A. S., Margaritis, M., Shirodaria, C., and Antoniades, C. (2012). Translating the effects of statins: from redox regulation to suppression of vascular wall inflammation. *Thromb. Haemost.* 108 (5), 840–848. doi: 10.1160/TH12-05-0337

Armas-Padilla, M. C., Armas-Hernandez, M. J., Sosa-Canache, B., Cammarata, R., Pacheco, B., Guerrero, J., et al. (2007). Nitric oxide and malondialdehyde in human hypertension. *Am. J. Ther.* 14 (2), 172–176. doi: 10.1097/01.pap.0000249914.75895.48

Awad, A. B., Alappat, L., and Valerio, M. (2012). Vitamin d and metabolic syndrome risk factors: evidence and mechanisms. *Crit. Rev. Food Sci. Nutr.* 52 (2), 103–112. doi: 10.1080/10408391003785458

Bagi, Z., Koller, A., and Kaley, G. (2003). Superoxide-NO interaction decreases flow- and agonist-induced dilations of coronary arterioles in Type 2 diabetes mellitus. *Am. J. Physiol. Heart Circ. Physiol.* 285 (4), 1404–1410. doi: 10.1152/ajpheart.00235.2003

Bakker, W., Eringa, E. C., Sipkema, P., and van Hinsbergh, V. W. (2009). Endothelial dysfunction and diabetes: roles of hyperglycemia, impaired insulin signaling and obesity. *Cell Tissue Res.* 335 (1), 165–189. doi: 10.1007/s00441-008-0685-6

Ban, K., Noyan-Ashraf, M. H., Hoefer, J., Bolz, S. S., Drucker, D. J., and Husain, M. (2008). Cardioprotective and vasodilatory actions of glucagon-like peptide 1 receptor are mediated through both glucagon-like peptide 1 receptor-dependent and -independent pathways. *Circulation* 117 (18), 2340–2350. doi: 10.1161/CIRCULATIONAHA.107.739938

Beckman, J. A., Creager, M. A., and Libby, P. (2002). Diabetes and atherosclerosis: epidemiology, pathophysiology, and management. *JAMA* 287 (19), 2570–2581. doi: 10.1001/jama.287.19.2570

Bleakley, C., Hamilton, P. K., Pumb, R., Harbinson, M., and McVeigh, G. E. (2015). endothelial function in hypertension: victim or culprit? *J. Clin. Hypertens.* 17 (8), 651–654. doi: 10.1111/jch.12546

Bonetti, P. O., Lerman, L. O., Napoli, C., and Lerman, A. (2003). Statin effects beyond lipid lowering–are they clinically relevant? *Eur. Heart J.* 24 (3), 225–248. doi: 10.1016/S0195-668X(02)00419-0

Buettner, R., Parhofer, K. G., Woenckhaus, M., Wrede, C. E., Kunz-Schughart, L. A., Scholmerich, J., et al. (2006). Defining high-fat-diet rat models: metabolic and molecular effects of different fat types. *J. Mol. Endocrinol.* 36 (3), 485–501. doi: 10.1677/jme.1.01909

Cai, H., and Harrison, D. G. (2000). Endothelial dysfunction in cardiovascular diseases: the role of oxidant stress. *Circ. Res.* 87 (10), 840–844. doi: 10.1161/01.RES.87.10.840

Chinen, I., Shimabukuro, M., Yamakawa, K., Higa, N., Matsuzaki, T., Noguchi, K., et al. (2007). Vascular lipotoxicity: endothelial dysfunction *via* fatty-acid-induced reactive oxygen species overproduction in obese zucker diabetic fatty rats. *Endocrinology* 148 (1), 160–165. doi: 10.1210/en.2006-1132

Cominacini, L., Pasini, A. F., Garbin, U., Davoli, A., Tosetti, M. L., Campagnola, M., et al. (2000). Oxidized low density lipoprotein (ox-LDL) binding to ox-LDL receptor-1 in endothelial cells induces the activation of NF-kappaB through an increased production of intracellular reactive oxygen species. *J. Biol. Chem.* 275 (17), 12633–12638. doi: 10.1074/jbc.275.17.12633

Davis, B. J., Xie, Z., Viollet, B., and Zou, M. H. (2006). Activation of the AMP-activated kinase by antidiabetes drug metformin stimulates nitric oxide synthesis *in vivo* by promoting the association of heat shock protein 90 and endothelial nitric oxide synthase. *Diabetes* 55 (2), 496–505. doi: 10.2337/diabetes.55.02.06.db05-1064

De Ferranti, S., and Mozaffarian, D. (2008). The perfect storm: obesity, adipocyte dysfunction, and metabolic consequences. *Clin. Chem.* 54 (6), 945–955. doi: 10.1373/clinchem.2007.100156

Deanfield, J. E., Halcox, J. P., and Rabelink, T. J. (2007). Endothelial function and dysfunction: testing and clinical relevance. *Circulation* 115 (10), 1285–1295. doi: 10.1161/CIRCULATIONAHA.106.652859

Dong, Y. F., Liu, L., Kataoka, K., Nakamura, T., Fukuda, M., Tokutomi, Y., et al. (2010). Aliskiren prevents cardiovascular complications and pancreatic injury in a mouse model of obesity and type 2 diabetes. *Diabetologia* 53 (1), 180–191. doi: 10.1007/s00125-009-1575-5

Elrashidy, R. A., Zhang, J., and Liu, G. (2019). Long-term consumption of western diet contributes to endothelial dysfunction and aortic remodeling in rats: implication of Rho-kinase signaling. *Clin. Exp. Hypertens.* 41 (2), 174–180. doi: 10.1080/10641963.2018.1462375

Emini Veseli, B., Perrotta, P., De Meyer, G. R. A., Roth, L., Van der Donckt, C., Martinet, W., et al. (2017). Animal models of atherosclerosis. *Eur. J. Pharmacol.* 816, 3–13. doi: 10.1016/j.ejphar.2017.05.010

Endemann, D. H., and Schiffrin, E. L. (2004). Endothelial dysfunction. *J. Am. Soc. Nephrol.* 15 (8), 1983–1992. doi: 10.1097/01.ASN.0000132474.50966.DA

Enseleit, F., Lüscher, T. F., and Ruschitzka, F. (2003). Angiotensin-converting enzyme inhibition and endothelial dysfunction: focus on ramipril. *Eur. Heart J. Suppl.* 5 (suppl_A), A31–AA6. doi: 10.1016/S1520-765X(03)90061-7

Eriksson, L., and Nystrom, T. (2014). Activation of AMP-activated protein kinase by metformin protects human coronary artery endothelial cells against diabetic lipoapoptosis. *Cardiovasc. Diabetol.* 13, 1–9 152. doi: 10.1186/s12933-014-0152-5

Eringa, E. C., Stehouwer, C. D., Roos, M. H., Westerhof, N., and Sipkema, P. (2007). Selective resistance to vasoactive effects of insulin in muscle resistance arteries of obese Zucker (fa/fa) rats. *Am. J. Physiol. Endocrinol. Metab.* 293 (5), 1134–1139. doi: 10.1152/ajpendo.00516.2006

Farquharson, C. A., and Struthers, A. D. (2000). Spironolactone increases nitric oxide bioactivity, improves endothelial vasodilator dysfunction, and suppresses vascular angiotensin I/angiotensin II conversion in patients with chronic heart failure. *Circulation* 101 (6), 594–597. doi: 10.1161/01.CIR.101.6.594

Ferrario, C. M., and Schiffrin, E. L. (2015). Role of mineralocorticoid receptor antagonists in cardiovascular disease. *Circ. Res.* 116 (1), 206–213. doi: 10.1161/CIRCRESAHA.116.302706

Gao, M., Zhao, W., Li, C., Xie, X., Li, M., Bi, Y., et al. (2018). Spermidine ameliorates non-alcoholic fatty liver disease through regulating lipid

metabolism *via* AMPK. *Biochem. Biophys. Res. Commun.* 505 (1), 93–98. doi: 10.1016/j.bbrc.2018.09.078

Gendron, M. E., Thorin-Trescases, N., Villeneuve, L., and Thorin, E. (2007). Aging associated with mild dyslipidemia reveals that COX-2 preserves dilation despite endothelial dysfunction. *Am. J. Physiol. Heart Circ. Physiol.* 292 (1), 451–458. doi: 10.1152/ajpheart.00551.2006

Ghosh, S., Lakshmanan, A. P., Hwang, M. J., Kubba, H., Mushannen, A., Triggle, C. R., et al. (2015). Metformin improves endothelial function in aortic tissue and microvascular endothelial cells subjected to diabetic hyperglycaemic conditions. *Biochem. Pharmacol.* 98 (3), 412–421. doi: 10.1016/j.bcp.2015.10.008

Gil-Ortega, M., Condezo-Hoyos, L., Garcia-Prieto, C. F., Arribas, S. M., Gonzalez, M. C., Aranguez, I., et al. (2014). Imbalance between pro and anti-oxidant mechanisms in perivascular adipose tissue aggravates long-term high-fat diet-derived endothelial dysfunction. *PloS One* 9 (4), 953. doi: 10.1371/journal.pone.0095312

Gordon, S. M., Li, H., Zhu, X., Shah, A. S., Lu, L. J., and Davidson, W. S. (2015). A comparison of the mouse and human lipoproteome: suitability of the mouse model for studies of human lipoproteins. *J. Proteome Res.* 14 (6), 2686–2695. doi: 10.1021/acs.jproteome.5b00213

Grundy, S. M., Cleeman, J. I., Daniels, S. R., Donato, K. A., Eckel, R. H., Franklin, B. A., et al. (2005). Diagnosis and management of the metabolic syndrome: an american heart association/national heart, lung, and blood institute scientific statement. *Circ* 112 (17), 2735–2752. doi: 10.1161/CIRCULATIONAHA.105.169404

Guzik, T. J., West, N. E., Black, E., McDonald, D., Ratnatunga, C., Pillai, R., et al. (2000). Vascular superoxide production by NAD(P)H oxidase: association with endothelial dysfunction and clinical risk factors. *Circ. Res.* 86 (9), 85–90. doi: 10.1161/01.RES.86.9.e85

Guzik, T. J., West, N. E., Pillai, R., Taggart, D. P., and Channon, K. M. (2002). Nitric oxide modulates superoxide release and peroxynitrite formation in human blood vessels. *Hypertension* 39 (6), 1088–1094. doi: 10.1161/01.HYP.0000018041.48432.B5

Hadi, H. A., Carr, C. S., and Al Suwaidi, J. (2005). Endothelial dysfunction: cardiovascular risk factors, therapy, and outcome. *Vasc. Health Risk Manage.* 1 (3), 183–198.

Hattori, T., Murase, T., Ohtake, M., Inoue, T., Tsukamoto, H., Takatsu, M., et al. (2011). Characterization of a new animal model of metabolic syndrome: the DahlS.Z-Lepr(fa)/Lepr(fa) rat. *Nutr. Diabetes* 1, e1–e6. doi: 10.1038/nutd.2010.1

Hayashi, T., Juliet, P. A., Matsui-Hirai, H., Miyazaki, A., Fukatsu, A., Funami, J., et al. (2005). l-Citrulline and l-arginine supplementation retards the progression of high-cholesterol-diet-induced atherosclerosis in rabbits. *Proc. Natl. Acad. Sci. U. S. A* 102 (38), 13681–13686. doi: 10.1073/pnas.0506595102

Heart Protection Study Collaborative G (2002). MRC/BHF heart protection study of antioxidant vitamin supplementation in 20,536 high-risk individuals: a randomised placebo-controlled trial. *Lancet* 360 (9326), 23–33. doi: 10.1016/S0140-6736(02)09328-5

Heitzer, T., Krohn, K., Albers, S., and Meinertz, T. (2000). Tetrahydrobiopterin improves endothelium-dependent vasodilation by increasing nitric oxide activity in patients with type ii diabetes mellitus. *Diabetologia* 43 (11), 1435–1438. doi: 10.1007/s001250051551

Hsu, C. L., Wu, C. H., Huang, S. L., and Yen, G. C. (2009). Phenolic compounds rutin and o-coumaric acid ameliorate obesity induced by high-fat diet in rats. *J. Agric. Food Chem.* 57 (2), 425–431. doi: 10.1021/jf802715t

Jeremy, R. W., McCarron, H., and Sullivan, D. (1996). Effects of dietary L-arginine on atherosclerosis and endothelium-dependent vasodilatation in the hypercholesterolemic rabbit. response according to treatment duration, anatomic site, and sex. *Circulation* 94 (3), 498–506. doi: 10.1161/01.cir.94.3.498

Jiang, F., Lim, H. K., Morris, M. J., Prior, L., Velkoska, E., Wu, X., et al. (2011). Systemic upregulation of NADPH oxidase in diet-induced obesity in rats. *Redox Rep.* 16 (6), 223–229. doi: 10.1179/174329211X13049558293713

Johnson, R. J., Segal, M. S., Sautin, Y., Nakagawa, T., Feig, D. I., Kang, D. H., et al. (2007). Potential role of sugar (fructose) in the epidemic of hypertension, obesity and the metabolic syndrome, diabetes, kidney disease, and cardiovascular disease. *Am. J. Clin. Nutr.* 86 (4), 899–906. doi: 10.1093/ajcn/86.4.899

Kanda M, S. K., and Ichihara, K. (2003). Effects of atorvastatin and pravastatin on glucose tolerance in diabetic rats mildly induced by streptozotocin. *Biol. Pharm. Bull.* 26 (12), 1681–1684. doi: 10.1248/bpb.26.1681

Kobayasi, R., Akamine, E. H., Davel, A. P., Rodrigues, M. A., Carvalho, C. R., and Rossoni, L. V. (2010). Oxidative stress and inflammatory mediators contribute to endothelial dysfunction in high-fat diet-induced obesity in mice. *J. Hypertens.* 28 (10), 2111–2119. doi: 10.1097/HJH.0b013e32833ca68c

Konukoglu, D., and Uzun, H. (2017). Endothelial dysfunction and hypertension. *Adv. Exp. Med. Biol.* 956, 511–540. doi: 10.1007/5584_2016_90

La Cava, A. (2017). Leptin in inflammation and autoimmunity. *Cytokine* 98, 51–58. doi: 10.1016/j.cyto.2016.10.011

Leal Vde, O., and Mafra, D. (2013). Adipokines in obesity. *Clin. Chim Acta* 419, 87–94. doi: 10.1016/j.cca.2013.02.003

Lerman, A., and Zeiher, A. M. (2005). Endothelial function: cardiac events. *Circulation* 111 (3), 363–368. doi: 10.1161/01.CIR.0000153339.27064.14

Li, Q., Youn, J. Y., and Cai, H. (2015). Mechanisms and consequences of endothelial nitric oxide synthase dysfunction in hypertension. *J. Hypertens.* 33 (6), 1128–1136. doi: 10.1097/HJH.0000000000000587

Liu, C., Chang, C., Lee, H., Chen, Y., Tsai, T., Chiang Chiau, J., et al. (2016). Metabolic damage presents differently in young and early-aged C57BL/6 mice fed a high-fat diet. *Int. J. Gerontol.* 10 (2), 105–111. doi: 10.1016/j.ijge.2015.10.004

Lobato, N. S., Filgueira, F. P., Akamine, E. H., Tostes, R. C., Carvalho, M. H., and Fortes, Z. B. (2012). Mechanisms of endothelial dysfunction in obesity-associated hypertension. *Braz. J. Med. Biol. Res.* 45 (5), 392–400. doi: 10.1590/S0100-879X2012007500058

Lowette, K., Roosen, L., Tack, J., and Vanden Berghe, P. (2015). Effects of high-fructose diets on central appetite signaling and cognitive function. *Front. Nutr.* 2, 1–5. doi: 10.3389/fnut.2015.00005

Makki, K., Froguel, P., and Wolowczuk, I. (2013). Adipose tissue in obesity-related inflammation and insulin resistance: cells, cytokines, and chemokines. *ISRN Inflamm.* 2013, 139–239. doi: 10.1155/2013/139239

Marcotorchino, J., Gouranton, E., Romier, B., Tourniaire, F., Astier, J., Malezet, C., et al. (2012). Vitamin D reduces the inflammatory response and restores glucose uptake in adipocytes. *Mol. Nutr. Food Res.* 56 (12), 1771–1782. doi: 10.1002/mnfr.201200383

Mark, A. L., Shaffer, R. A., Correia, M. L., Morgan, D. A., Sigmund, C. D., and Haynes, W. G. (1999). Contrasting blood pressure effects of obesity in leptin-deficient ob/ob mice and agouti yellow obese mice. *J. Hypertens.* 17 (12), 1949–1953. doi: 10.1097/00004872-199917121-00026

Marsh, S. A., Powell, P. C., Agarwal, A., Dell'Italia, L. J., and Chatham, J. C. (2007). Cardiovascular dysfunction in zucker obese and zucker diabetic fatty rats: role of hydronephrosis. *Am. J. Physiol. Heart Circ. Physiol.* 293 (1), 292–298. doi: 10.1152/ajpheart.01362.2006

Matsumoto, T., Sato, A., Suenaga, H., Kobayashi, T., and Kamata, K. (2004). Modulations of shear stress-induced contractile responses and agonist-induced vasodilation in hypercholesterolemic rats. *Atherosclerosis* 175 (1), 31–38. doi: 10.1016/j.atherosclerosis.2004.02.017

Michel, F. S., Man, G. S., Man, R. Y., and Vanhoutte, P. M. (2008). Hypertension and the absence of EDHF-mediated responses favour endothelium-dependent contractions in renal arteries of the rat. *Br. J. Pharmacol.* 155 (2), 217–226. doi: 10.1038/bjp.2008.256

Mollnau, H., Wendt, M., Szocs, K., Lassegue, B., Schulz, E., Oelze, M., et al. (2002). Effects of angiotensin II infusion on the expression and function of NAD(P)H oxidase and components of nitric oxide/cGMP signaling. *Circ. Res.* 90 (4), E58–E65. doi: 10.1161/01.RES.0000012569.55432.02

Morrow, V. A., Foufelle, F., Connell, J. M., Petrie, J. R., Gould, G. W., and Salt, I. P. (2003). Direct activation of AMP-activated protein kinase stimulates nitric-oxide synthesis in human aortic endothelial cells. *J. Biol. Chem.* 278 (34), 31629–31639. doi: 10.1074/jbc.M212831200

Mundy, A. L., Haas, E., Bhattacharya, I., Widmer, C. C., Kretz, M., Baumann, K., et al. (2007). Endothelin stimulates vascular hydroxyl radical formation: effect of obesity. *Am. J. Physiol. Regul. Integr. Comp. Physiol.* 293 (6), 2218–2224. doi: 10.1152/ajpregu.00295.2007

O'Neill, S., and O'Driscoll, L. (2015). Metabolic syndrome: a closer look at the growing epidemic and its associated pathologies. *Obes Rev.* 16 (1), 1–12. doi: 10.1111/obr.12229

Okon, E. B., Szado, T., Laher, I., McManus, B., and van Breemen, C. (2003). Augmented contractile response of vascular smooth muscle in a diabetic mouse model. *J. Vasc. Res.* 40 (6), 520–530. doi: 10.1159/000075238

Oparil, S., Zaman, M. A., and Calhoun, D. A. (2003). Pathogenesis of hypertension. *Ann. Intern Med.* 139 (9), 761–776. doi: 10.7326/0003-4819-139-9-200311040-00011

Pacher, P., Beckman, J. S., and Liaudet, L. (2007). Nitric oxide and peroxynitrite in health and disease. *Physiol. Rev.* 87 (1), 315–424. doi: 10.1152/physrev.00029.2006

Panchal, S. K., and Brown, L. (2011). Rodent models for metabolic syndrome research. *J. BioMed. Biotechnol.* 2011, 351–982. doi: 10.1155/2011/351982

Paniagua, J. A., Lopez-Miranda, J., Escribano, A., Berral, F. J., Marin, C., Bravo, D., et al. (2002). Cerivastatin improves insulin sensitivity and insulin secretion in early-state obese type 2 diabetes. *Diabetes* 51 (8), 2596–2603. doi: 10.2337/diabetes.51.8.2596

Pannirselvam, M., Verma, S., Anderson, T. J., and Triggle, C. R. (2002). Cellular basis of endothelial dysfunction in small mesenteric arteries from spontaneously diabetic (db/db -/-) mice: role of decreased tetrahydrobiopterin bioavailability. *Br. J. Pharmacol.* 136 (2), 255–263. doi: 10.1038/sj.bjp.0704683

Rajendran, P., Rengarajan, T., Thangavel, J., Nishigaki, Y., Sakthisekaran, D., Sethi, G., et al. (2013). The vascular endothelium and human diseases. *Int. J. Biol. Sci.* 9 (10), 1057–1069. doi: 10.7150/ijbs.7502

Saklayen, M. G. (2018). The global epidemic of the metabolic syndrome. *Curr. Hypertens. Rep.* 20 (2), 1–8. doi: 10.1007/s11906-018-0812-z

Sangle, G. V., and Shen, G. X. (2010). Signaling mechanisms for oxidized LDL-induced oxidative stress and the upregulation of plasminogen activator inhibitor-1 in vascular cells. *Clin. Lipidology.* 5 (2), 221–232. doi: 10.2217/clp.10.6

Santilli, F., D'Ardes, D., and Davi, G. (2015). Oxidative stress in chronic vascular disease: from prediction to prevention. *Vascul Pharmacol.* 74, 23–37. doi: 10.1016/j.vph.2015.09.003

Saraswathi, V., and Hasty, A. H. (2006). The role of lipolysis in mediating the proinflammatory effects of very low density lipoproteins in mouse peritoneal macrophages. *J. Lipid Res.* 47 (7), 1406–1415. doi: 10.1194/jlr.M600159-JLR200

Sasaki, S., Higashi, Y., Nakagawa, K., Kimura, M., Noma, K., Sasaki, S., et al. (2002). A low-calorie diet improves endothelium-dependent vasodilation in obese patients with essential hypertension. *Am. J. Hypertens.* 15 (4), 302–309. doi: 10.1016/S0895-7061(01)02322-6

Senaphan, K., Kukongviriyapan, U., Sangartit, W., Pakdeechote, P., Pannangpetch, P., Prachaney, P., et al. (2015). Ferulic acid alleviates changes in a rat model of metabolic syndrome induced by high-carbohydrate, high-fat diet. *Nutrients* 7 (8), 6446–6464. doi: 10.3390/nu7085283

Serpillon, S., Floyd, B. C., Gupte, R. S., George, S., Kozicky, M., Neito, V., et al. (2009). Superoxide production by NAD(P)H oxidase and mitochondria is increased in genetically obese and hyperglycemic rat heart and aorta before the development of cardiac dysfunction. The role of glucose-6-phosphate dehydrogenase-derived NADPH. *Am. J. Physiol. Heart Circ. Physiol.* 297 (1), 153–162. doi: 10.1152/ajpheart.01142.2008

Sharma, P. (2011). Inflammation and the metabolic syndrome. *Indian J. Clin. Biochem.* 26 (4), 317–318. doi: 10.1007/s12291-011-0175-6

Shenouda, S. M., Widlansky, M. E., Chen, K., Xu, G., Holbrook, M., Tabit, C. E., et al. (2011). Altered mitochondrial dynamics contributes to endothelial dysfunction in diabetes mellitus. *Circulation* 124 (4), 444–453. doi: 10.1161/CIRCULATIONAHA.110.014506

Shi, Y., Luscher, T. F., and Camici, G. G. (2014). Dual role of endothelial nitric oxide synthase in oxidized LDL-induced, p66Shc-mediated oxidative stress in cultured human endothelial cells. *PloS One* 9 (9), e107787. doi: 10.1371/journal.pone.0107787

Silver, A. E., Beske, S. D., Christou, D. D., Donato, A. J., Moreau, K. L., Eskurza, I., et al. (2007). Overweight and obese humans demonstrate increased vascular endothelial NAD(P)H oxidase-p47(phox) expression and evidence of endothelial oxidative stress. *Circulation* 115 (5), 627–637. doi: 10.1161/CIRCULATIONAHA.106.657486

Snijder, M. B., van Dam, R. M., Visser, M., Deeg, D. J., Dekker, J. M., Bouter, L. M., et al. (2005). Adiposity in relation to vitamin D status and parathyroid hormone levels: a population-based study in older men and women. *J. Clin. Endocrinol. Metab.* 90 (7), 4119–4123. doi: 10.1210/jc.2005-0216

Stankevicius, E., Martinez, A. C., Mulvany, M. J., and Simonsen, U. (2002). Blunted acetylcholine relaxation and nitric oxide release in arteries from renal hypertensive rats. *J. Hypertens.* 20 (8), 1571–1579. doi: 10.1097/00004872-200208000-00020

Taguchi, K., Kobayashi, T., Matsumoto, T., and Kamata, K. (2011). Dysfunction of endothelium-dependent relaxation to insulin *via* PKC-mediated GRK2/Akt activation in aortas of ob/ob mice. *Am. J. Physiol. Heart Circ. Physiol.* 301 (2), H571–H583. doi: 10.1152/ajpheart.01189.2010

Tang, E. H., and Vanhoutte, P. M. (2010). Endothelial dysfunction: a strategic target in the treatment of hypertension? *Pflugers Arch.* 459 (6), 995–1004. doi: 10.1007/s00424-010-0786-4

Taylor, P. D., McCarthy, A. L., Thomas, C. R., and Poston, L. (1992). Endothelium-dependent relaxation and noradrenaline sensitivity in mesenteric resistance arteries of streptozotocin-induced diabetic rats. *Br. J. Pharmacol.* 107 (2), 393–399. doi: 10.1111/j.1476-5381.1992.tb12757.x

Taylor, P. D., Wickenden, A. D., Mirrlees, D. J., and Poston, L. (1994). Endothelial function in the isolated perfused mesentery and aortae of rats with streptozotocin-induced diabetes: effect of treatment with the aldose reductase inhibitor, ponalrestat. *Br. J. Pharmacol.* 111 (1), 42–48. doi: 10.1111/j.1476-5381.1994.tb14021.x

Taylor, L. E., Gillis, E. E., Musall, J. B., Baban, B., and Sullivan, J. C. (2018). High-fat diet-induced hypertension is associated with a proinflammatory T cell profile in male and female dahl salt-sensitive rats. *Am. J. Physiol. Heart Circ. Physiol.* 315 (6), 1713–1723. doi: 10.1152/ajpheart.00389.2018

Teff, K. L., Elliott, S. S., Tschop, M., Kieffer, T. J., Rader, D., Heiman, M., et al. (2004). Dietary fructose reduces circulating insulin and leptin, attenuates postprandial suppression of ghrelin, and increases triglycerides in women. *J. Clin. Endocrinol. Metab.* 89 (6), 2963–2972. doi: 10.1210/jc.2003-031855

Traupe, T., Lang, M., Goettsch, W., Munter, K., Morawietz, H., Vetter, W., et al. (2002). Obesity increases prostanoid-mediated vasoconstriction and vascular thromboxane receptor gene expression. *J. Hypertens.* 20 (11), 2239–2245. doi: 10.1097/00004872-200211000-00024

Tune, J. D., Goodwill, A. G., Sassoon, D. J., and Mather, K. J. (2017). Cardiovascular consequences of metabolic syndrome. *Transl. Res.* 183, 57–70. doi: 10.1016/j.trsl.2017.01.001

Vandanmagsar, B., Youm, Y.-H., Ravussin, A., Galgani, J. E., Stadler, K., Mynatt, R. L., et al. (2011). The NLRP3 inflammasome instigates obesity-induced inflammation and insulin resistance. *Nat. Med.* 17 (2), 179–188. doi: 10.1038/nm.2279

Vanhoutte, P. M., and Tang, E. H. (2008). Endothelium-dependent contractions: when a good guy turns bad! *J. Physiol.* 586 (22), 5295–5304. doi: 10.1113/jphysiol.2008.161430

Vanhoutte, P. M., Feletou, M., and Taddei, S. (2005). Endothelium-dependent contractions in hypertension. *Br. J. Pharmacol.* 144 (4), 449–458. doi: 10.1038/sj.bjp.0706042

Versari, D., Daghini, E., Virdis, A., Ghiadoni, L., and Taddei, S. (2009). Endothelial dysfunction as a target for prevention of cardiovascular disease. *Diabetes Care* 32, Suppl 2:S314–21. doi: 10.2337/dc09-S330

Wang, B., Chandrasekera, P. C., and Pippin, J. J. (2014). Leptin- and leptin receptor-deficient rodent models: relevance for human type 2 diabetes. *Curr. Diabetes Rev.* 10 (2), 131–145. doi: 10.2174/1573399810666140508121012

Wang, X., DuBois, D. C., Sukumaran, S., Ayyar, V., Jusko, W. J., and Almon, R. R. (2014). Variability in zucker diabetic fatty rats: differences in disease progression in hyperglycemic and normoglycemic animals. *Diabetes Metab. Syndr. Obes.* 7, 531–541. doi: 10.2147/DMSO.S69891

Wassmann, S., Laufs, U., Muller, K., Konkol, C., Ahlbory, K., Baumer, A. T., et al. (2002). Cellular antioxidant effects of atorvastatin *in vitro* and *in vivo*. *Arterioscler. Thromb. Vasc. Biol.* 22 (2), 300–305. doi: 10.1161/hq0202.104081

Wattanapitayakul, S. K., Weinstein, D. M., Holycross, B. J., and Bauer, J. A. (2000). Endothelial dysfunction and peroxynitrite formation are early events in angiotensin-induced cardiovascular disorders. *FASEB J.* 14 (2), 271–278. doi: 10.1096/fasebj.14.2.271

Widlansky, M. E., and Gutterman, D. D. (2011). Regulation of endothelial function by mitochondrial reactive oxygen species. *Antioxid Redox Signal.* 15 (6), 1517–1530. doi: 10.1089/ars.2010.3642

Wind, S., Beuerlein, K., Armitage, M. E., Taye, A., Kumar, A. H., Janowitz, D., et al. (2010). Oxidative stress and endothelial dysfunction in aortas of aged spontaneously hypertensive rats by NOX1/2 is reversed by NADPH oxidase inhibition. *Hypertension* 56 (3), 490–497. doi: 10.1161/HYPERTENSIONAHA.109.149187

Winters, B., Mo, Z., Brooks-Asplund, E., Kim, S., Shoukas, A., Li, D., et al. (2000). Reduction of obesity, as induced by leptin, reverses endothelial dysfunction in

obese (Lep(ob)) mice. *J. Appl. Physiol. (1985)* 89 (6), 2382–2390. doi: 10.1152/jappl.2000.89.6.2382

Wong, V., Stavar, L., Szeto, L., Uffelman, K., Wang, C. H., Fantus, I. G., et al. (2006). Atorvastatin induces insulin sensitization in Zucker lean and fatty rats. *Atherosclerosis* 184 (2), 348–355. doi: 10.1016/j.atherosclerosis.2005.05.009

Wong, S. K., Chin, K. Y., Suhaimi, F. H., Fairus, A., and Ima-Nirwana, S. (2016). Animal models of metabolic syndrome: a review. *Nutr. Metab.* 13, 65 1–12. doi: 10.1186/s12986-016-0123-9

Xu, J., and Zou, M. H. (2009). Molecular insights and therapeutic targets for diabetic endothelial dysfunction. *Circulation* 120 (13), 1266–1286. doi: 10.1161/CIRCULATIONAHA.108.835223

Yang, D., Gluais, P., Zhang, J. N., Vanhoutte, P. M., and Feletou, M. (2004). Endothelium-dependent contractions to acetylcholine, ATP and the calcium ionophore A 23187 in aortas from spontaneously hypertensive and normotensive rats. *Fundam Clin. Pharmacol.* 18 (3), 321–326. doi: 10.1111/j.1472-8206.2004.00247.x

Yee A, M. S., Simpson, S. H., McAlister, F. A., Tsuyuki, R. T., and Johnson, J. A. (2004). Statin use in Type 2 diabetes mellitus is associated with a delay in starting insulin. *Diabetes Med.* 21, 962–967. doi: 10.1111/j.1464-5491.2004.01263.x

Yokoi, N., Hoshino, M., Hidaka, S., Yoshida, E., Beppu, M., Hoshikawa, R., et al. (2013). A novel rat model of type 2 diabetes: the zucker fatty diabetes mellitus ZFDM rat. *J. Diabetes Res.* 2013, 103–731. doi: 10.1155/2013/103731

Yoshizumi, M., Perrella, M. A., Burnett, J. C.Jr., and Lee, M. E. (1993). Tumor necrosis factor downregulates an endothelial nitric oxide synthase mRNA by shortening its half-life. *Circ. Res.* 73 (1), 205–209. doi: 10.1161/01.RES.73.1.205

Zhang, Y. H. (2017). Nitric oxide signalling and neuronal nitric oxide synthase in the heart under stress. *Res* 6, (742) 1–12. doi: 10.12688/f1000research.10128.1

Zhuang, H., Lin, Y., and Yang, G. (2007). Effects of 1,25-dihydroxyvitamin D3 on proliferation and differentiation of porcine preadipocyte *in vitro*. *Chem. Biol. Interact.* 170 (2), 114–123. doi: 10.1016/j.cbi.2007.07.012

Zucker, L. M., and Zucker, T. F. (1961). Fatty, a new mutation in the rat. *J. Hered.* 52 (6), 275–278. doi: 10.1093/oxfordjournals.jhered.a107093

Conflict of Interest: The authors declare that the research was conducted in the absence of any commercial or financial relationships that could be construed as a potential conflict of interest.

The handling editor declared a shared affiliation, though no other collaboration, with one of the authors MJ at time of review.

frontiers in Pharmacology

REVIEW
published: 04 March 2020
doi: 10.3389/fphar.2020.00129

Roles and Mechanisms of Interleukin-12 Family Members in Cardiovascular Diseases: Opportunities and Challenges

Jing Ye[1†], Yuan Wang[2†], Zhen Wang[1†], Ling Liu[3], Zicong Yang[3], Menglong Wang[1], Yao Xu[1], Di Ye[1], Jishou Zhang[1], Yingzhong Lin[3], Qingwei Ji[3*] and Jun Wan[1*]*

[1] Hubei Key Laboratory of Cardiology, Department of Cardiology, Renmin Hospital of Wuhan University, Cardiovascular Research Institute, Wuhan University, Wuhan, China, [2] Department of Thyroid Breast Surgery, Renmin Hospital of Wuhan University, Wuhan, China, [3] Department of Cardiology, the People's Hospital of Guangxi Zhuang Autonomous Region, Nanning, China

Cardiovascular diseases represent a complex group of clinical syndromes caused by a variety of interacting pathological factors. They include the most extensive disease population and rank first in all-cause mortality worldwide. Accumulating evidence demonstrates that cytokines play critical roles in the presence and development of cardiovascular diseases. Interleukin-12 family members, including IL-12, IL-23, IL-27 and IL-35, are a class of cytokines that regulate a variety of biological effects; they are closely related to the progression of various cardiovascular diseases, including atherosclerosis, hypertension, aortic dissection, cardiac hypertrophy, myocardial infarction, and acute cardiac injury. This paper mainly discusses the role of IL-12 family members in cardiovascular diseases, and the molecular and cellular mechanisms potentially involved in their action in order to identify possible intervention targets for the prevention and clinical treatment of cardiovascular diseases.

Keywords: cardiovascular diseases, IL-12 family members, atherosclerosis, coronary artery disease, hypertension, aortic dissection, viral myocarditis

OPEN ACCESS

Edited by:
Chen Huei Leo, Singapore University of Technology and Design, Singapore

Reviewed by:
Carlos F. Sánchez-Ferrer, Autonomous University of Madrid, Spain
Cees Korstanje, KorstanjePharmaConsultancy, Netherlands

***Correspondence:**
Yingzhong Lin
yingzhonglin@126.com
Qingwei Ji
jqw124@163.com
Jun Wan
whuwanjun@163.com;
wanjun@whu.edu.cn

†These authors have contributed equally to this work

Specialty section:
This article was submitted to Cardiovascular and Smooth Muscle Pharmacology, a section of the journal Frontiers in Pharmacology

Received: *28 November 2019*
Accepted: *30 January 2020*
Published: *04 March 2020*

Citation:
Ye J, Wang Y, Wang Z, Liu L, Yang Z, Wang M, Xu Y, Ye D, Zhang J, Lin Y, Ji Q and Wan J (2020) Roles and Mechanisms of Interleukin-12 Family Members in Cardiovascular Diseases: Opportunities and Challenges. Front. Pharmacol. 11:129. doi: 10.3389/fphar.2020.00129

INTRODUCTION

To date, cardiovascular disease remains the leading killer worldwide, especially in less-developed areas (Leong et al., 2017). It is not only a serious threat to patients' lives, but also poses a serious psychological burden to patients and their families. Although a large number of useful drugs and new technologies have been widely used in clinical treatment over recent years and have significantly improved survival rates, the overall prognosis of cardiovascular diseases is still very poor, and the death rate related to cardiovascular diseases is far higher than that of other diseases, even malignant tumors (Donofrio et al., 2014; Dukkipati et al., 2017; Bethel et al., 2018).

There are four members of the interleukin-12 (IL-12) family, including IL-12, IL-23, IL-27, and IL-35. An obvious feature of IL-12 family members is that each consists of two heterogeneous dimers, including an α subunit (p19, p28, and p35) and a β subunit [p40 and Epstein-Barr virus-induced protein 3 (EBI3)] (Vignali and Kuchroo, 2012; Sun et al., 2015). Therefore, deletion of either an α or β subunit can cancel the biological effects of the IL-12 family cytokines. Interestingly, the receptor for IL-

12 family members also consists of two protein chains. Among them, the IL-12 receptor (IL-12R) utilizes IL-12Rβ1 and IL-12Rβ2, IL-23 signaling employs IL-12Rβ1 and IL-23R, and IL-27 signals through gp130 and WSX-1; however, an exception is IL-35R, which consists of two downstream signals, including gp130-gp130 or IL-12Rβ1-IL-12Rβ1 (Presky et al., 1996; Oppmann et al., 2000; Pflanz et al., 2004; Collison et al., 2012). Molecular signaling mechanisms involving IL-12 family members are basically similar, and are all mediated by members of the Janus kinase (JAK) signal transducers and activators of transcription (STAT) family, especially JAK1/2-STAT1/3/4 (Ihle, 1995; O'Shea et al., 2002; Delgoffe et al., 2011). All IL-12 family members can be secreted by both immune and non-immune cells (Vignali and Kuchroo, 2012; Sun et al., 2015). For the immune cells, IL-12, IL-23, and IL-27 are mainly derived from effector T lymphocytes, macrophages, and dendritic cells, while IL-35 is mainly secreted by T helper cells (Tregs) (Langrish et al., 2004; Hunter, 2005; Collison et al., 2009; Collison et al., 2010; Andrews et al., 2016; Wei et al., 2017). IL-12 and IL-23 are considered to be pro-inflammatory factors that amplify downstream inflammatory signals. IL-35 plays an anti-inflammatory role and protects against tissue damage mediated by inflammatory responses, while IL-27 has a two-sided effect on the regulation of inflammation, in which it can not only play an anti-inflammatory role, but also a pro-inflammatory role, depending on the inflammatory environment (Ma and Trinchieri, 2001; Kastelein et al., 2007; Collison and Vignali, 2008; Vignali et al., 2008; Cox et al., 2011; Vignali and Kuchroo, 2012; Wojno and Hunter, 2012; Sun et al., 2015). The subunits, receptors, signaling pathways, and regulatory roles of the members of the IL-12 family in inflammation are listed in **Table 1**.

INTERLEUKIN-12 FAMILY MEMBERS AND CARDIOVASCULAR DISEASE

Interleukin-12 Family Members and Atherosclerosis, Coronary Artery Disease

Atherosclerosis and coronary artery diseases due to atherosclerosis are chronic inflammatory disorders, and infiltration by immune cells and inflammatory factors can be observed at all stages of disease development (Peter et al., 2009; Longenecker et al., 2016; Rahman and Fisher., 2018). IL-12

TABLE 1 | The subunits, receptors, signaling pathways of the IL-12 family members.

	IL-12	IL-23	IL-27	IL-35	References
Subunits	α: p35 β: p40	α: p19 β: p40	α: p28 β: EBI3	α: p35 β: EBI3	Vignali and Kuchroo, 2012; Sun et al., 2015
Receptors	IL-12Rβ1+IL12-Rβ2	IL-12Rβ1+IL-23R	gp130+ WSX-1	1. gp130+IL-12Rβ2 2. gp130+gp130 3. IL-12Rβ2+IL-12Rβ2	Presky et al., 1996; Oppmann et al., 2000; Pflanz et al., 2004; Vignali and Kuchroo, 2012; Collison et al., 2012; Sun et al., 2015
Pathways	JAKs: JAK2, TYK2 STATs: STAT4	JAKs: JAK2, TYK2 STATs: STAT3, STAT4	JAKs: JAK1, JAK2 STATs: STAT1, STAT3	JAKs: JAK1, JAK2 STATs: STAT1, STAT3, STAT4	Ihle, 1995; O'Shea et al., 2002; Delgoffe et al., 2011; Vignali and Kuchroo, 2012; Sun et al., 2015
Main sources	Mø, Th1	Mø, activated DCs,	Myeloid cells, such as Mø and activated DCs	Treg	Langrish et al., 2004; Hunter, 2005; Collison et al., 2009; Collison et al., 2010; Vignali and Kuchroo, 2012; Sun et al., 2015; Andrews et al., 2016; Wei et al., 2017
Other sources	activated DCs, NK, B cells, Th9, Th17	γδ T cells, B cells, NK cells, ECs, innate lymphoid cells	T cells, B cells, epithelial cells, plasma cells, and ECs	Activated DCs, Mø, placental trophoblast cells	Langrish et al., 2004; Hunter, 2005; Collison et al., 2009; Collison et al., 2010; Vignali and Kuchroo, 2012; Sun et al., 2015; Andrews et al., 2016; Wei et al., 2017
Role in immune response	Induce Th1 and Mø1 differentiation	Induce and promote th17 differentiation	IL-27 alone has no apparent stimulatory properties, collaboration with other ILs promote or inhibit T cell differentiation and proliferation	Promote Treg activity, suppress the Teff cell (Th1, and Th17) activity	Ma and Trinchieri, 2001; Kastelein et al., 2007; Collison and Vignali, 2008; Vignali et al., 2008; Cox et al., 2011; Vignali and Kuchroo, 2012; Wojno and Hunter, 2012; Sun et al., 2015
Regulation of inflammation	Except inflammatory environment induced by DOX or Ang II, all play pro-inflammatory role	Always play a pro-inflammatory roles, no anti-inflammatory effects had been reported	Not only play an anti-inflammatory role, but also play a pro-inflammatory effects, may be associated with inflammatory microenvironment	Always relieves the inflammatory response	Davenport and Tipping, 2003; Vignali and Kuchroo, 2012; Jin et al., 2012; Koltsova et al., 2012; Li et al., 2012; Yan et al., 2012; Jääskeläinen et al., 2013; Abbas et al., 2015; Subramanian et al., 2015; Sun et al., 2015; Andrews et al., 2016; Tao et al., 2016; Hu et al., 2016; Gregersen et al., 2017; Fatkhullina et al., 2018; Ye et al., 2018b; Jia et al., 2019; Liu et al., 2019; Vargas-Alarcón et al., 2019; Ye et al., 2019

Mø, macrophages, Mø1, M1 macrophages; DCs, dendritic cells; natural killer cell; endothelial cells; DOX; doxorubicin.

family members have significantly higher levels of expression in patients with atherosclerosis and coronary artery disease, and are closely related to the progression of these diseases.

Clinical Data

Previous studies reported that plasma IL-12 concentrations are significantly increased in many types of atherosclerosis and atherosclerotic cardiovascular disease, including stable angina pectoris (SAP), non-ST segment elevation myocardial infarction (NSTEMI), ST-elevation myocardial infarction (STEMI), acute myocardial infarction (AMI), and gradually increased SAP, unstable angina pectoris (UAP), and AMI (Zhou et al., 2001; Correia et al., 2010; Lin et al., 2012; Yong et al., 2013; Chistiakov et al., 2015; Opstad et al., 2016; Zykov et al., 2016). Clinical data showed that patients with coronary artery disease exhibit higher circulating IL-23 levels (Lin et al., 2012; Abbas et al., 2015; Sun et al., 2019a). In coronary artery disease patients who underwent percutaneous coronary intervention (PCI) with drug-eluting stents (DES), subjects with in-stent restenosis show higher circulating IL-23 levels in peripheral blood mononuclear cells (PBMCs) (Khojasteh-Fard et al., 2012). Numerous studies have confirmed that IL-27 expression is increased in plasma and plaques in the coronary and carotid arteries of coronary artery disease patients (Kempe et al., 2009; Jin et al., 2012; Lin et al., 2012; A Shahi et al., 2015; Gregersen et al., 2017). Abundant evidence identifies that IL-35 expression is significantly reduced in patients with coronary artery disease; plasma IL-35 levels are gradually reduced in SAP, UAP, and AMI patients, and decreased plasma IL-35 levels are inversely correlated with the left ventricular ejection fraction (LVEF) in coronary artery diseases (Lin et al., 2012; Rasa et al., 2018; Zhu et al., 2018).

Gene polymorphisms in members of the IL-12 family have been reported to be associated with the occurrence or progression of coronary artery disease. An IL-23R polymorphism was observed to be related to coronary artery disease, and the IL-23R rs6682925T/C polymorphism may independently relate to the presence of coronary artery disease (Zhang et al., 2014a). *IL-27* gene polymorphism had no effect on the presence of subclinical atherosclerosis, while closely related to atherosclerosis and coronary artery disease, rs26528 T and rs40837 A alleles significantly reduced the risk of coronary artery disease (Posadas-Sánchez et al., 2017; Vargas-Alarcón et al., 2019). No research about gene polymorphisms of IL-12 and IL-35 and the presence of coronary artery disease was reported yet.

Animal Studies

Elevated serum IL-12 levels are observed of atherosclerosis in ApoE-KO mice, and increased IL-12 levels are associated with the progression of atherosclerosis (Jääskeläinen et al., 2013). Accumulating animal study reports also demonstrate that treatment with exogenous recombinant murine IL-12 significantly aggravates the progression of atherosclerosis, and increases aortic atherosclerotic plaque areas in both ApoE-knockout mice and in low density lipoprotein (LDL) receptor-deficient mice, while cancelation the biological effects of IL-12 can significantly diminish such effects (Lee et al., 1999; Davenport and Tipping, 2003; Hauer et al., 2005). In a murine myocardial infarction model, canceling the biological effects of IL-12 alleviates cardiac dysfunction by promoting angiogenesis (Kan et al., 2016). In a recent study, Shi et al. reported that knockout of IL-12p35 subunit, which can cancel the biological effects of IL-12 and IL-35, significantly aggravated Th1/Th2 and Th17/Treg imbalance and increased atherosclerotic plaque areas in ApoE mice, which may suggest that the pro-atherosclerotic effects of IL-12 can be mediated by promoting the CD4+ T lymphocyte differentiation imbalance (Huang et al., 2019).

The role of IL-23 in atherosclerosis is controversial. Therapy involving IL-23p19, a subunit of IL-23, had no significant effect on atherosclerosis development in ApoE-deficient mice, although inflammatory responses were reduced (Wang et al., 2019). Another study reported that there was no significant difference in atherosclerotic area between low-density lipoprotein receptor (LDLR) knockout mice and IL-23 + LDLR double-knockout mice, after they were all fed with high-fat diet (Engelbertsen et al., 2018). A recent study reported that deficiency of IL-23 significantly decreased IL-22 expression in ApoE-knockout mice, and also reduced expression of IL-22, thereby relieving the release of inflammatory substances, and thus alleviating the process of atherosclerosis (Fatkhullina et al., 2018). Subramanian et al. reported that granulocyte-macrophage colony stimulating factor (GM-CSF) up-regulates the expression of IL-23, which further promotes the differentiation of macrophages and atherosclerosis development (Subramanian et al., 2015). These studies suggest that IL-23 has a strong regulatory effect on inflammation mediated by a high-fat diet in both ApoE-knockout mice and LDL-R-knockout mice (Subramanian et al., 2015; Engelbertsen et al., 2018; Fatkhullina et al., 2018; Wang et al., 2019), while the special role of IL-23 in atherosclerotic progression is unclear and further studies are needed to clarify this aspect.

Both the effects of IL-27R and IL-27 on atherosclerosis were reported. Koltsova et al. found that knockout of IL-27R significantly enhanced Th17 immune responses, up-regulated inflammatory responses, promoted the expression of tumor necrosis factor (TNF) and IL-17A, and further promoted the development of atherosclerosis in ApoE-deficient mice (Koltsova et al., 2012). Hirase et al. also reported that knockout of IL-27 plays similar roles in atherosclerosis development in LDLR-knockout mice; the mechanism may be related to the promotion of macrophage differentiation (Hirase et al., 2013). Ryu et al. found that in a high-fat diet-treated ApoE-knockout mouse atherosclerotic model, blockade of IL-27 signaling increased the plaque area *via* promotion of autoimmune follicular helper T cell responses (Ryu et al., 2018). These results suggest that IL-27 may be an important target for the treatment and prevention of atherosclerosis and coronary artery disease by inhibiting the differentiation of various immune cells and reducing inflammatory responses, thereby alleviating atherosclerotic progression. Hence, IL-27 may be an important target for the treatment and prevention of atherosclerosis and coronary artery disease.

Contrary to clinical experiments, as an anti-inflammatory cytokine, IL-35 expression in mouse atherosclerotic plaques was significantly increased (Wang et al., 2014). A small number of other studies, however, have reported increased IL-35 expression in atherosclerotic plaques and serum in ApoE mice fed with a high-fat diet, as well as in the plasma of patients with coronary artery disease (Gorzelak-Pabiś et al., 2017; Li et al., 2018). Using a mouse model of atherosclerosis, administration of recombinant mouse IL-35 significantly decreased plaque area in the aortic root, and Treg immune responses were also found to be enhanced (Tao et al., 2016). In a recent study, Shi et al. reported that knockout of IL-12p35 subunit, which can cancel the biological effects of IL-12 and IL-35, significantly aggravated Th1/Th2 and Th17/Treg imbalance and increased atherosclerotic plaque areas in ApoE mice, given that mouse IL-35 reverses Th35/Treg imbalance and up-regulates atherosclerosis development, whereas there were no effects on Th1/Th2 imbalance (Huang et al., 2019). In a recently published study, two subunits of IL-35 found in the left anterior descending branch following its ligation induced myocardial infarction in the heart tissues in mice. In addition, exogenous IL-35 treatment can significantly reduce infarct area of the left ventricle and reduce the incidence of left ventricular rupture; the mechanisms underlying this phenomenon may be related to the inhibitory role of IL-35 in the apoptosis of myocardial macrophages, thus increasing the differentiation of M2 macrophages and augmenting the expression of collagen (Jia et al., 2019). In rat models of coronary artery disease, IL-35 treatment significantly promotes early drug-eluting stent endothelialization; its mechanism may be related to the regulation of the activation of M2 macrophages (Liu et al., 2019). These studies have demonstrated that IL-35 regulates the differentiation of various immune cells involved in the progression of atherosclerotic heart disease.

Interleukin-12 Family Members and Hypertension

Hypertension is a complex group of clinical syndromes. Although the specific mechanisms remain unclear, it has been demonstrated that a variety of pathological factors are involved in the process of hypertension, among which immune responses and inflammation are most closely related to hypertension (Kirabo et al., 2014; Pober, 2014; Guzik and Touyz, 2017).

So far, little research has been conducted on IL-12 family members and hypertension. Data from clinical experiments reported that plasma IL-12 levels are significantly increased in hypertensive patients, and are positively correlated with both systolic blood pressure (SBP) and diastolic blood pressure (DBP) (Ye et al., 2019). IL-12 polymorphism is closely related to the incidence of hypertension-induced complications: hypertension patients who carry the *IL12B* 1159 A/A genotype exhibit a lower risk of incidence of stroke, while *IL12B* A/A carriers have an elevated risk of stroke (Timasheva et al., 2008).

In an animal study, angiotensin II (Ang II) infusion significantly increased aortic IL-12p35 expression and macrophages were the primary source (Ye et al., 2019). In an Ang II-induced mouse hypertension model, IL-12p35 knockout promoted M1 macrophage differentiation and elevated blood pressure, while IL-12 treatment unexpectedly lowered blood pressure (Ye et al., 2019). Another study reported that knockdown of IL-12p35 did not affect Ang II-induced hypertension (Li et al., 2012). One possible reason for this is that the IL-12p35 knockout mice in that study were treated for only a week, which is too short a period for blood pressure to change. Little research has been conducted regarding IL-23, IL-27, and IL-35 in relation to hypertension. One group reported that in deoxycorticosterone acetate and Ang II-treated mice, deficiency of IL-17 could decrease IL-23 expression and accelerate kidney injury (Krebs et al., 2014), and another study found that treatment with recombinant mouse IL-35 had no effects on blood pressure in Ang II-treated mice (Ye et al., 2019).

Interleukin-12 Family Members and Aortic Aneurysms and Aortic Dissection

Aortic aneurysms and aortic dissection are both degenerative lesions of the aorta and share the same pathological mechanisms, such as the excessive loss of aortic extracellular matrix mediated by multiple pathological factors, especially local aortic inflammation (Mallat et al., 2016; Rabkin, 2017; Raffort et al., 2017; Sherifova and Holzapfel, 2019).

There have been few studies regarding IL-12 family members, aortic aneurysms, and aortic dissection. Davis et al. reported that IL-12 levels in aortic tissue and serum were not significantly different in patients with abdominal aortic aneurysms compared to those in patients without abdominal aortic aneurysms (Davis et al., 2001). In aortic dissection patients, decreased plasma IL-35 concentrations were observed compared to non-aortic dissection patients (Ye et al., 2018a). In addition, no studies have been conducted on IL-12 family members and aortic aneurysms and aortic dissection.

Only one recent animal study reported that deletion of IL-27R reduced the formation of abdominal aortic aneurysm in ApoE deficiency mice, the mechanisms may be associated with a blunted accumulation of myeloid cells in the aorta (Peshkova et al., 2019).

Interleukin-12 Family Members and Cardiac Fibrosis

Cardiac fibrosis is a common feature of many heart diseases and is closely related to deterioration in cardiac function. The essence of cardiac fibrosis is that pathological factors activate cardiac fibroblasts, leading to abnormal deposition and increased numbers of cardiac collagen fibers (Moore-Morris et al., 2015; Gorabi et al., 2019).

All studies on IL-12 family members and cardiac fibrosis have been focused on animal studies and no related clinical studies have been reported. In an earlier report, the authors reported that infusion with Ang II increases cardiac IL-12 expression derived from cardiac macrophages; detection of IL-12 promotes the activation of CD4+ T lymphocytes and increases differentiation of M2 macrophages, thereby up-regulating the activation of the

transforming growth factor-β1 (TGF-β1) signaling pathway, which then aggravates cardiac fibrosis (Li et al., 2012). In mouse models of myocardial infarction, deletion of *IL-23* significantly reduces the expression of multiple fibrosis markers, including α-smooth muscle actin (α-SMA), collagen I, and collagen III (Savvatis et al., 2014). Unexpectedly, Yan et al. also reported that IL-23 deficiency amplifies the inflammatory response and promotes the release of various inflammatory factors, especially IL-17, which further promotes the infiltration and deposition of γδT cells in the left ventricle, promotes the apoptosis of cardiomyocytes, and aggravates cardiac fibrosis in a murine myocardial infarction model (Yan et al., 2012). In addition, IL-12p35 knockout increased the levels of cardiac mitochondrial reactive oxygen species (ROS) and calcium ion overload, which further aggravated mitochondrial dysfunction and energy failure, increased myocardial cell apoptosis, worsened cardiac dysfunction, and increased cardiac fibrosis in 25-month-old aging mice (Ye et al., 2020). However, how the cytokines IL-12 and IL-35 mediate these biological effects is currently unknown. Furthermore, no studies concerning IL-27 and IL-35 related to cardiac fibrosis have been reported.

Interleukin-12 Family Members and Cardiac Ischemia Reperfusion Injury

Ischemia reperfusion injury of the heart is an important issue that cannot be ignored in heart transplantation. A large number of studies have confirmed that myocardial apoptosis mediated by inflammatory responses after cardiac reperfusion is one of the most important mechanisms of ischemia reperfusion injury of the heart (Shin et al., 2017; Schanze et al., 2019).

Numerous animal studies have reported that members of the IL-12 family are involved in cardiac ischemia-reperfusion injury. In a recent study, Yan found that dectin-2 deficiency could protect against cardiac ischemia-reperfusion injury *via* alleviating Th1 immune responses and further decreasing IL-12 expression (Yan et al., 2017). An earlier study reported that high-mobility group box 1 (Hmgb-1) promoted ischemia-reperfusion injury in a mouse cardiac transplantation model (Zhu et al., 2013). In subsequent studies, pentraxin-3 and necrostatin-1 were also found to attenuate ischemic reperfusion injury by decreasing the expression of IL-23 (Zhang et al., 2014b; Zhu et al., 2014). Hu et al. reported that administration of mouse anti-IL-23 neutralizing antibody significantly reduced the expression of inflammatory markers such as IL-6, tumor necrosis factor α (TNF-α), and pro-oxidant markers such as malondialdehyde (MDA), and decreased the levels of superoxide dismutase (SOD), thereby relieving cardiac ischemia reperfusion injury (Hu et al., 2016). Up-regulation of cardiac IL-23 expression by adenovirus significantly increased the expression of serum lactate dehydrogenase (LDH) and creatine kinase myocardial band (CK-MB), elevated the expression of apoptosis-related proteins and infarcted areas, and these effects could be reversed by AG490, an inhibitor of the JAK2-STAT pathway (Liao et al., 2017). However, the roles of both IL-27 and IL-35 in cardiac ischemia and reperfusion injury have not been studied to date.

Interleukin-12 Family Members and Atrial Fibrillation

Atrial fibrillation is one of the most common arrhythmias and can lead to vascular embolizations, the most serious of which is cerebral artery embolization. Literature reports confirm that the mechanism of atrial fibrillation may be closely related to the occurrence of atrial fibrosis (Jalife and Kaur, 2015; Nattel, 2017).

Previous clinical studies have reported that elevated IL-12 expression is observed in left atrial tissues of atrial fibrillation patients (Stein et al., 2008; Lappegård et al., 2013). Chen et al. found that *IL-27* genetic variants, including the rs153109 G allele and GG genotype, increased the occurrence of atrial fibrillation in the Chinese Han population (Chen et al., 2017a).

Recent animal studies have reported that inhibition of Ang II-induced M1 macrophage differentiation and reduction of IL-12 release can reduce the occurrence of atrial fibrosis and atrial fibrillation (Sun et al., 2019b). No studies on the expression and mechanisms of the involvement of IL-23 and IL-35 in atrial fibrillation have been reported.

Interleukin-12 Family Members and Viral Myocarditis

Viral myocarditis is an uncommon heart disease. The death rate involving severe myocarditis exceeds that of AMI. Immune responses induced by viral infection are an important cause of myocardial injury in viral myocarditis (Chen et al., 2013; Pollack et al., 2015).

So far, although no clinical experiments have been reported on IL-12 family members and viral myocarditis, a large number of animal experiments have confirmed that all IL-12 family members are associated with viral myocarditis. Substantial evidence indicates that IL-12 expression is increased in both plasma and heart tissue of coxsackievirus B3-induced viral myocarditis in mice. In addition, elevated IL-12R levels were also found in heart tissue of mice with viral myocarditis (Fairweather et al., 2003; Nyland et al., 2012; Jenke et al., 2014; Zha et al., 2015; Miteva et al., 2017; Zhang et al., 2017). In an earlier study, the authors found that treatment with coxsackievirus B3 significantly increased both cardiac IL-12p35 and IL-12p40 expression, and treatment with recombinant mouse IL-12 and anti-IL-12 neutralizing antibodies reduced and increased mortality, respectively, in mice with viral myocarditis (Shioi et al., 1997). In a subsequent study, Nishio et al. reported that carvedilol treatment increases both IL-12 and interferon-γ (IFN-γ) expression, thereby reducing virus replication and thus improving survival rates in viral myocarditis mice (Nishio et al., 2003). In another study, Fairweather et al. demonstrated that the protective effect of IL-12 in viral myocarditis is mediated by activation of the STAT4 pathway and promotion of IFN-γ release. Knockout of the STAT4 pathway and IFN-γ can significantly reverse the protective effects of IL-12 and aggravate myocardial cell injury and mortality (Fairweather et al., 2005). Similarly, circulating IL-23 levels were also observed to be increased in coxsackievirus B3-induced mouse viral myocarditis (Yang et al., 2011; Sesti-Costa et al., 2017). Although there are no direct reports concerning the

effects of IL-23 on viral myocarditis, emodin can reduce myocardial injury and mortality mediated by viral myocarditis by reducing the expression of IL-23, indicating that IL-23 can aggravate myocardial injury in viral myocarditis (Jiang et al., 2014). In an initial study, Kong et al. found that IL-27 levels were elevated in mice with viral myocarditis, and regulated IL-17 expression, suggesting that IL-27 may be involved in the development of viral myocarditis (Kong et al., 2014). In a follow-up study, Zhu et al. found that IL-27 inhibited immune responses to Th17 and reduced the expression of IL-17, thereby protecting against coxsackievirus B3-induced viral myocarditis (Zhu et al., 2015). Unlike other members of the IL-12 family, IL-35 levels were found to be reduced in a mouse model of viral myocarditis, and were negatively correlated with the severity of viral myocarditis, as was the frequency of Tregs (Hu et al., 2014; Ouyang et al., 2017; Xu et al., 2018). In addition, up-regulation of IL-35 expression can significantly reduce Th17-mediated immune responses, and decrease IL-17 expression, thereby alleviating cardiac injury caused by viral myocarditis (Hu et al., 2014). These studies have confirmed that all IL-12 family members are involved in the course of viral myocarditis, and the mechanisms involved in their action are related to the regulation of Th1 and Th17 immune responses. Whether other immune cells are involved needs further confirmation.

Interleukin-12 Family Members and Cardiomyopathy

Cardiomyopathy is a rare heart disease characterized by enlarged ventricular spaces with unknown etiology. Its pathological mechanisms are very complex, and many factors, including genetic variation, can induce its occurrence (Heinig et al., 2017).

Data from previous clinical experiment reported that IL-12 expression was found to be unchanged in patients with idiopathic dilated cardiomyopathy and their relatives (Marriott et al., 1996), whereas IL-12 expression was found to be elevated in patients with autoimmune cardiomyopathy or alcoholic cardiomyopathy (Izumi et al., 2000; Jenke et al., 2013; Panchenko et al., 2015). *IL-12R* gene polymorphisms, including *IL-12B* 3' UTR C and *IL-12B* 3' UTR CC, result in significantly higher gene expression, and may increase the incidence of Chagas cardiomyopathy (Zafra et al., 2007). Similar to the IL-12 expression trends, circulating or cardiac IL-23 levels were found to be increased in patients with dilated cardiomyopathy, and with idiopathic dilated cardiomyopathy (Yi et al., 2009; Li et al., 2010; Myers et al., 2016). Individuals with *IL-12, IL-23R* polymorphisms, such as SNP rs10889677, are more susceptible to dilated cardiomyopathy among the Chinese Han population, rather than those with rs1884444 and rs11465817 (Chen et al., 2009). Elevated *IL-27* mRNA levels were observed in the heart tissue of human dilated cardiomyopathy patients, and an *IL-27* gene polymorphism involving SNP rs153109, rather than SNP rs17855750, predisposes to dilated cardiomyopathy in the Chinese Han population (Noutsias et al., 2011; Chen et al., 2017b). The expression of IL-35 in human cardiomyopathy has not been reported.

In a mouse model of cardiac myosin immunized-mice, the absence of IL-12R significantly reduced cardiac immune responses and delayed the progression of autoimmune cardiomyopathy, whereas knockout of the STAT4 pathway and IFN-γ significantly reversed the protective effect of IL-12 in autoimmune cardiomyopathy (Afanasyeva et al., 2001). In another study, Fairweather et al. found that knockout of IL-12R significantly slowed the progression of dilated cardiomyopathy in murine chronic viral myocarditis (Fairweather et al., 2004). Using IL-12p35 and IL-12p40 knockout mice and anti-IL-23 neutralizing antibodies, other researchers found that IL-23, rather than IL-12, exacerbated the progression of a localized underwear purchase response in the heart and autoimmune myocarditis, which could be blocked by anti-IL-17 neutralizing antibodies (Sonderegger et al., 2006). In a recent study, Wu et al. demonstrated that IL-23 is necessary to initiate cardiac autoimmunity by stimulating the activation and differentiation of CD4+ T lymphocytes (Wu et al., 2016). In contrast there have been no studies regarding cardiomyopathy and involvement of IL-27 and IL-35.

Interleukin-12 Family Members and Other Cardiovascular Diseases

IL-12 family members are also implicated in other cardiovascular diseases that are less common, such as congenital heart disease, ventricular fibrillation, and rejection after cardiac transplantation.

In earlier studies, it was reported that in young children with congenital heart disease, circulating IL-12 levels did not exhibit significant change after surgery (Madhok et al., 2006). Furthermore, the *IL-27* gene polymorphism, SNP rs153109, rather than rs17855750, is associated with congenital atrial septal defects and congenital ventricular septal defects (Zhang et al., 2016). In addition, IL-12 levels in plasma and brain tissue are significantly increased in an animal model of cardiac arrest after ventricular fibrillation. (Janata et al., 2014; Heo et al., 2017). In a mouse model of heart transplantation, administration of an anti-IL-12p40 antibody significantly reduced invasion by γδT cells, reduced the expression of various inflammatory factors, and greatly improved the survival of mice (Wang et al., 2012). In an animal model of acute myocardial injury induced by the chemotherapeutic drug doxorubicin, deletion of *IL-12p35* significantly increased cardiac injury, which was associated with increased inflammatory responses, oxidative stress, apoptosis, and autophagy. Treatment with recombinant mouse IL-12 significantly reversed these effects, suggesting that both IL-12 and IL-35 may play protective roles in cardiac injury induced by doxorubicin (Jia, 2018; Ye et al., 2018b; Ye et al., 2018c).

CONCLUSIONS

The current review sought to describe the composition, structure, molecular receptors, signaling pathways, and regulatory roles of each IL-12 family member. The expression of IL-12 family members in different cardiovascular diseases in humans and animals, and the regulatory effect of IL-12 family members on inflammatory response in different cardiovascular models are also

summarized in this paper in **Tables 2** and **3**. In addition, we also described the roles and possible mechanisms of involvement of IL-12 members in different cardiovascular diseases. Among these IL-12 family members, IL-12 can aggravate a variety of cardiovascular diseases, in addition to acute cardiac injury induced by doxorubicin, and hypertension prompted by Ang II. IL-23 mostly plays a role in injury. IL-27 has a two-sided regulatory effect in cardiovascular disease, with both protective and damaging effects; while IL-35 has been found to play a protective role in all cardiovascular diseases. Just as **Table 4**. Although IL-12 family

TABLE 2 | Expression of IL-12 family members in cardiovascular diseases.

	Diseases	IL-12	IL-23	IL-27	IL-35	References
Mouse	AS	Increase	Increase	–	Contro	Jääskeläinen et al., 2013; Wang et al., 2014; Subramanian et al., 2015
	IR	Increase	Increase	–	–	Zhu et al., 2013; Zhang et al., 2014b; Zhu et al., 2014; Yan et al., 2017
	CAD	Increase	–	–	Decrease	Wang et al., 2014; Kan et al., 2016
	Hypertension	Increase	Increase	–	–	Li et al., 2012; Krebs et al., 2014; Ye et al., 2019
	Viral myocarditis	Increase	Increase	Increase	Decrease	Fairweather et al., 2003; Yang et al., 2011; Nyland et al., 2012; Jenke et al., 2014; Kong et al., 2014; Hu et al., 2014; Zha et al., 2015; Zhang et al., 2017; Miteva et al., 2017; Sesti-Costa et al., 2017; Ouyang et al., 2017; Xu et al., 2018
	CM	–	–	–	–	–
	AA, AD	–	–	–	–	–
	AF	–	–	–	–	–
Human	AS	–	–	Increase	–	Gregersen et al., 2017
	IR	–	–	–	–	–
	CAD	Increase	Increase	Increase	Contro	Zhou et al., 2001; Kempe et al., 2009; Correia et al., 2010; Lin et al., 2012; Khojasteh-Fard et al., 2012; Jin et al., 2012; Yong et al., 2013; Chistiakov et al., 2015; Abbas et al., 2015; A Shahi et al., 2015; Zykov et al., 2016; Opstad et al., 2016; Zhu et al., 2018; Rasa et al., 2018; Sun et al., 2019a
	Hypertension	Increase	–	–	–	Ye et al., 2019
	Viral myocarditis	–	–	–	–	–
	CM	Increase	Increase	Increase	–	Marriott et al., 1996; Izumi et al., 2000; Yi et al., 2009; Li et al., 2010; Jenke et al., 2013; Panchenko et al., 2015; Myers et al., 2016; Wu et al., 2016
	AA, AD	Unchanged	–	–	Decrease	Davis et al., 2001; Ye et al., 2018a
	AF	Increase	–	–	–	Stein et al., 2008; Lappegård et al., 2013

AS, atherosclerosis; IR, ischemia-reperfusion; CAD, coronary artery diseases; CM, cardiomyopathy; AA, arterial aneurysm; AD, aortic dissection; AF, atrial fibrillation; Contro, controversial.

TABLE 3 | Regulation of different inflammatory environments by members of the interleukin-12 family.

Organ	Mouse	Model	IL-12	IL-23	IL-27	IL-35	References
Heart	Wild type	Ang II	Down	–	–	–	Li et al., 2012
	Wild type	CVB3	Both	Up	Down	–	Shioi et al., 1997; Nishio et al., 2003; Fairweather et al., 2005; Jiang et al., 2014; Zhu et al., 2015
	Wild type	LLDB	Up	–		Down	Kan et al., 2016; Jia et al., 2019; Liu et al., 2019
	Wild type	IR	Up	Up	–	–	Zhu et al., 2013; Zhang et al., 2014b; Zhu et al., 2014; Hu et al., 2016; Yan et al., 2017; Liao et al., 2017
	Wild type	DOX	Down	–	–	Down	Jia, 2018; Ye et al., 2018b; Ye et al., 2018c
Aorta	Wild type	Ang II	Down	–	–	–	Ye et al., 2019
	ApoE-/-, LDLR-/-	HFD	Up	Both	Both	Down	Lee et al., 1999; Davenport and Tipping, 2003; Hauer et al., 2005; Koltsova et al., 2012; Hirase et al., 2013; Subramanian et al., 2015; Kan et al., 2016; Tao et al., 2016; Engelbertsen et al., 2018; Fatkhullina et al., 2018; Ryu et al., 2018; Huang et al., 2019; Huang et al., 2019; Wang et al., 2019; Jia et al., 2019; Liu et al., 2019

Ang II, angiotensin II; CVB3, Coxsackievirus B3; LLDB, ligation of left anterior descending branch; IR, ischemia-reperfusion; DOX, doxorubicin; HFD, high-fat diet.
Up: magnify inflammatory response.
Down: alleviate inflammatory response.
Both: both the magnification and reduction of inflammatory response were reported.

TABLE 4 | Regulation of IL-12 family members on cardiovascular diseases.

Diseases	IL-12	IL-23	IL-27	IL-35	References
Atherosclerosis	Aggravate	Contro	Aggravate	Alleviate	Lee et al., 1999; Davenport and Tipping, 2003; Hauer et al., 2005; Koltsova et al., 2012; Hirase et al., 2013; Wang et al., 2014; Subramanian et al., 2015; Tao et al., 2016; Gorzelak-Pabiś et al., 2017; Engelbertsen et al., 2018; Fatkhullina et al., 2018; Li et al., 2018; Ryu et al., 2018; Huang et al., 2019; Wang et al., 2019
Cardiac ischemia reperfusion	Aggravate	Aggravate	–	–	Zhu et al., 2013; Zhang et al., 2014b; Zhu et al., 2014; Hu et al., 2016; Liao et al., 2017; Yan et al., 2017
CAD	Aggravate	–	–	Alleviate	Kan et al., 2016; Jia et al., 2019; Liu et al., 2019
Hypertension	Alleviate	–	–	No effect	Li et al., 2012; Krebs et al., 2014; Ye et al., 2019
Aortic dissection	–	–	Aggravate	–	Peshkova et al., 2019
Viral myocarditis	Contro	Aggravate	Alleviate	Alleviate	Shioi et al., 1997; Nishio et al., 2003; Fairweather et al., 2005; Yang et al., 2011; Jiang et al., 2014; Kong et al., 2014; Hu et al., 2014; Zhu et al., 2015; Sesti-Costa et al., 2017; Ouyang et al., 2017; Xu et al., 2018
Cardiomyopathy	Aggravate	Aggravate	–	–	Afanasyeva et al., 2001; Fairweather et al., 2004; Sonderegger et al., 2006; Zafra et al., 2007; Chen et al., 2009; Noutsias et al., 2011; Wu et al., 2016; Chen et al., 2017b
Cardiac fibrosis	Aggravate	Aggravate	–	–	Li et al., 2012; Yan et al., 2012; Savvatis et al., 2014; Ye et al., 2020
Cardiac injury	Alleviate	–	–	Alleviate	Jia, 2018; Ye et al., 2018b; Ye et al., 2018c
Heart transplantation	Aggravate	–	–	–	Wang et al., 2012

Contro, controversial.

members are involved in various biological effects such as inflammatory responses, oxidative stress, and apoptosis, the regulation of immune cell differentiation and inflammation is still the most important mechanism for the involvement of IL-12 in the development of cardiovascular diseases. In view of this, IL-12 family members may be potential targets for clinical prevention, intervention, and treatment of cardiovascular diseases. Hence, when considering IL-12 family members as potential targets for cardiovascular disease therapy, the influence of other cytokines and interactions involving interleukin family members should be considered.

AUTHOR CONTRIBUTIONS

JY, YW, and ZW wrote this article. LL, ZY, MW, YX, DY, and JZ searched literatures. YL, QJ, and JW provided ideas and financial support.

FUNDING

This work was supported by the National Natural Science Foundation of China (No. 81770472 and No. 81560085 to QJ; No. 81760051 to YL).

REFERENCES

A Shahi, H., Shimada, K., Miyauchi, K., Yoshihara, T., Sai, E., Shiozawa, T., et al. (2015). Elevated circulating levels of inflammatory markers in patients with acute coronary syndrome. *Int. J. Vasc. Med.* 2015, 805375. doi: 10.1155/2015/805375

Abbas, A., Gregersen, I., Holm, S., Daissormont, I., Bjerkeli, V., Krohg-Sørensen, K., et al. (2015). Interleukin 23 levels are increased in carotid atherosclerosis: possible role for the interleukin 23/interleukin 17 axis. *Stroke* 46 (3), 793–799. doi: 10.1161/STROKEAHA.114.006516

Afanasyeva, M., Wang, Y., Kaya, Z., Stafford, E. A., Dohmen, K. M., Sadighi Akha, A. A., et al. (2001). Interleukin-12 receptor/STAT4 signaling is required for the development of autoimmune myocarditis in mice by an interferon-gamma-independent pathway. *Circulation* 18104 (25), 3145–3151. doi: 10.1161/hc5001.100629

Andrews, C., McLean, M. H., and Durum, S. K. (2016). Interleukin-27 as a novel therapy for inflammatory bowel disease: a critical review of the literature. *Inflamma. Bowel Dis.* 22 (9), 2255–2264. doi: 10.1097/MIB.0000000000000818

Bethel, M. A., Patel, R. A., Merrill, P., Lokhnygina, Y., Buse, J. B., Mentz, R. J., et al. (2018). Cardiovascular outcomes with glucagon-like peptide-1 receptor agonists in patients with type 2 diabetes: a meta-analysis. *Lancet Diabetes Endocrinol.* 6 (2), 105–113. doi: 10.1016/S2213-8587(17)30412-6

Chen, Y., Zhou, B., Peng, Y., Wang, Y., Li, C., Ding, X., et al. (2009). Interleukin-23 receptor gene polymorphisms is associated with dilated cardiomyopathy in Chinese Han population. *Tissue Antigens* 73 (4), 330–334. doi: 10.1111/j.1399-0039.2009.01217.x

Chen, H. S., Wang, W., Wu, S. N., and Liu, J. P. (2013). Corticosteroids for viral myocarditis. *Cochrane Database Syst. Rev.* 10, CD004471. doi: 10.1002/14651858.CD004471.pub3

Chen, Y., Zeng, J., Zhang, R., Zeng, L., Li, Y., Wei, H., et al. (2017a). Effect of interleukin-27 genetic variants on atrial fibrillation susceptibility. *Genet. Test Mol. Biomarkers* 21 (2), 97–101. doi: 10.1089/gtmb.2016.0219

Chen, Y., Zhang, R., Zeng, L., Wei, H., Chen, Y., and Zeng, J. (2017b). IL-27 genetic variation and susceptibility of dilated cardiomyopathy in Chinese Han population. *Per. Med.* 14 (5), 401–408. doi: 10.2217/pme-2017-0013

Chistiakov, D. A., Bobryshev, Y. V., and Orekhov, A. N. (2015). Heterogeneity of Tregs and the complexity in the IL-12 cytokine family signaling in driving T-cell immune responses in atherosclerotic vessels. *Mol. Immunol.* 65 (1), 133–138. doi: 10.1016/j.molimm.2015.01.013

Collison, L. W., and Vignali, D. A. (2008). Interleukin-35: odd one out or part of the family? *Immunol. Rev.* 226, 248–262. doi: 10.1111/j.1600-065X.2008.00704.x

Collison, L. W., Pillai, M. R., Chaturvedi, V., and Vignali, D. A. (2009). Regulatory T cell suppression is potentiated by target T cells in a cell contact, IL-35- and

IL-10-dependent manner. *J. Immunol.* 182 (10), 6121–6128. doi: 10.4049/jimmunol.0803646

Collison, L. W., Chaturvedi, V., Henderson, A. L., Giacomin, P. R., Guy, C., Bankoti, J., et al. (2010). IL-35-mediated induction of a potent regulatory T cell population. *Nat. Immunol.* 11 (12), 1093–1101. doi: 10.1038/ni.1952

Collison, L. W., Delgoffe, G. M., Guy, C. S., Vignali, K. M., Chaturvedi, V., Fairweather, D., et al. (2012). The composition and signaling of the IL-35 receptor are unconventional. *Nat. Immunol.* 13 (3), 290–299. doi: 10.1038/ni.2227

Correia, L. C., Andrade, B. B., Borges, V. M., Clarêncio, J., Bittencourt, A. P., Freitas, R., et al. (2010). Prognostic value of cytokines and chemokines in addition to the GRACE Score in non-ST-elevation acute coronary syndromes. *Clin. Chim. Acta* 411 (7-8), 540–545. doi: 10.1016/j.cca.2010.01.011

Cox, J. H., Kljavin, N. M., Ramamoorthi, N., Diehl, L., Batten, M., and Ghilardi, N. (2011). IL-27 promotes T cell-dependent colitis through multiple mechanisms. *J. Exp. Med.* 208 (1), 115–1123. doi: 10.1084/jem.20100410

Davenport, P., and Tipping, P. G. (2003). The role of interleukin-4 and interleukin-12 in the progression of atherosclerosis in apolipoprotein E-deficient mice. *Am. J. Pathol.* 163 (3), 1117–1125. doi: 10.1016/S0002-9440(10)63471-2

Davis, V. A., Persidskaia, R. N., Baca-Regen, L. M., Fiotti, N., Halloran, B. G., and Baxter, B. T. (2001). Cytokine pattern in aneurysmal and occlusive disease of the aorta. *J. Surg. Res.* 101 (2), 152–156. doi: 10.1006/jsre.2001.6281

Delgoffe, G. M., Murray, P. J., and Vignali, D. A. (2011). Interpreting mixed signals: the cell's cytokine conundrum. *Curr. Opin. Immunol.* 23 (5), 632–638. doi: 10.1016/j.coi.2011.07.013

Donofrio, M. T., Moon-Grady, A. J., Hornberger, L. K., Copel, J. A., Sklansky, M. S., Abuhamad, A., et al. (2014). Diagnosis and treatment of fetal cardiac disease: a scientific statement from the American Heart Association. *Circulation* 129 (21), 2183–2242. doi: 10.1161/01.cir.0000437597.44550.5d

Dukkipati, S. R., Koruth, J. S., Choudry, S., Miller, M. A., Whang, W., and Reddy, V. Y. (2017). Catheter ablation of ventricular tachycardia in structural heart disease: indications, strategies, and outcomes-part II. *J. Am. Coll. Cardiol.* 70 (23), 2924–2941. doi: 10.1016/j.jacc.2017.10.030

Engelbertsen, D., Depuydt, M. A. C., Verwilligen, R. A. F., Rattik, S., Levinsohn, E., Edsfeldt, A., et al. (2018). IL-23R deficiency does not impact atherosclerotic plaque development in mice. *J. Am. Heart Assoc.* 7 (8). doi: 10.1161/JAHA.117.008257

Fairweather, D., Yusung, S., Frisancho, S., Barrett, M., Gatewood, S., Steele, R., et al. (2003). IL-12 receptor beta 1 and Toll-like receptor 4 increase IL-1 beta- and IL-18-associated myocarditis and coxsackievirus replication. *J. Immunol.* 170 (9), 4731–4737. doi: 10.4049/jimmunol.170.9.4731

Fairweather, D., Frisancho-Kiss, S., Yusung, S. A., Barrett, M. A., Davis, S. E., Gatewood, S. J., et al. (2004). Interferon-gamma protects against chronic viral myocarditis by reducing mast cell degranulation, fibrosis, and the pro-fibrotic cytokines transforming growth factor-beta 1, interleukin-1 beta, and interleukin-4 in the heart. *Am. J. Pathol.* 165 (6), 1883–1894. doi: 10.1016/S0002-9440(10)63241-5

Fairweather, D., Frisancho-Kiss, S., Yusung, S. A., Barrett, M. A., Davis, S. E., Steele, R. A., et al. (2005). IL-12 protects against coxsackievirus B3-induced myocarditis by increasing IFN-gamma and macrophage and neutrophil populations in the heart. *J. Immunol.* 174 (1), 261–269. doi: 10.4049/jimmunol.174.1.261

Fatkhullina, A. R., Peshkova, I. O., Dzutsev, A., Aghayev, T., McCulloch, J. A., Thovarai, V., et al. (2018). An interleukin-23-interleukin-22 axis regulates intestinal microbial homeostasis to protect from diet-induced atherosclerosis. *Immunity* 49 (5), 943–957. doi: 10.1016/j.immuni.2018.09.011

Gorabi, A. M., Hajighasemi, S., Kiaie, N., Rosano, G. M. C., Sathyapalan, T., Al-Rasadi, K., et al. (2019). Anti-fibrotic effects of curcumin and some of its analogues in the heart. *Heart Fail. Rev.* doi: 10.1007/s10741-019-09854-6

Gorzelak-Pabiś, P., Chalubinski, M., Wojdan, K., Luczak, E., Duraj, I., Mozdzan, M., et al. (2017). Increased plasma concentrations of interleukin 35 in patients with coronary artery disease. *Arch. Med. Sci.* 13 (4), 778–784. doi: 10.5114/aoms.2016.63751

Gregersen, I., Sandanger, Ø., Askevold, E. T., Sagen, E. L., Yang, K., Holm, S., et al. (2017). Interleukin 27 is increased in carotid atherosclerosis and promotes NLRP3 inflammasome activation. *PloS One* 12 (11), e0188387. doi: 10.1371/journal.pone.0188387

Guzik, T. J., and Touyz, R. M. (2017). Oxidative Stress, inflammation, and vascular aging in hypertension. *Hypertension* 70 (4), 660–667. doi: 10.1161/HYPERTENSIONAHA.117.07802

Hauer, A. D., Uyttenhove, C., de Vos, P., Stroobant, V., Renauld, J. C., van Berkel, T. J., et al. (2005). Blockade of interleukin-12 function by protein vaccination attenuates atherosclerosis. *Circulation* 112 (7), 1054–1062. doi: 10.1161/CIRCULATIONAHA.104.533463

Heinig, M., Adriaens, M. E., Schafer, S., van Deutekom, H. W. M., Lodder, E. M., Ware, J. S., et al. (2017). Natural genetic variation of the cardiac transcriptome in non-diseased donors and patients with dilated cardiomyopathy. *Genome Biol.* 18 (1), 170. doi: 10.1186/s13059-017-1286-z

Heo, J. C., Kim, B., Kim, Y. N., Kim, D. K., and Lee, J. H. (2017). Induction of inflammation *in vivo* by electrocardiogram sensor operation using wireless power transmission. *Sens. (Basel)* 17 (12). doi: 10.3390/s17122905

Hirase, T., Hara, H., Miyazaki, Y., Ide, N., Nishimoto-Hazuku, A., Fujimoto, H., et al. (2013). Interleukin 27 inhibits atherosclerosis *via* immune regulation of macrophages in mice. *Am. J. Physiol. Heart Circ. Physiol.* 305 (3), H420–H429. doi: 10.1152/ajpheart.00198.2013

Hu, Y., Dong, C., Yue, Y., and Xiong, S. (2014). In vivo delivery of interleukin-35 relieves coxsackievirus-B3-induced viral myocarditis by inhibiting Th17 cells. *Arch. Virol.* 159 (9), 2411–2419. doi: 10.1007/s00705-014-2098-z

Hu, X., Ma, R., Lu, J., Zhang, K., Xu, W., Jiang, H., et al. (2016). IL-23 promotes myocardial I/R injury by increasing the inflammatory responses and oxidative stress reactions. *Cell Physiol. Biochem.* 38 (6), 2163–2172. doi: 10.1159/000445572

Huang, Y., Hu, H., Liu, L., Ye, J., Wang, Z., Que, B., et al. (2019). Interleukin-12p35 deficiency reverses the Th1/Th2 imbalance, aggravates the Th17/Treg imbalance, and ameliorates atherosclerosis in ApoE-/- mice. *Mediators Inflamm.* 2019, 3152040. doi: 10.1155/2019/3152040

Hunter, C. A. (2005). New IL-12-family members: IL-23 and IL-27, cytokines with divergent functions. *Nat. Rev. Immunol.* 5 (7), 521–531. doi: 10.1038/nri1648

Ihle, J. N. (1995). The Janus protein tyrosine kinase family and its role in cytokine signaling. *Adv. Immunol.* 60, 1–35. doi: 10.1016/S0065-2776(08)60582-9

Izumi, T., Takehana, H., Matsuda, C., Yokoyama, H., Kohno, K., Suzuki, K., et al. (2000). Experimental autoimmune myocarditis and its pathomechanism. *Herz* 25 (3), 274–278. doi: 10.1007/s000590050020

Jääskeläinen, A. E., Seppälä, S., Kakko, T., Jaakkola, U., and Kallio, J. (2013). Systemic treatment with neuropeptide Y receptor Y1-antagonist enhances atherosclerosis and stimulates IL-12 expression in ApoE deficient mice. *Neuropeptides* 47 (2), 67–73. doi: 10.1016/j.npep.2012.11.001

Jalife, J., and Kaur, K. (2015). Atrial remodeling, fibrosis, and atrial fibrillation. *Trends Cardiovasc. Med.* 25 (6), 475–484. doi: 10.1016/j.tcm.2014.12.015

Janata, A., Magnet, I. A., Uray, T., Stezoski, J. P., Janesko-Feldman, K., Tisherman, S. A., et al. (2014). Regional TNFα mapping in the brain reveals the striatum as a neuroinflammatory target after ventricular fibrillation cardiac arrest in rats. *Resuscitation* 85 (5), 694–701. doi: 10.1016/j.resuscitation.2014.01.033

Jenke, A., Wilk, S., Poller, W., Eriksson, U., Valaperti, A., Rauch, B. H., et al. (2013). Adiponectin protects against Toll-like receptor 4-mediated cardiac inflammation and injury. *Cardiovasc. Res.* 99 (3), 422–431. doi: 10.1093/cvr/cvt118

Jenke, A., Holzhauser, L., Löbel, M., Savvatis, K., Wilk, S., Weithäuser, A., et al. (2014). Adiponectin promotes coxsackievirus B3 myocarditis by suppression of acute anti-viral immune responses. *Basic Res. Cardiol.* 109 (3), 408. doi: 10.1007/s00395-014-0408-y

Jia, D., Jiang, H., Weng, X., Wu, J., Bai, P., Yang, W., et al. (2019). Interleukin-35 promotes macrophage survival and improves wound healing after myocardial infarction in mice. *Circ. Res.* 124 (9), 1323–1336. doi: 10.1161/CIRCRESAHA.118.314569

Jia, Z. (2018). The Clinical potential of IL-12/IL-35 in treating chemotherapy drug-induced cardiac injury. *EBioMedicine* 35, 2–3. doi: 10.1016/j.ebiom.2018.08.018

Jiang, N., Liao, W., and Kuang, X. (2014). Effects of emodin on IL-23/IL-17 inflammatory axis, Th17 cells and viral replication in mice with viral myocarditis. *Nan Fang Yi Ke Da Xue Xue Bao.* 34 (3), 373–378. doi: 10.3969/j.issn.1673-4254.2014.03.17

Jin, W., Zhao, Y., Yan, W., Cao, L., Zhang, W., Wang, M., et al. (2012). Elevated circulating interleukin-27 in patients with coronary artery disease is associated with dendritic cells, oxidized low-density lipoprotein, and severity of coronary artery stenosis. *Mediators Inflamm.* 2012, 506283. doi: 10.1155/2012/506283

Kan, X., Wu, Y., Ma, Y., Zhang, C., Li, P., Wu, L., et al. (2016). Deficiency of IL-12p35 improves cardiac repair after myocardial infarction by promoting angiogenesis. *Cardiovasc. Res.* 109 (2), 249–259. doi: 10.1093/cvr/cvv255

Kastelein, R. A., Hunter, C. A., and Cua, D. J. (2007). Discovery and biology of IL-23 and IL-27: related but functionally distinct regulators of inflammation. *Annu. Rev. Immunol.* 25, 221–242. doi: 10.1146/annurev.immunol.22.012703.104758

Kempe, S., Heinz, P., Kokai, E., Devergne, O., Marx, N., and Wirth, T. (2009). Epstein-barr virus-induced gene-3 is expressed in human atheroma plaques. *Am. J. Pathol.* 175 (1), 440–447. doi: 10.2353/ajpath.2009.080752

Khojasteh-Fard, M., Abolhalaj, M., Amiri, P., Zaki, M., Taheri, Z., Qorbani, M., et al. (2012). IL-23 gene expression in PBMCs of patients with coronary artery disease. *Dis. Markers* 33 (6), 289–293. doi: 10.1155/2012/629814

Kirabo, A., Fontana, V., de Faria, A. P., Loperena, R., Galindo, C. L., Wu, J., et al. (2014). DC isoketal-modified proteins activate T cells and promote hypertension. *J. Clin. Invest.* 124 (10), 4642–4656. doi: 10.1172/JCI74084

Koltsova, E. K., Kim, G., Lloyd, K. M., Saris, C. J., von Vietinghoff, S., Kronenberg, M., et al. (2012). Interleukin-27 receptor limits atherosclerosis in Ldlr-/- mice. *Circ. Res.* 111 (10), 1274–1285. doi: 10.1161/CIRCRESAHA.112.277525

Kong, Q., Gao, M., Xue, Y., Pan, X., Lai, W., and Wu, W. (2014). Interleukin-17 contributes to the macrophage secretion of interleukin-27 in a murine model of viral myocarditis. *Zhonghua Xin Xue Guan Bing Za Zhi* 42 (5), 428–432. doi: 10.3760/cma.j.issn.0253–3758.2014.05.017

Krebs, C. F., Lange, S., Niemann, G., Rosendahl, A., Lehners, A., Meyer-Schwesinger, C., et al. (2014). Deficiency of the interleukin 17/23 axis accelerates renal injury in mice with deoxycorticosterone acetate +angiotensin II-induced hypertension. *Hypertension* 63 (3), 565–571. doi: 10.1161/HYPERTENSIONAHA.113.02620

Langrish, C. L., McKenzie, B. S., Wilson, N. J., de Waal Malefyt, R., Kastelein, R. A., and Cua, D. J. (2004). IL-12 and IL-23: master regulators of innate and adaptive immunity. *Immunol. Rev.* 202, 96–105. doi: 10.1111/j.0105-2896.2004.00214.x

Lappegård, K. T., Pop-Purceleanu, M., van Heerde, W., Sexton, J., Tendolkar, I., and Pop, G. (2013). Improved neurocognitive functions correlate with reduced inflammatory burden in atrial fibrillation patients treated with intensive cholesterol lowering therapy. *J. Neuroinflammation* 10, 78. doi: 10.1186/1742-2094-10-78

Lee, T. S., Yen, H. C., Pan, C. C., and Chau, L. Y. (1999). The role of interleukin 12 in the development of atherosclerosis in ApoE-deficient mice. *Arterioscler. Thromb. Vasc. Biol.* 19 (3), 734–742. doi: 10.1161/01.ATV.19.3.734

Leong, D. P., Joseph, P. G., McKee, M., Anand, S. S., Teo, K. K., Schwalm, J. D., et al. (2017). Reducing the global burden of cardiovascular disease, part 2: prevention and treatment of cardiovascular disease. *Circ. Res.* 121 (6), 695–710. doi: 10.1161/CIRCRESAHA.117.311849

Li, J., Wang, L., Wang, S., Zhu, H., Ye, P., Xie, A., et al. (2010). The Treg/Th17 imbalance in patients with idiopathic dilated cardiomyopathy. *Scand. J. Immunol.* 71 (4), 298–303. doi: 10.1111/j.1365-3083.2010.02374.x

Li, Y., Zhang, C., Wu, Y., Han, Y., Cui, W., Jia, L., et al. (2012). Interleukin-12p35 deletion promotes CD4 T-cell-dependent macrophage differentiation and enhances angiotensin II-Induced cardiac fibrosis. *Arterioscler. Thromb. Vasc. Biol.* 32 (7), 1662–1674. doi: 10.1161/ATVBAHA.112.249706

Li, X., Shao, Y., Sha, X., Fang, P., Kuo, Y. M., Andrews, A. J., et al. (2018). IL-35 (interleukin-35) suppresses endothelial cell activation by inhibiting mitochondrial reactive oxygen species-mediated site-specific acetylation of H3K14 (Histone 3 Lysine 14). *Arterioscler. Thromb. Vasc. Biol.* 38 (3), 599–609. doi: 10.1161/ATVBAHA.117.310626

Liao, Y., Hu, X., Guo, X., Zhang, B., Xu, W., and Jiang, H. (2017). Promoting effects of IL–23 on myocardial ischemia and reperfusion are associated with increased expression of IL–17A and up-regulation of the JAK2–STAT3 signaling pathway. *Mol. Med. Rep.* 16 (6), 9309–9316. doi: 10.3892/mmr.2017.7771

Lin, Y., Huang, Y., Lu, Z., Luo, C., Shi, Y., Zeng, Q., et al. (2012). Decreased plasma IL-35 levels are related to the left ventricular ejection fraction in coronary artery diseases. *PloS One* 7 (12), e52490. doi: 10.1371/journal.pone.0052490

Liu, X., Zhang, R., Hou, J., Wu, J., Zhang, M., Fang, S., et al. (2019). Interleukin-35 promotes early endothelialization after stent implantation by regulating macrophage activation. *Clin. Sci. (Lond.)* 133 (7), 869–884. doi: 10.1042/CS20180879

Longenecker, C. T., Sullivan, C., and Baker., J. V. (2016). Immune activation and cardiovascular disease in chronic HIV infection. *Curr. Opin. HIV AIDS* 11 (2), 216–225. doi: 10.1097/COH.0000000000000227

Ma, X., and Trinchieri, G. (2001). Regulation of interleukin-12 production in antigen-presenting cells. *Adv. Immunol.* 79, 55–92. doi: 10.1016/S0065-2776(01)79002-5

Madhok, A. B., Ojamaa, K., Haridas, V., Parnell, V. A., Pahwa, S., and Chowdhury, D. (2006). Cytokine response in children undergoing surgery for congenital heart disease. *Pediatr. Cardiol.* 27 (4), 408–413. doi: 10.1007/s00246-006-0934-y

Mallat, Z., Tedgui, A., and Henrion, D. (2016). Role of microvascular tone and extracellular matrix contraction in the regulation of interstitial fluid: implications for aortic dissection. *Arterioscler. Thromb. Vasc. Biol.* 36 (9), 1742–1747. doi: 10.1161/ATVBAHA.116.307909

Marriott, J. B., Goldman, J. H., Keeling, P. J., Baig, M. K., Dalgleish, A. G., and McKenna, W. J. (1996). Abnormal cytokine profiles in patients with idiopathic dilated cardiomyopathy and their asymptomatic relatives. *Heart* 75 (3), 287–290. doi: 10.1136/hrt.75.3.287

Miteva, K., Pappritz, K., El-Shafeey, M., Dong, F., Ringe, J., Tschöpe, C., et al. (2017). Mesenchymal stromal cells modulate monocytes trafficking in coxsackievirus B3-induced myocarditis. *Stem Cells Transl. Med.* 6 (4), 1249–1261. doi: 10.1002/sctm.16-0353

Moore-Morris, T., Guimarães-Camboa, N., Yutzey, K. E., Pucéat, M., and Evans, S. M. (2015). Cardiac fibroblasts: from development to heart failure. *J. Mol. Med. (Berl.)* 93 (8), 823–830. doi: 10.1007/s00109-015-1314-y

Myers, J. M., Cooper, L. T., Kem, D. C., Stavrakis, S., Kosanke, S. D., Shevach, E. M., et al. (2016). Cardiac myosin-Th17 responses promote heart failure in human myocarditis. *JCI Insight* 1 (9). doi: 10.1172/jci.insight.85851

Nattel, S. (2017). Molecular and cellular mechanisms of atrial fibrosis in atrial fibrillation. *JACC Clin. Electrophysiol.* 3 (5), 425–435. doi: 10.1016/j.jacep.2017.03.002

Nishio, R., Shioi, T., Sasayama, S., and Matsumori, A. (2003). Carvedilol increases the production of interleukin-12 and interferon-gamma and improves the survival of mice infected with the encephalomyocarditis virus. *J. Am. Coll. Cardiol.* 41 (2), 340–345. doi: 10.1016/S0735-1097(02)02711-0

Noutsias, M., Rohde, M., Göldner, K., Block, A., Blunert, K., Hemaidan, L., et al. (2011). Expression of functional T-cell markers and T-cell receptor Vbeta repertoire in endomyocardial biopsies from patients presenting with acute myocarditis and dilated cardiomyopathy. *Eur. J. Heart Fail.* 13 (6), 611–618. doi: 10.1093/eurjhf/hfr014

Nyland, J. F., Fairweather, D., Shirley, D. L., Davis, S. E., Rose, N. R., and Silbergeld, E. K. (2012). Low-dose inorganic mercury increases severity and frequency of chronic coxsackievirus-induced autoimmune myocarditis in mice. *Toxicol. Sci.* 125 (1), 134–143. doi: 10.1093/toxsci/kfr264

O'Shea, J. J., Gadina, M., and Schreiber, R. D. (2002). Cytokine signaling in 2002: new surprises in the Jak/Stat pathway. *Cell* 109, S121–S131. doi: 10.1016/s0092-8674(02)00701-8

Oppmann, B., Lesley, R., Blom, B., Timans, J. C., Xu, Y., Hunte, B., et al. (2000). Novel p19 protein engages IL-12p40 to form a cytokine, IL-23, with biological activities similar as well as distinct from IL-12. *Immunity* 13 (5), 715–725. doi: 10.1016/S1074-7613(00)00070-4

Opstad, T. B., Arnesen, H., Pettersen, A. Å., and Seljeflot, I. (2016). Combined elevated levels of the pro-inflammatory cytokines IL-18 and IL-12 are associated with clinical events in patients with coronary artery disease: an observational study. *Metab. Syndr. Relat. Disord.* 14 (5), 242–248. doi: 10.1089/met.2015.0130

Ouyang, H., Xiang, L., Chen, J., Xu, W., Jiao, Y., and Shen, H. (2017). Significant reduction of peripheral blood interleukin-35 and CD4+EBI3+ T cells, which are negatively correlated with an increase in the plasma IL-17 and cTnI level, in viral myocarditis patients. *Cent. Eur. J. Immunol.* 42 (1), 91–96. doi: 10.5114/ceji.2016.65892

Panchenko, L. F., Moiseev, V. S., Pirozhkov, S. V., Terebilina, N. N., Naumova, T. A., Baronets, V., et al. (2015). Blood content of markers of inflammation and cytokines in patients with alcoholic cardiomyopathy and ischemic heart disease at various stages of heart failure. *Kardiologiia* 55 (3), 41–48. doi: 10.18565/cardio.2015.3.41-48

Peshkova, I. O., Aghayev, T., Fatkhullina, A. R., Makhov, P., Titerina, E. K., Eguchi, S., et al. (2019). IL-27 receptor-regulated stress myelopoiesis drives abdominal aortic aneurysm development. *Nat. Commun.* 10 (1), 5046. doi: 10.1038/s41467-019-13017-4

Peter, L., Paul, M. R., and Göran, K. H. (2009). Inflammation in atherosclerosis: from pathophysiology to practice. *J. Am. Coll. Cardiol.* 54 (23), 2129–2138. doi: 10.1016/j.jacc.2009.09.009

Pflanz, S., Hibbert, L., Mattson, J., Rosales, R., Vaisberg, E., Bazan, J. F., et al. (2004). WSX-1 and glycoprotein 130 constitute a signal-transducing receptor for IL-27. *J. Immunol.* 172 (4), 2225–2231. doi: 10.4049/jimmunol.172.4.2225

Pober, J. S. (2014). Is hypertension an autoimmune disease? *J. Clin. Invest.* 124 (10), 4234–4236. doi: 10.1172/JCI77766

Pollack, A., Kontorovich, A. R., Fuster, V., and Dec, G. W. (2015). Viral myocarditis–diagnosis, treatment options, and current controversies. *Nat. Rev. Cardiol.* 12 (11), 670–680. doi: 10.1038/nrcardio.2015.108

Posadas-Sánchez, R., Pérez-Hernández, N., Rodríguez-Pérez, J. M., Coral-Vázquez, R. M., Roque-Ramírez, B., Llorente, L., et al. (2017). Interleukin-27 polymorphisms are associated with premature coronary artery disease and metabolic parameters in the Mexican population: the genetics of atherosclerotic disease (GEA) Mexican study. *Oncotarget* 8 (38), 64459–64470. doi: 10.18632/oncotarget.16223

Presky, D. H., Yang, H., Minetti, L. J., Chua, A. O., Nabavi, N., Wu, C. Y., et al. (1996). A functional interleukin 12 receptor complex is composed of two beta-type cytokine receptor subunits. *Proc. Natl. Acad. Sci. U. S. A.* 93 (24), 14002–14007. doi: 10.1073/pnas.93.24.14002

Rabkin, S. W. (2017). The role matrix metalloproteinases in the production of aortic aneurysm. *Prog. Mol. Biol. Transl. Sci.* 147, 239–265. doi: 10.1016/bs.pmbts.2017.02.002

Raffort, J., Lareyre, F., Clément, M., Hassen-Khodja, R., Chinetti, G., and Mallat, Z. (2017). Monocytes and macrophages in abdominal aortic aneurysm. *Nat. Rev. Cardiol.* 14 (8), 457–471. doi: 10.1038/nrcardio.2017.52

Rahman, K., and Fisher., E. A. (2018). Insights from pre-clinical and clinical studies on the role of innate inflammation in atherosclerosis regression. *Front. Cardiovasc. Med.* 5, 32. doi: 10.3389/fcvm.2018.00032

Rasa, F., Naderi, N., Eftekhar, E., Mansoori, E., and Rahimzadeh, M. (2018). Vitamin D status in coronary artery disease: association with IL-35 and TGF-β1 and disease severity. *Endocr. Metab. Immune Disord. Drug Targets* 18 (5), 522–529. doi: 10.2174/1871530318666180426101756

Ryu, H., Lim, H., Choi, G., Park, Y. J., Cho, M., Na, H., et al. (2018). Atherogenic dyslipidemia promotes autoimmune follicular helper T cell responses *via* IL-27. *Nat. Immunol.* 19 (6), 583–593. doi: 10.1038/s41590-018-0102-6

Savvatis, K., Pappritz, K., Becher, P. M., Lindner, D., Zietsch, C., Volk, H. D., et al. (2014). Interleukin-23 deficiency leads to impaired wound healing and adverse prognosis after myocardial infarction. *Circ. Heart Fail.* 7 (1), 161–171. doi: 10.1161/CIRCHEARTFAILURE.113.000604

Schanze, N., Bode, C., and Duerschmied, D. (2019). Platelet contributions to myocardial ischemia/reperfusion Injury. *Front. Immunol.* 10, 1260. doi: 10.3389/fimmu.2019.01260

Sesti-Costa, R., Françozo, M. C. S., Silva, G. K., Proenca-Modena, J. L., and Silva, J. S. (2017). TLR3 is required for survival following Coxsackievirus B3 infection by driving T lymphocyte activation and polarization: the role of dendritic cells. *PloS One* 12 (10), e0185819. doi: 10.1371/journal.pone.0185819

Sherifova, S., and Holzapfel, G. A. (2019). Biomechanics of aortic wall failure with a focus on dissection and aneurysm: a review. *Acta Biomater.* 99, 1–17. doi: 10.1016/j.actbio.2019.08.017

Shin, B., Cowan, D. B., Emani, S. M., Del Nido, P. J., and McCully, J. D. (2017). Mitochondrial transplantation in myocardial ischemia and reperfusion injury. *Adv. Exp. Med. Biol.* 982, 595–619. doi: 10.1007/978-3-319-55330-6_31

Shioi, T., Matsumori, A., Nishio, R., Ono, K., Kakio, T., and Sasayama, S. (1997). Protective role of interleukin-12 in viral myocarditis. *J. Mol. Cell Cardiol.* 29 (9), 2327–2334. doi: 10.1006/jmcc.1997.0445

Sonderegger, I., Röhn, T. A., Kurrer, M. O., Iezzi, G., Zou, Y., Kastelein, R. A., et al. (2006). Neutralization of IL-17 by active vaccination inhibits IL-23-dependent autoimmune myocarditis. *Eur. J. Immunol.* 36 (11), 2849–2856. doi: 10.1002/eji.200636484

Stein, A., Wessling, G., Deisenhofer, I., Busch, G., Steppich, B., Estner, H., et al. (2008). Systemic inflammatory changes after pulmonary vein radiofrequency ablation do not alter stem cell mobilization. *Europace* 10 (4), 444–449. doi: 10.1093/europace/eun041

Subramanian, M., Thorp, E., and Tabas, I. (2015). Identification of a non-growth factor role for GM-CSF in advanced atherosclerosis: promotion of macrophage apoptosis and plaque necrosis through IL-23 signaling. *Circ. Res.* 116 (2), e13–e24. doi: 10.1161/CIRCRESAHA.116.304794

Sun, L., He, C., Nair, L., Yeung, J., and Egwuagu, C. E. (2015). Interleukin 12 (IL-12) family cytokines: role in immune pathogenesis and treatment of CNS autoimmune disease. *Cytokine* 75 (2), 249–255. doi: 10.1016/j.cyto.2015.01.030

Sun, J., Yu, H., Liu, H., Pu, D., Gao, J., Jin, X., et al. (2019a). Correlation of pre-operative circulating inflammatory cytokines with restenosis and rapid angiographic stenotic progression risk in coronary artery disease patients underwent percutaneous coronary intervention with drug-eluting stents. *J. Clin. Lab. Anal.*, e23108. doi: 10.1002/jcla.23108

Sun, F., Guo, Z., Zhang, C., Che, H., Gong, W., Shen, Z., et al. (2019b). LncRNA NRON alleviates atrial fibrosis through suppression of M1 macrophages activated by atrial myocytes. *Biosci. Rep.* 39 (11). doi: 10.1042/BSR20192215

Tao, L., Zhu, J., Chen, Y., Wang, Q., Pan, Y., Yu, Q., et al. (2016). IL-35 improves Treg-mediated immune suppression in atherosclerotic mice. *Exp. Ther. Med.* 12 (4), 2469–2476. doi: 10.3892/etm.2016.3649

Timasheva, Y. R., Nasibullin, T. R., Zakirova, A. N., and Mustafina, O. E. (2008). Association of interleukin-6, interleukin-12, and interleukin-10 gene polymorphisms with essential hypertension in Tatars from Russia. *Biochem. Genet.* 46 (1-2), 64–74. doi: 10.1007/s10528-007-9130-x

Vargas-Alarcón, G., Pérez-Hernández, N., Rodríguez-Pérez, J. M., Fragoso, J. M., Posadas-Romero, C., López-Bautista, F., et al. (2019). Interleukin 27 polymorphisms, their association with insulin resistance and their contribution to subclinical atherosclerosis. The GEA Mexican study. *Cytokine* 114, 32–37. doi: 10.1016/j.cyto.2018.11.028

Vignali, D. A., and Kuchroo, V. K. (2012). IL-12 family cytokines: immunological playmakers. *Nat. Immunol.* 13 (8), 722–728. doi: 10.1038/ni.2366

Vignali, D. A. A., Collison, L. W., and Workman, C. J. (2008). How regulatory T cells work. *Nat. Rev. Immunol.* 8, 523–532. doi: 10.1038/nri2343

Wang, S., Xu, X., Xie, A., Li, J., Ye, P., Liu, Z., et al. (2012). Anti-interleukin-12/23p40 antibody attenuates chronic rejection of cardiac allografts partly *via* inhibition γδT cells. *Clin. Exp. Immunol.* 169 (3), 320–329. doi: 10.1111/j.1365-2249.2012.04612.x

Wang, B., Dai, S., Dong, Z., Sun, Y., Song, X., Guo, C., et al. (2014). The modulation of endoplasmic reticulum stress by chemical chaperone up-regulates immune negative cytokine IL-35 in apolipoprotein E-deficient mice. *PloS One* 9 (1), e87787. doi: 10.1371/journal.pone.0087787

Wang, J., Zhao, P., Gao, Y., Zhang, F., Yuan, X., Jiao, Y., et al. (2019). The effects of anti-IL-23p19 therapy on atherosclerosis development in ApoE-/- mice. *J. Interferon Cytokine Res.* 39 (9), 564–571. doi: 10.1089/jir.2019.0050

Wei, X., Zhang, J., Gu, Q., Huang, M., Zhang, W., Guo, J., et al. (2017). Reciprocal expression of IL-35 and IL-10 defines two distinct effector Treg subsets that are required for maintenance of immune tolerance. *Cell Rep.* 21 (7), 1853–1869. doi: 10.1016/j.celrep.2017.10.090

Wojno, E. D., and Hunter, C. A. (2012). New directions in the basic and translational biology of interleukin-27. *Trends Immunol.* 33, 91–97. doi: 10.1016/j.it.2011.11.003

Wu, L., Diny, N. L., Ong, S., Barin, J. G., Hou, X., Rose, N. R., et al. (2016). Pathogenic IL-23 signaling is required to initiate GM-CSF-driven autoimmune myocarditis in mice. *Eur. J. Immunol.* 46 (3), 582–592. doi: 10.1002/eji.201545924

Xu, P., Ji, L., Tian, S., and Li, F. (2018). Clinical effects of tanshinone IIA sodium sulfonate combined with trimetazidine and levocarnitine in the treatment of AVMC and its effects on serum TNF-α, IL-18 and IL-35. *Exp. Ther. Med.* 16 (5), 4070–4074. doi: 10.13194/j.issn.1673-842x.2016.02.064

Yan, X., Shichita, T., Katsumata, Y., Matsuhashi, T., Ito, H., Ito, K., et al. (2012). Deleterious effect of the IL-23/IL-17A axis and γδT cells on left ventricular remodeling after myocardial infarction. *J. Am. Heart Assoc.* 1 (5), e004408. doi: 10.1161/JAHA.112.004408

Yan, X., Zhang, H., Fan, Q., Hu, J., Tao, R., Chen, Q., et al. (2017). Dectin-2 deficiency modulates Th1 differentiation and improves wound healing after myocardial infarction. *Circ. Res.* 120 (7), 1116–1129. doi: 10.1161/CIRCRESAHA.116.310260

Yang, F., Wu, W. F., Yan, Y. L., Pang, Y., Kong, Q., and Huang, Y. L. (2011). Expression of IL-23/Th17 pathway in a murine model of Coxsackie virus B3-induced viral myocarditis. *Virol. J.* 8, 301. doi: 10.1186/1743-422X-8-301

Ye, J., Wang, Y., Wang, Z., Ji, Q., Huang, Y., Zeng, T., et al. (2018a). Circulating Th1, Th2, Th9, Th17, Th22, and Treg levels in aortic dissection patients. *Mediators Inflamm.* 2018, 5697149. doi: 10.1155/2018/5697149

Ye, J., Huang, Y., Que, B., Chang, C., Liu, W., Hu, H., et al. (2018b). Interleukin-12p35 knock out aggravates doxorubicin-induced cardiac injury and dysfunction by aggravating the inflammatory response, oxidative stress, apoptosis and autophagy in mice. *EBioMedicine* 35, 29–39. doi: 10.1016/j.ebiom.2018.06.009

Ye, J., Wang, Z., Huang, Y., Wang, M., Que, B., Ye, D., et al. (2018c). The clinical potential of IL-12/IL-35 in treating chemotherapy drug-induced cardiac injury - authors' reply. *EBioMedicine* 35, 4–5. doi: 10.1016/j.ebiom.2018.08.049

Ye, J., Que, B., Huang, Y., Lin, Y., Chen, J., Liu, L., et al. (2019). Interleukin-12p35 knockout promotes macrophage differentiation, aggravates vascular dysfunction, and elevates blood pressure in angiotensin II-infused mice. *Cardiovasc. Res.* 115 (6), 1102–1113. doi: 10.1093/cvr/cvy263

Ye, J., Wang, Y., Wang, Z., Liu, L., Yang, Z., Ye, D., et al. (2020). Interleukin-12p35 deficiency enhances mitochondrial dysfunction and aggravates cardiac remodeling in aging mice. *Aging (Albany NY).* 11. doi: 10.18632/aging.102609

Yi, A., Jian, L., Xiaojing, H., and Hui, X. (2009). The prevalence of Th17 cells in patients with dilated cardiomyopathy. *Clin. Invest. Med.* 32 (2), E144–E150. doi: 10.25011/cim.v32i2.6032

Yong, K., Dogra, G., Boudville, N., Chan, D., Adams, L., Ching, H., et al. (2013). Interleukin-12 is associated with arterial stiffness in healthy individuals. *Am. J. Hypertens.* 26 (2), 159–162. doi: 10.1093/ajh/hps032

Zafra, G., Morillo, C., Martín, J., González, A., and González, C. I. (2007). Polymorphism in the 3' UTR of the IL12B gene is associated with Chagas' disease cardiomyopathy. *Microbes Infect.* 9 (9), 1049–1052. doi: 10.1016/j.micinf.2007.04.010

Zha, X., Yue, Y., Dong, N., and Xiong, S. (2015). Endoplasmic reticulum stress aggravates viral myocarditis by raising inflammation through the IRE1-associated NF-κB pathway. *Can. J. Cardiol.* 31 (8), 1032–1040. doi: 10.1016/j.cjca.2015.03.003

Zhang, M., Cai, Z. R., Zhang, B., Cai, X., Li, W., Guo, Z., et al. (2014a). Functional polymorphisms in interleukin-23 receptor and susceptibility to coronary artery disease. *DNA Cell Biol.* 33 (12), 891–897. doi: 10.1089/dna.2014.2573

Zhang, A., Mao, X., Li, L., Tong, Y., Huang, Y., Lan, Y., et al. (2014b). Necrostatin-1 inhibits Hmgb1-IL-23/IL-17 pathway and attenuates cardiac ischemia reperfusion injury. *Transpl. Int.* 27 (10), 1077–1085. doi: 10.1111/tri.12349

Zhang, D., Ma, M., Yang, Y., Wan, L., Yang, Z., Lv, J., et al. (2016). Association between polymorphisms in IL27 and risk for CHD in a Chinese population. *Cardiol. Young.* 26 (2), 237–243. doi: 10.1017/S1047951115000037

Zhang, H., Yue, Y., Sun, T., Wu, X., and Xiong, S. (2017). Transmissible endoplasmic reticulum stress from myocardiocytes to macrophages is pivotal for the pathogenesis of CVB3-induced viral myocarditis. *Sci. Rep.* 7, 42162. doi: 10.1038/srep42162

Zhou, R. H., Shi, Q., Gao, H. Q., and Shen, B. J. (2001). Changes in serum interleukin-8 and interleukin-12 levels in patients with ischemic heart disease in a Chinese population. *J. Atheroscler. Thromb.* 8 (1), 30–32. doi: 10.5551/jat1994.8.30

Zhu, H., Li, J., Wang, S., Liu, K., Wang, L., and Huang, L. (2013). Hmgb1-TLR4-IL-23-IL-17A axis promote ischemia-reperfusion injury in a cardiac transplantation model. *Transplantation* 95 (12), 1448–1454. doi: 10.1097/TP.0b013e318293b7e1

Zhu, H., Cui, D., Liu, K., Wang, L., Huang, L., and Li, J. (2014). Long pentraxin PTX3 attenuates ischemia reperfusion injury in a cardiac transplantation model. *Transpl. Int.* 27 (1), 87–95. doi: 10.1111/tri.12197

Zhu, H., Lou, C., and Liu, P. (2015). Interleukin-27 ameliorates coxsackievirus-B3-induced viral myocarditis by inhibiting Th17 cells. *Virol. J.* 12, 189. doi: 10.1186/s12985-015-0418-x

Zhu, Z., Zhang, Y., Ye, J., Wang, X., Fu, X., Yin, Y., et al. (2018). IL-35 promoted STAT3 phosphorylation and IL-10 production in B cells, but its production was reduced in patients with coronary artery diseases. *Hum. Immunol.* 79 (12), 869–875. doi: 10.1016/j.humimm.2018.10.009

Zykov, M. V., Barbarash, O. L., Kashtalap, V. V., Kutikhin, A. G., and Barbarash, L. S. (2016). Interleukin-12 serum level has prognostic value in patients with ST-segment elevation myocardial infarction. *Heart Lung.* 45 (4), 336–340. doi: 10.1016/j.hrtlng.2016.03.007

Conflict of Interest: The authors declare that the research was conducted in the absence of any commercial or financial relationships that could be construed as a potential conflict of interest.

frontiers in Pharmacology

ORIGINAL RESEARCH
published: 18 March 2020
doi: 10.3389/fphar.2020.00203

The Anti-inflammatory Mediator Resolvin E1 Protects Mice Against Lipopolysaccharide-Induced Heart Injury

Jishou Zhang[1,2,3†], Menglong Wang[1,2,3†], Jing Ye[1,2,3†], Jianfang Liu[1,2,3], Yao Xu[1,2,3], Zhen Wang[1,2,3], Di Ye[1,2,3], Mengmeng Zhao[1,2,3] and Jun Wan[1,2,3]*

[1] Department of Cardiology, Renmin Hospital of Wuhan University, Wuhan, China, [2] Cardiovascular Research Institute, Wuhan University, Wuhan, China, [3] Hubei Key Laboratory of Cardiology, Wuhan, China

OPEN ACCESS

Edited by:
Owen Llewellyn Woodman,
Monash University, Australia

Reviewed by:
Roberta d'Emmanuele di Villa Bianca,
University of Naples Federico II, Italy
Jason Hellmann,
University of Louisville, United States

***Correspondence:**
Jun Wan
wanjun@whu.edu.cn

[†] These authors have contributed equally to this work

Specialty section:
This article was submitted to Cardiovascular and Smooth Muscle Pharmacology, a section of the journal Frontiers in Pharmacology

Received: 21 October 2019
Accepted: 14 February 2020
Published: 18 March 2020

Citation:
Zhang J, Wang M, Ye J, Liu J, Xu Y, Wang Z, Ye D, Zhao M and Wan J (2020) The Anti-inflammatory Mediator Resolvin E1 Protects Mice Against Lipopolysaccharide-Induced Heart Injury. Front. Pharmacol. 11:203. doi: 10.3389/fphar.2020.00203

Background: Sepsis-induced cardiomyopathy (*SIC*) is a common severe complication of sepsis that contributes to mortality. *SIC* is closely associated with excessive inflammatory responses, failed inflammation resolution, and apoptotic damage. Resolvin E1 (RvE1), an omega-3 polyunsaturated fatty acid (PUFA)-derived metabolite, has been reported to exert anti-inflammatory or proresolving activity in multiple animal models of inflammatory disease. However, the therapeutic potential of RvE1 in *SIC* remains undetermined, which was, therefore, the aim of the present study.

Methods: C57BL/6J mice were randomly divided into three groups: control, lipopolysaccharide (LPS), and LPS + RvE1. Echocardiography, Western blotting (WB), quantitative real-time (QRT)-PCR, histological analyses, and flow cytometry were used to evaluate cardiac function, myocardial inflammation, and the underlying mechanisms.

Results: The RvE1-injected group showed improved left ventricular (LV) function and reduced serum lactate dehydrogenase (LDH) and creatine kinase myocardial bound (CK-MB) levels. Compared to LPS treatment alone, RvE1 treatment inhibited the infiltration of neutrophils and macrophages into the heart and spleen and suppressed the secretion of pro-inflammatory cytokines, including interleukin (IL)-1β, IL-6, and monocyte chemoattractant protein (MCP)-1, in the heart. We also observed that the activation of the mitogen-activated protein kinase (MAPK) and nuclear factor (NF)-κB signaling pathways was blocked by RvE1 treatment, and this inhibition contributed to the improvement in the inflammatory response induced by LPS. RvE1 inhibited LPS-induced M1 macrophage polarization and promoted macrophage polarization toward the M2-like phenotype in both the heart and spleen. In addition, LPS administration dysregulated cyclooxygenase (COX) and lipoxygenase (LOX) in the heart, which were rectified by RvE1 treatment. RvE1 also reduced myocardial apoptosis rate in response to LPS-induced heart injury.

Conclusion: RvE1 protects the heart against *SIC* possibly through the inhibition of the MAPK and NF-κB inflammatory signaling pathways, modulation of macrophage polarization, and reduction in myocardial apoptosis. RvE1 may be a novel lipid mediator for the treatment of *SIC*.

Keywords: sepsis-induced cardiomyopathy, resolvin E1, inflammation, mitogen-activated protein kinase, macrophage polarization, apoptosis

INTRODUCTION

Sepsis is defined as life-threatening organ dysfunction and is caused by a dysregulated host response to infection. LPS from the bacterial cell wall is frequently used for the induction of sepsis (Xianchu et al., 2018). Sepsis-induced cardiomyopathy is a common complication of severe sepsis and is closely associated with the prognosis of patients. Evidence has suggested that myocardial injury caused by sepsis has characteristics of an excessive inflammatory response, failed resolution of inflammation, and apoptotic damage, which may ultimately bring about qualitative and quantitative myocardial alterations (Sharma, 2007; Deutschman and Tracey, 2014; Kong et al., 2017). Therefore, it is imperative that a novel strategy to protect patients against sepsis-induced myocardial injury *via* the inhibition of inflammation, promotion of inflammation resolution, or inhibition of cardiac myocyte apoptosis is found. In fact, promoting the switch from the inflammation phase to the resolution phase is a significant method to prevent heart injury (Cheng et al., 2017) and has become a hotpot about popular approach for regulating inflammation.

Anti-inflammatory lipid chemokines, including lipoxins, resolvins, protectins, and maresins, have shown remarkable beneficial effects in several animal models of disease, including atherosclerosis, diabetes, and obesity (Serhan, 2017). Resolvin E1 (RvE1) is one such chemokine. RvE1 is biosynthesized from EPA, which is metabolized to produce 18R-hydroxy-5Z,8Z,11Z,14Z,16E-EPA (18R-HEPE) *via* aspirin-acetylated COX-2 in endothelial cells or *via* a COX-independent pathway involving cytochrome P450 and is subsequently transformed by 5-LOX in neutrophils (Arita et al., 2005). The proresolving activity of RvE1 is mediated by the receptor ERV1/ChemR23, which is a G-protein-coupled receptor (Arita et al., 2005; Pirault and Back, 2018). The overexpression of ERV1/ChemR23 enhances the protective impact of RvE1 in several animal models of inflammation (Gao et al., 2013; Herrera et al., 2015; Sima et al., 2017). In addition, RvE1, showing as an antagonist, interacts with the BLT1 and ultimately attenuates LB4-dependent inflammation (Arita et al., 2007).

Previous studies indicated that RvE1 has remarkable anti-inflammatory and proresolution effects in many diseases, such as keratitis, periodontitis, allergic asthma, bacterial pneumonia, and acute lung injury (Seki et al., 2010; Flesher et al., 2014; Lee et al., 2015, 2016). Recent trials have shown that in the cardiovascular system, RvE1 prevents vascular inflammation, attenuates atherogenesis (Hasturk et al., 2015; Salic et al., 2016), and facilitates myocardial recovery from ischemia in the early stage by suppressing the infiltration of dominant Ly6C^{hi} monocytes/macrophages and the secretion of pro-inflammatory cytokines (Liu et al., 2018b).

Based on these effects of RvE1, in this study, we examined whether RvE1 protects against LPS-induced acute heart injury and further investigated its underlying mechanism.

Abbreviations: BLT1, leukotriene B4 (LB4) receptor 1; CAD, cardiovascular disease; COX, cyclooxygenase; EPA, eicosapentaenoic acid; HEPE, hydroxy-5Z,8Z,11Z,14Z,16E-eicosapentaenoic acid; HETE, hydroxy-eicosatetraenoic acid; LOX, lipoxygenase; LPS, lipopolysaccharide; MI, myocardial infarction; PG, prostaglandin; PUFA, polyunsaturated fatty acid; *SIC*, sepsis-induced cardiomyopathy.

MATERIALS AND METHODS

Reagents

RvE1 (5S, 12R, 18R-trihydroxy-6Z, 8E, 10E, 14Z, 16E-EPA, purity ≥ 95%, λ_{max}, 272 nm) was purchased from Cayman Chemical (Ann Arbor, MI, United States). LPS was obtained from Sigma-Aldrich (St. Louis, MO, United States).

Animals

All experimental procedures complied with the National Institutes of Health (NIH) Guide for the Care and Use of Laboratory Animals and were approved by the Animal Care and Use Committee of Renmin Hospital of Wuhan University (Wuhan, China).

Adult male C57BL/6 mice (aged 6–8 weeks) were purchased from Vital River Laboratory Animal Technology Co. Ltd. (Beijing, China). Mice were maintained in a humidity/temperature-controlled environment (70% relative humidity, 22°C) in a standard laboratory of the Cardiovascular Research Institute of Wuhan University with a 12:12-h light–dark cycle and were supplied with rodent food and water. These animals were acclimatized to the environment for 2 weeks and then randomly assigned into three groups: the control group, LPS exposure group, and LPS + RvE1 group. Mice were treated with LPS (10 mg/kg) *via* once intraperitoneal (i.p.) injection and pretreated i.p. with RvE1 (25 μg/kg) or vehicle (0.9% endotoxin-free saline) 30 min prior to LPS administration. Mice were sacrificed after 6 h of LPS treatment.

Echocardiography

After 6 h of LPS treatment, mice anesthetized with 1.5–2% isoflurane, were subjected to echocardiographic analysis using a Mylab 30CV ultrasound (Esaote S.P.A., Genoa, Italy) with a 10-MHz linear array ultrasound transducer. The heart rate (HR) and the left ventricular (LV) function, which included

the LV ejection fraction (LVEF), fractional shortening (FS), LV end-systolic diameter (LVESD), and LV end-diastolic diameter (LVEDD), were assessed.

Biochemical Determination

After the echocardiography analysis, animals were maintained under anesthesia, blood samples were taken from each mouse and centrifuged for 15 min at 3,000 × *g*. Then, the serum was used to detect lactate dehydrogenase (LDH) activity and creatine kinase myocardial bound (CK-MB) levels following the manufacturer's protocols (all from Nanjing Jiancheng Bioengineering Institute, Nanjing, China).

Histological Analysis

Hearts were isolated and arrested in 10% KCl solution, and spleens were subsequently isolated. Then, after fixation with 4% paraformaldehyde for 5 days, the hearts and spleens were embedded in paraffin and sliced into approximately 5 μm sections. Subsequently, the sections were stained with hematoxylin and eosin (H&E) for histological analysis.

Immunofluorescence

For immunofluorescence, each heart or spleen section was deparaffinized and blocked with 10% bovine serum albumin. Subsequently, the heart or spleen sections were incubated overnight at 4°C with one of the following primary antibodies: (a) anti-Ly6G antibody, (b) anti-CD68 antibody (R&D Systems), (c) anti-CD206 antibody (R&D Systems), and (d) anti-CD80 antibody (R&D Systems). Then, the sections were washed in phosphate-buffered saline (PBS) and incubated for 1 h at 37°C with secondary antibodies [horseradish peroxidase (HRP) goat anti-rabbit immunoglobulin G (IgG)]. Nuclei were counterstained with 4′,6-diamidino-2-phenylindole (DAPI).

TdT-Mediated dUTP Nick-End Labeling Assay

TdT-mediated dUTP nick-end labeling (TUNEL) staining was performed as previously described (Ye et al., 2018). Briefly, apoptosis of the left ventricle was assessed with a TUNEL kit (Millipore, United States) following the manufacturer's instructions. Light microscopy was used to evaluate apoptosis.

Quantitative Real-Time PCR

Total heart or splenic RNA was extracted with TRIzol reagent (Invitrogen Life Technologies, United States). Oligo(dT) primers and a Transcriptor First Strand cDNA Synthesis kit (Roche, Germany) were used to synthesize cDNA. For the PCR amplification, LightCycler 480 SYBR Green Master Mix (Roche, Germany) was used. The mRNA expression levels of the target genes were normalized to those of glyceraldehyde 3-phosphate dehydrogenase (GAPDH). The quantitative real-time (QRT)-PCR primers are shown in **Table 1**.

Western Blotting

The cardiac tissue protein was extracted, and the protein concentration was assessed, as previously described (Ye et al., 2018). Protein was separated by electrophoresis using Laemmli sodium dodecyl sulfate (SDS)-polyacrylamide gels and then transferred to Immobilon-FL polyvinylidene fluoride (PVDF) membranes (Millipore, United States). Subsequently, after being blocked with 5% non-fat milk for 1 h, the membranes were incubated at 4°C overnight with the following primary antibodies: ChemR23 (Santa Cruz Biotechnology, United States), Bax [Cell Signaling Technology (CST), United States], Bcl-2 (Abcam, United States), c-caspase 3 (CST, United States), phosphorylated/total-p65 (p/T-P65; CST, United States), phosphorylated/total-extracellular signal-regulated kinase (p/T-ERK; CST, United States), phosphorylated/total-c-Jun N-terminal kinase (p/T-JNK; CST, United States), phosphorylated/total-p38 mitogen-activated protein kinase (p/T-P38 MAPK; CST, United States), and GAPDH (CST, United States). Then, the membranes were treated with a second antibody at room temperature for 1 h. Finally, antibody binding was detected with a two-color infrared imaging system (Odyssey, LI-COR Biosciences, Lincoln, United Kingdom). The protein expression intensity was normalized to that of GAPDH.

Flow Cytometry

Flow cytometry of mice heart tissue was performed as previously described in our study (Wang et al., 2018). Briefly, isolated cell suspensions from hearts were filtered, centrifuged, resuspended, and blocked with a CD16/32 antibody. Samples were then incubated with primary antibodies for 1 h at 4°C in dark. The antibodies include anti-CD45, PE (BD Bioscience), and anti-CD11b+, FITC (BD Bioscience).

Statistical Analysis

All results are presented as the mean ± standard error of the mean (SEM). Differences between groups were determined by Student's *t*-test (two groups) or one-way analysis of variance (ANOVA) followed by Dunnett's test or Tukey's test (three groups). The significance criterion was set at a p-value < 0.05.

RESULTS

Lipopolysaccharide Upregulates the Expression of ChemR23 and BLT1 in the Heart

We first examined the expression of ChemR23 and BLT1 in the heart after LPS treatment. According to the QRT-PCR results, LPS treatment significantly increased the cardiac expression of BLT1 (**Figure 1A**) and ChemR23 (**Figure 1B**). In addition, Western blotting (WB) results showed that the expression of ChemR23 was increased by the administration of LPS (**Figure 1C**).

Resolvin E1 Attenuates Lipopolysaccharide-Induced Myocardial Dysfunction

Compared to that in the control group, LVEF (**Figure 2C**) and FS (**Figure 2D**) in the LPS group were markedly reduced,

TABLE 1 | Primers for quantitative real-time PCR.

Gene	Forward primer (5′–3′)	Reverse primer (5′–3′)
IL-1β	GGGCCTCAAAGGAAAGAATC	TACCAGTTGGGGAACTCTGC
IL-6	AGTTGCCTTCTTGGGACTGA	TCCACGATTTCCCAGAGAAC
MCP-1	ACTGAAGCCAGCTCTCTCTTCCTC	TTCCTTCTTGGGGTCAGCACAGAC
BLT1	GGCTGCAAACACTACATCTCC	TCAGGATGCTCCACACTACAA
ChemR23	ATGGAGTACGACGCTTACAACG	GGTGGCGATGACAATCACCA
CD80	GGCCTGAAGAAGCATTAGCTG	GAGGCTTCACCTAGAGAACCG
CD86	GCTTCAGTTACTGTGGCCCT	TGTCAGCGTTACTATCCCGC
CD163	TCCACACGTCCAGAACAGTC	CCTTGGAAACAGAGACAGGC
CD206	CAGGTGTGGGCTCAGGTAGT	TGTGGTGAGCTGAAAGGTGA
CD38	TCTCTAGGAAAGCCCAGATCG	GTCCACACCAGGAGTGAGC
CD36	ATGGGCTGTGATCGGAACTG	TTTGCCACGTCATCTGGGTTT
i-NOS	CGAAACGCTTCACTTCCAA	TGAGCCTATATTGCTGTGGCT
Arg-1	AACACGGCAGTGGCTTTAACC	GGTTTTCATGTGGCGCATTC
COX-1	GATTGTACTCGCACGGGCTAC	GGATAAGGTTGGACCGCACT
COX-2	AACCGCATTGCCTCTGAAT	CATGTTCCAGGAGGATGGAG
5-LOX	TGTTCCCATTGCCATCCAG	CACCTCAGACACCAGATGCG
ALOX-15	AAAGGCACTCTGTTTGAAGCG	CACCAA GTGTCCCCTCAGAAG
Bax	TGAGCGAGTGTCTCCGGCGAAT	GCACTTTAGTGCACAGGGCCTTG
BCL-2	TGGTGGACAACATCGCCCTGTG	GGTCGCATGCTGGGGCCATATA

ALOX-15, arachidonate 15-lipoxygenase; BLT1, leukotriene B4 (LB4) receptor 1; COX, cyclooxygenase; IL, interleukin; LOX, lipoxygenase; MCP, monocyte chemoattractant protein.

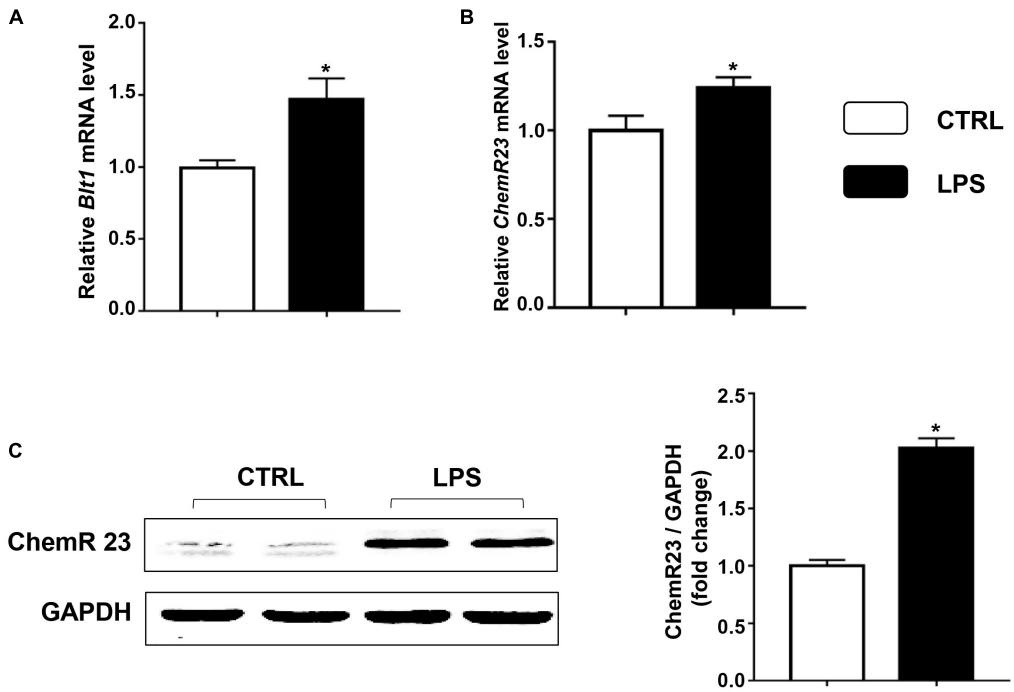

FIGURE 1 | Lipopolysaccharide (LPS) increases the expression of leukotriene B4 (LB4) receptor 1 (BLT1) and ChemR23 in the heart. Relative mRNA levels of BLT1 **(A)** and ChemR23 **(B)** in the control and LPS group ($n = 5$). **(C)** Representative Western blotting bands and quantitative results of protein levels of ChemR23 in the left ventricular (LV) tissue ($n = 5$) (the raw western blotting bands can be found in the **Supplementary Data Sheet 1**). Data are presented as the mean ± SEM. *$P < 0.05$ compared with the control (CTRL) group.

whereas LVEDD (**Figure 2A**) and LVESD (**Figure 2B**) were obviously increased, which suggest that LPS treatment reduces LV function. In contrast, these changes were significantly reversed by RvE1 (25 μg/kg) treatment (**Figures 2A–D**), which indicates that RvE1 protects LV function in LPS-induced heart injury.

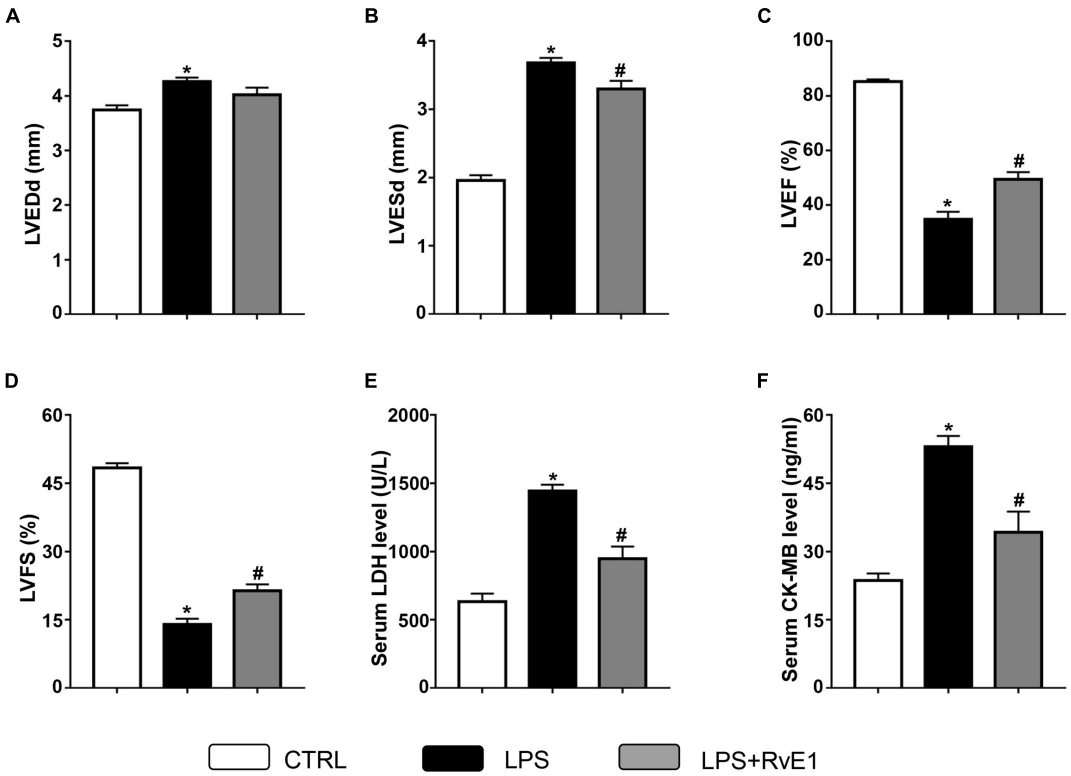

FIGURE 2 | Resolvin E1 ameliorates cardiac function in mice challenged with lipopolysaccharide (LPS). Left ventricular end-diastolic diameter (LVEDD) **(A)**, LV end-systolic diameter (LVESD) **(B)**, LV ejection fraction (LVEF) **(C)**, and LV fractional shortening (LVFS) **(D)** were evaluated by echocardiography in each group ($n = 6$). Serum levels of lactate dehydrogenase (LDH) **(E)** and creatine kinase myocardial bound (CK-MB) **(F)** were measured in each group ($n = 5$). Data are presented as the mean ± SEM. $^{*}P < 0.05$ compared with the control (CTRL) group, $^{\#}P < 0.05$ compared with the LPS group.

Resolvin E1 Reduces the Serum Levels of Creatine Kinase Myocardial Bound and Lactate Dehydrogenase in a Lipopolysaccharide-Induced Sepsis Model

To test the effect of RvE1 on LPS-induced myocardial injury, we examined the levels of marker enzymes of myocardial injury in the serum. Compared to those in the control group, the CK-MB and LDH levels in the LPS treatment group were significantly increased (**Figures 2E,F**). However, pretreatment with RvE1 notably mitigated these changes (**Figures 2E,F**), which suggests that RvE1 pretreatment alleviates LPS-induced myocardial injury in mice.

Resolvin E1 Reduces Inflammatory Cytokine Production Induced by Lipopolysaccharide in Cardiac Tissue

Left ventricular tissue from the three groups was further analyzed for the expression of a panel of inflammatory cytokines, including IL-1β, IL-6, and MCP-1. Compared to those in the control group, the mRNA levels of these inflammatory cytokines were markedly increased after 6 h of LPS exposure. However, the increase in inflammatory cytokine levels was observably inhibited by supplementation with RvE1 (**Figure 3A**). Similarly, compared to the cecal ligation and puncture (CLP) group, the mRNA levels of IL-1β and IL-6 were significantly reduced by treatment of RvE1 (**Supplementary Figures 1A,B**).

Resolvin E1 Reduces the Infiltration of Inflammatory Cells in the Heart

We also evaluated the infiltration of inflammatory cells in the heart by immunofluorescence. Compared to that in the control group, the infiltration of CD68+ macrophages and Ly6G+ neutrophils in the heart in the LPS group were significantly increased (**Figures 3B,C**). Interestingly, these changes were obviously mitigated by RvE1 treatment (**Figures 3B,C**). Similarly, these trends were also observed in CLP mouse models (**Supplementary Figures 1E,F**). Flow cytometry results also showed that LPS increased the infiltration of CD45+ cells and CD45+ CD11b+ cells in the heart, which was reversed by pretreatment of RvE1 (**Figures 3D,E**). These results indicate that RvE1 reduces the infiltration of inflammatory cells in the heart.

Resolvin E1 Mediates Macrophage Polarization in the Heart

To analyze the effect of RvE1 on macrophage differentiation in LPS-induced myocardial injury, we first detected the expression

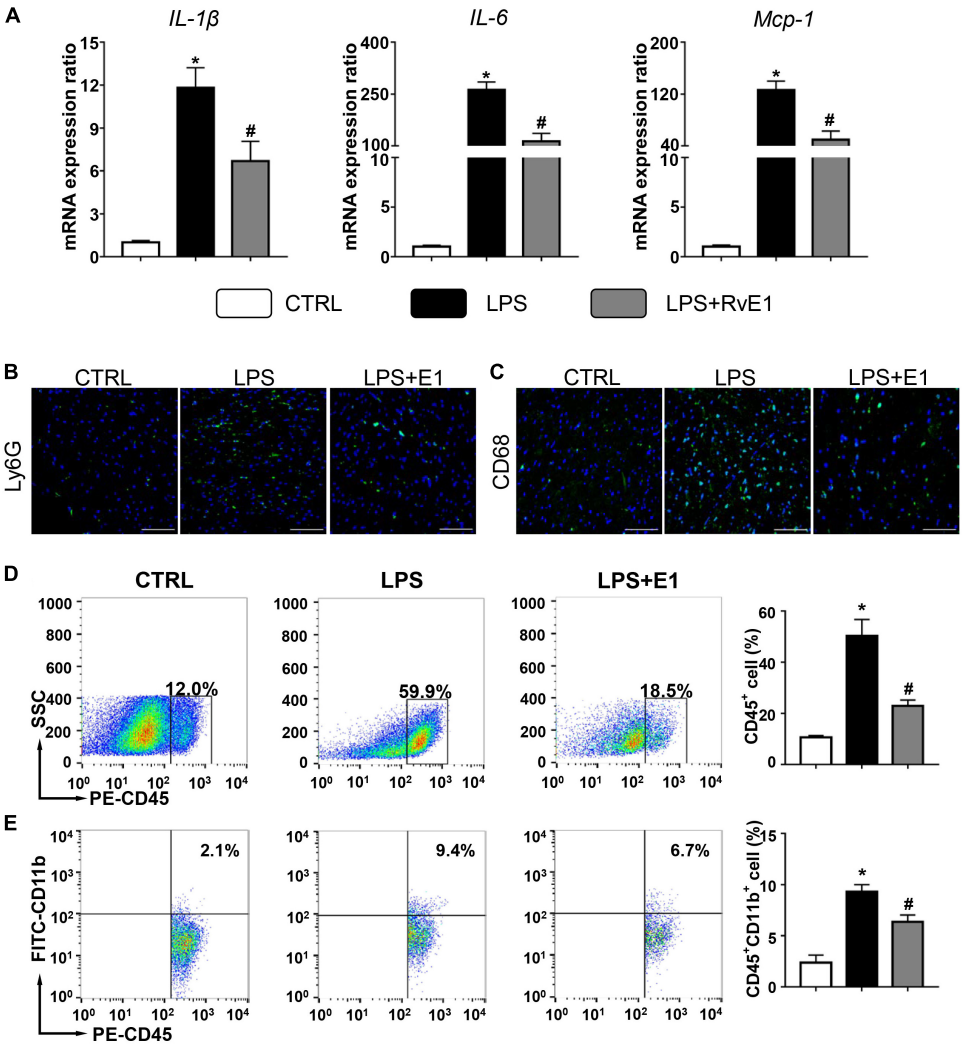

FIGURE 3 | Resolvin E1 inhibits the inflammation response in the heart. **(A)** mRNA levels of pro-inflammatory cytokines [interleukin (IL)-1β, IL-6, and monocyte chemoattractant protein (MCP)-1] were assessed in cardiac tissue (n = 5). Infiltration of neutrophils **(B)** and macrophages **(C)** in the heart in different groups (n = 4) (scale bar, 50 μm). **(D)** Flow cytometry analysis of CD45+ cells (n = 3). **(E)** Flow cytometry analysis of CD45 + CD11b + cells (n = 3). Data are presented as the mean ± SEM. $^{*}P < 0.05$ compared with the control (CTRL) group, $^{\#}P < 0.05$ compared with the lipopolysaccharide (LPS) group.

of surface markers or soluble regulators of macrophages in the heart using QRT-PCR. The mRNA levels of M1 markers, including CD80, CD86, CD38, and i-NOS, were observably increased in the LPS group, but pretreatment with RvE1 significantly inhibited this increase (**Figure 4A**). Conversely, treatment with LPS reduced the expression of M2 markers (CD163, CD206, and CD36), and RvE1 treatment significantly reversed this trend (**Figure 4B**). In addition, compared to the CLP group, RvE1 also reduced the mRNA level of CD38 and increased the level of Arg-1 (**Supplementary Figures 1C,D**). Then, we also evaluated the expression levels of i-NOS by WB; the results revealed that the levels of i-NOS were lower in the LPS + RvE1 group than those in the LPS group (**Figure 4C**). In addition, immunofluorescence staining showed similar results: lower CD80 expression (**Figure 4D**) and higher CD206 expression (**Figure 4E**) were observed in the LPS + RvE1 group than the LPS group. These results suggest that in cardiac tissue, RvE1 may inhibit LPS or CLP-induced MI polarization and promote macrophage polarization toward the M2 phenotype, which suppresses inflammation and promotes the resolution of inflammation.

Resolvin E1 Reduces the Infiltration of Inflammatory Cells and Mediates Macrophage Polarization in the Spleen

Immunofluorescence results showed that RvE1 reduced the infiltration of CD68+ macrophages and Ly6G+ neutrophils in the spleen challenged with LPS (**Figures 5A,B**). We also evaluated the effect of RvE1 on macrophage polarization in the spleen. Treatment with LPS increased the mRNA levels of M1 markers (CD80, CD86, and i-NOS) and reduced the levels of M2 markers

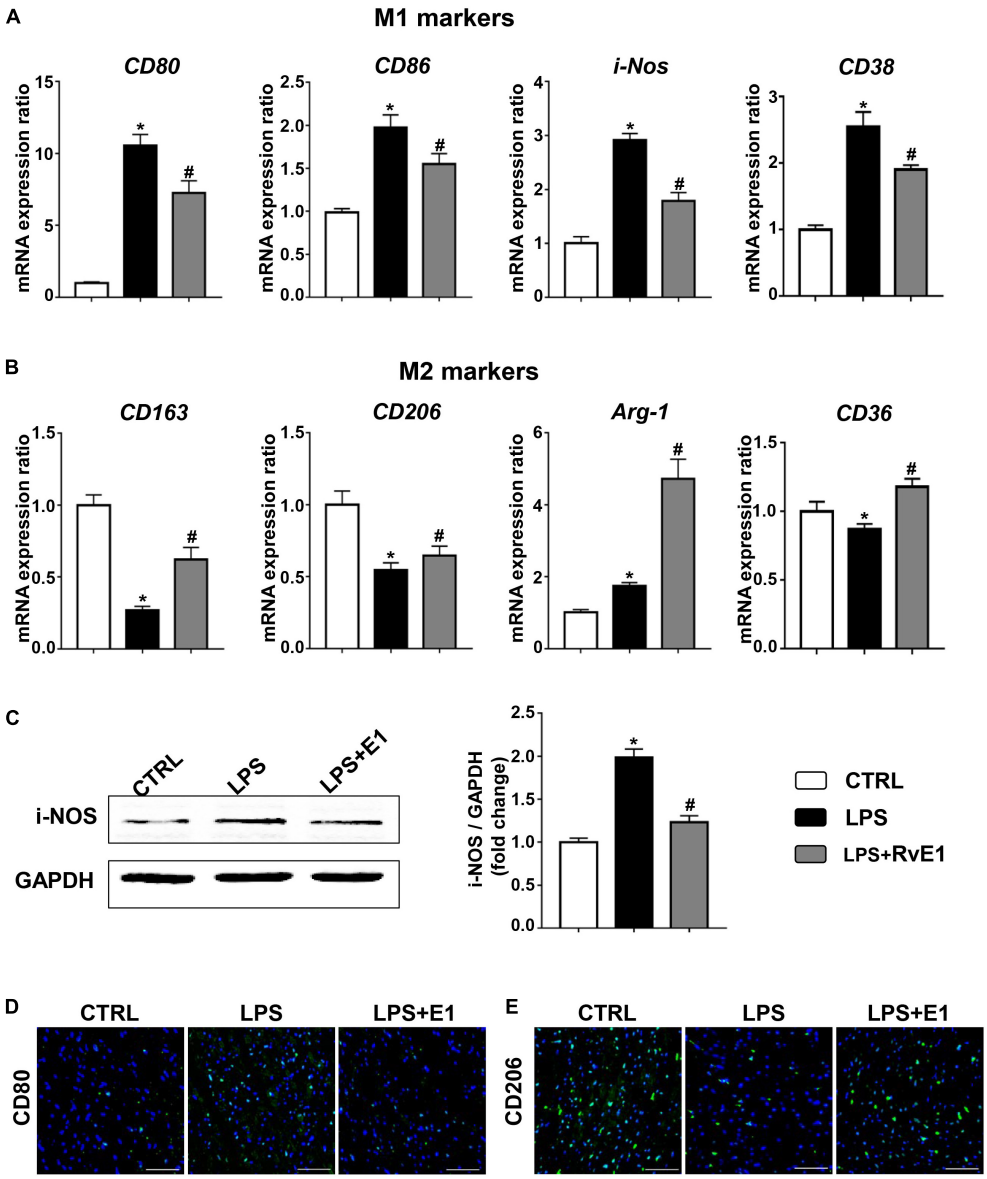

FIGURE 4 | Resolvin E1 protects mice against lipopolysaccharide (LPS)-induced heart injury through the reprogramming of macrophage polarization in the heart. **(A)** mRNA levels of M1 markers, including CD80, CD86, CD38, and i-NOS, in the left ventricular (LV) tissue of each group (n = 5). **(B)** mRNA levels of M2 markers, including CD163, CD206, CD36, and Arg-1, in the LV tissue of each group (n = 5). **(C)** i-NOS was assessed by Western blotting in the LV tissue of each group (n = 4) (the raw western blotting bands can be found in the **Supplementary Data Sheet 1**). **(D)** CD80 was assessed by immunofluorescence in the LV tissue of each group (n = 4) (scale bar, 50 μm). **(E)** CD206 was assessed by immunofluorescence in the LV tissue of each group (n = 4) (scale bar, 50 μm). Data are presented as the mean ± SEM. $^{*}P < 0.05$ compared with the control (CTRL) group, $^{\#}P < 0.05$ compared with the LPS group.

(CD163, CD206, and Arg-1). However, pretreatment with RvE1 significantly diminished these trends (**Figures 5C,D**). Similarly, immunofluorescence staining revealed that the expression levels of CD80 (**Figure 5E**) were notably reduced, and the expression levels of CD206 (**Figure 5F**) were significantly increased in the LPS + RvE1 group compared to those in the LPS group. These results reveal that RvE1 may also suppress the inflammation of the spleen by promoting macrophage M2 polarization and inhibiting M1 polarization, ultimately accelerating the resolution of systemic inflammation induced by LPS.

Resolvin E1 Mediates the Expression of Cyclooxygenase and Lipoxygenase in the Myocardial Tissue of Lipopolysaccharide-Treated Mice

Previous studies have suggested that COX and LOX may play a critical role in the formation of lipid mediators and the regulation of inflammation (Kain et al., 2014). In the present study, QRT-PCR was used to evaluate the expression of these immune-sensitive enzymes. We found that LPS

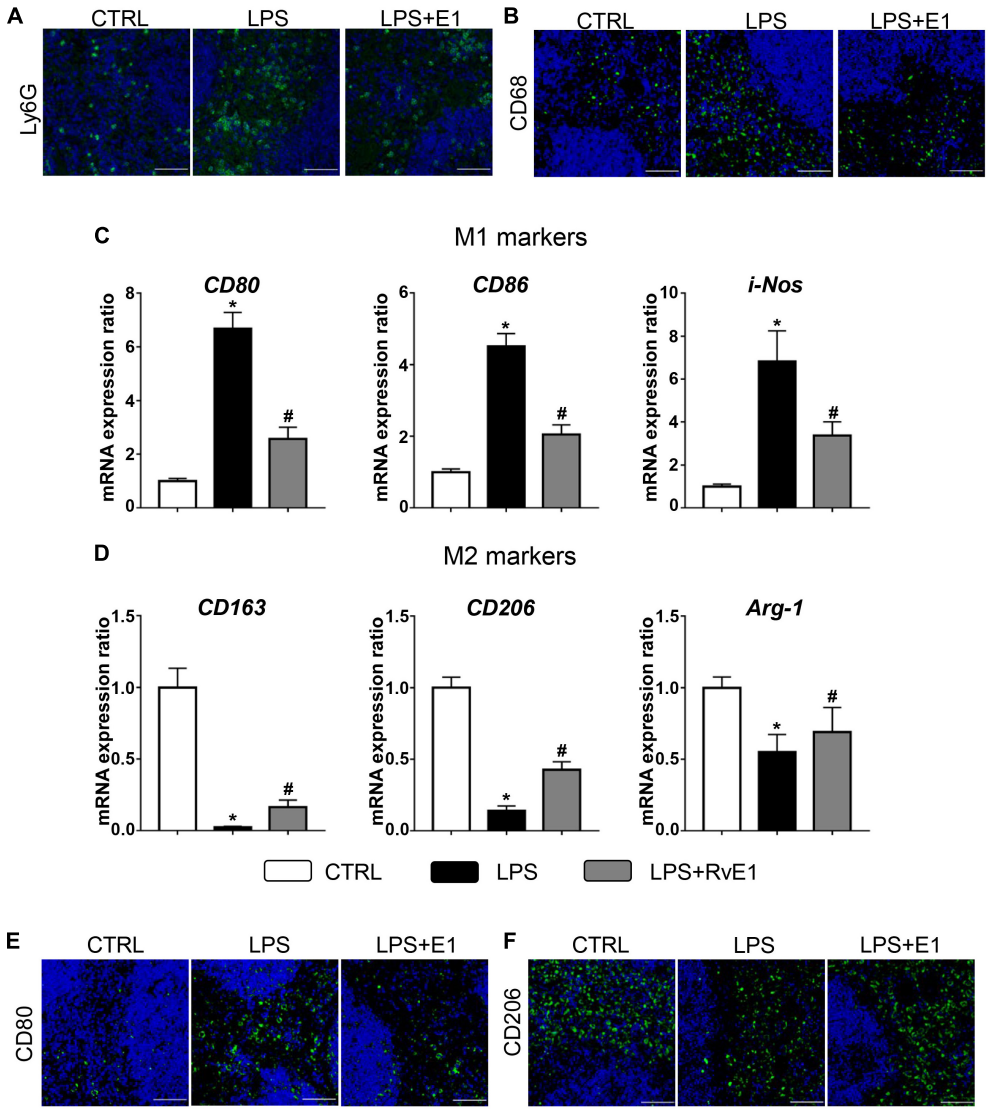

FIGURE 5 | Resolvin E1 reduces the infiltration of inflammatory cells and mediates macrophage polarization in the spleen. **(A,B)** Infiltration of neutrophils and macrophages in the spleen in different groups (n = 4) (scale bar, 50 μm). **(C)** mRNA levels of M1 markers, including CD80, CD86, and i-NOS, in the spleen of each group (n = 5). **(D)** mRNA levels of M2 markers, including CD163, CD206, and Arg-1, in the spleen of each group (n = 5). **(E)** CD80 was assessed by immunofluorescence in the spleen of each group (n = 4) (scale bar, 50 μm). **(F)** CD206 was assessed by immunofluorescence in the spleen of each group (n = 4) (scale bar, 50 μm). Data are presented as the mean ± SEM. $^{*}P < 0.05$ compared with the control (CTRL) group, $^{\#}P < 0.05$ compared with the lipopolysaccharide (LPS) group.

treatment significantly reduced the mRNA levels of COX-1 and 5-LOX in the heart, and this effect was reversed by RvE1 (**Figures 6A,C**). On the contrary, arachidonate 15-LOX (ALOX-15) levels were increased in the myocardial tissue of LPS-treated mice, and pretreatment with RvE1 obviously mitigated the trend compared to LPS treatment alone (**Figure 6D**). In addition, the mRNA levels of COX-2 were significantly increased in the LPS group and further increased in the LPS + RvE1 group (**Figure 6B**). These results suggest that RvE1 mitigates the inflammation of cardiac tissue possibly associated with the modulation of lipid mediator-related enzymes. However, the association between RvE1 and lipid mediator-related enzymes in spleen remains to be further studied (**Figures 6E–H**).

Resolvin E1 Reduced Lipopolysaccharide-Induced Myocardial Apoptosis *in vivo* and *in vitro*

To assess whether RvE1 prevents LPS-induced cardiomyocyte apoptosis, we first detected the activation of apoptosis-related signaling pathways. The QRT-PCR results revealed that the mRNA levels of Bax were higher and the levels of Bcl-2 were lower in the LPS group than those in the control group

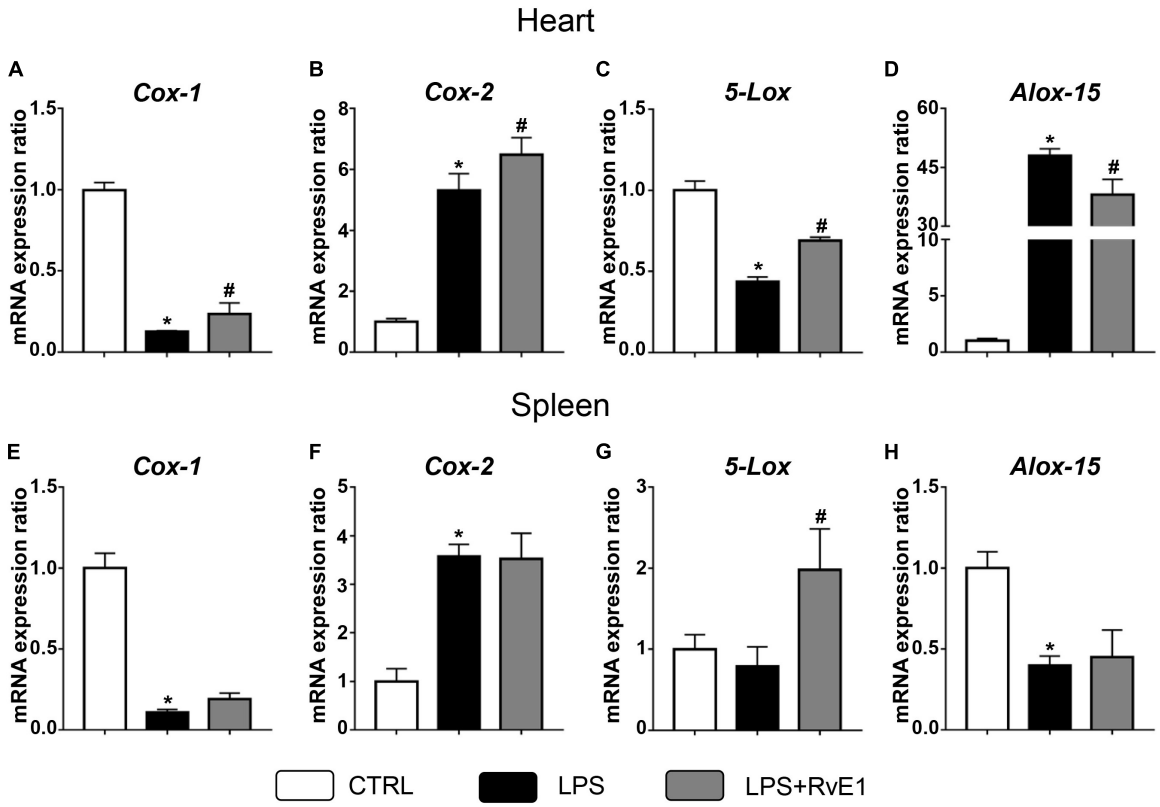

FIGURE 6 | Resolvin E1 mediates the expression of cyclooxygenase (COX) and lipoxygenase (LOX) in the myocardial tissue of lipopolysaccharide (LPS)-treated mice. **(A–D)** COX-1, COX-2, 5-LOX, and arachidonate 15-lipoxygenase (ALOX-15) in the left ventricular (LV) tissue were evaluated by QRT-PCR in each group ($n = 5$). **(E–H)** COX-1, COX-2, 5-LOX, and ALOX-15 in the spleen were evaluated by QRT-PCR in each group ($n = 5$). Data are presented as the mean ± SEM. $^{*}P < 0.05$ compared with the control (CTRL) group, $^{\#}P < 0.05$ compared with the LPS group.

(**Figure 7A**). However, the expression of Bax was reduced and the expression of Bcl-2 was increased in the RvE1-pretreatment group compared to those in the LPS group (**Figure 7A**). Similarly, WB results also suggested that Bax and c-caspase 3 levels were lower and the Bcl-2 level was higher in the LPS + RvE1 group than those in the LPS group (**Figures 7B,C**). In addition, after treatment with LPS for 6 h, an increase in the number of TUNEL-positive cells was observed in mice, and pretreatment with RvE1 alleviated this trend (**Figure 7D**). *In vitro*, WB results showed similar results (**Supplementary Figures 2A–C**).

Resolvin E1 Inhibits the Activation of the Mitogen-Activated Protein Kinase and Nuclear Factor-κB Signaling Pathways in the Myocardial Tissue of Lipopolysaccharide-Treated Mice

We further examined the activation of MAPK and NF-κB signaling pathways, which play a key role in regulating the production of inflammatory mediators, in cardiac tissue. Our results revealed that phosphorylation of P38, c-Jun N-terminal kinase (JNK), extracellular signal-regulated kinase (ERK), and P65 were increased in LV myocardial tissue from the LPS group (**Figures 8A–E**). However, levels of these LPS-activated signaling molecules were markedly reduced by RvE1 treatment (**Figures 8A–E**).

DISCUSSION

In the present study, we reveal that RvE1 attenuates LPS-induced cardiomyocyte injury, as evidenced by the improvement in cardiac function, decrease in the expression of myocardial damage markers, and reduction in the levels of pro-inflammatory cytokines. We also observed that the expression of the RvE1 receptors ChemR23 and BLT1 was increased after treatment with LPS, indicating that RvE1 might exert a protective effect by interacting with these receptors. In addition, RvE1 treatment inhibited the infiltration of inflammatory cells, regulated M1/M2 macrophage polarization in the heart and spleen, and modulated the expression of COX and LOX in the heart, which correlated with the resolution of inflammation. In addition, RvE1 also inhibited the MAPK and NF-κB inflammatory signaling pathways and mitigated the apoptosis of myocardial cells. In summary, these findings indicate that RvE1 might be a potent lipid metabolite that exerts protective effects against sepsis-induced cardiac injury by inhibiting local and systemic

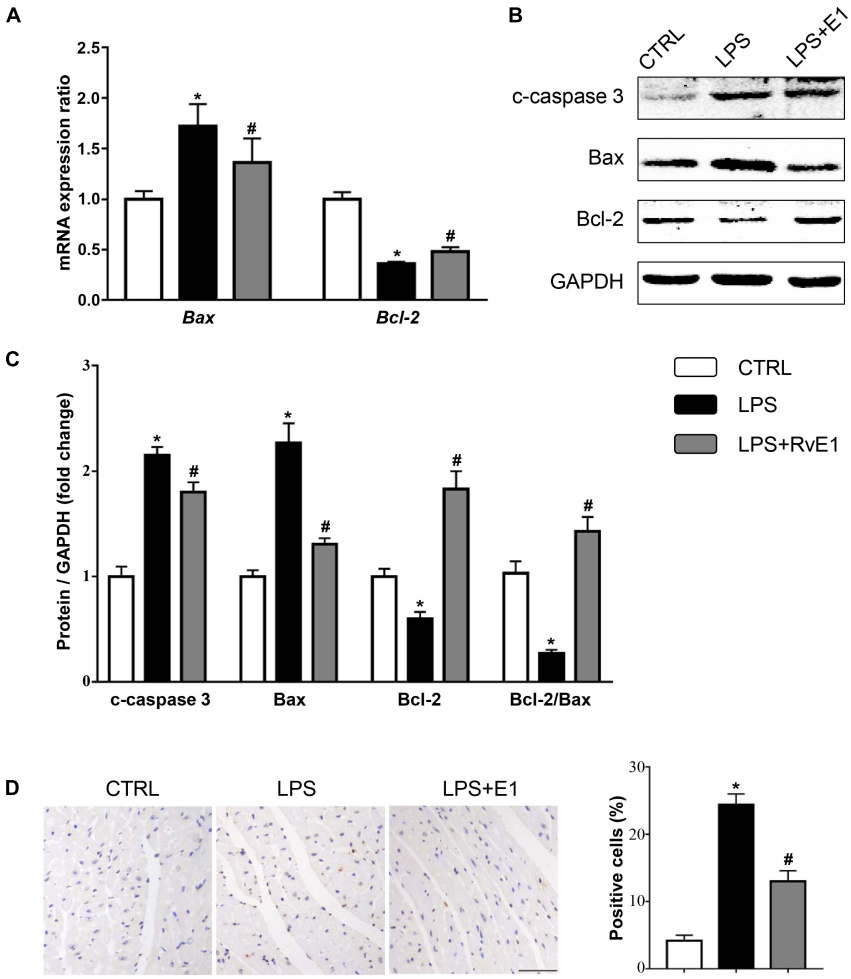

FIGURE 7 | Resolvin E1 attenuates lipopolysaccharide (LPS)-induced cardiomyocyte apoptosis. **(A)** mRNA levels of Bax and Bcl-2 in each group (n = 5). **(B,C)** Representative Western blotting bands **(B)** (the raw western blotting bands can be found in the **Supplementary Data Sheet 1**) and quantitative results **(C)** of c-caspase-3, Bax, and Bcl-2 in each group (n = 5). **(D)** Representative images of TdT-mediated dUTP nick-end labeling (TUNEL) staining and the quantitative results in each group (n = 4) (scale bar, 50 μm). Data are presented as the mean ± SEM. $^{*}P < 0.05$ compared with the control (CTRL) group, $^{\#}P < 0.05$ compared with the LPS group.

inflammatory responses, modulating macrophages polarization and reducing the rate of myocardial apoptosis.

Sepsis-induced cardiomyopathy is associated with high morbidity and mortality rates in critically ill patients (Romero-Bermejo et al., 2011; Deutschman and Tracey, 2014). LPS is frequently used to induce *SIC* in mice. It has been proposed that experimental septic myocardial injury was mainly evidenced by myocardial dysfunction and elevation of myocardial injury markers, including LDH, CK, and CK-MB (Chen et al., 2017, 2018). RvE1, an omega-3 polyunsaturated fatty acid (PUFA)-derived metabolite, exhibits anti-inflammatory or proresolving activity in multiple animal models of inflammatory diseases, such as periodontal inflammation, psoriatic dermatitis, and acute allergic asthma (Flesher et al., 2014; Balta et al., 2017; Sawada et al., 2018). In addition, previous research has indicated that RvE1 attenuates LPS-induced inflammation *in vitro* (Baker et al., 2018). As previously mentioned, RvE1 also plays a protective role in multiple CVDs [coronary artery disease (CAD)], including atherosclerosis, MI, and reperfusion injury (Keyes et al., 2010; Hasturk et al., 2015; Liu et al., 2018b). Therefore, it is highly necessary to clarify the functional roles of RvE1 in *SIC*. Interestingly, we found that LPS treatment increased serum LDH and CK-MB levels, and this increase was reversed by pretreatment with RvE1. In addition, RvE1 improved LVEF and FS in hearts challenged with LPS. These results suggest that RvE1 plays a protective role in septic heart injury.

Inflammatory cells and inflammatory cytokines play an important role in the inflammatory response to pathologic stimuli. Myocardial infiltration by immune cells, especially neutrophils and macrophages, contributes to sepsis-induced cardiac dysfunction, which is attenuated by the inhibition of the influx of these cells (Chen J. et al., 2016; Zheng et al., 2017). The levels of pro-inflammatory cytokines, including tumor necrosis factor (TNF)-α, IL-1β, IL-6, and MCP-1, have been observed to

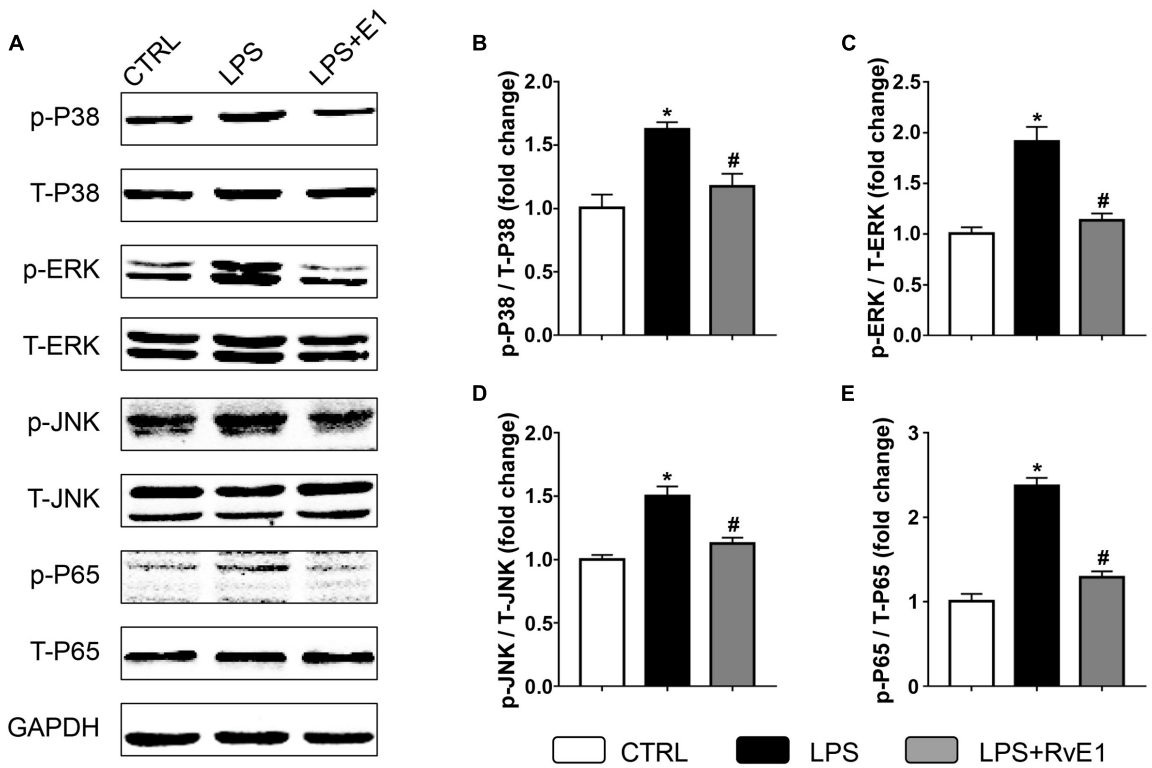

FIGURE 8 | Resolvin E1 inhibits the activation of the mitogen-activated protein kinase (MAPK) and nuclear factor (NF)-κB signaling pathways in the myocardial tissue of lipopolysaccharide (LPS)-treated mice. **(A)** Representative Western blotting bands of p/T-p38, p/T-ERK, p/T-JNK, and p/T-p65 in each group (the raw western blotting bands can be found in the **Supplementary Data Sheet 1**). Quantitative results of p-P38 **(B)**, p-ERK **(C)**, p-JNK **(D)**, and p-P65 **(E)** in each group ($n = 5$). Data are presented as the mean ± SEM. $^{*}P < 0.05$ compared with the control (CTRL) group, $^{\#}P < 0.05$ compared with the LPS group.

increase in the myocardium in response to sepsis (Chen J. et al., 2016; Huang et al., 2018). These cytokines are considered to be myocardial depression factors and exert an injurious effect on cardiomyocytes. Additionally, the neutralization of IL-6 and IL-1β contributes to the inhibition of the inflammatory response (Eger et al., 2018). In the present study, LPS treatment increased the mRNA levels of IL-1β, IL-6, and MCP-1 in cardiac tissue, and this increase was reduced by RvE1 pretreatment. Similarly, RvE1 reduced the sepsis-induced infiltration of neutrophils and macrophages in myocardial tissues. Consistent with this research, a previous study suggested that the anti-inflammatory mediator RvE1 reduces LPS-induced inflammation *in vitro* (Baker et al., 2018). Therefore, RvE1 may protect mouse hearts from septic injury by suppressing inflammation. In addition, the overexpression of the RvE1 receptors BLT1 and ChemR23 enhances the anti-inflammatory effect of RvE1 (Arita et al., 2007; Gao et al., 2013; Herrera et al., 2015; Sima et al., 2017). In this study, LPS treatment increased the expression of BLT1 and ChemR23 in the myocardium, which contributed to the protective effect of RvE1 against *SIC*.

The production of pro-inflammatory mediators is closely regulated by the activation of multiple signaling pathways, including MAPKs (ERK, JNK, and p38) and NF-κB. In the heart, LPS promotes the phosphorylation of ERK, JNK, p38, and p65, which enhances the production of pro-inflammatory mediators (Chen R.C. et al., 2016; Zhao et al., 2016). *In vitro*, RvE1 suppresses the production of cytokines in pulmonary macrophages by reducing the nuclear translocation of NF-κB p65 (Flesher et al., 2014). However, whether RvE1 prevents the phosphorylation of MAPK and p65 in *SIC* is still unknown. Our results revealed that the expression levels of p-ERK, p-JNK, p-P38, and p-P65 were lower in the RvE1 + LPS group than those in the LPS group, which occurred in parallel with the reduction in the levels of pro-inflammatory mediators. Therefore, the protective effect of RvE1 in LPS-induced heart injury may be closely associated with the inhibition of MAPK and NF-κB signaling pathways.

Modulation of the macrophage phenotype plays a crucial role in inflammatory processes and might be a novel strategy for the treatment of sepsis (Mahajan et al., 2015; Guo et al., 2018). LPS induces macrophage polarization to the M1 phenotype, which is associated with pro-inflammatory mediator production and heart injury. In contrast, M2 macrophages secrete increased amounts of anti-inflammatory cytokines and protect the heart against LPS-induced injury (Dai et al., 2015). Previous studies have suggested that protectin D1 regulates macrophage function and that RvD1 stimulates the M2 macrophage phenotype, which is associated with the resolution of lung inflammation and adipose tissue inflammation (Titos et al., 2011; Serhan et al., 2014). RvE1 was found to promote macrophage polarization toward an

M2-like phenotype, and these macrophages exerted a protective effect against vascular inflammation induced by mechanical injury (Liu et al., 2018a). Interestingly, our results revealed that RvE1 promotes macrophage polarization toward the M2-like phenotype (CD163, CD206, and Arg-1) and inhibited LPS-induced M1 macrophage polarization (CD80, CD86, and i-NOS). Therefore, RvE1 might reduce the LPS-induced inflammation response by regulating the reprogramming of macrophages. In addition, recent studies have demonstrated that CD163 plays a potentially proresolution role in models of resolving inflammation possibly by mediating IL-10 release and heme oxygenase-1 synthesis (Gilroy and De Maeyer, 2015). In this study, the expression of CD163 was increased in the RvE1 group compared to that in the LPS group, which indicates that RvE1 might play an important role in the resolution phase of LPS-induced heart injury.

Immunometabolism, primarily driven by COX and LOX, is closely associated with inflammation, especially following MI (Kain et al., 2014). Previous research has suggested that COX-1 might play a significant anti-inflammatory role in diabetes-impaired wound tissue by driving PG synthesis, which contributes to the tightly controlled resolution of inflammation (Goren et al., 2006). In our study, RvE1 treatment significantly increased the expression of COX-1, indicating that RvE1 contributes to the resolution of inflammation in *SIC*. The inhibition of COX-2 has a protective effect in many inflammatory diseases, whereas COX-2 still exerts biological activities to resolve inflammation in the resolution phase. The RvD1-induced activation of COX-2 expedites the resolution of inflammation and has therapeutic potential for the management of acute respiratory distress syndrome (Gao et al., 2017). Consistent with the results of previous studies, we found that the expression of COX-2 was increased after 6 h of LPS administration and was further increased by RvE1 treatment, suggesting that RvE1 improves the resolution of inflammation by enhancing the activation of COX-2 in the resolution phase. 5-LOX contributed to the synthesis of resolvins. Previous studies revealed that omega-3-enriched lipid emulsions enhanced macrophage efferocytosis and phagocytosis through 5-LOX (Korner et al., 2018). ALOX-15 is an enzyme that can produce 12-hydroxy-eicosatetraenoic acid (HETE) from arachidonic acid. The inhibition of ALOX-15 might inhibit inflammation and reduce vascular permeability by eliminating 12-HETE production in acute lung injury (Zarbock et al., 2009). Interestingly, RvE1 also reduced the expression of ALOX-15 and increased the expression of 5-LOX, which was consistent with the improvement in cardiac function. Therefore, RvE1 might be tightly associated with the modulation of lipid mediator-related enzymes in *SIC*.

Myocardial apoptosis is also a crucial process during *SIC*, and inhibition of apoptosis has been found to be protective (Sharma, 2007). RvE1 administration protected cardiomyocytes against apoptosis and improved cardiac function by reducing the secretion of pro-inflammatory cytokines in the peri-infarct zones (Liu et al., 2018b). Therefore, we used TUNEL staining, QRT-PCR, and WB to detect cardiomyocyte apoptosis in *SIC*. Our results showed that the number of TUNEL-positive nuclei and the expression of Bax and c-caspase 3 were reduced by RvE1 treatment, whereas the expression of Bcl-2 was increased. These results demonstrate that RvE1 significantly protects cardiomyocytes against sepsis-induced apoptosis.

The spleen is an important peripheral immune organ that is a critical reservoir of immune phagocytes, including neutrophils and monocytes/macrophages, and has been reported to play a crucial role in the clearance of pathogens in sepsis (Jahng et al., 2016; Kapellos et al., 2017). Previous studies have reported that the reduction in the number of neutrophils in the spleen is closely associated with the improvement of cardiac function and inhibition of the inflammatory response (Kain et al., 2015). In addition, M2 macrophage polarization in the spleen has a significantly beneficial effect on inflammation post-MI and sepsis (Kain et al., 2015; Taratummarat et al., 2018). Therefore, the crosstalk between the heart and spleen may affect the regulation of inflammation. In this study, the LPS-induced increase in neutrophil and macrophage densities in the spleen was attenuated by RvE1; this effect was also observed in the heart. In addition, the inhibition of M1 polarization and the induction of M2 polarization have been observed to contribute to the improvement of sepsis after RvE1 administration.

CONCLUSION

In conclusion, our results indicate that RvE1 protects the heart from sepsis-induced heart injury. The mechanism is possibly associated with the inhibition of MAPK and NF-κB inflammatory signaling pathways, modulation of macrophage polarization, and reduction in myocardial apoptosis. These findings suggest that RvE1 might be a high potential lipid mediator for the treatment of *SIC*.

DATA AVAILABILITY STATEMENT

All datasets generated for this study are included in the article/**Supplementary Material**.

ETHICS STATEMENT

The animal study was reviewed and approved by the Animal Care and Use Committee of Renmin Hospital of Wuhan University (Wuhan, China).

AUTHOR CONTRIBUTIONS

JZ and MW contributed to the experimental design and wrote the manuscript. JY, ZW, and YX contributed to the acquisition and analysis of the data. DY, YX, JL, MZ, and JW reviewed the manuscript.

FUNDING

This work was supported by the Fundamental Research Funds for the Central Universities, China (No. 2042019kf0065).

ACKNOWLEDGMENTS

The authors acknowledge the support received from the Renmin Hospital of Wuhan University. They also thank some friends in their lab for their help.

SUPPLEMENTARY MATERIAL

The Supplementary Material for this article can be found online at: https://www.frontiersin.org/articles/10.3389/fphar.2020.00203/full#supplementary-material

REFERENCES

Arita, M., Bianchini, F., Aliberti, J., Sher, A., Chiang, N., Hong, S., et al. (2005). Stereochemical assignment, antiinflammatory properties, and receptor for the omega-3 lipid mediator resolvin E1. *J. Exp. Med.* 201, 713–722. doi: 10.1084/jem.20042031

Arita, M., Ohira, T., Sun, Y. P., Elangovan, S., Chiang, N., and Serhan, C. N. (2007). Resolvin E1 selectively interacts with leukotriene B4 receptor BLT1 and ChemR23 to regulate inflammation. *J. Immunol.* 178, 3912–3917. doi: 10.4049/jimmunol.178.6.3912

Baker, L. A., Martin, N., Kimber, M. C., Pritchard, G. J., Lindley, M. R., and Lewis, M. P. (2018). Resolvin E1 (Rv E1) attenuates LPS induced inflammation and subsequent atrophy in C2C12 myotubes. *J. Cell. Biochem.* 119, 6094–6103. doi: 10.1002/jcb.26807

Balta, M. G., Loos, B. G., and Nicu, E. A. (2017). Emerging concepts in the resolution of periodontal inflammation: a role for resolvin E1. *Front. Immunol.* 8:1682. doi: 10.3389/fimmu.2017.01682

Chen, H., Wang, X., Yan, X., Cheng, X., He, X., and Zheng, W. (2018). LncRNA MALAT1 regulates sepsis-induced cardiac inflammation and dysfunction via interaction with miR-125b and p38 MAPK/NFkappaB. *Int. Immunopharmacol.* 55, 69–76. doi: 10.1016/j.intimp.2017.11.038

Chen, J., Lai, J., Yang, L., Ruan, G., Chaugai, S., Ning, Q., et al. (2016). Trimetazidine prevents macrophage-mediated septic myocardial dysfunction via activation of the histone deacetylase sirtuin 1. *Br. J. Pharmacol.* 173, 545–561. doi: 10.1111/bph.13386

Chen, L., Liu, P., Feng, X., and Ma, C. (2017). Salidroside suppressing LPS-induced myocardial injury by inhibiting ROS-mediated PI3K/Akt/mTOR pathway in vitro and in vivo. *J. Cell. Mol. Med.* 21, 3178–3189. doi: 10.1111/jcmm.12871

Chen, R. C., Wang, J., Yang, L., Sun, G. B., and Sun, X. B. (2016). Protective effects of ginsenoside Re on lipopolysaccharide-induced cardiac dysfunction in mice. *Food Funct.* 7, 2278–2287. doi: 10.1039/c5fo01357g

Cheng, Y., Feng, Y., Xia, Z., Li, X., and Rong, J. (2017). omega-Alkynyl arachidonic acid promotes anti-inflammatory macrophage M2 polarization against acute myocardial infarction via regulating the cross-talk between PKM2, HIF-1alpha and iNOS. *Biochim. Biophys. Acta* 1862, 1595–1605. doi: 10.1016/j.bbalip.2017.09.009

Dai, M., Wu, L., He, Z., Zhang, S., Chen, C., Xu, X., et al. (2015). Epoxyeicosatrienoic acids regulate macrophage polarization and prevent LPS-induced cardiac dysfunction. *J. Cell. Physiol.* 230, 2108–2119. doi: 10.1002/jcp.24939

Deutschman, C. S., and Tracey, K. J. (2014). Sepsis: current dogma and new perspectives. *Immunity* 40, 463–475. doi: 10.1016/j.immuni.2014.04.001

Eger, M., Hiram-Bab, S., Liron, T., Sterer, N., Carmi, Y., Kohavi, D., et al. (2018). Mechanism and prevention of titanium particle-induced inflammation and Osteolysis. *Front. Immunol.* 9:2963. doi: 10.3389/fimmu.2018.02963

Flesher, R. P., Herbert, C., and Kumar, R. K. (2014). Resolvin E1 promotes resolution of inflammation in a mouse model of an acute exacerbation of allergic asthma. *Clin. Sci.* 126, 805–814. doi: 10.1042/CS20130623

Gao, L., Faibish, D., Fredman, G., Herrera, B. S., Chiang, N., Serhan, C. N., et al. (2013). Resolvin E1 and chemokine-like receptor 1 mediate bone preservation. *J. Immunol.* 190, 689–694. doi: 10.4049/jimmunol.1103688

Gao, Y., Zhang, H., Luo, L., Lin, J., Li, D., Zheng, S., et al. (2017). Resolvin D1 improves the resolution of inflammation via activating NF-kappaB p50/p50-mediated cyclooxygenase-2 expression in acute respiratory distress syndrome. *J. Immunol.* 199, 2043–2054. doi: 10.4049/jimmunol.1700315

Gilroy, D., and De Maeyer, R. (2015). New insights into the resolution of inflammation. *Semin. Immunol.* 27, 161–168. doi: 10.1016/j.smim.2015.05.003

Goren, I., Muller, E., Pfeilschifter, J., and Frank, S. (2006). Severely impaired insulin signaling in chronic wounds of diabetic ob/ob mice: a potential role of tumor necrosis factor-alpha. *Am. J. Pathol.* 168, 765–777. doi: 10.2353/ajpath.2006.050293

Guo, L., Meng, M., Wei, Y., Lin, F., Jiang, Y., Cui, X., et al. (2018). Protective effects of live combined *B. subtilis* and *E. faecium* in polymicrobial sepsis through modulating activation and transformation of macrophages and mast cells. *Front. Pharmacol.* 9:1506. doi: 10.3389/fphar.2018.01506

Hasturk, H., Abdallah, R., Kantarci, A., Nguyen, D., Giordano, N., Hamilton, J., et al. (2015). Resolvin E1 (RvE1) attenuates atherosclerotic plaque formation in diet and inflammation-induced atherogenesis. *Arterioscler. Thromb. Vasc. Biol.* 35, 1123–1133. doi: 10.1161/ATVBAHA.115.305324

Herrera, B. S., Hasturk, H., Kantarci, A., Freire, M. O., Nguyen, O., Kansal, S., et al. (2015). Impact of resolvin E1 on murine neutrophil phagocytosis in type 2 diabetes. *Infect. Immun.* 83, 792–801. doi: 10.1128/IAI.02444-2414

Huang, S. H., Xu, M., Wu, H. M., Wan, C. X., Wang, H. B., Wu, Q. Q., et al. (2018). Isoquercitrin attenuated cardiac dysfunction via AMPKalpha-dependent pathways in LPS-treated mice. *Mol. Nutr. Food Res.* 62:e1800955. doi: 10.1002/mnfr.201800955

Jahng, J. W., Song, E., and Sweeney, G. (2016). Crosstalk between the heart and peripheral organs in heart failure. *Exp. Mol. Med.* 48:e217. doi: 10.1038/emm.2016.20

Kain, V., Ingle, K. A., Colas, R. A., Dalli, J., Prabhu, S. D., Serhan, C. N., et al. (2015). Resolvin D1 activates the inflammation resolving response at splenic and ventricular site following myocardial infarction leading to improved ventricular function. *J. Mol. Cell. Cardiol.* 84, 24–35. doi: 10.1016/j.yjmcc.2015.04.003

Kain, V., Prabhu, S. D., and Halade, G. V. (2014). Inflammation revisited: inflammation versus resolution of inflammation following myocardial infarction. *Basic Res. Cardiol.* 109:444. doi: 10.1007/s00395-014-0444-447

Kapellos, T. S., Recio, C., Greaves, D. R., and Iqbal, A. J. (2017). Cannabinoid receptor 2 modulates neutrophil recruitment in a murine model of endotoxemia. *Mediat. Inflamm.* 2017:4315412. doi: 10.1155/2017/4315412

Keyes, K. T., Ye, Y., Lin, Y., Zhang, C., Perez-Polo, J. R., Gjorstrup, P., et al. (2010). Resolvin E1 protects the rat heart against reperfusion injury. *Am. J. Physiol. Heart Circ. Physiol.* 299, H153–H164. doi: 10.1152/ajpheart.01057.2009

Kong, W., Kang, K., Gao, Y., Liu, H., Meng, X., Yang, S., et al. (2017). Dexmedetomidine alleviates LPS-induced septic cardiomyopathy via the cholinergic anti-inflammatory pathway in mice. *Am. J. Transl. Res.* 9, 5040–5047.

Korner, A., Schlegel, M., Theurer, J., Frohnmeyer, H., Adolph, M., Heijink, M., et al. (2018). Resolution of inflammation and sepsis survival are improved by dietary Omega-3 fatty acids. *Cell Death. Differ.* 25, 421–431. doi: 10.1038/cdd.2017.177

Lee, C. T., Teles, R., Kantarci, A., Chen, T., McCafferty, J., Starr, J. R., et al. (2016). Resolvin E1 reverses experimental Periodontitis and Dysbiosis. *J. Immunol.* 197, 2796–2806. doi: 10.4049/jimmunol.1600859

Lee, J. E., Sun, Y., Gjorstrup, P., and Pearlman, E. (2015). Inhibition of corneal inflammation by the resolvin E1. *Invest. Ophthalmol. Vis. Sci.* 56, 2728–2736. doi: 10.1167/iovs.14-15982

Liu, G., Gong, Y., Zhang, R., Piao, L., Li, X., Liu, Q., et al. (2018a). Resolvin E1 attenuates injury-induced vascular neointimal formation by inhibition of inflammatory responses and vascular smooth muscle cell migration. *FASEB J.* 32, 5413–5425. doi: 10.1096/fj.201800173R

Liu, G., Liu, Q., Shen, Y., Kong, D., Gong, Y., Tao, B., et al. (2018b). Early treatment with Resolvin E1 facilitates myocardial recovery from ischaemia in mice. *Br. J. Pharmacol.* 175, 1205–1216. doi: 10.1111/bph.14041

Mahajan, S., Saini, A., Chandra, V., Nanduri, R., Kalra, R., Bhagyaraj, E., et al. (2015). Nuclear receptor Nr4a2 promotes alternative polarization of macrophages and confers protection in sepsis. *J. Biol. Chem.* 290, 18304–18314. doi: 10.1074/jbc.M115.638064

Pirault, J., and Back, M. (2018). Lipoxin and resolvin receptors transducing the resolution of inflammation in cardiovascular disease. *Front. Pharmacol.* 9:1273. doi: 10.3389/fphar.2018.01273

Romero-Bermejo, F. J., Ruiz-Bailen, M., Gil-Cebrian, J., and Huertos-Ranchal, M. J. (2011). Sepsis-induced cardiomyopathy. *Curr. Cardiol. Rev.* 7, 163–183. doi: 10.2174/157340311798220494

Salic, K., Morrison, M. C., Verschuren, L., Wielinga, P. Y., Wu, L., Kleemann, R., et al. (2016). Resolvin E1 attenuates atherosclerosis in absence of cholesterol-lowering effects and on top of atorvastatin. *Atherosclerosis* 250, 158–165. doi: 10.1016/j.atherosclerosis.2016.05.001

Sawada, Y., Honda, T., Nakamizo, S., Otsuka, A., Ogawa, N., Kobayashi, Y., et al. (2018). Resolvin E1 attenuates murine psoriatic dermatitis. *Sci. Rep.* 8:11873. doi: 10.1038/s41598-018-30373-30371

Seki, H., Fukunaga, K., Arita, M., Arai, H., Nakanishi, H., Taguchi, R., et al. (2010). The anti-inflammatory and proresolving mediator resolvin E1 protects mice from bacterial pneumonia and acute lung injury. *J. Immunol.* 184, 836–843. doi: 10.4049/jimmunol.0901809

Serhan, C. N. (2017). Treating inflammation and infection in the 21st century: new hints from decoding resolution mediators and mechanisms. *FASEB J.* 31, 1273–1288. doi: 10.1096/fj.201601222R

Serhan, C. N., Chiang, N., Dalli, J., and Levy, B. D. (2014). Lipid mediators in the resolution of inflammation. *Cold Spring Harb. Perspect. Biol.* 7:a016311. doi: 10.1101/cshperspect.a016311

Sharma, A. C. (2007). Sepsis-induced myocardial dysfunction. *Shock* 28, 265–269. doi: 10.1097/01.shk.0000235090.30550.fb

Sima, C., Montero, E., Nguyen, D., Freire, M., Norris, P., Serhan, C. N., et al. (2017). ERV1 overexpression in myeloid cells protects against high fat diet induced obesity and glucose intolerance. *Sci. Rep.* 7:12848. doi: 10.1038/s41598-017-13185-13187

Taratummarat, S., Sangphech, N., Vu, C., Palaga, T., Ondee, T., Surawut, S., et al. (2018). Gold nanoparticles attenuates bacterial sepsis in cecal ligation and puncture mouse model through the induction of M2 macrophage polarization. *BMC Microbiol.* 18:85. doi: 10.1186/s12866-018-1227-1223

Titos, E., Rius, B., Gonzalez-Periz, A., Lopez-Vicario, C., Moran-Salvador, E., Martinez-Clemente, M., et al. (2011). Resolvin D1 and its precursor docosahexaenoic acid promote resolution of adipose tissue inflammation by eliciting macrophage polarization toward an M2-like phenotype. *J. Immunol.* 187, 5408–5418. doi: 10.4049/jimmunol.1100225

Wang, Z., Xu, Y., Wang, M., Ye, J., Liu, J., Jiang, H., et al. (2018). TRPA1 inhibition ameliorates pressure overload-induced cardiac hypertrophy and fibrosis in mice. *eBio Med.* 36, 54–62. doi: 10.1016/j.ebiom.2018.08.022

Xianchu, L., Lan, Z., Ming, L., and Yanzhi, M. (2018). Protective effects of rutin on lipopolysaccharide-induced heart injury in mice. *J. Toxicol. Sci.* 43, 329–337. doi: 10.2131/jts.43.329

Ye, J., Huang, Y., Que, B., Chang, C., Liu, W., Hu, H., et al. (2018). Interleukin-12p35 knock out aggravates doxorubicin-induced cardiac injury and dysfunction by aggravating the inflammatory response, oxidative stress, apoptosis and autophagy in mice. *eBio Med.* 35, 29–39. doi: 10.1016/j.ebiom.2018.06.009

Zarbock, A., Distasi, M. R., Smith, E., Sanders, J. M., Kronke, G., Harry, B. L., et al. (2009). Improved survival and reduced vascular permeability by eliminating or blocking 12/15-lipoxygenase in mouse models of acute lung injury (ALI). *J. Immunol.* 183, 4715–4722. doi: 10.4049/jimmunol.0802592

Zhao, H., Zhang, M., Zhou, F., Cao, W., Bi, L., Xie, Y., et al. (2016). Cinnamaldehyde ameliorates LPS-induced cardiac dysfunction via TLR4-NOX4 pathway: the regulation of autophagy and ROS production. *J. Mol. Cell. Cardiol.* 101, 11–24. doi: 10.1016/j.yjmcc.2016.10.017

Zheng, Z., Ma, H., Zhang, X., Tu, F., Wang, X., Ha, T., et al. (2017). Enhanced glycolytic metabolism contributes to cardiac dysfunction in polymicrobial sepsis. *J. Infect. Dis.* 215, 1396–1406. doi: 10.1093/infdis/jix138

Conflict of Interest: The authors declare that the research was conducted in the absence of any commercial or financial relationships that could be construed as a potential conflict of interest.

frontiers in Pharmacology

ORIGINAL RESEARCH
published: 27 March 2020
doi: 10.3389/fphar.2020.00373

Aldehyde Dehydrogenase 2 Protects Against Post-Cardiac Arrest Myocardial Dysfunction Through a Novel Mechanism of Suppressing Mitochondrial Reactive Oxygen Species Production

Rui Zhang[1,2,3,4], *Baoshan Liu*[1,2,3,4], *Xinhui Fan*[1,2,3,4], *Wenjun Wang*[1,2,3,4], *Tonghui Xu*[1,2,3,4], *Shujian Wei*[1,2,3,4], *Wen Zheng*[1,2,3,4], *Qiuhuan Yuan*[1,2,3,4], *Luyao Gao*[1,2,3,4], *Xinxin Yin*[1,2,3,4], *Boyuan Zheng*[1,2,3,4], *Chuanxin Zhang*[1,2,3,4], *Shuai Zhang*[1,2,3,4], *Kehui Yang*[1,2,3,4], *Mengyang Xue*[1,2,3,4], *Shuo Wang*[1,2,3,4], *Feng Xu*[1,2,3,4], *Jiali Wang*[1,2,3,4*], *Yihai Cao*[5*] and *Yuguo Chen*[1,2,3,4*]

[1] Department of Emergency Medicine, Qilu Hospital, Shandong University, Jinan, China, [2] Shandong Provincial Clinical Research Center for Emergency and Critical Care Medicine, Institute of Emergency and Critical Care Medicine of Shandong University, Qilu Hospital, Shandong University, Jinan, China, [3] Key Laboratory of Emergency and Critical Care Medicine of Shandong Province, Key Laboratory of Cardiopulmonary-Cerebral Resuscitation Research of Shandong Province, Shandong Provincial Engineering Laboratory for Emergency and Critical Care Medicine, Qilu Hospital, Shandong University, Jinan, China, [4] The Key Laboratory of Cardiovascular Remodeling and Function Research, Chinese Ministry of Education, Chinese Ministry of Health and Chinese Academy of Medical Sciences, The State and Shandong Province Joint Key Laboratory of Translational Cardiovascular Medicine, Qilu Hospital, Shandong University, Jinan, China, [5] Department of Microbiology, Tumor and Cell Biology, Karolinska Institute, Stockholm, Sweden

OPEN ACCESS

Edited by:
Owen Llewellyn Woodman,
Monash University, Australia

Reviewed by:
Didier Morin,
Centre National de la Recherche Scientifique (CNRS), France
Ana Cipak Gasparovic,
Rudjer Boskovic Institute, Croatia

***Correspondence:**
Yuguo Chen
chen919085@sdu.edu.cn
Yihai Cao
yihai.cao@ki.se
Jiali Wang
wangjiali_2000@126.com

Specialty section:
This article was submitted to Cardiovascular and Smooth Muscle Pharmacology, a section of the journal Frontiers in Pharmacology

Received: 29 October 2019
Accepted: 11 March 2020
Published: 27 March 2020

Citation:
Zhang R, Liu B, Fan X, Wang W, Xu T, Wei S, Zheng W, Yuan Q, Gao L, Yin X, Zheng B, Zhang C, Zhang S, Yang K, Xue M, Wang S, Xu F, Wang J, Cao Y and Chen Y (2020) Aldehyde Dehydrogenase 2 Protects Against Post-Cardiac Arrest Myocardial Dysfunction Through a Novel Mechanism of Suppressing Mitochondrial Reactive Oxygen Species Production. Front. Pharmacol. 11:373. doi: 10.3389/fphar.2020.00373

Post-cardiac arrest myocardial dysfunction significantly contributes to early mortality after the return of spontaneous circulation. However, no effective therapy is available now. Aldehyde dehydrogenase 2 (ALDH2) enzyme has been shown to protect the heart from aldehyde toxicity such as 4-hydroxy-2-nonenal (4-HNE) and oxidative stress. In this study, we evaluated the effect of enhanced activity or expression of ALDH2 on post-cardiac arrest myocardial dysfunction and survival in a rat cardiac arrest model. Furthermore, we elucidated the underlying mechanisms with a focus on mitochondrial reactive oxygen species (ROS) production in a cell hypoxia/reoxygenation model. A total of 126 rats were used for the ALDH2 activation or cardiac overexpression of ALDH2 studies. Randomization was done 10 min before the respective agonist injection or *in vivo* gene delivery. We showed that enhanced activity or expression of ALDH2 significantly improved contractile function of the left ventricle and survival rate in rats subjected to cardiac arrest-cardiopulmonary resuscitation procedure. Moreover, ALDH2 prevented cardiac arrest-induced cardiomyocyte death from apoptosis and mitochondrial damage. Mechanistically, 4-HNE, a representative substrate of ALDH2, was dominantly increased in the hypoxia/reoxygenation-exposed cardiomyocytes. Direct addition of 4-HNE led to significantly augmented succinate accumulation and mitochondrial ROS

production. Through metabolizing 4-HNE, ALDH2 significantly inhibited mitochondrial ROS production. Our findings provide compelling evidence of the cardioprotective effects of ALDH2 and therapeutic targeting this enzyme would provide an important approach for treating post-cardiac arrest myocardial dysfunction.

Keywords: aldehyde dehydrogenase 2, cardiopulmonary resuscitation, post-cardiac arrest myocardial dysfunction, cardiomyocyte death, mitochondrial reactive oxygen species

INTRODUCTION

Sudden cardiac arrest remains a major public health burden in terms of high mortality and morbidity worldwide (Hayashi et al., 2015). While efforts to initiate rapid cardiopulmonary resuscitation (CPR), e.g., establishment of medical emergency outreach teams, have improved the return of spontaneous circulation (ROSC) to 30–40% of patients with cardiac arrest, the mortality thereafter remains >50% (Neumar et al., 2008; Hazinski et al., 2015). Post-cardiac arrest myocardial dysfunction is an important cause of circulatory failure and early mortality after ROSC (Kern et al., 1996; Stub et al., 2011). Among the multiple factors, ischemia/reperfusion injury plays an essential role in the pathological progression of myocardial dysfunction. However, there is currently no effective therapeutic approach for post-cardiac arrest myocardial dysfunction as well as ischemia/reperfusion injury.

Mitochondria, as the center of energy supply and reactive oxygen species (ROS) production, play a crucial role as targets and drivers of ischemia/reperfusion injury after cardiac arrest (Penna et al., 2013; Matsuura et al., 2017). One mitochondrial feature during the ischemia/reperfusion processes is the ROS production (Zweier et al., 1987; Murphy and Steenbergen, 2008; Chouchani et al., 2014). Recently, mitochondrial ROS have been shown to be an important factor in contributing sudden cardiac death and myocardial dysfunction (Dey et al., 2018). However, the mechanism of mitochondrial ROS production and mitochondria-targeted treatments designed to ameliorate mitochondrial oxidative stress are still under study (Murphy, 2016; Dey et al., 2018).

Aldehydes are generated through lipid peroxidation on mitochondrial and plasma membranes in response to oxidative stress and have been observed in the heart after cardiac arrest (Hayashida et al., 2012). Aldehydes can easily diffuse from the side of their origin (i.e., membranes) and reach and attack targets intracellularly and extracellularly, forming adducts with macromolecules including proteins, DNA, and lipids which usually modulates or disrupts their functions (Roede and Jones, 2010; Li et al., 2018). Aldehydes can impair mitochondria by attacking on Cys, Lys, or Arg amino acid residues of mitochondrial proteins, but the underlying mechanism is still unclear (Roede and Jones, 2010; Li et al., 2018). Therefore, clarifying the role of aldehydes in mitochondrial injury and effectively clearing these highly harmful aldehydes is crucial to protect mitochondria from ischemia/reperfusion injury and alleviate post-cardiac arrest myocardial dysfunction.

Aldehyde dehydrogenase 2 (ALDH2) has recently emerged as a critical health-promoting enzyme, which is primarily expressed in the mitochondria in a wide variety of organs, including the heart (Li et al., 2018). Previous studies have suggested that ALDH2 plays a central protective role in several types of cardiac diseases and global cellular oxidative stress mainly through metabolizing various aldehydes, such as 4-hydroxy-2-nonenal (4-HNE) which is the most abundant and reactive carbonyl species (Chen et al., 2014; Ji et al., 2016; Liu et al., 2018). However, the influence of ALDH2 on post-cardiac arrest myocardial dysfunction and mitochondrial ROS has not been investigated yet. Thus, the aims of this study are (1) to evaluate the effect of enhanced activity or expression of ALDH2 on myocardial dysfunction and survival after cardiac arrest, (2) to examine the importance of ALDH2 in reducing cardiomyocyte death and mitochondrial injury, and (3) to elucidate the underlying mechanisms by which ALDH2 exerts cardioprotection with a focus on mitochondrial ROS production.

METHODS

Animals

Adult male Wistar rats were purchased from the Department of Experimental Animals of Shandong University (Jinan, China) and acclimatized in the housing facility for at least 1 week before the cardiac arrest and CPR (CA-CPR) procedure. Rats were fed with normal chow and were free to access tap water at a constant temperature of 21.0°C ± 1.0°C, with a fixed 12-h light/dark cycle. A total of 126 rats were assigned to 1 of 3 animal study frameworks: (1) protocol 1 of the ALDH2 activation study (n = 53)—Alda-1 (10 mg/kg, Sigma-Aldrich, St. Louis, Missouri) was administered *via* intraperitoneal injection 30 min before cardiac arrest; (2) protocol 2 of the ALDH2 activation study (n = 28)— Alda-1 (10 mg/kg) was administered *via* intraperitoneal injection at the start of resuscitation; and (3) cardiac overexpression of ALDH2 study (n = 45)—adeno-associated virus (serotype 9) (AAV9)-ALDH2 or AAV9-Veh was delivered *via* tail vein injection at 2.5×10^{11} vector genomes/rat 4 weeks before cardiac arrest. In each animal cohort, rats were randomized respectively to CA-CPR group and CA-CPR+Alda-1 group, or AAV9-Veh+CA-CPR group and AAV9-ALDH2+CA-CPR group 10 min before the injection. Furthermore, rats in protocol 1 of the ALDH2 activation study were assigned to 1 of 3 tissue collection time points. At 1 h after ROSC, rats were euthanized for assessing mitochondrial morphology of heart. At 4 h after ROSC, rats were euthanized

for myocardial functional and histological assessment. At 72 h after ROSC, rats were euthanized for assessing survival rate, myocardial function, and histology. In protocol 2 of the ALDH2 activation, rats with ROSC were followed up for 72 h for survival rate analysis. The myocardial function was detected within 4 h and at 72 h after ROSC. In the cardiac overexpression of ALDH2 study, rats were assigned to two tissue collection time points. At 1 h after ROSC, rats were euthanized for assessing mitochondrial morphology of heart. At 4 h after ROSC, rats were euthanized for myocardial functional and histological studies. Additional details about animal study can be found in the flowchart in **Figure 1**. The study was approved by the Institutional Animal Care and Use Committee of Shandong University, in accordance with National Institutes of Health Guidelines.

Cardiac Arrest and CPR Procedure

CA-CPR procedure was performed in rats as previously described with minor modifications (Huang et al., 2008; Kim et al., 2016; Wang et al., 2016). Briefly, rats were anesthetized with pentobarbital sodium (45 mg/kg, intraperitoneal injection). The oral trachea intubation with a 14-G cannula was performed and ventilator settings included a tidal volume of 0.7 ml/100 g, a respiratory rate of 70 breaths/min and FiO2 of 21%. PE-50 tubes filled with heparinized saline were inserted into the right femoral artery for blood pressure monitoring and blood gas sampling, and into the right femoral vein for epinephrine administration. The Millar pressure-volume catheter (ADInstruments, Sydney, Australia) was inserted through the right carotid artery and advanced into the left ventricle, as appropriate. The rectal temperature was monitored and maintained at 37°C ± 0.5°C by a heating pad. Blood pressure, left ventricular pressure, and needle-probe electrocardiogram monitoring data were recorded with the PowerLab acquisition system (ADInstruments). CA was induced by asphyxia *via* turning off the ventilator and clamping the endotracheal tube. CA was defined as the femoral mean arterial pressure (MAP) < 30 mmHg. After 8 min of asphyxia, the mechanical ventilator was reinitiated. The epinephrine (2 μg/100 g, once every 3 min) was administered, and chest compression (200 beats/min) was performed, attempting for 10 min at most. ROSC was defined as the return of sinus rhythm with a MAP ≥60 mmHg lasting for at least 5 min.

Cells and Hypoxia/Reoxygenation Procedure

Rat cardiomyoblasts cell line (H9c2) and primary cardiomyocytes isolated from adult male wild type (WT) mice and ALDH2 knockout (KO) mice were used. Cells were cultured normally in a humidified incubator with 95% air/5% CO_2 at 37°C. Hypoxia/reoxygenation procedure was induced by exposing cells in a hypoxic workstation (H35, Don Whitley Scientific, Bingley, United Kingdom) containing 94% N_2, 5% CO_2, and 1% O_2 at 37°C with serum-deprived media for 4 h and then culturing cells under normal conditions with complete media for another 2 h. Alda-1 (20 mmol/L) or Daidzin (60 mmol/L, Sigma-Aldrich) was added to the media 30 min before hypoxia/reoxygenation.

In Vivo Gene Delivery

The recombinant AAV9 vector carrying rat *ALDH2* with a cardiac troponin T (cTNT) promoter and green fluorescent protein (GFP) (AAV9-ALDH2) (Hanbio Inc, Shanghai, China) or carrying only cTNT and GFP (AAV9-Veh) as a negative

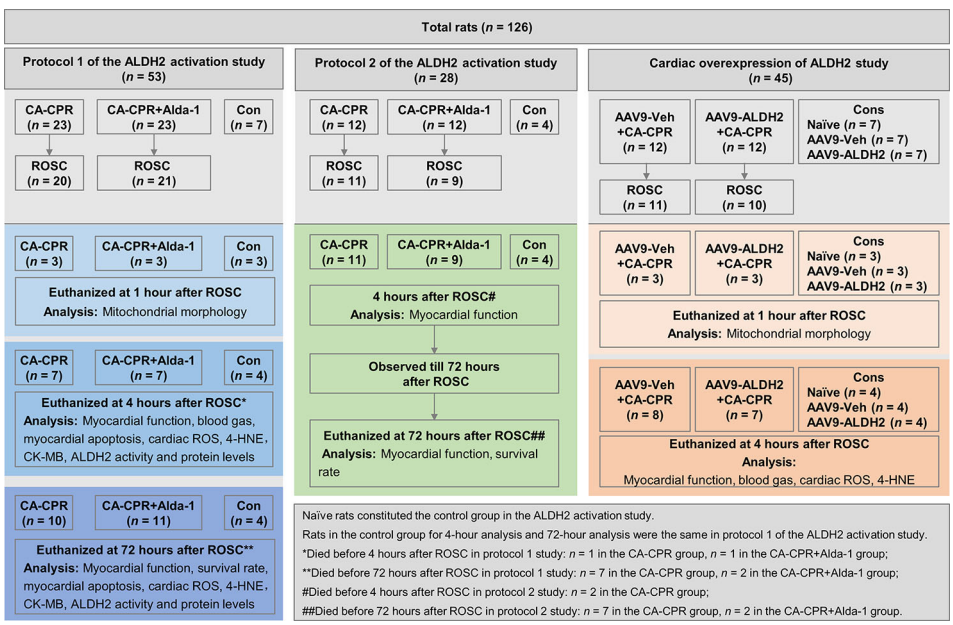

FIGURE 1 | The flowchart of the animal study.

control was delivered to male rats *via* a bolus tail vein injection at 2.5×10^{11} vector genomes/rat. After 4 weeks, the expression of GFP in the liver, skeletal muscle, and heart tissue in rats receiving gene delivery was observed under a fluorescence microscope (Olympus Corporation, Tokyo, Japan), and the expression levels of ALDH2 were detected by western blot analysis.

Measurement of Myocardial Function

Left ventricular cardiac output (CO) and ejection fraction (EF) were measured by Millar pressure-volume catheter (ADInstruments). Left ventricular end diastolic diameter (LVEDD) and left ventricular end systolic diameter (LVESD) were measured to calculate EF, fractional shortening (FS), left ventricular end diastolic volume (LVEDV), and left ventricular end systolic volume (LVESV) by echocardiography (VisualSonics, Toronto, Canada) as described previously (Wang et al., 2011).

Tissue Collection and Processing at Pre-Specified Time Points

Rats were euthanized by transcardial perfusion with saline and then hearts were harvested rapidly. At 1 h after ROSC, the left ventricular tissue was cut into ~1 mm^3 pieces and each piece was fixed with glutaraldehyde overnight for the transmission electron microscope (TEM) exanimation. At 4 h and 72 h after ROSC, the left ventricular tissue was washed in saline, snap frozen in liquid nitrogen and stored at −80°C for ALDH2 activity, ALDH2 expression, and cardiac ROS analysis; otherwise, the left ventricular tissue was fixed in 4% formaldehyde, embedded in paraffin, and cut into sections of 6 μm in thickness to assess apoptosis.

Fluorescently-Labeled Alda-1

Alda-1 was combined with lissamine rhodamine B200, a red natural luciferin, by electrostatic adherence (Jieyi Biotech, Shanghai, China) and administered to rats *via* intraperitoneal injection. After 4 h, the left ventricular tissue was observed under a fluorescence microscope (Olympus Corporation).

Measurement of Myocardial Apoptosis

Apoptosis was assessed by transferase mediated dUTP nick-end labeling (TUNEL) staining using ApopTag® In Situ Apoptosis Detection Kits (Millipore, Burlington, Massachusetts) (Tan et al., 2012; Liu et al., 2017). After staining, the sections were observed under a fluorescence microscope (Olympus Corporation) and measured by Image-Pro Plus 6.0 (Media Cybernetics, Rockville, Maryland).

Examination of Mitochondrial Morphology

Thin sections (70 nm) of left ventricular tissue were stained and examined using a scanning TEM (JEOL Ltd., Tokyo, Japan) (Huang et al., 2011). The severity of mitochondrial structural damage was semi-quantified using Flameng grading of 1 through 5 as described previously (Flameng et al., 1980; Hawong et al., 2015).

Determination of Plasma Creatine Kinase-MB (CK-MB)

Blood samples were centrifuged at 1000 × g for 20 min to collect plasma. The levels of CK-MB were measured using enzyme-linked immunosorbent assay (ELISA) (Cloud-clone, Wuhan, China).

Determination of Blood Gas

Arterial blood was obtained at 15 min, 1 h, and 4 h after ROSC and blood gas profiles (pH, PaO_2, $PaCO_2$, glucose, and lactate) were measured immediately using automated blood gas analyzer (Instrumentation Laboratory, Bedford, Massachusetts).

Measurement of ALDH2 Activity

The mitochondria were isolated from myocardial tissue using the Tissue Mitochondria Isolation Kit (Beyotime, Nanjing, China). The mitochondria were sonicated, centrifuged at 11,000 × g for 10 min at 4°C and the supernatant was collected to measure ALDH2 activity. The supernatant was incubated with 50 mmol/L sodium pyrophosphate, 2.5 mmol/L NAD^+, and 10 mmol/L propionaldehyde for 10 min. Acetaldehyde as the substrate of ALDH2 was oxidized to acetic acid, whereas NAD^+ was reduced to NADH which was used to determine ALDH2 activity. Production of NADH was determined by spectrophotometric absorbance at 340 nm (Thermo Scientific, Waltham, Massachusetts) (Wang et al., 2011; Tan et al., 2012).

Isolation of Primary Cardiomyocytes From Adult Mice

The ALDH2 KO mice were provided by University of Occupational and Environmental Health (Fukuoka, Japan). The cardiomyocytes were isolated from adult male WT mice and ALDH2 KO mice (all were C57BL/6 background) as described previously (Ackers-Johnson et al., 2016; Pang et al., 2016). Briefly, mice were sacrificed after anaesthetized with 2% isoflurane, and hearts were rapidly excised and mounted onto a temperature-controlled (37°C) Langendorff system (ADInstruments). The hearts were perfused retrogradely through the aorta with collagenase II (Sigma-Aldrich), collagenase IV (Sigma-Aldrich), and collagenase IV (Sigma-Aldrich) for about 20 min until digestion was apparent. The digested left ventricles were then cut into ~1 mm^3 pieces and dissociated by pipetting 2 min. After four sequential rounds of gravity settling using three intermediate calcium reintroduction buffers to gradually restore calcium concentration to physiological levels, the cell pellet which was enriched with myocytes was collected and used for the experiments within 8 h after isolation.

Measurement of Mitochondrial ROS, Cellular ROS, and Cardiac ROS

The mitochondrial ROS levels in H9c2 cells and primary cardiomyocytes were measured with MitoSOX Red reagent, a mitochondrial superoxide (O_2^-) indicator (Invitrogen, Carlsbad, California) (Roberge et al., 2014; Ji et al., 2016). Cells were incubated with 5 μmol/L MitoSOX Red for 10 min at 37°C

protected from light. The cellular ROS levels in H9c2 cells were measured by incubating with 10 μmol/L 2′,7′-dichlorofluorescin diacetate (DCFH-DA) (Beyotime) for 30 min at 37°C protected from light which was converted to fluorescent 2′,7′-dichlorofluorescein (DCF) by ROS (Ji et al., 2016). The O_2^- levels in cardiac tissue were measured using dihydroethidium (DHE) (Beyotime), an oxidative fluorescent dye (Ji et al., 2016; Zhang et al., 2016). Frozen sections (6 μm) of myocardium were incubated with 10 μmol/L DHE for 30 min at 37°C protected from light and incubated with DAPI (Boster, Wuhan, China) for 2 min to label nuclei. After incubation, cells and tissue sections were observed under a fluorescence microscope (Olympus Corporation). The intensity of fluorescence was quantified by ImageJ software (U.S. National Institutes of Health, Bethesda, Maryland). Three samples of each group were studied and five randomly selected fields of each sample were evaluated. The mean intensity of fluorescence of the five fields for each sample was used for statistical analysis.

Measurement of Mitochondrial Respiratory Function

Mitochondrial respiratory function evaluated by oxygen consumption rate (OCR) was assessed using a Seahorse XF^{e}24 analyzer with the Seahorse XF Cell Mito Stress Test Kit (Agilent Technologies, Santa Clara, California) as described previously (Ikeda et al., 2016; Tsushima et al., 2018). Briefly, ~10^5 cells were seeded in a 24-well plate specific for the Seahorse XF^{e}24 instrument and underwent hypoxia/reoxygenation procedure. After the hypoxia/reoxygenation procedure, cells were equilibrated with XF assay media supplemented with 25 mmol/L glucose, 1 mmol/L sodium pyruvate, and 2 mmol/L L-glutamine. Then, the OCR was analyzed by Seahorse XF^{e}24 analyzer with the following inhibitors: 1 μmol/L oligomycin (Oligo), 1 μmol/L carbonyl cyanide 4-(trifluoromethoxy) phenylhydrazone (FCCP), and 0.5 μmol/L rotenone/antimycin A (Rot/Ant).

Adenosine 5'-Triphosphate (ATP) Assay

Cellular ATP contents were measured by a firefly luciferase-based ATP assay kit (Beyotime) according to the manufacturer's instructions. Briefly, cells were schizolysized and centrifuged at 12,000 × g for 5 min at 4°C to collect the cell supernatant which was then mixed with ATP detection working solution. The protein concentration of sample was measured and the standard curve of ATP concentration was prepared. The ATP level was measured based on the emitted light by a luminescence plate reader (Thermo Scientific).

Measurement of Succinate Levels

The levels of succinate were assessed colorimetrically using the established Succinate Assay Kit (Abcam, Cambridge, UK) according to the manufacturer's instructions (Karlstaedt et al., 2016). Briefly, cells were washed with cold PBS, resuspended in succinate assay buffer, homogenized, and centrifuged for 12,000 × g for 5 min at 4°C to collect supernatant. The samples were then incubated with the reaction mix for 30 min at 37°C. The standard curve of succinate concentration was prepared. The level of succinate was measured colorimetrically at 450nm (Thermo Scientific).

Measurement of Mitochondrial Membrane Potential

The mitochondrial membrane potential was measured by incubating cells with 100 nmol/L TMRM (Invitrogen) for 30 min at 37°C. After rinsed twice, cells were observed under a fluorescence microscope (Olympus Corporation). The intensity of fluorescence was quantified by ImageJ software (U.S. National Institutes of Health) and was used to indicate the mitochondrial membrane potential. Three samples of each group were studied and five randomly selected fields of each sample were evaluated. The mean value of the five fields for each sample was used for statistical analysis.

Assessment of Succinate Dehydrogenase (SDH) Carbonylation

To detect the levels of SDH carbonylation, SDH was immunoprecipitated by incubating 500 μg cell lysate with 2–10 μg anti-SDHA antibody (Abcam) overnight at 4°C, followed by incubation with 20 μl protein A/G agarose (Beyotime) for 2 h at 4°C. Immunoprecipitates were washed, resuspended in 1× sample buffer, boiled for 5 min, and analyzed by western blot analysis.

Cell Treatment With 4-HNE

When detecting the level of mitochondrial ROS, cellular succinate, and mitochondrial membrane potential, 4-HNE (BioVision, Milpitas, California) with different concentrations (10 μM, 20 μM, or 40 μM) was incubated with ~10^6 cells for 4 h. And when detecting SDH carbonylation, 40 μM 4-HNE was incubated with ~5×10^6 cells for 4 h.

Western Blot Analysis

Protein samples were separated by SDS-PAGE and transferred to nitrocellulose membranes (Millipore). After blocked with 5% milk, the blots were probed with antibodies against ALDH2 (1:1,000, Abcam), β-actin (1:1,000, Cell Signaling Technology, Danvers, Massachusetts), and 4-HNE-protein adducts (1:1,000, Abcam). For assessment of SDH carbonylation, blots were probed with anti-DNPH antibody (1:1,000, Abcam) after incubated with 0.5 mmol/L 2, 4-dinitro phenylhydrazine (DNPH, Sigma-Aldrich) for 30 min or probed with anti-SDHA antibody (1:1,000, Abcam) (Wu et al., 2016; Li et al., 2018). Membranes were washed and incubated with horseradish peroxidase-conjugated secondary antibodies (1:10,000) for 2 h and detected using the chemiluminescence method. The intensity of the bands was quantified by ImageJ software (U.S. National Institutes of Health).

Immunofluorescence Staining

The distribution of 4-HNE-protein adducts in cells was detected using immunofluorescence staining. Briefly, cells grown on cover slip were fixed with 4% formaldehyde and permeated with 0.5% Triton X-100. After blocked with goat serum, cells were incubated with primary antibody against 4-HNE-protein

adducts (1:1,000, Abcam) overnight. Cells were washed and incubated with secondary antibody for 1 h. Then, cells were incubated with 100 nmol/L Mito-tracker Red (Beyotime) for 30 min at 37°C protected from light and incubated with DAPI (Boster) for 2 min to label nuclei. The fluorescence of 4-HNE-protein adducts, Mito-tracker Red and DAPI was observed under a fluorescence microscope (Olympus Corporation).

Statistical Analysis

The continuous data were presented as mean ± SEM. Group comparisons were performed by one-way analysis of variances (ANOVA) with Tukey's *post hoc* test or Student's t-test. Comparisons between time-based measurements within each group were performed by repeated-measures ANOVA. Survival was presented by Kaplan-Meier curves, and the log-rank test was used for comparing survival rate between groups. A P value <0.05 was considered statistically significant (2-tailed).

RESULTS

Baseline and Procedural Characteristics of the Animal Study

There were no significant differences in the baseline body weight, heart rate, MAP, left ventricular CO, EF or FS between the CA-CPR group and the CA-CPR+Alda-1 group in the ALDH2 activation study (**Supplemental Table 1**). In addition, no differences were observed in cardiac arrest duration, CPR duration, or ROSC rate between the CA-CPR group and the CA-CPR+Alda-1 group in the ALDH2 activation study (**Supplemental Table 2**). Similar results with regard to the baseline and procedural features were found in the cardiac overexpression of ALDH2 study (**Supplemental Tables 3** and **4**).

Activation of ALDH2 Effectively Improves Post-Cardiac Arrest Myocardial Dysfunction and Survival Rate

Myocardial function within 4 h after ROSC, as evaluated by left ventricular CO and EF using Millar pressure-volume catheter, was markedly reduced in all rats subjected to CA-CPR procedure (**Figure 2A**) compared with their respective baseline in protocol 1 of the ALDH2 activation study (**Supplemental Table 1**). Alda-1 reached the heart after intraperitoneal administration (**Supplemental Figure 1**) and significantly increased both left ventricular CO and EF, with the improvement in left ventricular CO occurring as early as 15 min after ROSC and the improvement in left ventricular EF occurring at 1 h after ROSC (**Figure 2A**). Similar trends for 4-h myocardial function after ROSC, as evaluated by left ventricular EF and FS using echocardiography, were observed in protocol 2 of the ALDH2 activation study (**Figure 2B**). Taken together, these results demonstrate that upregulation of ALDH2 activity by Alda-1 improves myocardial function within 4 h after ROSC.

We further evaluated left ventricular EF and FS at 72 h after ROSC using echocardiography in the CA-CPR group and the CA-CPR+Alda-1 group in the two protocols of the ALDH2 activation study. The impairment of left ventricular EF and FS remained significant in the CA-CPR group compared with their respective baseline in both protocol 1 and protocol 2; however, left ventricular EF and FS in the CA-CPR+Alda-1 group were restored to 92.0 and 89.7% of their baseline levels, respectively, in protocol 1 and restored to 86.3 and 82.5% of their baseline levels, respectively, in protocol 2 (P > 0.05 versus their respective

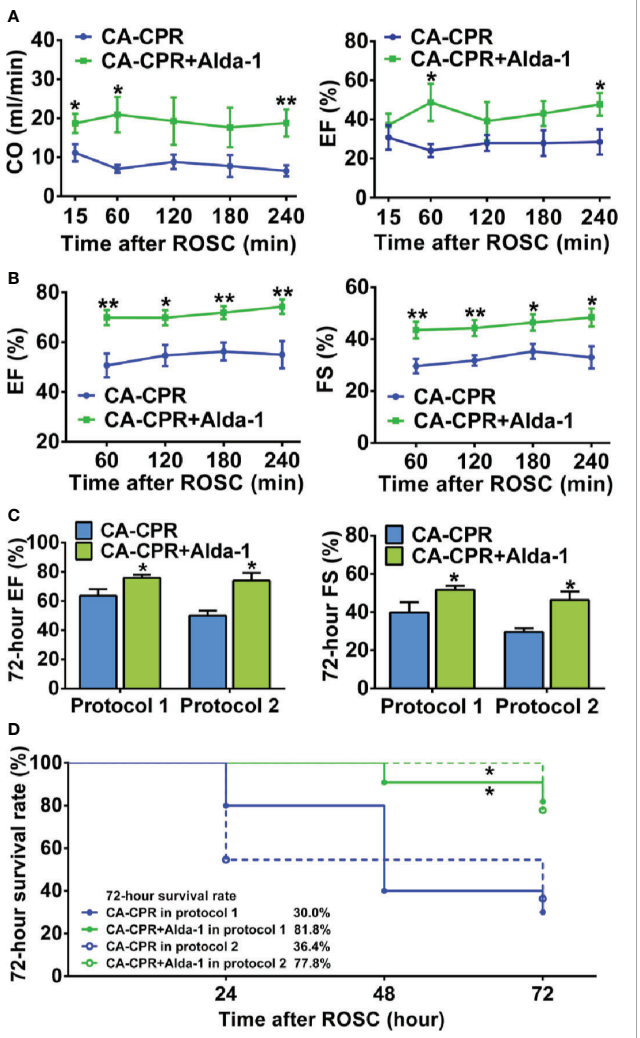

FIGURE 2 | The effect of ALDH2 activation by Alda-1 on post-cardiac arrest myocardial dysfunction and survival rate. **(A)** Left ventricular cardiac output (CO) and ejection fraction (EF) evaluated by Millar pressure-volume catheter within 4 h after ROSC in protocol 1 of the ALDH2 activation study (n = 6 animals per group). **(B)** Left ventricular EF and fractional shortening (FS) evaluated by echocardiography within 4 h after ROSC in protocol 2 of the ALDH2 activation study (n = 9 animals per group). **(C)** Left ventricular EF and FS evaluated by echocardiography at 72 h after ROSC in the two protocols of the ALDH2 activation study (n = 3–9 animals per group). **(D)** Kaplan-Meier survival curves within 72 h after ROSC in the two protocols of the ALDH2 activation study. Myocardial function between groups was compared by Student's t-test and time-based measurements within each group were compared by repeated-measures ANOVA. The survival rate between groups was compared by the log-rank test. Data are presented as mean ± SEM. *P < 0.05, **P < 0.01 versus CA-CPR group.

baselines, **Figure 2C** and **Supplemental Table 1**). The 72-h survival rate was 30.0% in the CA-CPR group, whereas it was 81.8% in the CA-CPR+Alda-1 group in protocol 1. The log-rank test revealed markedly improved survival rate in the CA-CPR +Alda-1 group compared with the CA-CPR group ($P < 0.05$, **Figure 2D**). The same trend for survival rate between the CA-CPR group and CA-CPR+Alda-1 group was observed in protocol 2 (**Figure 2D**). Collectively, these results demonstrate that upregulation of ALDH2 activity reveals significant improvement in the 72-h myocardial function and survival rate.

We also determined the activity and expression levels of ALDH2 in myocardium in rats subjected to CA-CPR procedure. The results showed that the activity of ALDH2 was reduced by 58.8% at 4 h and 64.8% at 72 h after ROSC, respectively, which was significantly elevated by Alda-1; however, the expression levels of ALDH2 did not alter during the observation periods (**Supplemental Figure 2**). These findings can explain why upregulation of ALDH2 activity has a protective effect on post-cardiac arrest myocardial dysfunction.

Activation of ALDH2 Attenuates Cardiac Arrest-Induced Cardiomyocyte Death and Mitochondrial Injury

Because we saw no differences of the cardioprotection effect between these two protocols of ALDH2 activation study and in order to keep consistence with the ALDH2 overexpression study which enhanced ALDH2 activity before cardiac arrest, the rats in protocol 1 of the ALDH2 activation study were used for the following mitochondrial morphology and biomedical investigations. As expected, cardiac myocyte apoptosis was increased sharply at both 4 h and 72 h after ROSC in the CA-CPR group, which was significantly attenuated by Alda-1 (**Figure 3A**). The levels of plasma CK-MB were increased 3.0-fold at 72 h after ROSC, which were abolished by Alda-1 (**Figure**

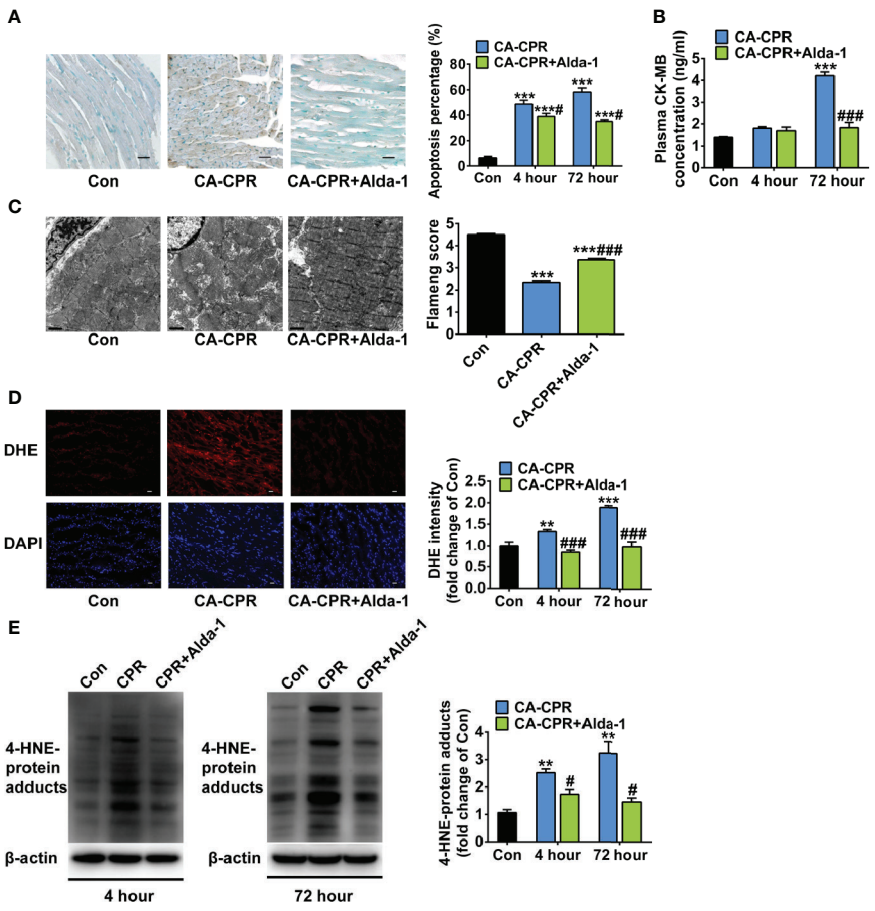

FIGURE 3 | The effect of ALDH2 activation by Alda-1 on post-cardiac arrest cardiomyocyte death, mitochondrial structural damage, and cardiac ROS levels. **(A)** Representative photographs of cardiomyocyte apoptosis by TUNEL staining at 4 h after ROSC and quantification at 4 h and 72 h after ROSC (n = 3–4 animals per group). Scale bar = 100 μm. **(B)** The plasma levels of CK-MB at 4 h and 72 h after ROSC (n = 3–4 animals per group). **(C)** Representative photographs and quantification of mitochondrial morphology by TEM examination at 1 h after ROSC (n = 3 animals per group). Scale bar = 1 μm. **(D)** Representative photographs of dihydroethidium (DHE) staining at 4 h after ROSC and quantification at 4 h and 72 h after ROSC (n = 3–4 animals per group). Scale bar = 100 μm. **(E)** Representative immunoblots and quantification of 4-HNE-protein adducts at 4 h and 72 h after ROSC (n = 3–4 animals per group). Group comparisons were performed by ANOVA with Tukey's *post hoc* test. Data are presented as mean ± SEM. $^{**}P < 0.01$, $^{***}P < 0.001$ versus Con group; $^{\#}P < 0.05$, $^{\#\#\#}P < 0.001$ versus CA-CPR group.

3B). Consisted with these findings, obvious mitochondrial structural damage was observed at 1 h after ROSC in the CA-CPR group, which was partially reversed by Alda-1 (**Figure 3C**). The elevated cellular ROS levels (**Figure 3D**) and 4-HNE-protein adducts (**Figure 3E**) were also inhibited by Alda-1. However, there were no significant differences in the levels of blood gas (pH, PaO_2, $PaCO_2$, glucose, and lactate) between the CA-CPR group and the CA-CPR+Alda-1 group at 15 min, 1 h, or 4 h after ROSC, respectively (**Supplemental Table 5**). These results suggest that myocardial cell death and mitochondrial damage should be the disordered physiological processes that cause post-cardiac arrest myocardial dysfunction, whereas upregulation of ALDH2 activity could attenuate these disorders.

Enhanced Expression of ALDH2 Improves Post-Cardiac Arrest Myocardial Dysfunction

To further validate the cardioprotective effect of ALDH2 activation, we examined whether enhancing the expression of ALDH2 had protective effect on post-cardiac arrest myocardial dysfunction. The AAV9 vector carrying ALDH2 with a cTNT promoter was constructed, which led to the increased expression of ALDH2 in the heart, but not in the liver or skeletal muscle (**Figure 4A** and **Supplemental Figure 3**). Cardiac specific overexpression of ALDH2 significantly improved left ventricular EF, evaluated by echocardiography, within 4 h after ROSC compared with that in the CA-CPR group (**Figure 4B**). The mitochondrial structural damage at 1 h after ROSC was significantly prevented by cardiac specific overexpression of ALDH2 (**Figure 4C**). The elevated cellular ROS levels (**Figure 4D**) and 4-HNE-protein adducts (**Figure 4E**) were also inhibited by cardiac specific overexpression of ALDH2. However, ALDH2 overexpression did not affect the levels of blood gas at 15 min, 1 h, or 4 h after ROSC (**Supplemental Table 6**). These findings indicate that enhancement of ALDH2 through both enzymatic activation and protein overexpression attenuates post-cardiac arrest myocardial dysfunction.

Alda-1 Specifically Activates ALDH2 and Suppresses Hypoxia/Reoxygenation-Induced Mitochondrial ROS

We explored the molecular mechanisms by which ALDH2 exerted cardioprotection after cardiac arrest through regulation of its activity in a rat cardiomyoblast hypoxia/reoxygenation model, focusing on mitochondrial ROS. The levels of mitochondrial ROS were increased 5.7-fold during hypoxia/reoxygenation, the extent of which was significantly reduced by Alda-1; inhibition of ALDH2 by Daidzin did not further increase the mitochondrial ROS levels (**Figure 5A**). Similar inverse trends were observed for the cellular ATP levels (**Figure 5B**). The overall cellular ROS levels were also elevated during hypoxia/reoxygenation, which were inhibited by Alda-1 (**Supplemental Figure 4**). Additionally, mitochondrial respiratory dysfunction reflected by the reduced OCR under hypoxia/reoxygenation was markedly reversed by Alda-1 (**Figure 5C**). These results show the dramatically increased levels of mitochondrial ROS and the concomitant disorders of mitochondrial energy generation during reoxygenation could be inhibited by Alda-1, suggesting control of mitochondrial ROS should be an important function of ALDH2.

Furthermore, we assessed the specificity of Alda-1 on ALDH2, which has not been proved in the previous studies yet. Primary cardiomyocytes were obtained from ALDH2 KO mice and its background WT mice, respectively. ALDH2 KO cardiomyocytes generated more mitochondrial ROS under hypoxia/reoxygenation compared with the cardiomyocytes from WT mice; however, Alda-1 had no effect on the levels of mitochondrial ROS in ALDH2 KO cardiomyocytes (**Figure 5D**). Similar findings were observed for hypoxia/reoxygenation-induced mitochondrial respiratory dysfunction (**Figure 5E**). These results indicate that Alda-1 has no other targets in mitochondrial protection except interacting with ALDH2.

4-HNE Is Increased Under Hypoxia/Reoxygenation and Promotes Mitochondrial ROS Production

We further examined whether the effect of ALDH2 on inhibiting mitochondria ROS production during hypoxia/reoxygenation was attributed to its enzymatic function against toxic aldehyde overload. 4-HNE, a representative substrate of ALDH2, was selectively investigated. The 4-HNE-protein adducts were increased 2.1-fold after 4 h of hypoxia followed by 2 h of reoxygenation, which were distributed in both the mitochondria and the cytoplasm (**Figure 6A** and **Supplemental Figure 5**). Importantly, 4-HNE increased the levels of mitochondrial ROS 3.2-fold (**Figure 6B**). Since previous evidence has shown that the accumulated succinate is the main driver of mitochondrial ROS production (Chouchani et al., 2014), we hypothesized that 4-HNE may interfere with this process. We observed that the levels of mitochondrial ROS were aggravated by addition of succinate during hypoxia/reoxygenation (**Figure 6C**), which were blocked by dimethyl malonate (DMM), a membrane-permeable precursor of the SDH competitive inhibitor and SDH is a critical enzyme responsible for succinate generation (**Figure 6D**). It was interesting that 4-HNE stimulation resulted in the elevated succinate accumulation in a concentration-dependent manner (**Figure 6E**) and increased mitochondrial membrane potential (**Figure 6F**). Additionally, augmented SDH carbonylation was observed with 4-HNE treatment (**Figure 6G**). Treatment with DMM inhibited 4-HNE-induced increase of mitochondrial ROS levels (**Figure 6B**). Taken together, these data suggest that aldehydes play an essential role in mediating succinate accumulation and mitochondrial ROS production, which may explain why enhancement of ALDH2 inhibits mitochondrial ROS production during hypoxia/reoxygenation (**Figure 7**).

DISCUSSION

In this study, we demonstrate that enhanced activity or expression of ALDH2 attenuates myocardial dysfunction, cardiomyocyte

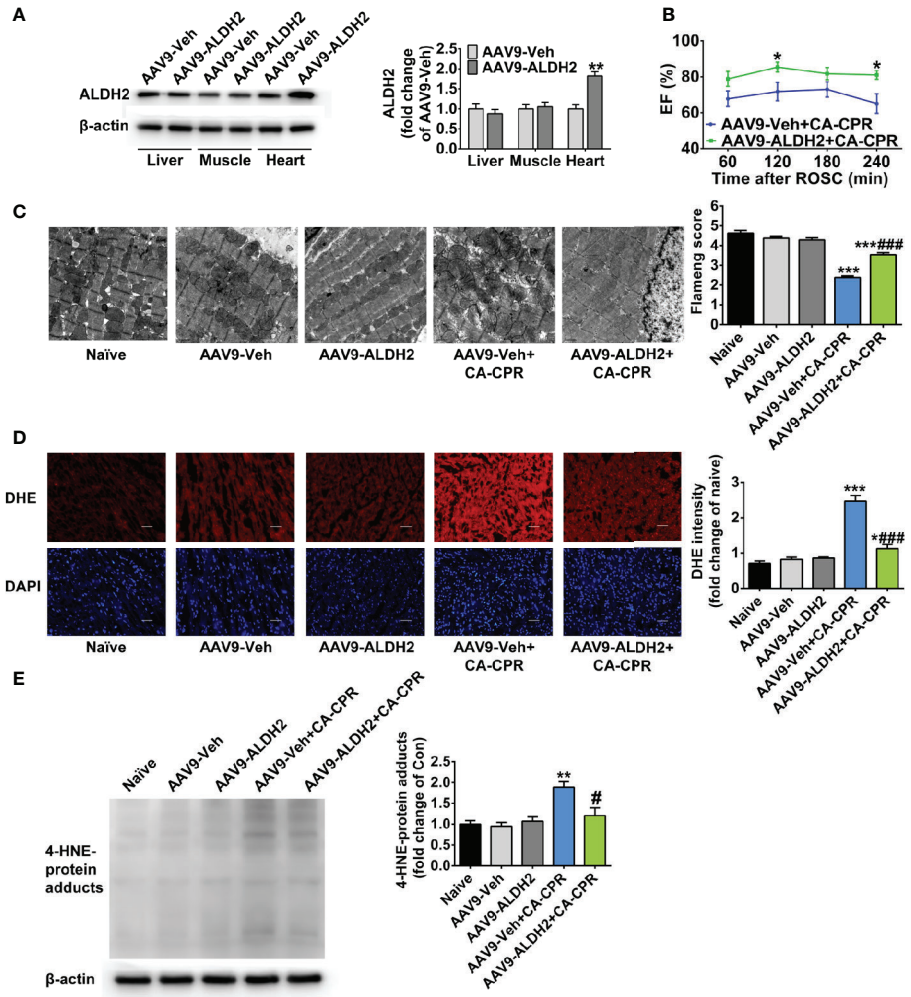

FIGURE 4 | The effect of cardiac overexpression of ALDH2 on post-cardiac arrest myocardial dysfunction and mitochondrial structural damage. **(A)** Representative immunoblots and quantification of ALDH2 expression in the liver, skeletal muscle, and heart tissue (n = 5 animals per group). $^{**}P < 0.01$ versus AAV9-Veh group. **(B)** Left ventricular EF within 4 h after ROSC in AAV9-Veh+CA-CPR and AAV9-ALDH2+CA-CPR group (n = 7–8 animals per group). $^{*}P < 0.05$ versus AAV9-Veh +CA-CPR group. **(C)** Representative photographs and quantification of mitochondrial morphology by TEM examination at 1 h after ROSC (n = 3 animals per group). Scale bar = 1 μm. $^{***}P < 0.001$ versus Naïve group; $^{###}P < 0.001$ versus AAV9-Veh+CA-CPR group. **(D)** Representative photographs of dihydroethidium (DHE) staining at 4 h after ROSC (n = 4 animals per group). Scale bar = 100 μm. $^{*}P < 0.05$, $^{***}P < 0.001$ versus Naïve group; $^{###}P < 0.001$ versus AAV9-Veh+CA-CPR group. **(E)** Representative immunoblots and quantification of 4-HNE-protein adducts at 4 h after ROSC (n = 4 animals per group). Myocardial function between groups was compared by Student's t-test and time-based measurements within each group were compared by repeated-measures ANOVA. The mitochondrial morphology, DHE intensity, and 4-HNE-protein adducts between groups were compared by ANOVA with Tukey's *post hoc* test. Data are presented as mean ± SEM. $^{**}P < 0.01$ versus naïve group; $^{#}P < 0.05$ versus AAV9-Veh+CA-CPR group.

death, and mitochondrial injury in a rat cardiac arrest model. Importantly, ALDH2 restores 72-h myocardial contractile function and substantially improves the survival rate after cardiac arrest. In the mechanistic studies, we reveal that aldehydes, 4-HNE, increased after ischemia/reperfusion injury which promotes succinate accumulation and mitochondrial ROS production. By clearing 4-HNE, ALDH2 suppresses mitochondrial ROS. Therefore, our results clearly suggest the protective role of ALDH2 in post-cardiac arrest myocardial dysfunction through a novel mechanism of suppressing aldehydes-mediating mitochondrial ROS production.

We used the asphyxia-induced cardiac arrest model in this study which is a well-established model to study cardiovascular dysfunction after cardiac arrest and the baseline cardiovascular parameters in this study are consistent with previous reports (Huang et al., 2007; Huang et al., 2008; Oh et al., 2017). We evaluated the effect of ALDH2 on post-cardiac arrest myocardial dysfunction through either upregulation of ALDH2 enzymatic activity or cardiac specific overexpression of ALDH2 in the animal studies. The cardioprotective performance of ALDH2 was established through these complete evaluations. Therefore, the beneficial role of ALDH2 in heart diseases is extended to the

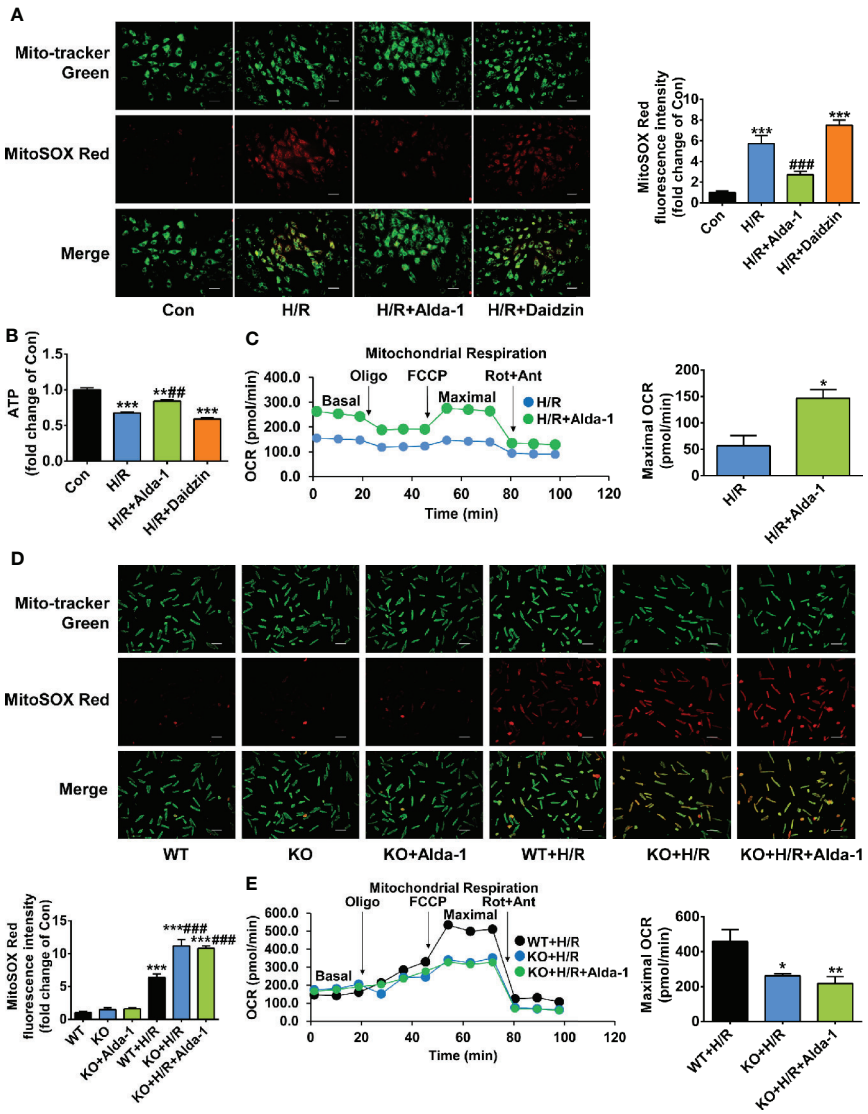

FIGURE 5 | The effect of Alda-1 on mitochondrial ROS levels and mitochondrial energy generation capacity during hypoxia/reoxygenation (H/R). **(A–C)** Data are from H9c2 cells and are presented as mean ± SEM. **(A)** Representative photographs and quantification of mitochondrial ROS levels (n = 3 samples per group). Scale bar = 250 μm. $^{***}P < 0.001$ versus Con group; $^{\#\#\#}P < 0.001$ versus H/R group. **(B)** The levels of cellular ATP (n = 3 samples per group). $^{**}P < 0.01$, $^{***}P < 0.001$ versus Con group; $^{\#\#}P < 0.01$ versus H/R group. **(C)** Mitochondrial respiratory function evaluated by OCR and quantification of maximal OCR (n = 3 samples per group). The maximal OCR was calculated by subtracting non-mitochondrial respiration rate (the final rate after Rot/Ant) from the maximal FCCP rate. $^{*}P < 0.05$ versus H/R group. **(D, E)** Data are from primary cardiomyocytes isolated from adult male WT mice and ALDH2 KO mice, and are presented as mean ± SEM. **(D)** Representative photographs and quantification of mitochondrial ROS levels (n = 3 samples per group). Scale bar = 250 μm. $^{***}P < 0.001$ versus WT group; $^{\#\#\#}P < 0.001$ versus WT+H/R group. **(E)** Mitochondrial respiratory function evaluated by OCR and quantification of maximal OCR (n = 5–6 samples per group). $^{*}P < 0.05$, $^{**}P < 0.01$ versus WT+H/R group. Group comparisons were performed by ANOVA with Tukey's *post hoc* test or Student's t-test.

life-threatening cardiac arrest thus far. In addition, the unifying characteristics of these strategies are that the interventions were applied before the restoration of blood flow to the myocardium in rats subjected to cardiac arrest (Eltzschig and Eckle, 2011; Patil et al., 2015). While pharmacologic interventions before cardiac arrest are impossible due to the unexpected occurrence of cardiac events in routine settings, our results offer an original concept that therapies targeting ALDH2 in treating cardiac arrest could be initiated at an early time window, e.g., during basic life support. It is notable that although the mechanisms by which Alda-1 increases ALDH2 activity have been clarified in the previous literature (Perez-Miller et al., 2010), we first showed the specificity of Alda-1 on ALDH2, especially in mitochondrial protection. Our results suggest it is worth the effort to translate Alda-1 into clinical therapies or to explore new candidates which can enhance ALDH2 activity.

There are several other potentially therapeutic approaches that have been shown to be effective in improving post-cardiac

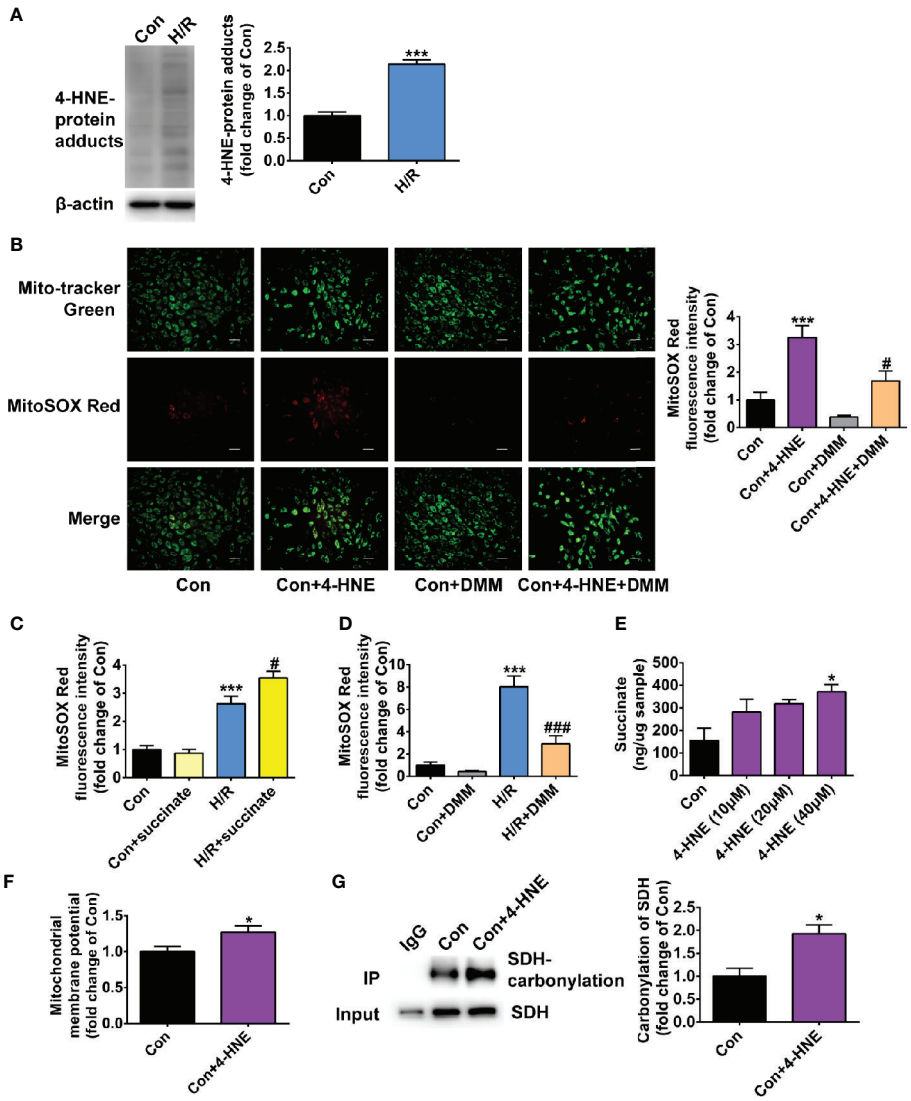

FIGURE 6 | The effect of 4-HNE on mitochondrial ROS levels, succinate accumulation, mitochondrial membrane potential and SDH carbonylation. **(A)** Representative immunoblots and quantification of 4-HNE-protein adducts under hypoxia/reoxygenation (H/R) (n = 3 samples per group). **(B)** Representative photographs and quantification of mitochondrial ROS levels under the treatment of 4-HNE (40 μM) and 4-HNE (40 μM) +dimethyl malonate (DMM) (n = 3 samples per group). **(C, D)** The mitochondrial ROS levels after the addition of succinate or dimethyl malonate (DMM) during hypoxia/reoxygenation (H/R) (n = 4 samples per group). **(E)** The levels of succinate under the treatment of 4-HNE (n = 3 samples per group). **(F)** The quantification of mitochondrial membrane potential under the treatment of 4-HNE (40 μM) (n = 3 samples per group). **(G)** Representative immunoblots and quantification of SDH carbonylation under the treatment of 4-HNE (40 μM) (n = 3 samples per group). Group comparisons were performed by ANOVA with Tukey's *post hoc* test or Student's t-test. Data are presented as mean ± SEM. $^{*}P < 0.05$, $^{***}P < 0.001$ versus Con group; $^{\#}P < 0.05$ versus Con +4-HNE group or H/R group; $^{\#\#\#}P < 0.001$ versus H/R group.

arrest myocardial dysfunction. Pharmacological inhibition of mitochondrial permeability transition pore with cyclosporine A at the onset of resuscitation or after ROSC preserves myocardial function and attenuates post-cardiac arrest myocardial injury in the rabbit and rat models of cardiac arrest (Cour et al., 2011; Knapp et al., 2015). Natural hibernation signaling central mediator pentazocine, a δ-opioid receptor agonist, improves cardiac index after ROSC, which is returned to ~95% of baseline in a rat cardiac arrest model (Fang et al., 2006). In this study, we provide a new target for attenuating post-cardiac arrest myocardial dysfunction, which exhibits similar effects with previous studies. This evidence is all from animal studies; however, whether anyone could protect human victims of cardiac arrest requires further investigation.

We observed 4-HNE-overload and mitochondrial injury in heart after cardiac arrest. Aldehydes were found in heart and brain after cardiac arrest as reactive stress markers, however how aldehydes lead to cardiac injury and how to clear them were still

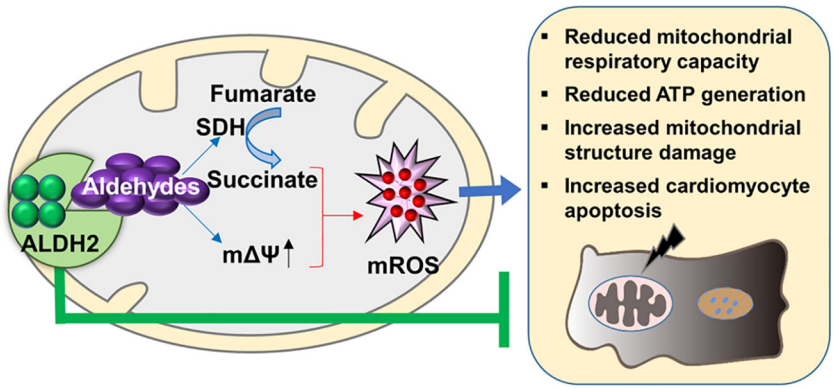

FIGURE 7 | The proposed molecular mechanisms of the protective effect of ALDH2 on post-cardiac arrest myocardial dysfunction. The aldehydes, e.g. 4-HNE, which are accumulated during ischemia/reperfusion result in mitochondrial ROS (mROS) burst. The latter triggers a series of orchestrated events including reduced mitochondrial respiratory capacity, reduced ATP generation, increased mitochondrial structure damage, and cardiomyocyte death, thereby contributing to myocardial dysfunction. Evidence from this study show that targeting ALDH2 would provide an important approach for treating post-cardiac arrest myocardial dysfunction through inhibiting mitochondrial ROS production.

indefinite (Hayashida et al., 2012; Liu et al., 2016). Mitochondrial damage in heart was observed from 1 min to 1 h after ROSC (Tsai et al., 2011; Huang et al., 2015). We found that mitochondrial ROS was involved in the mitochondrial dysfunction, impaired mitochondrial morphology, and cardiomyocytes apoptosis. Additionally, mitochondrial ROS were able to drive both acute emergent events, such as electrical instability responsible for sudden cardiac arrest, and chronic heart failure remodeling (Dey et al., 2018). However, protective treatments specifically targeted to mitochondria are still under study (Murphy, 2016; Dey et al., 2018). In this study, we found that ALDH2 could reduce mitochondrial ROS, therefore protecting mitochondria and heart after cardiac arrest.

Additionally, we provided a new understanding about the mechanisms of mitochondrial ROS production after cardiac arrest. In the present, there has no agreed conclusion about how mitochondrial ROS are produced. Some people believed that electron "leakage" from damaged mitochondrial electron transport chain during ischemia/reperfusion constituted a major source of mitochondrial ROS (Han et al., 2008). Recently, it was reported that there was a common pathway, that succinate oxidation and a high mitochondrial membrane potential were two essential requirements for mitochondrial ROS production (Chouchani et al., 2014; Chouchani et al., 2016; Mills et al., 2016). In this study, we found that 4-HNE mediate mitochondrial ROS production and amplify the ROS-induced ROS systems. 4-HNE is one of the lipid peroxidation-derived aldehydes which has been most intensively studied. We observed the 4-HNE could induce the carbonylation of SDH which is a critical enzyme responsible for succinate generation. Additionally, 4-HNE promoted succinate accumulation and led to increase in mitochondrial membrane potential and mitochondrial ROS levels. These findings provide novel evidence for the role of aldehydes in mitochondrial ROS production.

Several limitations should be considered. Firstly, although we identify the significant improvement of ALDH2 on post-cardiac arrest myocardial dysfunction and 72-h survival rate in a rat cardiac arrest model, we do not assess the long-term outcome. Secondly, we are unable to determine definitively whether the protective effect of ALDH2 is through suppressing mitochondrial ROS production during cardiac arrest due to the technique challenge for detecting mitochondrial ROS in living organisms as accurately as in cells. Thirdly, we did not test the dose-response study or more therapeutic windows within which enhancing ALD2 activity is beneficial after cardiac arrest. Thus, further investigations are needed to answer these questions.

In summary, we demonstrate that enhanced activity or expression of ALDH2 reduces cardiomyocyte death and mitochondrial injury, attenuates post-cardiac arrest myocardial dysfunction, and improves 72-h survival rate in a rat cardiac arrest model. Our results also imply that the protective role of ALDH2 may be through suppressing 4-HNE-mediating mitochondrial ROS production. These findings suggest therapeutic targeting ALDH2 would provide an important approach for treating post-cardiac arrest myocardial dysfunction and warrants clinical validation.

DATA AVAILABILITY STATEMENT

The datasets generated for this study are available on request to the corresponding authors.

ETHICS STATEMENT

The animal study was reviewed and approved by the Institutional Animal Care and Use Committee of Shandong University.

AUTHOR CONTRIBUTIONS

YCh, YCa, JW, FX, RZ, BL, WW, SWe, QY, MX, and SWa designed research. RZ, BL, XF, WW, TX, WZ, LG, XY, BZ, CZ, SZ, and KY performed research. RZ, JW, BL, WW, and XF analyzed data. JW, YCh, YCa, RZ, BL, SWe, and QY wrote and revised the paper.

FUNDING

This study was supported by the National Key Research and Development Program of China (2017YFC0908700, 2017YFC0908703), National Natural Science Foundation of China (81772036, 81671952, 81873950, 81873953, 81570401, 81571934), National Science and Technology Fundamental Resources Investigation Project (2018FY100600, 2018FY100602), Taishan Pandeng Scholar Program of Shandong Province (tspd20181220), Taishan Young Scholar Program of Shandong Province (tsqn20161065, tsqn201812129), Key Research and Development Program of Shandong Province (2018GSF118003), the Fundamental Research Funds of Shandong University (2018JC011), Science Foundation of Qilu Hospital of Shandong University (2015QLQN13), and the Natural Science Foundation of Shandong Province (ZR2014HP035).

SUPPLEMENTARY MATERIAL

The Supplementary Material for this article can be found online at: https://www.frontiersin.org/articles/10.3389/fphar.2020.00373/full#supplementary-material

REFERENCES

Ackers-Johnson, M., Li, P. Y., Holmes, A. P., O'Brien, S. M., Pavlovic, D., and Foo, R. S. (2016). A Simplified, Langendorff-Free Method for Concomitant Isolation of Viable Cardiac Myocytes and Nonmyocytes From the Adult Mouse Heart. *Circ. Res.* 119 (8), 909–920. doi: 10.1161/CIRCRESAHA.116.309202

Chen, C. H., Ferreira, J. C., Gross, E. R., and Mochly-Rosen, D. (2014). Targeting aldehyde dehydrogenase 2: new therapeutic opportunities. *Physiol. Rev.* 94 (1), 1–34. doi: 10.1152/physrev.00017.2013

Chouchani, E. T., Pell, V. R., Gaude, E., Aksentijevic, D., Sundier, S. Y., Robb, E. L., et al. (2014). Ischaemic accumulation of succinate controls reperfusion injury through mitochondrial ROS. *Nature.* 515 (7527), 431–435. doi: 10.1038/nature13909

Chouchani, E. T., Pell, V. R., James, A. M., Work, L. M., Saeb-Parsy, K., Frezza, C., et al. (2016). A Unifying Mechanism for Mitochondrial Superoxide Production during Ischemia-Reperfusion Injury. *Cell Metab.* 23 (2), 254–263. doi: 10.1016/j.cmet.2015.12.009

Cour, M., Loufouat, J., Paillard, M., Augeul, L., Goudable, J., Ovize, M., et al. (2011). Inhibition of mitochondrial permeability transition to prevent the post-cardiac arrest syndrome: a pre-clinical study. *Eur. Heart J.* 32 (2), 226–235. doi: 10.1093/eurheartj/ehq112

Dey, S., DeMazumder, D., Sidor, A., Foster, D. B., and O'Rourke, B. (2018). Mitochondrial ROS Drive Sudden Cardiac Death and Chronic Proteome Remodeling in Heart Failure. *Circ. Res.* 123 (3), 356–371. doi: 10.1161/CIRCRESAHA.118.312708

Eltzschig, H. K., and Eckle, T. (2011). Ischemia and reperfusion–from mechanism to translation. *Nat. Med.* 17 (11), 1391–1401. doi: 10.1038/nm.2507

Fang, X., Tang, W., Sun, S., Huang, L., Huang, Z., and Weil, M. H. (2006). Mechanism by which activation of delta-opioid receptor reduces the severity of postresuscitation myocardial dysfunction. *Crit. Care Med.* 34 (10), 2607–2612. doi: 10.1097/01.CCM.0000228916.81470.E1

Flameng, W., Borgers, M., Daenen, W., and Stalpaert, G. (1980). Ultrastructural and cytochemical correlates of myocardial protection by cardiac hypothermia in man. *J. Thorac. Cardiovasc. Surg.* 79 (3), 413–424. doi: doi: 10.1016/S0022-5223(19)37950-4

Han, F., Da, T., Riobo, N. A., and Becker, L. B. (2008). Early mitochondrial dysfunction in electron transfer activity and reactive oxygen species generation after cardiac arrest. *Crit. Care Med.* 36 (11 Suppl), S447–S453. doi: doi: 10.1097/CCM.0b013e31818a8a51

Hawong, H. Y., Patterson, J. R., Winner, B. M., Goudreau, J. L., and Lookingland, K. J. (2015). Comparison of the structure, function and autophagic maintenance of mitochondria in nigrostriatal and tuberoinfundibular dopamine neurons. *Brain Res.* 1622, 240–251. doi: 10.1016/j.brainres.2015.06.030

Hayashi, M., Shimizu, W., and Albert, C. M. (2015). The spectrum of epidemiology underlying sudden cardiac death. *Circ. Res.* 116 (12), 1887–1906. doi: 10.1161/CIRCRESAHA.116.304521

Hayashida, K., Sano, M., Kamimura, N., Yokota, T., Suzuki, M., Maekawa, Y., et al. (2012). H(2) gas improves functional outcome after cardiac arrest to an extent comparable to therapeutic hypothermia in a rat model. *J. Am. Heart Assoc.* 1 (5), e003459. doi: 10.1161/JAHA.112.003459

Hazinski, M. F., Nolan, J. P., Aickin, R., Bhanji, F., Billi, J. E., Callaway, C. W., et al. (2015). Part 1: Executive Summary: 2015 International Consensus on Cardiopulmonary Resuscitation and Emergency Cardiovascular Care Science With Treatment Recommendations. *Circulation.* 132 (16 Suppl 1), S2–39. doi: 10.1161/CIR.0000000000000270

Huang, C. H., Hsu, C. Y., Chen, H. W., Tsai, M. S., Cheng, H. J., Chang, C. H., et al. (2007). Erythropoietin improves the postresuscitation myocardial dysfunction and survival in the asphyxia-induced cardiac arrest model. *Shock.* 28 (1), 53–58. doi: 10.1097/shk.0b013e31802f0218

Huang, C. H., Hsu, C. Y., Tsai, M. S., Wang, T. D., Chang, W. T., and Chen, W. J. (2008). Cardioprotective effects of erythropoietin on postresuscitation myocardial dysfunction in appropriate therapeutic windows. *Crit. Care Med.* 36 (11 Suppl), S467–S473. doi: doi: 10.1097/CCM.0b013e31818a8cec

Huang, C. H., Tsai, M. S., Hsu, C. Y., Su, Y. J., Wang, T. D., Chang, W. T., et al. (2011). Post-cardiac arrest myocardial dysfunction is improved with cyclosporine treatment at onset of resuscitation but not in the reperfusion phase. *Resuscitation.* 82 (Suppl 2), S41–S47. doi: 10.1016/S0300-9572(11)70150-2

Huang, C. H., Tsai, M. S., Chiang, C. Y., Su, Y. J., Wang, T. D., Chang, W. T., et al. (2015). Activation of mitochondrial STAT-3 and reduced mitochondria damage during hypothermia treatment for post-cardiac arrest myocardial dysfunction. *Basic Res. Cardiol.* 110 (6), 59. doi: 10.1007/s00395-015-0516-3

Ikeda, K., Liu, X., Kida, K., Marutani, E., Hirai, S., Sakaguchi, M., et al. (2016). Thiamine as a neuroprotective agent after cardiac arrest. *Resuscitation.* 105, 138–144. doi: 10.1016/j.resuscitation.2016.04.024

Ji, W., Wei, S., Hao, P., Xing, J., Yuan, Q., Wang, J., et al. (2016). Aldehyde Dehydrogenase 2 Has Cardioprotective Effects on Myocardial Ischaemia/Reperfusion Injury via Suppressing Mitophagy. *Front. Pharmacol.* 7, 1–15. 101. doi: 10.3389/fphar.2016.00101

Karlstaedt, A., Zhang, X., Vitrac, H., Harmancey, R., Vasquez, H., Wang, J. H., et al. (2016). Oncometabolite d-2-hydroxyglutarate impairs alpha-ketoglutarate dehydrogenase and contractile function in rodent heart. *Proc. Natl. Acad. Sci. U. S. A.* 113 (37), 10436–10441. doi: 10.1073/pnas.1601650113

Kern, K. B., Hilwig, R. W., Rhee, K. H., and Berg, R. A. (1996). Myocardial dysfunction after resuscitation from cardiac arrest: an example of global myocardial stunning. *J. Am. Coll. Cardiol.* 28 (1), 232–240. doi: doi: 10.1016/0735-1097(96)00130-1

Kim, T., Paine, M. G., Meng, H., Xiaodan, R., Cohen, J., Jinka, T., et al. (2016). Combined intra- and post-cardiac arrest hypothermic-targeted temperature management in a rat model of asphyxial cardiac arrest improves survival and neurologic outcome compared to either strategy alone. *Resuscitation.* 107, 94–101. doi: 10.1016/j.resuscitation.2016.07.232

Knapp, J., Roewer, J., Bruckner, T., Bottiger, B. W., and Popp, E. (2015). Evaluation of cyclosporine a as a cardio- and neuroprotective agent after cardiopulmonary resuscitation in a rat model. *Shock.* 43 (6), 576–581. doi: 10.1097/SHK.0000000000000357

Li, C., Sun, W., Gu, C., Yang, Z., Quan, N., Yang, J., et al. (2018). Targeting ALDH2 for Therapeutic Interventions in Chronic Pain-Related Myocardial Ischemic Susceptibility. *Theranostics.* 8 (4), 1027–1041. doi: 10.7150/thno.22414

Liu, J., Wang, Y., Zhuang, Q., Chen, M., Wang, Y., Hou, L., et al. (2016). Protective effects of cyclosporine A and hypothermia on neuronal mitochondria in a rat asphyxial cardiac arrest model. *Am. J. Emerg. Med.* 34 (6), 1080–1085. doi: 10.1016/j.ajem.2016.02.066

Liu, B., Wang, J., Li, M., Yuan, Q., Xue, M., Xu, F., et al. (2017). Inhibition of ALDH2 by O-GlcNAcylation contributes to the hyperglycemic exacerbation of myocardial ischemia/reperfusion injury. *Oncotarget.* 8 (12), 19413–19426. doi: 10.18632/oncotarget.14297

Liu, W., Zhai, X., Wang, W., Zheng, B., Zhang, Z., Fan, X., et al. (2018). Aldehyde dehydrogenase 2 activation ameliorates cyclophosphamide-induced acute cardiotoxicity via detoxification of toxic aldehydes and suppression of cardiac cell death. *J. Mol. Cell Cardiol.* 121, 134–144. doi: 10.1016/j.yjmcc.2018.07.006

Matsuura, T. R., Bartos, J. A., Tsangaris, A., Shekar, K. C., Olson, M. D., Riess, M. L., et al. (2017). Early Effects of Prolonged Cardiac Arrest and Ischemic Postconditioning during Cardiopulmonary Resuscitation on Cardiac and Brain Mitochondrial Function in Pigs. *Resuscitation.* 116, 8–15. doi: 10.1016/j.resuscitation.2017.03.033

Mills, E. L., Kelly, B., Logan, A., Costa, A. S. H., Varma, M., Bryant, C. E., et al. (2016). Succinate Dehydrogenase Supports Metabolic Repurposing of Mitochondria to Drive Inflammatory Macrophages. *Cell.* 167 (2), 457–470 e413. doi: 10.1016/j.cell.2016.08.064

Murphy, E., and Steenbergen, C. (2008). Mechanisms underlying acute protection from cardiac ischemia-reperfusion injury. *Physiol. Rev.* 88 (2), 581–609. doi: 10.1152/physrev.00024.2007

Murphy, M. P. (2016). Understanding and preventing mitochondrial oxidative damage. *Biochem. Soc. Trans.* 44 (5), 1219–1226. doi: 10.1042/BST20160108

Neumar, R. W., Nolan, J. P., Adrie, C., Aibiki, M., Berg, R. A., Bottiger, B. W., et al. (2008). Post-cardiac arrest syndrome: epidemiology, pathophysiology, treatment, and prognostication. A consensus statement from the International Liaison Committee on Resuscitation (American Heart Association, Australian and New Zealand Council on Resuscitation, European Resuscitation Council, Heart and Stroke Foundation of Canada, InterAmerican Heart Foundation, Resuscitation Council of Asia, and the Resuscitation Council of Southern Africa); the American Heart Association Emergency Cardiovascular Care Committee; the Council on Cardiovascular Surgery and Anesthesia; the Council on Cardiopulmonary, Perioperative, and Critical Care; the Council on Clinical Cardiology; and the Stroke Council. *Circulation.* 118 (23), 2452–2483. doi: 10.1161/CIRCULATIONAHA.108.190652

Oh, J. S., Tulasi, J., Xiaodan, R., Stacey, W. C., and Neumar, R. W. (2017). Valproic Acid Combined With Postcardiac Arrest Hypothermic-Targeted Temperature Management Prevents Delayed Seizures and Improves Survival in a Rat Cardiac Arrest Model. *Crit. Care Med.* 45 (11), e1149–e1156. doi: 10.1097/CCM.0000000000002690

Pang, J., Fuller, N. D., Hu, N., Barton, L. A., Henion, J. M., Guo, R., et al. (2016). Alcohol Dehydrogenase Protects against Endoplasmic Reticulum Stress-Induced Myocardial Contractile Dysfunction via Attenuation of Oxidative Stress and Autophagy: Role of PTEN-Akt-mTOR Signaling. *PloS One* 11 (1), e0147322. doi: 10.1371/journal.pone.0147322

Patil, K. D., Halperin, H. R., and Becker, L. B. (2015). Cardiac arrest: resuscitation and reperfusion. *Circ. Res.* 116 (12), 2041–2049. doi: 10.1161/CIRCRESAHA.116.304495

Penna, C., Perrelli, M. G., and Pagliaro, P. (2013). Mitochondrial pathways, permeability transition pore, and redox signaling in cardioprotection: therapeutic implications. *Antioxid. Redox Signal.* 18 (5), 556–599. doi: 10.1089/ars.2011.4459

Perez-Miller, S., Younus, H., Vanam, R., Chen, C. H., Mochly-Rosen, D., and Hurley, T. D. (2010). Alda-1 is an agonist and chemical chaperone for the common human aldehyde dehydrogenase 2 variant. *Nat. Struct. Mol. Biol.* 17 (2), 159–164. doi: 10.1038/nsmb.1737

Roberge, S., Roussel, J., Andersson, D. C., Meli, A. C., Vidal, B., Blandel, F., et al. (2014). TNF-alpha-mediated caspase-8 activation induces ROS production and TRPM2 activation in adult ventricular myocytes. *Cardiovasc. Res.* 103 (1), 90–99. doi: 10.1093/cvr/cvu112

Roede, J. R., and Jones, D. P. (2010). Reactive species and mitochondrial dysfunction: mechanistic significance of 4-hydroxynonenal. *Environ. Mol. Mutagen.* 51 (5), 380–390. doi: 10.1002/em.20553

Stub, D., Bernard, S., Duffy, S. J., and Kaye, D. M. (2011). Post cardiac arrest syndrome: a review of therapeutic strategies. *Circulation.* 123 (13), 1428–1435. doi: 10.1161/CIRCULATIONAHA.110.988725

Tan, Y., Li, X., Prabhu, S. D., Brittian, K. R., Chen, Q., Yin, X., et al. (2012). Angiotensin II plays a critical role in alcohol-induced cardiac nitrative damage, cell death, remodeling, and cardiomyopathy in a protein kinase C/nicotinamide adenine dinucleotide phosphate oxidase-dependent manner. *J. Am. Coll. Cardiol.* 59 (16), 1477–1486. doi: 10.1016/j.jacc.2011.12.034

Tsai, M. S., Huang, C. H., Tsai, C. Y., Chen, H. W., Lee, H. C., Cheng, H. J., et al. (2011). Ascorbic acid mitigates the myocardial injury after cardiac arrest and electrical shock. *Intensive Care Med.* 37 (12), 2033–2040. doi: 10.1007/s00134-011-2362-6

Tsushima, K., Bugger, H., Wende, A. R., Soto, J., Jenson, G. A., Tor, A. R., et al. (2018). Mitochondrial Reactive Oxygen Species in Lipotoxic Hearts Induce Post-Translational Modifications of AKAP121, DRP1, and OPA1 That Promote Mitochondrial Fission. *Circ. Res.* 122 (1), 58–73. doi: 10.1161/CIRCRESAHA.117.311307

Wang, J., Wang, H., Hao, P., Xue, L., Wei, S., Zhang, Y., et al. (2011). Inhibition of aldehyde dehydrogenase 2 by oxidative stress is associated with cardiac dysfunction in diabetic rats. *Mol. Med.* 17 (3-4), 172–179. doi: 10.2119/molmed.2010.00114

Wang, P., Jia, L., Chen, B., Zhang, L., Liu, J., Long, J., et al. (2016). Hydrogen Inhalation is Superior to Mild Hypothermia in Improving Cardiac Function and Neurological Outcome in an Asphyxial Cardiac Arrest Model of Rats. *Shock.* 46 (3), 312–318. doi: 10.1097/SHK.0000000000000585

Wu, B., Yu, L., Wang, Y., Wang, H., Li, C., Yin, Y., et al. (2016). Aldehyde dehydrogenase 2 activation in aged heart improves the autophagy by reducing the carbonyl modification on SIRT1. *Oncotarget.* 7 (3), 2175–2188. doi: 10.18632/oncotarget.6814

Zhang, T., Zhang, Y., Cui, M., Jin, L., Wang, Y., Lv, F., et al. (2016). CaMKII is a RIP3 substrate mediating ischemia- and oxidative stress-induced myocardial necroptosis. *Nat. Med.* 22 (2), 175–182. doi: 10.1038/nm.4017

Zweier, J. L., Flaherty, J. T., and Weisfeldt, M. L. (1987). Direct measurement of free radical generation following reperfusion of ischemic myocardium. *Proc. Natl. Acad. Sci. U. S. A.* 84 (5), 1404–1407. doi: doi: 10.1073/pnas.84.5.1404

Conflict of Interest: The authors declare that the research was conducted in the absence of any commercial or financial relationships that could be construed as a potential conflict of interest.

frontiers in Pharmacology

ORIGINAL RESEARCH
published: 17 April 2020
doi: 10.3389/fphar.2020.00392

Bazedoxifene Attenuates Abdominal Aortic Aneurysm Formation *via* Downregulation of Interleukin-6/Glycoprotein 130/Signal Transducer and Activator of Transcription 3 Signaling Pathway in Apolipoprotein E–Knockout Mice

Dan Yan[1,2†], Haiyan Ma[1,3†], Wei Shi[1], Pengcheng Luo[1], Tianshu Liu[1], Junyi Guo[1], Maocai Zhai[1], Jingwen Tao[1], Shengqi Huo[1], Chenglong Li[4], Jiayuh Lin[5], Sheng Li[1], Jiagao Lv[1], Cuntai Zhang[2] and Li Lin[1*]*

[1] Division of Cardiology, Department of Internal Medicine, Tongji Hospital, Tongji Medical College, Huazhong University of Science and Technology, Wuhan, China, [2] Department of Geriatrics, Tongji Hospital, Tongji Medical College, Huazhong University of Science and Technology, Wuhan, China, [3] Division of Cardiology, Department of Internal Medicine, First People's Hospital of Shangqiu, Shangqiu, China, [4] Department of Medicinal Chemistry, College of Pharmacy, University of Florida, Gainesville, FL, United States, [5] Department of Biochemistry and Molecular Biology, University of Maryland School of Medicine, Baltimore, MD, United States

Abdominal aortic aneurysm (AAA) is a chronic inflammatory disease characterized by aortic dilatation and predominantly affects an elderly population. Accumulating evidence suggests that Interleukin-6 (IL-6) and the signal transducer and activator of transcription 3 (STAT3) play an important role in formation of AAAs. However, it remains unclear whether Bazedoxifene (BAZ) could suppress the activation of IL-6/GP130/STAT3 in vascular cells and the formation of AAA. Here we explored the effect of BAZ on AngII-stimulated AAA formation. ApoE$^{-/-}$ mice infused with AngII for 28 days using osmotic minipumps were treated with placebo or 5mg/kg BAZ. In our results most of the AngII-induced mice developed AAA with exacerbated inflammation, degradation of elastin fibers, STAT3 phosphorylation, and increased expression of matrix metalloproteinases (MMPs). These effects were markedly attenuated by BAZ. Furthermore, BAZ suppressed the stimuli-induced (IL-6 or AngII) expression of P-STAT3, MMP2 and MMP9 in vascular smooth muscle cells (VSMCs). BAZ inhibited wound healing, colony formation and suppressed STAT3 nuclear translocation *in vitro*. In conclusion, these results indicated that BAZ downregulated IL-6/GP130/STAT3 signaling and interfered with AAA formation induced by AngII in ApoE$^{-/-}$ mice, which indicates a novel potential strategy for the prevention and therapy of AAA.

Keywords: abdominal aortic aneurysm, inflammation, bazedoxifene, IL-6, STAT3

OPEN ACCESS

Edited by:
Cheng Xue Helena Qin,
Baker Heart and Diabetes Institute, Australia

Reviewed by:
Neil Macritchie,
University of Glasgow, United Kingdom
InKyeom Kim,
Kyungpook National University, South Korea
De-Pei Liu,
Peking Union Medical College Hospital (CAMS), China

***Correspondence:**
Cuntai Zhang
ctzhang@tjh.tjmu.edu.cn;
ctzhang0425@163.com
Li Lin
linlee271227@163.com;
linli@tjh.tjmu.edu.cn

†These authors have contributed equally to this work

Specialty section:
This article was submitted to Cardiovascular and Smooth Muscle Pharmacology, a section of the journal Frontiers in Pharmacology

Received: *08 December 2019*
Accepted: *16 March 2020*
Published: *17 April 2020*

Citation:
Yan D, Ma H, Shi W, Luo P, Liu T, Guo J, Zhai M, Tao J, Huo S, Li C, Lin J, Li S, Lv J, Zhang C and Lin L (2020) Bazedoxifene Attenuates Abdominal Aortic Aneurysm Formation via Downregulation of Interleukin-6/Glycoprotein 130/Signal Transducer and Activator of Transcription 3 Signaling Pathway in Apolipoprotein E–Knockout Mice. Front. Pharmacol. 11:392. doi: 10.3389/fphar.2020.00392

INTRODUCTION

Abdominal aortic aneurysm (AAA) is a potentially life-threatening degenerative vascular disease affecting 6% to 9% of men over the age of 65 years, with an annual death toll of more than 15,000 (Baxter et al., 2008; Wang et al., 2013; Argyriou et al., 2018). Although in most patients no symptoms manifest, AAA progresses over time and eventually ruptures, leading to a high mortality rate (Hoornweg et al., 2008; Ohno et al., 2018). Currently, there is no pharmaceutical strategy that diminishes aneurysm progression during the early stages. Surgery and endovascular repair with stents are the main treatments for AAA (Wang et al., 2013; Ijaz et al., 2016). There is an existing gap in the study of the occurrence and development of AAA, suggesting that exploring potential mechanisms could play a critical role in the prevention and treatment of abdominal aortic aneurysm in clinical work.

The formation of AAA is a complex process, involving remodeling of the extracellular matrix (ECM), chronic inflammation and the degradation of elastin fibers regulated by matrix metalloproteinases (Nordon et al., 2011). A number of reports have demonstrated an increased expression of matrix metalloproteinases (MMPs) in AAA and genetic variants have been proposed to be associated with AAA (Dilme et al., 2014). MMPs, particularly MMP2 and MMP9, degrade the extracellular matrix and elastic fibers leading to the development and progression of AAA (Dilme et al., 2014; Ghosh et al., 2015).

Recently, aortic wall inflammation, which is considered to be the most significant causative factor contributing to the degradation and remodeling of the ECM, has been highlighted in the development and progression of AAA (Ohno et al., 2018). Interleukin-6 (IL-6), one of the proinflammatory cytokines, exerts its effect *via* the IL-6 receptors (IL-6R) and induces homodimerization with its co-receptor gp130, resulting in the phosphorylation of the transcription factor STAT3 (Ferreira et al., 2013). It has been reported that IL-6 signaling – including the expression of IL-6 and phosphorylation of STAT3 (P-STAT3) – is over-activated in AAA lesions (Liao et al., 2012). Genetic studies have shown an association between genetic variation in IL-6R and the risk of developing AAA (Harrison et al., 2013), indicating that targeting IL-6R may be a useful strategy in combatting AAA. These studies suggest that the IL-6/GP130/STAT3 signaling pathway may play an important role in the formation and development of AAA. Inhibition of the IL-6/GP130 interface, and hence influencing the phosphorylation of STAT3, may be a new therapeutic option for AAA.

Bazedoxifene (BAZ) has been approved by the FDA (Food and Drug Administration) for the prevention and treatment of postmenopausal osteoporosis. In our previous study, using multiple ligand simultaneous docking (MLSD) and drug repositioning approaches, we identified that BAZ exhibited a new function targeting the IL-6/GP130 protein-protein interface (Li et al., 2014). BAZ could suppress tumor growth and induce apoptosis in human cancer cells and in a tumor xenograft mice model (Li et al., 2014; Chen et al., 2018). Whether BAZ is effective at suppressing IL-6/GP130/STAT3 signaling or inhibiting the formation of AAA is still unclear. Herein, we reported the suppressive effect of BAZ on the formation and development of AAA. We found that BAZ attenuated the development and severity of AngII-stimulated AAA in $ApoE^{-/-}$ mice and that BAZ could suppress the phosphorylation of STAT3 and the expression of MMP2 and MMP9. Moreover, a similar effect of BAZ was shown in mouse vascular smooth muscle cells (VSMCs). These results may indicate that BAZ exhibits inhibition against the IL-6/GP130/STAT3 signaling pathway and may be promising for use in the prevention or treatment of AAA patients in future.

MATERIALS AND METHODS

Animal Experiment

All animal experiments were carried out in accordance with National Institute of Health guidelines and approved by the Experimental Animal Research Committee of Tongji Medical College, Huazhong University of Science and Technology. Mice were anesthetized using 2% isoflurane mixed with 0.5-1.0 L/min 100% O_2. We used a classic AAA model in which a continuous AngII infusion in 8-week-old male apolipoprotein-E-deficient ($ApoE^{-/-}$) mice induces AAA formation after implantation by subcutaneously implanted mini-osmotic pumps (Model 2004, Alzet, CA, USA) (Vorkapic et al., 2016). All $ApoE^{-/-}$mice were randomly divided into three groups: control (n=12), AngII (n=13), BAZ (n=12). AngII powder (Sigma) was solubilized in 0.9% sodium chloride and loaded into mini-osmotic pumps for systemic hormone delivery (1000 ng/kg/min infusion rate and 28-day duration) following subcutaneous implantation in the dorsum of mice. $ApoE^{-/-}$ mice in the control group were infused with 0.9% NaCl. The AngII-infused mice were then randomized into two groups (both were fed a normal diet), one group was treated with a vehicle control and the other was given 5mg/kg BAZ (purchased from Cayman Chemical Company, Ann Arbor, Michigan, USA) every day during Ang II infusion. BAZ was dissolved in a PBS solution containing 20% hydroxypropyl-beta-cyclodextrin (HPBCD) and 5% DMSO. After 28 days, aorta tissues were harvested from euthanized mice.

Histology

The aortas were embedded in paraffin and cut into 5–10μm cross-sections, then stained with hematoxylin and eosin (H&E), or elastica van Gieson (EVG) staining for elastin.

Immunohistochemistry

The tissue sections were deparaffinized and dehydrated by fractionation using xylene and ethanol. The sections were incubated for 1h at room temperature or overnight at 4°C with the following primary antibodies: IL-6 (anti-rabbit, D220828, Sangon, Shanghai, China), P-STAT3 (Tyrosine 705, #9145, CST), MMP2 (sc-8835, Santa Cruz), MMP9 (sc-6841, Santa Cruz), α-smooth muscle actin (α-SMA, Clone 1A4, DAKO) and CD68 (#76437, CST). After washing with PBS, tissue sections were incubated with biotinylated secondary antibody for 90 min at room temperature. Then an avidin-biotin peroxidase complex was added for another 30 minutes. Then diaminobenzidine was

added as a substrate that reacts with immune cells to make stain and then the tissue sections counterstained with hematoxylin.

Cell Culture and Treatment

The mouse vascular smooth muscle cell (VSMC) line was purchased from American Type Culture Collection. All cells were cultured in a humidified 37°C incubator grown with 5% CO_2, using DMEM (Dulbecco's modified Eagle's medium) containing 10% fetal bovine serum (FBS, Gibico) and 1% penicillin/streptomycin (Sigma).

Western Blot Analysis

After pretreatment with different concentrations of BAZ (10, 15, 20 μmol/L) or DMSO for 2h, VSMCs were induced by IL-6 or AngII for 30 minutes or 12h before collection. The collected cells lysed in a modified RIPA buffer containing phosphatase inhibitors and protease inhibitors. The protein concentration was detected by a BCA protein assay kit. Proteins in each sample were subjected to SDS-PAGE, then the following primary antibodies were used for western blotting: MMP2 (sc-8835, Santa Cruz), P-STAT3 (Tyrosine 705, #9131, CST), MMP9 (sc-6841, Santa Cruz), and GAPDH (#2118, CST). Blots were developed with horseradish peroxidase-conjugated conjugated secondary antibodies and protein detection was performed using an enhanced chemiluminescence (ECL) western blot kit according to the manufacturer's instructions.

ELISA

Vascular smooth muscle cell lines were seeded in 48-well plates (3×10^4 cells/well) and starved for 10h. Cells were treated with AngII (10^{-7}mol/L) or DMSO for 0h, 2h, 4h, 8h, 12h or 24h. Then cell culture medium was collected for ELISA (Rat intact PTH ELISA Kit, Elabscience, Wuhan, China).

Colony Formation Assay

VSMCs were plated with 1×10^3 cells/well in 6-well plates then BAZ (15, 20 μM) or DMSO was added for 4 h. After treatment 5000 live cells were reseeded on 10 cm plates with no-drug medium and incubated for 14 days. Colonies were then washed with PBS for three times and stained with crystal violet (0.5%), after fixing with paraformaldehyde (4%) for 20 min. After the crystal violet was removed, plates were washed with PBS and dried.

Wound Healing

Approximately 2×10^5 cells were seeded in 6-well plates. A linear scratch was generated with a 10-μl pipette tip after the cells reached 100% confluence and were then washed with PBS to remove non-adherent cells. After treatment with 10μmol/L or 15μmol/L BAZ or DMSO for 2 hours, the medium was changed and fresh medium containing 10% FBS was added. The distance migrated was observed after 12 h or 24 h under the microscope. The cell migration ratio was calculated as following: Cell migration ratio (%) = (specific day wound surface area − initial wound area)/initial wound area × 100%.

Immunofluorescence Staining Analysis

VSMCs cells were seeded into 6-well plates with pre-placed sides. After the cells are attached, the cells were pretreated with BAZ for 2h, then stimulated by IL-6 for 30 mins. After processing, the cells were washed and then fixed with paraformaldehyde for 15 minutes at room temperature. After two washes with PBS, a PBS buffer containing 0.3% Triton X-100 and 5% normal goat serum was added to permeabilize cells at room temperature for one hour. Next the cells were incubated with a polyclonal rabbit antibody P-STAT3 (1:50 dilution) or STAT3 (1:100 dilution) overnight at 4°C. The cells were washed with a PBS buffer supplemented with 0.1% Tween-20 three times after the overnight incubation. Subsequently, the cells were incubated with Cy3-conjugated anti-rabbit secondary antibody (1:100; Jackson ImmunoResearch Laboratories, West Grove, PA) at room temperature for 1 h and then stained with nuclear –specific DAPI (vector Laboratories, Burlingame, CA, USA) for 5 min. Digital images were captured by fluorescent microscopy.

Quantitative PCR Analysis

VSMCs were treated with BAZ (20 μmol/L) or DMSO for 2 hours. Then AngII or IL-6 was added for 30 minutes or 4 hours before cells were collected. Total RNA was extracted with an HI Pure RNA extract Kit (Magen, China) and converted to cDNA using a Rever Tra Ace qPCR RT kit (TOYOBO, Japan). The silencing efficiency was detected by RT-PCR performed on the ABI Step One Plus (Applied Biosystems, USA) with SYBR green PCR mix (TOYOBO, Japan) according to the manufacturer's instructions. The specific oligos used in the study were as follows: MMP2 (forward): 5′-ACACCAAGAACTTCCGACTATCCA ATG-3′, MMP2 (reverse): 5′-CAGTACCAGTGTCAGTATCA GCATCAG -3′; MMP9(forward): 5′-CTCCTGGTGCTCCTGG CTCTAG-3′, MMP9(reverse): 5′-GTGTAACCATAGCGGTAC AGGTAATCC-3′, GAPDH (forward): 5′-AGTGCCAGCCTCG TCTCATA-3′, GAPDH (reverse): **5**-′AGAGAAGGCAGCCC TGGTAA-3′. The fold change of relative mRNA expression was calculated using the 2-ΔΔCt method.

Cell Viability Assay

Cell Counting Kit-8 (CCK-8) assay kits (Promoter Biotechnology Ltd, Nanjing, China) were used to detect the cell viability. Cells were planted in a 96-well plate with 1×10^4 cells/well. After attachment, VSMCs were treated with different dosages of BAZ (5, 10, 15, 20 μM) or DMSO for 24 h. CCK-8 was added (10 μL/well), and the absorbance was measured at a wavelength of 450 nm.

Statistical Analysis

Data were presented as the mean ± SEM. The difference between groups was evaluated by one-way ANOVA (Analysis of variance) with Bonferroni's *post hoc*. Statistical significance was defined as $P < 0.05$ or $P < 0.01$. Statistical analysis was performed using SPSS software (version 13.0). All experiments were performed at least three times independently.

RESULTS

BAZ Attenuates the Formation and Severity of Aneurysms of AngII-Induced AAA in ApoE$^{-/-}$ Mice

We detected the suppressive effect of BAZ in the development of abdominal aortic aneurysm in AngII-induced mice. As shown in **Figure 1A**, compared to the AngII-induced group, BAZ significantly attenuated the formation and severity of abdominal aortic aneurysm. An aortic diameter increase of approximately 50% was defined as the development of AAA (Tsai et al., 2013). As shown in **Figure 1C**, the incidence of AAA was calculated from all the animals in each group. Continuous infusion of AngII in mice increased the incidence of AAA (7/13, 53.84%) compared with the control group (0/12, 0%). However, the incidence of AAA significantly decreased with BAZ treatment (3/12, 25%) in comparison to the AngII group (7/13, 53.84%). Moreover, the external diameter of the aorta was also attenuated by treatment with BAZ when compared with AngII-induced group in APOE$^{-/-}$, as shown in **Figure 1D**. During the intervention period of 28 days, there were four deaths (4/13, 30.77%) in the AngII group, three deaths (3/12, 25%) in the BAZ group and no deaths or aneurysms were observed in the control group (**Supplementary Figure 1**). The survival curves were analyzed with Logrank test. The mortality rate of AngII-induced mice was slightly decreased by treatment with BAZ, when compared to the AngII group at the end of the experiment (day 28). Although there was no significant difference between the AngII and BAZ groups (P=0.23). These results indicated that treatment with BAZ attenuated the formation of AAA in Ang II-induced mice and decreased the expansion of the aorta. The structure of BAZ was shown in **Figure 1F**.

The part of the aortas with maximum diameter were collected and embedded. H&E staining of cross-sections showed that AngII infusion led to a significant thickening of the abdominal aortic wall. While BAZ treatment markedly reduced wall thicknesses (**Figure1Ba**). The relative thickness of the aortic wall was further determined. As shown in **Figure1E**, Baz treatment significantly decreased the aortic wall thickness compared with AngII. In addition, BAZ treatment significantly reduced elastin degradation in AAA lesions of AngII-infused ApoE$^{-/-}$ mice. EVG stained sections suggested that elastin fibers exhibited apparent discontinuity and disintegration in the aortic wall of the AngII-infused mice. While treatment with BAZ obviously reversed the degradation of elastin induced by AngII (**Figure 1Bb**). These results indicated that BAZ could significantly attenuate the development and severity of aneurysms in AngII-infused ApoE$^{-/-}$ mice.

BAZ Inhibits Expression of P-STAT3, MMPs and Attenuates Aortic Wall Remodeling and Inflammation in AngII Treated ApoE$^{-/-}$ Mice

It has been reported that AngII-infused ApoE knock-out mice mostly present AAAs around the suprarenal area immediately distal to the branch of the renal artery (Daugherty et al., 2006). So, we selected aortic sections from the aneurysm-prone areas for histological characteristics analysis. Representative immunohistochemical staining was shown in **Figure 2**. To detect the effect of BAZ on IL-6/GP130/STAT3 signaling, the expression of P-STAT3 in abdominal aortas of three groups of mice was compared. Western blot analysis showed that AngII infusion led to increased phosphorylation of STAT3 at Tyr705, however, BAZ could inhibit the expression of P-STAT3 (**Figures 1G–I**). Immunohistochemistry showed similar results. As in **Figure 2Ab**, the expression of P-STAT3 was increased (brown nuclei represent P-STAT3 positive) in the vascular wall of AngII-induced mice. BAZ could decrease the expression of P-STAT3. As shown in **Figure 2Aa**, the level of IL-6 was increased in the vessel wall of abdominal aortic aneurysms in AngII-infused ApoE$^{-/-}$ mice compared to similar sections of aorta in saline-infused control mice. While treatment with BAZ could significantly decrease the expression of IL-6 in the same vessel wall section of aortas. Simultaneously, we also tested the expression of IL-6 in mouse serum *via* ELISA. As shown in **Supplementary Figure 2**, the expression of IL-6 in serum was increased dramatically in Ang II-induced mice. However, BAZ treatment deceased the expression of IL-6 in serum compared with only AngII-infused mice. MMPs, especially MMP2 and MMP9, whose expressions were increased in the abdominal aortas of AngII-induced ApoE$^{-/-}$ mice, participate in the process of AAA development. Immunohistochemical staining and western blotting showed that administration of BAZ significantly down-regulated the expression of MMP2 and MMP9 (**Figures 1G, J, K**, **2B**). Abundant infiltration by CD68-positive macrophages was detected in the adventitia and media of the aortic aneurysms from the AngII-infused mice. Increased expression of CD68 was detected in the suprarenal section of aortas in AngII-induced group without BAZ, while the expression of CD68 was significantly inhibited by BAZ (**Figure 2C**). Hyperproliferation of VSMCs in the aortic wall plays an important role in AAA. Our results indicated that BAZ inhibited the over-proliferation of VSMCs in AAA lesions of AngII-infused ApoE$^{-/-}$ mice. As shown in **Figure 2D**, treatment with BAZ decreased the expression of α-SMA when compared with AngII-infused mice.

Bazedoxifene Inhibits the Phosphorylation of STAT3 Induced by IL-6

Vascular smooth muscle cells, which act as a major component of the aortic wall, play an important role in AAA (Yao et al., 2019). VSMCs were used to test the effect of BAZ *in vitro*. Our results showed that Interleukin-6 could induce the phosphorylation of STAT3 in VSMCs (**Figures 3A, B**). BAZ inhibited the phosphorylation of STAT3 induced by IL-6 but had no significant effect on the overall expression of STAT3 in VSMCs (**Figures 3A–D**).

Bazedoxifene Suppresses the Phosphorylation of STAT3 Induced by AngII

We also found that AngII could induce phosphorylation of STAT3 in VSMCs (**Figures 3E, F**). Similarly, BAZ, which has been reported to inhibit the IL-6/GP130 interface, could also

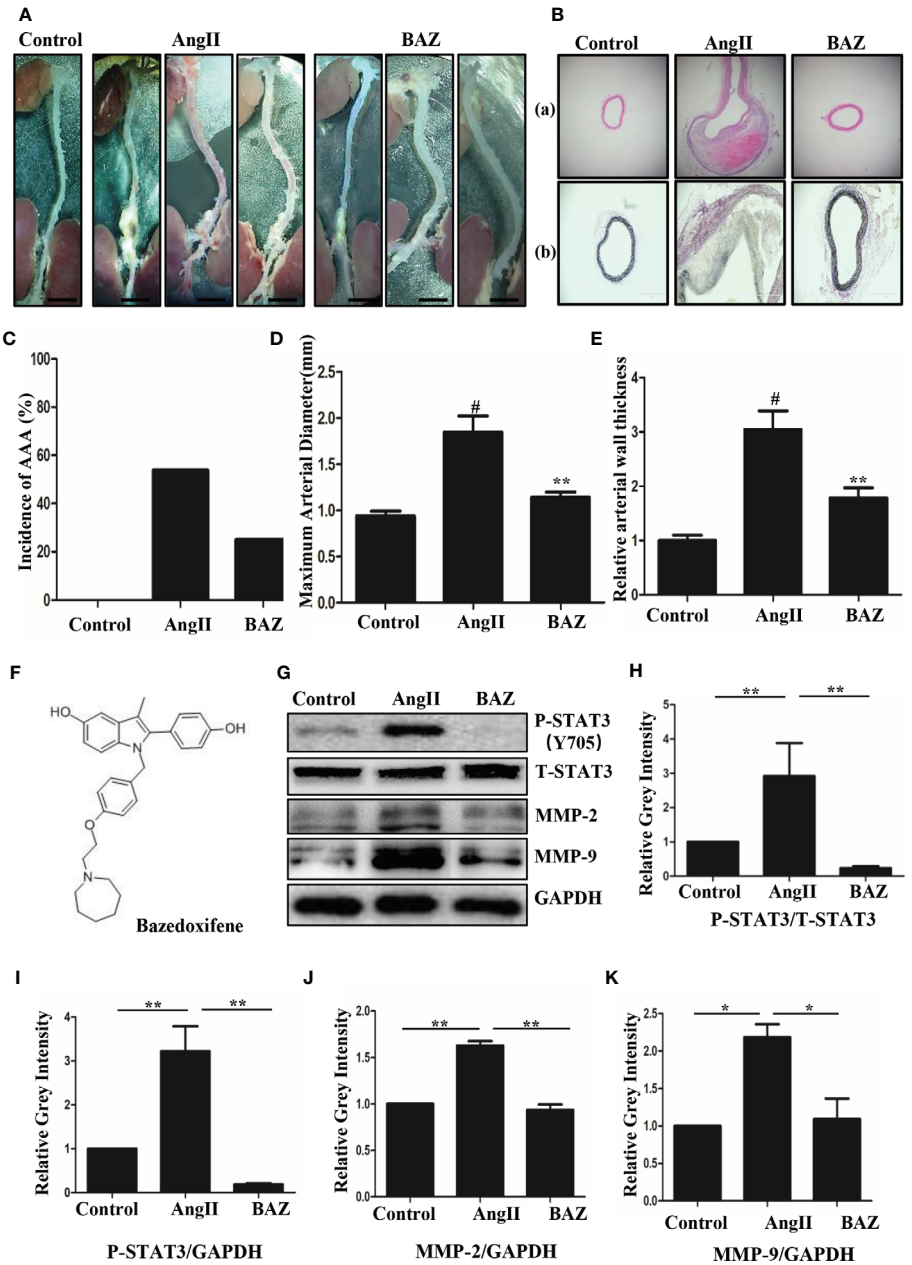

FIGURE 1 | The structure of BAZ and the effect of BAZ on the development of Ang-II-induced abdominal aortic aneurysm **(A)** Morphometrical change of AAA in ApoE$^{-/-}$ mice. Representative images of macroscopic features in aneurysms from sacrificed mice after 28 days. Scale bar denotes 2 mm. **(B)** Histological change of aneurysms in mice shown by hematoxylin eosin (H&E) **(Ba)** and elastin van Gieson (EVG) **(Bb)** staining. Scale bar denotes 400 mm. **(C)** The incidence of AAA was calculated from all of the animals in each group. **(D)** BAZ treatment significantly deceased the external diameter of the aorta (n=9). **(E)** Relative aortic wall thickness of each group (n=9). **(F)** The structure of Bazedoxifene (BAZ). **(G)** Western blots for the expression of P-STAT3, T-STAT3, MMP2 and MMP9 in mice aneurysms. **(H)** Relative gray intensity to STAT3 and **(I–K)** relative gray intensity to GAPDH was calculated (n = 3). Data were expressed as mean ± standard error of the mean. $^{\#}P < 0.05$ compared with the control group, $^{*}p < 0.05$, $^{**}p < 0.01$ compared with the AngII group.

suppress the phosphorylation of STAT3 as induced by AngII and without an effect on overall STAT3 levels (**Figures 3E–H**).

To explore the mechanism, we first detected the effect of AngII on IL-6 secretion. When the cells were stimulated with AngII, the concentration of IL-6 was increased in the supernatant. This result suggested that AngII could induce the secretion of IL-6 in VSMCs (**Figure 3I**). It has been reported that in the classic IL-6 signaling pathway IL-6 binds to the membrane-bound IL-6 receptor (IL-6R) and then recruits GP130 to form the IL-6/IL-6Rα/GP130 heterotrimer which is

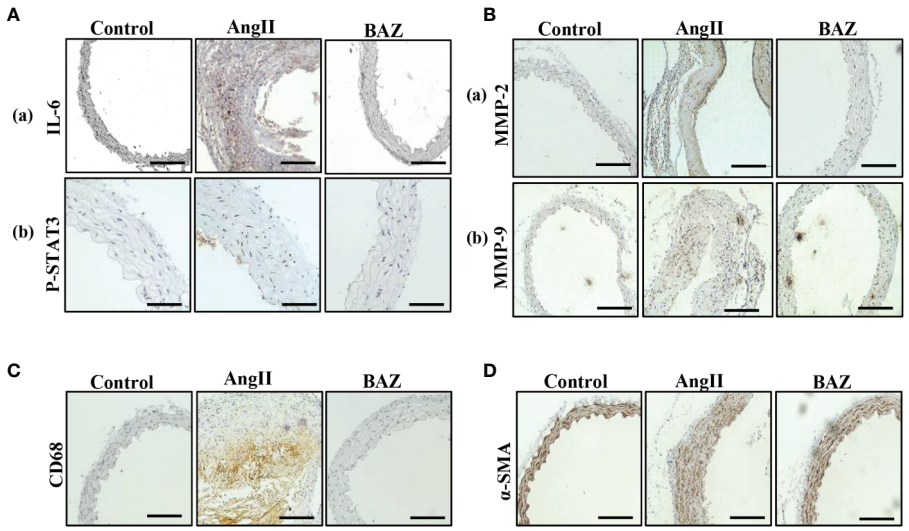

FIGURE 2 | Effect of BAZ on the abdominal aorta *via* immunohistochemical staining in mice. **(A)** Expression and distribution of P-STAT3 and IL-6 (both brown-stained) in cross-sections of aorta from ApoE$^{-/-}$mice. **(B)** The expression of MMP2 and MMP9 was detected *via* immunohistochemical staining in the abdominal aorta of ApoE$^{-/-}$ mice. **(C)** Representative immunohistochemical staining of CD68 in aortic cross-sections. **(D)** Representative images showing a-SMA expression in aortic cross-sections. The scale depicts 100μm for each interval in **A(b)** and 200μm in **A(a) B, C, D**.

followed by the activation and phosphorylation of STAT3. However, in IL-6 trans signaling IL-6 can also bind to soluble forms of IL-6R (sIL-6R) and then bind to gp130 (Ferreira et al., 2013; Aparicio-Siegmund et al., 2019). So we further detected the effects of sIL-6R on IL-6 or Ang II induced STAT3 phosphorylation. As shown in our results, sIL-6R could slightly decrease IL-6-induced STAT3 phosphorylation at lower concentrations but increased STAT3 phosphorylation at higher concentrations (**Figures 3J–L**). It was very interesting to find that the phosphorylation of STAT3 induced by AngII could be inhibited by sIL-6R (**Figures 3N–P**). The density of pSTAT3 was normalized by the total density of STAT3 (**Figures 3D, H, M, Q**). These data indicated that AngII-induced activation of STAT3 was at least partially mediated by the IL-6 signaling pathway.

BAZ Suppresses the Expression of MMP2, MMP9 Induced by IL-6 and AngII

In our results, western blotting showed that BAZ suppressed the expression of MMP2 and MMP9 induced by IL-6 and AngII (**Figures 4A, D**). Relative gray intensity to GAPDH was shown in **Figures 4B-F**. Moreover, we found the mRNA expression of MMP2 and MMP9 induced by IL-6 and AngII was decreased by BAZ (**Figures 4G–J**).

BAZ Inhibits STAT3 Activation in the Nucleus in VSMCs

After pretreatment with BAZ for 2 hours, VSMCs were induced with IL-6 for another 30 minutes and P-STAT3 or STAT3 was detected by immunofluorescence staining. After stimulation by IL-6, STAT3 was phosphorylated and translocated into the nucleus in VSMCs. However, most of the STAT3 was retained in the cytoplasm of cells treated with BAZ (**Figure 5B**). In addition, IL-6 induced STAT3 phosphorylation in the nucleus, which was blocked by BAZ in VSMCs (**Figure 5A**). Thus, these data suggested that the suppression of STAT3 phosphorylation by BAZ might impair STAT3 transcriptional functions in VSMCs.

BAZ Suppresses Cell Migration, Colony Forming Capacity and Cell Viability in VSMCs

STAT3 phosphorylation was involved in the over-activation of vascular smooth muscle cells. We next evaluated whether BAZ could inhibit cell migration and colony formation, which are important processes in the development of abdominal aortic aneurysms. As shown in **Figure 6A**, VSMCs were pretreated with BAZ for 4 h, then the same number of viable cells were planted at the same cell densities in 10 cm plates. After incubation for two weeks, cells were stained with crystal violet. BAZ could clearly inhibit colony formation in VSMCs. Wound healing assays were used to detect the effect of BAZ on cell migration in vascular smooth muscle cells. Our results showed that treatment with BAZ caused a reduction in wound healing (**Figures 6B, C**). Meanwhile, the CCK-8 assay suggested that BAZ suppressed cell viability in VSMCs (**Figure 6D**). These results may indicate BAZ could suppress the formation of AAA *via* the inhibitory effect on over-proliferation in VSMCs.

DISCUSSION

Abdominal aortic aneurysm is a serious vascular disease with a high mortality rate and no effective therapeutic treatment is available except for aneurysmectomy (Erbel et al., 2015).

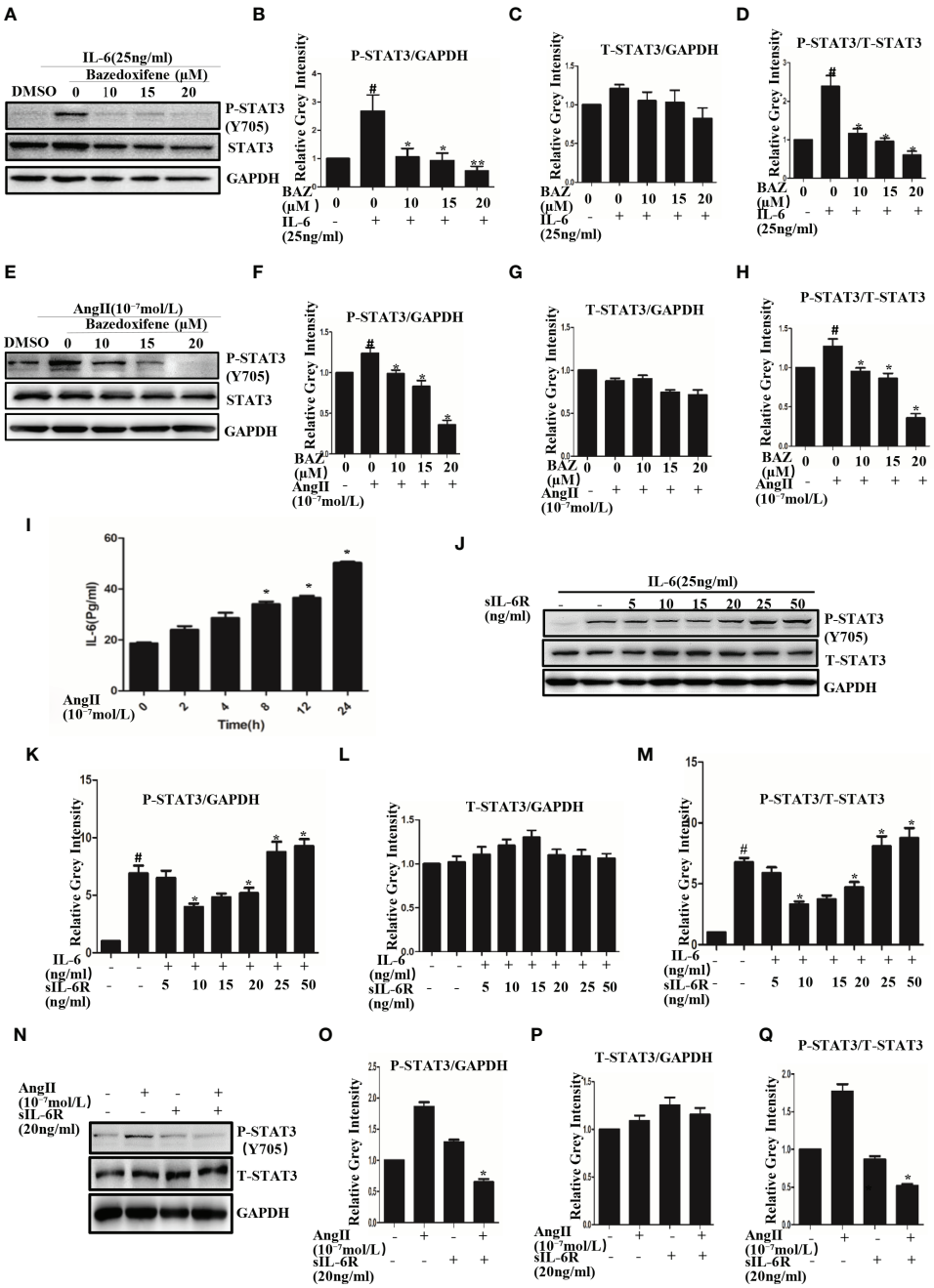

FIGURE 3 | BAZ suppresses the phosphorylation of STAT3 induced by IL-6 and AngII in VSMCs. Cells were pretreated with BAZ for 2 hours and then stimulated with IL-6 **(A)** and AngII **(E)**, western blotting was used to show the expression of P-STAT3 and STAT3. **(I)** ELISA was used to exam the effect of AngII on the secretion of IL-6 *in vitro*. **(J)** The effect of sIL-6R at different concentrations on IL-6 signaling transduction. **(N)** The effect of AngII or sIL-6R on the expression of P-STAT3. **(B, C, F, G, K, L, O, P)** Relative gray intensity to GAPDH was calculated. **(D, H, M, Q)** Relative gray intensity to T–STAT3 was calculated. Data were expressed as mean ± standard error of the mean (n = 3). $^{\#}P < 0.05$ compared with the control; *P< 0.05, **P< 0.01compared with IL-6 or AngII.

Despite the fact that animal studies have identified several potential therapeutic targets in the pathogenesis of AAA, pharmacotherapy for AAA is yet to be established (Baxter et al., 2008; Ohno et al., 2018). It has been reported that there was no significant association between AAA progression and the use of statins, beta blockers, angiotensin-converting enzyme inhibitors or angiotensin II receptor blockers (Baxter et al., 2008; Kokje et al., 2015), which indicated that there may be other mechanisms involved in the progression of AAA. In our results, BAZ could inhibit the activity of the IL-6/GP130/STAT3 signaling pathway and significantly decreased the severity of AAA in an AngII-induced ApoE$^{-/-}$ mice model. BAZ could also

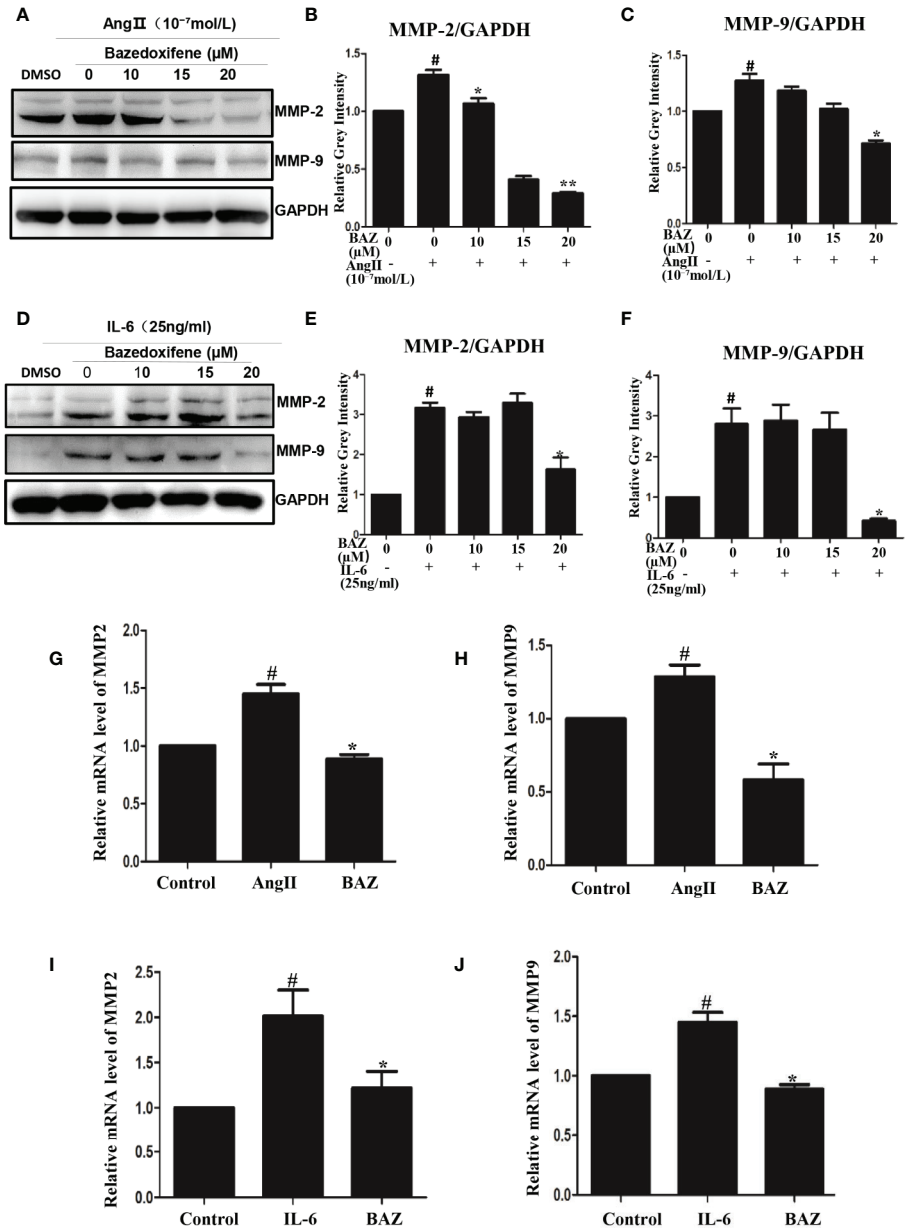

FIGURE 4 | BAZ suppresses the expression of MMP2 and MMP9 induced by IL-6 and AngII in VSMCs. Pretreatment of BAZ for 2 hours suppressed the increase in both MMP2 and MMP9 expression induced by IL-6 **(A)** and AngII **(D)**. Relative gray intensity to GAPDH was calculated (n = 3) **(B, C, E, F)**. The mRNA expression of MMP2 and MMP9 was assessed by qRT-PCR and normalized to GAPDH and is expressed in arbitrary units. BAZ suppressed the mRNA expression of MMP2 and MMP9 induced by IL-6 **(I, J)** and AngII **(G, H)**. Data were presented as the mean ± SEM. $^{\#}P < 0.05$ compared with the control; *P< 0.05, **P< 0.01 compared with IL-6 or AngII.

inhibit the expression of P-STAT3, MMP2 and MMP9 *in vivo* and *in vitro*. It could also inhibit the proliferation of VSMCs and maladaptive responses to inflammation which accompanied the overexpression of pro-inflammatory mediators *in vivo* (Butoi et al., 2016; Das et al., 2017). These results suggest that BAZ may have a protective effect on the treatment of AAA by inhibition of the IL-6/GP130/STAT3 signaling pathway. That may provide a new option for the prevention and treatment of AAA.

Although the pathogenesis of AAA remains unclear, a large body of evidence supports the critical role of inflammation (Aoki et al., 2007). IL-6 as a multicellular cytokine has been reported to participate in cell proliferation, apoptosis and various inflammatory responses (Hunter and Jones, 2015). In an inflammatory response, IL-6 exerts its function through binding to its receptor (IL-6R, located on cell membranes, or stays in a soluble state in plasma) by forming a binary complex

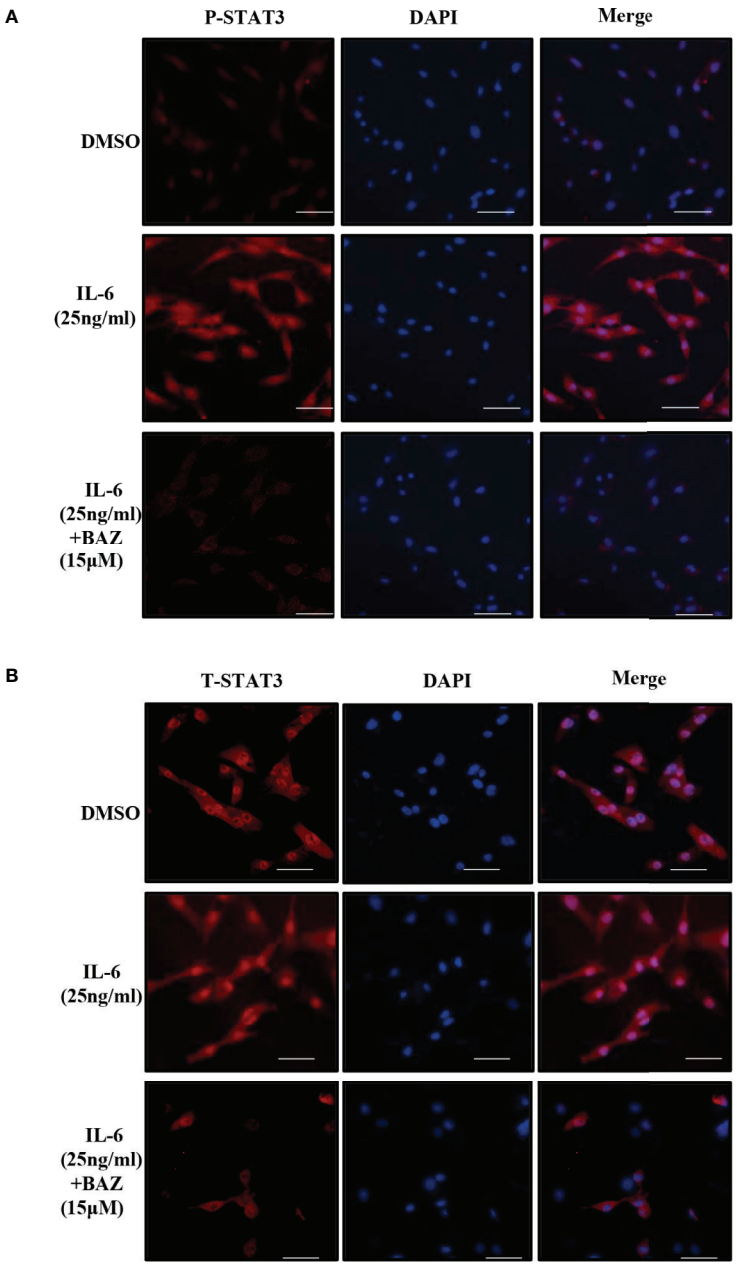

FIGURE 5 | BAZ suppresses STAT3 activation in nucleus and the nuclear translocation induced by IL-6 in VSMCs. After pretreatment with BAZ for 2 hours, cells were stimulated with IL-6 for another 30 minutes, and then STAT3 activation **(A)** and STAT3 nuclear translocation **(B)** were detected by immunofluorescence staining as described. Scale bar represents 200μm.

and then recruiting glycoprotein 130 (GP130) leading to the formation of the IL-6/IL-6R/GP130 heterotrimer. The homodimerization of the IL-6/IL-6Rα/GP130 trimers initiate an intracellular signaling cascade of phosphorylation of Janus kinases (JAKs), thereby activating a downstream effector STAT3 *via* phosphorylation (Li et al., 2014). Genetic and observational associations imply a link between IL-6 and AAA disease (Hunter and Jones, 2015). Furthermore, a systematic review and meta-analysis suggested that the IL-6 receptor pathway might be a causal signaling in human AAA pathogenesis and inhibition of IL-6R may contribute to AAA treatment (Harrison et al., 2013). STAT3, one of the significant downstream target genes of IL-6, has been documented in the pathogenesis of AAA (Ohno et al., 2018; Yao et al., 2019). It has been reported that an increased expression of P-STAT3 is identified in AAA tissues compared with non-aneurysmal controls (Liao et al., 2012). Moreover, in

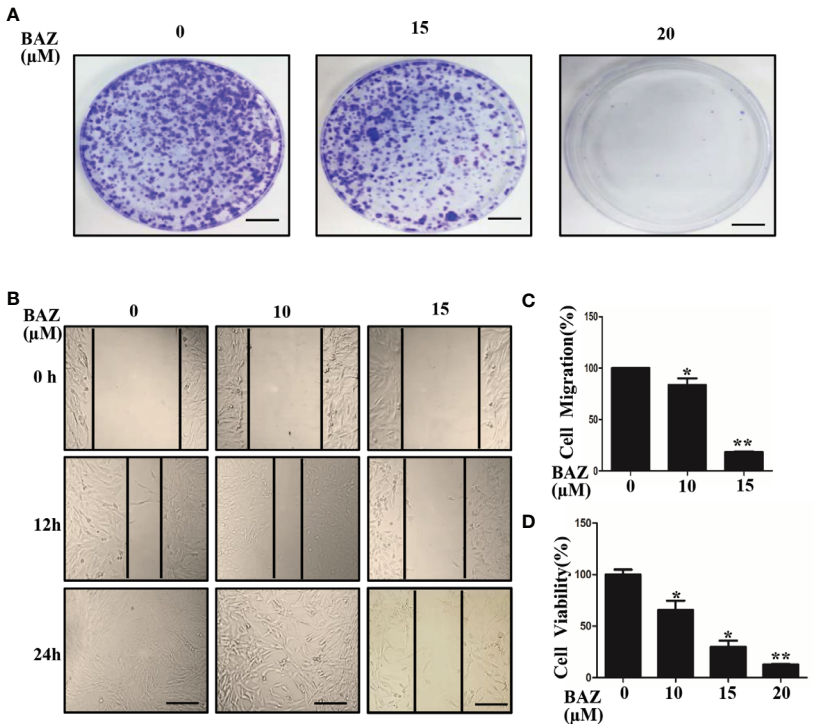

FIGURE 6 | BAZ inhibits colony formation and wound healing in VSMCs. **(A)** Cells were pretreated with BAZ (15 or 20 mM) or DMSO for 4 h, then colony formation was evaluated after two weeks. Scale bar denotes 1 cm. **(B)** After BAZ treatment for 2h, the migration ability of VSMCs was detected using wound-healing assays. Scale bar represents 400 μm. **(C)** Cell migration was assessed. **(D)** BAZ reduced cell viability of VSMCs. *P< 0.05, **P< 0.01 compared with the control.

our results, BAZ, which has been reported to inhibit the IL-6/GP130 protein-protein interface, significantly decreased the severity of AAA in ApoE$^{-/-}$ mice. Furthermore, BAZ could suppress the phosphorylation of STAT3 *in vitro* and *in vivo*. These results may suggest that the IL-6/GP130/STAT3 pathway may take a significant role in the pathogenesis of abdominal aortic aneurysm. More importantly, the inhibition of the IL-6/GP130/STAT3 pathway might become a new target for the prevention or treatment of AAA.

A number of studies have shown that AngII induces AAA by increasing the inflammatory profile, however, its specific molecular pathway remains unclear (Weiss et al., 2014). Despite the fact that animal studies have shown that the use of AT1 receptor inhibitors may protect against abdominal aortic aneurysms, the outcomes of clinical research has been unsatisfying and often remains inconsistent (Maekawa et al., 2017). Use of AT1-receptor antagonists does not affect AAA growth (Weiss et al., 2014). It indicates that there may be other molecular pathways involved in the occurrence and development of abdominal aortic aneurysms induced by AngII. However, our results demonstrated that AngII-induced activation of STAT3 was mediated by IL-6, at least in part. We found P-STAT3 induced by AngII could be inhibited by soluble IL-6 receptors (sIL-6R), a specific constituent of the trans-signaling of IL-6, which could limit IL-6-induced P-STAT3 at low concentrations but increase P-STAT3 at higher concentrations. Furthermore, BAZ, which could impede the IL-6/GP130 interface, could also inhibit the phosphorylation of STAT3 induced by AngII. These results indicate that IL-6/GP130/STAT3 may participate, albeit partially, in the response to AngII in VSMCs. This may provide a theoretical basis for the treatment of AAA by targeting the IL-6/GP130/STAT3 signaling pathway.

Bazedoxifene has been approved by the FDA for use as a treatment for osteoporosis in clinics. It has been reported that BAZ could reduce cerebral aneurysm ruptures in rats in a blood pressure-independent manner and that BAZ has no significant effect on blood pressure (Maekawa et al., 2017). Moreover, in our previous research, we demonstrated that Bazedoxifene could bind to the GP130 D1 domain and inhibit the IL-6/GP130 protein-protein interface (Li et al., 2014). Subsequently, it suppresses STAT3 phosphorylation and transcription induced by IL6. Various studies have shown Bazedoxifene could inhibit tumor growth by targeting the IL-6/GP130/STAT3 signaling pathway (Wu et al., 2016; Xiao et al., 2017; Chen et al., 2019; Ma et al., 2019). Based on our study, we found Bazedoxifene could attenuate the formation and severity of aneurysms, which may expand the application of Bazedoxifene to the prevention and treatment of abdominal aortic aneurysms in clinics. Despite reports that some small molecule compounds, such as Ursolic acid (Zhai et al., 2018) and S31-201 (Qin et al., 2015), could decrease the incidence and severity of AAAs by inhibiting the phosphorylation of STAT3 in an AngII-infused

ApoE$^{-/-}$ mouse model, to date no small molecule STAT3 inhibitor is available for clinical therapy. Compared with these compounds (which are not used clinically), Bazedoxifene has advantages in terms of stability, security and oral absorbency. Drug repurposing is a valuable approach in delivering new AAA therapeutics rapidly into clinics.

The limitations of our study require consideration. Several animal models of AAA have been developed in mice including injury of the aortic wall with calcium chloride or elastase (Patelis et al., 2017). Compared with other models, the AngII-infused model supports an imbalance of the renin-angiotensin system in the pathogenesis of AAA (Zhang et al., 2009). Infusion of AngII *via* subcutaneous osmotic minipumps in ApoE$^{-/-}$ mice has also been shown to result in the formation of AAAs, which could mimic the inflammatory microenvironment and exhibit many characteristics of human AAA including rupture of the elastic layer, activation of matrix metalloproteinases, macrophage infiltration and so on (Senemaud et al., 2017). Differences between species and individuals perhaps lead to diverse consequences. For example, unlike humans, mice often present suprarenal AAAs and their relevance remains somewhat limited by their inability to expand indefinitely with time (Patelis et al., 2017). So further experiments might be needed to evaluate the effect of BAZ in human AAA. On the other hand, although our results suggested a significant effect of BAZ on AAA in VSMCs and in animals, whether the *in vivo* effect of BAZ was dependent on the IL-6/GP130/STAT3 signaling pathway was still unclear in our work due to the complicated mechanisms of AAA.

In summary, we demonstrated that BAZ might play a protective role in the pathology of AAA in AngII-induced mice. As an FDA-approved drug with known pharmacokinetics and safety, Bazedoxifene has great potential to be used in clinics for the treatment of AAA. Moreover, considering BAZ as a pharmacological template, we established a basis for increasing the rate of development of drugs that selectively target the IL-6/GP130/STAT3 pathway with better bioavailability and fewer side effects. It may provide a novel strategy for the prevention and therapy of AAA in clinics.

DATA AVAILABILITY STATEMENT

All datasets generated for this study are included in the article/**Supplementary Material**.

ETHICS STATEMENT

All animal experiments were carried out in accordance with National Institute of Health guidelines and approved by the Experimental Animal Research Committee of Tongji Medical College, Huazhong University of Science and Technology.

AUTHOR CONTRIBUTIONS

CZ and LL contributed to the design of this study, coordinated the experiments and provided funding sources. DY and HM performed animal experiments and biological molecular experiments. WS, PL, TL, and MZ contributed to the cellular experiments. JG, JT, and SH contributed to the collection and analysis of the data. CL and JL provided extensive support. SL and JGL contributed to the manuscript draft. All authors have contributed significantly and approved the final manuscript.

FUNDING

This research was supported by the National Natural Science Foundation of China to LL (81570416) and SL (81570337), the Fundamental Research Fund for the Central Universities (HUST) to JGL (2017KFYXJJ099), the Science and Technology Project Foundation of Wuhan to JGL (2017060201010175), Hubei Province health and family planning scientific research project to JGL (WJ2019M120), Natural Science Foundation of Hubei Province to LL (2019CFB668) and the Outstanding Young Investigator Foundation of Tongji Hospital to LL (YXQN009).

SUPPLEMENTARY MATERIAL

The Supplementary Material for this article can be found online at: https://www.frontiersin.org/articles/10.3389/fphar.2020.00392/full#supplementary-material

FIGURE S1 | Kaplane-Meier curves of the survival of APOE$^{-/-}$. Data represent the Kaplan-Meier curve depicting mouse survival. (n=13 for the AngII group, n=12 for the control group and BAZ group. P=0.23, for AngII vs BAZ, log-rank test).

FIGURE S2 | The expression of IL-6 in mice serum. The expression of IL-6 in mice serum was decreased by BAZ treatment compared with AngII-induced (n=9). Data were expressed as mean ± standard error of the mean. #P < 0.05 compared with the control group, *p < 0.05, compared with the AngII group.

REFERENCES

Aoki, H., Yoshimura, K., and Matsuzaki, M. (2007). Turning back the clock: regression of abdominal aortic aneurysms via pharmacotherapy. *J. Mol. Med. (Berl)* 85 (10), 1077–1088. doi: 10.1007/s00109-007-0213-2

Aparicio-Siegmund, S., Garbers, Y., Flynn, C. M., Waetzig, G. H., Gouni-Berthold, I., Krone, W., et al. (2019). The IL-6-neutralizing sIL-6R-sgp130 buffer system is disturbed in patients with type 2 diabetes. *Am. J. Physiol. Endocrinol. Metab.* 317 (2), E411–E420. doi: 10.1152/ajpendo.00166.2019

Argyriou, C., Georgiadis, G. S., Kontopodis, N., Pherwani, A. D., Van Herwaarden, J. A., Hazenberg, C., et al. (2018). Screening for Abdominal Aortic Aneurysm During Transthoracic Echocardiography: A Systematic Review and Meta-analysis. *Eur. J. Vasc. Endovasc Surg.* 55 (4), 475–491. doi: 10.1016/j.ejvs.2018.01.003

Baxter, B. T., Terrin, M. C., and Dalman, R. L. (2008). Medical Management of Small Abdominal Aortic Aneurysms. *Circulation* 117 (14), 1883–1889. doi: 10.1161/circulationaha.107.735274

Butoi, E., Gan, A. M., Tucureanu, M. M., Stan, D., Macarie, R. D., Constantinescu, C., et al. (2016). Cross-talk between macrophages and smooth muscle cells impairs collagen and metalloprotease synthesis and promotes angiogenesis. *Biochim. Biophys. Acta* 1863 (7 Pt A), 1568–1578. doi: 10.1016/j.bbamcr.2016.04.001

Chen, X., Wei, J., Li, C., Pierson, C. R., Finlay, J. L., and Lin, J. (2018). Blocking interleukin-6 signaling inhibits cell viability/proliferation, glycolysis, and

colony forming activity of human medulloblastoma cells. *Int. J. Oncol.* 52 (2), 571–578. doi: 10.3892/ijo.2017.4211

Chen, X., Tian, J., Su, G. H., and Lin, J. (2019). Blocking IL-6/GP130 Signaling Inhibits Cell Viability/Proliferation, Glycolysis, and Colony Forming Activity in Human Pancreatic Cancer Cells. *Curr. Cancer Drug Targets* 19 (5), 417–427. doi: 10.2174/1568009618666180430123939

Das, S., Senapati, P., Chen, Z., Reddy, M. A., Ganguly, R., Lanting, L., et al. (2017). Regulation of angiotensin II actions by enhancers and super-enhancers in vascular smooth muscle cells. *Nat. Commun.* 8 (1),1467. doi: 10.1038/s41467-017-01629-7

Daugherty, A., Rateri, D. L., and Cassis, L. A. (2006). Role of the renin-angiotensin system in the development of abdominal aortic aneurysms in animals and humans. *Ann. N Y Acad. Sci.* 1085, 82–91. doi: 10.1196/annals.1383.035

Dilme, J. F., Bellmunt, S., Camacho, M., Sola-Villa, D., Romero, J. M., Escudero, J. R., et al. (2014). Influence of cardiovascular risk factors on levels of matrix metalloproteinases 2 and 9 in human abdominal aortic aneurysms. *Eur. J. Vasc. Endovasc Surg.* 48 (4), 374–381. doi: 10.1016/j.ejvs.2014.05.023

Erbel, R., Aboyans, V., Boileau, C., Bossone, E., Di Bartolomeo, R., Eggebrecht, H., et al. (2015). Corrigendum to: 2014 ESC Guidelines on the diagnosis and treatment of aortic diseases. *Eur. Heart J.* 36 (41), 2779. doi: 10.1093/eurheartj/ehv178

Ferreira, R. C., Freitag, D. F., Cutler, A. J., Howson, J. M., Rainbow, D. B., Smyth, D. J., et al. (2013). Functional IL6R 358Ala allele impairs classical IL-6 receptor signaling and influences risk of diverse inflammatory diseases. *PloS Genet.* 9 (4), e1003444. doi: 10.1371/journal.pgen.1003444

Ghosh, A., Pechota, A., Coleman, D., Upchurch, G. R.Jr., and Eliason, J. L. (2015). Cigarette smoke-induced MMP2 and MMP9 secretion from aortic vascular smooth cells is mediated via the Jak/Stat pathway. *Hum. Pathol.* 46 (2), 284–294. doi: 10.1016/j.humpath.2014.11.003

Harrison, S. C., Smith, A. J., Jones, G. T., Swerdlow, D. I., Rampuri, R., Bown, M. J., et al. (2013). Interleukin-6 receptor pathways in abdominal aortic aneurysm. *Eur. Heart J.* 34 (48), 3707–3716. doi: 10.1093/eurheartj/ehs354

Hoornweg, L. L., Storm-Versloot, M. N., Ubbink, D. T., Koelemay, M. J., Legemate, D. A., and Balm, R. (2008). Meta analysis on mortality of ruptured abdominal aortic aneurysms. *Eur. J. Vasc. Endovasc Surg.* 35 (5), 558–570. doi: 10.1016/j.ejvs.2007.11.019

Hunter, C. A., and Jones, S. A. (2015). IL-6 as a keystone cytokine in health and disease. *Nat. Immunol.* 16 (5), 448–457. doi: 10.1038/ni.3153

Ijaz, T., Tilton, R. G., and Brasier, A. R. (2016). Cytokine amplification and macrophage effector functions in aortic inflammation and abdominal aortic aneurysm formation. *J. Thorac. Dis.* 8 (8), E746–E754. doi: 10.21037/jtd.2016.06.37

Kokje, V. B., Hamming, J. F., and Lindeman, J. H. (2015). Editor's Choice - Pharmaceutical Management of Small Abdominal Aortic Aneurysms: A Systematic Review of the Clinical Evidence. *Eur. J. Vasc. Endovasc Surg.* 50 (6), 702–713. doi: 10.1016/j.ejvs.2015.08.010

Li, H., Xiao, H., Lin, L., Jou, D., Kumari, V., Lin, J., et al. (2014). Drug design targeting protein-protein interactions (PPIs) using multiple ligand simultaneous docking (MLSD) and drug repositioning: discovery of raloxifene and bazedoxifene as novel inhibitors of IL-6/GP130 interface. *J. Med. Chem.* 57 (3), 632–641. doi: 10.1021/jm401144z

Liao, M., Xu, J., Clair, A. J., Ehrman, B., Graham, L. M., and Eagleton, M. J. (2012). Local and systemic alterations in signal transducers and activators of transcription (STAT) associated with human abdominal aortic aneurysms. *J. Surg. Res.* 176 (1), 321–328. doi: 10.1016/j.jss.2011.05.041

Ma, H., Yan, D., Wang, Y., Shi, W., Liu, T., Zhao, C., et al. (2019). Bazedoxifene exhibits growth suppressive activity by targeting interleukin-6/glycoprotein 130/signal transducer and activator of transcription 3 signaling in hepatocellular carcinoma. *Cancer Sci.* 110 (3), 950–961. doi: 10.1111/cas.13940

Maekawa, H., Tada, Y., Yagi, K., Miyamoto, T., Kitazato, K. T., Korai, M., et al. (2017). Bazedoxifene, a selective estrogen receptor modulator, reduces cerebral aneurysm rupture in Ovariectomized rats. *J. Neuroinflammation* 14 (1), 197. doi: 10.1186/s12974-017-0966-7

Nordon, I. M., Hinchliffe, R. J., Loftus, I. M., and Thompson, M. M. (2011). Pathophysiology and epidemiology of abdominal aortic aneurysms. *Nat. Rev. Cardiol.* 8 (2), 92–102. doi: 10.1038/nrcardio.2010.180

Ohno, T., Aoki, H., Ohno, S., Nishihara, M., Furusho, A., Hiromatsu, S., et al. (2018). Cytokine Profile of Human Abdominal Aortic Aneurysm: Involvement of JAK/STAT Pathway. *Ann. Vasc. Dis.* 11 (1), 84–90. doi: 10.3400/avd.oa.17-00086

Patelis, N., Moris, D., Schizas, D., Damaskos, C., Perrea, D., Bakoyiannis, C., et al. (2017). Animal models in the research of abdominal aortic aneurysms development. *Physiol. Res.* 66 (6), 899–915. doi: 10.33549/physiolres.933579

Qin, Z., Bagley, J., Sukhova, G., Baur, W. E., Park, H.-J., Beasley, D., et al. (2015). Angiotensin II-induced TLR4 mediated abdominal aortic aneurysm in apolipoprotein E knockout mice is dependent on STAT3. *J. Mol. Cell. Cardiol.* 87, 160–170. doi: 10.1016/j.yjmcc.2015.08.014

Senemaud, J., Caligiuri, G., Etienne, H., Delbosc, S., Michel, J. B., and Coscas, R. (2017). Translational Relevance and Recent Advances of Animal Models of Abdominal Aortic Aneurysm. *Arterioscler. Thromb. Vasc. Biol.* 37 (3), 401–410. doi: 10.1161/ATVBAHA.116.308534

Tsai, S. H., Huang, P. H., Peng, Y. J., Chang, W. C., Tsai, H. Y., Leu, H. B., et al. (2013). Zoledronate attenuates angiotensin II-induced abdominal aortic aneurysm through inactivation of Rho/ROCK-dependent JNK and NF-kappaB pathway. *Cardiovasc. Res.* 100 (3), 501–510. doi: 10.1093/cvr/cvt230

Vorkapic, E., Dugic, E., Vikingsson, S., Roy, J., Mayranpaa, M. I., Eriksson, P., et al. (2016). Imatinib treatment attenuates growth and inflammation of angiotensin II induced abdominal aortic aneurysm. *Atherosclerosis* 249, 101–109. doi: 10.1016/j.atherosclerosis.2016.04.006

Wang, Y., Krishna, S., and Golledge, J. (2013). The calcium chloride-induced rodent model of abdominal aortic aneurysm. *Atherosclerosis* 226 (1), 29–39. doi: 10.1016/j.atherosclerosis.2012.09.010

Weiss, N., Rodionov, R. N., and Mahlmann, A. (2014). Medical management of abdominal aortic aneurysms. *Vasa* 43 (6), 415–421. doi: 10.1024/0301-1526/a000388

Wu, X., Cao, Y., Xiao, H., Li, C., and Lin, J. (2016). Bazedoxifene as a Novel GP130 Inhibitor for Pancreatic Cancer Therapy. *Mol. Cancer Ther.* 15 (11), 2609–2619. doi: 10.1158/1535-7163.MCT-15-0921

Xiao, H., Bid, H. K., Chen, X., Wu, X., Wei, J., Bian, Y., et al. (2017). Repositioning Bazedoxifene as a novel IL-6/GP130 signaling antagonist for human rhabdomyosarcoma therapy. *PloS One* 12 (7), e0180297. doi: 10.1371/journal.pone.0180297

Yao, F., Yao, Z., Zhong, T., Zhang, J., Wang, T., Zhang, B., et al. (2019). Imatinib prevents elastase-induced abdominal aortic aneurysm progression by regulating macrophage-derived MMP9. *Eur. J. Pharmacol.* 860, 172559. doi: 10.1016/j.ejphar.2019.172559

Zhai, M., Guo, J., Ma, H., Shi, W., Jou, D., Yan, D., et al. (2018). Ursolic acid prevents angiotensin II-induced abdominal aortic aneurysm in apolipoprotein E-knockout mice. *Atherosclerosis* 271, 128–135. doi: 10.1016/j.atherosclerosis.2018.02.022

Zhang, Y., Naggar, J. C., Welzig, C. M., Beasley, D., Moulton, K. S., Park, H. J., et al. (2009). Simvastatin inhibits angiotensin II-induced abdominal aortic aneurysm formation in apolipoprotein E-knockout mice: possible role of ERK. *Arterioscler. Thromb. Vasc. Biol.* 29 (11), 1764–1771. doi: 10.1161/ATVBAHA.109.192609

Conflict of Interest: The authors declare that the research was conducted in the absence of any commercial or financial relationships that could be construed as a potential conflict of interest.

frontiers in Pharmacology

REVIEW
published: 19 May 2020
doi: 10.3389/fphar.2020.00727

Nitroxyl: A Novel Strategy to Circumvent Diabetes Associated Impairments in Nitric Oxide Signaling

Anida Velagic[1,2,3], *Chengxue Qin*[1,2,3], *Owen L. Woodman*[3], *John D. Horowitz*[4], *Rebecca H. Ritchie*[1,2,3,5] *and Barbara K. Kemp-Harper*[5]*

[1] Heart Failure Pharmacology, Baker Heart and Diabetes Institute, Melbourne, VIC, Australia, [2] Central Clinical School, Monash University, Melbourne, VIC, Australia, [3] Drug Discovery Biology, Monash Institute of Pharmaceutical Sciences, Monash University, Melbourne, VIC, Australia, [4] Basil Hetzel Institute, Queen Elizabeth Hospital, University of Adelaide, Adelaide, SA, Australia, [5] Department of Pharmacology, Biomedicine Discovery Institute, Monash University, Melbourne, VIC, Australia

Diabetes is associated with an increased mortality risk due to cardiovascular complications. Hyperglycemia-induced oxidative stress underlies these complications, leading to an impairment in endogenous nitric oxide (NO•) generation, together with reductions in NO• bioavailability and NO• responsiveness in the vasculature, platelets and myocardium. The latter impairment of responsiveness to NO•, termed NO• resistance, compromises the ability of traditional NO•-based therapeutics to improve hemodynamic status during diabetes-associated cardiovascular emergencies, such as acute myocardial infarction. Whilst a number of agents can ameliorate (e.g. angiotensin converting enzyme [ACE] inhibitors, perhexiline, statins and insulin) or circumvent (e.g. nitrite and sGC activators) NO• resistance, nitroxyl (HNO) donors offer a novel opportunity to circumvent NO• resistance in diabetes. With a suite of vasoprotective properties and an ability to enhance cardiac inotropic and lusitropic responses, coupled with preserved efficacy in the setting of oxidative stress, HNO donors have intact therapeutic potential in the face of diminished NO• signaling. This review explores the major mechanisms by which hyperglycemia-induced oxidative stress drives NO• resistance, and the therapeutic potential of HNO donors to circumvent this to treat cardiovascular complications in type 2 diabetes mellitus.

Keywords: nitric oxide, diabetes, type 2 diabetes, cardiovascular disease, nitroxyl, HNO, nitric oxide resistance

OPEN ACCESS

Edited by:
Ebru Arioglu Inan, Ankara University, Turkey

Reviewed by:
Nazareno Paolocci, Johns Hopkins University, United States
Carlo Gabriele Tocchetti, University of Naples Federico II, Italy

***Correspondence:**
Barbara K. Kemp-Harper
Barbara.Kemp@monash.edu

Specialty section:
This article was submitted to Cardiovascular and Smooth Muscle Pharmacology, a section of the journal Frontiers in Pharmacology

Received: *01 March 2020*
Accepted: *01 May 2020*
Published: *19 May 2020*

Citation:
Velagic A, Qin C, Woodman OL, Horowitz JD, Ritchie RH and Kemp-Harper BK (2020) Nitroxyl: A Novel Strategy to Circumvent Diabetes Associated Impairments in Nitric Oxide Signaling. Front. Pharmacol. 11:727. doi: 10.3389/fphar.2020.00727

INTRODUCTION

Globally, over 460 million individuals have diabetes, and this figure is projected to increase to 700 million by the year 2045 (Saeedi et al., 2019). It is estimated that 90% of these individuals have type 2 diabetes mellitus (T2DM), and approximately 10% have type 1 diabetes mellitus (T1DM) (International Diabetes Federation, 2019). The leading cause of morbidity and mortality in individuals with either diabetes subtype is cardiovascular disease (Htay et al., 2019). Individuals with diabetes have an elevated risk of coronary artery disease, peripheral vascular disease, ischemic stroke and heart failure (Almourani et al., 2019). These cardiovascular complications arise largely as a consequence of hyperglycemia-induced oxidative stress, which impairs nitric oxide (NO•)

signaling at the level of synthesis and responsiveness (Fiorentino et al., 2013). This loss in NO• responsiveness, termed 'NO• resistance,' results largely due to "scavenging" of NO• by superoxide and inactivation of its target, soluble guanylyl cyclase (sGC) (Paolocci et al., 2001a; Worthley et al., 2007; Ritchie et al., 2017). NO• resistance affects multiple sites in the cardiovascular system, including the myocardium, vasculature and platelets (Qin et al., 2020). As such, patients with diabetes fail to respond to the anti-aggregatory and vasodilator effects of NO•-based pharmacotherapies during cardiovascular emergencies, such as acute myocardial infarction, transient myocardial ischemia and acute decompensated heart failure (Dautov et al., 2013). Several pharmacotherapies including statins, some angiotensin-converting enzyme (ACE) inhibitors, perhexiline, and insulin (in the presence of severe hyperglycemia) ameliorate NO• resistance (Chirkov and Horowitz, 2007), while sGC activators primarily circumvent the problem (Costell et al., 2012). However, there are limitations associated with their clinical utility, particularly as these amelioration strategies are not instantaneously effective, and thus unsuitable for emergency situations. On the contrary, nitroxyl (HNO) donors circumvent NO• resistance and thus promote vasodilation, while uniquely inducing positive inotropic and lusitropic responses that persist in conditions of oxidative stress (e.g. heart failure, diabetes) where responses to NO• are diminished (Paolocci et al., 2003; Chin et al., 2016; Tare et al., 2017; Qin et al., 2020). Although the aforementioned cardiovascular changes are associated with both T1DM and T2DM, due to the prevalence of the latter, this review will explore the major mechanisms that drive impairments in NO• signaling in T2DM, and highlight the therapeutic potential of HNO donors to circumvent this problem, in order to alleviate acute hemodynamic complications in T2DM.

NITRIC OXIDE SIGNALING IN THE CARDIOVASCULAR SYSTEM

Nitric Oxide Synthesis

NO• plays an important role in maintaining cardiovascular homeostasis. This occurs through its vasodilator capacity, inhibition and reversal of platelet aggregation, suppression of inflammation and oxidative stress, inhibition of thrombosis and modulation of vascular smooth muscle cell (VSMC) proliferation and vascular remodeling (Napoli et al., 2006; Ignarro, 2019). NO• is endogenously synthesized by three isoforms of the NO• synthase (NOS) enzyme, specifically, neuronal NOS (nNOS), inducible NOS (iNOS) and endothelial NOS (eNOS), also known as NOS1, NOS2 and NOS3, respectively (Salerno et al., 2018). All three enzymes consist of two subunits, an N-terminal oxygenase domain that binds the substrate L-arginine, cofactor tetrahydrobiopterin (BH_4) and a heme iron group, and a C-terminal reductase domain that binds nicotinamide adenine dinucleotide phosphate (NADPH), flavin adenine dinucleotide phosphate (FAD) and flavin mononucleotide (FMN) (Qian and Fulton, 2013). Between these domains, exists a calmodulin binding sequence, that binds calcium (Ca^{2+}) (Förstermann and Sessa, 2012).

eNOS is considered the predominant isoform constitutively expressed in the cardiovascular system, where it is responsible for the synthesis of NO• in endothelial cells, cardiomyocytes and platelets (Radziwon-Balicka et al., 2017; Ritchie et al., 2017). In endothelial cells, eNOS produces NO• in response to stimulation by shear stress or receptor agonists including bradykinin, acetylcholine, substance P, thrombin, histamine or β-adrenoceptor agonists (Premer et al., 2019). Under basal conditions, eNOS is present in an inactive state bound to either caveolin-1 or caveolin-3, which are located in small invaginations of the plasma membrane known as caveolae, in endothelial cells or cardiomyocytes, respectively (Massion et al., 2003). Upon stimulation by shear stress or agonists, intracellular Ca^{2+} levels increase, leading to recruitment of the Ca^{2+}-calmodulin sequence, which displaces caveolin-1 or caveolin-3 from the enzyme leading to eNOS activation (Förstermann and Sessa, 2012). Subsequently, the cofactor BH_4 and heat shock protein 90 (hsp90) are recruited, together with protein kinase B/Akt, which phosphorylates Ser^{1177}, thereby activating eNOS (Sharma et al., 2012). This leads to electron transfer from NADPH by FAD and FMN, allowing O_2 to bind to the heme iron group on eNOS, resulting in the conversion of L-arginine to NO• and L-citrulline (Stuehr et al., 2004; Mancardi et al., 2005). NO• is also generated from NOS-independent sources such as from nitrite and dietary nitrate. In brief, following absorption of dietary nitrate from the gastrointestinal tract, salivary commensal bacteria reduce nitrate to nitrite. Nitrite can then circulate and be converted to NO• via the nitrite reductase activity of several proteins (e.g. deoxyhemoglobin, xanthine oxidoreductase), providing a NOS-independent pathway for NO• generation (Farah et al., 2018). The major physiological modulator of eNOS activity appears to be tissue concentrations of the competitive NOS antagonist asymmetric dimethylarginine (ADMA) (Böger, 2004; Cooke, 2005).

Nitric Oxide Signaling in the Vasculature

NO• signals predominantly via its intracellular receptor, sGC. In the vasculature, endothelium-derived NO• diffuses into underlying VSMCs in a paracrine manner, where it binds to the ferrous (Fe^{2+}) heme iron on sGC (Mancardi et al., 2005; Korkmaz et al., 2018). Activation of sGC leads to the production of 3,5-cyclic guanosine monophosphate (cGMP), intracellular levels of which are regulated by phosphodiesterases (PDEs), which hydrolyze cGMP to GMP (Kass et al., 2007). cGMP effectors include cGMP-dependent protein kinases (cGKs), PDEs and cGMP-gated ion channels (Kemp-Harper and Schmidt, 2009). cGKs phosphorylate target proteins leading to a reduction in intracellular Ca^{2+} concentration, resulting in VSMC relaxation and vasodilation, and suppression of VSMC proliferation (Kemp-Harper and Schmidt, 2009) (**Figure 1**). Similarly, the anti-aggregatory actions of NO• are mediated predominantly via the sGC/cGMP signaling pathway. Thus NO• generated by the endothelium diffuses into the blood vessel lumen where it inhibits platelet aggregation, platelet adhesion to the vascular wall, and thrombosis (Förstermann and Sessa, 2012).

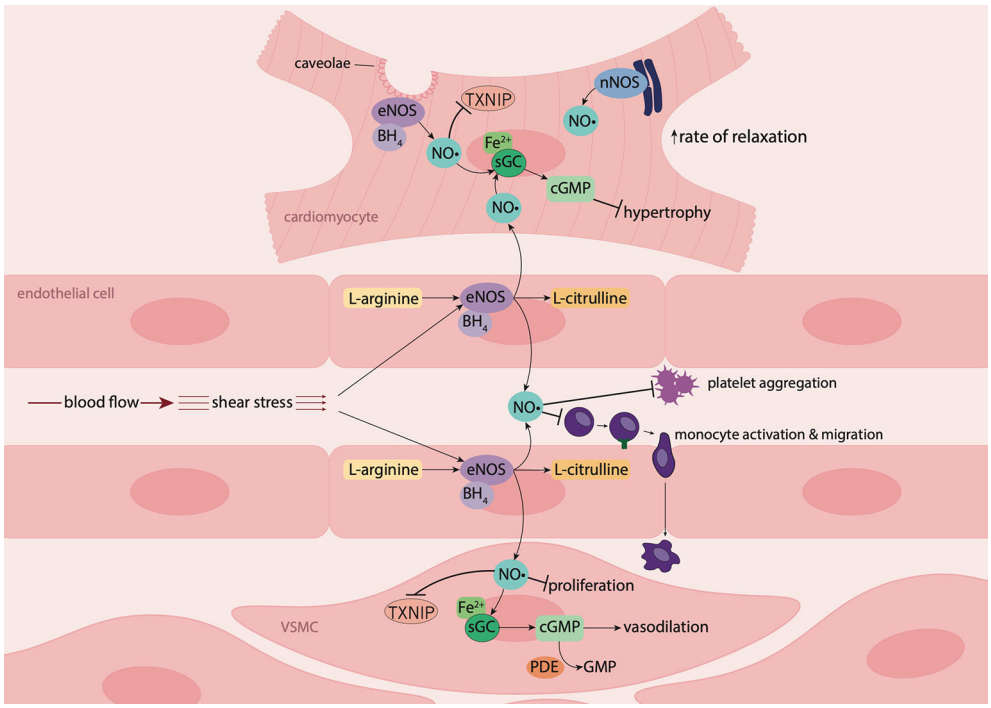

FIGURE 1 | Nitric oxide signaling in the vasculature and myocardium. In endothelial cells and cardiomyocytes, nitric oxide (NO•) is produced by endothelial nitric oxide synthase (eNOS) following stimulation by shear stress (blood flow) or the presence of agonists such as bradykinin. Upon stimulation, the cofactor tetrahydrobiopterin (BH_4) is recruited, resulting in the conversion of L-arginine to NO• and L-citrulline. In the vascular lumen, NO• inhibits platelet aggregation and leukocyte adhesion and migration. NO• produced by endothelial cells diffuses into underlying vascular smooth muscle cells (VSMCs) where it suppresses proliferation and binds to the ferrous (Fe^{2+}) heme group on its biological target, soluble guanylyl cyclase (sGC). Activation of sGC leads to the production of 3',5'-cyclic guanosine monophosphate (cGMP) resulting in vasodilation. NO• produced by endothelial cells from coronary vessels, diffuses into cardiomyocytes, where in combination with NO• produced intracellularly by eNOS and neuronal nitric oxide synthase (nNOS), induces myocardial relaxation, and has anti-hypertrophic effects. NO• also suppresses thioredoxin-interacting protein (TXNIP) formation in cardiomyocytes and the vasculature.

NO• also signals independently of sGC via direct protein S-nitrosylation: NO• reacts with thiols on cysteine residues of target proteins, resulting in modulation of their biological functions (Mancardi et al., 2005; Lima et al., 2010). This is of particular relevance in the vasculature whereby NO• limits superoxide generation via S-nitrosylation of $p47^{phox}$, a critical subunit of the reactive oxygen species (ROS)-generating enzyme, nicotinamide adenine dinucleotide phosphate (NADPH) oxidase 2 (Nox2) (Selemidis et al., 2007), thus protecting against vascular oxidative stress.

Moreover, NO• plays a key anti-inflammatory/anti-atherogenic role, with an ability to limit the activation and transmigration of monocytes through the endothelium to the site of vascular injury via the reduction of endothelial adhesion molecules [e.g. vascular adhesion molecule-1 (VCAM-1); (Spiecker et al., 1997)], chemokine [e.g. monocyte chemoattractant protein-1 (MCP-1); (Zeiher et al., 1995)] and cytokine expression (e.g. interleukin-6 (IL-6); (De Caterina et al., 1995)). These actions of NO• may be explained, in part, by its inhibitory effects on nuclear factor kappa-B (NF-κB) and NLRP3 inflammasome activation. NO• suppresses NF-κB signaling via S-nitrosylation of its regulatory subunit and transcription factor, IKKβ and p65, respectively (Qian and Fulton, 2012). This leads to decreased expression of pro-inflammatory and pro-atherogenic mediators including intracellular adhesion molecule-1 (ICAM-1), VCAM-1 (Spiecker et al., 1997; Qian and Fulton, 2012), MCP-1 and IL-6 (De Caterina et al., 1995; Zeiher et al., 1995). Moreover, NO• regulates the NLRP3 inflammasome, which is a multiprotein signaling complex expressed in macrophages, that activates caspase-1, resulting in the maturation and secretion of the pro-inflammatory cytokines, interleukin-1β (IL-1β) and interleukin-18 (IL-18) (Chen and Sun, 2013). NO• inhibits NLRP3 inflammasome activation, likely via suppression of expression of the NLRP3 activator thioredoxin-interacting protein (TXNIP) (Sverdlov et al., 2013; Chong et al., 2015), thus decreasing caspase-1 activation and secretion of mature IL-1β and IL-18 (Hernandez-Cuellar et al., 2012; Mao et al., 2013). In addition, NO• also has the capacity to limit mast cell degranulation, reducing the release of inflammatory mediators and cytokines and thereby inhibiting the initiation of acute vascular inflammatory processes (Coleman, 2002).

Overall, the entire spectrum of endogenous NO• effects is pro-homeostatic, and confers protection against both atherosclerotic plaque development and rupture. Indeed, NO• normally functions as a 'firehose', dousing out the flames of

incipient plaque rupture and protecting against acute cardiovascular events.

Nitric Oxide Signaling in the Myocardium

As in the vasculature, NO• plays a key role in the regulation of heart function. NO•, generated by endothelial cells lining the coronary vasculature, diffuses into cardiomyocytes where, in combination with cardiomyocyte nNOS and eNOS-derived NO•, it has anti-hypertrophic effects, enhances myocardial relaxation and improves left ventricular diastolic distensibility (Rosenkranz et al., 2002; Paulus and Bronzwaer, 2004). These actions of NO• are mediated via sGC/cGMP signaling, and are cGK-dependent. cGK modulates excitation-contraction coupling through phosphorylation of troponin I, myosin-binding protein C and titin, thus decreasing myofilament Ca^{2+} sensitivity (Farah et al., 2018). cGK also phosphorylates phospholamban on the sarcoplasmic reticulum Ca^{2+}-ATPase pump (SERCA2a) pump, increasing Ca^{2+} reuptake into the sarcoplasmic reticulum (Ritchie et al., 2009). Moreover, cGK suppresses L-type calcium channel activity, further decreasing intracellular Ca^{2+} levels, which attenuates the positive inotropic effects of beta-adrenergic signaling, thus promoting cardiomyocyte relaxation (Massion et al., 2003). cGK also has anti-hypertrophic effects, due to its ability to regulate Ca^{2+} current by modulating L-type Ca^{2+} channel activity, suppress mitogen-activated protein kinases, and inhibit myocyte growth and expression of hypertrophic genes (Ritchie et al., 2009). NO• also modulates myocardial energetic production through its actions on mitochondria, where it inhibits mitochondrial respiration and glucose uptake, and promotes free fatty acid uptake (Massion et al., 2003; Paulus and Bronzwaer, 2004).

IMPAIRED CARDIOVASCULAR NITRIC OXIDE SIGNALING IN DIABETES

Impaired NO• signaling is present in a wide range of forms of cardiovascular pathologies and has been documented in obesity, diabetes, hypertension, atherosclerosis, congestive cardiac failure, aortic stenosis, angina pectoris, unstable angina, hyperglycemia/diabetes, myocardial infarction, acute atrial fibrillation, ageing and polycystic ovarian syndrome (Lees et al., 1998; Chirkov and Horowitz, 2007; Sverdlov et al., 2014). In the presence of most coronary risk factors, NO• signaling is impacted with evidence of a reduction in both synthesis of and responsiveness to NO• (Worthley et al., 2007; Ito et al., 2015).

Impaired Nitric Oxide Generation

With regard to NO• generation, severe hyperglycemia can lead to an impairment via reduction of the critical eNOS cofactor BH_4, increased ADMA, eNOS uncoupling, increased arginase activity and decreased nitrite reduction (Tousoulis et al., 2013; Kövamees et al., 2016). Reduced BH_4 levels have been identified in human umbilical vein endothelial cells exposed to high glucose conditions, and in aortae isolated from diabetic mice (Xu et al., 2007). In this study, hyperglycemia decreased BH_4 levels via inhibition of 26S proteasome activity of guanosine 5'-triphosphate cyclohydrolase I (GTPCH), which is a rate-limiting enzyme of BH_4 synthesis, and increased levels of peroxynitrite, which oxidizes BH_4 to dihydrobiopterin (BH_2), thereby uncoupling eNOS (Xu et al., 2007). The authors also found attenuated endothelium-dependent vasodilation in response to acetylcholine in aortae from diabetic mice, indicating impaired vascular generation or responsiveness to NO• per se (Xu et al., 2007). Similarly, increases in forearm blood flow in response to acetylcholine, measured by venous occlusion plethysmography, were impaired in individuals with T2DM, when compared to non-diabetic controls (Heitzer et al., 2000). Interestingly, concomitant infusion of BH_4 improved forearm blood flow responses to acetylcholine in T2DM, indicating that the observed impairment in endothelium-dependent vasodilation, and hence NO• generation, may be due to decreased BH_4 (Heitzer et al., 2000).

NOS competes with arginases and arginine methyltransferases (PRMT), for its substrate, L-arginine. Arginase converts L-arginine into L-ornithine or urea, and arginase activity is elevated in disease states associated with endothelial dysfunction, including T2DM (Shemyakin et al., 2012; Kövamees et al., 2016). Similarly, PRMT catalyze the methylation of L-arginine to monomethylarginine (MMA), which is converted to ADMA by type 1 PRMT (Zakrzewicz and Eickelberg, 2009). ADMA is a competitive NOS inhibitor, reducing NO• generation (Vallance et al., 1992). Indeed, plasma ADMA levels have been proposed as a clinically relevant biomarker of endothelial dysfunction and cardiovascular disease (Zhou et al., 2017). Thus, a reduction in endothelium-dependent vasodilation in patients with T2DM, following ingestion of a high fat meal, has been associated with increased levels of ADMA (Fard et al., 2000). However, surprisingly ADMA concentrations are paradoxically lower in diabetic than non-diabetic patients (Horowitz et al., 2018), suggesting that NO• generation by NOS activation is not a major problem in such individuals.

An interesting point for consideration is that endothelial dysfunction has a component of NO• resistance that is difficult to dissect in individual patients by NOS-dependent activation, such as administration of acetylcholine and salbutamol. Thus, it is unclear whether the observed "endothelial dysfunction" is predominantly a reflection of decreased eNOS activity and/or of impaired ability of NO• to signal per se. This distinction between "endothelial dysfunction" and isolated NO• resistance was highlighted in a study by Okon et al., where sensitivity to the endothelium-dependent vasodilator acetylcholine was 10-fold lower in mammary arteries from patients with T2DM, compared to non-diabetic patients, indicating endothelial dysfunction (Okon et al., 2005). Moreover, eNOS gene and protein expression was decreased in T2DM mammary arteries by approximately 50 and 30%, respectively, compared to non-diabetic counterparts (Okon et al., 2005). However, while this reduction in vasodilator response to acetylcholine in T2DM could be due to impaired NO• generation as a consequence of decreased eNOS expression and activity, the authors also found

that the vasodilator responses to the endothelium-independent NO• donor, sodium nitroprusside (SNP), were also attenuated in T2DM mammary arteries, indicating reduced vascular responsiveness to NO•, and hence the presence of NO• resistance. Similarly, brachial-artery flow-mediated vasodilation was found to be impaired in patients with T2DM with or without coronary heart disease, when compared to age- and sex-matched non-diabetic controls (Ito et al., 2015). However, the authors did not examine endothelium-independent vasodilation via the use of a NO• donor such as SNP. Therefore, in this study, it is unclear whether the impairment in brachial-artery flow mediated vasodilation in patients with T2DM was due to impaired vascular NO• generation or signaling or both. This highlights the importance of testing vascular responsiveness to a NO• donor to delineate the bases for impaired responses to NOS activators.

Nitric Oxide Resistance

NO• resistance represents a multifaceted disorder, in which impairments in NO• signaling lead to diminished NO•-responsiveness in platelets, the vasculature and myocardium, resulting in a loss in the vaso- and cardio-protective effects of endogenous and exogenous NO• (Chirkov and Horowitz, 2007). In patients with cardiovascular disease, the presence of NO• resistance is an independent predictor of adverse cardiovascular events and mortality risk (Schachinger et al., 2000; Willoughby et al., 2012). Several studies have identified NO• resistance in T2DM (Williams et al., 1996; van Etten et al., 2002; Anderson et al., 2005; Okon et al., 2005; Shemyakin et al., 2012). In platelets, the NO• donor SNP inhibited aggregation by 15.4 ± 7% in T2DM, compared to 73.1 ± 5.9% in healthy controls, indicating decreased platelet responsiveness to NO• in T2DM, and thus the presence of NO• resistance (Anderson et al., 2005). In studies by Williams et al., and van Etten et al., patients with T2DM displayed vascular NO• resistance, indicated by reduced brachial artery flow-mediated vasodilation in response to SNP, compared to healthy controls (Williams et al., 1996; van Etten et al., 2002). Similarly, vasodilator response of the brachial artery in response to intra-arterial infusion of SNP was lower in patients with coronary artery disease and T2DM, compared to healthy controls, indicating decreased VSMC responsiveness to NO•, and thus NO• resistance (Shemyakin et al., 2012). To the best of our knowledge, the presence of myocardial NO• resistance has not thus far been examined in T2DM. However, in a rat model of T1DM, both myocardial contractile and relaxation responses to the NO• donor diethylamine-NONOate (DEA/NO) were impaired, establishing the presence of myocardial NO• resistance in T1DM (Qin et al., 2020). Thus, it is probable that NO• resistance also occurs at the level of the human myocardium in T2DM, particularly as platelet and vascular responsiveness to NO• is diminished in these patients. Although the pathogenesis of T2DM is different to that of T1DM, they are both characterized by hyperglycemia, and associated with oxidative stress, both of which can contribute to impairment of NO• signaling (Fiorentino et al., 2013).

OXIDATIVE STRESS AS A CONTRIBUTOR TO NITRIC OXIDE RESISTANCE

NO• resistance occurs largely due to oxidative stress, where ROS scavenge NO• and reversibly inactivate sGC, resulting in impaired tissue responsiveness to endogenous or exogenous NO• (Dautov et al., 2013; Tare et al., 2017). Oxidative stress refers to an imbalance between the generation of ROS and their clearance by endogenous antioxidants, such as superoxide dismutase, catalase and glutathione peroxidase (Wink et al., 2001). ROS consist of free-radical species, including superoxide, peroxyl, hydroxyl and hydroperoxyl, and non-radicals, such as hydrogen peroxide, peroxynitrite and hypochlorous acid (Phaniendra et al., 2015). They are generated by the mitochondrial electron transport chain, in addition to several other sources including xanthine oxidase, NADPH oxidases, iNOS, and uncoupled eNOS (Brownlee, 2005; Pignatelli et al., 2018).

ROS have a marked impact on NO• generation and signaling. Specifically, NO• reacts rapidly with superoxide forming the powerful oxidant peroxynitrite, which reduces the bioavailability of NO• (Ritchie et al., 2017). In Langendorff-perfused rat hearts, superoxide directly quenches NO•, reducing basal- and agonist-induced NO• release and subsequent vasodilation of the coronary vasculature, in the absence of modifications in eNOS expression or activity (Paolocci et al., 2001a). Peroxynitrite uncouples eNOS by oxidizing BH_4 to BH_2, which leads to electron donation to molecular oxygen (O_2), resulting in the generation of superoxide, further exacerbating oxidative stress (Farah et al., 2018). In addition, peroxynitrite is able to oxidize the ferrous (Fe^{2+}) heme group on sGC to its ferric (Fe^{3+}) state, desensitizing the enzyme to NO•. Furthermore, oxidation of the heme group weakens its binding, resulting in a heme-free form of sGC which is susceptible to ubiquitin-dependent degradation (Meurer et al., 2009). Consequently, tissue responsiveness to endogenous and exogenous NO• is impaired, resulting in NO• resistance (Ritchie et al., 2017) (**Figure 3**).

Hyperglycemia-Induced Oxidative Stress

In T2DM, hyperglycemia can lead to oxidative stress via increased NADPH oxidase activity, overproduction of mitochondrial ROS and elevated expression of TXNIP (**Figure 2**) (Aon et al., 2015). Elevated myocardial NADPH oxidase-derived superoxide production has been identified in a mouse model of T2DM, and was found to exacerbate left ventricular remodeling and heart failure post-myocardial infarction, when compared to non-diabetic controls (Matsushima et al., 2009). Moreover, internal mammary arteries from patients with T2DM undergoing coronary bypass surgery, displayed elevated NADPH oxidase-derived superoxide levels, and increased membrane translocation of the Nox1/2 regulatory subunits $p47^{phox}$ and Rac1 (Antonopoulos et al., 2015). Nox1 and Nox2 are the major sources of ROS in the vascular wall (Drummond et al., 2011). Therefore, increased membrane translocation of their regulatory subunits $p47^{phox}$ and

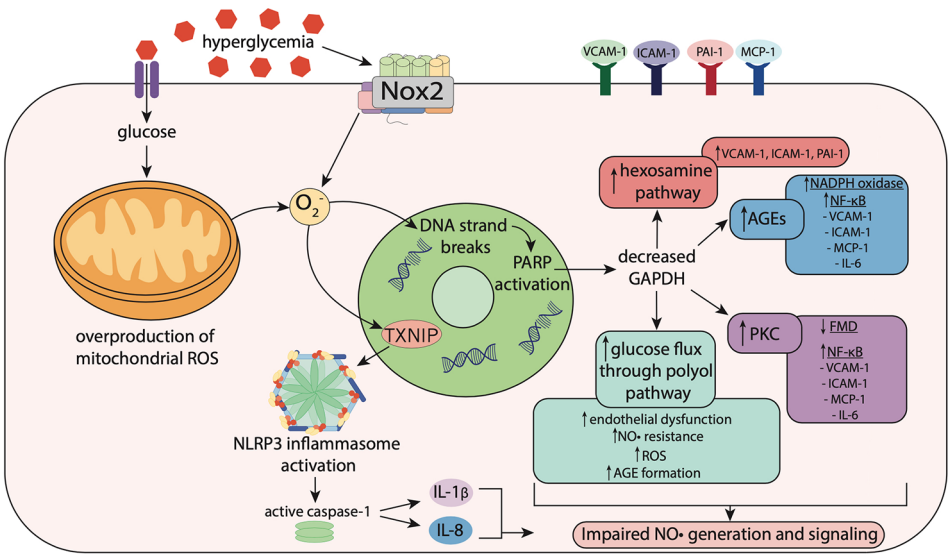

FIGURE 2 | Hyperglycemia-induced oxidative stress impairs nitric oxide signaling. Hyperglycemia induces oxidative stress via increased activity of nicotinamide adenine dinucleotide phosphate (NADPH) oxidase (Nox) enzymes including Nox2, resulting in superoxide (O_2^-) generation. In mitochondria, hyperglycemia increases reactive oxygen species (ROS) production including O_2^-, which stimulates thioredoxin-interacting protein (TXNIP) expression. TXNIP promotes activation of the NLRP3 inflammasome, which activates caspase-1, resulting in the maturation and secretion of the pro-inflammatory cytokines, interleukin-1β (IL-1β) and interleukin-18 (IL-18). O_2^- also causes strand breaks in DNA, leading to activation of poly (ADP-ribose) polymerase (PARP), which reduces activity of glyceraldehyde-3 phosphate dehydrogenase (GAPDH). Decreased GAPDH activity leads to overactivation of the hexosamine pathway, upregulation of protein kinase C (PKC), elevated glucose flux through the polyol pathway and increased formation of advanced glycation end-products (AGEs). This leads to activation of Nox and NF-κB signaling, resulting in increased expression of pro-inflammatory and pro-atherogenic mediators including vascular adhesion molecule-1 (VCAM-1), intracellular adhesion molecule-1 (ICAM-1), monocyte chemoattractant protein-1 (MCP-1), plasminogen activator inhibitor-1 (PAI-1) and interleukin-6 (IL-6). Upregulation of these pathways results in impaired flow-mediated vasodilation, reflecting both endothelial dysfunction and nitric oxide (NO•) resistance.

Rac1 suggests that activation of Nox1/2 is elevated in the vasculature in T2DM.

Hyperglycemia can also stimulate overproduction of mitochondrial ROS, as higher levels of intracellular glucose-derived pyruvate increase flux of electron donors NADH and $FADH_2$ into the electron transport chain (Giacco and Brownlee, 2010). This increases the voltage gradient across the mitochondrial membrane, preventing electron transfer within complex III (Giacco and Brownlee, 2010). Consequently, electrons accumulate at coenzyme Q_{10}, which donates electrons to molecular oxygen, resulting in superoxide generation, which combined with superoxide generated from other sources such as NADPH oxidase, causes DNA strand breaks (Pacher and Szabó, 2005; Giacco and Brownlee, 2010). This results in activation of poly (ADP-ribose) polymerase (PARP), an enzyme involved in DNA repair, which under normal conditions, resides within the nucleus in an inactive state (Brownlee, 2005). Once activated, PARP modifies the glycolytic enzyme glyceraldehyde-3 phosphate dehydrogenase (GAPDH), reducing its activity (Brownlee, 2005). Decreased GAPDH activity leads to overactivation of the hexosamine pathway, upregulation of protein kinase C (PKC), elevated glucose flux through the polyol pathway and increased formation of advanced glycation end-products (AGEs), all of which can promote impairments in NO• generation and/or signaling (Fiorentino et al., 2013) (**Figure 2**).

Hexosamine Pathway

In the hexosamine pathway, O-GlcNAc transferase (OGT) catalyzes a post-translational modification, known as O-GlcNAcylation, of proteins modulating their biological activity (Qin et al., 2017). Increased O-GlcNAcylation has been identified in patients with T2DM (Degrell et al., 2009; Springhorn et al., 2012). Overactivation of this pathway can lead to elevated endothelial expression of the pro-inflammatory and pro-atherogenic mediators VCAM-1, ICAM-1 and plasminogen activator inhibitor-1 (PAI-1) (Fiorentino et al., 2013) (**Figure 2**). A recent study identified decreased NO• production, reduced eNOS expression, and increased O-GlcNAcylation of eNOS in perivascular adipose tissue from thoracic aortae from rats with metabolic syndrome (da Costa et al., 2018). As a result, the anti-contractile capacity of the perivascular adipose tissue was diminished (da Costa et al., 2018). Moreover, increased O-GlcNAcylation of myocardial proteins has been associated with cardiac dysfunction in mouse models of T2DM (Fülöp et al., 2007; Marsh et al., 2011).

Protein Kinase C

PKC consists of a family of serine/threonine kinases, which play an important role in signal transduction of several vascular functions, including regulation of angiogenesis, endothelial cell permeability, extracellular matrix deposition and vasoconstriction (Kizub et al., 2014). In a study by Tabit et al., in patients with T2DM, endothelial

expression of PKCβ was elevated and associated with impaired flow-mediated dilation of the brachial artery (Tabit et al., 2013). The authors also found increased endothelial levels of the peroxynitrite derivative nitrotyrosine, and elevated activity of NF-κB, indicating the presence of endothelial inflammation and nitrosative/oxidative stress in T2DM (Tabit et al., 2013).

The Polyol Pathway

In the polyol pathway, glucose is reduced to sorbitol by aldose reductase, which consumes NADPH in the process (Chandra et al., 2002). NADPH consumption limits NO• production and exacerbates oxidative stress, as NADPH is required for the production of NO• and the antioxidant reduced glutathione (Ramana et al., 2003; Lorenzi, 2007). The deleterious effects of sorbitol on the microvasculature have been demonstrated in rat gracilis arterioles, where exposure to sorbitol stimulated vascular production of ROS, and impaired endothelium-dependent and endothelium-independent vasodilation to a NO• donor, indicating that sorbitol can induce endothelial dysfunction with a substantial component of NO• resistance (Toth et al., 2007) (**Figure 2**). In addition, methylglyoxal, an intermediate of this pathway, is implicated in endothelial dysfunction and elevated in patients with T2DM (Wang et al., 2007; Lund et al., 2011). Methylglyoxal is also a potent glycating agent that reacts with intracellular and extracellular proteins, resulting in the formation of AGEs (Lund et al., 2011).

Advanced Glycation End-Products

AGEs are formed during non-enzymatic reactions between reducing sugars or sugar-derived products and amino groups on proteins, lipids or nucleic acids (Barlovic et al., 2010). AGEs and their receptor (receptor for AGEs; RAGE) play a central role in the pathogenesis of vascular complications (Thomas et al., 2005). In patients with T2DM, plasma levels of AGEs are elevated, and negatively correlated with endothelium-dependent and endothelium-independent vasodilation (Tan et al., 2002). Moreover, plasma levels of AGEs are approximately 74% higher in patients with T2DM with vascular complications, compared to those with T2DM without vascular complications (Farhan and Hussain, 2019). Activation of RAGE by AGEs also stimulates NADPH oxidase, increasing intracellular ROS generation, subsequently activating NF-κB, resulting in the production of pro-inflammatory and pro-atherogenic mediators, including IL-6, VCAM-1, ICAM-1 and MCP-1 (Barlovic et al., 2010) (**Figure 2**). Consequently, oxidative stress and inflammation are exacerbated, leading to further impairments in NO• signaling (Andrews et al., 2016). NF-κB activation also stimulates NO• generation by iNOS, however, when superoxide levels are elevated, superoxide anions react with NO• forming peroxynitrite (Wright et al., 2006). This leads to a loss of the inhibitory effects of iNOS-derived NO• on mast cell stabilization (Coleman, 2002), which is critical for prevention of plaque rupture and coronary vasospasm, which precede most ischemic emergencies (Kovanen et al., 1995; Laine et al., 1999).

Thioredoxin-Interacting Protein (TXNIP)

Hyperglycemia is also associated with increased expression of TXNIP via the glucose-response element in its gene (Turturro et al., 2007). Thioredoxin (TRX) is a key modulator of intracellular redox stress, possessing antioxidant activity. TXNIP serves as a negative regulator of TRX and contributes to oxidative stress in diabetes, in addition to promoting inflammation with a key role in NLRP3 inflammasome activation (Schulze et al., 2004; Zhou et al., 2010) (**Figure 2**). TXNIP gene expression is elevated in peripheral bone mononuclear cells from patients with T2DM, compared to patients with T1DM and non-diabetic controls (Szpigel et al., 2018). This increase in TXNIP was accompanied by elevated gene expression of NLRP3 and IL-1β, indicating that TXNIP promotes inflammation in T2DM through activation of the NLRP3 inflammasome (Szpigel et al., 2018). These actions of TXNIP are likely to negatively impact NO• signaling in T2DM. Indeed, a reciprocal relationship between platelet NO• responsiveness and TXNIP expression has been demonstrated (Sverdlov et al., 2013).

Collectively, these data provide robust evidence for a key role of oxidative stress and inflammation in the development of cardiovascular complications in T2DM. Central to the disease pathology is an impairment in endogenous and exogenous NO• signaling. Taking into consideration the more prominent role of NO• resistance in impaired NO• signaling in diabetes, there is a strong therapeutic focus on overcoming NO• resistance in this disease setting.

CURRENT AND EMERGING PHARMACOTHERAPIES TO OVERCOME IMPAIRED NITRIC OXIDE SIGNALING: A FOCUS ON NITRIC OXIDE RESISTANCE

As highlighted, NO• resistance is particularly debilitating in T2DM, where the mortality risk associated with cardiovascular emergencies is increased (e.g. acute myocardial infarction, transient myocardial ischemia, acute pulmonary edema) (Lindholm et al., 2005). In these circumstances, rapid vasodilator and anti-aggregatory actions are required yet NO•-based pharmacotherapies are ineffective. Thus, whilst nitrovasodilators, including the organic nitrate glyceryl trinitrate (GTN), have been clinically utilized since 1876 for the treatment of angina pectoris and heart failure (Sun et al., 2011), their effectiveness is diminished in the very conditions for which they are most needed. As such, NO•-independent therapeutic approaches aimed at ameliorating or circumventing NO• resistance, particularly to manage cardiovascular emergencies, are urgently required for the diabetic population.

Amelioration Strategies

A number of treatments, including some ACE inhibitors, perhexiline, statins, and reversal of severe hyperglycemia have been shown to ameliorate NO• resistance (**Table 1**).

ACE Inhibitors

Increased activity of the renin-angiotensin system and the generation of angiotensin II, which possesses pro-oxidative, pro-inflammatory and vasoconstrictive properties, is associated with many cardiovascular diseases (Ruszkowski et al., 2019). The ACE inhibitors ramipril and perindopril decrease the formation

of angiotensin II, and in large clinical trials (HOPE, Heart Outcomes Prevention Evaluation; EUROPA, European Trial on Reduction of Cardiac Events with Perindopril), have been shown to reduce the incidence of myocardial infarction, cardiac arrest, heart failure, stroke and diabetes-related complications in aging, high-risk adults with vascular disease or diabetes (Yusuf et al., 2000; Fox, 2003).

Whilst the precise mechanisms underlying the improved cardiovascular outcomes following treatment with ramipril or perindopril remain unclear, an ability of these ACE inhibitors to ameliorate NO• resistance may contribute to treatment benefit. Ramipril and perindopril have been shown to improve NO• donor responsiveness, at least at the level of the platelet. In individuals with chronic heart failure, treatment with perindopril for 4 days improved platelet responsiveness to SNP, reducing the proportion of subjects with platelet NO• resistance from 40 to 0% (Chirkov et al., 2004). Similarly, the effect of ramipril on platelet responsiveness to SNP was assessed in a randomized, placebo-controlled, blinded study in older adults (aged ≥50 years) of high cardiovascular risk (history of stroke, coronary artery disease, peripheral vascular disease and/or diabetes) (Willoughby et al., 2012). In this study, 3 months of ramipril therapy decreased systolic and diastolic pressure, and reduced augmentation index (Aix) and plasma levels of ADMA, markers of arterial stiffness and endothelial dysfunction, respectively (Willoughby et al., 2012). The authors also identified a separate group of participants with diabetes, who displayed severe platelet NO• resistance at baseline, in which ramipril therapy for 2 weeks improved platelet responsiveness to SNP, suggesting improved sensitivity of sGC to NO• (Willoughby et al., 2012).

Based on these findings, it is clear that long-term therapy with the ACE inhibitors ramipril or perindopril overcomes NO• resistance and provides protection against adverse cardiovascular events in high-risk populations. However, ACE inhibitor-mediated reversal of NO• resistance is not an option for patients who are intolerant of ACE inhibition, many of whom are diabetic (Neutel, 2010; DuMond and King, 2011). Moreover, the use of ACE inhibitors to attenuate NO• resistance in a cardiovascular emergency is clinically impracticable with the CONSENSUS II study (Cooperative New Scandinavian Enalapril Survival Study II) showing that the intravenous administration of the ACE inhibitor, enalaprilat, within 24 h of an acute myocardial infarct, increased mortality (Swedberg et al., 1992).

Perhexiline

The anti-anginal agent, perhexiline, has shown some promise with regard to ameliorating NO• resistance. Used in patients refractory to commonly used antianginal therapies, the anti-ischemic properties of perhexiline are attributed to its ability to inhibit the mitochondrial enzyme carnitine palmitoyltransferase, leading to the reduction in fatty acid metabolism and a shift to greater carbohydrate metabolism by the myocardium (oxygen sparing effect) (Ashrafian et al., 2007). In addition, perhexiline limits oxidative stress via inhibition of NADPH oxidase (Kennedy et al., 2006). Studies have demonstrated an ability of perhexiline to improve platelet SNP responsiveness in patients with stable angina pectoris (Chirkov et al., 2001), acute coronary syndromes (Willoughby et al., 2002) and aortic stenosis (Chirkov et al., 2002). However, the clinical utility of perhexiline is limited due to its complex pharmacokinetics and potential to cause hepatic- and neuro-toxicity, necessitating close therapeutic monitoring (Chong et al., 2016).

Statins

Statins are lipid-lowering drugs that are primarily used to treat hypercholesterolemia and prevent the progression of cardiovascular disease (Ko et al., 2019). Whilst statin therapy is associated with improvement in endothelial function in patients with cardiovascular disease (Reriani et al., 2011), evidence in support of an ability of statins to ameliorate vascular NO• resistance is conflicting. Thus, in patients with T1DM, atorvastatin (40 mg/day; 6 weeks) was shown to improve nitroglycerin-mediated dilatation in the brachial artery (Dogra et al., 2005). Similarly, following an acute coronary syndrome, atorvastatin treatment (80 mg/day, 16 weeks) lead to an improvement in GTN-mediated dilation (Dupuis et al., 2005). By contrast, atorvastatin (40 mg/day; 6 weeks) therapy in patients with non-ischemic chronic heart failure, did not lead to an improvement in GTN-mediated dilation in the brachial artery (Strey et al., 2006). At the level of the platelet there is data, albeit limited, to suggest that statin therapy ameliorates NO• resistance. For example, in patients with acute coronary syndrome, pharmacotherapy with statins was associated with improved anti-aggregatory actions of SNP (Chirkov et al., 2001). In addition, in individuals with mild hypercholesterolemia, treatment with pravastatin (40 mg/day) for 3 months, improved inhibition of platelet aggregation in response to SNP (Stepien et al., 2003). Of note, the ability of statins to ameliorate NO• resistance is unlikely due to their cholesterol lowering actions per se, rather their pleiotropic effects such as an ability to reduce superoxide generation and oxidative stress may be responsible. However, acute introduction of statins during evolving acute myocardial infarction has not convincingly improved outcomes (Ostadal, 2012; Vavuranakis et al., 2017).

Reversal of Severe Hyperglycemia

As discussed, hyperglycemia is a key contributor to the endothelial dysfunction and macrovascular complications associated with diabetes. Moreover, hyperglycemia contributes to vascular NO• resistance, such that glucose lowering, with long-term insulin treatment (3.5 years), improves brachial artery vasodilatation to SNP in patients with T2DM (Vehkavaara and Yki-Järvinen, 2004). Similarly, in diabetic patients with severe hyperglycemia and acute coronary syndromes, rapid correction of hyperglycemia via intravenous insulin (12 h) increases platelet responsiveness to NO• (Worthley et al., 2007). Such protective actions of insulin are likely due to its ability to reduce oxidative stress, independently of the potential for acute modulation of platelet TXNIP expression (Chong et al., 2015). Indeed, in the DIGAMI study (Diabetes Mellitus Insulin-Glucose Infusion in Acute Myocardial Infarction), insulin infusion post-acute myocardial infarction, followed by multi-dose subcutaneous insulin administration, decreased mortality rate in patients with diabetes (Malmberg et al., 1995). These findings suggest that the relatively rapid effects

TABLE 1 | Current and emerging therapies to ameliorate and circumvent nitric oxide resistance.

Therapy	Properties	Limitations	References
Amelioration strategies			
ACE inhibitors: Ramipril & Perindopril	•Decrease angiotensin II formation •Improve endothelial function by decreasing bradykinin degradation	•Benefits observed following prolonged use (days to months) •Limited utility during cardiovascular emergencies	(Murphey et al., 2003; Chirkov et al., 2004; Lob et al., 2006; Willoughby et al., 2012)
Perhexiline	•Anti-ischemic •Inhibits mitochondrial enzyme carnitine palmitoyltransferase	•Potential neuro- & hepato-toxicity •Variable pharmacokinetics: close therapeutic monitoring required	(Ashrafian et al., 2007; Chong et al., 2016)
Statins	•Lower cholesterol •Increase hepatic LDL uptake •Enhance eNOS gene expression •Enhance eNOS activity by reducing caveolin-1 expression	•Benefits observed following prolonged use (days to months) •Limited utility during cardiovascular emergencies	(Willoughby et al., 2002; Stepien et al., 2003; Chirkov et al., 2004; Lundberg et al., 2015; Go et al., 2019)
Insulin (in presence of severe hyperglycemia)	•Lower plasma glucose •Reduce oxidative stress and superoxide production	•NO• resistance can persist following acute, aggressive glycaemic control •Beneficial effects on mortality unclear	(Vehkavaara and Yki-Järvinen, 2004; Mehta et al., 2005; Worthley et al., 2007)
Circumvention strategies			
sGC activators	•Bind to heme pocket of sGC •Heme-independent •Activate sGC if heme is oxidized or detached	•Can cause hypotension	(Follmann et al., 2013; Buys et al., 2018; Elgert et al., 2019)
Nitrite	•Converted to NO• via reductases •Vasodilator & anti-aggregatory actions potentiated in hypoxia	•Anti-platelet effect diminished in patients with IHD •Does not reduce infarct size post-acute myocardial infarction	(Dautov et al., 2013; Siddiqi et al., 2014; Jones et al., 2015)
Nitroxyl donors	•Vasodilator, anti-aggregatory, positive cardiac inotropic/lusitropic actions •sGC-dependent & -independent signaling •Resistant to oxidative stress	•May cause coronary steal •Long-term benefits remain to be elucidated	(Irvine et al., 2007; Kemp-Harper, 2011; Dautov et al., 2013)

of infused insulin on platelet NO• responsiveness are of use in patients experiencing acute myocardial infarction, however, it should be noted that a component of NO• resistance may persist following acute, aggressive glycemic control (12 h insulin i.v. infusion) (Worthley et al., 2007).

Whilst the pharmacotherapies discussed have the potential to ameliorate NO• resistance at the level of the vasculature and platelet, all of these strategies have delayed onset of activity, taking hours to days to take effect. As such they are unsuitable for emergency situations (e.g. acute MI, transient myocardial ischemia or acute pulmonary edema), in which rapid circumvention of NO• resistance is required. This is of particular relevance in the diabetic population in which cardiovascular emergencies occur with greater frequency.

Circumvention Strategies

Emerging therapeutic strategies to circumvent NO• resistance, include sGC activators, nitrite and HNO donors (**Table 1**).

sGC Activators

Since NO• resistance is associated with sGC oxidation to the NO•-insensitive Fe^{3+}-sGC and subsequent heme-deplete sGC forms, the use of NO•- and heme-independent sGC activators to overcome this limitation has gained considerable attention. sGC activators target sGC in its oxidized (Fe^{3+}) or heme-free states and as such have greater efficacy under conditions of oxidative stress (Sandner et al., 2019). Pre-clinical studies have identified protective effects of sGC activators against ischemia/reperfusion injury, myocardial infarction, diabetic cardiomyopathy and diabetic nephropathy (Mátyás et al., 2015; Boustany-Kari et al., 2016; Lee et al., 2017). Furthermore, sGC activators may ameliorate NO• resistance. Thus, chronic treatment of rats with heart failure with the sGC activator, ataciguat (10 mg/kg/twice daily, 10 weeks) improved the vascular response to exogenous NO• in aortic rings and reduced platelet activation (Schäfer et al., 2010). Importantly, sGC activators themselves are anti-aggregatory agents and their anti-platelet actions in both humans (Mendes-Silverio et al., 2012) and rodents (Roger et al., 2010) are augmented when sGC is oxidized. Such findings suggest that sGC activators have the potential to circumvent NO• resistance. Currently, however, the clinical utility of this class of compound is unclear given their profound, and sustained, blood pressure lowering effects in patients with acute decompensated heart failure (Breitenstein et al., 2017) and peripheral arterial occlusive disease (Sandner et al., 2019), in the absence of a clear therapeutic benefit.

Nitrite

There is growing interest in the therapeutic potential of nitrite, both as an alternate source of NO• and a signaling molecule in its

own right. Importantly, the vasodilator and anti-aggregatory responses to nitrite are potentiated in the setting of hypoxia, suggesting that it may have considerable advantages in the treatment of acute cardiovascular disorders (Dautov et al., 2014). However, current evidence in support of an ability of nitrite to circumvent NO• resistance is limited, and hinges on the concept that part of the effects of nitrite are NO•- and sGC-independent. Thus, in platelets from patients with ischemic heart disease, in whom NO• resistance is evident, the anti-aggregatory effects of nitrite were found also to be diminished (Dautov et al., 2014). By contrast, in heart failure patients with preserved ejection fraction (HFpEF), resistance to the anti-aggregatory actions of SNP was evident, yet the ability of nitrite to inhibit platelet aggregation was maintained (Borgognone et al., 2018). Whilst these anti-aggregatory actions of nitrite were mediated via sGC activation, they were only due, in part, to NO•. The clinical utility of nitrite in the circumvention of NO• resistance is also tempered by the finding that in two clinical trials in patients with acute myocardial infarction (NIAMI and NITRITE-AMI), nitrite administration prior to reperfusion, did not reduce infarct size (Siddiqi et al., 2014; Jones et al., 2015).

Nitroxyl-Based Therapies

HNO is the one-electron reduced and protonated form of NO•. Using the prototypical HNO donors Angeli's salt (which is also a source of nitrite) and iso-propylamine-NONOate (IPA-NO), HNO has been shown to have distinct pharmacological properties and therapeutic advantages when compared to its redox sibling (Irvine et al., 2008; Bullen et al., 2011a). Specifically, unlike NO•, the actions of HNO are preserved during oxidative stress, as HNO is resistant to scavenging by superoxide (Irvine et al., 2007; Kemp-Harper et al., 2016). Moreover, HNO causes venous and arterial dilation (Tare et al., 2017), suppresses vascular generation of ROS via rapid (within minutes), and direct, inhibition of Nox2 oxidase (Miller et al., 2013) and is resistant to tolerance development (unlike organic nitrates) (Irvine et al., 2007). HNO also inhibits VSMC proliferation and platelet aggregation (Tsihlis et al., 2010; Bullen et al., 2011b; Dautov et al., 2013), and reduces endothelial expression of adhesion molecules, monocyte activation and leukocyte adhesion (Andrews et al., 2016). In the vasculature, HNO induces vasodilation predominantly through sGC/cGMP signaling and the preference of HNO for ferric (Fe^{3+}) versus ferrous (Fe^{2+}) heme groups (Miranda et al., 2003) raises the interesting possibility that HNO may preferentially target the oxidized (Fe^{3+}) versus reduced (Fe^{2+}) forms of sGC. Such a property may contribute to the preserved efficacy of HNO in the face of oxidative stress, yet studies to date have not provided evidence in support of an ability of HNO to activate oxidized sGC (Miller et al., 2009; Zeller et al., 2009). In comparison to NO•, HNO can also signal via distinct vascular pathways, including the activation of voltage-dependent K^+ channels (Irvine et al., 2003; Andrews et al., 2009), ATP-sensitive K^+ channels and the release of calcitonin gene-related peptide (**Figure 3**) (Favaloro and Kemp-Harper, 2007; Chin et al., 2014). Interestingly, HNO might also be endogenously generated, however, in the absence of a validated method to measure tissue levels, this is yet to be established conclusively (Andrews et al., 2009; Kahlberg et al., 2016; Fukuto, 2019). Another unique feature of HNO in comparison to NO•, is the ability of HNO to react directly with thiols and thiol-containing proteins (i.e. cysteines), independently of sGC/cGMP signaling (Kemp-Harper, 2011). In the myocardium, this property allows HNO to serve as a positive cardiac inotrope, interacting with cysteine residues on thiol-containing proteins including ryanodine receptors (Tocchetti et al., 2007) and phospholamban, the regulatory phosphoprotein of the sarcoplasmic reticulum Ca^{2+}-ATPase pump (SERCA2a), to enhance Ca^{2+} cycling (Keceli et al., 2019). HNO also increases myofilament calcium sensitivity by promoting the formation of disulfide bonds between myofilament cysteine residues (Gao et al., 2012), Together, these actions of HNO result in enhanced myocardial contractility and relaxation (**Figure 3**) (Paolocci et al., 2007; Tocchetti et al., 2007). It should also be noted that differently from legacy inotropes, the inotropic response to HNO does not require the entry of extracellular Ca^{2+} (Kohr et al., 2010).

These unique properties of HNO, together with its preserved efficacy in the setting of oxidative stress, suggest that HNO donors may circumvent NO• resistance and be of clinical utility in a cardiovascular emergency.

Indeed, HNO donor compounds have displayed vaso- and cardio-protective efficacy, particularly in disease states where endothelial dysfunction and NO• resistance is present (Andrews et al., 2016). At the level of the vasculature, there is evidence to support an ability of both endogenous and exogenous HNO to circumvent NO• resistance. Thus, in the diabetic rat aorta (Leo et al., 2012) and small mesenteric arteries (Kahlberg et al., 2016; Tare et al., 2017), endothelium-dependent relaxation mediated by HNO is preserved, yet that mediated by NO• is impaired. Moreover, in pre-clinical studies, vasorelaxation to the HNO donors, Angeli's salt and IPA/NO are maintained in the diabetic (Leo et al., 2012; Tare et al., 2017), hypercholesterolemic (Bullen et al., 2011b) and hypertensive (Wynne et al., 2012; Irvine et al., 2013) vasculature. Importantly, HNO can also circumvent platelet NO• resistance. Thus, in hypercholesterolemic mice we have shown that the anti-aggregatory actions of the HNO donor, IPA/NO are preserved, yet those to the NO• donor, GTN are impaired (Bullen et al., 2011b). Moreover, in patients with coronary artery disease, the impaired anti-platelet response to the NO• donor, SNP, is circumvented by the HNO donor, IPA/NO (Dautov et al., 2013).

Whilst the discussion so far has focused on circumventing NO• resistance in the vasculature and platelets, it is pertinent to note that the myocardium is also susceptible to NO• resistance, such that NO• can no longer enhance left ventricular (LV) relaxation (Qin et al., 2020). Thus, following ischemia–reperfusion (I–R) injury (Chin et al., 2016) or the induction of T1DM (Qin et al., 2020) in rats, the ability of the NO• donor, DEA/NO to enhance myocardial relaxation is impaired. Such an impairment in myocardial responsiveness to NO• (endogenous or exogenous) may facilitate LV dysfunction, LV hypertrophy and cardiac remodelling

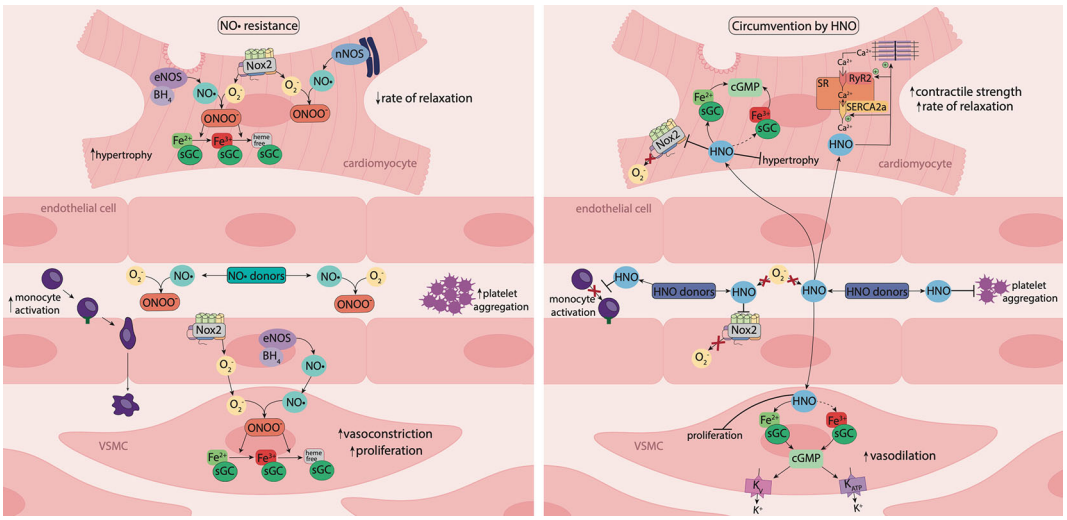

FIGURE 3 | Nitric oxide resistance and its circumvention by nitroxyl. Under oxidative stress, activity of nicotinamide adenine dinucleotide phosphate (NADPH) oxidase (Nox) enzymes, such as Nox2, is elevated, resulting in increased superoxide (O_2^-) generation. O_2^- reacts with nitric oxide (NO•), generating the powerful oxidant, peroxynitrite ($ONOO^-$), which oxidizes the ferrous (Fe^{2+}) heme group of sGC to the ferric (Fe^{3+}) or heme-free state, desensitizing the enzyme to NO•. Consequently, tissue responsiveness to NO• is impaired, resulting in NO• resistance. Nitroxyl (HNO) is resistant to scavenging by O_2^- and HNO donors offer an opportunity to circumvent NO• resistance. In the vasculature, HNO causes vasorelaxation, inhibits platelet aggregation and reduces monocyte activation. In vascular smooth muscle cells (VSMCs), HNO signals predominantly via activation of sGC and the subsequent increase in 3',5'-cyclic guanosine monophosphate (cGMP) and may activate the oxidized (Fe^{3+}) form of sGC. HNO also targets vascular voltage-dependent and ATP-sensitive K^+ channels through a cGMP-dependent mechanism. In the vasculature and myocardium, HNO interacts directly with Nox2 to suppresses O_2^- generation. In cardiomyocytes, HNO has anti-hypertrophic effects, and reacts directly with thiols and thiol-containing proteins including the sarcoplasmic reticulum Ca^{2+}-ATPase pump (SERCA2a) and ryanodine receptors (RyR2) to enhance Ca^{2+} cycling, together with increasing myofilament Ca^{2+} sensitivity, resulting in enhanced myocardial contractility and relaxation. The vaso- and cardio-protective actions of HNO are preserved in the setting of oxidative stress and HNO donors offer a new therapeutic approach to treat diabetes-associated cardiovascular complications.

(Nightingale et al., 2011; Sverdlov et al., 2011). Recent pre-clinical studies have demonstrated that HNO donors can circumvent myocardial NO• resistance. Specifically, unlike DEA/NO, myocardial relaxation to Angeli's salt is preserved following I–R injury in rat isolated hearts (Chin et al., 2016). In addition, Angeli's salt was found to reduce the duration of ventricular fibrillation following I–R injury (Chin et al., 2016). Similarly, the HNO donor IPA/NO enhanced myocardial relaxation and contraction responses in diabetic rat hearts, while responses to DEA/NO were attenuated (Qin et al., 2020).

Collectively these findings suggest that HNO donors may be particularly useful in acute cardiovascular emergencies associated with NO• resistance. Indeed, the ability of HNO to rapidly unload the heart (venous dilation) (Paolocci et al., 2001b), improve coronary blood flow (arterial dilation) (Paolocci et al., 2003; Andrews et al., 2015) and inhibit platelet aggregation (Bermejo et al., 2005; Bullen et al., 2011b; Dautov et al., 2013) is highly advantageous following an ischemic event. Moreover, the positive inotropic and lusitropic properties of HNO (Paolocci et al., 2003; Sabbah et al., 2013) provide a unique therapeutic approach in which an improvement in myocardial performance can also be achieved in this setting. Future studies should also determine if HNO donors have the ability to stabilize mast cells and if this action is preserved in the face of impaired NO• signaling. Indeed, mast cell stabilization is critical for the prevention of plaque rupture and coronary spasm, events which trigger most cardiac ischemic emergencies (Kovanen and Bot, 2017). A caveat of many nitrovasodilators is the coronary steal phenomenon, where non-specific vasodilators induce dilation in non-ischemic regions and reduce systemic blood pressure, causing blood flow to be directed away from ischemic regions of need (Harrison and Bates, 1993). Whilst there is no current evidence that HNO donors cause coronary steal, this concept has not been fully interrogated and whether HNO selectivity targets ischemic sites remains unknown. With the recent development of the next-generation HNO donors and their ongoing clinical evaluation, these concepts will need to be investigated.

To date, the therapeutic benefits of short-term HNO administration has been a key focus. However, many of the properties of HNO confer potential for long-term use in the treatment of cardiovascular pathologies associated with impaired NO• signaling. Thus in addition to the vasodilatory, anti-aggregatory and inotropic actions of HNO donors, their ability to attenuate oxidative stress (Lin et al., 2012; Miller et al., 2013), inflammation (Andrews et al., 2016) and cardiac hypertrophy (Lin et al., 2012; Irvine et al., 2013) and their resistance to tolerance development (Irvine et al., 2011; Andrews et al., 2015) is advantageous. Indeed, the long-term cardioprotective actions of HNO in the diabetic heart is supported by our finding that chronic *in vivo* administration of the HNO donor, 1-nitrosocyclohexyl acetate (1-NCA, daily i.p. injection for 4 weeks) to streptozotocin-treated mice, attenuated left ventricular diastolic dysfunction and

cardiomyocyte hypertrophy (Cao et al., 2015). With the recent development of HNO donors with more favorable pharmacokinetic properties (del Rio et al., 2014; Hartman et al., 2018), it is anticipated that the therapeutic potential of this class of compound in the treatment of both acute and chronic cardiovascular diseases will be rigorously investigated.

Next-Generation Nitroxyl Donors

Given the short half-life, poor aqueous solubility and active by-products released by the abovementioned HNO donors, novel synthetic pure HNO donors have now been developed. These include CXL-1020, which non-enzymatically decomposes to HNO with a half-life of approximately 2.1 min (Sabbah et al., 2013). CXL-1020 has been shown to induce positive inotropic and lusitropic effects in murine cardiomyocytes from healthy or failing hearts, and these effects were also observed *in vivo* in failing canine hearts (Sabbah et al., 2013). In patients with acute decompensated heart failure, intravenous infusion (4–6 h) of CXL-1020 enhanced cardiac function by reducing left and right ventricular pressures, decreasing systemic vascular resistance, and increasing cardiac output and stroke volume (Sabbah et al., 2013). These hemodynamic changes were not associated with alterations in heart rate, or the occurrence of arrhythmias, highlighting the safety, efficacy and potential therapeutic utility of CXL-1020 for the treatment of cardiovascular disease, where responsiveness to NO• is diminished (Sabbah et al., 2013).

These discoveries have led to the development of other HNO donors with greater tolerability and more suitable half-lives for therapeutic use in humans (Hartman et al., 2018). Of these, the HNO donor BMS-986231 (half-life; 40–144 min), has been shown to enhance cardiac contractile and relaxant responses, while promoting vasodilation and reducing myocardial oxygen consumption in canine models of heart failure (Hartman et al., 2018). Moreover, in a phase I clinical trial in healthy individuals, BMS-986231 (24- or 48-hour intravenous infusion) was well tolerated, as the only drug-related adverse event reported was the development of headaches, which were alleviated following hydration, and are a common side effect of vasodilator therapy (Cowart et al., 2019). Further, the vasodilator capacity of BMS-986231 was evident with the HNO donor causing dose-dependent reductions in systolic and diastolic blood pressure, which were sustained during infusion, and returned to baseline following infusion cessation (Cowart et al., 2019). Similar findings were also observed in patients with heart failure, where BMS-986231 reduced pulmonary arterial systolic and diastolic pressure, while decreasing total peripheral vascular resistance (Tita et al., 2017). Importantly, these hemodynamic changes were not associated with changes in heart rate or the presence of arrhythmias (Tita et al., 2017). In the StandUP-AHF study (Study Assessing Nitroxyl Donor Upon Presentation with Acute Heart Failure), patients hospitalized with heart failure with reduced ejection fraction (HF-rEF) will receive intravenous infusions of BMS-986231 at various doses or placebo for 48 h (Felker et al., 2019). The results of this multicenter, randomized, double-blind, placebo-controlled clinical trial will provide further information about the safety and tolerability of HNO donors with regard to hypotension (Felker et al., 2019).

Whilst the poor aqueous solubility of BMS-986231 limits its clinical use to intravenous administration, orally bioavailable HNO donors are on the horizon (Tita et al., 2017). CXL-1036 is an orally available HNO donor that also has a half-life (30 minutes) suitable for *in vivo* use and has been shown to enhance cardiac contraction and relaxation, and reduce myocardial demand, without altering heart rate in a canine model of heart failure (del Rio et al., 2014).

To date, much of the focus of HNO donors has been on their therapeutic potential in the treatment of acute decompensated heart failure. However, the novel vaso- and cardio-protective properties of HNO highlight the therapeutic potential of HNO donors in the treatment of a range of vascular and cardiac pathologies, particularly where NO• signaling and responsiveness is impaired, such as in T2DM. We eagerly await future studies which will examine the ability for HNO donors to overcome NO• resistance in patients with T2DM, and alleviate cardiovascular complications associated with this disease.

CONCLUSION

A loss in the generation, bioavailability and responsiveness to vasoprotective NO• is a key contributor to the cardiovascular dysfunction and propensity towards acute myocardial ischemia associated with T2DM. Underpinning the impairment in NO• signaling (termed NO• resistance) is an increase in oxidative stress, driven predominantly by hyperglycemia. The impact of elevated ROS generation is far reaching, leading not only to impaired vasodilator and anti-aggregatory capacity, but ab initio reduction in therapeutic utility of NO•-based therapeutics. NO• resistance constitutes an independent risk factor for subsequent cardiovascular morbidity and mortality, and there is an urgent need to treat diabetes associated endothelial dysfunction and NO• resistance. Although perhexiline, statins and some ACE inhibitors have shown promise in their ability to improve hemodynamic and vasodilator responses in diabetes, there are limitations associated with their use in emergency treatment of cardiovascular disorders. HNO donors, however, present novel pharmacological properties, including circumvention of NO• resistance, which may facilitate a new therapeutic approach to treat diabetes-associated cardiovascular complications.

AUTHOR CONTRIBUTIONS

AV and BK-H were responsible for the design and draft of the manuscript. CQ, OW, JH, and RR provided critical review and revision of the manuscript. All authors provide approval for publication of the content.

FUNDING

This work was supported in part by a National Health & Medical Research Council Project Grant (ID: APP1120859) to RR, JH, and BK-H.

REFERENCES

Almourani, R., Chinnakotla, B., Patel, R., Kurukulasuriya, L. R., and Sowers, J. (2019). Diabetes and cardiovascular disease: an update. *Curr. Diab. Rep.* 19, 1–13. doi: 10.1007/s11892-019-1239-x

Anderson, R. A., Ellis, G. R., Evans, L. M., Morris, K., Chirkov, Y. Y., Horowitz, J. D., et al. (2005). Platelet nitrate responsiveness in fasting and postprandial type 2 diabetes. *Diabetes Vasc. Dis. Res.* 2, 88–93. doi: 10.3132/dvdr.2005.015

Andrews, K. L., Irvine, J. C., Tare, M., Apostolopoulos, J., Favaloro, J. L., Triggle, C. R., et al. (2009). A role for nitroxyl (HNO) as an endothelium-derived relaxing and hyperpolarizing factor in resistance arteries. *Br. J. Pharmacol.* 157, 540–550. doi: 10.1111/j.1476-5381.2009.00150.x

Andrews, K. L., Lumsden, N. G., Farry, J., Jefferis, A.-M., Kemp-Harper, B. K., and Chin-Dusting, J. P. F. (2015). Nitroxyl: a vasodilator of human vessels that is not susceptible to tolerance. *Clin. Sci. (Lond).* 129, 179–187. doi: 10.1042/CS20140759

Andrews, K. L., Sampson, A. K., Irvine, J. C., Shihata, W. A., Michell, D. L., Lumsden, N. G., et al. (2016). Nitroxyl (HNO) reduces endothelial and monocyte activation and promotes M2 macrophage polarization. *Clin. Sci.* 130, 1629–1640. doi: 10.1042/cs20160097

Antonopoulos, A. S., Margaritis, M., Coutinho, P., Shirodaria, C., Psarros, C., Herdman, L., et al. (2015). Adiponectin as a link between type 2 diabetes and vascular NADPH oxidase activity in the human arterial wall: The regulatory role of perivascular adipose tissue. *Diabetes* 64, 2207–2219. doi: 10.2337/db14-1011

Aon, M. A., Tocchetti, C. G., Bhatt, N., Paolocci, N., and Cortassa, S. (2015). Protective Mechanisms of Mitochondria and Heart Function in Diabetes. *Antioxid. Redox Signal.* 22, 1563–1586. doi: 10.1089/ars.2014.6123

Ashrafian, H., Horowitz, J. D., and Frenneaux, M. P. (2007). Perhexiline. *Cardiovasc. Drug Rev.* 25, 76–97. doi: 10.1111/j.1527-3466.2007.00006.x

Barlovic, D. P., Thomas, M. C., and Jandeleit-Dahm, K. (2010). Cardiovascular disease: what's all the AGE/RAGE about? *Cardiovasc. Hematol. Disord. Targets* 10, 7–15. doi: 10.2174/187152910790780050

Bermejo, E., Sáenz, D. A., Alberto, F., Rosenstein, R. E., Bari, S. E., and Lazzari, M. A. (2005). Effect of nitroxyl on human platelets function. *Thromb. Haemost.* 94, 578–584. doi: 10.1160/TH05-01-0062

Böger, R. H. (2004). Asymmetric dimethylarginine, an endogenous inhibitor of nitric oxide synthase, explains the "l-arginine paradox" and acts as a novel cardiovascular risk factor. *J. Nutr.* 134, 2842S–2847S. doi: 10.1093/jn/134.10.2842S

Borgognone, A., Shantsila, E., Worrall, S. M., Prompunt, E., Loka, T., Loudon, B. L., et al. (2018). Nitrite circumvents platelet resistance to nitric oxide in patients with heart failure preserved ejection fraction and chronic atrial fibrillation. *Cardiovasc. Res.* 114, 1313–1323. doi: 10.1093/cvr/cvy087

Boustany-Kari, C. M., Harrison, P. C., Chen, H., Lincoln, K. A., Qian, H. S., Clifford, H., et al. (2016). A soluble guanylate cyclase activator inhibits the progression of diabetic nephropathy in the ZSF1 rat. *J. Pharmacol. Exp. Ther.* 356, 712–719. doi: 10.1124/jpet.115.230706

Breitenstein, S., Roessig, L., Sandner, P., and Lewis, K. S. (2017). *"Novel sGC Stimulators and sGC Activators for the Treatment of Heart Failure BT - Heart Failure,"*. Eds. J. Bauersachs, J. Butler and P. Sandner ((Cham: Springer International Publishing)), 225–247. doi: 10.1007/164_2016_100

Brownlee, M. (2005). The pathobiology of diabetic complications. *Diabetes* 54, 1615. doi: 10.2337/diabetes.54.6.1615

Bullen, M. L., Miller, A. A., Andrews, K. L., Irvine, J. C., Ritchie, R. H., Sobey, C. G., et al. (2011a). Nitroxyl (HNO) as a vasoprotective signaling molecule. *Antioxid. Redox Signal.* 14, 1675–1686. doi: 10.1089/ars.2010.3327

Bullen, M. L., Miller, A. A., Dharmarajah, J., Drummond, G. R., Sobey, C. G., and Kemp-Harper, B. K. (2011b). Vasorelaxant and antiaggregatory actions of the nitroxyl donor isopropylamine NONOate are maintained in hypercholesterolemia. *Am. J. Physiol. Circ. Physiol.* 301, H1405–H1414. doi: 10.1152/ajpheart.00489.2011

Buys, E. S., Zimmer, D. P., Chickering, J., Graul, R., Chien, Y. T., Profy, A., et al. (2018). Discovery and development of next generation sGC stimulators with diverse multidimensional pharmacology and broad therapeutic potential. *Nitric. Oxide - Biol. Chem.* 78, 72–80. doi: 10.1016/j.niox.2018.05.009

Cao, N., Wong, Y. G., Rosli, S., Kiriazis, H., Huynh, K., Qin, C., et al. (2015). Chronic administration of the nitroxyl donor 1-nitrosocyclo hexyl acetate limits left ventricular diastolic dysfunction in a mouse model of diabetes mellitus in vivo. *Circ. Hear. Fail.* 8, 572. doi: 10.1161/CIRCHEARTFAILURE.114.001699

Chandra, D., Jackson, E. B., Ramana, K. V., Kelley, R., Srivastava, S. K., and Bhatnagar, A. (2002). Nitric oxide prevents aldose reductase activation and sorbitol accumulation during diabetes. *Diabetes* 51, 3095. doi: 10.2337/diabetes.51.10.3095

Chen, S., and Sun, B. (2013). Negative regulation of NLRP3 inflammasome signaling. *Protein Cell* 4, 251–258. doi: 10.1007/s13238-013-2128-8

Chin, K. Y., Qin, C., Cao, N., Kemp-Harper, B. K., Woodman, O. L., and Ritchie, R. H. (2014). The concomitant coronary vasodilator and positive inotropic actions of the nitroxyl donor Angeli's salt in the intact rat heart: Contribution of soluble guanylyl cyclase-dependent and -independent mechanisms. *Br. J. Pharmacol.* 171, 1722–1734. doi: 10.1111/bph.12568

Chin, K. Y., Michel, L., Qin, C. X., Cao, N., Woodman, O. L., and Ritchie, R. H. (2016). The HNO donor Angeli's salt offers potential haemodynamic advantages over NO or dobutamine in ischaemia-reperfusion injury in the rat heart ex vivo. *Pharmacol. Res.* 104, 165–175. doi: 10.1016/j.phrs.2015.12.006

Chirkov, Y. Y., and Horowitz, J. D. (2007). Impaired tissue responsiveness to organic nitrates and nitric oxide: A new therapeutic frontier? *Pharmacol. Ther.* 116, 287–305. doi: 10.1016/j.pharmthera.2007.06.012

Chirkov, Y. Y., Holmes, A. S., Willoughby, S. R., Stewart, S., Wuttke, R. D., Sage, P. R., et al. (2001). Stable angina and acute coronary syndromes are associated with nitric oxide resistance in platelets. *J. Am. Coll. Cardiol.* 37, 1851–1857. doi: 10.1016/S0735-1097(01)01238-4

Chirkov, Y. Y., Holmes, A. S., Willoughby, S. R., Stewart, S., and Horowitz, J. D. (2002). Association of aortic stenosis with platelet hyperaggregability and impaired responsiveness to nitric oxide. *Am. J. Cardiol.* 90, 551–554. doi: 10.1016/s0002-9149(02)02536-5

Chirkov, Y. Y., Holmes, A. S., Martelli, J. D., and Horowitz, J. D. (2004). Effect of perindopril on platelet nitric oxide resistance in patients with chronic heart failure secondary to ischemic left ventricular dysfunction. *Am. J. Cardiol.* 93, 1438–1440. doi: 10.1016/j.amjcard.2004.02.052

Chong, C.-R., Liu, S., Licari, G., Heresztyn, T., Chirkov, Y. Y., Ngo, D. T., et al. (2015). Reversal of hyperglycemia: effects on nitric oxide signaling. *Am. J. Med.* 128, 427–430. doi: 10.1016/j.amjmed.2014.11.007

Chong, C.-R., Sallustio, B., and Horowitz, J. D. (2016). Drugs that affect cardiac metabolism: focus on perhexiline. *Cardiovasc. Drugs Ther.* 30, 399–405. doi: 10.1007/s10557-016-6664-3

Coleman, J. W. (2002). Nitric oxide: A regulator of mast cell activation and mast cell-mediated inflammation. *Clin. Exp. Immunol.* 129, 4–10. doi: 10.1046/j.1365-2249.2002.01918.x

Cooke, J. P. (2005). ADMA: Its role in vascular disease. *Vasc. Med.* 10, 11–17. doi: 10.1191/1358863x05vm598oa

Costell, M. H., Ancellin, N., Bernard, R. E., Zhao, S. F., Upson, J. J., Morgan, L. A., et al. (2012). Comparison of soluble guanylate cyclase stimulators and activators in models of cardiovascular disease associated with oxidative stress. *Front. Pharmacol.* 3, 1–14. doi: 10.3389/fphar.2012.00128

Cowart, D., Venuti, R. P., Lynch, K., Guptill, J. T., Noveck, R. J., and Foo, S. Y. (2019). A phase 1 randomized study of single intravenous infusions of the novel nitroxyl donor BMS-986231 in healthy volunteers. *J. Clin. Pharmacol.* 59, 717–730. doi: 10.1002/jcph.1364

da Costa, R. M., da Silva, J. F., Alves, J. V., Dias, T. B., Rassi, D. M., Garcia, L. V., et al. (2018). Increased O-GlcNAcylation of endothelial nitric oxide synthase compromises the anti-contractile properties of perivascular adipose tissue in metabolic syndrome. *Front. Physiol.* 9, 1–16. doi: 10.3389/fphys.2018.00341

Dautov, R. F., Ngo, D. T. M., Licari, G., Liu, S., Sverdlov, A. L., Ritchie, R. H., et al. (2013). The nitric oxide redox sibling nitroxyl partially circumvents impairment of platelet nitric oxide responsiveness. *Nitric. Oxide - Biol. Chem.* 35, 72–78. doi: 10.1016/j.niox.2013.08.006

Dautov, R. F., Stafford, I., Liu, S., Cullen, H., Madhani, M., Chirkov, Y. Y., et al. (2014). Hypoxic potentiation of nitrite effects in human vessels and platelets. *Nitric. Oxide Biol. Chem.* 40, 36–44. doi: 10.1016/j.niox.2014.05.005

De Caterina, R., Libby, P., Peng, H. B., Thannickal, V. J., Rajavashisth, T. B., Gimbrone, M. A., et al. (1995). Nitric oxide decreases cytokine-induced endothelial activation: Nitric oxide selectively reduces endothelial expression of adhesion molecules and proinflammatory cytokines. *J. Clin. Invest.* 96, 60–68. doi: 10.1172/JCI118074

Degrell, P., Cseh, J., Mohás, M., Molnár, G. A., Pajor, L., Chatham, J. C., et al. (2009). Evidence of O-linked N-acetylglucosamine in diabetic nephropathy. *Life Sci.* 84, 389–393. doi: 10.1016/j.lfs.2009.01.007

del Rio, C. L., Robert, G. S., Youngblood, B. L., Ueyama, Y., May, J. R., Humphries, D. J., et al. (2014). Abstract 13228: nitroxyl (HNO) donated via slow-release oral pro-drug improves ventriculo-arterial coupling in conscious dogs with induced heart failure: enhanced load-independent mechano-energetics. *Circulation* 130, A13228–A13228. doi: 10.1161/circ.130.suppl_2.13228

Dogra, G. K., Watts, G. F., Chan, D. C., and Stanton, K. (2005). Statin therapy improves brachial artery vasodilator function in patients with Type 1 diabetes and microalbuminuria. *Diabet. Med.* 22, 239–242. doi: 10.1111/j.1464-5491.2004.01382.x

Drummond, G. R., Selemidis, S., Griendling, K. K., and Sobey, C. G. (2011). Combating oxidative stress in vascular disease: NADPH oxidases as therapeutic targets. *Nat. Rev. Drug Discovery* 10, 453–471. doi: 10.1038/nrd3403

DuMond, J. F., and King, S. B. (2011). The chemistry of nitroxyl-releasing compounds. *Antioxid. Redox Signal.* 14, 1637–1648. doi: 10.1089/ars.2010.3838

Dupuis, J., Tardif, J.-C., Rouleau, J.-L., Ricci, J., Arnold, M., Lonn, E., et al. (2005). Intensity of lipid lowering with statins and brachial artery vascular endothelium reactivity after acute coronary syndromes (from the BRAVER trial). *Am. J. Cardiol.* 96, 1207–1213. doi: 10.1016/j.amjcard.2005.06.057

Elgert, C., Rühle, A., Sandner, P., and Behrends, S. (2019). A novel soluble guanylyl cyclase activator, BR 11257, acts as a non-stabilising partial agonist of sGC. *Biochem. Pharmacol.* 163, 142–153. doi: 10.1016/j.bcp.2019.02.007

Förstermann, U., and Sessa, W. C. (2012). Nitric oxide synthases: regulation and function. *Eur. Heart J.* 33, 829–837d. doi: 10.1093/eurheartj/ehr304

Fülöp, N., Mason, M. M., Dutta, K., Wang, P., Davidoff, A. J., Marchase, R. B., et al. (2007). Impact of Type 2 diabetes and aging on cardiomyocyte function and O-linked N-acetylglucosamine levels in the heart. *Am. J. Physiol. - Cell Physiol.* 292, 1370–1378. doi: 10.1152/ajpcell.00422.2006

Farah, C., Michel, L. Y. M., and Balligand, J. L. (2018). Nitric oxide signalling in cardiovascular health and disease. *Nat. Rev. Cardiol.* 15, 292–316. doi: 10.1038/nrcardio.2017.224

Fard, A., Tuck, C. H., Donis, J. A., Sciacca, R., Di Tullio, M. R., Wu, H. D., et al. (2000). Acute elevations of plasma asymmetric dimethylarginine and impaired endothelial function in response to a high-fat meal in patients with type 2 diabetes. *Arterioscler. Thromb. Vasc. Biol.* 20, 2039–2044. doi: 10.1161/01.ATV.20.9.2039

Farhan, S. S., and Hussain, S. A. (2019). Advanced glycation end products (AGEs) and their soluble receptors (sRAGE) as early predictors of reno-vascular complications in patients with uncontrolled type 2 diabetes mellitus. *Diabetes Metab. Syndr. Clin. Res. Rev.* 13, 2457–2461. doi: 10.1016/j.dsx.2019.06.019

Favaloro, J. L., and Kemp-Harper, B. K. (2007). The nitroxyl anion (HNO) is a potent dilator of rat coronary vasculature. *Cardiovasc. Res.* 73, 587–596. doi: 10.1016/j.cardiores.2006.11.018

Felker, G. M., Borentain, M., Cleland, J. G., DeSouza, M. M., Kessler, P. D., O'Connor, C. M., et al. (2019). Rationale and design for the development of a novel nitroxyl donor in patients with acute heart failure. *Eur. J. Heart Fail.* 21, 1022–1031. doi: 10.1002/ejhf.1504

Fiorentino, T. V., Prioletta, A., Zuo, P., and Folli, F. (2013). Hyperglycemia-induced oxidative stress and its role in diabetes mellitus related cardiovascular diseases. *Curr. Pharm. Des.* 19, 5695–5703. doi: 10.2174/1381612811319320005

Follmann, M., Griebenow, N., Hahn, M. G., Hartung, I., Mais, F. J., Mittendorf, J., et al. (2013). The chemistry and biology of soluble guanylate cyclase stimulators and activators. *Angew. Chemie - Int. Ed.* 52, 9442–9462. doi: 10.1002/anie.201302588

Fox, K. M. (2003). Efficacy of perindopril in reduction of cardiovascular events among patients with stable coronary artery disease: randomised, double-blind, placebo-controlled, multicentre trial (the EUROPA study). *Lancet* 362, 782–788. doi: 10.1016/s0140-6736(03)14286-9

Fukuto, J. M. (2019). A recent history of nitroxyl chemistry, pharmacology and therapeutic potential. *Br. J. Pharmacol.* 176, 135–146. doi: 10.1111/bph.14384

Gao, W. D., Murray, C. I., Tian, Y., Zhong, X., DuMond, J. F., Shen, X., et al. (2012). Nitroxyl-mediated disulfide bond formation between cardiac myofilament cysteines enhances contractile function. *Circ. Res.* 111, 1002–1011. doi: 10.1161/CIRCRESAHA.112.270827

Giacco, F., and Brownlee, M. (2010). Oxidative stress and diabetic complications. *Circ. Res.* 107, 1058–1070. doi: 10.1161/CIRCRESAHA.110.223545

Go, A. S., Ambrosy, A. P., Kheder, K., Fan, D., Sung, S. H., Inveiss, A. I., et al. (2019). Statin therapy and risk of incident diabetes mellitus in adults with cardiovascular risk factors. *Am. J. Cardiol.* 125, 534–541. doi: 10.1016/j.amjcard.2019.11.011

Harrison, D. G., and Bates, J. N. (1993). The nitrovasodilators: new ideas about old drugs. *Circulation* 87, 1461–1467. doi: 10.1161/01.cir.87.5.1461

Hartman, J. C., del Rio, C. L., Reardon, J. E., Zhang, K., and Sabbah, H. N. (2018). Intravenous infusion of the novel HNO donor BMS-986231 is associated With beneficial inotropic, lusitropic, and vasodilatory properties in 2 canine models of heart failure. *JACC Basic to Transl. Sci.* 3, 625–638. doi: 10.1016/j.jacbts.2018.07.003

Heitzer, T., Krohn, K., Albers, S., and Meinertz, T. (2000). Tetrahydrobiopterin improves endothelium-dependent vasodilation by increasing nitric oxide activity in patients with Type II diabetes mellitus. *Diabetologia* 43, 1435–1438. doi: 10.1007/s001250051551

Hernandez-Cuellar, E., Tsuchiya, K., Hara, H., Fang, R., Sakai, S., Kawamura, I., et al. (2012). Cutting edge: nitric oxide inhibits the NLRP3 inflammasome. *J. Immunol.* 189, 5113–5117. doi: 10.4049/jimmunol.1202479

Horowitz, J. D., De Caterina, R., Heresztyn, T., Alexander, J. H., Andersson, U., Lopes, R. D., et al. (2018). Asymmetric and symmetric dimethylarginine predict outcomes in patients with atrial fibrillation: an ARISTOTLE substudy. *J. Am. Coll. Cardiol.* 72, 721–733. doi: 10.1016/j.jacc.2018.05.058

Htay, T., Soe, K., Lopez-Perez, A., Doan, A. H. A., Romagosa, M. A., and Aung, K. K. (2019). Mortality and cardiovascular disease in type 1 and type 2 diabetes. *Curr. Cardiol. Rep.* 21, 1–7. doi: 10.1007/s11886-019-1133-9

Ignarro, L. J. (2019). Nitric oxide is not just blowing in the wind. *Br. J. Pharmacol.* 176, 131–134. doi: 10.1111/bph.14540

International Diabetes Federation (2019). Latest figures show 463 million people now living with diabetes worldwide as numbers continue to rise. *Diabetes Res. Clin. Pract.* 157, 107932. doi: 10.1016/j.diabres.2019.107932

Irvine, J. C., Favaloro, J. L., and Kemp-Harper, B. K. (2003). NO- activates soluble guanylate cyclase and Kv channels to vasodilate resistance arteries. *Hypertension* 41, 1301–1307. doi: 10.1161/01.HYP.0000072010.54901.DE

Irvine, J. C., Favaloro, J. L., Widdop, R. E., and Kemp-Harper, B. K. (2007). Nitroxyl anion donor, Angeli's salt, does not develop tolerance in rat isolated aortae. *Hypertension* 49, 885–892. doi: 10.1161/01.Hyp.0000259328.04159.90

Irvine, J. C., Ritchie, R. H., Favaloro, J. L., Andrews, K. L., Widdop, R. E., and Kemp-Harper, B. K. (2008). Nitroxyl (HNO): the Cinderella of the nitric oxide story. *Trends Pharmacol. Sci.* 29, 601–608. doi: 10.1016/j.tips.2008.08.005

Irvine, J. C., Kemp-Harper, B. K., and Widdop, R. E. (2011). Chronic administration of the HNO donor Angeli's salt does not lead to tolerance, cross-tolerance, or endothelial dysfunction: comparison with GTN and DEA/NO. *Antioxid. Redox Signal.* 14, 1615–1624. doi: 10.1089/ars.2010.3269

Irvine, J. C., Cao, N., Gossain, S., Alexander, A. E., Love, J. E., Qin, C., et al. (2013). HNO/cGMP-dependent antihypertrophic actions of isopropylamine-NONOate in neonatal rat cardiomyocytes: Potential therapeutic advantages of HNO over NO. *Am. J. Physiol. - Hear. Circ. Physiol.* 305, H365–H377. doi: 10.1152/ajpheart.00495.2012

Ito, H., Nakashima, M., Meguro, K., Furukawa, H., Yamashita, H., Takaki, A., et al. (2015). Flow mediated dilatation is reduced with the progressive stages of glomerular filtration rate and albuminuria in type 2 diabetic patients without coronary heart disease. *J. Diabetes Res.* 2015, 1–9. doi: 10.1155/2015/728127

Jones, D. A., Pellaton, C., Velmurugan, S., Rathod, K. S., Andiapen, M., Antoniou, S., et al. (2015). Randomized phase 2 trial of intracoronary nitrite during acute myocardial infarction. *Circ. Res.* 116, 437–447. doi: 10.1161/CIRCRESAHA.116.305082

Kövamees, O., Shemyakin, A., and Pernow, J. (2016). Amino acid metabolism reflecting arginase activity is increased in patients with type 2 diabetes and associated with endothelial dysfunction. *Diabetes Vasc. Dis. Res.* 13, 354–360. doi: 10.1177/1479164116643916

Kahlberg, N., Qin, C. X., Anthonisz, J., Jap, E., Ng, H. H., Jelinic, M., et al. (2016). Adverse vascular remodelling is more sensitive than endothelial dysfunction to hyperglycaemia in diabetic rat mesenteric arteries. *Pharmacol. Res.* 111, 325–335. doi: 10.1016/j.phrs.2016.06.025

Kass, D. A., Takimoto, E., Nagayama, T., and Champion, H. C. (2007). Phosphodiesterase regulation of nitric oxide signaling. *Cardiovasc. Res.* 75, 303–314. doi: 10.1016/j.cardiores.2007.02.031

Keceli, G., Majumdar, A., Thorpe, C. N., Jun, S., Tocchetti, C. G., Lee, D. I., et al. (2019). Nitroxyl (HNO) targets phospholamban cysteines 41 and 46 to enhance cardiac function. *J. Gen. Physiol.* 151, 758–770. doi: 10.1085/jgp.201812208

Kemp-Harper, B. K., and Schmidt, H. H. H. W. (2009). *"cGMP in the vasculature,"*. Eds. H. H. H. W. Schmidt, F. Hofmann and J.-P. Stasch (Berlin, Heidelberg: Springer Berlin Heidelberg), 447–467. doi: 10.1007/978-3-540-68964-5_19

Kemp-Harper, B. K., Horowitz, J. D., and Ritchie, R. H. (2016). Therapeutic potential of nitroxyl (HNO) donors in the management of acute decompensated heart failure. *Drugs* 76, 1337–1348. doi: 10.1007/s40265-016-0631-y

Kemp-Harper, B. K. (2011). Nitroxyl (HNO): A novel redox signaling molecule. *Antioxid. Redox Signal.* 14, 1609–1613. doi: 10.1089/ars.2011.3937

Kennedy, J. A., Beck-Oldach, K., McFadden-Lewis, K., Murphy, G. A., Wong, Y. W., Zhang, Y., et al. (2006). Effect of the anti-anginal agent, perhexiline, on neutrophil, valvular and vascular superoxide formation. *Eur. J. Pharmacol.* 531, 13–19. doi: 10.1016/j.ejphar.2005.11.058

Kizub, I. V., Klymenko, K. I., and Soloviev, A. I. (2014). Protein kinase C in enhanced vascular tone in diabetes mellitus. *Int. J. Cardiol.* 174, 230–242. doi: 10.1016/j.ijcard.2014.04.117

Ko, M. J., Jo, A. J., Kim, Y. J., Kang, S. H., Cho, S., Jo, S. H., et al. (2019). Time- and dose-dependent association of statin use with risk of clinically relevant new-onset diabetes mellitus in primary prevention: a nationwide observational cohort study. *J. Am. Hear. Assoc.* 8, e011320. doi: 10.1161/jaha.118.011320

Kohr, M. J., Kaludercic, N., Tocchetti, C. G., Gao, W. D., Kass, D. A., Janssen, P. M. L., et al. (2010). Nitroxyl enhances myocyte Ca2+ transients by exclusively targeting SR Ca2+-cycling. *Front. Biosci. - Elit.* 2 E, 614–626. doi: 10.2741/e118

Korkmaz, Y., Roggendorf, H. C., Siefer, O. G., Seehawer, J., Imhof, T., Plomann, M., et al. (2018). Downregulation of the α1- and β1-subunit of sGC in arterial smooth muscle cells of OPSCC Is HPV-Independent. *J. Dent. Res.* 97, 1214–1221. doi: 10.1177/0022034518774531

Kovanen, P. T., and Bot, I. (2017). Mast cells in atherosclerotic cardiovascular disease - Activators and actions. *Eur. J. Pharmacol.* 816, 37–46. doi: 10.1016/j.ejphar.2017.10.013

Kovanen, P. T., Maija, K., and Timo, P. (1995). Infiltrates of activated mast cells at the site of coronary atheromatous erosion or rupture in myocardial infarction. *Circulation* 92, 1084–1088. doi: 10.1161/01.CIR.92.5.1084

Laine, P., Kaartinen, M., Penttilä, A., Panula, P., Paavonen, T., and T, K. P. (1999). Association between myocardial infarction and the mast cells in the adventitia of the infarct-related coronary artery. *Circulation* 99, 361–369. doi: 10.1161/01.CIR.99.3.361

Lee, K. H., Lee, S. R., Cho, H., Woo, J. S., Kang, J. H., Jeong, Y. M., et al. (2017). Cardioprotective effects of PKG activation by soluble GC activator, BAY 60-2770, in ischemia-reperfusion-injured rat hearts. *PloS One* 12, 1–12. doi: 10.1371/journal.pone.0180207

Lees, C., Jurkovic, D., Zaidi, J., and Campbell, S. (1998). Unexpected effect of a nitric oxide donor on uterine artery Doppler velocimetry in oligomenorrheic women with polycystic ovaries. *Ultrasound Obstet. Gynecol.* 11, 129–132. doi: 10.1046/j.1469-0705.1998.11020129.x

Leo, C. H., Joshi, A., Hart, J. L., and Woodman, O. L. (2012). Endothelium-dependent nitroxyl-mediated relaxation is resistant to superoxide anion scavenging and preserved in diabetic rat aorta. *Pharmacol. Res.* 66, 383–391. doi: 10.1016/j.phrs.2012.07.010

Lima, B., Forrester, M. T., Hess, D. T., and Stamler, J. S. (2010). S-nitrosylation in cardiovascular signaling. *Circ. Res.* 106, 633–646. doi: 10.1161/CIRCRESAHA.109.207381

Lin, E. Q., Irvine, J. C., Cao, A. H., Alexander, A. E., Love, J. E., Patel, R., et al. (2012). Nitroxyl (HNO) stimulates soluble guanylyl cyclase to suppress cardiomyocyte hypertrophy and superoxide generation. *PloS One* 7, 6–16. doi: 10.1371/journal.pone.0034892

Lindholm, M. G., Boesgaard, S., Torp-Pedersen, C., and Kober, L. (2005). Diabetes mellitus and cardiogenic shock in acute myocardial infarction. *Eur. J. Heart Fail.* 7, 834–839. doi: 10.1016/j.ejheart.2004.09.007

Lob, H., Rosenkranz, A. C., Breitenbach, T., Berkels, R., Drummond, G., and Roesen, R. (2006). Antioxidant and nitric oxide-sparing actions of dihydropyridines and ACE inhibitors differ in human endothelial cells. *Pharmacology* 76, 8–18. doi: 10.1159/000088854

Lorenzi, M. (2007). The polyol pathway as a mechanism for diabetic retinopathy: attractive, elusive, and resilient. *Exp. Diabetes Res.* 2007, 61038. doi: 10.1155/2007/61038

Lund, T., Svindland, A., Pepaj, M., Jensen, A.-B., Berg, J. P., Kilhovd, B., et al. (2011). Fibrin(ogen) may be an important target for methylglyoxal-derived AGE modification in elastic arteries of humans. *Diabetes Vasc. Dis. Res.* 8, 284–294. doi: 10.1177/1479164111416831

Lundberg, J. O., Gladwin, M. T., and Weitzberg, E. (2015). Strategies to increase nitric oxide signalling in cardiovascular disease. *Nat. Rev. Drug Discovery* 14, 623–641. doi: 10.1038/nrd4623

Mátyás, C., Németh, B. T., Oláh, A., Hidi, L., Birtalan, E., Kellermayer, D., et al. (2015). The soluble guanylate cyclase activator cinaciguat prevents cardiac dysfunction in a rat model of type-1 diabetes mellitus. *Cardiovasc. Diabetol.* 14, 1–13. doi: 10.1186/s12933-015-0309-x

Malmberg, K., Rydén, L., Efendic, S., Herlitz, J., Nicol, P., Waldenstrom, A., et al. (1995). Randomized trial of insulin-glucose infusion followed by subcutaneous insulin treatment in diabetic patients with acute myocardial infarction (DIGAMI study): Effects on mortality at 1 year. *J. Am. Coll. Cardiol.* 26, 57 LP–57 65. doi: 10.1016/0735-1097(95)00126-K

Mancardi, D., Ridnour, L., Thomas, D., Katori, T., Tocchetti, C., Espey, M., et al. (2005). The Chemical Dynamics of NO and Reactive Nitrogen Oxides: A Practical Guide. *Curr. Mol. Med.* 4, 723–740. doi: 10.2174/1566524043359854

Mao, K., Chen, S., Chen, M., Ma, Y., Wang, Y., Huang, B., et al. (2013). Nitric oxide suppresses NLRP3 inflammasome activation and protects against LPS-induced septic shock. *Cell Res.* 23, 201–212. doi: 10.1038/cr.2013.6

Marsh, S. A., Dell'Italia, L. J., and Chatham, J. C. (2011). Activation of the hexosamine biosynthesis pathway and protein O-GlcNAcylation modulate hypertrophic and cell signaling pathways in cardiomyocytes from diabetic mice. *Amino Acids* 40, 819–828. doi: 10.1007/s00726-010-0699-8

Massion, P. B., Feron, O., Dessy, C., and Balligand, J. L. (2003). Nitric oxide and cardiac function: Ten years after, and continuing. *Circ. Res.* 93, 388–398. doi: 10.1161/01.RES.0000088351.58510.21

Matsushima, S., Kinugawa, S., Yokota, T., Inoue, N., Ohta, Y., Hamaguchi, S., et al. (2009). Increased myocardial NAD(P)H oxidase-derived superoxide causes the exacerbation of postinfarct heart failure in type 2 diabetes. *Am. J. Physiol. - Hear. Circ. Physiol.* 297, 409–416. doi: 10.1152/ajpheart.01332.2008

Mehta, S. R., Yusuf, S., Diaz, R., Zhu, J., Pais, P., Xavier, D., et al. (2005). Effect of glucose-insulin-potassium infusion on mortality in patients with acute ST-segment elevation myocardial infarction: the CREATE-ECLA randomized controlled trial. *JAMA* 293, 437–446. doi: 10.1001/jama.293.4.437

Mendes-Silverio, C. B., Leiria, L. O. S., Morganti, R. P., Anhê, G. F., Marcondes, S., Mónica, F. Z., et al. (2012). Activation of haem-oxidized soluble guanylyl cyclase with BAY 60-2770 in human platelets lead to overstimulation of the cyclic GMP signaling pathway. *PloS One* 7, e47223. doi: 10.1371/journal.pone.0047223

Meurer, S., Pioch, S., Pabst, T., Opitz, N., Schmidt, P. M., Beckhaus, T., et al. (2009). Nitric oxide-independent vasodilator rescues heme-oxidized soluble guanylate cyclase from proteasomal degradation. *Circ. Res.* 105, 33–41. doi: 10.1161/CIRCRESAHA.109.198234

Miller, T. W., Cherney, M. M., Lee, A. J., Francoleon, N. E., Farmer, P. J., King, S. B., et al. (2009). The effects of nitroxyl (HNO) on soluble guanylate cyclase activity: interactions at ferrous heme and cysteine thiols. *J. Biol. Chem.* 284, 21788–21796. doi: 10.1074/jbc.M109.014282

Miller, A. A., Maxwell, K. F., Chrissobolis, S., Bullen, M. L., Ku, J. M., Michael De Silva, T., et al. (2013). Nitroxyl (HNO) suppresses vascular Nox2 oxidase activity. *Free Radic. Biol. Med.* 60, 264–271. doi: 10.1016/j.freeradbiomed.2013.02.025

Miranda, K. M., Nims, R. W., Thomas, D. D., Espey, M. G., Citrin, D., Bartberger, M. D., et al. (2003). Comparison of the reactivity of nitric oxide and nitroxyl with heme proteins: A chemical discussion of the differential biological effects of these redox related products of NOS. *J. Inorg. Biochem.* 93, 52–60. doi: 10.1016/S0162-0134(02)00498-1

Murphey, L., Vaughan, D., and Brown, N. (2003). Contribution of bradykinin to the cardioprotective effects of ACE inhibitors. *Eur. Hear. J. Suppl.* 5, A37–A41. doi: 10.1016/S1520-765X(03)90062-9

Napoli, C., de Nigris, F., Williams-Ignarro, S., Pignalosa, O., Sica, V., and Ignarro, L. J. (2006). Nitric oxide and atherosclerosis: An update. *Nitric. Oxide - Biol. Chem.* 15, 265–279. doi: 10.1016/j.niox.2006.03.011

Neutel, J. M. (2010). Choosing among renin-angiotensin system blockers for the management of hypertension: From pharmacology to clinical efficacy. *Curr. Med. Res. Opin.* 26, 213–222. doi: 10.1185/03007990903444434

Nightingale, A. K., Sverdlov, A. L., Rajendran, S., Mishra, K., Heresztyn, T., Ngo, D. T. M., et al. (2011). Lack of association between aortic sclerosis and left ventricular hypertrophy in elderly subjects. *Int. J. Cardiol.* 150, 33–38. doi: 10.1016/j.ijcard.2010.02.024

Okon, E. B., Chung, A. W. Y., Rauniyar, P., Padilla, E., Tejerina, T., McManus, B. M., et al. (2005). Compromised arterial function in human type 2 diabetic patients. *Diabetes* 54, 2415–2423. doi: 10.2337/diabetes.54.8.2415

Ostadal, P. (2012). Statins as first-line therapy for acute coronary syndrome? *Exp. Clin. Cardiol.* 17, 227–236.

Pacher, P., and Szabó, C. (2005). Role of poly(ADP-ribose) polymerase-1 activation in the pathogenesis of diabetic complications: endothelial dysfunction, as a common underlying theme. *Antioxid. Redox Signal.* 7, 1568–1580. doi: 10.1089/ars.2005.7.1568

Paolocci, N., Biondi, R., Bettini, M., Lee, C., Berlowitz, C. O., Rossi, R., et al. (2001a). Oxygen radical-mediated reduction in basal and agonist-evoked no release in isolated rat heart. *J. Mol. Cell. Cardiol.* 33, 671–679. doi: 10.1006/jmcc.2000.1334

Paolocci, N., Saavedra, W. F., Miranda, K. M., Martignani, C., Isoda, T., Hare, J. M., et al. (2001b). Nitroxyl anion exerts redox-sensitive positive cardiac inotropy in vivo by calcitonin gene-related peptide signaling. *Proc. Natl. Acad. Sci. U. S. A.* 98, 10463–10468. doi: 10.1073/pnas.181191198

Paolocci, N., Katori, T., Champion, H. C., St. John, M. E., Miranda, K. M., Fukuto, J. M., et al. (2003). Positive inotropic and lusitropic effects of HNO/NO- in failing hearts: Independence from β-adrenergic signaling. *Proc. Natl. Acad. Sci.* 100, 5537 LP– 5542. doi: 10.1073/pnas.0937302100

Paolocci, N., Jackson, M. I., Lopez, B. E., Miranda, K., Tocchetti, C. G., Wink, D. A., et al. (2007). The pharmacology of nitroxyl (HNO) and its therapeutic potential: not just the janus face of NO. *Pharmacol. Ther.* 113, 442–458. doi: 10.1016/j.pharmthera.2006.11.002

Paulus, W. J., and Bronzwaer, J. G. F. (2004). Nitric oxide's role in the heart: Control of beating or breathing? *Am. J. Physiol. - Hear. Circ. Physiol.* 287, 8–13. doi: 10.1152/ajpheart.01147.2003

Phaniendra, A., Jestadi, D. B., and Periyasamy, L. (2015). Free radicals: properties, sources, targets, and their implication in various diseases. *Indian J. Clin. Biochem.* 30, 11–26. doi: 10.1007/s12291-014-0446-0

Pignatelli, P., Menichelli, D., Pastori, D., and Violi, F. (2018). Oxidative stress and cardiovascular disease: new insights. *Kardiol Pol.* 76, 713–722. doi: 10.5603/KP.a2018.0071

Premer, C., Kanelidis, A. J., Hare, J. M., and Schulman, I. H. (2019). Rethinking endothelial dysfunction as a crucial target in fighting heart failure. *Mayo Clin. Proc. Innov. Qual. Outcomes* 3, 1–13. doi: 10.1016/j.mayocpiqo.2018.12.006

Qian, J., and Fulton, D. J. R. (2012). Exogenous, but not endogenous nitric oxide inhibits adhesion molecule expression in human endothelial cells. *Front. Physiol.* 3, 1–7. doi: 10.3389/fphys.2012.00003

Qian, J., and Fulton, D. (2013). Post-translational regulation of endothelial nitric oxide synthase in vascular endothelium. *Front. Physiol.* 4, 1–11. doi: 10.3389/fphys.2013.00347

Qin, C. X., Sleaby, R., Davidoff, A. J., Bell, J. R., De Blasio, M. J., Delbridge, L. M., et al. (2017). Insights into the role of maladaptive hexosamine biosynthesis and O-GlcNAcylation in development of diabetic cardiac complications. *Pharmacol. Res.* 116, 45–56. doi: 10.1016/j.phrs.2016.12.016

Qin, C. X., Anthonisz, J., Leo, C. H., Kahlberg, N., Velagic, A., Li, M., et al. (2020). Nitric oxide resistance, induced in the myocardium by diabetes, is circumvented by the nitric oxide redox sibling, nitroxyl. *Antioxid. Redox Signal.* 32, 60–77. doi: 10.1089/ars.2018.7706

Radziwon-Balicka, A., Lesyk, G., Back, V., Fong, T., Loredo-Calderon, E. L., Dong, B., et al. (2017). Differential eNOS-signalling by platelet subpopulations regulates adhesion and aggregation. *Cardiovasc. Res.* 113, 1719–1731. doi: 10.1093/cvr/cvx179

Ramana, K. V., Chandra, D., Srivastava, S., Bhatnagar, A., and Srivastava, S. K. (2003). Nitric oxide regulates the polyol pathway of glucose metabolism in vascular smooth muscle cells. *FASEB J.* 17, 417–425. doi: 10.1096/fj.02-0722com

Reriani, M. K., Dunlay, S. M., Gupta, B., West, C. P., Rihal, C. S., Lerman, L. O., et al. (2011). Effects of statins on coronary and peripheral endothelial function in humans: a systematic review and meta-analysis of randomized controlled trials. *Eur. J. Cardiovasc. Prev. Rehabil.* 18, 704–716. doi: 10.1177/1741826711398430

Ritchie, R. H., Irvine, J. C., Rosenkranz, A. C., Patel, R., Wendt, I. R., Horowitz, J. D., et al. (2009). Exploiting cGMP-based therapies for the prevention of left ventricular hypertrophy: NO• and beyond. *Pharmacol. Ther.* 124, 279–300. doi: 10.1016/j.pharmthera.2009.08.001

Ritchie, R. H., Drummond, G. R., Sobey, C. G., De Silva, T. M., and Kemp-Harper, B. K. (2017). The opposing roles of NO and oxidative stress in cardiovascular disease. *Pharmacol. Res.* 116, 57–69. doi: 10.1016/j.phrs.2016.12.017

Roger, S., Paysant, J., Badier-Commander, C., Cordi, A., Verbeuren, T. J., and Feletou, M. (2010). Anti-aggregating effect of BAY 58-2667, an activator of soluble guanylyl cyclase. *Vasc. Pharmacol.* 53, 281–287. doi: 10.1016/j.vph.2010.09.008

Rosenkranz, A. C., Hood, S. G., Woods, R. L., Dusting, G. J., and Ritchie, R. H. (2002). Acute antihypertrophic actions of bradykinin in the rat heart: Importance of cyclic GMP. *Hypertension* 40, 498–503. doi: 10.1161/01.HYP.0000032854.74042.CF

Ruszkowski, P., Masajtis-Zagajewska, A., and Nowicki, M. (2019). Effects of combined statin and ACE inhibitor therapy on endothelial function and blood pressure in essential hypertension - a randomised double-blind, placebo controlled crossover study. *JRAAS - J. Renin-Angiotensin-Aldosterone Syst.* 20, 1–9. doi: 10.1177/1470320319868890

Sabbah, H. N., Tocchetti, C. G., Wang, M., Daya, S., Gupta, R. C., Tunin, R. S., et al. (2013). Nitroxyl (HNO) a novel approach for the acute treatment of heart failure. *Circ. Heart Fail.* 6, 1250–1258. doi: 10.1161/CIRCHEARTFAILURE.113.000632

Saeedi, P., Petersohn, I., Salpea, P., Malanda, B., Karuranga, S., Unwin, N., et al. (2019). Global and regional diabetes prevalence estimates for 2019 and projections for 2030 and 2045: Results from the International Diabetes Federation Diabetes Atlas, 9th edition. *Diabetes Res. Clin. Pract.* 157, 107843. doi: 10.1016/j.diabres.2019.107843

Salerno, J. C., Hopper, B. L., Ghosh, D. K., Scott, I. M., and McMurry, J. L. (2018). Control of eNOS and nNOS through regulation of obligatory conformational changes in the reductase catalytic cycle. *bioRxiv* 410571, 1–35. doi: 10.1101/410571

Sandner, P., Zimmer, D. P., Milne, G. T., Follmann, M., Hobbs, A., and Stasch, J.-P. (2019). Soluble Guanylate Cyclase Stimulators and Activators. *Handb. Exp. Pharmacol.* 249, 1–40. doi: 10.1007/164_2018_197

Schäfer, A., Fraccarollo, D., Werner, L., and Bauersachs, J. (2010). Guanylyl cyclase activator ataciguat improves vascular function and reduces platelet activation in heart failure. *Pharmacol. Res.* 62, 432–438. doi: 10.1016/j.phrs.2010.06.008

Schachinger, V., Britten, M. B., and Zeiher, A. M. (2000). Prognostic impact of coronary vasodilator dysfunction on adverse long-term outcome of coronary heart disease. *Circulation* 101, 1899–1906. doi: 10.1161/01.CIR.101.16.1899

Schulze, P. C., Yoshioka, J., Takahashi, T., He, Z., King, G. L., and Lee, R. T. (2004). Hyperglycemia promotes oxidative stress through inhibition of thioredoxin function by thioredoxin-interacting protein. *J. Biol. Chem.* 279, 30369–30374. doi: 10.1074/jbc.M400549200

Selemidis, S., Dusting, G. J., Peshavariya, H., Kemp-Harper, B. K., and Drummond, G. R. (2007). Nitric oxide suppresses NADPH oxidase-dependent superoxide production by S-nitrosylation in human endothelial cells. *Cardiovasc. Res.* 75, 349–358. doi: 10.1016/j.cardiores.2007.03.030

Sharma, A., Bernatchez, P. N., and de Haan, J. B. (2012). Targeting endothelial dysfunction in vascular complications associated with diabetes. *Int. J. Vasc. Med.* 2012, 750126. doi: 10.1155/2012/750126

Shemyakin, A., Kövamees, O., Rafnsson, A., Böhm, F., Svenarud, P., Settergren, M., et al. (2012). Arginase inhibition improves endothelial function in patients with coronary artery disease and type 2 diabetes mellitus. *Circulation* 126, 2943–2950. doi: 10.1161/CIRCULATIONAHA.112.140335

Siddiqi, N., Neil, C., Bruce, M., MacLennan, G., Cotton, S., Papadopoulou, S., et al. (2014). Intravenous sodium nitrite in acute ST-elevation myocardial infarction: a randomized controlled trial (NIAMI). *Eur. Heart J.* 35, 1255–1262. doi: 10.1093/eurheartj/ehu096

Spiecker, M., Peng, H. B., and Liao, J. K. (1997). Inhibition of endothelial vascular cell adhesion molecule-1 expression by nitric oxide involves the induction and nuclear translocation of IκBα. *J. Biol. Chem.* 272, 30969–30974. doi: 10.1074/jbc.272.49.30969

Springhorn, C., Matsha, T. E., Erasmus, R. T., and Essop, M. F. (2012). Exploring leukocyte O-GlcNAcylation as a novel diagnostic tool for the earlier detection of type 2 diabetes mellitus. *J. Clin. Endocrinol. Metab.* 97, 4640–4649. doi: 10.1210/jc.2012-2229

Stepien, J. M., Prideaux, R. M., Willoughby, S. R., Chirkov, Y. Y., and Horowitz, J. D. (2003). Pilot study examining the effect of cholesterol lowering on platelet nitric oxide responsiveness and arterial stiffness in subjects with isolated mild hypercholesterolaemia. *Clin. Exp. Pharmacol. Physiol.* 30, 507–512. doi: 10.1046/j.1440-1681.2003.03859.x

Strey, C. H., Young, J. M., Lainchbury, J. H., Frampton, C. M., Nicholls, M. G., Richards, A. M., et al. (2006). Short-term statin treatment improves endothelial function and neurohormonal imbalance in normocholesterolaemic patients with non-ischaemic heart failure. *Heart* 92, 1603 LP– 1609. doi: 10.1136/hrt.2005.082560

Stuehr, D. J., Santolini, J., Wang, Z. Q., Wei, C. C., and Adak, S. (2004). Update on mechanism and catalytic regulation in the NO synthases. *J. Biol. Chem.* 279, 36167–36170. doi: 10.1074/jbc.R400017200

Sun, L., Ferreira, J. C. B., and Mochly-Rosen, D. (2011). ALDH2 activator inhibits increased myocardial infarction injury by nitroglycerin tolerance. *Sci. Transl. Med.* 3, 107ra111–107ra111. doi: 10.1126/scitranslmed.3002067

Sverdlov, A. L., Ngo, D. T. M., Nightingale, A. K., Rajendran, S., Mishra, K., Heresztyn, T., et al. (2011). The endogenous NOS inhibitor asymmetric dimethylarginine (ADMA) predicts LV mass independent of afterload. *Nitric. Oxide - Biol. Chem.* 25, 41–46. doi: 10.1016/j.niox.2011.04.009

Sverdlov, A. L., Chan, W. P. A., Procter, N. E. K., Chirkov, Y. Y., Ngo, D. T. M., and Horowitz, J. D. (2013). Reciprocal regulation of NO signaling and TXNIP expression in humans: Impact of aging and ramipril therapy. *Int. J. Cardiol.* 168, 4624–4630. doi: 10.1016/j.ijcard.2013.07.159

Sverdlov, A. L., Ngo, D. T. M., Chan, W. P. A., Chirkov, Y. Y., and Horowitz, J. D. (2014). Aging of the nitric oxide system: Are we as old as our NO? *J. Am. Heart Assoc.* 3, 1–12. doi: 10.1161/JAHA.114.000973

Swedberg, K., Held, P., Kjekshus, J., Rasmussen, K., Ryden, L., and Wedel, H. (1992). Effects of the early administration of enalapril on mortality in patients with acute myocardial infarction. Results of the Cooperative New Scandinavian Enalapril Survival Study II (CONSENSUS II). *N. Engl. J. Med.* 327, 678–684. doi: 10.1056/NEJM199209033271002

Szpigel, A., Hainault, I., Carlier, A., Venteclef, N., Batto, A. F., Hajduch, E., et al. (2018). Lipid environment induces ER stress, TXNIP expression and inflammation in immune cells of individuals with type 2 diabetes. *Diabetologia* 61, 399–412. doi: 10.1007/s00125-017-4462-5

Tabit, C. E., Shenouda, S. M., Holbrook, M., Fetterman, J. L., Kiani, S., Frame, A. A., et al. (2013). Protein kinase C-β contributes to impaired endothelial insulin signaling in humans with diabetes mellitus. *Circulation* 127, 86–95. doi: 10.1161/CIRCULATIONAHA.112.127514

Tan, K. C. B., Chow, W.-S., Ai, V. H. G., Metz, C., Bucala, R., and Lam, K. S. L. (2002). Advanced glycation end products and endothelial dysfunction in type 2 diabetes. *Diabetes Care* 25, 1055. doi: 10.2337/diacare.25.6.1055

Tare, M., Kalidindi, R. S. R., Bubb, K. J., Parkington, H. C., Boon, W. M., Li, X., et al. (2017). Vasoactive actions of nitroxyl (HNO) are preserved in resistance arteries in diabetes. *Naunyn. Schmiedebergs. Arch. Pharmacol.* 390, 397–408. doi: 10.1007/s00210-016-1336-1

Thomas, M. C., Baynes, J. W., Thorpe, S. R., and Cooper, M. E. (2005). The role of AGEs and AGE inhibitors in diabetic cardiovascular disease. *Curr. Drug Targets* 6, 453–474. doi: 10.2174/1389450054021873

Tita, C., Gilbert, E. M., Van Bakel, A. B., Grzybowski, J., Haas, G. J., Jarrah, M., et al. (2017). A phase 2a dose-escalation study of the safety, tolerability, pharmacokinetics and haemodynamic effects of BMS-986231 in hospitalized patients with heart failure with reduced ejection fraction. *Eur. J. Hear. Fail* 19, 1321–1332. doi: 10.1002/ejhf.897

Tocchetti, C. G., Wang, W., Froehlich, J. P., Huke, S., Aon, M. A., Wilson, G. M., et al. (2007). Nitroxyl improves cellular heart function by directly enhancing cardiac sarcoplasmic reticulum Ca2+ cycling. *Circ. Res.* 100, 96–104. doi: 10.1161/01.RES.0000253904.53601.c9

Toth, E., Racz, A., Toth, J., Kaminski, P. M., Wolin, M. S., Bagi, Z., et al. (2007). Contribution of polyol pathway to arteriolar dysfunction in hyperglycemia. Role of oxidative stress, reduced NO, and enhanced PGH2/TXA2 mediation. *Am. J. Physiol. Circ. Physiol.* 293, H3096–H3104. doi: 10.1152/ajpheart.01335.2006

Tousoulis, D., Papageorgiou, N., Androulakis, E., Siasos, G., Latsios, G., Tentolouris, K., et al. (2013). Diabetes mellitus-associated vascular impairment: Novel circulating biomarkers and therapeutic approaches. *J. Am. Coll. Cardiol.* 62, 667–676. doi: 10.1016/j.jacc.2013.03.089

Tsihlis, N. D., Murar, J., Kapadia, M. R., Ahanchi, S. S., Oustwani, C. S., Saavedra, J. E., et al. (2010). Isopropylamine NONOate (IPA/NO) moderates neointimal hyperplasia following vascular injury. *J. Vasc. Surg.* 51, 1248–1259. doi: 10.1016/j.jvs.2009.12.028

Turturro, F., Friday, E., and Welbourne, T. (2007). Hyperglycemia regulates thioredoxin-ROS activity through induction of thioredoxin-interacting protein (TXNIP) in metastatic breast cancer-derived cells MDA-MB-231. *BMC Cancer* 7, 1–7. doi: 10.1186/1471-2407-7-96

Vallance, P., Leone, A., Calver, A., Collier, J., and Moncada, S. (1992). Accumulation of an endogenous inhibitor of nitric oxide synthesis in chronic renal failure. *Lancet (London England)* 339, 572–575. doi: 10.1016/0140-6736(92)90865-z

van Etten, R., de Koning, E., Verhaar, M., Gaillard, C., and Rabelink, T. (2002). Impaired NO-dependent vasodilation in patients with Type II (non-insulin-dependent) diabetes mellitus is restored by acute administration of folate. *Diabetologia* 45, 1004–1010. doi: 10.1007/s00125-002-0862-1

Vavuranakis, M., Kariori, M., Siasos, G., Kalogeras, K., and Tousoulis, D. (2017). Statins in acute coronary syndromes. *Curr. Pharm. Des.* 23, 547–553. doi: 10.2174/1381612823666170816114403

Vehkavaara, S., and Yki-Järvinen, H. (2004). 3.5 years of insulin therapy with insulin glargine improves in vivo endothelial function in type 2 diabetes. *Arterioscler. Thromb. Vasc. Biol.* 24, 325–330. doi: 10.1161/01.ATV.0000113817.48983.c5

Wang, H., Meng, Q. H., Gordon, J. R., Khandwala, H., and Wu, L. (2007). Proinflammatory and proapoptotic effects of methylglyoxal on neutrophils from patients with type 2 diabetes mellitus. *Clin. Biochem.* 40, 1232–1239. doi: 10.1016/j.clinbiochem.2007.07.016

Williams, S. B., Cusco, J. A., Roddy, M. A., Johnstone, M. T., and Creager, M. A. (1996). Impaired nitric oxide-mediated vasodilation in patients with non-insulin-dependent diabetes mellitus. *J. Am. Coll. Cardiol.* 27, 567–574. doi: 10.1016/0735-1097(95)00522-6

Willoughby, S. R., Stewart, S., Chirkov, Y. Y., Kennedy, J. A., Holmes, A. S., and Horowitz, J. D. (2002). Beneficial clinical effects of perhexiline in patients with stable angina pectoris and acute coronary syndromes are associated with potentiation of platelet responsiveness to nitric oxide. *Eur. Heart J.* 23, 1946–1954. doi: 10.1053/euhj.2002.3296

Willoughby, S. R., Rajendran, S., Chan, W. P., Procter, N., Leslie, S., Liberts, E. A., et al. (2012). Ramipril sensitizes platelets to nitric oxide: implications for therapy in high-risk patients. *J. Am. Coll. Cardiol.* 60, 887–894. doi: 10.1016/j.jacc.2012.01.066

Wink, D. A., Miranda, K. M., Espey, M. G., Pluta, R. M., Hewett, S. J., Colton, C., et al. (2001). Mechanisms of the antioxidant effects of nitric oxide. *Antioxid. Redox Signal.* 3, 203–213. doi: 10.1089/152308601300185179

Worthley, M. I., Holmes, A. S., Willoughby, S. R., Kucia, A. M., Heresztyn, T., Stewart, S., et al. (2007). The deleterious effects of hyperglycemia on platelet function in diabetic patients with acute coronary syndromes: mediation by superoxide production, resolution with intensive insulin administration. *J. Am. Coll. Cardiol.* 49, 304–310. doi: 10.1016/j.jacc.2006.08.053

Wright, E., Scism-Bacon, J. L., and Glass, L. C. (2006). Oxidative stress in type 2 diabetes: The role of fasting and postprandial glycaemia. *Int. J. Clin. Pract.* 60, 308–314. doi: 10.1111/j.1368-5031.2006.00825.x

Wynne, B. M., Labazi, H., Tostes, R. C., and Webb, R. C. (2012). Aorta from angiotensin II hypertensive mice exhibit preserved nitroxyl anion mediated relaxation responses. *Pharmacol. Res.* 65, 41–47. doi: 10.1016/j.phrs.2011.07.002

Xu, J., Wu, Y., Song, P., Zhang, M., Wang, S., and Zou, M. H. (2007). Proteasome-dependent degradation of guanosine 5′-triphosphate cyclohydrolase I causes tetrahydrobiopterin deficiency in diabetes mellitus. *Circulation* 116, 944–953. doi: 10.1161/CIRCULATIONAHA.106.684795

Yusuf, S., Sleight, P., Pogue, J., Bosch, J., Davies, R., and Dagenais, G. (2000). Effects of an angiotensin-converting-enzyme inhibitor, ramipril, on cardiovascular events in high-risk patients. *N. Engl. J. Med.* 342, 145–153. doi: 10.1056/nejm200001203420301

Zakrzewicz, D., and Eickelberg, O. (2009). From arginine methylation to ADMA: A novel mechanism with therapeutic potential in chronic lung diseases. *BMC Pulm. Med.* 9, 1–7. doi: 10.1186/1471-2466-9-5

Zeiher, A. M., Fisslthaler, B., Schray-Utz, B., and Busse, R. (1995). Nitric oxide modulates the expression of monocyte chemoattractant protein 1 in cultured human endothelial cells. *Circ. Res.* 76, 980–986. doi: 10.1161/01.res.76.6.980

Zeller, A., Wenzl, M. V., Beretta, M., Stessel, H., Russwurm, M., Koesling, D., et al. (2009). Mechanisms underlying activation of soluble guanylate cyclase by the nitroxyl donor Angeli's salt. *Mol. Pharmacol.* 76, 1115–1122. doi: 10.1124/mol.109.059915

Zhou, R., Tardivel, A., Thorens, B., Choi, I., and Tschopp, J. (2010). Thioredoxin-interacting protein links oxidative stress to inflammasome activation. *Nat. Immunol.* 11, 136–140. doi: 10.1038/ni.1831

Zhou, S., Zhu, Q., Li, X., Chen, C., Liu, J., Ye, Y., et al. (2017). Asymmetric dimethylarginine and all-cause mortality: A systematic review and meta-analysis. *Sci. Rep.* 7, 1–9. doi: 10.1038/srep44692

Conflict of Interest: The authors declare that the research was conducted in the absence of any commercial or financial relationships that could be construed as a potential conflict of interest.

frontiers in Pharmacology

REVIEW
published: 29 September 2020
doi: 10.3389/fphar.2020.535395

Epigenetics and Vascular Senescence–Potential New Therapeutic Targets?

Qian Ding[1,2], *Chunhong Shao*[3]*, *Peter Rose*[4] *and Yi Zhun Zhu*[1]*

[1] State Key Laboratory of Quality Research in Chinese Medicine and School of Pharmacy, Macau University of Science and Technology, Macau, China, [2] School of Basic Medicine, Guizhou University of Traditional Chinese Medicine, Guiyang, China, [3] Department of Psychiatry, Huashan Hospital, Fudan University, Shanghai, China, [4] School of Biosciences, University of Nottingham, Loughborough, United Kingdom

Epigenetics is defined as the heritable alterations of gene expression without changes to the coding sequence of DNA. These alterations are mediated by processes including DNA methylation, histone modifications, and non-coding RNAs mechanisms. Vascular aging consists of both structural and functional changes in the vasculature including pathological processes that drive progression such as vascular cell senescence, inflammation, oxidation stress, and calcification. As humans age, these pathological conditions gradually accumulate, driven by epigenetic alterations, and are linked to various aging-related diseases. The development of drugs targeting a spectrum of epigenetic processes therefore offers novel treatment strategies for the targeting of age-related diseases. In our previous studies, we identified HDAC4, JMJD3, Fra-1, and GATA4 as potential pharmacological targets for regulating vascular inflammation, injury, and senescence.

Keywords: vascular aging, epigenetics, cell senescence, inflammation, oxidation stress, calcification

OPEN ACCESS

Edited by:
Cheng Xue Helena Qin,
Monash University, Australia

Reviewed by:
Hou-Zao Chen,
Chinese Academy of Medical Sciences, China
Christina Yan Ru Tan,
*Agency for Science, Technology and Research (A*STAR), Singapore*

***Correspondence:**
Yi Zhun Zhu
yzzhu@must.edu.mo
Chunhong Shao
chunhongshao@fudan.edu.cn

Specialty section:
This article was submitted to Cardiovascular and Smooth Muscle Pharmacology, a section of the journal Frontiers in Pharmacology

Received: *15 February 2020*
Accepted: *31 August 2020*
Published: *29 September 2020*

Citation:
Ding Q, Shao C, Rose P and Zhu YZ (2020) Epigenetics and Vascular Senescence–Potential New Therapeutic Targets?. Front. Pharmacol. 11:535395. doi: 10.3389/fphar.2020.535395

INTRODUCTION

In the 19th century, the father of modern medicine William Osler stated, "a man is only as old as his arteries." During vascular aging, pathological processes drive changes in the structure and function of blood vessels including dysregulation in vascular homeostasis and vascular remodeling, leading to lumen dilation, vascular stiffness, and thickening. At the molecular level dysregulation in vascular homeostasis is promoted by vascular cell senescence, widespread inflammation, oxidation stress, and calcification (Ding et al., 2018). It is now widely recognized that vascular aging is intimately linked with cardiovascular diseases (CVD) including atherosclerosis (AS), hypertension, coronary heart disease, and stroke (Lakatta and Levy, 2003b). Aside from high mortality rates, CVD also leads to reduce quality of life in afflicted individuals and high burden on society and families (Van Camp, 2014).

Epigenetics is defined as processes that governs the expression of a gene(s) without altering the sequence of coding DNA. These heritable changes in expression are controlled by distinct chemical modifications to bases present in DNA including DNA methylation and histone modification in

addition to non-coding RNA (ncRNA) mechanisms. In healthy tissues, normal gene expression occurs as a result of interactions between genetic and environmental factors *viz*. smoking, obesity, or alcohol consumption, which can cause dysregulation in cellular homeostasis, having negative impacts on health. Epigenetics changes can explained many of the interaction between genes and environment cues and can explain altered risk of developing diseases in humans (Feinberg, 2018). Indeed, as age increases the cumulative effects of stress and environmental impacts promotes the gradual accumulation of epigenetic changes in tissues. These epigenetic changes could serve by increasing an individuals susceptibility and risk of developing chronic diseases. Fortunately, many of these epigenetic modifications can be reversed, and targeting the respective enzymes that control methylation or histone modifications has been proposed as useful drug target in the treatment of age-related diseases. Therefore, in the current review, coverage of vascular aging and associated epigenetics processes will be covered. In addition, a summary of the main pathological drivers of vascular cell senescence, inflammation, oxidation stress, and calcification will be provided. A better perspective of epigenetic changes that occur during vascular aging will help to better understand the process of vascular damage that occurs with age. This information could be used to better development therapeutics or strategies to delay or treat aging-related cardiovascular diseases (Sen et al., 2016).

VASCULAR AGING

Vascular aging is characterized by changes in both structural and functional elements associated with blood vessels. Over the course of time, vascular aging leads to lumen dilation, vascular stiffness, and thickening, these changes being largely driven by pathological processes including vascular cell senescence, widespread inflammation, oxidation stress, and tissue calcification (Ding et al., 2018). The structural and functional changes of blood vessels that occurs during vascular aging are shown in **Figure 1**.

Structural Changes

Blood vessels (excluding capillaries) are composed of distinct anatomical features comprising the intima, media, and adventitia. The intima is largely composed of endothelial cells (ECs) and is the first defensive layer important in mitigating the development of vascular diseases. The media consists of vascular smooth muscle cells (VSMCs), elastic fibers, and extracellular matrix, and the adventitia, the outermost layer, is composed of loose connective tissue. This region is consists of thick collagen fibers and disordered elastin fibers. It is widely known that during aging, significant change occur in the intima, and this alters the function properties of this layer and, importantly, how the intima interacts with adjacent regions like the media (Lakatta et al., 2009). These changes promote altered responses to luminal dilation,

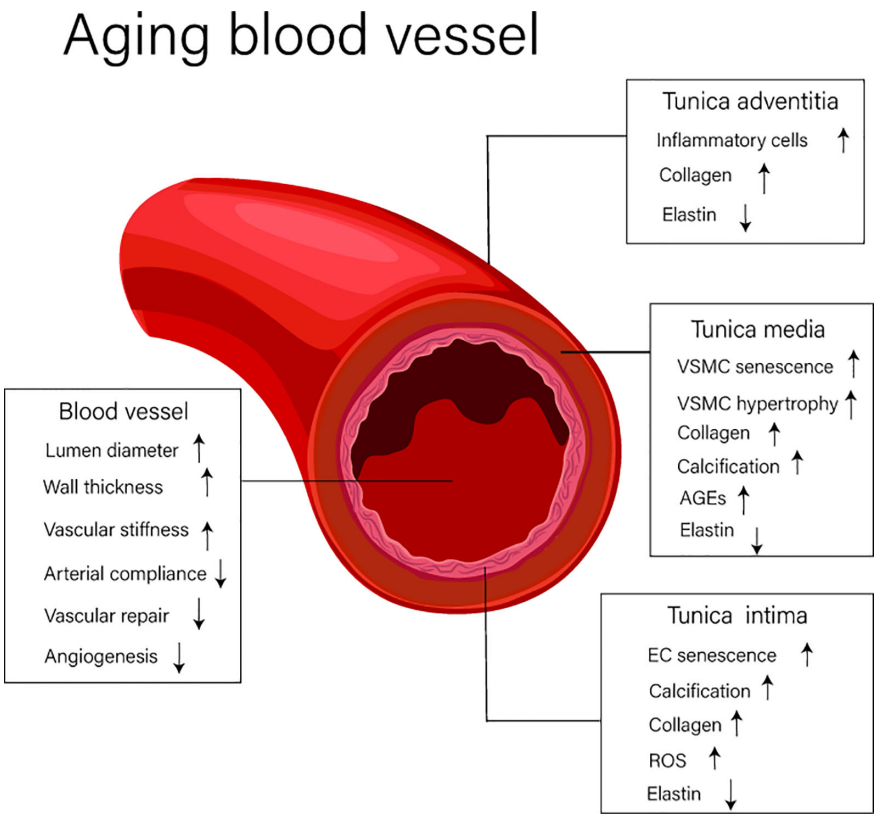

FIGURE 1 | The structure and functional changes of blood vessels. EC, endothelial cell; VSMC, vascular smooth muscle cell; AGEs, advanced glycation end products; ROS, reactive oxygen species.

vascular stiffness, and the thickening of blood vessels. Indeed, research has shown that the diameter of the aorta of elderly people, those over 65 years of age, increases by 15–20% compared with that of tissues from younger individuals (Lakatta, 2003). In addition, increased thickening of the arterial wall, largely driven by thickening of the arterial intima and media (Lakatta and Levy, 2003a), is associated with increased abundance of hypertrophic smooth muscle cells. Other common structural changes associated with aged blood vessels include elastin breaks, increased collagen abundance, and elevated levels of advanced glycation end products (AGEs). Combined these changes have a dramatic impact on the severity of vascular aging (Lakatta, 2003; Lakatta and Levy, 2003a).

Functional Changes

Increased arterial stiffness, decreased arterial compliance (AC), reductions in vascular repair, and diminished capacity to control processes like angiogenesis are important features of aging blood vessels. Arterial stiffness and decreased AC can be attributed to smooth muscle cell hypertrophy, arterial calcification, and ECM remolding. One of the key reasons for the decline in the ability of vessels to repair tissue damage is thought to be due to vascular endothelial cell senescence (Lakatta and Levy, 2003a; Novella et al., 2012).

Pathological Process During Vascular Aging and Cardiovascular Diseases

Aging blood vessels promote the development of vascular diseases and in turn accelerates the process of vascular aging. Numerous epidemiological studies indicate that lipid levels, diabetes, sedentary lifestyles, and various genetic factors increase the risk of coronary heart disease, hypertension, heart failure, and stroke. Underpining these changes are distinct biochemical and physiological changes that drive changes in the cardiovascular system. In recent times, the conventional cardiovascular continuum (CCC) in 2006 (Dzau et al., 2006a; Dzau et al., 2006b) has proposed that CVD begins with risk factors and progresses to terminal stage cardiac disease through a series of steps. The main characteristics of CCC are viewed as coronary artery atherosclerosis (AS), leading to coronary stenosis, and myocardial ischemia and myocardial infarction. However, one aspect not considered by the CCC criteria is the role of aging, especially vascular aging in the occurrence and development of CVD. Therefore, in 2010, the aging cardiovascular continuum (ACC) suggested that a key component of CVD should include aging (O'Rourke et al., 2010). Therefore, the ACC describes the stages of cardiovascular disease (CVD) as vascular aging, which promotes aorta dilation and sclerosis. In turn, these pathoglogical changes lead to heart failure, terminal stage cardiac disease, and death. In essence, the basic characteristics proposed by the ACC are the progressive degradation of the proximal aorta with arterial dilatation and sclerosis that has an adverse effects on the heart. If we consider that aortic pulsation, then the repetitive stretching and relaxation of arteries has occured 3 billion times in elderly people over 80 years old; it is clear that aging is an important factor in this process. As such, aging should be viewed as a risk factor for CVD, since it explains 50% of all clinical CVD cases in senior citizen (Cunha et al., 2017).

Vascular aging and CVD have several common pathological features when viewed at the molecular and cellular levels *viz.* increased oxidative stress, a pro-inflammatory environment, dysregulation in cell signaling, and altered response to infiltrating immune cell types. These feactures, as mentioned, provide sufficient conditions in the aged artery for the development of cardiovascular disease. For example, arterial aging and atherosclerosis have similar structural and biochemical characteristics. Indeed, research has shown that abnormal plasma cholesterol levels of young people is related to arterial wall thickening, VSMCs, collagen proliferation, and collagen deposition. These changes are similar to those observed in elderly people with altered cholesterol levels (McGill et al., 2008; Wang et al., 2010a). However, some animal studies show that plasma lipid levels do not change with aging; however, the prevalence, severity, and negative impact of atherosclerosis still increase in aged animals (Eto et al., 2008). These observations suggesting other molecular events are also important in driving CVD. One clue then may be that many proteins that are highly expressed in atherosclerotic tissues are also increased in aging arterial walls such as MFG-E8 and MMPs (Fu et al., 2009).

The pathological processes assocociated with vascular aging are characterized by vascular cell senescence, widespread inflammation, oxidation stress, and calcification, and these processes are summarized in **Figure 2**. As ECs age, the cells become flattened and enlarged, the rates of proliferation is diminished, and rates of apoptosis increased. In addition, enrichment of the surrounding environment with inflammatory mediators including interleukins-6 and tumour necrosis factor-α results in the decreased ability to control vascular repair and angiogenesis. Similalrly, the numbers of hypertrophic VSMCs begin to increase, as do the rates of cell proliferation and migration, and combined, this cellular transition drives extracellular matrix (ECM) remolding. Critically, as rates of inflammation increases over time, so do changes in cell populations of EC and VSMCs, and this, in turn, stimulates vascular aging and ultimately the endothelium damage. A widely recognized key driver of chronic inflammation in the vascularite, especially during aging, is the renin-angiotensin II (Ang II) signaling pathway. Changes in this signaling system initiates a cascde of events leading to the activation of downstream pro-inflammatory transcription factors like nuclear factor kappa beta (NF-kB), the production of reactive oxygen species (ROS) leading to oxidative damage, and the induction of endoplasmic reticulum (ER) stress. ER and sarcoplasmic reticulum are important pools of calcium; therefore, this could promote dysregulation in Ca^{2+} signaling. Collectively, these molecular events accelerate vascular remodeling (Cavallaro et al., 2000; Lakatta et al., 2009; Wang et al., 2010a; Wang et al., 2010b; Krebs et al., 2015). Under normal physiological conditions, ROS are produced in the vascular system through two routes, the mitochondrial and non-mitochondrial pathways. Importantly, in healthy or younger cells, oxidative stress is controlled by cells having the capacity to remove excess ROS *via* antioxidant system, and this could potentially reduce the rates of oxidative damage to mtDNA, respiratory chain complex proteins, and other important

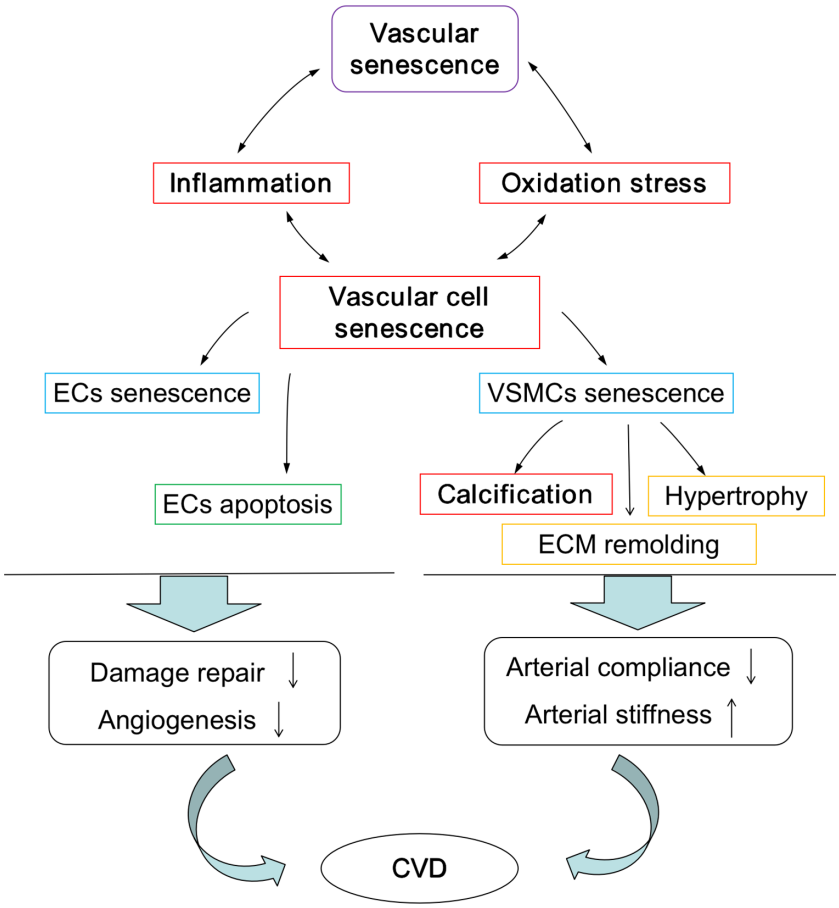

FIGURE 2 | Pathological process during vascular aging. Pathological process promote the development of vascular aging and vascular aging accelerates the pathological process. EC, endothelial cell; VSMC, vascular smooth muscle cell; ECM, extracellular matrix; CVD, cardiovascular diseases.

cellular components, therefore maintaining adequate cellular and tissue redox homeostasis (Kadlec et al., 2016). However, during aging, mitochondrial function can diminish, and this results in a cumulative increase of mitochondrial damage and excessive ROS production. Consequently, increased levels of ROS are generated *via* active oxygen release mechanism, resulting in further damage to the mitochondrial outer membrane and causing membranes to rupture, intracellular calcium overload, DNA damage, and the release of pro-apoptotic proteins like cytochrome C. This cascade ultimately leads to the induction of apoptosis or necrosis and further amplifies damage to aged or aging tissues fueling age-related degenerative diseases (Mikhed et al., 2015).

Tissue calcification is also common in the aged cardiovascular system, and researchers have demonstrated that senescent VSMCs are associated with a calcification phenotype. Aging VSMCs produce appreciable levels of calpain-1, and these promote blood vessels calcification, a process commonly referred to as biomineralization (Jiang et al., 2012). Calcification activates tissue transglutaminase (TG2) and upregulates calcification promoter genes such as the osteoblast transcription factor Runt-related transcription factor 2 (Runx2) and bone morphogenetic protein-2 (BMP-2). These systems participate in driving arterial calcification and sclerosis in the aging blood vessel wall. It is now realized that vascular calcification is an important cause of the increase in the incidence and mortality of cardiovascular diseases (Leopold, 2013) and that calcification, VSMCs hypertrophy, ECM remolding promote arterial stiffness and decreased AC.

EPIGENETIC CONTROL OF GENE EXPRESSION

Epigenetics is the heritable alterations of gene expression without changing the DNA sequence and determines whether a gene is turned on or off (Handy et al., 2011). Mounting evidence shows that epigenetic mechanisms play an important role in phenotypes and behavioral changes. Indeed, these mechanisms go someway to explain why twins who grew up in different locations and under differing environmental conditions, yet having the same genetic background, can have differences in lifespans or altered risks of chronic diseases such as diabetes or

hypertension (Fraga et al., 2005; Tan et al., 2013). Similarly, dietary influences like caloric restriction can delay the occurrence of age-dependent diseases *via* epigenetic mechanisms. Again, these examples exemplify the intimate association between how environmental factors can drive changes in epigenetic events that control gene expression (Maegawa et al., 2017).

DNA Methylation

DNA methylation, the direct addition of a methyl group to the 5th carbon atom of cytosine, is one the most widely recognised epigenetic mechanims known to regulate gene expression. CpG islands, characterized as short interspersed DNA sequences that are GC-rich regions. In mammalian cells, most of these CpG regions can be methylated (Jeltsch, 2008). Importantly, *de novo* DNA methylation status is governed by a family of enzymes known as DNA methyltransferases that include DNMT3a and DNMT3b, along with DNMT1 that is important during replication (Okano et al., 1999). The activities of these enzymes are readily influenced by environmental cues making DNA methylation a dynamic process in cells and tissues (Tsaprouni et al., 2014). Generally speaking, high methylation rates in the gene promoter region of genes inhibit gene expression. Inhibition in this instance is caused by altered (reduced) transcription factors binding to promoters consensus regions or by reducing the recruitment of chromatin modifying enzymes (Kohli and Zhang, 2013). To date, a wide range of abnormal DNA methylation patterns have been characterized in aged cells, with many seen in various age-related diseases (Hai and Zuo, 2016).

Histone Modifications

Histone modifications is another important epigenetic mechanism that regulates gene transcription by changing how histones proteins interact with DNA. Changes in DNA histone interactions is important in controlling gene expression during processes such as replication, transcription, and repair. Common mechanisms of histone modification include methylation, acetylation, phosphorylation, and ubiquitination. Unlike DNA methylation, the effect of histone modifications on gene expression may vary due to the specific type of chemical modifications (Shahbazian and Grunstein, 2007). Enzymes that regulate histone modifications include histone deacetylase (HDAC), histone methyltransferase, and histone acetyltransferase, and it is widely known that these enzymes play an important roles in the process of vascular aging (Calvanese et al., 2009).

ncRNA Mechanisms

ncRNA is RNA that lacks the capacity to code for a protein. Examples of ncRNA include microRNA (miRNA), long ncRNA (lncRNA), and small interfering RNA (siRNA). Although ncRNA has no direct affect on chromatin structure, it does play an important role in post-transcriptional control of gene expression (Gurha and Marian, 2013). Genome-wide RNA sequencing shows that ncRNAs are differentially expressed in both senescent and normal cells (Wu et al., 2015; Anderson et al., 2016).

DO EPIGENETICS MECHANISMS CONTRIBUTE TO VASCULAR AGING?

The following introduces the pathological steps that are involved in the epigenetic regulation of vascular aging. A summary of these events and epigenetic targets are shown in **Table 1**.

Are Epigenetic Mechanisms Involved in the Regulation of Vascular Cell Senescence?

NAD-dependent deacetylase sirtuin-1 (SIRT1), is the most thoroughly studied member of the Nuclear-localized type III histone deacetylases (Situin) family. This protein is involved at multiple levels during the stages of vascular aging, and plays an important role vascular cell senescence as demonstrated by the following observations: (1) the expression of SIRT1 in VSMCs of mice is decreased with advancing age; (2) smooth muscle-specific knockout of SIRT1 in animals promotes Angiotensin II (Ang II) induced vascular senescence (Chen et al., 2016); (3) SIRT1 is important in the deacetylation of histone H4K16, and that this process inhibits senescence of ECs and is protective against vascular aging (Wan et al., 2014); (4) SIRT1 can increase ECs Kruppel-like factor 2 (KLF2) expression, which causes vascular ECs to enter a "vaso-protective" state (Gracia-Sancho et al., 2010); (5) energy restriction promotes increased SIRT1 expression in VSMCs and tissues and fights abdominal aortic aneurysm (Liu et al., 2016); and finally, (6) nuclear-localized SIRT6 protects telomeres in vascular ECs, tempering reductions in replication capacity and premature cell senescence following DNA damage (Cardus et al., 2013).

ncRNAs, especially miRNAs, are involved in vascular cell senescence. miRNAs are short single-stranded ribonucleic acids that can negatively regulate gene expression by base-pairing to target mRNA and causing mRNA cleavage or translation repression (Carthew and Sontheimer, 2009). For example, the expression of miR-217 in ECs is seen to increase with age and can inhibit the expression of SIRT1. Subsequent reductions in the expression of SIRT1 increases the levels of senescent and dysfunction ECs. Interestingly, miR-217 inhibition reportedly slows the rates of cellular senescence in ECs (Menghini et al., 2009). Similarly, miR-145 and miR-143 can regulate the phenotypic transition of smooth muscle cells during vascular aging and during the differentiation of smooth muscle. The miR-143 and miR-145 work together targeted transcription factors network, such as Klf4 (Kruppel-like factor 4) and myocardin and Elk-1 (member of ETS oncogene family) and, on the one hand, form a positive feedback mechanism to promote the differentiation of smooth muscle cells, and on the other hand, repress the proliferation of smooth muscle cells (Cordes et al., 2009). The lncRNA H19 is expressed in the adult endothelium and is reduced with advanced age. H19 inhibits the STAT3 signaling pathway, a key pathway regulating endothelial cell senescence (Hofmann et al., 2019). Other lcRNAs such as MEG3 prevent miR-128–dependent Girdin down regulation and inhibits vascular endothelial cell senescence (Lan et al., 2019). More recently, our research group has shown that Fos-

TABLE 1 | Vascular aging related epigentics targets.

Targets	Major findings	Effects	References
SIRT1	Decreases in VSMC of aged mice	Enhance vascular inflammation	(Chen et al., 2016)
	Deacetylate histone H4K16	Improves the function of endothelial cells	(Wan et al., 2014)
	Increase ECs KLF2 expressions	Vaso-protective	(Gracia-Sancho et al., 2010)
	Increased by energy limitation	Fight abdominal aortic aneurysm	(Liu et al., 2016)
	Activation by SIRT1 activators	Inhibit vascular remodeling, stiffness and calcification	(Takemura et al., 2011; Winnik et al., 2015; Fry et al., 2016; Badi et al., 2018)
SIRT2	Deacetylate p65Lys310	Regulates inflammmation *via* NF-κB-dependent gene expression	(Rothgiesser et al., 2019)
SIRT3	Missing will lead to the high acetylation and inactivation of SOD2	Leading to an imbalance of redox homeostasis in blood vessels	(Dikalova et al., 2017)
SIRT6	Protect telomere	Avoiding premature cell senescence caused by DNA damage	(Cardus et al., 2013)
HDAC3	Inhibit the activation of macrophages	Lacking HDAC3 will be easily activated by IL-4 and accelerate blood vessel's inflammation	(Mullican et al., 2011)
HDAC4	Deacetylate FoxO3a	Regulates vascular inflammation *via* activation of autophagy	(Yang et al., 2018)
JMJD3	Deficiency of JMJD3 and Nox4 prohibits autophagic activation	Attenuates neointima and vascular remodelling following carotid injury	(Luo et al., 2018)
Fra-1	Directly binding and transcriptionally activating p21 and p16 signaling	Promoting vascular aging	(Yang et al., 2019)
GATA4	Directly binding to the the angiogenic factors VEGFA and VEGFC promoter and enhancing transcription.	Regulates Angiogenesis and Persistence of Inflammation	(Jia et al., 2018b)
MCP-1	Hypomethylation of the promoter region in atherosclerosis	Increases the expression of MCP-1, promotes the recruitment of inflammatory cells	(Liu et al., 2012)
eNOS	Hypermethylation of promoter region appears in pathological conditions	Inhibiting the expression of eNOS and NO production	(Chan et al., 2004)
p66Shc	Contains a large number of methylation modification sites	Modifying the methylation level to regulate the gene expression in order to control mitochondrial produce hydrogen peroxide	(Ventura et al., 2002; Cencioni et al., 2013)
miR-217	Combined with the (3'-UTR) of SIRT1 to inhibit the expression of SIRT1	Causing senescence and dysfunction of ECs	(Menghini et al., 2009)
miR-143/miR-145	miR-143 and miR-145 are activated in differentiated smooth muscle cells	Inhibits the proliferation of smooth muscle cells	(Cordes et al., 2009)
miR-210	Reduce the overproduction of ROS	Regulates oxidation stress	(Ma et al., 2018)
miR-135a/miR-714/miR-762/ miR-712	Inhibit the outflow of calcium ions by disrupting Ca2+ efflux proteins NCX1, PMCA1, and NCKX4	Promote VSMC calcification	(Gui et al., 2012)
Long non-coding RNA H19	Decreased expressed along with aging in the adult endothelium	Inhibits STAT3 signaling pathway to regulate endothelial cell senescence	(Hofmann et al., 2019)
Long noncoding RNA MEG3	Impairing miR-128-dependent girdin down regulation	Prevents vascular endothelial cell senescence	(Lan et al., 2019)

SIRT, type III histone deacetylases (Sirtuin); VSMC, vascular smooth muscle cell; H4K16, histone4 Lysine16; KLF2, endothelial cells Kruppel-like factor 2. SOD2, superoxide dismutase 2; HDAC, histone deacetylase; FoxO3a, Forkhead boxO3;MCP-1, monocyte chemoattractant protein-1; P66Shc, member of Shc (src homology and collagen homology) family; 3'-UTR, 3'-untranslated region; eNOS, endothelial nitric oxide synthase; NO, nitric oxide; ROS, reactive oxygen species; JMJD3, histone demethylase; GATA4, a member of GATA zinc-finger transcription factor family; Fra-1, Fos-related antigen1; NF-κB, nuclear factor kappa-B; miR, micro RNA; NCX1, Na^{+}-Ca^{2+} exchanger isoform 1; NCKX4, $Na^{+}/K^{+/}Ca^{2+}$-exchange protein 4; PMCA1, plasma membrane calcium ATPase 1; STAT3, signal transducers and activators of transcription.

related antigen 1 (Fra-1) plays an important role in Ang II–induced vascular senescence. Fra-1 expression is dramatically increased in Ang II–induced rat aortic endothelial cell (RAEC) senescence (Yang et al., 2019).

Epigenetic Regulation of Inflammation in Vascular Aging

Typically, an individuals inflammatory status increases with age (Fulop et al., 2018). Studies on the methylation patterns in the human genome have shown that hypermethylation of DNA appears to correlated with chronic inflammation associated with many aging-related diseases (Cutolo et al., 2014). For example, in pathophysiological conditions such as atherosclerosis, hypomethylation of the promoter region of monocyte chemoattractant protein-1 (MCP-1) leads to increased expression of MCP-1 and promotes the recruitment of inflammatory cells accelerating the disease process (Liu et al., 2012).

In other research, the activation of SIRT1 in smooth muscle cells reduces the stiffness of blood vessels; a process associate with crosstalk with the NF-κB inflammatory signaling pathway and the inhibition of inflammatory signaling (Fry et al., 2016). Loss of functional SIRT1 resulted in hyperacetylated of NF-$_K$B and drives increased transcription of pro-inflammatory genes. Similarly, cytoplasmic SIRT2 induces the deacetylate of p65 Lys310 and regulates NF-κB–dependent gene expression *viz.* reduces transcription of pro-inflammation genes (Rothgiesser

et al., 2019). These finding showing that acetylation status of NF-κB is an important driver of rates of inflammation in cells and tissues. Additional support comes from the knowledge that the inhibition of histone deacetylases (HDAC) increases tumor necrosis factor α (TNF-α) levels, the activation of the NF-κB signaling pathway, and resultant increase in IL-8 expression (Ashburner et al., 2001). Other members of the HDAC family such as HDAC3 have been shown to inhibit the activation of macrophages. In macrophages lacking HDAC3, there is an increased response to stimulation by interleukin 4 (IL-4) that likely drives increased rates of inflammation in blood vessel leading to aging (Mullican et al., 2011). In addition, our research on vascular aging points to a possible role of HDAC4 in mitigating inflammatory responses in the vascular system. HDAC4 appears to play an essential role in vascular inflammation by regulates Ang II–induced autophagy *via* the activation of FoxO3a deacetylation (Yang et al., 2018), work recently communicated as an editorial focusing on cardiovascular epigenetics (Tarun and Antoniades, 2018). Additional research from our group has identified histone demethylase Jumonji domain-containing protein 3 (JMJD3) as a key epigenetic regulator of the inflammatory response in cells (Liu et al., 2018). JMJD3 playing a pivitol role in rheumatoid synovial hyperplasia in rheumatoid arthritis (RA) (Jia et al., 2018a; Wu et al., 2019). Moreover, evidence also points to potential roles for JMJD3 in vascular remodeling (Luo et al., 2018) and in the regulation of the transcription factor GATA4. GATA4 functioning in inflammation persistence and angiogenesis in rheumatoid arthritis (RA) (Jia et al., 2018).

Other mechanisms linking epigenetic processes and inflammatory status include the ncRNA molecule, miR-155. miR-155 is a positive regulator of vascular inflammation, and is abundant in activated macrophages and monocytes, and potentially leaves blood vessels in a chronic inflammatory state. Increased levels of miR-155 induce the expression of MCP-1, and could encourage the recruitment of monocytes to vascular tissues thus exacerbating the inflammatory response (Wu et al., 2014). In contrast, miR-194 has opposing effects in that this miRNA can inhibit inflammation. While the mechanisms for this still required additional research, it is known that miR-194 overexpression can inhibit tumor necrosis factor receptor-associated factor 6 (TRAF6), and this reduces the production of monocyte inflammatory factors (Tian et al., 2015).

Regulation of Oxidation Stress in Vascular Aging

Links between vascular aging, DNA methylation patterns and oxidative stress are also seen in blood vessels. Regulation in the expression of endothelial nitric oxide synthase (eNOS), which encodes an endogenous nitric oxide synthase and is a source of the vasoactive molecule nitric oxide (NO), is altered by methylation status. Lower methylation patterns in the promoter region of eNOS allow for gene transcription and is therefore important in the production of NO and associated physiological processes involving this gaseous signaling molecule. In pathological situations hypermethylation in the eNOS promoter region inhibits eNOS expression and causes diminished levels of NO (Chan et al., 2004). Other proteins such as p66Shc, a protein associated with endothelial dysfunction, are also regulated *via* methylation status. The p66Shc protein is important in signaling systems linked to the production of hydrogen peroxide (H_2O_2), and the gene encoding for this protein is known to contains a large number of methylation sites. Modification of the methylation pattern is thus seen as a means to control the expression of this protein (Ventura et al., 2002; Cencioni et al., 2013).

Potential roles of SIRT1 in mitigating oxidative stress in smooth muscle cells has recently been proposed and suggested to be important in reducing blood vessels stiffness (Fry et al., 2016). Similarly, expression of SIRT3 a protein known to decline in tissues by as much as 40% by the age of 65 also appears to be important in mitigating oxidative stress. In cells lacking SIRT3, the activity of the mitochondrial antioxidant enzyme superoxide dismutase 2 (SOD2) is impaired due to hyperacetylation. Consequently, elevated mitochondrial $O_2^{\bullet}$ and diminished endothelial NO are observed, leading to an imbalance of redox homeostasis in blood vessels (Dikalova et al., 2017). Building on this area of research are roles for miRNA and associated impacts on redox systems linked to vascular ageing. To date, miR-210 has recently been demonstrated to reduce the overproduction of mitochondrial reactive oxygen species (ROS) (Ma et al., 2018).

Epigenetics Systems and Calcification in Vascular Aging

SIRT1 can inhibit vascular remodeling, stiffness, and functions in protection against atherosclerosis and vascular calcification in mice and is indicative that SIRT1 has protective roles in vascular injury diseases (Winnik et al., 2015). Evidence to support protective roles come from several important pieces of research. Firstly, that *in vitro* culture of VSMCs using media containing high levels of phosphate (Pi) stimulates cell senescence and calcification. These changes related to the down-regulation of SIRT1 expression and the activation of p21 (WAF1/Cip1). Activation of p21(WAF1/Cip1) drives replicative senescent in VSMC cells, a process that can be reversed in cells in which p21(WAF1/Cip1) has been knockdown using molecular approaches. Moreover, loss of functional p21(WAF1/Cip1) abolishes Pi induced senescence and calcification in VSCMs. Thirdly, knockdown of SIRT1 in cells promotes a transformation to a calcification phenotype and promotes Pi-induced VSMC senescence calcification. Interestingly, treatment of cells with the SIRT1 induce resveratrol activates the protein and inhibits VSMC calcification (Takemura et al., 2011). In allied areas of research, the expression of the miRNA molecule miR-34a is elevated in the aorta of aged mice and is associated with rates of calcification. miR-34a is downregulating by SIRT1, this serving to temper miR-34a induced VSMCs calcification (Badi et al., 2018). Futhermore, the lncRNA-ES3/miR-34c-5p/BMF axis has recently been shown to regulate high-glucose-induced VSMCs calcification/senescence (Lin et al., 2019), and miR-135a, miR-714, miR-762, and miR-712 are involved in VSMC calcification by disrupting Ca^{2+} efflux proteins like NCX1, PMCA1, and NCKX4 (Gui et al., 2012).

EPIGENETICS REGULATION AND TREATMENT OF VASCULAR AGING AND CVD

As discussed in the previous sections, vascular aging contributes to cardiovascular disease(s) including atherosclerosis, hypertension, coronary heart diseases, and stroke. Vascular aging encompasses many biochemical and physiological changes associated with vascular remodeling, vascular homeostasic imbalance, vascular cell senescence, a pro-inflammation state and increased rates of oxidative stress, and tissue calcification. The interplay between each of these conditions is complex and makes the development of robust treatment strategies targetting vascular aging challenging. Indeed, the targeting of a single vascular cell type or population or a specific signaling system is difficult. However, the recognized association between epigenetic regulation of multiple gene targets coding for proteins regulating biochemical or physiological processes linked to vascular aging may be achievable. Epigenetic targets could serve as appropriate therapeutic targets suitable for the management of vascular aging and related diseases in humans. These treatments, if explored and developed further, may be more effective, span several risk factors linked to the development of vascular aging, and would have the added benefit that they are reversible processes. Such systems could be exploited in the future development of novel therapeutics. For example, our research has demonstrated that JMJD3 could be a useful therapeutic target. JMJD3 is a crucial epigenetic regulator involved in the inflammatory response to LPS in macrophages. JMJD3 expression is controlled by the transcription factor Sp-1 and is responsible for changes in the expression of cystathionine gamma-lyase (CSE). This system negatively regulates the inflammatory response in cells and tissues and reduce the progression of rheumatoid arthritis (RA). Moreover, deficiency of JMJD3 reduces neointima formation after vascular injury by inhibits the Nox4-autophagy signaling pathway. These observations suggesting that JMJD3 may represent a novel target for the development of new anti-inflammatory therapeutics for treating RA, the prevention and treatment of intima hyperplasia-related vascular diseases, and other pro-inflammatory conditions (Liu et al., 2018; Jia et al., 2018a; Luo et al., 2018; Wu et al., 2019). Likewise, the transcription factor GATA4, a key regulator of angiogenesis and persistence of inflammation in RA may also hold promise as a therapeutic target (Jia et al., 2018). We also show that Fos-related antigen 1 (Fra-1) plays a novel and key role in promoting vascular aging by directly binding and activating the target proteins p21(WAF1/Cip1) and p16(INK4A) protein signaling systems. Intervention of Fra-1 is a potential strategy for the prevention of aging-related cardiovascular disorders (Yang et al., 2019).

The development of epigenetically targeted therapeutics has received considerable attention over the last decade and has lead to the identification of several important epigenetic modified protein inhibitors including the FDA-approved molecule azacytidine and various inhibitors of DNMT1, HDAC, and histone acetyltransferases (HAT) (Voelter-Mahlknecht, 2016). These therapeutics could be adopted for use in the treatment of specific CVD conditions. To date, epidrugs-based therapeutics for the treatment of CVD mainly include compounds widely used in the clinical that function through epigenetics-related mechanisms, numerous natural compounds, and various newly synthesized molecules. Our group has reported on the anti-inflammation effects of the HDAC4 inhibitor Tasquinimod and its use in the treatment of vascular inflammation-related diseases (Yang et al., 2018). Other molecules of interest include common statins used to lower serum cholesterol to prevent major cardiovascular problems. Some statins may function as HDAC inhibitor (Voelter-Mahlknecht, 2016). Likewise, trichostatin A, an inhibitor of HDAC, prevents ventricular remodeling by inhibiting TNF-α transcription and by promoting cardiomyocyte survival by enhancing Akt phosphorylation (Zhang et al., 2012). In addition, in experimental models of myocardial infarction and atherosclerosis, the HDAC inhibitor sodium butyrate inhibits NF-κB signal transduction and the production of inflammatory molecules including TNF-α, interleukin-6, vascular cell adhesion molecule-1, and intercellular adhesion molecule-1, pointing to potential pharmacological effects (Hu et al., 2014). The natural product curcumin functions as an HAT inhibitor in rodent models of heart failure preserving systolic function and preventing ventricular hypertrophy (Pan et al., 2013). Similarly, molecules like folic acid and B vitamins are DNMT inhibitors and deficiencies in folic acid causes global DNA hypomethylation that is associated with increased risk of CVD including coronary heart disease, atherosclerosis, and anemia (Kim et al., 2007; McNulty et al., 2008). The common analgesic, acetylsalicylic acid appears to reduces ATP-binding cassette transporter A1 gene methylation rates in the pathophysiology conditions associated with coronary heart disease and thus points to a potentially new therapeutic strategy for this disease (Guay et al., 2014). Likewise, the molecule 5- aza-2-deoxycytidinede (DAC), an inhibitor of DNMT that can reverse rates of DNA methylation, has been shown to re-active genes silenced by hypermethylation *viz.* estrogen receptors α and β in normal ECs and smooth muscle. Importantly, the failure of some estrogen therapies to protect cardiac tissues from damage could be due to epigenetic silencing of the female estrogen receptor. The discovery of natural products that can be used to alter SIRT1 activity in cells has also gained some interest. SIRT1 expression and activity can reduce during senescence-related diseases and re-activation of SIRT1 in tissues may offer new opportunities in the development of future drug candidates. Indeed, one potential drug for disease intervention, is the stilbene resveratrol, an activator of SIRT1. Resveratrol has been repeatedly shown to effectively delay vascular senescence in mice, and to improve cardiometabolic health (da Luz et al., 2012; Pollack and Crandall, 2013; Kim et al., 2018). Finally, rapamycin-induced miR-30a down-regulation is mediated *via* the targeting of beclin1 and can inhibit the senescence of VSMCs (Tan et al., 2019). It is clear that more research is needed to further address the anti-aging effects of many of these molecules and in the discovery of other compounds that could be used to manipulate epigenetic systems in mammalian cells and tissues. In particular,

pharmacologist should focus on research to assess the role of other types of epigenetic targeting drugs. Identified molecules could then drive developments in combined approaches to treat CVD using epigenetic-based therapeutics coupled with hormone replacement therapy (Schiano et al., 2015).

CONCLUSION AND PROSPECTS

Our understanding of the molecular mechanism controlling the epigenetic regulation of gene expression has progressed significantly over the last two decades. However, much has still to be learnt, and our perceived ideas of epigenetic modulation and its manipulation *in vivo* is far more complicated than previously thought. Aging is an irreversible biological process while epigenetic alternations are reversible and may offer novel treatment strategies in patients with age-related CVD. New methods and experimental research techniques are needed to facilitate the manipulation of epigenetic processes in cells and tissues. Indeed, recently a newly emerging epigenetic mechanism involving RNA methylation has been reported (Yue et al., 2015); however, its role in vascular biology is not yet clear and requires further research. Another important problem to be solved in the future is how to manipulate histone modification in specific tissues like the vascular endothelium. This problem is critical because systemic inhibition or activation of HDAC, or other epigenetic enzymes may cause adverse reactions (Heerboth et al., 2014). Building on these advances will be the ability to monitor epigenetic changes in cells, this will be critical in making advances in this field. Interestingly, the progressive development of single-cell sequencing and single-cell epigenetic technologies like scATAC-seq, scDNase-seq, and scChic-seq can be used to study the mode of epigenetic regulation at the single-cell level, and these technologies will offers exciting opportunities in the near future (Nawy, 2014; Ku et al., 2019). In particular, these systems will aid in the development of more elaborate models of epigenetic regulation and will allow for the development of more accurately therapeutics for use in epigenetic research. With regards to vascular aging, a good start here would be research on newer epigenetic pharmaceuticals, developed using drug repurposing approaches; a safe and low-cost way to support future vascular drug discovery (Xu et al., 2019). In addition, since epigenetic mechanisms work in concert to regulate gene networks, there may also be requirements for the development of epigenetic "cocktail" therapies that can be exploited to target a spectrum of age-related genes for treating age-related diseases.

AUTHOR CONTRIBUTIONS

All authors contributed to the article and approved the submitted version.

FUNDING

This work was supported by the National Natural Science Foundation of China (81973320), Macau Science and Technology Development fund (FDCT) (067/2018/A2,033/2017/AMJ, 0007/2019/AKP, 0052/2020/A), and the Key Laboratory Program of the Education Commission of Shanghai Municipality (no. ZDSYS14005).

REFERENCES

Anderson, K. M., Anderson, D. M., McAnally, J. R., Shelton, J. M., Bassel-Duby, R., and Olson, E. N. (2016). Transcription of the non-coding RNA upperhand controls Hand2 expression and heart development. *Nature* 539 (7629), 433–436. doi: 10.1038/nature20128

Ashburner, B. P., Westerheide, S. D., and Baldwin, A. S.Jr (2001). The p65 (RelA) subunit of NF-kappaB interacts with the histone deacetylase (HDAC) corepressors HDAC1 and HDAC2 to negatively regulate gene expression. *Mol. Cell Biol.* 21 (20), 7065–7077. doi: 10.1128/MCB.21.20.7065-7077.2001

Badi, I., Mancinelli, L., Polizzotto, A., Ferri, D., Zeni, F., Burba, I., et al (2018). miR-34a Promotes Vascular Smooth Muscle Cell Calcification by Downregulating SIRT1 (Sirtuin 1) and Axl (AXL Receptor Tyrosine Kinase). *Arterioscler. Thromb. Vasc. Biol.* 38 (9), 2079–2090. doi: 10.1161/ATVBAHA.118.311298

Calvanese, V., Lara, E., Kahn, A., and Fraga, M. F. (2009). The role of epigenetics in aging and age-related diseases. *Ageing Res. Rev.* 8 (4), 268–276. doi: 10.1016/j.arr.2009.03.004

Cardus, A., Uryga, A. K., Walters, G., and Erusalimsky, J. D. (2013). SIRT6 protects human endothelial cells from DNA damage, telomere dysfunction, and senescence. *Cardiovasc. Res.* 97 (3), 571–579. doi: 10.1093/cvr/cvs352

Carthew, R. W., and Sontheimer, E. J. (2009). Origins and Mechanisms of miRNAs and siRNAs. *Cell* 136 (4), 642–655. doi: 10.1016/j.cell.2009.01.035

Cavallaro, U., Castelli, V., Del Monte, U., and Soria, M. R. (2000). Phenotypic alterations in senescent large-vessel and microvascular endothelial cells. *Mol. Cell Biol. Res. Commun.* 4 (2), 117–121. doi: 10.1006/mcbr.2000.0263

Cencioni, C., Spallotta, F., Martelli, F., Valente, S., Mai, A., Zeiher, A. M., et al. (2013). Oxidative stress and epigenetic regulation in ageing and age-related diseases. *Int. J. Mol. Sci.* 14 (9), 17643–17663. doi: 10.3390/ijms140917643

Chan, Y., Fish, J. E., D'Abreo, C., Lin, S., Robb, G. B., Teichert, A. M., et al. (2004). The cell-specific expression of endothelial nitric-oxide synthase: a role for DNA methylation. *J. Biol. Chem.* 279 (33), 35087–35100. doi: 10.1074/jbc.M405063200

Chen, H. Z., Wang, F., Gao, P., Pei, J. F., Liu, Y., Xu, T. T., et al. (2016). Age-Associated Sirtuin 1 Reduction in Vascular Smooth Muscle Links Vascular Senescence and Inflammation to Abdominal Aortic Aneurysm. *Circ. Res.* 119 (10), 1076–1088. doi: 10.1161/CIRCRESAHA.116.308895

Cordes, K. R., Sheehy, N. T., White, M. P., Berry, E. C., Morton, S. U., Muth, A. N., et al. (2009). miR-145 and miR-143 regulate smooth muscle cell fate and plasticity. *Nature* 460 (7256), 705–710. doi: 10.1038/nature08195

Cunha, P. G., Boutouyrie, P., Nilsson, P. M., and Laurent, S. (2017). Early Vascular Ageing (EVA): Definitions and Clinical Applicability. *Curr. Hypertens. Rev.* 13 (1), 8–15. doi: 10.2174/1573402113666170413094319

Cutolo, M., Paolino, S., and Pizzorni, C. (2014). Possible contribution of chronic inflammation in the induction of cancer in rheumatic diseases. *Clin. Exp. Rheumatol.* 32 (6), 839–847. doi: 10.3177/jnsv.47.385

da Luz, P. L., Tanaka, L., Brum, P. C., Dourado, P. M., Favarato, D., Krieger, J. E., et al. (2012). Red wine and equivalent oral pharmacological doses of resveratrol delay vascular aging but do not extend life span in rats. *Atherosclerosis* 224 (1), 136–142. doi: 10.1016/j.atherosclerosis.2012.06.007

Dikalova, A. E., Itani, H. A., Nazarewicz, R. R., McMaster, W. G., Flynn, C. R., Uzhachenko, R., et al. (2017). Sirt3 Impairment and SOD2 Hyperacetylation in Vascular Oxidative Stress and Hypertension. *Circ. Res.* 121 (5), 564–574. doi: 10.1161/CIRCRESAHA.117.310933

Ding, Y. N., Tang, X., Chen, H. Z., and Liu, D. P. (2018). Epigenetic Regulation of Vascular Aging and Age-Related Vascular Diseases. *Adv. Exp. Med. Biol.* 1086, 55–75. doi: 10.1007/978-981-13-1117-8_4

Dzau, V. J., Antman, E. M., Black, H. R., Hayes, D. L., Manson, J. E., Plutzky, J., et al. (2006a). The cardiovascular disease continuum validated: clinical evidence of improved patient outcomes: part I: Pathophysiology and clinical trial evidence (risk factors through stable coronary artery disease). *Circulation* 114 (25), 2850–2870. doi: 10.1161/CIRCULATIONAHA.106.655688

Dzau, V. J., Antman, E. M., Black, H. R., Hayes, D. L., Manson, J. E., Plutzky, J., et al. (2006b). The cardiovascular disease continuum validated: clinical evidence of improved patient outcomes: part II: Clinical trial evidence (acute coronary syndromes through renal disease) and future directions. *Circulation* 114 (25), 2871–2891. doi: 10.1161/CIRCULATIONAHA.106.655761

Eto, H., Miyata, M., Shirasawa, T., Akasaki, Y., Hamada, N., Nagaki, A., et al. (2008). The long-term effect of angiotensin II type 1a receptor deficiency on hypercholesterolemia-induced atherosclerosis. *Hypertens. Res.* 31 (8), 1631–1642. doi: 10.1291/hypres.31.1631

Feinberg, A. P. (2018). The Key Role of Epigenetics in Human Disease Prevention and Mitigation. *N. Engl. J. Med.* 378 (14), 1323–1334. doi: 10.1056/NEJMra1402513

Fraga, M. F., Ballestar, E., Paz, M. F., Ropero, S., Setien, F., Ballestar, M. L., et al. (2005). Epigenetic differences arise during the lifetime of monozygotic twins. *Proc. Natl. Acad. Sci. U. S. A.* 102 (30), 10604–10609. doi: 10.1073/pnas.0500398102

Fry, J. L., Al Sayah, L., Weisbrod, R. M., VanRoy, I., Weng, X., Cohen, R. A., et al. (2016). Vascular Smooth Muscle Sirtuin-1 Protects Against Diet-Induced Aortic Stiffness. *Hypertension* 68 (3), 775–784. doi: 10.1161/HYPERTENSIONAHA.116.07622

Fu, Z., Wang, M., Gucek, M., Zhang, J., Wu, J., Jiang, L., et al. (2009). Milk fat globule protein epidermal growth factor-8: a pivotal relay element within the angiotensin II and monocyte chemoattractant protein-1 signaling cascade mediating vascular smooth muscle cells invasion. *Circ. Res.* 104 (12), 1337–1346. doi: 10.1161/CIRCRESAHA.108.187088

Fulop, T., Larbi, A., Dupuis, G., LePage, A., Frost, E. H., Cohen, A. A., et al. (2018). Immunosenescence and Inflamm-Aging As Two Sides of the Same Coin: Friends or Foes? *Front. Immunol.* 8:1960. doi: 10.3389/fimmu.2017.01960

Gracia-Sancho, J., Villarreal, G.Jr, Zhang, Y., and García-Cardeña, G. (2010). Activation of SIRT1 by resveratrol induces KLF2 expression conferring an endothelial vasoprotective phenotype. *Cardiovasc. Res.* 85 (3), 514–519. doi: 10.1093/cvr/cvp337

Guay, S. P., Légaré, C., Houde, A. A., Mathieu, P., Bossé, Y., and Bouchard, L. (2014). Acetylsalicylic acid, aging and coronary artery disease are associated with ABCA1 DNA methylation in men. *Clin. Epigenet.* 6 (1):14. doi: 10.1186/1868-7083-6-14

Gui, T., Zhou, G., Sun, Y., Shimokado, A., Itoh, S., Oikawa, K., et al. (2012). MicroRNAs that target Ca(2+) transporters are involved in vascular smooth muscle cell calcification. *Lab. Invest.* 92 (9), 1250–1259. doi: 10.1038/labinvest.2012.85

Gurha, P., and Marian, A. J. (2013). Noncoding RNAs in cardiovascular biology and disease. *Circ. Res.* 113 (12), e115–e120. doi: 10.1161/CIRCRESAHA.113.302988

Hai, Z., and Zuo, W. (2016). Aberrant DNA methylation in the pathogenesis of atherosclerosis. *Clin. Chim. Acta* 456, 69–74. doi: 10.1016/j.cca.2016.02.026

Handy, D. E., Castro, R., and Loscalzo, J. (2011). Epigenetic modifications: basic mechanisms and role in cardiovascular disease. *Circulation* 123 (19), 2145–2156. doi: 10.1161/CIRCULATIONAHA.110.956839

Heerboth, S., Lapinska, K., Snyder, N., Leary, M., Rollinson, S., and Sarkar, S. (2014). Use of epigenetic drugs in disease: an overview. *Genet. Epigenet.* 6, 9–19. doi: 10.4137/GEG.S12270

Hofmann, P., Sommer, J., Theodorou, K., Kirchhof, L., Fischer, A., Li, Y., et al. (2019). Long non-coding RNA H19 regulates endothelial cell aging via inhibition of STAT3 signalling. *Cardiovasc. Res.* 115 (1), 230–242. doi: 10.1093/cvr/cvy206

Hu, X., Zhang, K., Xu, C., Chen, Z., and Jiang, H. (2014). Anti-inflammatory effect of sodium butyrate preconditioning during myocardial ischemia/reperfusion. *Exp. Ther. Med.* 8 (1), 229–232. doi: 10.3892/etm.2014.1726

Jeltsch, A. (2008). Reading and writing DNA methylation. *Nat. Struct. Mol. Biol.* 15 (10), 1003–1004. doi: 10.1038/nsmb1008-1003

Jia, W., Wu, W., Yang, D., Xiao, C., Su, Z., Huang, Z., et al. (2018a). Histone demethylase JMJD3 regulates fibroblast-like synoviocyte-mediated proliferation and joint destruction in rheumatoid arthritis. *FASEB J.* 32 (7), 4031–4042. doi: 10.1096/fj.201701483R

Jia, W., Wu, W., Yang, D., Xiao, C., Huang, M., Long, F., et al. (2018b). GATA4 regulates angiogenesis and persistence of inflammation in rheumatoid arthritis. *Cell Death Dis.* 9 (5), 503. doi: 10.1038/s41419-018-0570-5

Jiang, L., Zhang, J., Monticone, R. E., Telljohann, R., Wu, J., Wang, M., et al. (2012). Calpain-1 regulation of matrix metalloproteinase 2 activity in vascular smooth muscle cells facilitates age-associated aortic wall calcification and fibrosis. *Hypertension* 60 (5), 1192–1199. doi: 10.1161/HYPERTENSIONAHA.112.196840

Kadlec, A. O., Chabowski, D. S., Ait-Aissa, K., and Gutterman, D. D. (2016). Role of PGC-1α in Vascular Regulation: Implications for Atherosclerosis. *Arterioscler. Thromb. Vasc. Biol.* 36 (8), 1467–1474. doi: 10.1161/ATVBAHA.116.307123

Kim, J., Kim, J. Y., Song, K. S., Lee, Y. H., Seo, J. S., Jelinek, J., et al. (2007). Epigenetic changes in estrogen receptor beta gene in atherosclerotic cardiovascular tissues and in-vitro vascular senescence. *Biochim. Biophys. Acta* 1772 (1), 72–80. doi: 10.1016/j.bbadis.2006.10.004

Kim, E. N., Kim, M. Y., Lim, J. H., Kim, Y., Shin, S. J., Park, C., et al. (2018). The protective effect of resveratrol on vascular aging by modulation of the renin-angiotensin system. *Atherosclerosis* 270, 123–131. doi: 10.1016/j.atherosclerosis.2018.01.043

Kohli, R. M., and Zhang, Y. (2013). TET enzymes, TDG and the dynamics of DNA demethylation. *Nature* 502 (7472), 472–479. doi: 10.1038/nature12750

Krebs, J., Agellon, L. B., and Michalak, M. (2015). Ca(2+) homeostasis and endoplasmic reticulum (ER) stress: An integrated view of calcium signaling. *Biochem. Biophys. Res. Commun.* 460 (1), 114–121. doi: 10.1016/j.bbrc.2015.02.004

Ku, W. L., Nakamura, K., Gao, W., Cui, K., Hu, G., Tang, Q., et al. (2019). Single-cell chromatin immunocleavage sequencing (scChIC-seq) to profile histone modification. *Nat. Methods* 16 (4), 323–325. doi: 10.1038/s41592-019-0361-7

Lakatta, E. G., and Levy, D. (2003a). Arterial and cardiac aging: major shareholders in cardiovascular disease enterprises: Part I: aging arteries: a "set up" for vascular disease. *Circulation* 107 (1), 139–146. doi: 10.1161/01.cir.0000048892.83521.58

Lakatta, E. G., and Levy, D. (2003b). Arterial and cardiac aging: major shareholders in cardiovascular disease enterprises: Part II: the aging heart in health: links to heart disease. *Circulation* 107 (2), 346–354. doi: 10.1161/01.cir.0000048893.62841.f7

Lakatta, E. G., Wang, M., and Najjar, S. S. (2009). Arterial aging and subclinical arterial disease are fundamentally intertwined at macroscopic and molecular levels. *Med. Clin. North Am.* 93 (3), 583–Contents. doi: 10.1016/j.mcna.2009.02.008

Lakatta, E. G. (2003). Arterial and cardiac aging: major shareholders in cardiovascular disease enterprises: Part III: cellular and molecular clues to heart and arterial aging. *Circulation* 107 (3), 490–497. doi: 10.1161/01.cir.0000048894.99865.02

Lan, Y., Li, Y. J., Li, D. J., Li, P., Wang, J. Y., Diao, Y. P., et al. (2019). Long noncoding RNA MEG3 prevents vascular endothelial cell senescence by impairing miR-128-dependent Girdin downregulation. *Am. J. Physiol. Cell Physiol.* 316 (6), C830–C843. doi: 10.1152/ajpcell.00262.2018

Leopold, J. A. (2013). Vascular calcification: an age-old problem of old age. *Circulation* 127 (24), 2380–2382. doi: 10.1161/CIRCULATIONAHA.113.003341

Lin, X., Zhan, J. K., Zhong, J. Y., Wang, Y. J., Wang, Y., Li, S., et al. (2019). lncRNA-ES3/miR-34c-5p/BMF axis is involved in regulating high-glucose-induced calcification/senescence of VSMCs. *Aging (Albany N. Y.)* 11 (2), 523–535. doi: 10.18632/aging.101758

Liu, X. L., Zhang, P. F., Ding, S. F., Wang, Y., Zhang, M., Zhao, Y. X., et al. (2012). Local gene silencing of monocyte chemoattractant protein-1 prevents vulnerable plaque disruption in apolipoprotein E-knockout mice. *PLoS One* 7 (3), e33497. doi: 10.1371/journal.pone.0033497

Liu, Y., Wang, T. T., Zhang, R., Fu, W. Y., Wang, X., Wang, F., et al. (2016). Calorie restriction protects against experimental abdominal aortic aneurysms in mice. *J. Exp. Med.* 213 (11), 2473–2488. doi: 10.1084/jem.20151794

Liu, S., Wang, X., Pan, L., Wu, W., Yang, D., Qin, M., et al. (2018). Endogenous hydrogen sulfide regulates histone demethylase JMJD3-mediated inflammatory response in LPS-stimulated macrophages and in a mouse model of LPS-induced septic shock. *Biochem. Pharmacol.* 149, 153–162. doi: 10.1016/j.bcp.2017.10.010

Luo, X., Yang, D., Wu, W., Long, F., Xiao, C., Qin, M., et al. (2018). Critical role of histone demethylase Jumonji domain-containing protein 3 in the regulation of neointima formation following vascular injury. *Cardiovasc. Res.* 114 (14), 1894–1906. doi: 10.1093/cvr/cvy176

Ma, X., Wang, J., Li, J., Ma, C., Chen, S., Lei, W., et al. (2018). Loading MiR-210 in Endothelial Progenitor Cells Derived Exosomes Boosts Their Beneficial Effects on Hypoxia/Reoxygeneation-Injured Human Endothelial Cells via Protecting

Mitochondrial Function. *Cell Physiol. Biochem.* 46 (2), 664–675. doi: 10.1159/000488635

Maegawa, S., Lu, Y., Tahara, T., Lee, J. T., Madzo, J., Liang, S., et al. (2017). Caloric restriction delays age-related methylation drift. *Nat. Commun.* 8 (1), 539. doi: 10.1038/s41467-017-00607-3

McGill, H. C.Jr, McMahan, C. A., and Gidding, S. S. (2008). Preventing heart disease in the 21st century: implications of the Pathobiological Determinants of Atherosclerosis in Youth (PDAY) study. *Circulation* 117 (9), 1216–1227. doi: 10.1161/CIRCULATIONAHA.107.717033

McNulty, H., Pentieva, K., Hoey, L., and Ward, M. (2008). Homocysteine, B-vitamins and CVD. *Proc. Nutr. Soc* 67 (2), 232–237. doi: 10.1017/S0029665108007076

Menghini, R., Casagrande, V., Cardellini, M., Martelli, E., Terrinoni, A., Amati, F., et al. (2009). MicroRNA 217 modulates endothelial cell senescence via silent information regulator 1. *Circulation* 120 (15), 1524–1532. doi: 10.1161/CIRCULATIONAHA.109.864629

Mikhed, Y., Daiber, A., and Steven, S. (2015). Mitochondrial Oxidative Stress, Mitochondrial DNA Damage and Their Role in Age-Related Vascular Dysfunction. *Int. J. Mol. Sci.* 16 (7), 15918–15953. doi: 10.3390/ijms160715918

Mullican, S. E., Gaddis, C. A., Alenghat, T., Nair, M. G., Giacomin, P. R., Everett, L. J., et al. (2011). Histone deacetylase 3 is an epigenomic brake in macrophage alternative activation. *Genes Dev.* 25 (23), 2480–2488. doi: 10.1101/gad.175950.111

Nawy, T. (2014). Single-cell sequencing. *Nat. Methods* 11 (1), 18. doi: 10.1038/nmeth.2771

Novella, S., Heras, M., Hermenegildo, C., and Dantas, A. P. (2012). Effects of estrogen on vascular inflammation: a matter of timing. *Arterioscler. Thromb. Vasc. Biol.* 32 (8), 2035–2042. doi: 10.1161/ATVBAHA.112.250308

Okano, M., Bell, D. W., Haber, D. A., and Li, E. (1999). DNA methyltransferases Dnmt3a and Dnmt3b are essential for de novo methylation and mammalian development. *Cell* 99 (3), 247–257. doi: 10.1016/s0092-8674(00)81656-6

O'Rourke, M. F., Safar, M. E., and Dzau, V. (2010). The Cardiovascular Continuum extended: aging effects on the aorta and microvasculature. *Vasc. Med.* 15 (6), 461–468. doi: 10.1177/1358863X10382946

Pan, M. H., Lai, C. S., Wu, J. C., and Ho, C. T. (2013). Epigenetic and disease targets by polyphenols. *Curr. Pharm. Des.* 19 (34), 6156–6185. doi: 10.2174/1381612811319340010

Pollack, R. M., and Crandall, J. P. (2013). Resveratrol: therapeutic potential for improving cardiometabolic health. *Am. J. Hypertens.* 26 (11), 1260–1268. doi: 10.1093/ajh/hpt165

Rothgiesser, K. M., Erener, S., Waibel, S., Lüscher, B., and Hottiger, M. O. (2019). Correction: SIRT2 regulates NF-κB-dependent gene expression through deacetylation of p65 Lys310 (doi:10.1242/jcs.073783). *J. Cell Sci.* 132 (8), jcs232801. doi: 10.1242/jcs.232801

Schiano, C., Vietri, M. T., Grimaldi, V., Picascia, A., De Pascale, M. R., and Napoli, C. (2015). Epigenetic-related therapeutic challenges in cardiovascular disease. *Trends Pharmacol. Sci.* 36 (4), 226–235. doi: 10.1016/j.tips.2015.02.005

Sen, P., Shah, P. P., Nativio, R., and Berger, S. L. (2016). Epigenetic Mechanisms of Longevity and Aging. *Cell* 166 (4), 822–839. doi: 10.1016/j.cell.2016.07.050

Shahbazian, M. D., and Grunstein, M. (2007). Functions of site-specific histone acetylation and deacetylation. *Annu. Rev. Biochem.* 76, 75–100. doi: 10.1146/annurev.biochem.76.052705.162114

Takemura, A., Iijima, K., Ota, H., Son, B. K., Ito, Y., Ogawa, S., et al. (2011). Sirtuin 1 retards hyperphosphatemia-induced calcification of vascular smooth muscle cells. *Arterioscler. Thromb. Vasc. Biol.* 31 (9), 2054–2062. doi: 10.1161/ATVBAHA.110.216739

Tan, Q., Christiansen, L., Thomassen, M., Kruse, T. A., and Christensen, K. (2013). Twins for epigenetic studies of human aging and development. *Ageing Res. Rev.* 12 (1), 182–187. doi: 10.1016/j.arr.2012.06.004

Tan, P., Wang, H., Zhan, J., Ma, X., Cui, X., Wang, Y., et al. (2019). Rapamycin□induced miR□30a downregulation inhibits senescence of VSMCs by targeting Beclin1. *Int. J. Mol. Med.* 43 (3), 1311–1320. doi: 10.3892/ijmm.2019.4074

Tarun, A., and Antoniades, C. (2018). The era of cardiovascular epigenetics: histone deacetylases and vascular inflammation. *Cardiovasc. Res.* 114 (7), 928–930. doi: 10.1093/cvr/cvy099

Tian, H., Liu, C., Zou, X., Wu, W., Zhang, C., and Yuan, D. (2015). MiRNA-194 Regulates Palmitic Acid-Induced Toll-Like Receptor 4 Inflammatory Responses in THP-1 Cells. *Nutrients* 7 (5), 3483–3496. doi: 10.3390/nu7053483

Tsaprouni, L. G., Yang, T. P., Bell, J., Dick, K. J., Kanoni, S., Nisbet, J., et al. (2014). Cigarette smoking reduces DNA methylation levels at multiple genomic loci but the effect is partially reversible upon cessation. *Epigenetics* 9 (10), 1382–1396. doi: 10.4161/15592294.2014.969637

Van Camp, G. (2014). Cardiovascular disease prevention. *Acta Clin. Belg.* 69 (6), 407–411. doi: 10.1179/2295333714Y.0000000069

Ventura, A., Luzi, L., Pacini, S., Baldari, C. T., and Pelicci, P. G. (2002). The p66Shc longevity gene is silenced through epigenetic modifications of an alternative promoter. *J. Biol. Chem.* 277 (25), 22370–22376. doi: 10.1074/jbc.M200280200

Voelter-Mahlknecht, S. (2016). Epigenetic associations in relation to cardiovascular prevention and therapeutics. *Clin. Epigenet.* 8, 4. doi: 10.1186/s13148-016-0170-0

Wan, Y. Z., Gao, P., Zhou, S., Zhang, Z. Q., Hao, D. L., Lian, L. S., et al. (2014). SIRT1-mediated epigenetic downregulation of plasminogen activator inhibitor-1 prevents vascular endothelial replicative senescence. *Aging Cell* 13 (5), 890–899. doi: 10.1111/acel.12247

Wang, M., Khazan, B., and Lakatta, E. G. (2010a). Central Arterial Aging and Angiotensin II Signaling. *Curr. Hypertens. Rev.* 6 (4), 266–281. doi: 10.2174/157340210793611668

Wang, M., Monticone, R. E., and Lakatta, E. G. (2010b). Arterial aging: a journey into subclinical arterial disease. *Curr. Opin. Nephrol. Hypertens.* 19 (2), 201–207. doi: 10.1097/MNH.0b013e3283361c0b

Winnik, S., Auwerx, J., Sinclair, D. A., and Matter, C. M. (2015). Protective effects of sirtuins in cardiovascular diseases: from bench to bedside. *Eur. Heart J.* 36 (48), 3404–3412. doi: 10.1093/eurheartj/ehv290

Wu, X. Y., Fan, W. D., Fang, R., and Wu, G. F. (2014). Regulation of microRNA-155 in endothelial inflammation by targeting nuclear factor (NF)-κB P65. *J. Cell Biochem.* 115 (11), 1928–1936. doi: 10.1002/jcb.24864

Wu, C. L., Wang, Y., Jin, B., Chen, H., Xie, B. S., and Mao, Z. B. (2015). Senescence-associated Long Non-coding RNA (SALNR) Delays Oncogene-induced Senescence through NF90 Regulation. *J. Biol. Chem.* 290 (50), 30175–30192. doi: 10.1074/jbc.M115.661785

Wu, W., Qin, M., Jia, W., Huang, Z., Li, Z., Yang, D., et al. (2019). Cystathionine-γ-lyase ameliorates the histone demethylase JMJD3-mediated autoimmune response in rheumatoid arthritis. *Cell Mol. Immunol.* 16 (8), 694–705. doi: 10.1038/s41423-018-0037-8

Xu, S., Kamato, D., Little, P. J., Nakagawa, S., Pelisek, J., and Jin, Z. G. (2019). Targeting epigenetics and non-coding RNAs in atherosclerosis: from mechanisms to therapeutics. *Pharmacol. Ther.* 196, 15–43. doi: 10.1016/j.pharmthera.2018.11.003

Yang, D., Xiao, C., Long, F., Su, Z., Jia, W., Qin, M., et al. (2018). HDAC4 regulates vascular inflammation via activation of autophagy. *Cardiovasc. Res.* 114 (7), 1016–1028. doi: 10.1093/cvr/cvy051

Yang, D., Xiao, C., Long, F., Wu, W., Huang, M., Qu, L., et al. (2019). Fra-1 plays a critical role in angiotensin II-induced vascular senescence. *FASEB J.* 33 (6), 7603–7614. doi: 10.1096/fj.201801671RRRR

Yue, Y., Liu, J., and He, C. (2015). RNA N6-methyladenosine methylation in post-transcriptional gene expression regulation. *Genes Dev.* 29 (13), 1343–1355. doi: 10.1101/gad.262766.115

Zhang, L., Qin, X., Zhao, Y., Fast, L., Zhuang, S., Liu, P., et al. (2012). Inhibition of histone deacetylases preserves myocardial performance and prevents cardiac remodeling through stimulation of endogenous angiomyogenesis. *J. Pharmacol. Exp. Ther.* 341 (1), 285–293. doi: 10.1124/jpet.111.189910

Conflict of Interest: The authors declare that the research was conducted in the absence of any commercial or financial relationships that could be construed as a potential conflict of interest.

Advantages of publishing in Frontiers

OPEN ACCESS
Articles are free to read for greatest visibility and readership

FAST PUBLICATION
Around 90 days from submission to decision

HIGH QUALITY PEER-REVIEW
Rigorous, collaborative, and constructive peer-review

TRANSPARENT PEER-REVIEW
Editors and reviewers acknowledged by name on published articles

Frontiers
Avenue du Tribunal-Fédéral 34
1005 Lausanne | Switzerland

Visit us: www.frontiersin.org
Contact us: info@frontiersin.org | +41 21 510 17 00

REPRODUCIBILITY OF RESEARCH
Support open data and methods to enhance research reproducibility

DIGITAL PUBLISHING
Articles designed for optimal readership across devices

FOLLOW US
@frontiersin

IMPACT METRICS
Advanced article metrics track visibility across digital media

EXTENSIVE PROMOTION
Marketing and promotion of impactful research

LOOP RESEARCH NETWORK
Our network increases your article's readership